



University of Zagreb

UNIVERSITY OF ZAGREB
FACULTY OF HUMANITIES AND SOCIAL SCIENCES

Katarina Gerometta

**LATE PLEISTOCENE TO HOLOCENE
CAVE GEOARCHAEOLOGY ON THE
EASTERN ADRIATIC COAST AND IN ITS
HINTERLAND**

DOCTORAL DISSERTATION

Zagreb, 2017



Sveučilište u Zagrebu

SVEUČILIŠTE U ZAGREBU
FILOZOFSKI FAKULTET

Katarina Gerometta

**GEOARHEOLOGIJA PLEISTOCENSKIH I
HOLOCENSKIH PEĆINSKIH NALAZIŠTA
ISTOČNE JADRANSKE OBALE I
ZALEĐA**

DOKTORSKI RAD

Zagreb, 2017.



University of Zagreb

UNIVERSITY OF ZAGREB
FACULTY OF HUMANITIES AND SOCIAL SCIENCES

KATARINA GEROMETTA

**LATE PLEISTOCENE TO HOLOCENE
CAVE GEOARCHAEOLOGY ON THE
EASTERN ADRIATIC COAST AND IN ITS
HINTERLAND**

DOCTORAL DISSERTATION

Supervisors:
Prof. Giovanni Boschian
Prof. Ivor Karavanić, Ph.D.

Zagreb, 2017



Sveučilište u Zagrebu

SVEUČILIŠTE U ZAGREBU
FILOZOFSKI FAKULTET

Katarina Gerometta

**GEOARHEOLOGIJA PLEISTOCENSKIH I
HOLOCENSKIH PEĆINSKIH NALAZIŠTA
ISTOČNE JADRANSKE OBALE I
ZALEĐA**

DOKTORSKI RAD

Mentori:
Prof. Giovanni Boschian
Prof. dr. sc. Ivor Karavanić

Zagreb, 2017.

Acknowledgements

The doctoral dissertation research has been funded from research projects *Špilja Zala, Velika pećina u Kličevici* (both financed by the Ministry of Culture of the Republic of Croatia), *Kremeni materijali, tehnologija i prilagodba u kamenom dobu Hrvatske* (Ministry of Science and Education of the Republic of Croatia), all led by Prof. dr. sc. Ivor Karavanić, Faculty of Humanities and Social Sciences, University of Zagreb; *Srednjovjekovna Istra: prostor zajedništva i suprotnosti (od VI. do XVI. st.)* (Ministry of Science and Education of the Republic of Croatia) led by Prof. dr. sc. Ivan Jurković, Faculty of Humanities, Juraj Dobrila University of Pula; *Fondi Ex 60% Dipartimento di Scienze Archeologiche*, Prof. Giovanni Boschian, University of Pisa; Vrsar Municipality scholarship, an Erasmus+ Grant, and my parents.

Information on supervisors

Prof. Giovanni Boschian graduated in Geological Sciences from the University of Trieste in 1985, after which he worked as consultant archaeologist and geoarchaeologist in various projects, mainly state archaeological heritage offices and universities. Since 1990 he works at the University of Pisa, first at the Department of Archaeological Sciences (1990-2010) as research technician, research engineer, researcher, all the time teaching courses on Geoarchaeology. Since 2011 he is Associate Professor at the Department of Biology, University of Pisa, teaching courses on environmental archaeology and geoarchaeology. His field research relates mostly to the stratigraphic, geoarchaeological and palaeoenvironmental aspects of the excavated sites. He has organised four meetings of geoarchaeologists in Pisa (1995, 1998, 2003, 2011). He is team member of various current projects in Italy, South Africa, Georgia, Croatia, Bosnia and Herzegovina, and co-director of two in Italy (Visogliano rock-shelter, Trieste; Grotta della Cala dei Santi, Tuscany). He was active in two INTERREG IIIA projects from 2000 to 2006: Italy – France and Italy – Slovenia and is now coordinator of the University of Pisa partner in the H2020-TWINN project “MendTheGap”. He has published numerous scientific papers in journals and congress proceedings (see: <http://arp.unipi.it/listedoc.php?ide=007571&ord=C>).

Prof. Ivor Karavanić, PhD graduated in Archeology in 1990, he obtained his MA in 1993 and PhD in 1999 from the Faculty of Humanities and Social Sciences in Zagreb. Professional interests include Paleolithic archeology, human evolution, prehistoric chipped stone techniques and prehistoric religion. The main scientific interest is focused on the study of adjustments of the Middle Paleolithic and Upper Paleolithic hunter-gatherers in Central Europe and the Mediterranean, in particular with regard to their lithic industry. Prof. Karavanić was principal investigator of Mujina Pećina, Zemunica, Zala, Velika Pećina (Kličevica) and the underwater Paleolithic site Kastel Štafilić - Resnik. He was awarded two grants from the French government, a Constantin-Jireček scholarship in Austria, and the Fulbright scholarship in the US. He was a visiting professor at the Muséum National d'Histoire Naturelle (IPH, Paris), University of Ljubljana, Jagiellonian University (Krakow), head of the Department of Archeology and Vice Dean of the Faculty of Humanities and Social Sciences in Zagreb. He has published numerous scientific papers and participated in conferences at home and abroad (see: <https://bib.irb.hr/lista-radova?autor=188740>).

SUMMARY

The dissertation deals with the interpretation of the archaeological layers of five cave archaeological sites: Mujina Pećina near Kaštela, Velika pećina-Kličevica near Benkovac, Zemunica in Bisko, Zala near Ogulin and Romualdova Pećina near Rovinj. The study is based on geoarchaeological analyses that include a detailed description of the stratigraphic sequence at each site, sedimentological laboratory analyses and micromorphological analysis of sediments. The subjects of this study are prehistoric layers from the mentioned caves, from the Middle Palaeolithic to the Bronze Age levels. The main goals of the geoarchaeological study were to understand the infilling and postdepositional processes of the five caves, and the environmental conditions that controlled them, as well as the use of the cave by humans and animals. The identified site formation processes are polygenetic in origin and can generally be divided in geogenic, non-human biogenic processes and processes derived by anthropogenic activities. The analyses confirmed the hypothesis of different cave use by Middle Paleolithic, Upper Paleolithic, Mesolithic, Neolithic and Bronze Age humans. The environmental data from the sediments do not show particular connection between climate and Neandertal presence in Romualdova and Velika Pećina-Kličevica. The data from Mujina Pećina differ in some extent. The human presence in the cave was more frequent during the earlier warmer phases and the rather arid event corresponding to loess deposition. The phase of more intense and continuous use of the cave by humans was during the deposition of unit E3C. The Upper Palaeolithic levels consist of domestic waste residues. The Mesolithic levels mostly comprise domestic waste deposits, including ash, bone fragments, and more or less crushed land snails. The Neolithic, Copper, and Bronze Age part of the sequences are characterised by continuous evidence of sheep/goat and probably cattle dung accumulations, and were used as pastoral sites.

Key words: geoarchaeology, sedimentology, soil micromorphology, site formation processes, caves, prehistory, Eastern Adriatic.

SAŽETAK

Arheologija se često definira kao znanost koja proučava prošle kulture na temelju materijalnih ostataka koje su one ostavile iza sebe. U te se ostatke ubrajaju razne konstrukcije, zatim alatke izrađene od raznolikih materijala, umjetnički predmeti, kosti te ostale rukotvorine i nalazi ljudskih aktivnosti. Svi su nam ti predmeti važni za proučavanje ljudskog ponašanja u prošlosti. Međutim, najveći dio materijala koji arheolozi iskopaju prilikom svojih istraživanja nisu samo ti objekti, već nadasve tlo ili sediment u kojem su se pronađeni objekti nalazili, odnosno njihov kontekst, koji se može također djelomično smatrati rukotvorinom, s obzirom da čovjek sudjeluje u njegovom formiranju putem raznolikih aktivnosti. U ovom doktorskom radu bit će riječ upravo o sedimentima i njihovoj važnosti pri interpretaciji arheoloških nalaza i nalazišta. Da bi razumijeli kontekst nalaza moramo razumijeti, između ostalog, i procese koji su doveli do njihovog nastanka.

Tema doktorskog rada je interpretacija arheoloških slojeva pet špiljskih arheoloških nalazišta: Mujine pećine kod Kaštela, Velike pećine u kanjonu Kličevice nedaleko Benkovca, Zemunice kod Biskog, Zale kod Ougulina i Romualdove špilje nedaleko Rovinja. Istraživanje se temelji na geoarheološkoj analizi koja uključuje detaljan opis stratigrafskog slijeda na pojedinom nalazištu, osnovne sedimentološke laboratorijske analize te mikromorfološke analize sedimenata. Predmet istraživanja jesu prapovijesni slojevi u navedenim špiljama, od srednjeg paleolitika do brončanoga doba. U radu je objašnjen međusobni utjecaj prapovijesnoga čovjeka i njegovog okoliša te razlike u upotrebi špiljskog prostora tijekom kasnoga pleistocena i holocena na prostoru istočnog Jadrana.

Cilj geoarheološkog istraživanja pet navedenih špilja jest ustanoviti procese taloženja sedimenata, postdepozicijske procese te uvjete u okolišu koji su ih kontrolirali, kao i ljudske aktivnosti u špiljama. Identificirani procesi formiranje primjene su poligenetsku osnovu porijekla i općenito se može podijeliti u geogene, neljudskih biogenih procesima i procesima dobivenih ljudskim aktivnostima. Analize su potvrđili hipotezu o različitim korištenja špilje srednjeg paleolitika, gornji paleolitik, mezolitik, neolitika i brončanog doba ljudi.

Podaci za zaštitu okoliša iz sedimenata ne pokazuju posebnu vezu između klime i neandertalca prisutnosti u Romualdova i Velike Pećina-Kličevica. Podaci iz Mujina Pećina

razlikuju u određenoj mjeri. Ljudska prisutnost u njoj je češća tijekom ranijih toplijim fazama i prilično sušno slučaju odgovara lesnom taloženju. Faza intenzivniju i kontinuirano korištenje špilje ljudi je tijekom depozicije jedinice E3C. Razine gornjeg paleolitika sastoje od ostataka domaćih otpada. Mezolitika razine uglavnom obuhvaćaju domaće depozite otpada, uključujući i pepela, koštanih ulomaka, te više ili manje zdrobljenim kopnenim puževima. Neolitika, bakra, a brončano doba dio sekvence karakterizira kontinuirani dokaz ovaca / koza i vjerojatno stoke izmeta akumulacije, te su korišteni kao pastoralnih stranicama.

Ključne riječi: geoarheologija, sedimentologija, mikromorfologija tla, procesi formiranja nalazišta, špilje, prapovijest, istočni Jadran

Table of Contents

| | |
|---|-----------|
| 1. Introduction | 1 |
| 2. Study area | 5 |
| 3. Materials and methods..... | 12 |
| 3.1. Fieldwork | 14 |
| 3.2. Laboratory methods..... | 15 |
| 3.2.1. Sedimentological analyses | 15 |
| 3.2.2. Soil micromorphology | 17 |
| 4. Mujina Pećina..... | 20 |
| 4.1. Introduction..... | 5 |
| 4.2. Site presentation..... | 21 |
| 4.3. Archaeological background | 22 |
| 4.4. Results | 24 |
| 4.4.1. Field observations | 24 |
| 4.4.2. Architecture of the stratigraphic units and sediment texture | 28 |
| 4.4.3. Micromorphology | 31 |
| 4.5. Discussion..... | 39 |
| 4.6. Concluding remarks..... | 41 |
| 5. Zala | 42 |
| 5.1. Introduction..... | 42 |
| 5.2. Site presentation..... | 42 |
| 5.3. Archaeological background | 45 |
| 5.4. Results | 46 |
| 5.4.1. Field observations | 46 |
| 5.4.2. Sediment texture of the stratigraphic units | 52 |
| 5.4.3. Micromorphology | 53 |
| 5.5. Discussion..... | 62 |
| 5.6. Concluding remarks | 65 |
| 6. Zemunica | 67 |
| 6.1. Introduction..... | 67 |
| 6.2. Site presentation..... | 67 |
| 6.3. Archaeological background | 68 |

| | |
|---|------------|
| 6.4. Results | 71 |
| 6.4.1. Field observations | 71 |
| 6.4.2. Architecture of the stratigraphic units and sediment texture | 76 |
| 6.4.3. Micromorphology | 80 |
| 6.5. Discussion..... | 99 |
| 6.6. Concluding remarks | 102 |
| 7. Romualdova Pećina..... | 103 |
| 7.1. Introduction..... | 103 |
| 7.2. Site presentation..... | 104 |
| 7.3. Archaeological background | 105 |
| 7.4. Results | 107 |
| 7.4.1. Field observations | 107 |
| 7.4.2. Architecture of the stratigraphic units and sediment texture | 108 |
| 7.4.3. Micromorphology | 110 |
| 7.5. Discussion..... | 119 |
| 7.6. Concluding remarks | 121 |
| 8. Velika Pećina - Kličevica | 122 |
| 8.1. Introduction..... | 122 |
| 8.2. Site presentation..... | 123 |
| 8.3. Archaeological background | 123 |
| 8.4. Results | 125 |
| 8.4.1. Field observations | 125 |
| 8.4.2. Sediment texture of the stratigraphic units | 128 |
| 8.4.3. Micromorphology | 130 |
| 8.5. Discussion..... | 140 |
| 8.6. Concluding remarks | 141 |
| 9. Conclusions | 142 |
| Bibliography | 146 |
| List of Figures | 153 |
| List of Tables..... | 157 |
| Biography | 158 |
| Appendix 1 | 160 |

| | |
|-------------------|-----|
| Appendix 2 | 172 |
| Appendix 3 | 184 |
| Appendix 4 | 199 |
| Appendix 5 | 214 |
| Appendix 6 | 238 |
| Appendix 7 | 261 |
| Appendix 8 | 272 |
| Appendix 9 | 283 |
| Appendix 10 | 290 |

1. INTRODUCTION

Archaeology is often referred to as the science that studies past cultures based on artefacts they left behind. These include various structures (e.g. houses, hearths, ovens, etc.), tools made from different materials, art objects, bones and other artefacts related to human activities. All these objects are important for the study of human behaviour in the past. However, most of the material found by archaeologists during their excavations is not comprised only of these objects, but also the sediment or soil in which they were found, i.e. their context, can also be considered itself an artifact, since humans contribute to its formation through a variety of activities. This thesis will discuss sediments and their importance in the interpretation of findings and archaeological sites. In order to understand the context, it is also necessary to understand the processes that led to its formation. The branch of archaeology that studies the processes that led to the deposition of archaeological layers is called geoarchaeology.

The stratigraphic sequences of sediments, the possible hiatuses, reworking and disturbing of sediments can be determined using geoarchaeological methods. The observations carried out on geoarchaeological samples also allow us to determine the origin of the sediments on an archaeological site, i.e. whether it is related to human activities (culturally conditioned) or formed by natural processes. What caused the deposition of sediments in a specific place? Why do some layers contain certain artefacts? What human behaviours or what natural processes have formed and modified the archaeological layers? All these and other questions can be answered through the study of site formation processes (Goldberg and Macphail, 2006; Butzer, 1964). One of the main objectives of geoarchaeology is to reconstruct the relationships that existed in the past between human groups and the environmental context in which they lived (Angelucci, 2009). Cave sediments allow us to understand to some extent the climate and environmental changes in the past. The possibility of obtaining paleoclimatic data from cave sediments depends on whether the climate was the deciding factor in the processes that led to the sedimentation of certain layers. Compared with the open-air sites, the entrances of caves and rock shelters represent a privileged environment of sedimentation for the reconstruction of the palaeo-environment and climate change.

The term geoarchaeology appears in the 1960's and involves a multidisciplinary scientific approach that uses the concepts and methods of archaeology and soil sciences to solve archaeological problems. Although I. W. Cornwall published his book *Soils for the*

Archaeologist already in 1958, geoarchaeology developed as a separate discipline in the late 1960's and 1970's (in this context, K. Butzer's book *Environment and Archaeology: An Introduction to Pleistocene Geography* from 1964 should be mentioned).

In 1938, the Austrian scientist W. L. Kubiëna published the book *Micropedology*, which represents a first attempt to introduce a terminology for the description of thin sections and a first synthesis of knowledge on the micromorphology. The interest for this discipline increased in the 1960 's when the need became more apparent for a new system for micromorphological descriptions of thin sections as well as the need for a new terminology, which was introduced by the Australian scientists R. Brewer and J. Sleeman (*Fabric and Mineral Analysis of Soils*, 1964). With new knowledge and discoveries in the field of micromorphology, and with new publications that appeared since the 1960's, in order to facilitate the understanding and communication among micromorphologists, a new terminology was proposed by Bullock et al. in the *Handbook for Soil Thin Section Description* (1985), which is now widely accepted. Based on this manual, but with somewhat modified terminology, G. Stoops published in 2003 the *Guidelines for Analysis and description of Soil and Regolith Thin Sections*, which represents the main textbook for morphological description of soil samples and sediments. Although since the 1960's many papers related to micromorphological analysis and interpretation were published, only in 2010 the manual *Interpretation of Micromorphological Features of Soils and Regoliths* (eds. G. Stoops, V. Marcelino and F. Mees) appeared, which includes not only the terminology for the description, but also interpretations of micromorphological samples.

During the 1970's archaeologists realised the importance of studying the context of the findings for the interpretation of past events on archaeological sites. They understood that the archaeological record cannot be considered only as a fossilised record of human behaviour because it suffered modifications due to various processes. It was necessary to find a way to identify such processes. Based on previous knowledge in geoarchaeology and the study of site formation processes, M. B. Schiffer developed the concept of the formation of archaeological sites and divided the processes into cultural (anthropogenic) and natural ones: the so-called C-transforms and N-transforms (Schiffer, 1983). His concept is based largely on observations done by Butzer (1982) such as the influence of water on the horizontal distribution of artefacts or changes in the soil as a result of ice activities. Butzer (1982) also noted that the processes that occur during population growth differ significantly from those during the negative demographic phase, i.e. during the abandonment of the settlement (e. g. layers forming a tell that belong to the time of the abandonment of the settlement, formed as a result

of decay and destruction of houses and other structures, are thicker than those from the period of the occupation, and the deposition is faster (Butzer, 1982; Miller Rosen, 1986).

Using standard geological methods, Malez, Paquette, An. Šimunić and Al. Šimunić studied the sediments containing archaeological remains from the cave Vindija with special reference to the climatic conditions during the sedimentation (Malez and Rukavina, 1975; Malez et al., 1984). The only systematic micromorphological study of sediments from Croatian caves has been published by G. Boschian for Pupićina Peć in Istria (Boschian, 2006).

Most of the archaeological research on sites in caves is carried out at the entrance of the cave, where sediments of various origins accumulate, often resulting in a complex stratigraphic sequence. Most of the caves analysed for this thesis have that kind of sediments.

The research objectives are: to identify postdepositional and depositional processes of archaeological layers in each of the studied caves (Mujina Pećina, Zala, Zemunica, Romualdova Pećina, Velika Pećina-Kličevica), to determine how and to what extent humans changed (influenced) their environment during prehistory and to provide a more complete picture of the archaeological context, also identifying possible sin- and postdepositional reworking of sediments.

The main hypotheses to be tested are:

- It is possible to observe differences in the use of caves (and their eventual abandonment) in different periods and these differences reflect different human behaviour and their relationship with the environment surrounding them.
- It is commonly assumed that the Neandertals were adapted to a cold climate; since it is possible to reconstruct the climate of the period of human occupation of the caves through the study of sediments, it will also be possible to verify if Neandertals used caves predominantly in cold or warm climate.

The study is based on geoarchaeological analysis that includes a detailed description of the stratigraphic sequence at each site, sedimentological laboratory analyses and micromorphological analysis of sediments. The subjects of this study are prehistoric layers from five caves, from the Middle Palaeolithic to the Bronze Age levels. Attempts will be made to explain the interaction of prehistoric humans with their environment, and to explain the differences in the use of the caves during the late Pleistocene and Holocene in the eastern Adriatic area.

By applying geoarchaeological methods to the study of archaeological sites, natural and cultural formation processes will be determined as well as eventual postdepositional

modifications on archaeological layers. The proposed research will provide new insights into the archaeological context, the relationship between humans and their environment and into the influence of the environment on human behaviour and will thus complete and improve the archaeological interpretation.

Since the micromorphological research related to archaeology is very rarely conducted in Croatia, this thesis should also contribute to the spreading of interest in such analyses, especially because micromorphology is used today as a standard method in archaeology and it represents a prerequisite for a more complete understanding of an archaeological site.

2. STUDY AREA

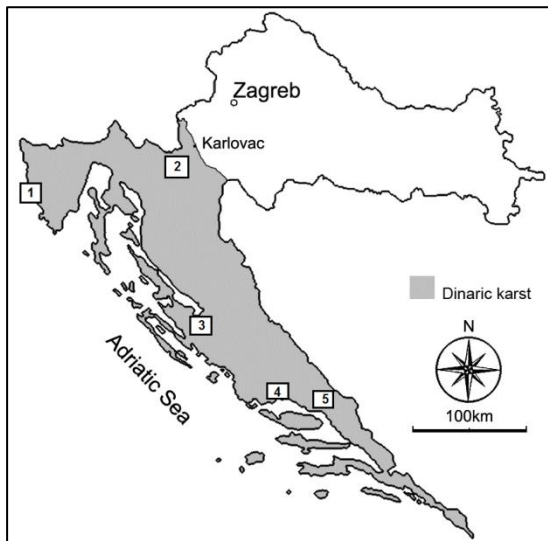


Figure 2.1 Study area: 1. Romualdova Pećina, 2. Pećina Zala, 3. Velika Pećina-Kličevica, 4. Mujina Pećina, 5. Pećina Zemunica.

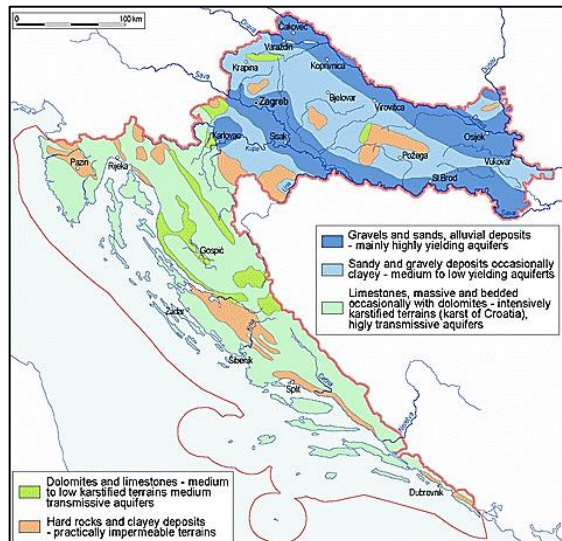


Figure 2.2 Hydrogeological map of Croatia (Bognar et al., 2012.).

The five caves studied in this thesis are situated in the Croatian karst (Fig. 2.1), which is part of the broader Dinaric karst, located between the Pannonian Basin and the Adriatic Sea. The main features include high plateaus and karst poljes oriented parallel to the typical Dinaric northwest-southeast direction of tectonic activity. The Dinaric karst consists predominantly of Triassic, Jurassic and Cretaceous limestones and dolomites (Fig. 2.2). The features of the Croatian karst are developed in the massively bedded Cretaceous limestones, the Promina Beds (alternating marls, sandstones, conglomerates, limestone and cherts, overlain by alluvial sediments, mostly made of conglomerates with marly beds including coal and plant remains), and the Jelar Breccia of unknown age.

During the Pleistocene, glacial processes affected only the higher parts of the Dinaric Mountains, above 1,100 m a. s. l (Mihevc and Prelovšek, 2010; Zupan Hajna, 2010).

The caves are situated in several geomorphological regions of the Dinaric Mountain Belt (after Bognar, 2001; Bognar et al., 2012), including:

1. Istrian Peninsula - South Istrian karst plateau (Romualdova Pećina),
2. Mountainous Croatia - area between Karlovac (Una-Korana) plateau and Ogulin-Plaški Valley (Pećina Zala),
3. North-Western Dalmatia - North Dalmatian karst plateau (Velika Pećina-Kličevica in Ravnici Kotari),

4. Central Dalmatia - coastal area of Central Dalmatia (Mujina Pećina),
5. Central Dalmatia - Middle Dalmatian Hinterland / Zagora (Pećina Zemunica).

According to its geomorphological and geological setting, the Istrian peninsula consists of three main regions. The *White Istria* covers the mountain ridge of Učka and the mountain group of Čićarija, it spreads in the northern and north-eastern part of the peninsula and is characterised by barren rocky karst surfaces. The north-western and central part of Istria is known as *Grey Istria*. It is composed of Eocene flysch consisting of impermeable marl, clay and sandstone (Riđanović, 1975); therefore most rivers and streams originate in this area. The southern and western part of Istria (*Red Istria*) consists of a limestone plateau where “terra rossa” soils (Alfisols and Ultisols) have developed, often with bauxite pockets (Roglić, 1975). The characteristics of “terra rossa” indicate its polygenetic origin (Roglić, 1975). “Materials other than the insoluble residue of limestones and dolomites that might have contributed to terra rossa are loess sediments, whose deposition was very important recurrent process in Istria probably since the early Middle Pleistocene, and flysch sediments which extended much more southwards from its present position” (Durn, Ottner and Slovenec, 1999, 126) (Fig. 2.5). “Quartz diagenetic sediments” (known also as “quartz sands” or “quartz sandstones”) occur within limestones in three separate layers (0.5 - 6 m thick) trending in two directions: NE-SW (Tinjan-Pula region) and NW-SE (Savudrija-Buje-Oprtalj region). These sediments are composed mostly of idiomorphic authigenic quartz crystals, microcrystalline quartz aggregates and cryptocrystalline to microcrystalline chert-like clusters (Durn et al., 2003).

The compressed core of the anticlinal structure of carbonate rocks (Upper Jurassic thick-bedded limestone) between Poreč and Rovinj directs water flow (Riđanović, 1975) (Fig. 2.4). Limska Draga (Lim Valley) is the 31 km long valley of the river Pazinčica (or Pazinski potok), which springs on the southern slopes of Učka, in a flysch area. Limska draga is the extension of a once permanent river that ran east of the present town of Pazin before the uplift of the Istrian limestone plateau and the formation of the Pazinski ponor. This was probably the course of the present Pazinčica River (Pazinski potok) whose course was later stopped by the elevated flysch hills around Mount Orljak and Veli Breh, and directed to the canyon of the present ponor at the border of flysch and limestone. Pazinčica directs its waters towards springs in the eastern and the southern part of the Istrian peninsula (Fig. 2.3).

Romualdova Pećina is situated on the southern side of the 10 km long Lim Bay, which is the continuation of the Limska Draga karst valley, now flooded by the Adriatic Sea.

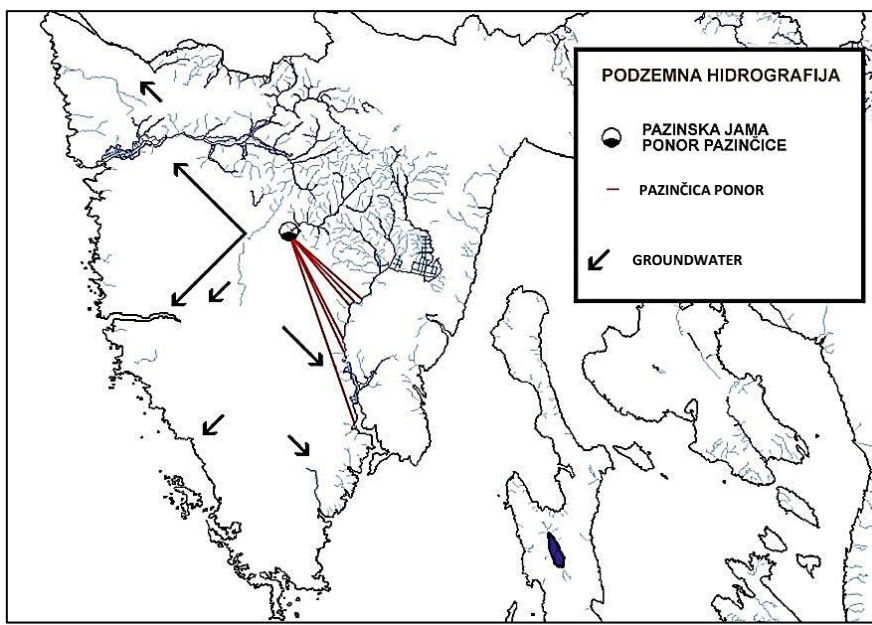


Figure 2.3 Underground hydrology of Istria (http://www.pazinska-jama.com/index_en.php?link=postanak).

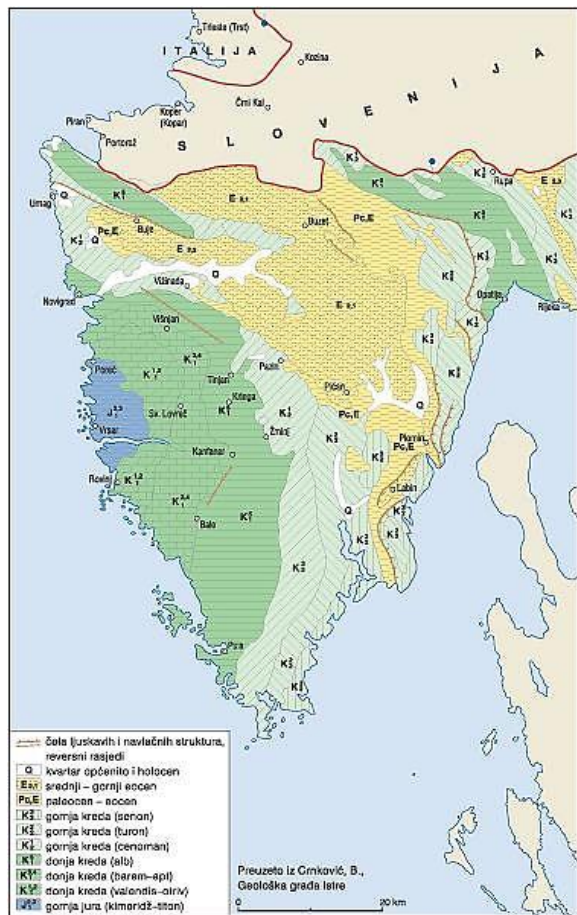


Figure 2.4 Geology of Istria (Vlahović et al., 2008).

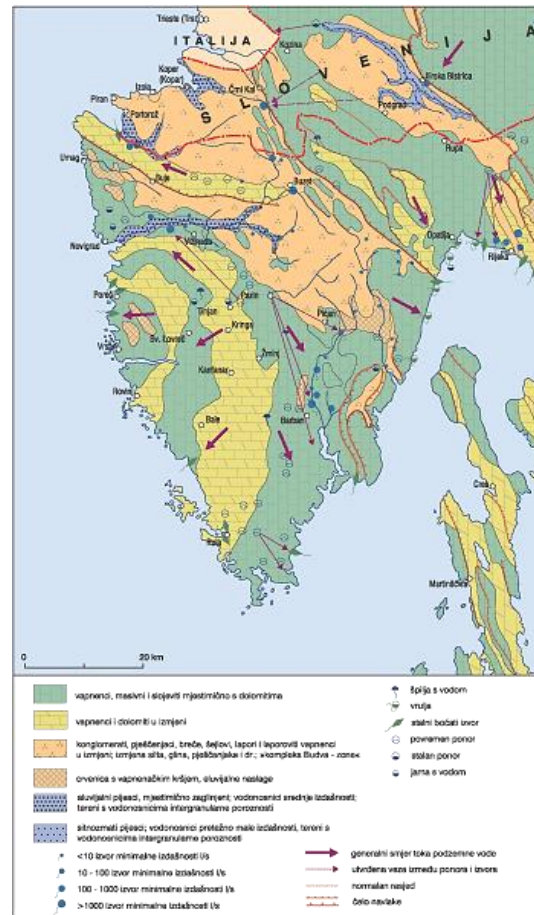


Figure 2.5 Hydrogeology of Istria (Božičević, 2008).

Pećina Zala is situated in the north-eastern part of the hilly-mountainous border of the Ogulin-Plaški Valley. It is located at the foot of the northern slopes of the Krpelj (or Krpel) Hill, which divides the Ogulin-Plaški Valley from the karstic valley of Dubrave, the area extending from the shallow karst of Pokuplje and Kordun (the transitional area between the Mountainous and Central Croatia) to Krpelj.

Four rock complexes can be distinguished in the Ogulin-Plaški microregion (Bahun, 1970).:

- clastic rocks of Upper Paleozoic and Triassic Age;
- Triassic and Jurassic dolomites;
- Jurassic dolomites with lenses of limestone;
- limestone almost exclusively of Cretaceous Age.

In addition to fluvial processes, dissolution was very important for the development of the morphology of the area, because it shaped a plateau at the foot of the slopes of Krpelj (between Ogulin and Oštarije) (Pavić, 1975). The whole area is characterized by elongated outcrops of limestone and dolomite, oriented NW-SE along a typical Dinaric trend; only in the Ogulinsko Zagorje there is a small outcrop of impermeable Triassic clastic rocks (Fig. 2.7). Several springs emerge along the eastern boundary of the dolomitic rocks outcrop, from Vitunj through Ogulin and up to Plaški, and feed the surface waters (Zagorska Mrežnica, Vrnjika, Dretulja). Few kilometres to the East, at the contact between dolomites and limestones, the surface waters sink into several ponors, and these waters re-emerge in neighbouring springs, after their underground course (Fig. 2.6). Water staining proved the connection between: Ogulinska Dobra and Gojačka Dobra, Zagorska Mrežnica and Bistrac, Zagorska Mrežnica with Tounjčica and Kukača, etc. (Riđanović, 1975).

The main types of soils in this area are rendzinas, brown soils, and podzolic soils; in small areas of carbonate rocks *terra rossa* also occurs (Pavić, 1975).

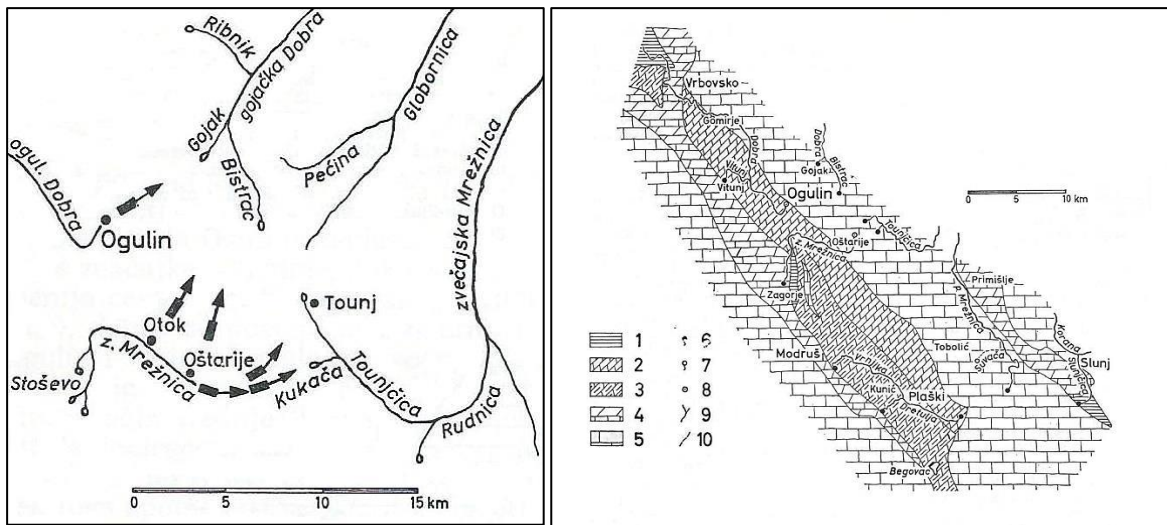


Figure 2.6 Underground hydrography of the Ogulin area (Pavić, 1975).

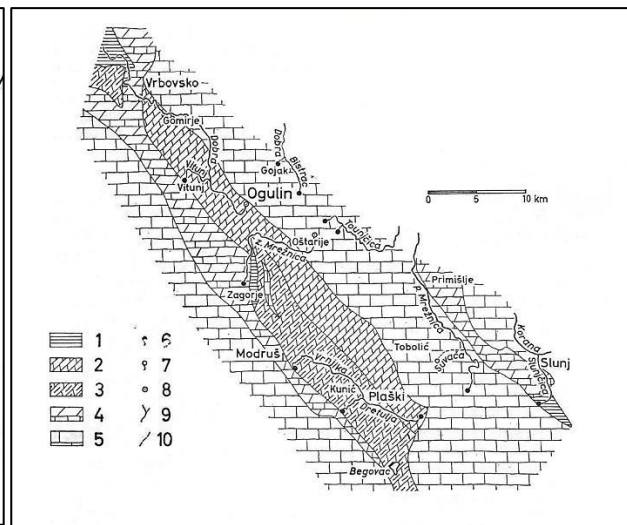


Figure 2.7 Geology of the Ogulin-Plaški Valley (Pavić, 1975). 1. Paleozoic and Triassic clastics, 2. Dogger and Malm and Lower Cretaceous dolomites, 3. Triassic, Liassic and partly Malm dolomites, 4. Malm dolomites and limestones, 5. Cretaceous limestones, 6. permanent spring, 7. periodical spring, 8. ponor, 9. permanent surface water stream, 10. periodical surface water stream.

Velika pećina is situated on the north-western side of the Kličevica river canyon, in the North Dalmatian karst plateau, in the area of Ravnici Kotari (Fig. 2.8).

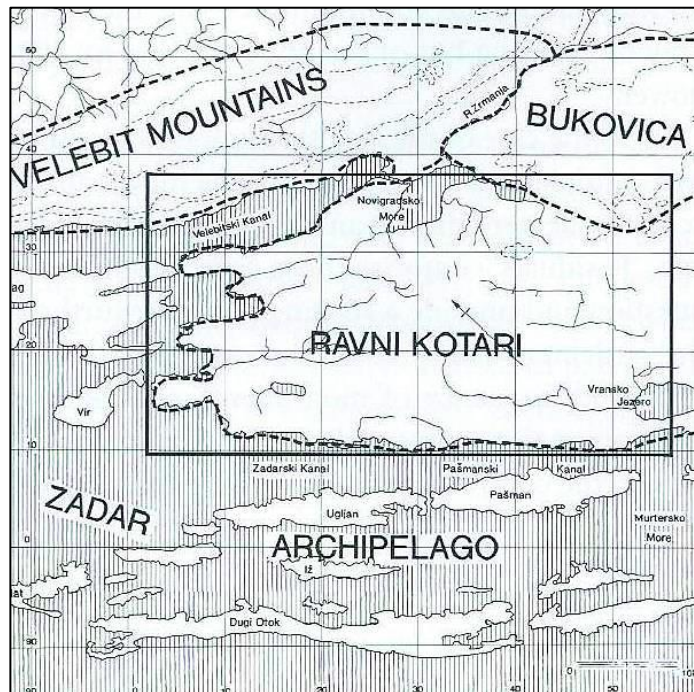


Figure 2.8 Ravnici Kotari and Bukovica (Chapman, J., Shields, R. and Batović, 1996).

The composition of the bedrock is zonal and affects the morphology of the landscape. Late Cretaceous and Tertiary limestones prevail in Ravnici Kotari, extending along the NW-SE Dinaric direction, while limestone ridges (anticline) alternate with valleys shaped on sandy marls in the transverse SW-NE direction. A higher limestone plateau – Bukovica-overhanged to the north by the Velebit mountain range lies in the direct hinterland of the cave. In Bukovica, Tertiary limestones (Promina) are the most common rock type, together with limestone breccias and conglomerates with marly intercalations and some bauxites (Obrovac bauxites) (Fig. 2.9). A series of small seasonal lakes, known as *blata*, occur in the higher valleys. The Benkovac valley drains into Nadinsko Blato through a deep gorge cut into a limestone ridge at Kličevica (Chapman, Shields and Batović, 1996).

The sedimentation in the valleys comprises the Eocene flysch, a series of Quaternary sands and gravels, and modern alluvium (Chapman, Shields and Batović, 1996). Soils on loess and sands are widespread and most fertile in Ravnici Kotari, especially in its western part, from Smilčić up to Nin. In the eastern part of Kotari, soils with limestone skeleton and marly soils prevail while scattered gravelly soil and *terra rossa* occur in Bukovica (Friganović, 1975).

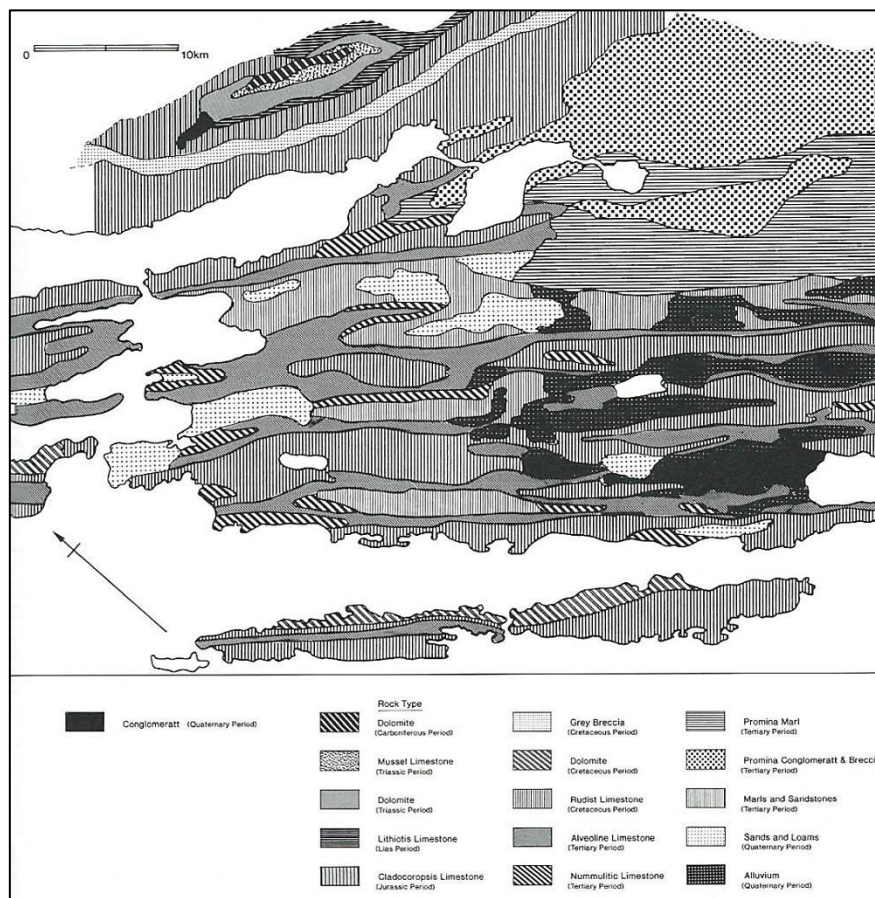


Figure 2.9 Geology of Ravnici Kotari and Bukovica (Chapman, J., Shields, R. and Batović, 1996).

Mujina Pećina and Pećina Zemunica are situated in Central Dalmatia, the first one in the coastal area of the Split region, the second one in the hinterland (Dalmatinska Zagora or Middle Dalmatian Hinterland), which is divided from the coast by the Kozjak and Mosor mountains.

Cretaceous and Paleogene limestones prevail in Zagora, with occasional intercalations of older Triassic sediments - Werfenian schists, and gypsum (on the edge of Muć fields, in the valleys of Vrba, on the slopes of Svilaja and Moseć). The limestone reefs of Opor (650 m), Perun (485 m), Kozjak (780 m) and Mosor (1340 m) form an anticlinal fold, running steeply towards the coast (Friganović, 1975). Pećina Zemunica is situated at the foot of the Mali Mosor Hills, in Turonian limestones with dolomite lenses, looking onto the Dicmo (Krušvarsko or Bisko) karstic polje - a fertile field with dominant *terra rossa* soils (Fig. 2.10).

In the area between the limestone reefs and the coast - in Kaštela, Solin, Split and Stobreč polje - a narrow belt of tertiary marls (flysch) is interbedded with Neogene limestones and Quaternary alluvium (Friganović, 1975).

Limestone cliffs, marl slopes and alluvial plains are characteristic of the natural basis of the Split coast. The area surrounding Mujina Pećina is tectonically complex, with stratified limestone and massive and stratified limestone overthrust on foraminiferal limestone (Marinčić, Magaš and Borović, 1971).

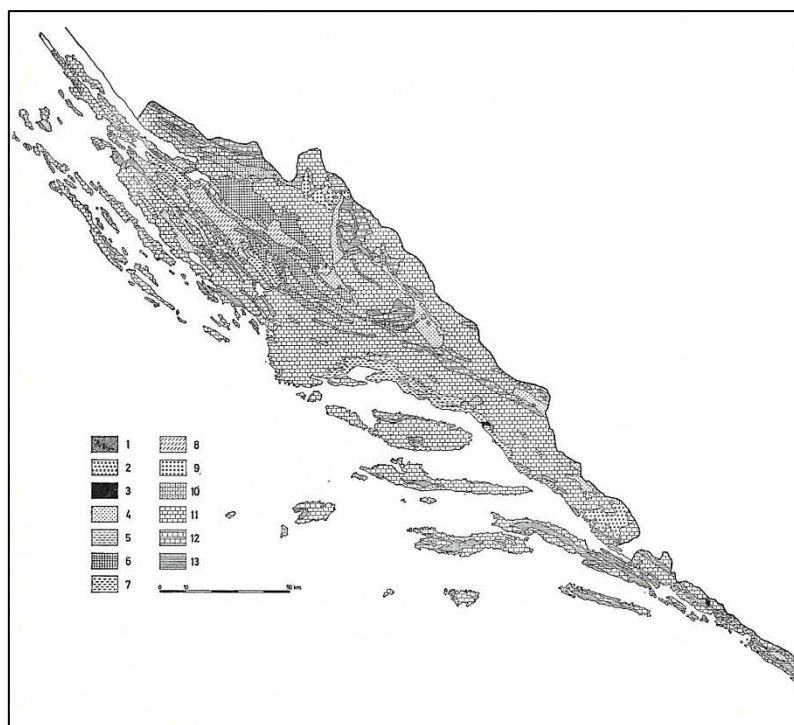


Figure 2.10 Geological sketch of Dalmatia: 1. sands and lacustrine deposits (Late Neogene), 2. recent alluvial sediments, 3. recent gravel and sandy debris, 4. alluvium and *terra rossa* (Quaternary), 5. lacustrine clay and marl deposits (Late Neogene), 6. limestone conglomerates (Paleogene) intercalated with sandstones and marl, 7. platy and stratified/layered flysch (Paleogene), 8. marls and conglomerates (Paleogene), 9. flysch-like deposits (Mesozoic), 10. limestone breccia (mostly Upper and Lower Cretaceous), 11. stratified and banked karstified limestone (Mesozoic), 12. limestones and dolomites (mostly Mesozoic), 13. dolomites (mostly Mesozoic) (Roglić, 1975).

3. MATERIALS AND METHODS

"Geoarchaeology begins in the field, for it is there where observations are made and initial data are generated. Missed opportunities in making sound field observations are very difficult to make up for, (...) since the archaeological record is extracted from the "geological" context..." (Goldberg and Macphail 2006, 299).

This thesis examines the archaeological sediments of five Late Pleistocene to Holocene cave sites (Mujina Pećina, Zala, Romualdova Pećina, Zemunica and Velika Pećina - Kličevica). Emphasis is put on the prehistoric horizons, from the Middle Paleolithic to the Bronze Age.

Mujina Pećina is located north of Kaštela, about 260 m above sea level. All layers of the cave belong to the Middle Late Pleistocene (45000 - 39000 BP) and contain finds of the Middle Paleolithic Mousterian culture (Rink et al., 2002; Karavanić et al., 2008). Samples were taken from two profiles (southern and western) of the archaeological trench inside the cave; a sample of red soil (*terra rossa*) was taken as a control sample in the vicinity of the cave. A total of 12 samples were analysed for grain-size analyses, and seven samples for micromorphological analysis.

The cave Zala (Mikašinovića Pećina / Savića Pećina) is located near the town of Ogulin, on the left side of the stream Bistrac. The stratigraphic sequence comprises numerous layers that belong to the Late Pleistocene (Late Upper Paleolithic) and Holocene (Mesolithic, Bronze Age, Iron Age, Roman period, and Middle Ages); 15 samples for grain size analyses and seven samples for micromorphological analysis were studied.

Romualdova Pećina is situated on the northern slope of the St. Martin's Hill (Sv. Martin), on the south coast of the Lim Bay (Lim Channel), close to its eastern end. The entrance to the cave is located about 120 metres above sea level (Malez). Most of the layers belong to the Middle Late Pleistocene; the findings were ascribed to the Middle and Upper Paleolithic according to the typological characteristics; Holocene layers are also present (including Bronze Age and more recent finds). The profiles of trench 1, excavated in 2007

(Komšo, 2011) and situated near the entrance of the cave were sampled; 11 samples for grain size analyses and 13 samples for micromorphological analysis were analysed.

The cave Zemunica is located at the foot of the northern part of the Mali Mosor, close to the village of Bisko, near Trilj. The stratigraphic sequence is formed by some Pleistocene (Late Upper Paleolithic) and numerous Holocene layers (Mesolithic, Neolithic, Copper Age, and Bronze Age) (Šošić-Klindžić et al., 2015); 24 samples were collected for grain size analyses and 31 samples for micromorphological analysis.

Velika Pećina is located on the northern slope of the canyon of the Kličevica creek, near the village of Raštević, near Benkovac. The stratigraphic sequence is relatively short: layer D was dated to $39240 + / -740$ BP ($^{14}\text{C} - \text{AMS}$, Beta-228733), belongs to the Late Pleistocene (with Mousterian finds) and overlaps chronologically with the upper layers of the Mujina pećina (Karavanić, Čondić and Vukosavljević, 2007). Two sections of the trench excavated in 2006 were sampled; seven samples for grain size analyses and 17 samples for micromorphological analysis were collected. The excavation of the site is still in progress, and other samples from new trenches will be collected in future.

Prior to fieldwork, a detailed study of topographic and geological maps was carried out, in order to gather information about the spatial context and elevations, and about rocks and sediments exposed at the surface (Goldberg and Macphail, 2006). When necessary, soil maps were also consulted. The study of the environment surrounding the caves is very important, since syn- and post-depositional processes may influence the sedimentation inside caves, especially at the entrance, where colluvia or taluses typically accumulate (Waters, 1996). These can include reworked soils, fluvial deposits, aeolian deposits, etc. The architecture of the units and the sedimentation processes were interpreted in relation to the geomorphologic characteristics of the caves and their outside catchment.

Although caves are often considered to be “sedimentary traps” protected from many post-depositional processes (Karkanas, 2013), dissolution, erosion and reworking can alter significantly the stratigraphic framework. An approach based on depositional systems can better explain sedimentation processes because it takes into consideration the stratigraphic relationships within the sequence, since the boundaries of the lithostratigraphic units are not always time-parallel.

3.1 Fieldwork

In order to understand the infilling processes, and consequently the environmental conditions that controlled them, as well as the use of the cave by humans and animals, different methods were applied.

Three of the caves, Mujina Pećina, Zemunica, and Romualdova Pećina were studied well after the end of the excavations; the lithostratigraphic sequence from Zala was examined during the last two seasons of excavations when little of the 3D geometry of the sedimentary units was available. The sequence from Velika Pećina – Kličevica was sampled a few years after the test excavations, and also during the first two seasons of the new excavations. Detailed information about the sampling of each of the caves will be presented in subsequent chapters dealing with each of the caves.

After cleaning the profiles exposed by the systematic excavations, one or more profiles were chosen for close examination and sampling.

Since most of the cave sediments were sampled after the end of the excavations, a good collaboration with field directors and the team of archaeologists excavating the sites, proved to be crucial for understanding the geometry of the units, and allowed a more reliable interpretation of the sequences.

Prior to sampling, the lithostratigraphic units were identified; several sketches and photographs were made, followed by a detailed description that allowed a preliminary interpretation in the field. The descriptions followed the standards established by Catt (1991); the architecture of the stratigraphic units and sediment texture (by field grading, colour (according to Munsell Soil Color Chart), the organization and orientation of skeleton elements and their shape, degree of sorting, and the thickness of the units were documented. The shape of the boundaries, and the postdepositional modifications, such as the degree of cementation, erosional features, bio- or cryoturbations, were also recorded.

Systematic sampling of the exposed profiles was carried out as follows: bulk samples for grain size analysis were collected for each of the units or sets of units, and intact, undisturbed oriented sediment or soil monoliths were collected for micromorphology. Intact blocks of sediment were cut when possible, wrapped in toilet paper and secured for transportation by adhesive tape; in some cases, when the sediments were too friable, the samples were collected by a metal Kubiena box. The position of all samples was indicated on profile sketches and photographs.

The coarse (>2 mm) component was measured on the whole sample at 1ϕ precision by dry sieving and direct weighing in the field only for Mujina Pećina due to the nature of its sediments, which are very stony. Two-dimensional estimates of clast shapes were carried out by image analysis techniques on photographs.

3.2 Laboratory methods

Sedimentological and micromorphological analyses were carried out at the “Laboratorio di Geoarcheologia” of the University of Pisa.

3.2.1 Sedimentological analyses

Detailed sedimentological analyses were conducted on the < 2 mm fraction, the size of the bulk samples depending on the grading of the unit, from about 50 g to 12-15 kg (for the stony sediments of Mujina Pećina).

Grain size analysis of fine fractions (<2000 μm) can be performed using a number of different and complementary methods. This section will describe the methods used to analyse the sediment samples from the five studied caves.

The sand fraction was measured by wet sieving and observed under a stereo microscope, while silt and clay fractions were measured using the Bouyoucos hydrometer method.

Particle size analysis provides information about the energy of sediment transport. The deposition of fine-grained sediments indicates lower energy of transport while coarse-grained sediments correspond to higher energy of transport. It is also used to determine the environment and source of deposition. The dimensions of the particles are determined by measuring three axes: a (corresponding to the maximum length), b (intermediate, measured perpendicular to the axis a) and c (minimum, perpendicular to axes a and b). In grain-size analysis, the dimension of the particles is commonly measured using the axis b, which controls its passage through the sieve. The sieves are used for the analysis of grains larger than 0.0625 mm. The grain size was measured using the Udden-Wentworth classification scheme (particle size: >2 mm gravel and debris; 2 mm - 0, 063 mm sand; 0, 063 mm - 0, 004 mm silt / powder; <0.004 mm clay). The weight of the analysed sample must be proportional

to the overall granulometry of the sediment, in order to be statistically significant (Cremaschi, 2000; Angelucci, 2010; Goldberg and Macphail, 2006).

All the samples were divided into three subsamples; one was stored as reference material, the second one was pre-treated with H₂O₂ (130 vol., diluted with H₂O) to remove organic matter, and the third one was pretreated with 10% HCl to remove the carbonates; to remove the HCl, the samples were “washed” with H₂O. Both analysed subsamples underwent the same procedure. During the first phase of the analysis the samples are divided by wet sieving into two main fractions, sand, and silt and clay, employing a 2000 µm, 1400 µm, 1000 µm, 710 µm, 500 µm, 355 µm, 250 µm, 180 µm, 125 µm, 90 µm, 63 µm sieves (phi/2 mesh interval). The < 63µm fraction of the sediment, i.e. silt and clay, is collected in a separate bucket, together with the water by which the > 63 µm sediment was washed. The silt and clay fraction is left in the bucket to sediment for 24h while the sand fraction has to be dried in an oven prior to weighing at 0.01 g precision. The < 63µm sediment fraction needs to be further chemically treated with a 5 g/l solution of sodium hexametaphosphate (NaPO₃)₆, in order to induce the dispersion of the clay particles. This fraction was further determined by the Bouyoucos hydrometer method using Stokes’ law. The method is based on the different rate of sedimentation of the particles in the aqueous sediment suspension; the larger are the particles (their diameter), the higher is their sedimentation (falling) velocity. It is also based on the fact that the density of the suspension is higher than the density of pure water, and density decreases proportionally with the deposition of the sediment. The density is measured at specific time intervals (1', 2', 5', 15', 45', 2h, 8h, 16h, and 24h). Since the viscosity of water is affected by temperature, a measurement correction is necessary for temperatures deviating from a standard temperature of 20°C. The samples are eventually dried out in an oven at 105°C and weighed. The weights of the silt and clay fractions are thus obtained.

3.2.2 Soil micromorphology

Samples for micromorphological analysis were collected mainly from the profiles of the trenches as undisturbed and oriented blocks, so that all the elements of the sediment retain their original positions. The samples were collected from the profiles, approximately one per unit, or at the boundary between units in order to observe the boundary morphology. The monoliths were air-dried at 30°C in a ventilated oven for 7 days, and then impregnated by low-viscosity acetone-diluted polyester resin under moderate suction; polymerisation was carried out under atmospheric pressure for about 90 days.

The thin sections were cut by a diamond disk and ground to 30 µm by corundum abrasive powders, using petroleum for cooling, and covered by a standard optic glass slide. The size of the slides is 90x55 mm, or 60x45 mm. With loose and unconsolidated sediment this kind of sampling was not possible; Kubiena metal boxes of approximately 60 mm diameter were thus used. All thin sections were made by the laboratory “Servizi per la geologia” (Piombino, Italy). These were observed under a standard polarising microscope at magnifications ranging from 2.5x to 100x. The thin sections were viewed under plane-polarised light (PPL), cross-polarised light (XPL) and oblique incident light (OIL) with supplemental use of the fluorescence illumination (blue light and ultraviolet-UV light). The descriptions follow the guidelines proposed by Stoops (2003), Bullock et al. (1985), Brewer (1964), and Stoops, Marcelino and Mees (2010). In this chapter, the most used descriptive terms of the study will be explained.

Regarding heterogeneity, the *fabric* of a soil or sediment can be described. Fabric deals with the disposition, shape, size, and frequency of all soil constituents (Stoops, 2003; Bullock et al., 1985). The most important characteristics of a soil fabric - *elements of fabric* – are spatial distribution and orientation, size, sorting, and shape. Although the colour is not a part of the fabric, it is also a descriptive criterion (Stoops, 2003). The birefringence fabric (b-fabric) describes the characteristics of clay in the micromass (fine material).

The c/f-related distribution (coarse vs. fine) of most of the samples analysed in this work is porphyric, i.e. “the larger fabric units occur in a dense groundmass of smaller units” (Stoops, 2003, 44). The part of the soil fabric that deals with the relation between the solid and the pores – *voids* (i.e. spaces not occupied by solid soil material) – is called microstructure (Bullock et al., 1985; Stoops, 2003; Stoops, Marcelino and Mees, 2010). The most common identified types are blocky, lenticular, granular, and complex microstructure.

The sediment constituents are divided into coarse and fine mineral and organic components. Coarse mineral components include single and compound mineral grains (or rock fragments), inorganic residues of biological origin, and anthropogenic elements (Stoops, 2003). The most abundant identified inorganic residues of biological origin are phytoliths, shells of mollusks and gastropods, bones, and mineral products of animal metabolism (coprolites and fecal spherulites). It must be pointed out that most of the identified inorganic residues of biological origin, although following Stoops (2003) are not included in anthropogenic elements in the description of the thin sections, have to be considered products of human use of the caves studied. This aspect will be considered in the following chapters.

Phytoliths are <1 mm bodies normally found in the groundmass or as infillings. Here, the term phytolith refers to the opal/silica (one of the minerals produced by plants) phytolith. Although not all plants produce phytoliths, they are the most durable biogenic plant material in archaeological sites. Some of the plants that produce phytoliths, and that are important in archaeology are cereals, grasses, and wood. Cereals from different taxa (wheat, barley, rye, oats, rice, etc.) can be differentiated upon the shape of their phytoliths. It is also possible to identify some plant parts (leaves, stems, and inflorescence). Interconnected phytoliths occur in soils with in situ decomposed or burned organic matter. All this characteristics can be used to reconstruct different uses of space (Gutiérrez-Castorena and Effland, 2010; Stoops, Marcelino and Mees, 2010; Weiner, 2010).

Another frequent inorganic residue, which remains after the combustion of organic material, and its partial conversion into carbon dioxide, is ash. The composition of ash depends on the plants, and other materials (bones, dung, etc.) used for combustion. Ash from wood and bark is dominated by calcite. At lower temperatures (500° to 600°C) the wood or bark ash crystals still retain the shape of the calcium oxalate monohydrate crystals originally present in the wood. Bone ash is composed of calcined carbonate hydroxyapatite, while the ash derived from animal dung is dominated by silica phytoliths characteristic for grasses and leaves (Weiner, 2010).

Fecal/dung spherulites are 5-15 µm calcium carbonate crystalline features that form in the intestine of some animals. Spherulites are mostly produced by ruminant herbivores (mostly sheep and goats, less cows), they are absent in caecal digesting herbivores, their number is low in omnivores and low-to-absent in carnivores. These spherulites can easily be recognised from other types of spherulites by their optical characteristics (Canti, 1999).

In addition to the terminology proposed by Stoops (2003), the term pedorelict, borrowed by Brewer (1964), will be used to indicate “features formed by erosion, transport,

and deposition of nodules of an older soil material, or by preservation of some part of a previously existing soil horizon within a newly formed horizon” (Stoops, 2003, 104). Since pedorelicts belong to the groundmass (groundmass comprises coarse and fine material-micromass, and packing voids), they will be described as part of the coarse material. At interpretation level, as fragments of a transported soil/sediment, pedorelicts can have relevant palaeoenvironmental significance. They indicate the previous existence of a soil/sediment, i.e. earlier climatic and environmental conditions; they indicate also erosional processes that dismantled the previous soil/sediment, and suggest that there was transport of particles ending with a mixed soil horizon.

Pedofeatures are units of fabric that differ from the surrounding soil material “in concentration in one or more components or by a difference in internal fabric” (Stoops, 2003, 101).

The interpretation of all the individuated components and features as anthropogenic or natural, and the processes they imply, will be presented in the following chapters, dealing with each of the cave sites.

4. MUJINA PEĆINA

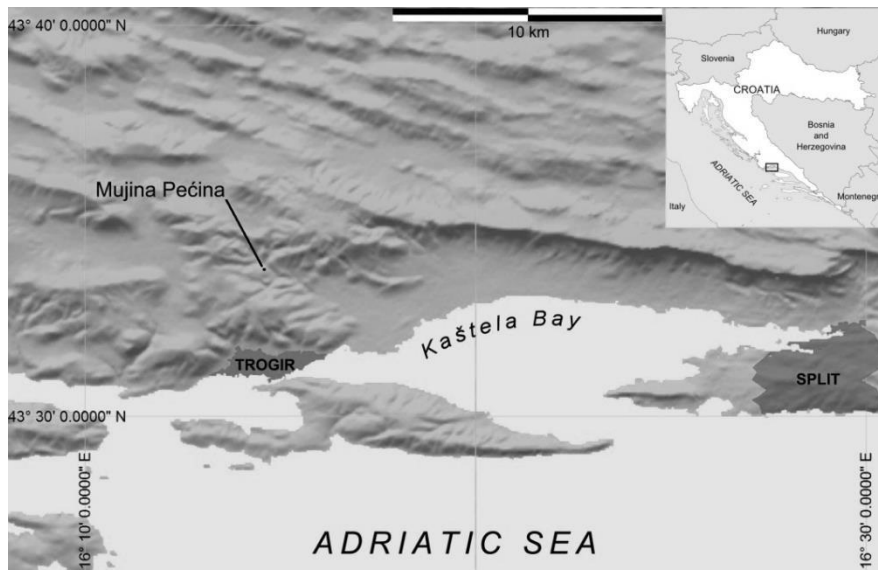


Figure 4.1 Location map of Mujina Pećina (Boschian et al., in prep.).

4.1 Introduction

Mujina pećina (Fig. 4.1) is known since the 1970s. In 1977, during a survey, M. Malez collected many lithic artefacts that can be attributed to the Middle Paleolithic. In 1979, N. Petrić published a report on test trenches conducted in 1978, but the first systematic excavations, directed by I. Karavanić, were carried out from 1995 to 2003 (Karavanić and Bilich-Kamenjarin, 1997).

Mujina Pećina is the only site of this area with a clear and relatively long stratigraphic sequence, and where the Mousterian was systematically excavated and chronometrically dated. The new excavations identified a sequence of at least eight levels (A, B, C, D1, D2, E1, E2, and E3) including a rich Mousterian industry. The total depth of the deposit is about 2 m. The upper part of this sequence was ^{14}C dated to an average age of $39'222 \pm 2956$ uncal years BP; however, these figures are somewhat uncertain because dates on bone do not fit perfectly the charcoal one, even if almost all these fall largely within the 39 ± 5 - 49 ± 9 (LU) or 46 ± 8 - 32 ± 4 (EU) ka span of the ESR age determination (Rink et al., 2002).

4.2 Site presentation

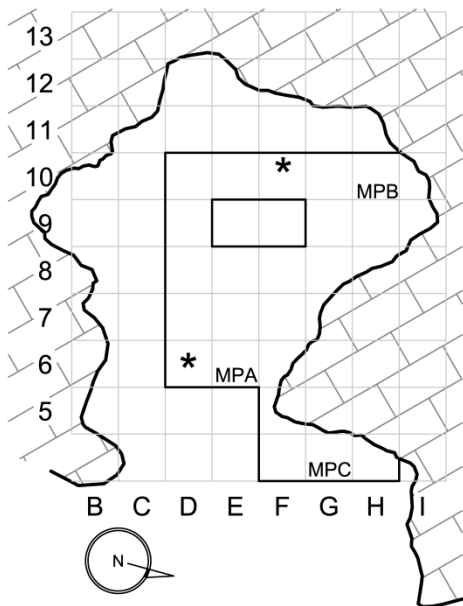


Figure 4.2 Plan of Mujina Pećina. Stars mark the main sampling locations for sedimentology and soil micromorphology.



Figure 4.3 View of the SW side of the karstic gorge crossing Labinštica hills. The cave is situated at the foot of a limestone cliff, close to the toe of a small scree. Continuous line: fault line (Boschian et al. in prep.).

Mujina pećina is situated in Dalmatia, north of Kaštela, near the road leading to Labinština. It is located about 260 m above sea level, and the cave mouth faces the Kaštela Bay. The cave is ca. 10 m long and 8 m wide, it has a sheltered northern niche and a small entrance chamber (Karavanić et al., 2008) (Fig. 4.2).

Mujina Pećina is located about 60 m above the present-day bottom of a deep karstic gorge, a few tens of metres below the overlying plateau. The area is tectonically complex, with stratified limestone and massive and stratified limestone overthrust on foraminiferal limestone (Marinčić, Magaš and Borović, 1971). The close surroundings of the cave are characterised by outcrops of deeply karstified limestone and moderately high cliffs deeply fractured by a minor fault that can be followed for several tens of metres on the gorge side; coarse screes and rockfall / debris fall deposits (*sensu* Blikra and Nemec, 1998) are active within the steep and often narrow spaces among the rocky outcrops, and are also widely developed all over the gorge side. The cave opens at the base of a 10-12 m-high, vertical and smooth cliff that is, in fact, the hanging wall of the above-mentioned fault, and a small debrisfall cone flowing out from a narrow couloir partly enters the cave from the southern side of its entrance (Fig. 4.3).

The cave consists of an inner, elliptically shaped chamber 6x8 m wide, connected with the exterior by a short and wide corridor. Walls and ceiling are rather smooth, but strong fracturing is evident within the overlying rock mass.

Chert deposits were identified in the immediate vicinity of Mujina Pećina: „*The western slope of a long gorge in the Plano area, in which Mujina Pećina is located, is composed of Upper Cretaceous deposits. The opposite side of the slope, i.e. the eastern side, is composed of thickly layered Eocene limestone with the frequent appearance of chert veins and nodules. Chert freed of limestone by corrosion juts out in spurs. It can also be found scattered along the slope and the bottom of the gorge. ... It is possible to find larger nodules of approximately two kilogrammes which are homogenous in composition...*“ (Karavanić et al. 2008, 49-51).

4.3 Archaeological background

All levels in the cave belong to the Late Middle Paleolithic (45000 - 39000 BP), to the Oxygen Isotope Stage 3, and are associated with a Late Mousterian archaeological context (Karavanić et al., 2008). Since all lithic production phases were established at the site, it seems that Neandertals used the cave as a workshop (Karavanić et al., 2008).

Faunal and lithic remains were determined and studied only for the uppermost (Levels B-D) part of the sequence (Miracle 2005; Karavanić et al. 2008), whereas the study of the lower part of the sequence is still in progress. The analysis of the vertical distribution of finds indicates that the archaeological material is most frequent in E levels, and it is least frequent in Levels D (Nizek and Karavanić, 2012).

Because of similar characteristics, lithic artefacts from Levels B and C, as those from Levels D1 and D2 were studied by Karavanić et al. (2008) as single units. A total of 404 artefacts (32.67 % of which are tools), were collected from Levels B and C. Different categories of flakes (flakes, small flakes, flakes with cortex, and Levallois flakes) are the most abundant artefacts in these levels (58.42%), followed by chunks with and without cortex (18.81%). Levallois débitage is rare, representing only 6.94% of all artefacts. The most common tool types are denticulates and notched pieces (39.69%), but retouched flakes (27.48%), Upper Paleolithic types (15.27%), and side-scrappers (12.21%) also occur. The main characteristic of these tools is their small size, and they resemble the Micromousterian (Karavanić et al., 2008; Karavanić et al., 2008a). Levels D1 and D2 contain 222 lithic artefacts, 47% of which are tools. Although Levels B-C contain much more tools, Levallois débitage is more frequent in

Levels D1-D2 (18.46%), and it includes flakes, points, blades, and one Microlevallois core. The most common artefacts in Levels D1 and D2 are flakes (25.68%), followed by small flakes (19.82%), flakes with cortex (11.26%), and chunks (8.1%). Retouched pieces dominate among tools (40.43%), followed by denticulates and notched pieces (29.79%), sidescrapers and Upper Palaeolithic types (10.64%) (Karavanić et al., 2008). Karavanić et al. (2008) analysed the raw material of 30 specimens, all of which are chert classified into five groups based on the structure, colour, and composition. In Levels B, C, D1, and D2 the most common type is a milky-light grey and dark grey chert (71.78% in Levels B-C, 78.83% in Levels D) that probably originated from calcareous deposits near Trogir (approximately 4 km from Mujina Pećina), followed by a light grey, dark grey, and light brown group of cherts (18.81% in Levels B-C, 13.06% in Levels D). This group, together with the third (brownish-grey with a sandy appearance) and fourth group (light brown and light grey chert with molluscan fragments, foraminifers, and radiolarians), less than 10% of specimens, can be found within a 15 km radius of the site. The nearest outcrop of the last, fifth group of dark, radiolarian cherts is situated on the SE slopes of the mountain Svilaja, ca. 40 km from Mujina Pećina (Karavanić et al., 2008; Karavanić et al., 2008a, 262-263).

Two localized areas of burning, probably representing open, unstructured and unpaved Mousterian hearths, were found in occupation level D2; anthracotomical analyses show that *Juniperus sp.* was used for fuel in both hearths (Karavanić et al., 2008).

The faunal composition shifts from a codominance of red deer and chamois-ibex in Levels D1-D2 that formed during relatively cold conditions to a clear dominance of wild caprines followed by large bovids and equids in Levels B-C that formed during relatively warm conditions (Miracle, 2005, 84). Faunal remains from Mujina pećina also show clear differences in species frequency between the two stratigraphic complexes (Miracle, 2005).

4.4 Results

The geoarchaeological study of the sequence of Mujina Pećina was carried out on the sequence put into light by the I. Karavanić excavations of years 1995-2003. The study of the sequence and the sampling of the lithologic units were carried out *a posteriori* on the excavation profiles, well after the end of the excavation. The deposit was divided into lithologic units - some more than the excavation units - that were observed at eye-scale and described in the field; the description is based on Catt (1991). The architecture of the units and their stratigraphic relationships were interpreted in relation to the geomorphologic characteristics of the cave and its outside catchment.

Samples were taken from two sections (southern and western) of the archaeological trench inside the cave; a sample of red soil (*terra rossa*) was taken as a control sample in the vicinity of the cave. A total of 12 samples were collected for grain size analyses and seven samples for micromorphological analysis.

Each lithologic unit was sampled for grain-size analyses, the size of the bulk samples depending on the grading of the unit, 15 to 20 kg because of the large number of stones. The coarse (>2 mm) component was measured on the whole sample at 1φ precision by dry sieving and direct weighing in the field. It must be pointed out that the clasts were sieved considering their minimum diameter, consequently, elements significantly longer than the lower mesh size may fall within each class.

Two-dimensional estimates of clast shapes were carried out by image analysis techniques on photographs of the whole 16-32 mm grain-size class, which is the most abundant in almost all units.

4.4.1 Field observations

The following descriptions are based on the southern and eastern profiles. These profiles do not contain Level C, visible in the published northern Profile A, excavated in 1995. The description of the Profile A will, therefore, is reported according to Rink et al., 2002, Karavanić and Bilich-Kamenjarin, 1997, Karavanić et al. 2008, and Karavanić et al., 2008a. The relative depth of each lithologic unit is indicated in the description.

Southern stratigraphic profile (Fig. 4.4):

1. 0 – 5 cm. Poorly sorted debris, composed of angular to subangular limestone fragments chaotically deposited on the surface of the cave; matrix is absent.
2. 5 – 10 cm. Angular, poorly sorted rubble up to 62 mm (average 15 – 32 mm), slightly platy and deposited chaotically. Brown silt loam matrix with strongly developed fine granular aggregates.
3. 10 – 15 cm. Concave lens comprising only the coarser fraction of the overlying level. Some clasts are arranged parallel to the depositional surface.
4. 15 – 33 cm. Angular poorly sorted rubble (rarely subangular) up to 32 mm; larger clasts are rare. The moderately platy clasts are chaotically arranged and are slightly parallel to the depositional surface. Abundant silt loam light brown matrix; strongly developed fine granular aggregates; partially cemented (CaCO_3).
5. 33 – 105 cm. Very angular poorly sorted rubble; 128 mm clasts are common, but the size is mostly 32 – 64 mm. Platy clasts and splinters are common. Although the clasts tend to be parallel to the depositional surface, some sloping clasts are present too, but almost no one is vertical (there are some verticalized clasts in the lower part of the bed, and a layer of platy clasts arranged parallel to the depositional surface at about - 45 cm). Skeleton supported, with relatively abundant matrix; strongly developed fine granular aggregates, moderately cemented.
6. 105 – 117 cm. Angular poorly sorted rubble; very rare clasts of 128 mm, clasts smaller than 32 mm prevail, other sizes are rare. Abundant silt loam matrix with moderately developed fine to medium granular aggregates. The skeleton is more or less parallel to the depositional surface; verticalised clasts are very rare (mostly the larger ones).
7. 117 – 131 cm. Angular poorly sorted rubble. Few clasts are larger than 128 mm; the most common are 32 to 64 mm; there are frequent platy clasts, rarely inclined, and mostly parallel to the depositional surface. Very rare matrix: very dark reddish-brown silt loam with fine, strongly developed aggregates.
8. 131 – 139 cm. Reddish silt loam matrix with angular and subangular clasts; poorly sorted; the maximum size of clasts is 32 – 64 mm (rare), mostly 16 – 32 mm. Moderately developed granular aggregates; the colour tends to lighten downwards. The lower boundary is slightly undulating. Matrix supported.
9. 139 – 151 cm. Poorly sorted rubble; angular to subangular clasts - their maximum size is 64 – 128 mm, more common 32 – 64 mm, some are platy. Very rare matrix, more

abundant on the top of the level, where it is lighter, and this upper limit is diffuse. Moderately developed crumb aggregates, skeleton supported. Rare platy clasts, concentrated at the bottom in some areas; the lower boundary is clear.

10. 155 – 168 cm. Poorly sorted rubble with frequent angular and common platy clasts parallel to the depositional surface. The maximum dimension of the clasts is 128 mm, more common 32 – 64 mm. Silt loam, greyish-black to black matrix; moderately developed coarse crumb aggregates; the boundary is clear.
11. 168 – 188 cm. Poorly sorted angular to subangular rubble with rare platy clasts; chaotical. Large clasts have more than 128 mm, but the 64 – 128 mm are more common. Rare reddish-brown to brown fine granular matrix with white speckles (CaCO_3); moderately cemented.
12. 188 – 215 cm. Silt loam dark brown to black matrix with angular to subangular clasts (64 mm very rare, 32 mm rare).

Eastern stratigraphic profile:

1. 0 cm. Poorly sorted rubble on the surface; no matrix.
2. 0 – 5 cm. Brown silt loam matrix with strongly developed fine granular aggregates. Skeleton supported, poorly sorted angular clasts chaotically arranged. Subhorizontal, very clear boundary.
3. 5 – 35 cm. Poorly sorted, angular rubble with common or frequent platy clasts (the size is 128 mm, but more frequent ones are 16 to 32 mm, and some 64 mm). Abundant yellowish-brown silt loam matrix with strongly developed crumb aggregates. Clasts are chaotically arranged, but rarely verticalized. Undulating limit; on the left the layer thins down progressively and becomes stonier.
4. 35 – 110 cm. Poorly sorted, more or less loose angular rubble, with abundant platy elements (size > 256 mm rare, 128 – 256 mm common, very small clasts are rare); the arrangement of the clasts is moderately organised, with elements that tend to horizontality, rare are vertical. There is a layer of large platy, horizontal stones at - 90 cm. Rare silt loam matrix, crumb. Openwork or skeleton supported.
5. Lithostratigraphic unit 5 is equivalent to the Level E1 of the southern profile.

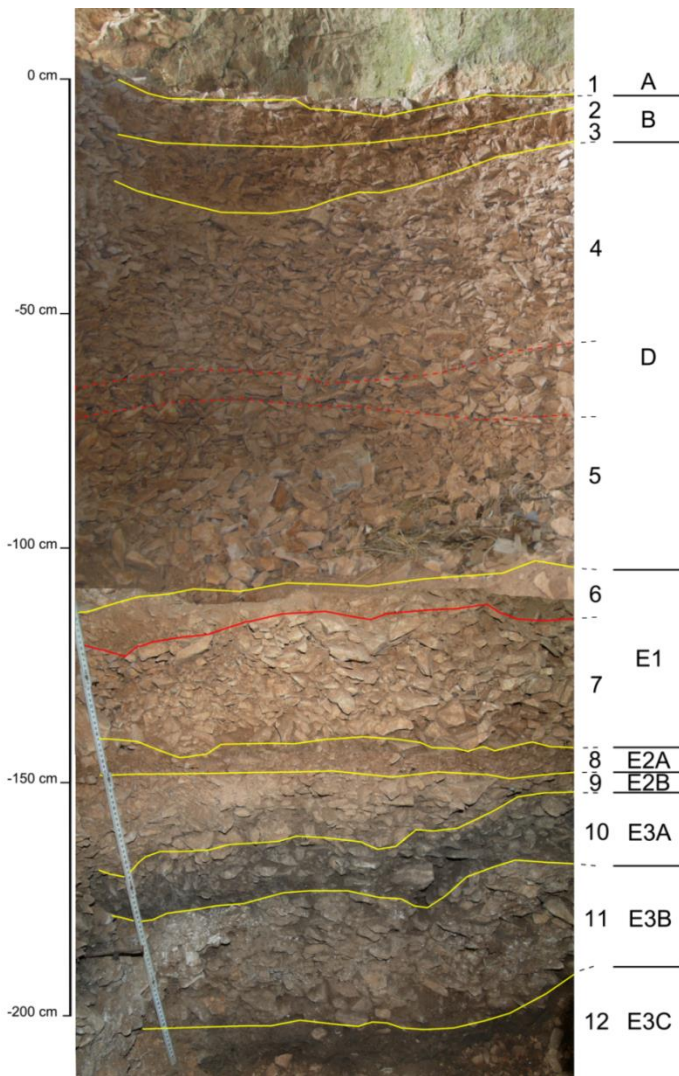


Figure 4.4 Reference stratigraphic sequence along the longitudinal profile, in excavation square D6 (Boschian et al., in prep.).

Northern Profile A (Fig. 4.5), according to Rink et al., 2002, Karavanić and Bilich-Kamenjarin, 1997, Karavanić et al., 2008, and Karavanić et al., 2008a:

1. Level A – dark brown (7.5YR3/3) humus with Mousterian lithics and bones, mixed with recent bones and artefacts, 2 to 4 cm thick.
2. Level B – brown (7.5YR5/6) sandy loam, 12 to 31 cm thick, with stone debris.
3. Level C – brown (7.5YR4/6) sandy sediment, 1 to 26 cm thick, with stone debris. The layer has a wedge-like shape and is only present in square metres E9, E10, F9, F10, G9 and G10.

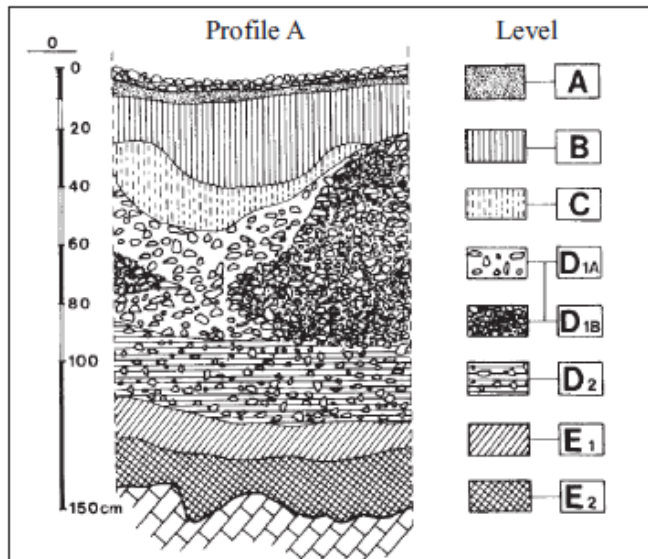


Figure 4.5 Stratigraphic Profile A from Mujina Pećina (Karavanić and Bilich-Kamenjarin, 1997).

- 4. Level D1A – cryoclastic stone debris with some gravel (somewhere calcified) with a small quantity of yellowish red (5YR5/6) sandy sediment 1 to 38 cm thick.
- 5. Level D1B – cryoclastic stone debris sporadically calcified with a very small quantity of fine sediment or without it, 1 to 71 cm thick.
- 6. Level D2 – cryoclastic stone debris with gravel and yellowish red (5YR4/6) sandy sediment, 25 to 28 cm thick.
- 7. Level E1 – reddish brown (5YR4/3) sandy sediment, 8 to 12 cm thick, with much stone debris and abundant organic material.
- 8. Level E2 – dark reddish brown (5YR3/3) sandy clay sediment, 12 to 18 cm thick, with stone debris and organic remains.
- 9. Level E3 appears above the floor of the cave at the entrance and is not visible in the northern profile. Very dark brown sandy clay sediment with some stone debris and considerable organic material.

4.4.2 Architecture of the stratigraphic units and sediment texture

The stratigraphic units of the Mujina Pećina infill are shaped as almost continuous layers or as lenses, all of which dip gently towards the outside of the cave. Along the transversal profiles the inclination of the units reflects the slope of the bedrock, but it decreases from the bottom upwards so that the uppermost units are roughly horizontal. Along the transversal profile of the cave infill, which is situated along the northern wall of the entrance, the units are approximately horizontal or dip gently towards the North or rise slightly towards the northern wall. The real shape of the boundaries is not always clear due to the coarse texture of the units. They are marked by undulations and erosional features (Boschian et al., in prep.).

Units comprised in level E3 occur above the bedrock in the entrance area of the cave and dip towards it. Unit E3A is moderately eroded and occurs only in the outermost part of the cave. Accordingly, the bottom limit of unit E2B is an erosional feature. Along the longitudinal profile of the cave, unit E2B is characterised by major undulations, but it is concave-upwards along the transversal direction in the entrance area where it dips towards the centre of the cave. The top of unit E1 is concave-upwards and dips gently outwards in the entrance area (Boschian et al., in prep.). The vertical distribution of flint artefacts and bones follows its shape (Nizek and Karavanić, 2012). The discontinuity marked by the top boundary of unit E1 divides the entire sequence into two parts: the upper part is characterised by thick, well-developed tabular layers with linear limits; the lower part of the sequence is made up of lenses tiled one upon the others towards the inside of the cave (Boschian et al., in prep.). In the inner part of the cave, the top of unit D is marked by an erosional feature which is filled up by unit C (only present in squares E/F/G 9-10).

The texture of the entire sequence of sediments is very stony; it is characterised by mostly fine to medium gravel classes without major differences between units. The matrix quantity is always less than 20%, and varies significantly throughout the sequence, in some cases also within the same unit. The lower part of the sequence, below the erosional surface at the top of unit E1, is much richer in matrix, ranging between 7% and 17%, with two peaks in units E3C and E3A; there is another peak in the reddish horizon that marks the top of E1. There is very few matrix in levels D and B: a minimum of 3% in D and 6-7% in B. Level D has much more matrix in the inner part of the cave, up to almost 20% (Boschian et al., in prep.). Fig. 5.7 represents the grain-size results from the profile close to the entrance, and Fig. 5.8 from the profile deep inside the cave.

The fine fraction (<2 mm) is poorly sorted, with a maximum in the <2 µm class and in the 31-23 µm class. The sand fraction is much more abundant in the undecalcified samples (Fig. 4.7), including limestone fragments and CaCO₃-cemented aggregates. The clay fraction is more abundant in the decalcified samples (Fig. 4.6) with a component of fine carbonates, apart from units E3C-12 and E3A-10. (Boschian et al., in prep.). The clay component is usually around 20% of the fine-grained component. Clay is minimum in unit E2B where the graphic mean is 14.6 µm, which is higher than in other units, where it is between 9 and 12 µm. In units D (in the part of the profile in the cave interior) and E1-6, where clay is >50%, there is a secondary maximum in the 11-7 µm class. The lowermost levels, up to E1-7 are silty, with clay between 20 and 40%, while the overlaying levels E1-6 and D are dominated

by clay (50-70%). The uppermost levels (D-4 and B) are again siltier, with clay around 25-30%.

The coarse elements tend to be organised in secondary horizons which differ regarding the size of the elements or by better sorting. This is evident mostly in levels D and B where the orientation of the platy and elongated clasts is parallel or subparallel to the unit boundaries. The size of the skeleton elements is largely included within the grain-size classes of the 16-32 and 32-50 mm, except from units E3B, E1, and D in square 10. The elongated elements are more common in the lower part of the sequence; a better orientation of the elements -somewhat parallel to the unit boundaries- is also a characteristic of these units. Some convoluted features can be observed between units E2A-E2B-E3B. Large pebbles and cobbles occur sparsely within units E1-7 and E3A-10, and sometimes also in other units (Boschian et al., in prep.).

The skeleton elements are angular or sometimes subangular because of surface dissolution. In most of the layers examined, limestone splinters and plaquettes dominate within the fine, 2000 – 63 µm fractions. Numerous bone fragments (micro fauna), limestone fragments coated by manganese, few goethite/limonite aggregates, chert, manganese and iron nodules, feldspar, calcite, quartz grains (some of which very rounded) were observed under the stereomicroscope; mica is common in the 125 µm and finer fractions, and in some of the samples CaCO₃ concretions were also present.

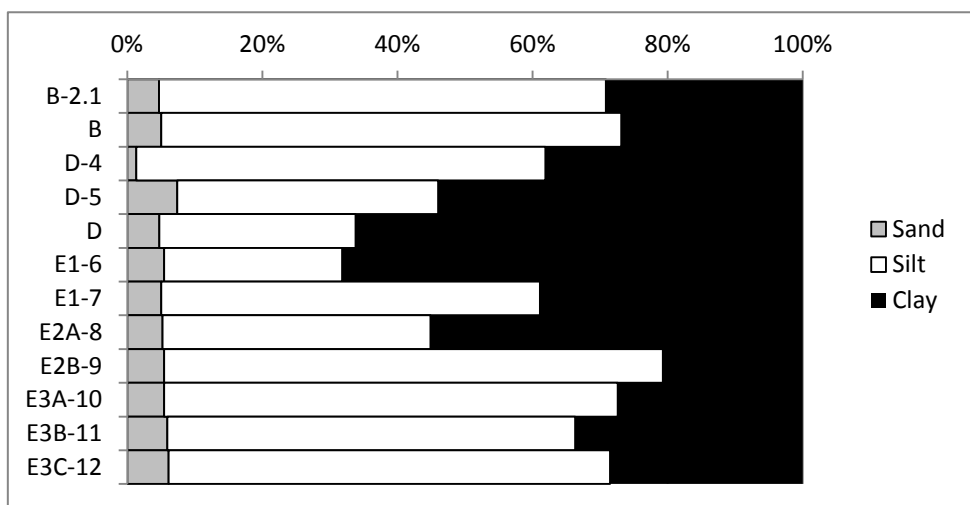


Figure 4.6 Grain-size (Wentworth, 1922) of the <2 mm fraction of decalcified samples.

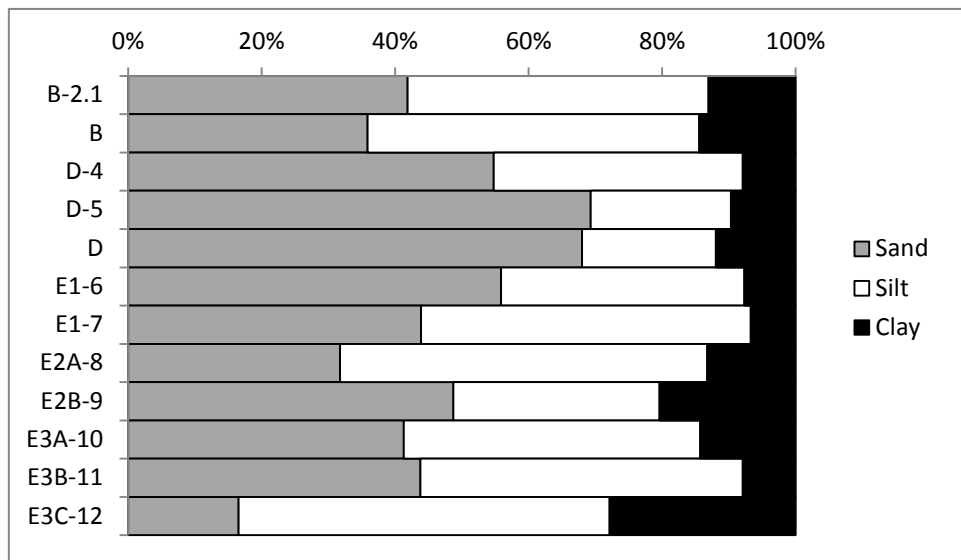


Figure 4.7 Grain-size (Wentworth, 1922) of the <2 mm fraction of undecalcified samples.

4.4.3 Micromorphology

Six samples for micromorphological analysis (Levels B, D-4, D-5, two samples from E2A, and E3C) were collected from the southern profile, located between squares D 7-8 and E 7-8. The main micromorphological characteristics of Mujina Pećina sediments are summarised here:

MP/9/B

Microstructure and porosity: poorly sorted to unsorted complex microstructure with compound packing voids, planes, chambers and channels: subangular blocky microstructure with moderately to highly separated peds, highly separated and well-developed granular microstructure with unaccommodated peds.

Groundmass: c/f-related distribution pattern is open porphyric.

Coarse material:

Rock fragments: frequent limestone fragments (mainly biomicritic, containing bryozoans, foraminifera etc.), common subrounded to angular chert fragments.

Minerals: frequent subangular to rounded phosphates, frequent subangular to subrounded sparitic calcite, common subangular quartz grains and muscovite flakes, few feldspars, very few biotite and rounded glauconite grains.

Inorganic residues of biological origin: common angular to subrounded bone fragments.

Organic: very few amorphous organic matter.

Micromass: yellowish brown dusty micromass (PPL) with amorphous, crystallitic, and granostriated b-fabric.

Pedofeatures: few Fe coatings, frequent Fe/Mn nodules, few cappings.

Organic material not included in the groundmass or in pedofeatures: infillings of loose discontinuous excrements.

MP/6/D4

Microstructure and porosity: granular microstructure with chambers and channels.

Groundmass: c/f-related distribution pattern is open porphyric.

Coarse material:

Rock fragments: frequent angular to rounded limestone fragments, few very angular chert fragments.

Minerals: frequent angular to subrounded calcite grains, common angular to subangular quartz, few angular feldspar, common muscovite flakes, frequent phosphates (greyish speckled in PPL), very few garnets?

Inorganic residues of biological origin: very few bone and shell fragments.

Micromass: greyish brown micromass (in PPL) with crystallitic b-fabric.

Pedofeatures: frequent Fe nodules, few Fe hypocoatings and coatings on phosphates, very few dusty clay and silt coatings, very few compound layered clay and silt hypocoatings, and clay coating fragments (called papules by Brewer 1964), silt cappings, including a link capping on limestone fragments, very few calcite infillings.

MP/8/D5

Microstructure and porosity: poorly sorted granular microstructure with moderately to highly separated peds and strongly developed ped and pellicular grain microstructure with chambers.

Groundmass: c/f-related distribution pattern: chitonic and gefuric.

Coarse material:

Rock fragments: frequent angular to rounded limestone fragments, very few subangular chert fragments.

Minerals: few subangular quartz grains, muscovite flakes, subrounded to rounded phosphates, angular calcite grains.

Inorganic residues of biological origin: very few bone fragments.

Micromass: greyish brown dusty (in PPL) clay with calcitic crystallitic b-fabric.

Pedofeatures: coarse clay and silt cappings, Fe hypocoatings, Fe nodules.

MP/1/E2A(1)

Microstructure and porosity: poorly to medium developed fine granular microstructure with chambers and channels.

Groundmass: c/f-related distribution pattern: porphyric.

Rock fragments: frequent angular to subrounded limestone fragments, common angular to subrounded chert fragments.

Minerals: common subangular quartz grains, few muscovite flakes, common angular to subrounded phosphates, frequent angular to subangular calcite grains, few feldspars, very few chalcedony.

Inorganic residues of biological origin: frequent bone fragments, very few shell fragments.

Micromass: yellowish brown speckled clay with granostriated b-fabric.

Pedofeatures: Fe/Mn nodules (matrix nodules), common calcite coatings and hypocoatings.

MP/3/E2A(2)

Microstructure and porosity: poorly to medium developed fine granular microstructure.

Groundmass: c/f-related distribution pattern: porphyric.

Coarse material:

Rock fragments: frequent angular to subrounded limestone fragments, common angular to rounded chert fragments.

Minerals: common angular to subrounded quartz grains, common muscovite flakes, frequent angular to subrounded phosphates, common subangular calcite grains.

Inorganic residues of biological origin: frequent bone fragments.

Micromass: yellowish brown (in PPL) speckled clay with granostriated and strial b-fabric.

Pedofeatures: frequent Fe/Mn nodules (matrix nodules), very few clay coatings, and few Fe hypocoatings.

MP/2/E3C

Microstructure and porosity: massive or well developed granular microstructure with planes and cracks.

Groundmass: c/f-related distribution pattern: porphyric.

Coarse material:

Rock fragments: frequent angular to rounded chert fragments.

Minerals: subangular mono- and polycrystalline quartz grains, common muscovite flakes, frequent angular to rounded phosphates, few opaques, very few glauconite grains.

Inorganic residues of biological origin: frequent bone fragments.

Organic: common charcoal fragments, common fine amorphous organic matter, common dark brown tissue residues, frequent punctuations.

Micromass: yellowish brown (in PPL) speckled clay with granostriated, porostriated and stipple-speckled b-fabric, and parallel striated b-fabric.

Pedofeatures: dense complete and incomplete infillings, frequent calcite hypocoatings and coatings, very few clay coatings (mostly fragmented), few intrusive and matrix typic Fe nodules, very few rolling pedofeatures.

Organic matter not included in groundmass: infillings of loose discontinuous excrements, and fungi.

Microstructure is always granular, weakly to well developed, more or less disturbed by channels and chambers. It is sometimes subangular blocky with moderately to highly separated peds (Level B) or pellicular grain microstructure (Level D.5). The related distribution pattern is porphyric (Level E2A, E3C) or open porphyric (Level B and D.4) with the exception of Level D.5 in which it is chitonic and gefuric. In upper levels – B, D.4 and D.5 the b-fabric is always crystallitic (mostly due to widespread microsparite), while in the lower, E complex speckled clay is characteristic, with striated (E2A) or parallel striated (E3C) b-fabric. The granostriated b-fabric is present in Levels B, E2A, and E3C. In E3C, it is more evident and in this layer porostriated b-fabric also occurs.

The assemblage of minerals identified in the thin sections of Mujina Pećina sediments is relatively uniform; the same minerals and rocks were found in almost all layers. The coarse skeleton consists mainly of limestone with visible skeletal particles/grains, foraminifera, bryozoans etc., micritic or biomicritic and sparitic limestone (Fig. 4.8 a-b; 4.9. e-f). Calcite occurs everywhere in the sediment, and quartz is the most important mineral among the silicates. There is a significant amount of chert fragments in Level B and the complex of Levels E, in particular in the lowermost Level E3C (Fig. 4.8 c-d). Muscovite is very common and occurs in silt-size laminae; small amounts of biotite were also observed. Among the organic components, fragmented bones are present, sometimes burnt, as well as sand and silt sized amorphous organic matter (Fig. 4.10 a-c), which occasionally gives a darker colour to the matrix and charcoal fragments. These organic fragments are frequent in E3C and E2A samples, and occasional in Level B. Nodules of Fe or Mn oxides, clay pedorelicts with a skeleton made of angular quartz particles (Fig. 4.8 e-f), reddish clay aggregates (papules) (Fig. 4.9 e-f) often occur in sediments and occasionally also “rolling pedofeatures” (Fig. 4.10 d). Together with a poor sorting of particles, these are all indicators of colluvial deposits (Courty et al., 1989, 93). Secondary carbonates were also observed in E3C and E2A samples. A large presence of phosphates should be pointed out, the most important ones being those which can be identified as carnivore coprolites (Levels B, D, and E2A).

The main characteristic of Mujina Pećina sediments is that natural processes largely formed the sediments. This, along with field observations, is supported by micromorphological analyses. First of all, a coarse calcareous skeleton, mainly composed of angular limestone

fragments of climatic origin can be recognized (cyclic freezing and thawing of the vault and cave walls resulted in the fragmentation of the limestone that consequently fell off the roof and walls of the cave). The freezing and thawing cycle is recognisable also upon pedofeatures in Levels D.4 and D.5, where silt cappings occur. Climatic conditions associated with postdepositional processes are also documented by secondary carbonates that must have formed in a wet period, and probably represent partially "melted" (i.e. dissolved and recrystallised) limestone. Another characteristic of Mujina Pećina sediments are pedorelicts indicating input of allochthonous sediments or soils, which were previously deposited outside the cave and penetrated inside the cave area probably because of colluvium. In some samples (especially in Levels E2A and E3C) small bone fragments are very frequent, some burnt or partially burnt at a relatively low temperature, which could indicate the characteristics of the Neanderthal diet. A possible explanation for bone splinters is that they were deliberately smashed, kneaded and heated to extract the bone marrow, activities that were performed *in situ* (Rabinovich and Hovers, 2004; Roebeoks and Villa, 2011). However, it is possible that the bones were gnawed by carnivores, although no carnivore coprolites were observed in Level E3C. Perhaps the most interesting information shown by the micromorphological analysis of Mujina Pećina sediments is the presence of detrital phosphate grains which can be identified as fragments of carnivore coprolites, possibly hyenas (Miller and Macphail, pers. comm.; Goldberg, 1980). It is noteworthy that in Level E3C, the one with the highest frequency of faunal remains and lithic artefacts, no carnivore coprolites were observed in thin section, although some other phosphate grains do occur.

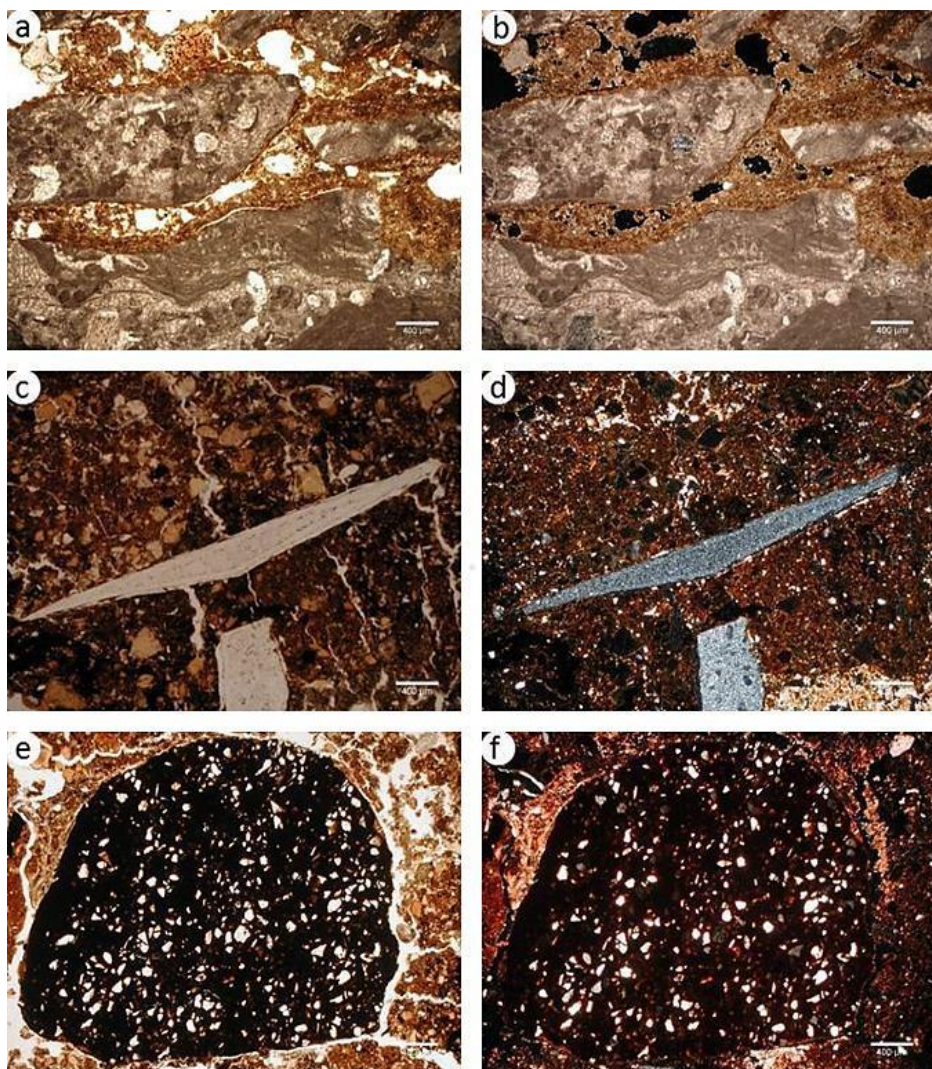


Figure 4.8 Microphotographs of sediment thin sections from Mujina Pećina. a: silt cappings on limestone fragments, PPL. b: as in a, XPL. c: chert, PPL. d: as in c, XPL. e: pedorelic with quartz skeleton, PPL. f: as in e, XPL (Boschian et al., in prep.).

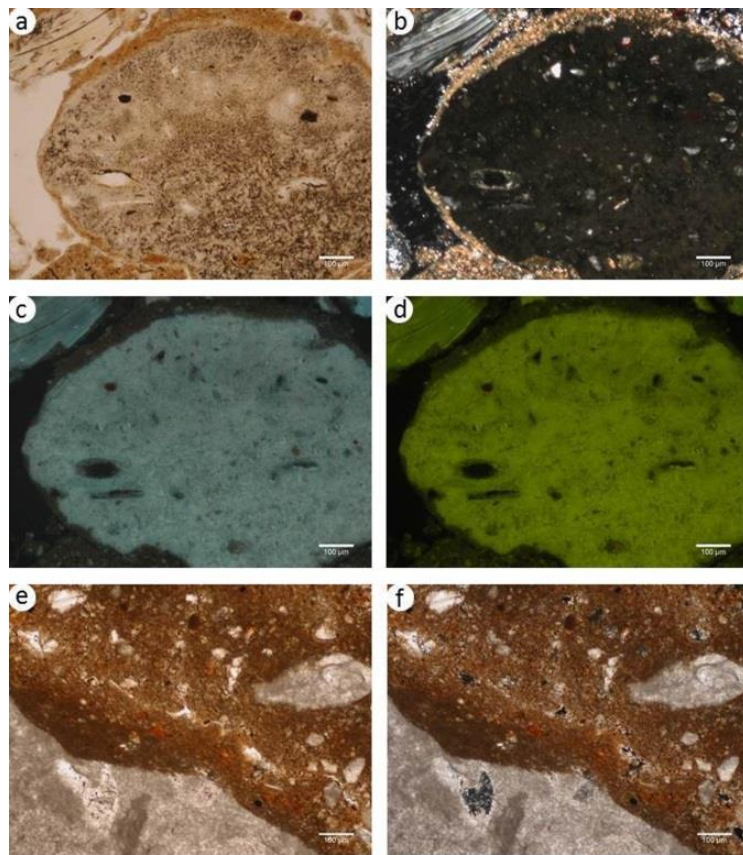


Figure 4.9 Microphotographs of sediment thin sections from Mujina Pećina. a: phosphate-probable carnivore coprolite and a bone fragment, PPL. b: as in a, XPL. c: as in a, infrared FLUO. d: as in a, blue FLUO. e: silt capping on limestone fragment with red clay pedorelic and muscovite flake inside, PPL. f: as in e, XPL (Boschian et al., in prep.).

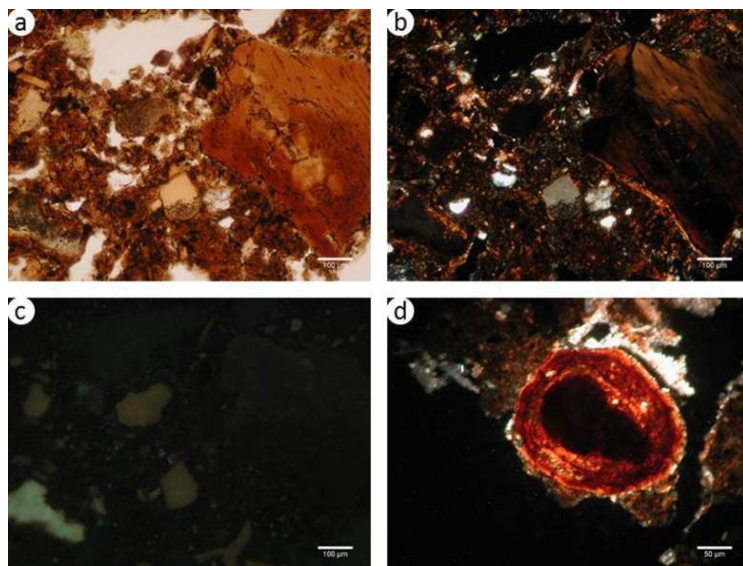


Figure 4.10 Microphotographs of sediment thin sections from Mujina Pećina. a: burnt bone, “bone sand”, amorphous organic matter, nodules, granostriated b-fabric, PPL. b: as in a, XPL. c: as in a, infrared fluorescence. d: “rolling” pedofeature, XPL (Boschian et al., in prep.).

4.5 Discussion

The main site formation processes that controlled the deposition of Mujina Pećina sediments are:

1. The accumulation of rubble inside the cave, deriving from roof spall.
2. External processes connected to the activity of the outside scree, or to the in-wash of fine material.

The origin of the coarse sedimentary component can be estimated by the shape of the elements of the skeleton. Elongated clasts derive from the breaking up of the ceiling and walls of the cave due to tectonic fracturing, while relatively equant clasts originate from the scree rubble accumulated outside the cave. The upper part of the sequence (levels D-4 to B) can be differentiated from the lower part (levels E3B-11 to D-5) according to this parameter. The mixture of both, internal and external components is visible in all the levels. However, since equant or moderately elongated elements are more frequent than the prolate ones, it can be concluded that external inputs were always more relevant than roof spall.

The differences in the sequences of samples B-2, B-2.1, B, and D-4 show that the composition of the sediments also depends on its position within the cave. The samples were collected in different parts of the profile, each one more to the inside of the cave. The elements are progressively more prolate, showing an increasing relevance of roof spall to the inside of the cave (Boschian et al., in prep.).

The upper part of the sequence (levels D to B) indicates that the outer scree activity increased and became more relevant during the last phases of deposition. These units tend to be subhorizontal or slightly dip towards the inside and North of the cave, and are also much thicker than the lower ones, indicating higher deposition rates. Some of the units (E2B-9 to E1-6) belonging to the lower part of the sequence are organised in relatively small lenses, which is an indication for distal debris flow deposition. These units are subhorizontal along a transversal profile of the cave located at the entrance, and tend to climb against the northern wall, which indicates that they are also connected with the outer scree. The lowermost units E3C-12 to E3A-10 are organised in thicker lenses that dip more steeply towards the outside of the cave, and are the richest in internal components. The top of this part of the sequence is marked by a clear erosional surface which indicates that part of the sediments accumulated because of roof spall, have been removed (Boschian et al., in prep.).

The grains size analysis of the fine fraction shows that the matrix is always less than 20%, and that it is more abundant in the lowermost levels. The grain-size distribution indicates different processes in the deposition of the fine fraction through time. The lowermost and uppermost parts of the sequence are characterised by silty clay loam matrix, with the exceptions of E2B-9 (silty loam) and E2A-8 (clay). The unit E2B-9 is the only one in the limits of the primary loess field. The texture fits the palaeosols in the loess sequences of Susak Island (Cremaschi, 1990b; Mikulčić Pavlaković et al., 2011; Wacha et al., 2011) with significantly lower sand component, which may indicate distal loess deposition and/or a loss of wind flow energy due to the relatively high location of the cave within the hills. The levels D-5, D, and E1-6 are dominated by clay. Its reddish hue derives from Fe-oxides, indicating colluvium of Alfisols developed outside the cave. This process is also confirmed by soil micromorphology: the pedorelicts and/or papules indicate inputs of allochthonous sediment or soil, previously deposited outside the cave and transported into it by inwash. The pedorelicts are common also in unit E2A, indicating the inwash of aggregated clay. Two layer couples E2A-8/E1-7 and E1-6/D-5 consisting of a thin matrix-rich layer and a thicker accumulation of rubble with few matrix probably represent phases of soil erosion and runoff followed by the reactivation of the scree. This indicates morphological instability under fresh and strongly variable wet/dry conditions (Di Maggio et al., 1999; Cottignoli et al., 2002). The uppermost level of the sequence, B-1.2, and B are again characterised by a loess-like percentage of silt. (Boschian et al., in prep.).

At microscopic level, silt cappings (Fig. 10 a-b) on coarse skeleton elements in layers D-4 and D-5 testify to freezing and thawing cycles, phases of deep seasonal frost subsequent to the deposition of the sediments (during the deposition of D4 or later).

All these characteristics indicate a strong variability of the environmental conditions, which were cold or fresh, and with oscillations between more or less arid régime. The lowermost units were deposited under steadier conditions, generally cold/arid favouring the sedimentation of aeolian dust, but with warmer episodes indicated by less coarse fraction in the lowermost E3C-12 and E3B-11 levels. The aeolian dust found in the cave is not primary, it is altered, and it entered the cave because of runoff a short time after its deposition outside the cave. Despite the previous preliminary interpretation of the sedimentological characteristics (Karavanić and Bilich-Kamenjarin, 1997; Rink et al., 2002) that contrasted with the faunal data, the hypotheses about paleoenvironmental change visible from the obtained data in fact match the change in faunal composition: chamois/ibex and equids fit well in an open and somewhat arid environment dominated by aeolian processes, whereas

discontinuous shrub cover is more likely than forest in phases of instability, as during the deposition of D. It is also possible that some part of the sequence, representing a colder maximum preceding the loess deposition of E2B-9 may have been removed by erosion, as indicated by the erosive boundary between E3A-10 and E2B-9 (Boschian et al., in prep.).

The human presence in the cave was more frequent during the earlier warmer phases and the rather arid event corresponding to loess deposition. Phosphate aggregates that can be identified at microscopic level as fragments of carnivore coprolites, possibly hyenas (Miller, Macphail, pers. comm.; Kolska Horwitz and Goldberg, 1979; Goldberg, 1980) are a relevant component of the sediments of almost all units, and can be considered as indicators of alternating frequentation of the cave by humans and carnivores. It is noteworthy that coprolites were not observed in unit E3C, which includes the highest density of faunal remains and lithic artefacts and may represent a phase of more intense and continuous use of the cave by humans.

4.6 Concluding remarks

The Mujina cave sequence was formed by two main natural processes, roof spall and scree input/inwash of fine material. These processes formed a homogeneous deposit comprised of limestone rubble and few matrix. Sedimentological and micromorphological analyses show that the fine component of the sediment is mainly made up of more or less moderately altered loess in the lower part of the sequence (levels E3C-12 to E2B-9), with a peak of poorly altered loess in level E2B-9, which may represent the cold and strongly arid Heinrich event H5, with age as in GICC05 coupled with GRIP, GISP2 and NGRIP records (Seierstad et al., 2014). The ^{14}C datings of these levels, though below the ^{14}C measure background, are consistent with this hypothesis, with a minimum age of about 47.8 ka BP (median deriving from bayesian modelling) (Boschian et al., in prep.). Hyena coprolites are a relevant component of the sediments, indicating alternating use of the cave by humans and carnivores. Frequent very small bone fragments, sometimes burnt or partially burnt, could indicate the characteristics of the Neanderthal diet, i.e. the extraction of the bone marrow. Another possible explanation for the burnt small bone fragments is the use of bones as fuel.

5. ZALA



Figure 5.1 Location map of Zala Cave

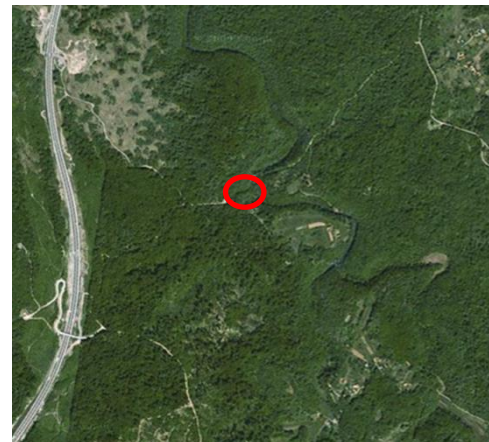


Figure 5.2 Location of Zala Cave (Google Earth).

5.1 Introduction

Zala Cave is situated in western Croatia; about 2 km to the E-NE of the town of Ogulin (Fig. 5.1). It is the only Upper Paleolithic and Mesolithic site discovered in Karlovac County.

Although many animal bones and a pottery shard were collected by S. Božičević in 1966 during speleological explorations of the cave (Jalžić and Božičević, 1971), the first archaeological trial excavations were carried out only in 2000 by D. Perkić, and yielded Iron Age, Bronze Age and Upper Paleolithic remains. The new systematic excavations, resumed in 2005 by I. Karavanić (Karavanić et al, 2007; Karavanić et al., 2008a), have brought to light a sedimentary sequence including numerous layers containing cultural remains whose age spans from the Late Upper Paleolithic to the Middle Ages, indicating a long and recurring use of the cave. The excavation lasted until 2011, and the study of the archaeological material is still in progress.

5.2 Site presentation

Zala is situated at the foot of the northern slopes of Krpelj hill, in the Tuk area (Karavanić et al., 2007). It lies on the left side of the canyon of the Bistrac stream, 1.5 km downstream of the source and about 100 m from the left bank of the stream (Fig. 5.2). The

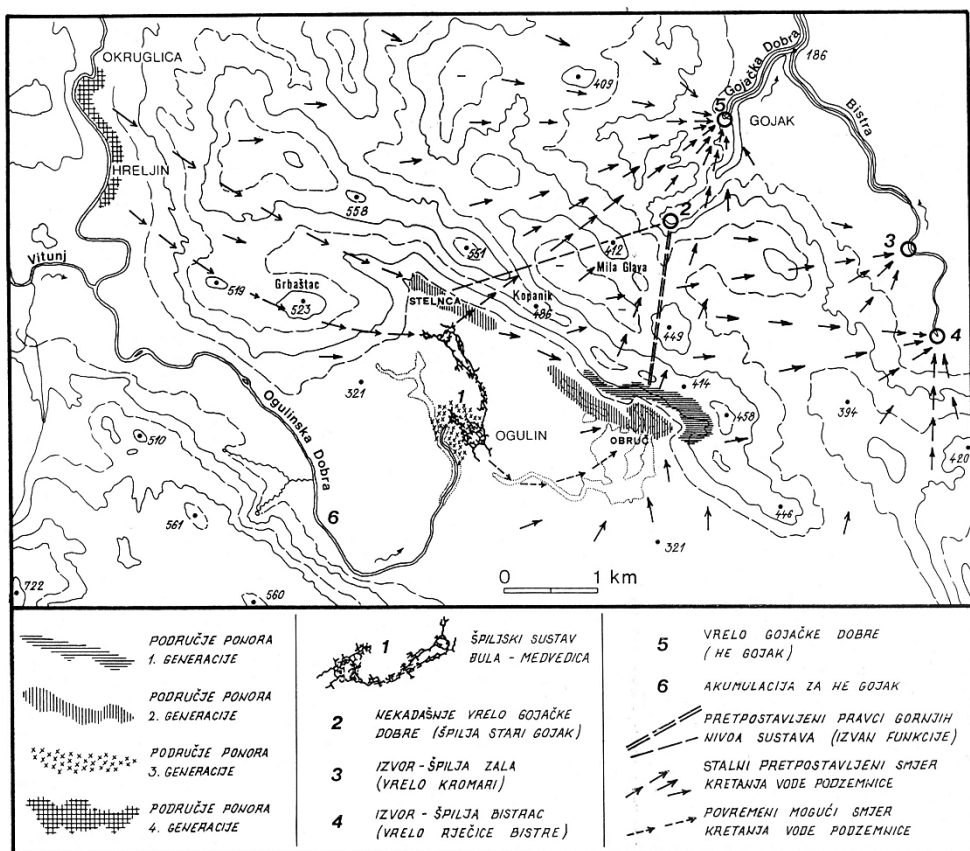


Figure 5.3 Cave system Đula - Medvedica with surface and underground hydrology
[\(<http://speleologija.eu/DjulaMedvedica/geologija.html>\)](http://speleologija.eu/DjulaMedvedica/geologija.html)

cave is probably connected to a large cave system called Đulin Ponor - Medvedica Cave - Izvor-Špilja Gojak spring (Fig. 5.3).

The cave is shaped within foraminiferous and algal-foraminiferous limestones of Aptian (Lower Cretaceous) age, and also Albian foraminiferous limestones are strictly associated with the cave systems connected to Zala. Neogene marls and sands can be found some hundred metres to the East of the cave. Mainly dolomitic rocks of Triassic to Jurassic age crop out to the West of Ogulin; to the South of the town, a limited outcrop of micaceous siltstones and sandstones can be observed (Vrsaljko et al., 2015).

The cave Zala opens at the bottom of the eastern side of a cliff surrounding a semi-cylindrical and flat-bottomed karstic depression; a secondary subvertical fault oriented NE-SW shapes the southern side of the depression, partly corresponding to the inner part of the cave. The depression is limited on its “open” side by a dam-like accumulation of large boulders organised in some irregular and coarse scree deposits that lean against the cliff.

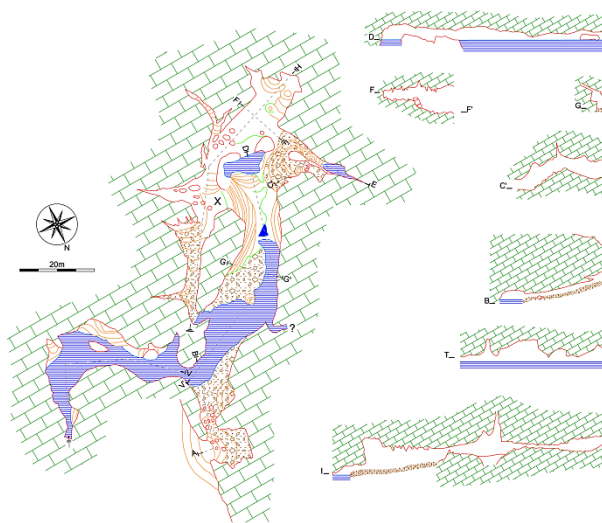


Figure 5.4 Cave plan, modified and redrawn from Jalžić & Božičević (1966).

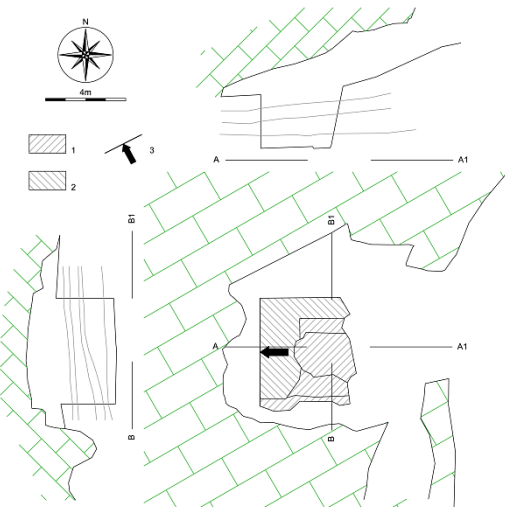


Figure 5.5 Plan and profiles of the entrance chamber. 1: old excavation area; 2: present-day excavation area; 3: main profile view. Modified and redrawn after Šošić Klindžić.

The entrance is oriented toward the East; it is 5 m wide and about 2.4 m high. Morphologically the cave can be divided into three parts: the entrance, a water channel and a large channel with siphon-lakes. In the outer part of the cave there is a small dry chamber (the entrance hall) which is connected to the inner system by a short and low passage (Fig. 5.4, profile A-B, 5.5). The entrance is approximately 12 m long and 10 m wide, and the height decreases from 2.4 m at the entrance to only 40 cm at the end of the entrance hall (Jalžić and Božićević, 1971; Karavanić et al., 2007). To the east, the underground lake extends for 75 m through a water channel which ends to the East with a narrow and submerged vertical crack in the direction of the exit siphon at the foot of the vertical rocks along the Bistrac stream. Though precise measurements are not yet available at present, the average level of the water in front of this exit siphon (which is normally flooded by the Bistrac waters) is probably almost the same or just a bit lower than inside Zala.

In the southern part of the cave, the siphon-lakes collect the water of the Zagorska Mrežnica River (Jalžić and Božićević, 1971); nevertheless, the communication with the Špiljski Sustav Đulin Ponor - Medvedica Cave - Izvor-Špilja Gojak must be active at vadose or phreatic level, because the water table inside the cave has systematically decreased after the construction of the Gojak hydropower plant.

About 2.5 km North-west of Zala, the Bistrica flows into the Gojačka Dobra River, which springs out from the Izvor-Špilja Gojak spring cave about 1 km to the South-east of the confluence.

At present, the domed ceilings of the entrance hall and of the inner side merge into a ridge, which is interrupted only above the passage. To the inside, this ridge is welded to the floor by a flowstone, while on the other side (entrance hall) the sediments fill up the space to a level about 1.5-2 m higher than the inside floor.

5.3 Archaeological background

The sedimentary sequence of Zala Cave spans from the Late Upper Pleistocene to the Late Holocene, and it includes Late Upper Paleolithic, Mesolithic, Bronze Age, Iron age, Roman and Medieval cultural remains. The Late Upper Palaeolithic dating was carried out on an animal bone sample by ^{14}C AMS, and gave an age of $13,840 \pm 50$ BP (Beta-228734); 16,986-16,509 cal BP (at 95.4% probability) (Karavanić et al., 2008b). The lithic assemblage, including backed bladelets and thumbnail endscrapers, suggests a Late Epigravettian cultural attribution; amongst animal bones, terrestrial fauna dominates, but perforated marine snail shells of *Cyclope neritea*, and a fragment of *Pecten jacobaeus* were also found. In Mesolithic layers large amounts of fish remains, pierced marine *Columbella rustica* shells, and pierced freshwater *Lithoglyphus naticoides* snail shells were found together with chipped stone artefacts. A large concentration of ash and charcoal also suggests the presence of hearths. A single available ^{14}C AMS date on bone 9430 ± 60 BP (Beta-235936; 11,066-10,504 cal BP at 95.4% probability) originates from a unit containing no typically Mesolithic artefacts, but indicates human presence in the cave during the early Mesolithic (Karavanić et al., 2008b). Numerous fragments of pottery, animal bones, bone needles, small bronze fragments, and two hearths indicate a more intense occupation of the cave during the Bronze Age. The pottery is characteristic for the Late Bronze Age, and a date obtained from a charcoal from one of the hearths (unit 69) gave $2,940 \pm 60$ BP (Beta-235935), 3,324-2,895 cal BP (at 95.4% probability) confirming this attribution. Late Iron Age/Roman layers are dated to $1,980 \pm 60$ BP (Beta-235934); 2115 – 1816 cal BP (at 95.4% probability). The surface layers yielded Medieval remains, mixed with recent ones (Karavanić et al., 2007; Karavanić et al., 2008b; Karavanić et al., 2008a; Komšo and Vukosavljević, 2011).

5.4 Results¹

5.4.1 Field observations

The archaeological excavations are situated in the entrance chamber of the cave, where a 5 m wide and about 2.5 m thick main profile was brought to light (Fig. 5.5, 5.6). The main lithological units (roughly corresponding from the theoretical point of view to the stratigraphic units used in the archaeological documentation) that were recognised at eye-scale observation during the excavation were described following the standard guidelines recommended by Catt (Ed.) (1991).

The thickness of the lithological units usually spans from 30-35 to 2-3 cm, apart the blocky unit (SU 101) that is about 1 m thick. The units are mostly layer-shaped, with common minor lenses interfingered within the main units; in general, all these slope gently towards the South (to the left of the profile in Fig. 5.6) and decrease their thickness upslope, sometimes thinning out at the top of the slope.

Some hiatuses can be identified within this sequence; these are usually evident at eye-scale examination of the stratigraphic sequence, and are often associated with gaps in the cultural sequence.

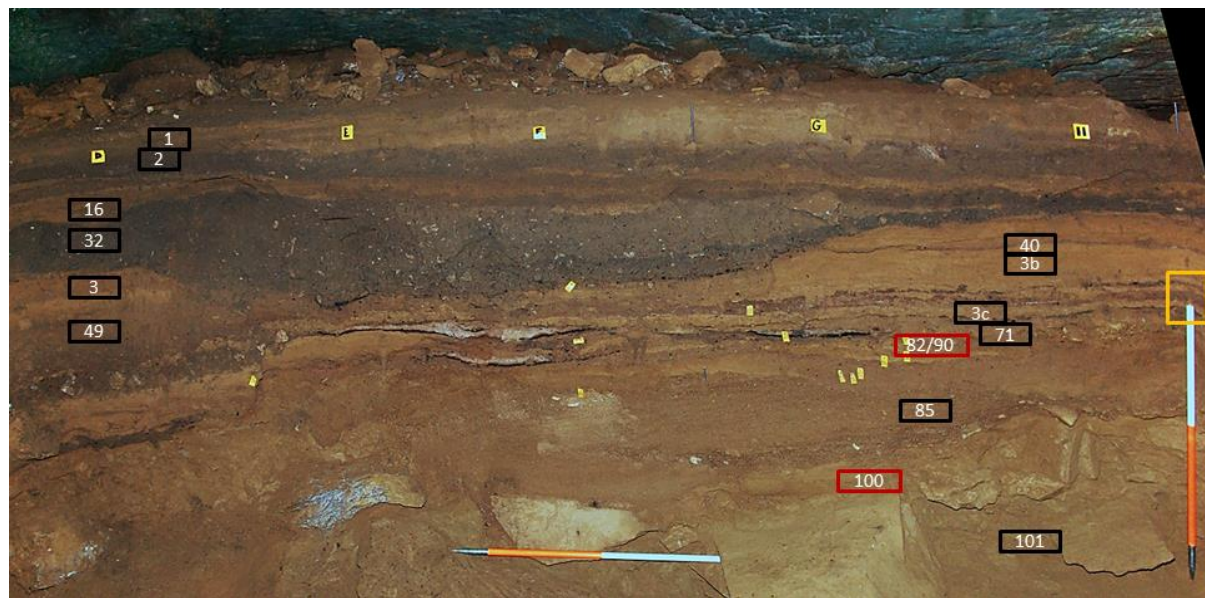


Figure 5.6 Main transversal profile across the entrance hall with the location of samples. In black – granulometry; in red – micromorphology. The details for the yellow square are given in Figure 5.9.

¹ Before the discussion of the thesis, the results were translated into Croatian and published in Arheologija šipilje Zale. Od paleolitičkih lovaca skupljača do rimskih osvajača (eds. N. Vukosavljević, I. Karavanić, 2015 (2016)).

Though the sequence comprises a large number of lithological units, these can be grouped in eight basic groups, which correspond also roughly to cultural horizons.

From the bottom upwards, the main groups are the following.

8 - Massive sandy silt loam, with few angular limestone skeleton, made up of large blocks that are sometimes in a vertical position. Darker or lighter chroma mark minor cm-thick layers and laminae; these levels are also strongly convoluted and wavy, with evident injection features. Few Epigravettian (Late Upper Palaeolithic) cultural remains (unit SU 102).

7 - Limestone rubble, large blocks and boulders up to 1 m large, angular and often platy, with sandy loam matrix; skeleton-supported structure. The thickness decreases towards the North and -more steeply- also toward the East (outside of the cave); here, a thick lens of sandy loam very similar to 8 and with strong convolutions and injection features (Figure 5.7.) is interfingered within the rubble. Thickness about 1-1.2 m, sharp subhorizontal boundary. Epigravetian (Late Upper Paleolithic) cultural remains (SU 101).



Figure 5.7 Strongly convoluted and disrupted laminae and possible ice wedge.

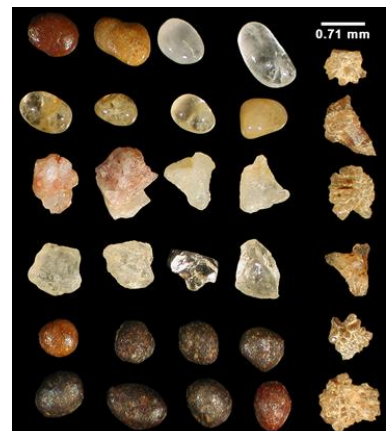


Figure 5.8 Stratigraphic unit SJ85, sand grains from the grain-size class 100-710 µm.

6 - This group includes some lithological units overlying a major unconformity that shapes the top of the underlying blocky level. The first two of these (SU 100 and SU 97-98) are relatively thin lenses lying inside shallow depressions of underlying layer; these are made up of fine to very fine sand or sandy loam, with poorly evident lamination. The third (SU 85) is an approximately 40 cm thick sigmoidal body with internal cross-bedding and subplanar lamination made up of medium-coarse sand to very fine gravel, which thins out upslope to the North of the profile and builds up a toplap. This unit was found on a large part of the excavation surface, evidently climbing and thinning out towards the entrance of the chamber. The grains of these units are mainly silicatic, including well-rounded to angular quartz (hyaline to pinkish-milky), drusae of authigenic minerals, and Fe-oxide pisolithes (Fig. 5.8).

Thickness 0-50 cm, sharp limit, gently sloping towards SW. SU 100 Late Upper Paleolithic. SU 97-98 no cultural remains.

5 - Homogeneous sand or sandy loam, sometimes with fine granular aggregation. Several levels and small lenses are included within this group, separated by disconformities. A sequence of small sandy to loamy concave-upwards units (SU 94-92, 84, 82) lies in a shallow depression on the top of SU 89, while SU 75 is a more or less tabular layer, sandy and with laminar sedimentary structures, that is somewhat thicker towards the south-western corner of the excavation area.

Units 82, 84, 92, 93 and 94 include abundant fishbone remains and/or Mesolithic industry, and can be roughly correlated with an *in situ* hearth (SU 90-92) that was found in squares 8-9/H. This hearth leans against the tips of blocks belonging to SU 101 and overlies SU 85, which in this area reaches its uppermost height and partly fills the gaps between the above-mentioned blocks. Some tens of centimetres towards the inside, SU 75 lies directly above SU 89 and/or SU 85 -the other intermediate ones or even SU 89 being absent here- and comes into lateral contact with the hearth by an erosion surface.

The whole thickness of this group is between 20 and 30 cm; the limit is abrupt, somewhat undulating, and gently dipping towards the South-western corner of the excavation area. Mesolithic cultural remains (SU 82, 84, 92-94). No cultural remains (SU 75).

4 - This group includes several layers 2-4 cm-thick, characterised by alternating yellowish and brownish colour, the former being thicker. Charcoal fragments are frequent within the brown layers, where also some very thin whitish laminae (probably ash) can be observed (SU 65). Along the Eastern (main) profile, the bottom of this group is marked by two well-preserved unstructured hearths (SU 83 and 78), including a blackish charcoal-rich layer at their bottom, and a thicker ash layer.

SU 75 lies above SU 83, and separates it from an overlying third Bronze Age hearth (SU 74). It must also be pointed out that the uniform interfingering of brown and yellowish layers is not present here, as well as to the outside of the cave, where it is substituted by an up to 50 cm-thick brownish layer divided into a lower coarser horizon overlain by a lighter and finer one.

Horizontally laminated aggregates can be observed throughout the group. Thickness about 30-35 cm average; sharp plane limit, gently sloping toward South-east. Units SU 65-SU 49. Bronze Age cultural remains.

3 - Brownish to yellowish stoneless silty loam, with several lighter 3-5 cm-thick horizons concentrated mostly in the upper part. One greyish horizon is also present. Very well

developed laminar aggregation, with subhorizontal aggregates, is common throughout the group, particularly well developed in the SW corner.

Thickness 5-40 cm; the limit is abrupt, plane and gently sloping towards South-east. Unit SU 56 includes Bronze Age remains, SU 49 Bronze or Iron Age, SU 40?, SU 3 no cultural remains.

2 - Greyish silty clay loam, with common unsorted angular limestone gravel and some blocks; well-developed coarse granular aggregation. Charcoal fragments are common throughout the unit. The level is relatively thin on the Northern side of the profile, and becomes thicker and thicker downslope; a very wide and shallow channel-like erosion feature can be observed in squares E-F-(G)/11 along the main profile. SU 32. Roman cultural remains?

Thickness 20-35 cm; sharp limit, moderately undulating and very gently sloping towards SW.

1 - Sequence of several loamy tabular layers, brownish to yellowish to greyish; few limestone skeleton, angular and unsorted. The limits between horizons are abrupt or slightly diffuse, with some undulations that occur mostly in the NW corner of the excavation area. Thickness 35-40 cm; sharp lower limit, plane or slightly undulating, subhorizontal to gently sloping.

Units 16-1. Medieval and recent cultural remains.



Figure 5.9 Bronze Age anthropogenic and geogenic units; detail of Figure 9 with the locations of the samples.

Table 5.1 Grouping and colour of the analysed lithologic units.

| Lithologic group | Unit | Cultural horizon | Munsell Soil Color Charts (under moist conditions) |
|------------------|------|--|--|
| 8 | 102 | Late Upper Paleolithic - Epigravettian | 10YR 5/4 yellowish brown |
| 7 | 101 | Late Upper Paleolithic - Epigravettian | 10YR 5/4 yellowish brown |
| 6 | 100 | Late Upper Paleolithic - Epigravettian | 10YR 5/4 yellowish brown |
| 6 | 85 | No cultural remains | 10YR 3/4 dark yellowish brown |
| | 82, | | 10 YR 5/6 yellowish brown |
| 5 | 80, | Mesolithic | 10 YR 5/3 brown |
| | 90 | | 10YR 5/2 grayish brown |
| 4-5 | 75 | No cultural remains. | 10YR 4/6 dark yellowish brown |
| 4 | 77 | Bronze Age | 10 YR 4/2 dark grayish brown |
| 4 | 71 | No cultural remains. | 10 YR 5/6 yellowish brown |
| 4 | 65 | Bronze Age | 10 YR 4/3 brown |
| 4 | 3c | Bronze Age | 10YR 4/6 dark yellowish brown |
| 4 | 49 | Bronze Age/Iron Age? | 5YR 4/2 dark reddish gray |
| 3 | 40 | Iron Age/Roman | 10YR 4/2 dark grayish brown |
| 3 | 3b | Iron Age/Roman | 10YR 4/6 dark yellowish brown |
| 2 | 32 | Roman | 7.5 YR 3/2 dark brown |
| 1 | 16 | Medieval | 10YR 3/3 dark brown |
| 1 | 2 | Medieval and recent | 7.5YR 2.5/2 very dark brown |
| 1 | 1 | Recent | 10YR 4/4 dark yellowish brown |

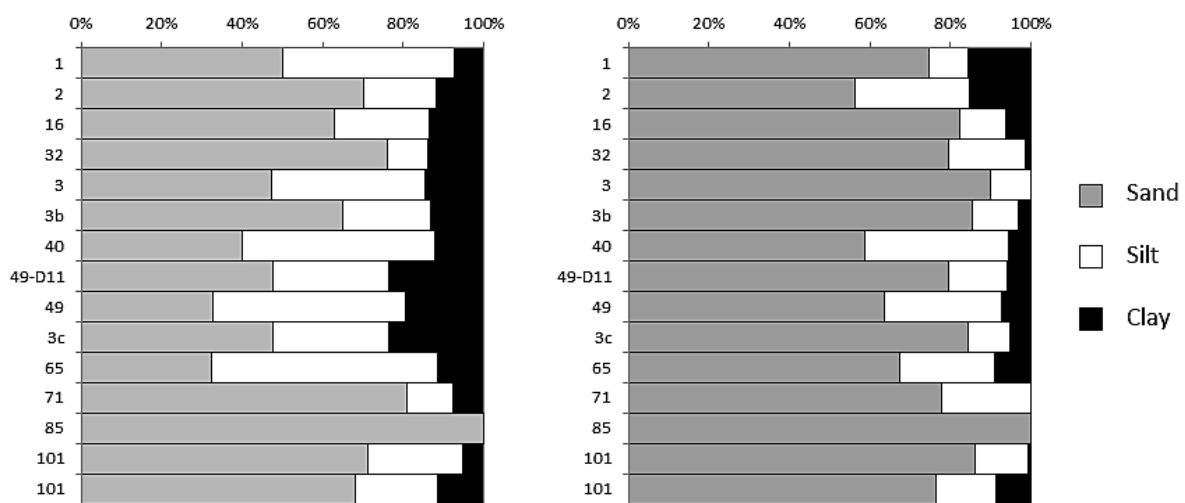


Figure 5.10 Granulometric analyses of Zala Cave sediments. 1. decalcified, 2. undecalcified.

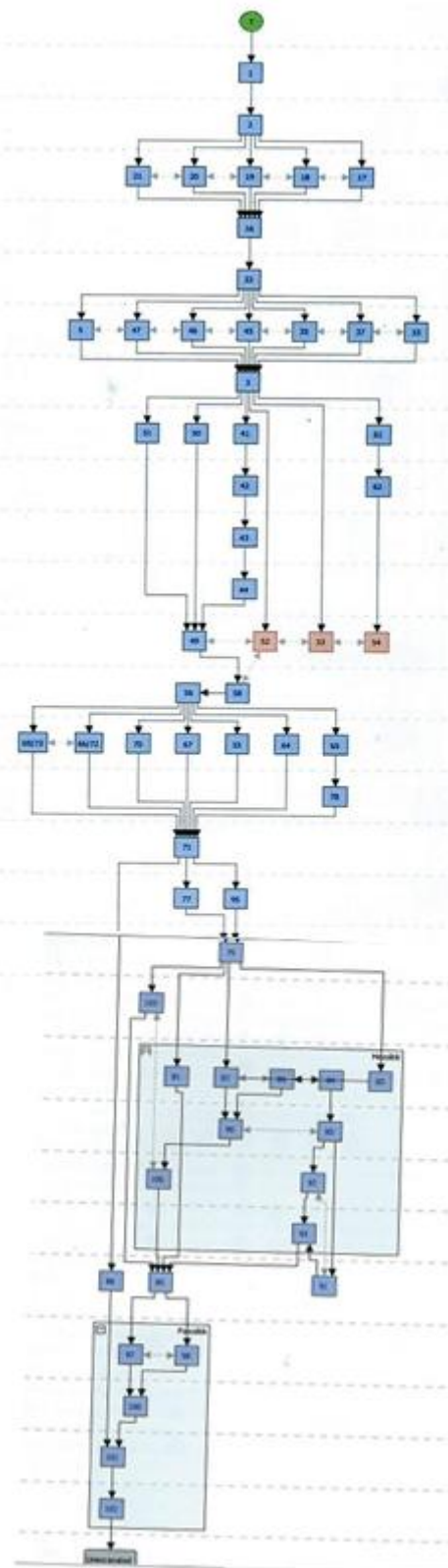


Figure 5.11 Harris matrix (Šošić Klindžić et al., 2015).

5.4.2. Sediment texture of the stratigraphic units

Each unit, or in some cases the most representative element of a set of similar units, was sampled for laboratory analyses; one or two samples *per* unit were collected in different locations in the sequence and within the excavation area. In each sampling location, a bag of bulk sediment ranging from 150 g to 500 g depending on the average texture was collected for particle-size determination and routine chemical analyses. For each of these samples, the particle-size analysis of the fine fraction (< 2 mm) was carried out at 1/2 φ precision on 100 g of sediment (50 g for the finer units).

The texture of the sediments is sandy to loamy, usually with minor clay percentage; the skeleton is usually rather rare, comprising sparse, medium gravel- to block-size elements. Fine to medium gravel-size elements are common in SU 32; conversely, SU 101 is made up of coarse angular limestone rubble and blocks, including metre-size boulders, and representing, therefore, a peculiarity in the sequence.

The coarse component of the sediments is usually calcareous, while the finer one - from sand downwards in the grain-size scale- is dominated by silicate minerals, mostly quartz, feldspar, plagioclase and very abundant mica; the last one is most common in the very fine sand- to silt-size textural fractions.

All the sediments can be roughly divided into three groups according to their fine fraction (< 2 mm) granulometry (Fig. 5.10). SU 85 is excluded from these grouping since it is composed entirely of sand.

1) The first group includes SU 1, 3-D11, 3c, 49-D11. The sand amount in the undecalcified samples ranges between 47% and 50%; the silt fraction is 39-42%.

2) The second group comprises SU 16, 3-H11, 75, and 101. SU 2 and 32 can also be included in this group despite some inconsistencies. The sand amount in the undecalcified samples is 63-81%, silt amount is 10-24%.

In the decalcified samples, the sand fraction is generally much more abundant (75-90% in the first group; 78-86% in the second group, except from SU 2 where it is somewhat lower, around 56%).

3) The third one includes granulometrically the most similar group of sediments. It has the most abundant silt amount (ranging between 48% and 56%), and the lowest percentage of sand (32-40%) of the whole sequence in both undecalcified and decalcified samples.

In the decalcified samples, all the units have a minor clay percentage, ranging from 0-15%.

5.4.3 Micromorphology

Micromorphological analyses were carried out on seven thin sections, prepared from the undisturbed monoliths of sediment collected during the 2009 and 2010 field seasons. The main micromorphological characteristics of Zala sediments are summarised in this chapter. One Paleolithic, three Mesolithic and three samples collected from the Bronze Age levels were studied. The location of the samples collected from the profile is given in Figure 5.6 and Figure 5.9.

Z 2010/6/T1

This thin section includes sediments from alternating levels SU 3, SU 49, and SU 65 (for the description of SU 65 see Z 2010/T/T2).

1a) SU 3 – microfacies 2

Microstructure and porosity: platy and channel microstructure.

Groundmass: c/f-related distribution pattern is close to double spaced porphyric.

Coarse material:

Rock fragments: few subrounded flint fragments.

Minerals: frequent angular to subangular spathic calcite, common subangular to subrounded quartz grains, common muscovite flakes.

Inorganic residues of biological origin: very few shell fragments.

Organic: very few tissue fragments, very few charcoal fragments.

Micromass: yellowish brown dusty clay (in PPL) with stipple speckled b-fabric.

Pedofeatures: few Fe/Mn nodules and punctuations.

1b) SU 3 – microfacies 1

Microstructure and porosity: intergrain microaggregate microstructure is rare.

Groundmass: c/f-related distribution pattern is close to single spaced fine or coarse enaulic.

Coarse material:

Rock fragments: very few subrounded flint fragments.

Minerals: dominant angular to subangular sparitic calcite, common subangular quartz grains, few muscovite flakes, few biotite

Inorganic residues of biological origin: very few shell fragments.

Organic: very few amorphous organic matter.

Micromass: very few clay with speckled b-fabric.

Pedofeatures: few clay papulae, common Fe/Mn nodules.

2) SU 49

The SU 49 is formed of two thin brownish levels separated by a thin discontinuous yellowish level (microfacies 1, but with ice lensing). The brownish levels will be described here.

Microstructure and porosity: crumb and granular microstructure with few channels.

Groundmass: c/f-related distribution pattern is open porphyric.

Coarse material:

Rock fragments: very few rounded flint fragments.

Minerals: frequent angular to subangular spathic calcite grains, common subangular to subrounded quartz grains, common muscovite flakes, very few biotite, few phosphatic fragments.

Inorganic residues of biological origin: common phytoliths (few interconnected), dominant faecal spherulites, very few shell fragments.

Anthropogenic elements: charcoal fragments, frequent micrite (ash).

Organic: frequent tissue, cells, amorphous organic matter, and punctuations, very few pollen (?).

Micromass: dusty clay and ash with calcitic crystallitic and speckled b-fabric.

Pedofeatures: few Fe/Mn nodules.

Z 2010/7/T2

This thin section comprises several SU: 3 (described above), 65, 75 (same as SU 3), and 77 (which will be described in the following thin section Z 2010/8/T3).

SU 65

The SU 65 is made of compact levels of spherulites, phytoliths and ash included between thicker levels consisting of small rounded aggregates of spherulites.

Microstructure and porosity: complex microstructure (fluid, crumb, granular, spheroidal) with channels, vesicles and simple packing voids.

Groundmass: c/f-related distribution pattern is close to double spaced enaulic.

Coarse material:

Rock fragments: very few subrounded sandstone fragments, very few subangular to rounded flint fragments.

Minerals: very frequent sparitic calcite, frequent angular to subrounded quartz grains, few muscovite flakes.

Inorganic residues of biological origin: burnt micritic organ and tissue residues, dominant faecal spherulites, frequent phytoliths, micritic drusae, very few bone fragments.

Anthropogenic elements: few charcoal fragments.

Organic: amorphous organic matter, punctuations.

Micromass: grayish brown micromass with calcitic crystallithic b-fabric.

Pedofeatures: common clay papulae, very few Fe/Mn nodules.

Z 2010/8/T3

This thin section includes sediments from SU 77 embedded in SU 75. For the description of SU 75 see SU 3.

SU 77

Microstructure and porosity: granular microstructure.

Groundmass: c/f-related distribution pattern is enaulic.

Coarse material:

Rock fragments: common rounded sandstone fragments, very few limestone frgs.

Minerals: frequent quartz, calcite, common muscovite.

Inorganic residues of biological origin: few phytoliths, spherulites.

Anthropogenic elements: frequent charcoal frgs, few pottery frgs, few slag, dominant ash.

Micromass:dusty fine ash and dusty clay with calcitic crystallitic b-fabric.

Pedofeatures:Fe/Mn nodules.

Z 2010/12/82-80

This thin section includes sediments from SU 82, and SU 80.

1) SU 82:

Microstructure and porosity: intergrain microaggregate microstructure (microfacies 1); massive and channel microstructure (microfacies 2).

Groundmass: c/f-related distribution pattern is close to single spaced fine or coarse enaulic (microfacies 1); close to single spaced porphyric (microfacies 2).

Coarse material:

Rock fragments: few rounded quartzitic fragments, few rounded flint fragments.

Minerals: common muscovite flakes, frequent angular to subangular sparitic calcite, frequent subangular to subrounded quartz grains, very few biotite, common angular to subangular opaques.

Inorganic residues of biological origin: very few shell fragments.

Micromass: yellowish dusty clay (PPL) with parallel striated and granostriated b-fabric.

Pedofeatures: common clay papulae, few Fe nodules, Fe coatings and hypocoatings.

2) SU 80

Microstructure and porosity: crumb and spongy microstructure with vughs.

Groundmass: c/f-related distribution pattern is single spaced to close enaulic.

Coarse material:

Rock fragments: few rounded sandstone fragments, few rounded flint fragments, few subrounded to rounded limestone fragments, common rounded quartzitic fragments (quartz aggregates).

Minerals: frequent angular to subangular sparitic calcite, common subangular to subrounded quartz grains, common muscovite flakes, few biotite.

Inorganic residues of biological origin: common angular to rounded bone fragments (burnt and unburnt).

Organic: few amorphous organic matter.

Anthropogenic elements: frequent charcoal fragments, very frequent angular to subangular micritic aggregates (ashes).

Pedorelicts: common pedorelicts (fragments of microfacies 2 fabric, and reddish pedorelicts with skeleton).

Micromass: stipple speckled b-fabric.

Pedofeatures: few concentric Fe/Mn nodules, common typic Fe/Mn nodules, few rolling pedofeatures, common clay papulae.

Includes also a thin layer of microfacies 2 fabric.

Z 2010/9/90

Microstructure and porosity: lenticular platy microstructure.

Groundmass: c/f-related distribution pattern is open porphyric.

Coarse material:

Rock fragments: common angular to subangular limestone fragments, frequent subrounded to rounded quartz aggregates, few subrounded to rounded flint fragments, few rounded sandstone fragments

Minerals: common angular to subangular sparitic calcite, common subangular to subrounded quartz grains, common muscovite flakes

Inorganic residues of biological origin: frequent subangular to rounded bone fragments (mostly burnt), few shell fragments.

Anthropogenic elements: common charcoal fragments, micritic aggregates (ashes), very few pottery fragments.

Pedorelicts: loess like pedorelicts (few).

Micromass: ash with banded fabric, calcitic crystallitic b-fabric.

Pedofeatures: common silt cappings, common Fe/Mn nodules (mostly typic, very few concentric, few Fe hypocoatings, few clay papulae.

Z 2010/13/80-89

Microstructure and porosity: moderately to highly separated lenticular microstructure with channels; granular microstructure.

Groundmass: c/f-related distribution pattern is

Coarse material:

Rock fragments: rare angular limestone fragments, common subangular to rounded quartzitic fragments, few rounded sandstone, and common angular to subangular flint fragments.

Minerals: frequent angular (sparitic) to rounded (micritic) calcite grains, quartz, common muscovite flakes, and few angular opaques.

Inorganic residues of biological origin: very few shells, few bone fragments

Organic: very few charred fragments.

Common pedorelicts.

Micromass: granostriated b-fabric and banded fabric.

Pedofeatures: concentric Fe/Mn nodules, common compound stratified cappings, rare link cappings, and few clay papulae, fecal spherulites (only in SU 80).

Z 2009/1/100

Microstructure and porosity: moderately to weakly separated lenticular microstructure, and granular microstructure with vesicles.

Groundmass: c/f-related distribution pattern is close to double-spaced porphyric.

Coarse material:

Rock fragments: very few rounded sandstone fragments, common angular to subrounded limestone fragmetns, common metamorphic? fragments,

Minerals: frequent quartz and feldspar, frequent muscovite flakes, frequent angular (sparitic) to rounded (micritic) calcite grains, very few clorite flakes.

Inorganic residues of biological origin: none.

Organic: none.

Rare pedorelicts.

Micromass: greyish brown (PPL) dusty micromass with banded fabric.

Pedofeatures: frequent Fe/Mn nodules (frequent typic, common concentric; few nucleic and disorthic nodules), common stratified silt cappings, common clay papulae, few dusty clay coatings.

The lowermost sample of the sequence, derived from the Late Upper Paleolithic layer SU 100, presents a moderately to weakly separated lenticular microstructure, occasionally granular, with rare channels and vesicles, and the micromass is dusty grayish brown in PPL, and with banded fabric (Fig. 5.12, a – b, e). The most abundant coarse components are angular to subrounded foraminiferal and/or sparite to micritic limestone fragments, quartz and calcite grains, although feldspar and muscovite are quite frequent. Other coarse material includes sandstone and metamorphic rock fragments, mostly rounded, and rare aggregates (pedorelicts). The most important pedofeatures are stratified silt cappings that occur on coarse fragments and are occasionally downturned or associated with banded fabric (accumulations of silt and coarse clay on the top of the lenses). Iron oxide/manganese nodules (typic, concentric, nucleic) are common, and disorthic nodules also occur.

Three thin sections were ground from samples collected in Mesolithic layers (SU 90, SU 89-80, SU 82-80). Rock fragments are the most abundant coarse material, ranging from angular to subangular limestone fragments (with foraminiferans, sparite or micritic) to well-rounded sandstone (often quartzitic sandstone) and metamorphic rock fragments. Bone fragments, angular to subrounded and frequently burned, are one of the most abundant types of coarse material. Ice lensing and silt cappings are the most evident pedofeatures in SU 90 (hearth), which is characterised by a lenticular platy microstructure (Fig. 5.12 c – d, f). The two thin sections comprising sediments from SU 89-90 and 82-80 have crumb and spongy microstructures, or an intergrain microaggregate microstructure. Fe/Mn nodules are common in all the studied units.

The Bronze Age sequence is characterized by alternating, few centimetres thick brownish (Bronze Age SU 77, SU 65, and Bronze/Iron Age SU 49) and fine yellowish layers (SU 3c, 71, 75). The yellowish sediments are geogenic and include two microfacies; the coarser, well sorted sediment (mostly composed of calcite, quartz and muscovite) always overlies the finer one (where calcite, quartz and muscovite are embedded in a clay

micromass). The brownish layers are anthropogenic, and their characteristics are the following:

- 1) SU 77 is a dark brown, 1.5-2 cm thick layer including frequent charcoal fragments, organic matter, pottery fragments, very few possible slag fragments, randomly dispersed wood ash and phytoliths, and very few fragments of sheep/goat droppings (faecal spherulites and phytoliths).
- 2) SU 65 comprises exclusively burnt sheep/goat dung (faecal spherulites and phytoliths). At least three ash (burnt plants and faecal pellets) microlayers can be recognised inside this 2.5 cm thick dung layer (Fig. 5.13).
- 3) SU 49 is made up of two discontinuous microlayers of sheep/goat dung (faecal spherulites and organic matter) divided by a thin (0.5-1 cm) discontinuous yellowish layer identical to the SU 3c, 71 and 75 fine-grained microfacies. The upper of the two brownish dung layers also contains droppings that differ from the ones ascribed to sheep/goats, very phosphatic with abundant phytoliths and very few spherulites, that can probably be ascribed to omnivores (Fig. 5.14).

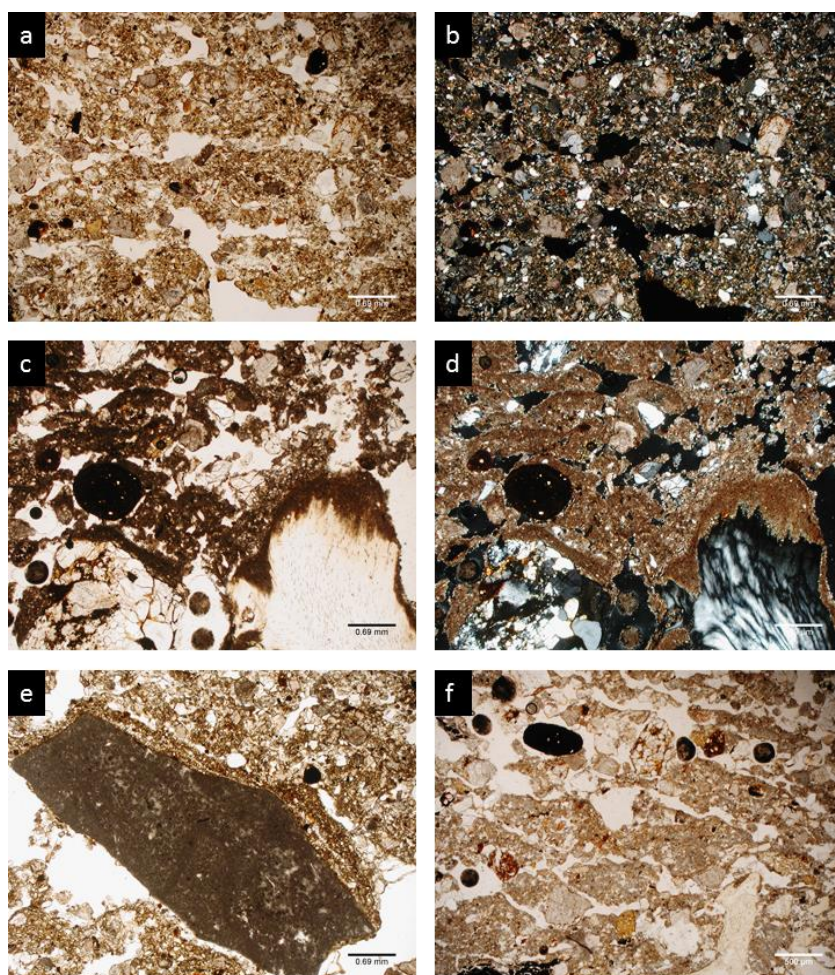


Figure 5.12 Photomicrographs: a) SU 100, lenticular microstructure, PPL; b) SU 100, lenticular microstructure, XPL; c) SU 90, banded fabric and silt cappings, PPL; d) SU 90, banded fabric and silt cappings, XPL; e) SU 100, stratified silt capping on limestone fragment; f) SU 90, lenticular microstructure, PPL.

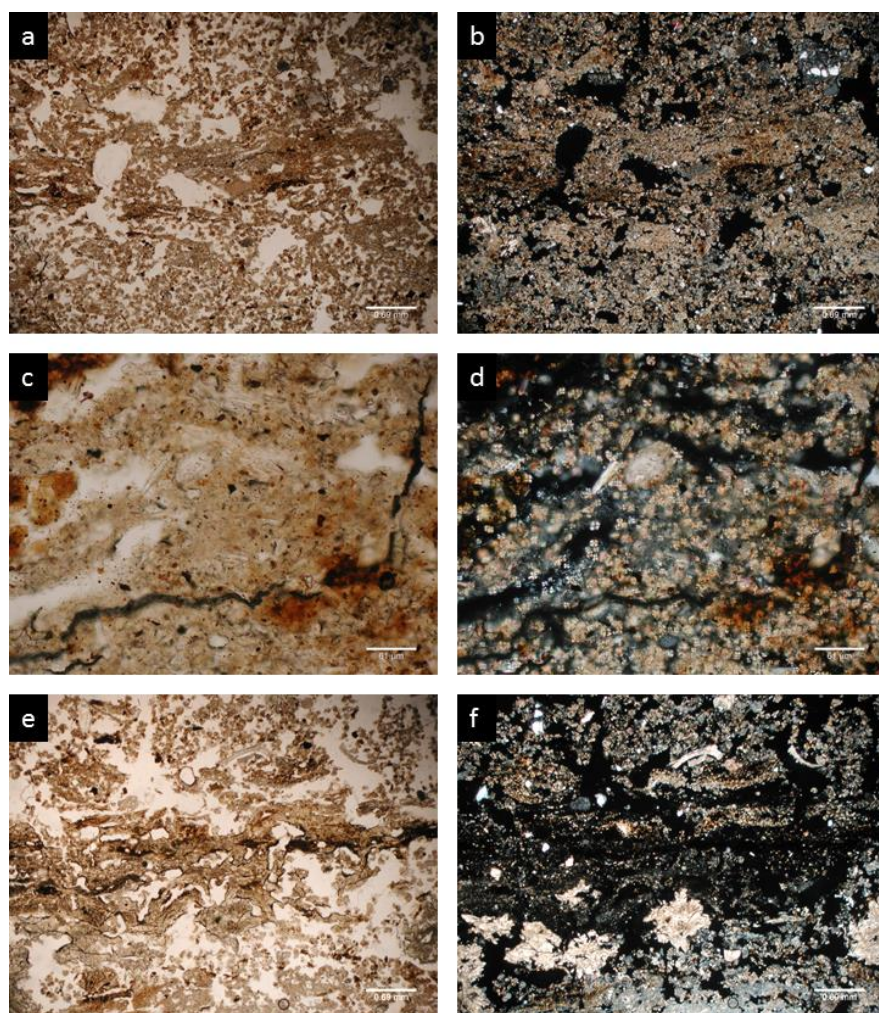


Figure 5.13 Photomicrographs, SU 65: a) spherulites, phytoliths and ash in PPL; b) spherulites, phytoliths and ash in XPL; c) same as a, detail; d) same as b, detail; e) recrystallized ashes, spherulites, phytoliths, PPL; f) recrystallized ashes, spherulites, phytoliths, XPL.

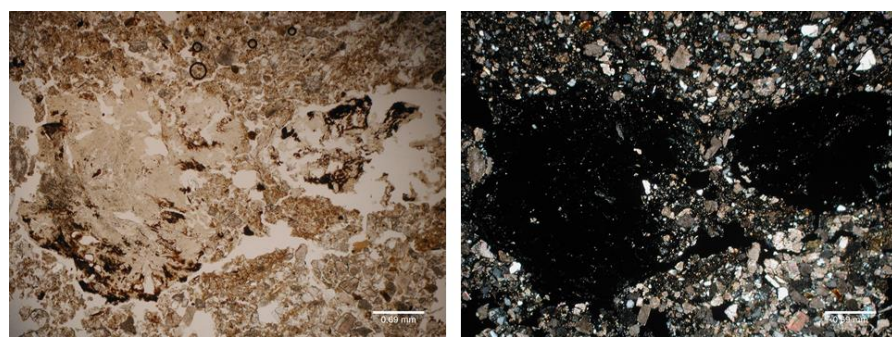


Figure 5.14 Photomicrographs, SU 49, phosphatic dropping.

5.5 Discussion

The most important issue about the formation processes of the Zala Cave infilling is the origin and the process of emplacement of the clastic sediments. A relevant topic is also to ascertain whether the cultural remains are *in situ* or reworked.

At Zala Cave, the mineral component of the sediment has three possible origins:

1. Strictly local, *i.e.* originated from the bedrock in which the cave is shaped; limestone blocks and rubble can be ascribed to this class. Part of these clasts may have rolled into the cave through the entrance, after having dropped from the cliff overhanging the cave entrance; this hypothesis may be supported by the roughly conical shape of the group of units 8 and by the partly imbricated arrangement of blocks inside it, which resemble a scree deposit. Nevertheless, it is also very likely that a large part of the blocks derive from ceiling breakdowns triggered by deep frost, as indicated by the occurrence of common frost slabs in the medium gravel-size fraction of the rubble.

Conversely, it is unlikely that large part of the fine fraction of the sediment may derive from the alteration of the bedrock because the local Cretaceous limestone is rather pure and does not include a remarkable quantity of silicate minerals.

2. Endokarstic, *i.e.* transported and deposited in the cave by underground river flow. A large part of the very fine gravel and sand components of the sediment probably have this origin. The most evident river deposit within the sequence of the Zala Cave is SU 85: its sigmoidal shape and internal cross-bedding are typical of side accretion bodies in fluvial environment, and similar deposits -even if finer- are being formed at present along the lake situated in the internal part of the cave. The relatively large grain-size of the particles in SU 85 suggests strong flow energy, which may have reworked and also removed the finer part of the underlying unit.

Unit 75 shares some characteristics with SU 85, *i.e.* some lamination, general shape and texture; consequently, it may be inferred that part of the Mesolithic cultural remains are embedded in a unit that was reworked *ab antiquo*. The corresponding unreworked deposits (including a hearth) are limited to the area where the unit lies higher on the underlying topographic surface, *i.e.* in the North-eastern portion of the excavation area. Micromorphology confirmed this hypothesis, showing that the Mesolithic hearth SU 90 in square H8 is *in situ*, while samples taken from the main transversal profile show mixing and reworking of sediments. It is noteworthy that no faecal spherulites were observed in

sediments with Mesolithic cultural remains, indicating that the reworking happened before the sedimentation of the Bronze Age layers.

A large part of the sequence, at least the portion overlying the blocky unit up to the bottom of SU 32, was affected by river processes. Laminated sands and erosion surfaces occur often among these levels, which are also sloping towards the southern side of the entrance hall, and indicate frequent river floods (erosion) followed by decreasing energy phases (sand deposition). Some evidence of ponding can probably be indicated by the small lenses SU 94 - SU 82 that are embedded within this part of the sequence.

The reasons why the internal river may have reached the entrance hall can be explained if the geometrical relationships between the hall and the internal cave, and also the shape of the ceiling, are observed. As described above, the ceiling in the inner cave is just a bit lower than in the entrance hall; both are slightly domed, and are probably divided by a sort of inverse ridge that results from the juxtaposition of the two domed shapes (Fig. 5.4, Fig. 5.5). On the side of the hall, the sediment fills up large part of the chamber and covers the shape of the ridge (which is indeed the southern wall of the hall), while to the inside the floor is 1-1.5 m lower, so that the shape of the ridge can be easily observed, even if it is partly covered by a flowstone connected to the floor. In the latest phases of Late Pleistocene or Early Holocene (when SU 85 was probably deposited), the sediment level was about 1.2-1.5 m lower in the entrance hall, and the flowstone had not yet (completely?) grown, so that there was direct communication between the two chambers and the water could easily flood the entrance hall.

Regarding the provenance of the silicate sediments, a large part of which comprises rounded grains, the problem is somewhat more complex. It is not unlikely that these may derive from the dismantling of sandstone formations, like the Triassic ones cropping out a couple of kilometres South of Ogulin in the Mrežnica basin, to which the Zala underground river is also supposed to be connected. Nevertheless, it may also occur that the Zala underground river itself eroded directly these formations in areas where they do not crop out on the surface.

3. Allochthonous, *i.e.* material coming from more or less distant areas outside the cave. Such sort of material is usually rather fine and includes colluvia deriving from the dismantling of soils and/or sediments deposited outside the cave, or -more rarely- windblown dust (loess).

Some evidence of slope processes may also be inferred from the undulating limits between units in groups 2 and 1, which may indicate sediment creep in a cold environment (Van Vliet-Lanoë, 1985; 1987).

The input of aeolian dust is questionable at Zala Cave; it would be normally indicated by the occurrence of remarkable quantities of windblown micas deriving from the metamorphic parageneses of the Alpine fringe (Cremaschi, 1990a; 1990b), but it must also be observed that the abundant micas (mostly muscovite) found in the Zala sediments may also derive from the Triassic pelitic formations situated South of Ogulin. Moreover, the grain-size curves of these sediments do not resemble the classical loess because of the too high sand percentage.

Eventually, referring to processes triggered by periglacial conditions, it must be pointed out that ice lensing (Coutard and Mücher, 1983; Van Vliet-Lanoë, 1976), attested by the well developed laminar aggregation occurring in group 3, is good evidence of deep seasonal frost. Even sounder evidence of frost is provided by the strongly convoluted laminations occurring in the basal levels underlying the blocky layer (SU 101), in the fine level interfingered in it, and to some extent also in the directly overlying unit 89 (on the Northern profile). This evidence is in accordance with very cold environmental conditions that also triggered the frost shattering and breakdown of the ceiling, originating the blocky unit SU 101. Deep seasonal frost is further confirmed at microscopic scale for SU 100 and 90 by the occurrence of pedofeatures such as silt cappings, ice lensing, banded fabric, as well as by frost shattered coarse limestone clasts.

It may be argued that deep seasonal frost may not fit the age and supposed warm climate corresponding to the deposition of groups 3-1, which took place during the Medium-Late Holocene (Bronze Age remains). Nonetheless, it can be observed that the depression where the Zala is situated is a peculiar ecotope, where the characteristics of the present-day floral biocenosis indicate average temperatures lower than in the surroundings. Such peculiarity may have also enhanced the effects of low temperatures during the Late Glacial and the Early Holocene, causing strong cryoturbation in the cave sediments.

Soil micromorphology revealed some anthropogenic component in the infilling processes, but this was limited to the upper Middle/Late Holocene part of the sequence which includes Bronze and/or Iron Age cultural remains. The anthropogenic units 77, 65, 49, and possibly 40, situated between the Bronze Age hearths (SU 83, 78, 74) and SU 32, alternate with yellowish fine river sediments. During the deposition of the lowermost of these three

layers (SU 77), the cave was used primarily as a domestic space. SU 65, which lies in the middle of this group of units, marks a shift in the use of the entrance chamber of Zala Cave; repeated cycles of burnt dung (confirmed by the abundance of faecal spherulites and phytoliths) together with the very small amount of pottery shards (pers. comment B. Olujić; Olujić and Perković, 2015) indicate that the cave was used almost exclusively seasonally as stock pen for ovicaprids. In the uppermost unit (SU 49) the dung was only partially burnt, at the top of the unit; conversely, the rest of it underwent natural mineralisation processes. As proven by Brochier et al. (1992), these processes can considerably reduce the volume of the layers and thus have to be taken into consideration. Geo-ethnoarchaeological studies conducted by Brochier et al. (1992) showed that burning reduces the dung volume by approximately 13-19%, while mineralisation causes loss of volume by up to 80%. This must be taken into consideration in archaeological interpretations, because these processes concentrate cultural remains originally distributed through a much thicker layer which represents a much longer span of time than a layer of burnt dung (Brochier et al., 1992). In SU 49 a total of 553 fragments of pottery was collected, which is much more if compared to SU 65, where only 32 fragments were found (Olujić, pers. comm.). It is noteworthy that grain size analyses showed that the thin brownish SU 40 is very similar to SU 65, 49 and 77, with smaller amount of sand (39.94%), and a greater percentage of silt (48.05%) if compared to the other two groups of sediments. This results could indicate another episode of stabling inside the cave, although we do not have micromorphological analysis that could confirm this hypothesis.

5.6 Concluding remarks

The geoarchaeological study of the Zala Cave deposits has brought into light some palaeoenvironmental peculiarities, mostly connected to an extremely cold climatic situation at the end of the Pleistocene and beginning of the Holocene. Despite the unfavourable conditions, the cave was visited by groups of hunters-gatherers, and this sort of use continued throughout the Holocene even if the environmental conditions of the site were not particularly favourable.

The entrance hall of the Zala Cave was in direct communication with the inside at least until the Early Holocene, when the underground flow partially reworked the Mesolithic levels; by the Bronze Age the communication was closed, and the cave was occasionally

flooded through the narrow eastern passage which still connects the entrance chamber to the inner part of the cave.

At present, there is no evidence of cave use by humans between the Mesolithic and the Bronze Age because the corresponding levels (except from maybe few Copper Age pottery fragments; Olujić and Perković, 2015) -if any- were removed by the erosional processes of the river. Nonetheless, it cannot be excluded that levels corresponding to this period may be found in the northernmost part of the entrance hall, upslope the dipping levels and at a higher level above the old river.

Finally, it must be pointed out that the underground river flow must have been much stronger than the present-day one (in fact, before the construction of the Gojak hydropower plant) during the late Late Pleistocene-Early Holocene, as demonstrated by the coarser grain-size of the sediments and by the well-developed lateral accretion deposits. The underground cave system Đulin Ponor - Medvedica Cave - Izvor-Šipilja Gojak may have been affected by periodical strong rainfall in the basin of the Gornja Dobra and Zagorska Mrežnica.

It must be first observed that the anthropogenic component was apparently minor at Zala during the Late Pleistocene and at the beginning of the Holocene, and it can be well identified at present only as hearths and cultural remains included in the sediments deposited by river flow. The sedimentological study indicates that several postdepositional processes affected the archaeological record of Zala Cave. The lower part of the sequence comprising Paleolithic and Mesolithic cultural remains was partially eroded and reworked by *ab antiquo* river flow. Convolutions, injection features and ice wedges indicate strong cryoturbations that most certainly moved the Paleolithic, and Mesolithic finds vertically and horizontally through the sequence during the Late Pleistocene and Early Holocene.

Soil micromorphology provided valuable information about the infilling processes and on-site Bronze Age human activities. This group of units is characterised by three brown anthropogenic layers, alternating with yellow geogenic sediments (fine river sand). During the Bronze Age, the cave was first used for short-term domestic activities, with a shift to seasonal pastoral activities in later stages of the Bronze Age.

6. ZEMUNICA

6.1 Introduction



Figure 6.1 Location map of Zemunica (Šošić Klindžić et al., 2015).

Zemunica Cave is situated in a karstic area, near the village of Bisko, 17 km east of Split (Fig. 6.1). The rescue excavations of the cave (on the route Dugopolje-Bisko of the Adriatic motorway) directed by I. Karavanić, were carried out in 2005 (Šošić and Karavanić, 2006). The sedimentary sequence of Zemunica Cave includes numerous layers containing cultural remains whose age spans from the Late Upper Paleolithic to the Early Bronze Age. Zemunica is one of a few middle dalmatian sites excavated on the Northern side of the Dinaric Alps, and therefore gives valuable information about prehistory in this area (Šošić Klindžić et al., 2015).

6.2 Site presentation

Zemunica Cave is situated at the foot of the Mali Mosor Hills, in Turonian limestones with dolomite lenses, looking onto the Dicmo (Krušvarska or Bisko) karstic polje - a fertile area with dominant *terra rossa* soils. The cave is 16 x 18 m wide (Fig. 6.2), with a maximum height of about 4 m, and there is a natural opening in the middle of its ceiling. The entrance of the cave is situated at the base of a cliff facing northwards. In their report, the excavators mention rocks scattered all over the surface of the cave, therefore they opened a trench (Trench 1) at the very entrance of the cave in order to deepen it for the removal of rocks and sediment (Šošić and Karavanić, 2006). Two more trenches were opened inside the cave, each 3 x 3 m at the top; Trench 2 in squares E-G 18-20, and Trench 3 in squares S-U 17-20. The

thickness of the stratigraphic sequence in Trench 2 is 4.6 m, while in Trench 3 it is about 3 m, but the bedrock was not reached in either of the two trenches (Šošić Klindžić et al., 2015).

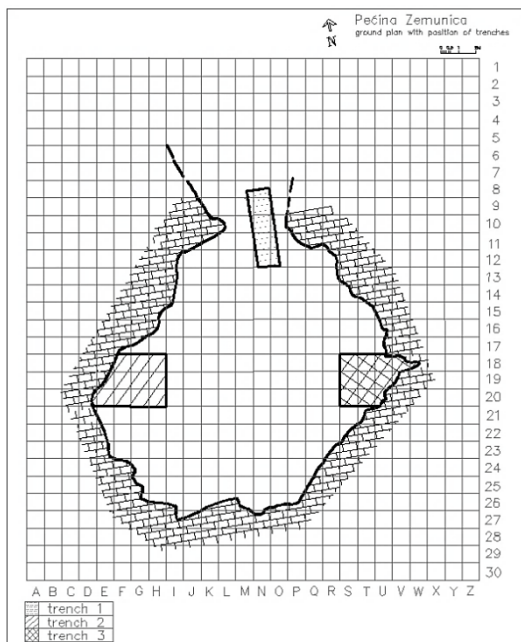


Figure 6.2 Cave plan (Šošić Klindžić et al., 2015).

6.3 Archaeological background

The sedimentary sequence of Zemunica Cave spans from the Late Upper Pleistocene to the early Late Holocene, and includes Late Upper Paleolithic, Mesolithic, Neolithic, Copper Age, and Bronze Age cultural remains. Preliminary results are available only for the Upper Paleolithic, Mesolithic, and Early Neolithic finds, while the study of the Late Neolithic, Copper, and Bronze Age archaeological material is still in progress.

The Late Upper Paleolithic was dated on charcoal to $11,740 \pm 90$ ^{14}C BP (12,110 – 11,490 cal. BC at 2σ ; Beta-218732); the faunal remains (mostly red deer, but also bovids, equids, wild boar, roe deer etc.) fit the Upper Pleistocene period, but the lithic assemblage lacks diagnostic elements. It includes long and wide blades that are not present in later periods in Zemunica (Šošić Klindžić et al., 2015). The Mesolithic levels were dated from $10,000 \pm 70$ ^{14}C BP (9,990–9,270 cal. BC at 2σ ; Beta-218733; charcoal) to $9,310 \pm 60$ BP (8,730 – 8,340 cal. BC at 2σ , Beta-236133; bone). They include abundant snail shells, red deer, roe deer and wild boar, which are typical for the Adriatic Early Mesolithic. The Mesolithic lithic assemblage lacks

diagnostic types; however, it can be placed in the group without trapezes. The lithic industry differs from the Neolithic one, and comprises some Epigravettian elements like backed bladelets and circular endscrapers (Šošić Klindžić et al., 2015). Late Mesolithic levels were not present in the cave. The Early Neolithic (Impressa culture) spans from $7,120 \pm 40$ BP (6,060 – 5,920 cal. BC, 2σ ; Beta-225630; bone) to $6,550 \pm 40$ BP (5600 – 5470 cal. BC, 2σ ; Beta-236134; bone) indicating that more than one phase of the Impressa culture may be present at the site (Šošić Klindžić et al., 2015). The lithic assemblage comprises 143 artefacts, but only eight are tools, mainly retouched pieces, and one backed bladelet. The majority of the Impressa culture pottery shards (74%) is decorated by impression, incision, and application; one pintadera made of clay was also found. Dispersed human remains were also recorded at the site, in Paleolithic, Mesolithic and Neolithic levels. All of the dated human remains are dated around 7,000 14C BP indicating significant level mixing and/or wrong attribution for some of the levels. This problems will be discussed in this section (Šošić Klindžić et al., 2015).

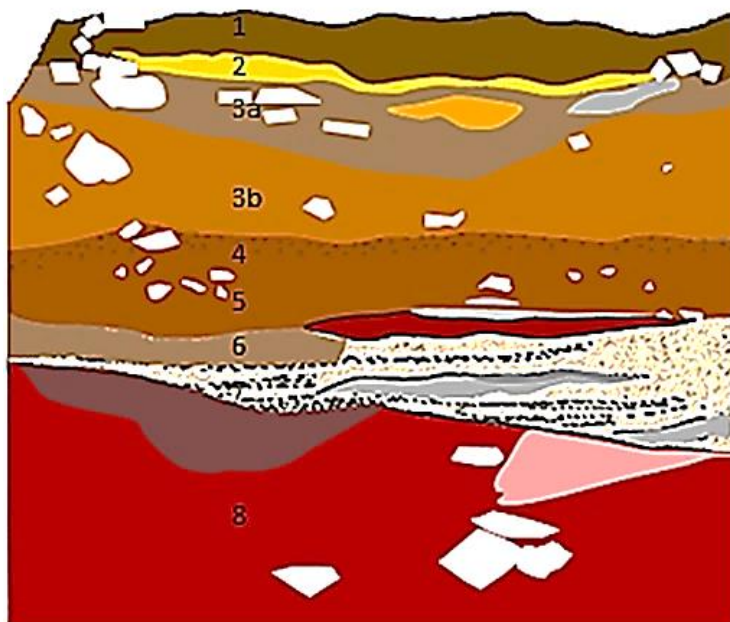


Figure 6.3 Profile V 17-18-19, trench 3a.

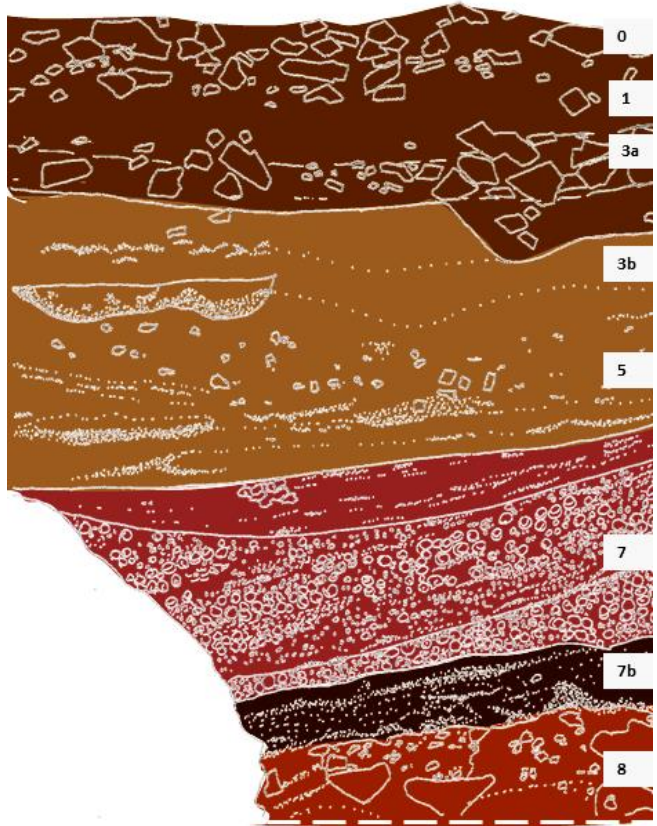


Figure 6.4 Profile S 19-20, trench 3b.

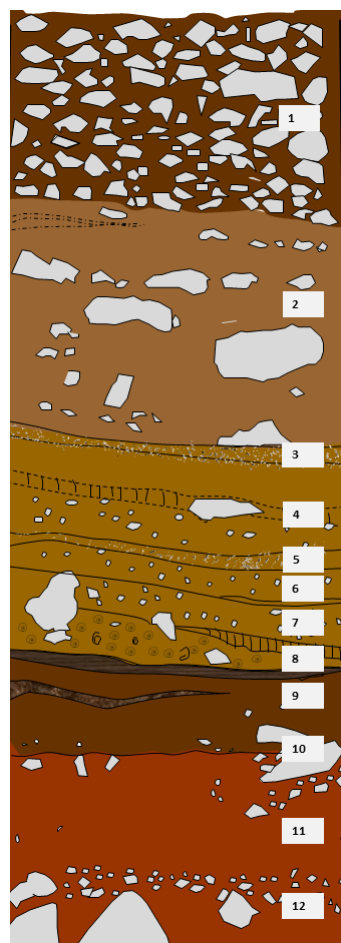


Figure 6.5 Profile G 18-19, trench 2.

6.4 Results

Samples were taken from two trenches (Trench 2 and Trench 3) inside the cave. A total of 24 samples were collected for grain size analyses and 31 samples for micromorphological analysis.

6.4.1 Field observations

The following descriptions of the lithostratigraphic groups are based on the profiles V 17-18-19 (Fig. 6.3) in trench 3a, S 19-20 in trench 3b (Fig. 6.4), and G 18-19 in trench 2 (Fig. 6.5) which were the only profiles available for sampling and studying. The sequences are described from the bottom upwards. The stratigraphic units are classified in archaeological cultures/periods according to the documentation of the excavations; however subsequent geoarchaeological analyses showed that some of the units labelled as Mesolithic based on the lack of pottery, must be attributed to the Neolithic.

Trench 3, profile V 17-18-19:

8. Reddish clay loam, with unsorted subangular to subrounded clasts and blocks (up to 1 m wide) concentrated at the bottom (SU-106/112). Medium developed polyhedral aggregation with Fe coatings on ped surfaces. Some patches of the unit are occasionally cemented. Includes units SU 112, 106, 142. Pleistocene cultural remains or sterile.

7. Greyish and reddish ashy sandy loam layers and lenses, complexely interfingered with the reddish SU 86 in the southern part of the profile. Red pedorelicts and small angular fine to medium-size gravel clasts (1-3 cm) are common. Sharp and erosive boundary, shaping the top of 8. SU 86, 91, 92, 98?, 105, 103. Mesolithic cultural remains.

6. Sandy loam with common small angular fine to medium gravel-size clasts and crushed shells. SU 83, 71?. Mesolithic cultural remains.

5. Light brown silty clay (SU 63), including grey and reddish lenses in the southern part of the profile (SU 64-Neolithic; SU 81, 82-Mesolithic?). Abrupt boundary.

4. Loose greyish brown silty clay loam with frequent fine gravel-size clasts and frequent crushed shells. SU 60; no pottery or lithics.

3b. Brown silty clay with rare medium to fine gravel-size angular clasts. Abrupt boundary, sub-horizontal and slightly undulating. SU 53; Neolithic cultural remains.

3a. Grayish brown silty clay with occasional angular clasts, arranged mostly parallel to the surface (SU 40). Includes an ashy lens (SU 52) and a yellowish wavy clay lens with reddish pedorelicts (SU N/D). Bronze Age cultural remains.

2. Thin layer of yellow clay loam, massive or poorly aggregated. Sharp, undulating boundary. SU 36; Bronze Age cultural remains.

1. Brown silt loam with occasional subangular stones; includes a thin layer of charcoal at the bottom. Fine granular aggregation. Clear boundary, undulating and subhorizontal. SU 35; Bronze Age.

Trench 3, profile S 19-20:

8. Reddish clay loam (SU 106); at the bottom (SU 112), it includes unsorted subangular to subrounded clasts and blocks (up to 1 m). Clear boundary. Pleistocene.

7b. SU 139 can be divided into two parts from a lithological point of view. Dark grayish brown loose silt loam, with angular to subangular medium to coarse-gravel size (5-20 cm), with frequent snail shells, bone fragments and charcoal. Clear to abrupt boundary (lower part of SU 139). Very dark grey silt loam, relatively compact, with very rare, angular fine to medium gravel-size clasts (2-3 cm), reddish pedorelicts and very frequent charcoal fragments (upper part of SU 139). Upper Paleolithic cultural remains.

7. Layers of reddish brown loose sandy silt loam, with abundant crushed land snail shells, alternating with layers of intact snail shells with abundant ash and charcoal. The layers are slightly inclined towards the south. Reddish pedorelicts are common. Clear boundary. SU 135, 134, 115 lower. Mesolithic cultural remains.

5. Grayish brown silty loam layers and ashy lenses. Clear to diffuse boundary. SU 115 upper, 116, 114. Neolithic cultural remains.

3b. Brown compact silty clay with rare angular fine gravel (1-5 cm); includes ash and charcoal lenses. Abrupt boundary, sub-horizontal and slightly undulating. SU 45. Bronze Age cultural remains.

3a. Dark brown silty loam with frequent angular to subangular calcareous rubble (7-30 cm) with a thin yellowish lens at the bottom. Lower part of SU 43. Bronze Age cultural remains.

1. Dark greyish brown silty loam with occasional subangular unsorted stones. Upper part of SU 43. Bronze Age cultural remains.

0. Reworked surface layer. Calcareous rubble (angular to subangular), skeleton-supported structure, with few dark brown silty matrix; poor sorting; abrupt limit. SU 7 upper; Bronze Age/Recent.

Trench 2, profile G 18-19:

12. Large blocks, terminating upwards with unsorted angular to subangular gravel; skeleton-supported; abundant light brown matrix with poorly developed medium granular aggregation. Boundary unobserved. SU 146. Pleistocene.

11. Dark reddish silty loam, with medium developed medium-coarse granular aggregation; very few unsorted angular to subangular skeleton (up to 35 cm), concentrated in clusters; clear evidence of decalcification. Abrupt limit, subhorizontal. SU 143, 136. Pleistocene.

10. Thin level of unsorted stones, fine gravel to blocks; matrix as in 9) (probably a facies of 9). SU 138. Pleistocene.

9. Dark brown silty clay loam, with very few skeleton mostly located at the bottom of the unit, subangular to subrounded, with clear evidence of decalcification. Some very dark brown to blackish subunits are also present, bounded by diffuse limits; the top limit one is particularly evident, with slightly variable thickness. Sharp limit, subhorizontal and smooth. SU 118 (archaeologically sterile layer), SU 122, SU 130. Mesolithic cultural remains.

8. Large-size land snails in dark reddish matrix, darkening downwards. The snails are more commonly broken on the southern side, where the layer is remarkably thinner (trampling?). Sharp sigmoidal limit, subhorizontal. SU 113. Neolithic.

7. Brown silty loam, with well-developed coarse granular aggregation; dominant, skeleton, angular to subangular, made up of unsorted fine to medium gravel (rubble); skeleton-supported structure, sometimes openwork. Common bone and charcoal, occurring throughout the unit. Abrupt limit, gently dipping southwards. At the bottom, there is a loamy lens-like feature, with a dark reddish level underlying a blackish one. Combustion feature?). SU 111, 110; Neolithic.

6. Brown clay or silty clay, massive and sticky; few angular skeleton, unsorted fine to medium gravel, chaotically dispersed; common to very common charcoal. Abrupt limit. This level corresponds to SU 109; Neolithic cultural remains.

5. Silty loam with common very fine angular gravel chaotically dispersed. Concave-upwards sigmoidal level, thickening eastwards; abrupt limit, gently dipping southwards. SU N/D

4. Silty clay loam, not very different from 2); it can be divided into some subunits with diffuse limits; the central one is light brown clay layer with some charcoal and almost no aggregation. SU N/D.

3. Greyish clay loam with common very fine gravel and few coarser elements (up to 10-12 cm) subangular to subrounded, chaotically dispersed. Frequent charcoal and amorphous organic matter. Thin layer (15-20 cm) with clear limit, gently dipping southwards. SU N/D.

2. Brown silty clay loam; it can be divided into several layer-like subunits following colour (darker brown, sometimes reddish) or texture (more or less clay or skeleton); limits between subunits are usually clear to diffuse. Common skeleton, unsorted, subangular to subrounded (due to dissolution). Clear limit, gently dipping southwards. SU N/D.

1. Surface layer. Calcareous rubble, with blocks; skeleton-supported structure, with few matrix (sometimes openwork); poor sorting, with smaller size elements at the bottom, usually well oriented along the unit limit. Sharp limit, probably dipping southwards. SU N/D.

Table 6.1 Sediment colour under wet and dry conditions.

| Sample/ Stratigraphic Unit | Munsell soil color - wet | Munsell soil color - dry |
|---|-----------------------------------|---------------------------------|
| 1/35 | 10 YR 3/3 dark brown | 10 YR 6/4 light yellowish brown |
| 2/40 | 7.5 YR 3/2 dark brown | 10 YR 6/3 pale brown |
| 3/53 | 7.5 YR 3/3 dark brown | 10 YR 6/4 light yellowish brown |
| 4/60 | 10 YR 3/3 dark brown | 10 YR 6/3 pale brown |
| 5/63 | 10 YR 3/4 dark yellowish brown | 10 YR 5/4 yellowish brown |
| 6/83 | 10 YR 3/2 very dark grayish brown | 10 YR 6/3 pale brown |
| 7/92 | 2.5 YR 2.5/4 dark reddish brown | 2.5 YR 3/4 dark reddish brown |
| 8/106 (Trench 3a) | 2.5 YR 3/4 dark reddish brown | 2.5 YR 3/4 dark reddish brown |
| 50/106 (Trench 3b) | 5 YR 5/6 yellowish red | 7.5 YR 6/8 reddish yellow |
| 51/139 lower | 7.5 YR 2.5/2 very dark brown | 10 YR 3/4 dark yellowish brown |
| 52/139 upper | 10 YR 2/2 very dark brown | 10 YR 4/3 brown |
| 53/135 | 7.5 YR 3/3 dark brown | 7.5 5/3 dark brown |
| 54/134 upper | 7.5 YR 2.5/3 very dark brown | 7.5 YR 4/2 brown |
| 55/115 lower | 7.5 YR 2.5/2 very dark brown | 7.5 YR 5/4 brown |
| 56/115 upper | 10 YR 3/3 dark brown | 10 YR 6/3 pale brown |
| 57/114 | 10 YR 4/2 dark grayish brown | 10 YR 5/4 yellowish brown |
| 58/45 | 10 YR 4/2 dark grayish brown | 10 YR 6/4 light yellowish brown |
| 100/12/146 | 10 YR 3/4 dark yellowish brown | 10 YR 5/4 yellowish brown |
| 101/11/136 | 7.5 YR 3/4 dark brown | 7.5 YR 4/4 brown |
| 102/10/138 | 10 YR 3/4 dark yellowish brown | 10 YR 4/6 dark yellowish brown |
| 103/9/122 | 7.5 YR 3/3 dark brown | 10 YR 4/4 dark yellowish brown |
| 105/7/110 lower | 10 YR 3/3 dark brown | 10 YR 5/3 brown |
| 106/7/110 upper | 10 YR 3/3 dark brown | 10 YR 5/3 brown |
| 107/6/109 | 10 YR 3/3 dark brown | 10 YR 5/3 brown |

6.4.2 Architecture of the stratigraphic units and sediment texture

The bedrock was not reached during the excavations in either of the trenches. The lowermost group of excavated units is reddish to yellow-reddish clay loam (SU 106). It can be divided into two parts, the lower part includes unsorted, medium to large-size limestone blocks (SU 112), while the upper one, overlying the large blocks, is less stony or stoneless (SU 142). The top surface of this reddish group of units in trench 3a is an erosional feature which dips southwards. In trench 3b the reddish units occur approximately 1 m deeper than in 3a. Here, the lower part of the large blocks is included in the red sediment, while the upper part emerges into the overlying layers; this indicates strong erosional processes that removed part of the reddish sediment. In trench 3b, SU 139 (Palaeolithic) is overlying the reddish layer 106; SU 139 is a brownish silty loam rich in charcoal and organic matter. The erosional shape at the top of the reddish layer in trench 3a is filled with a lens comprising crushed snails (SU 86), which laterally merges into a sequence of lenses of reworked ash (SU 103 and 91); all are ascribed to the Mesolithic. In trench 3b the Mesolithic units are represented by two stacked land snail shell middens (SU 134 and 135) including aggregates of reddish sediments similar to the sediment of SU 106; the reddish sediment is more abundant at the bottom of each of the snail middens. SU 81 and 82 were also ascribed to the Mesolithic by the excavators, but subsequent micromorphological analysis showed that, from the bottom of this group of units upwards, the sediments are mostly made up of sheep/goat, and cattle dung (see section 6.4.3.). Various groups of ashy lenses overlying relatively thin dark brown, and reddish lenses ascribed to the Neolithic (the overlying lenses SU 64-82-81 from trench 3a may tentatively be correlated with the lenses labelled as SU 116 in trench 3b), Copper, and Bronze Age occur between brown to grayish brown mostly homogeneous layers. The top brownish levels include few cm-thick yellowish lenses which differ from the other sediments of the cave (see section 6.4.3). Almost all of the post-Mesolithic units in Trench 3 are coprogenic, and are made of sheep/goat and possibly cattle dung (see section 6.4.3).

In trench 2, the reddish unit 106 is overlain by brownish to yellowish silty clay loam SU 146, SU 143, SU 136, and SU 138. The bottom of this group of units has few medium- to small-size stones. The upper limit of this group of units is sharp, probably erosional. In trench 2, the sequence includes only one snail midden SU 113, which includes Neolithic cultural remains. According to the excavators, this is the first post-Mesolithic unit in this part of the cave. The boundary between the Mesolithic and Neolithic units is an erosion surface. All of the post-Mesolithic units studied from Trench 2 are made of sheep/goat dung (from SU

110_upper upwards in the sequence), with the exception of the lowermost Neolithic unit 113, and a small lens SU 110_lower, directly overlying SU 113.

Grain size analyses (Fig. 6.6 and 6.7) have been carried out on the fine grained fraction (<2 mm) of the sediments. The sand fraction is more abundant (>28%) in the undecalcified samples of the SU 83 (28.6%), SU 115 lower (33.41%), SU 134 (34.9%), and SU 135 (35.86%). All the sediments with more than 28% sand fraction in undecalcified samples embed Mesolithic cultural remains. The silt fraction in the undecalcified samples is always more than 40% in all of the analysed units, with the exception of SU 106 in trench 3a where it is just slightly minor (39.43%). The clay percentage (>60%) is highest in the decalcified samples from SU 35 (61.73%) and SU 43 (63.45%), followed by SU 83 (54.89%), SU 40 (53.93%) and SU 63 (53.84%). It is noteworthy that all of these units come from Trench 3a, while in units from Trench 3b and Trench 2, the clay percentage is not higher than 29%, except from SU 139 lower (35.77%), and SU 106 (46.76%). The grain sizes of the reddish sediment SU 106 from Trench 3b (6.28% sand, 46.96% silt, 46.76% clay) are very similar to those from SU 106 (2.61% sand, 56.86% silt, 40.54% clay) and SU 92 (1.37% sand, 55.72% silt, 42.92% clay) in Trench 3a. Those units differ from all the other ones, where the sand amount is always higher than 11%. The grain size distribution of units 106 and 92 is in good accordance with the data available for *terra rossa* soil in Croatia. According to Durn et al. (1999) and Durn (2003) *terra rossa* in Istria (Croatia) is composed predominantly of clay and silt sized particles, with sand particles forming less than 4% (the clay content ranges from 32.1 to 77.2%).

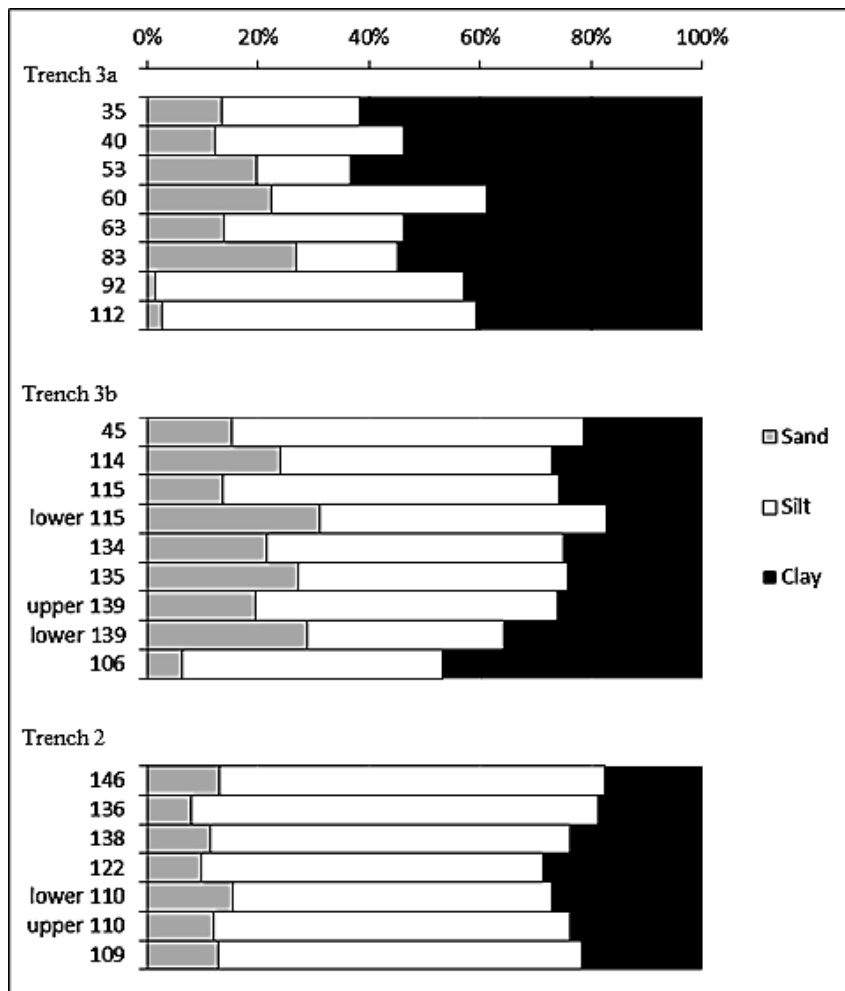


Figure 6.6 Grain-size (Wentworth, 1922) of the <2 mm fraction of decalcified samples.

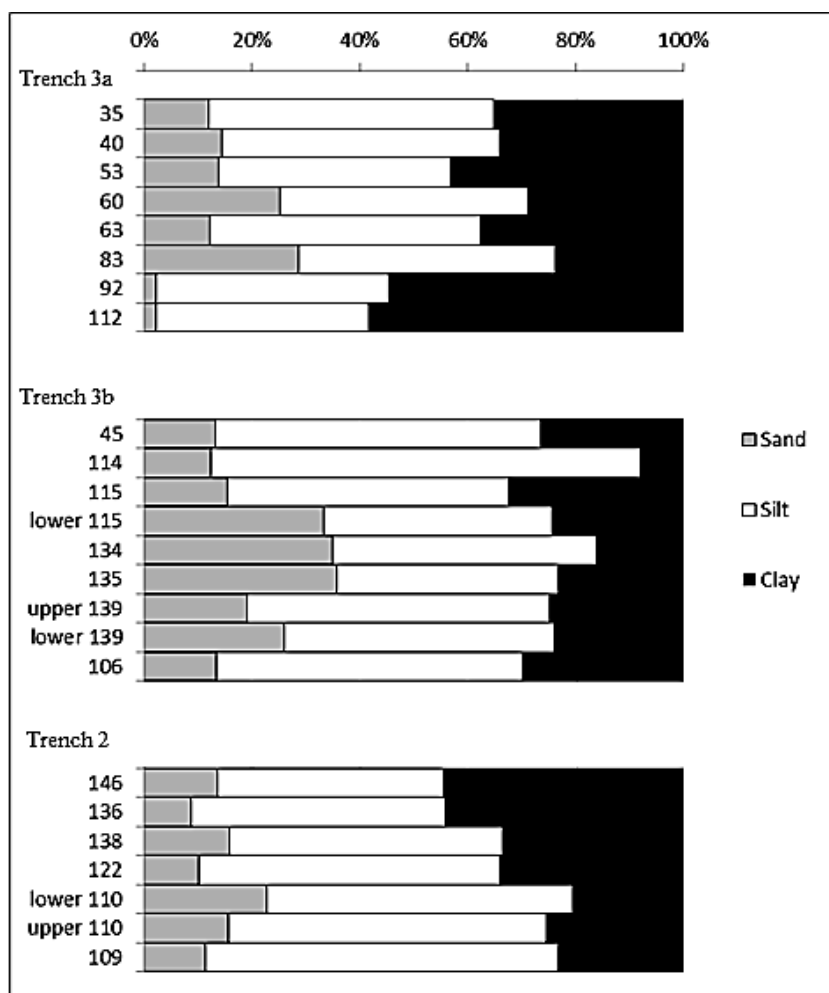


Figure 6.7 Grain-size (Wentworth, 1922) of the <2 mm fraction of undecalcified samples.

6.4.3 Micromorphology



Figure 6.8 Location of the samples for micromorphological analyses: a) SU 106, b) SU 139 lower, c) SU 139 upper, d) SU 135 (134 middle), e) SU 134 (134 upper), f) SU 115 lower, g) SU 115 upper, h) SU 114, i) SU 45, j) SU 43-45, k) SU 116lower-115 upper, l) SU116 upper.

Micromorphological analyses were carried out on 31 thin sections, approximately one per stratigraphic unit visible in the two sampled profiles; in some cases, the samples were collected at the boundary between units. The thin sections were prepared from the undisturbed monoliths of sediment (except from samples ZEM 7/92 and ZEM 8/102 which contain non oriented sediment fragments) collected in 2012, after the end of the excavations, so the same problems concerning the 3D geometry of the units arose in Zemunica, as explained in previous chapters. The main micromorphological characteristics of the sediments are summarised in this chapter. The location of the samples collected from the profile is given in Figure 6.8.

Eleven samples were studied from Trench 3a: Upper Paleolithic SU 112, 142; Mesolithic SU 92, 83/86, 103, 91; Neolithic Impressa culture 81/82/64, Neolithic Hvar culture SU 53; Bronze Age SU 40, 40B-yellow lens inside SU 40, and SU 40/36/35.

Twelve thin sections were analysed from Trench 3a: Upper Paleolithic? SU 106, Upper Paleolithic 139 lower, 139 upper, Mesolithic 135 (sample 134 middle), 134 upper, and 115 lower; Neolithic Impressa SU 115 upper/116, 114, 115, 116 upper; Bronze Age SU 45, and 45/43 .

Eight samples were studied from Trench 2: Paleolithic SU 136, 146, 136/138; Mesolithic SU 122; Sterile SU 118/Neolithic Impressa SU 113, Neolithic Impressa SU 110, and 109/overlying unit.

The most common characteristics of the thin sections are given below.

Trench 3a:

ZEM 7/92

This thin section comprises six unoriented sediment fragments from SU 92. They consist of dusty red clay with common quartz grains and mica flakes. Granostriated b-fabric is surrounding the angular to subangular blocky aggregates. They are often seen as pedorelicts in thin section from many stratigraphic units.

ZEM 8/102

This thin section includes two unoriented sediment fragments from SU 102. Same as ZEM 7/92, but the aggregates are rounded to subrounded and one has a calcitic core.

ZEM 16/142

Red clay aggregates embedded in calcitic groundmas. Red silty clay aggregates are also present, and red clayey aggregates with quartz and muscovite skeleton.

ZEM 15/103

Microstructure and porosity: granular microstructure with vesicles.

Groundmass: c/f-related distribution pattern is open porphyric.

Coarse material:

Rock fragments: few angular limestone fragments.

Minerals: common quartz grains, few muscovite flakes, few feldspars.

Inorganic residues of biological origin: common shell fragments

Anthropogenic elements: very frequent charcoal fragments, dominant calcite aggregates (wood ash)

Organic: burnt tissue

Pedorelicts: red clay aggregates with quartz and mica skeleton.

Micromass: calcitic (ash) and dusty clay.

Pedofeatures: Fe/Mn nodules.

ZEM 14/91

Microstructure and porosity: granular microstructure with vesicles.

Groundmass: c/f-related distribution pattern is open porphyric.

Coarse material:

Rock fragments: few angular limestone fragments.

Minerals: common quartz grains, few muscovite flakes, few feldspars.

Inorganic residues of biological origin: common shell fragments

Anthropogenic elements: very frequent charcoal fragments, dominant calcite aggregates (wood ash)

Organic: burnt tissue

Pedorelicts: red clay aggregates with quartz and mica skeleton.

Micromass: calcitic (ash) and dusty clay.

Pedofeatures: Fe/Mn nodules, ice lenses.

ZEM 12/83-86

This thin section comprises two stratigraphic units – SU 83 and the overlying SU 86. SU 86 has the same micromorphological characteristics as SU 115_lower, but the snail shells are more frequent.

SU 83

Microstructure and porosity: granular microstructure with vesicles.

Groundmass: c/f-related distribution pattern is open porphyric.

Coarse material:

Rock fragments: common subangular limestone fragments.

Minerals: aggregated microsparitic and sparitic calcite.

Inorganic residues of biological origin: frequent shells, bone fragments.

Anthropogenic elements: frequent charcoal fragments.

Organic: few amorphous organic matter.

Pedorelicts: red clay aggregates with quartz and mica skeleton, red silty clay aggregates.

Micromass: dusty clay and fine ash, calcitic crystallitic b-fabric.

Pedofeatures: Fe/Mn nodules.

ZEM 13/64, 82, 81

This thin section comprises units 64, 82, and 81. Stratigraphic unit 81 is made of mostly very well-articulated phytoliths in a micromass with undifferentiated or speckled b-fabric. At the bottom of SU 81, there is a thin dark brown layer mostly made up of herbivore dung; reddish pedorelicts also occur.

SU 64

Stratigraphic unit 64 is a mixture of burnt herbivore dung and burnt plant remains (wood ash, plant tissue).

Microstructure and porosity:

Groundmass: c/f-related distribution pattern is open porphyric.

Coarse material:

Rock fragments: common reddish brown pedorelicts with quartz skeleton, few subangular limestone fragments, very few rounded flint fragments

Minerals: few quartz grains, few muscovite flakes

Inorganic residues of biological origin: very frequent faecal spherulites and phytoliths

Anthropogenic elements: micritic aggregates (ash)

Organic:

Micromass: calcitic crystallitic or undifferentiated b-fabric

Pedofeatures:

ZEM 3/53

Microstructure and porosity: angular blocky and granular microstructure with channels and vughs.

Groundmass: c/f-related distribution pattern is close to double spaced porphyric.

Coarse material:

Rock fragments: common subangular to subrounded flint fragments.

Minerals: frequent angular to subrounded quartz, common feldspars, few muscovite flakes, very few pyroxenes (?), frequent calcite.

Inorganic residues of biological origin: micritic aggregates (burnt plant tissue and cells), dominant faecal spherulites and phytoliths.

Anthropogenic elements: frequent charcoal fragments.

Organic: common amorphous organic matter, punctuations,

Micromass: dusty clay with speckled b-fabric or undifferentiated b-fabric.

Pedofeatures: common clay papulae, Fe/Mn nodules, very few clay coatings

ZEM 10/40A (yellow lens)

Microstructure and porosity: subangular blocky to granular microstructure with channels, chambers and vesicles.

Groundmass: c/f-related distribution pattern is single spaced to open porphyric.

Coarse material:

Rock fragments: none.

Minerals: very frequent angular to subrounded quartz grains, few muscovite flakes

Inorganic residues of biological origin: few spherulites at the bottom of the thin section.

Anthropogenic elements: none.

Organic: none.

Pedorelicts: common almost pure red clay aggregates (very developed), very few reddish aggregates with quartz skeleton.

Micromass: dusty clay with granostriated, porostriated and circular striated b-fabric.

Pedofeatures: clay coatings and infillings, Fe oxides

ZEM 11/40

Microstructure and porosity: (sub)angular blocky to massive microstructure with vughs.

Groundmass: c/f-related distribution pattern is close porphyric.

Coarse material:

Rock fragments: common subrounded flint fragments, few quartz aggregates, few limestone fragments, few pedorelicts.

Minerals: frequent subangular quartz, few feldspars, common calcite, few phosphates

Inorganic residues of biological origin: few bone fragments, dominant faecal spherulites and phytoliths.

Anthropogenic elements: charcoal fragments, micritic aggregates (ash), pottery fragments.

Organic: punctuations, amorphous organic matter.

Micromass: dusty clay with calcitic crystallithic b-fabric.

Pedofeatures: few Fe/Mn nodules and intercalations, few clay papulae.

ZEM 9/36

This thin section consists of three stratigraphic units – SU 35, SU 36, and SU 40 (SU 40 was described in sample ZEM 11/40B).

1) SU 35

Microstructure and porosity: angular blocky to massive microstructure with vughs.

Groundmass: c/f-related distribution pattern is close to single spaced porphyric.

Coarse material:

Rock fragments: very few subangular flint fragments.

Minerals: common angular to subangular quartz grains and quartz aggregates, common sparitic calcite, very few muscovite flakes.

Inorganic residues of biological origin: dominant faecal spherulites and phytoliths.

Anthropogenic elements: charcoal fragments (discontinuous layer at the bottom of the unit and common though the unit), micritic aggregates (ash).

Organic: common amorphous organic matter and punctuations.

Micromass: dusty clay.

Pedofeatures: common clay papulae, common matrix intercalations, Fe/Mn nodules.

1) SU 36

Microstructure and porosity: angular blocky to massive microstructure with vughs.

Groundmass: c/f-related distribution pattern is open porphyric.

Coarse material:

Rock fragments: few limestone fragments, few pedorelicts.

Minerals: common muscovite flakes, common angular to subangular quartz, common sparitic calcite, few phosphates.

Inorganic residues of biological origin: few articulated phytoliths.

Anthropogenic elements: -.

Organic: -.

Micromass: dusty clay with speckled b-fabric.

Pedofeatures: common Fe/Mn nodules, hypocoatings and quasicoatings, few clay papulae.

Trench 3b:

ZEM 50/106

Microstructure and porosity: lenticular and granular microstructure with vesicles and channels.

Groundmass: c/f-related distribution pattern is open porphyric.

Coarse material:

Rock fragments: frequent angular to subrounded limestone fragments (often in vertical position).

Minerals: common angular to subangular quartz grains, common sparitic calcite, few muscovite flakes.

Inorganic residues of biological origin: few shell fragments.

Anthropogenic elements: none.

Organic: few tissue and amorphous organic matter.

Pedorelicts: aggregates of pure dusty red clay.

Micromass: dusty clay with calcitic crystallitic and granostriated b-fabric.

Pedofeatures: ice lenses, concentric calcitic nodules, clay papules, Fe/Mn nodules, calcite coatings

ZEM 51/139 lower

Microstructure and porosity: granular microstructure.

Groundmass: c/f-related distribution pattern is close to open porphyric.

Coarse material:

Rock fragments: few angular flint fragments, common subangular limestone fragments.

Minerals: few phosphates (possible carnivore coprolites), common quartz grains, few feldspars, few muscovite flakes.

Inorganic residues of biological origin: very frequent bone fragments.

Anthropogenic elements: frequent charcoal fragments.

Organic: amorphous organic matter.

Pedorelicts: red clay aggregates with quartz and mica skeleton, red silty clay aggregates.

Micromass: dusty clay with stipple speckled b-fabric.

Pedofeatures: clay papules.

ZEM 54/139 upper

Microstructure and porosity: granular microstructure.

Groundmass: c/f-related distribution pattern is close to open porphyric.

Coarse material:

Rock fragments: few angular flint fragments, very few subangular limestone fragments.

Minerals: few phosphates (possible carnivore coprolites), common quartz grains, few feldspars, few muscovite flakes.

Inorganic residues of biological origin: very frequent bone fragments.

Anthropogenic elements: very frequent charcoal fragments.

Organic: very frequent tissue and amorphous organic matter.

Pedorelicts: red clay aggregates with quartz and mica skeleton, red silty clay aggregates.

Micromass: dusty clay with stipple speckled b-fabric.

Pedofeatures: clay papules, Fe/Mn oxides.

ZEM 52/134 upper

Microstructure and porosity: granular microstructure with vesicles.

Groundmass: c/f-related distribution pattern is open porphyric.

Coarse material:

Rock fragments:

Minerals: few phosphates, common quartz grains, few muscovite flakes.

Inorganic residues of biological origin: frequent shell fragments

Anthropogenic elements: frequent charcoal fragments

Organic: amorphous organic matter

Pedorelicts: red clay aggregates with quartz and mica skeleton, red silty clay aggregates.

Micromass: ash and dusty clay, calcitic crystallitic b-fabric

Pedofeatures: clay papules, Fe/Mn oxides.

ZEM 53/134 middle

Microstructure and porosity: granular and lenticular microstructure.

Groundmass: c/f-related distribution pattern is open porphyric.

Coarse material:

Rock fragments:

Minerals: few phosphates, common quartz grains, few muscovite flakes.

Inorganic residues of biological origin: frequent shell fragments.

Anthropogenic elements: frequent charcoal fragments.

Organic: amorphous organic matter.

Pedorelicts: red clay aggregates with quartz and mica skeleton, red silty clay aggregates.

Micromass: ash and dusty clay, calcitic crystallitic b-fabric

Pedofeatures: clay papules, Fe/Mn oxides.

ZEM 55/115 lower

Microstructure and porosity: fine granular microstructure.

Groundmass: c/f-related distribution pattern is open porphyric.

Coarse material:

Rock fragments:

Minerals: few phosphates, common quartz grains, few muscovite flakes.

Inorganic residues of biological origin: frequent shell fragments

Anthropogenic elements: frequent charcoal fragments

Organic: amorphous organic matter

Pedorelicts: red clay aggregates with quartz and mica skeleton, red silty clay aggregates.

Micromass: ash and dusty clay, calcitic crystallitic b-fabric

Pedofeatures: clay papules, Fe/Mn oxides.

ZEM 60/115, 116

SU 115 upper

Microstructure and porosity: fluid with vesicles.

Groundmass: c/f-related distribution pattern is close porphyric.

Coarse material:

Rock fragments: few rounded flint fragments.

Minerals: few quartz grains.

Inorganic residues of biological origin: dominant spherulites, frequent phytoliths, few shells, few bone fragments.

Anthropogenic elements: frequent charcoal fragments, wood ash.

Organic: very frequent tissue and amorphous organic matter.

Micromass: ash.

Pedofeatures: clay papules.

ZEM 61/116 upper

The thin section comprises two microfacies. Microfacies 1 consists of a completely burnt, whitish unit, while microfacies 2 is made of partially burnt dark brown material.

Microstructure and porosity: fluid with vesicles.

Groundmass: c/f-related distribution pattern is close porphyric.

Coarse material:

Rock fragments: few rounded flint fragments, few angular to subangular limestone fragments.

Minerals: few quartz grains.

Inorganic residues of biological origin: dominant spherulites, frequent phytoliths, few shells, few bone fragments.

Anthropogenic elements: frequent charcoal fragments, wood ash.

Organic: very frequent tissue and amorphous organic matter.

Micromass: ash.

Pedofeatures: clay papules.

ZEM 56/115

Microstructure and porosity: highly to medium separated subangular blocky microstructure, and granular microstructure with channels and chambers.

Groundmass: c/f-related distribution pattern is porphyric.

Coarse material:

Rock fragments: few subrounded limestone fragments, very few angular to subangular flint fragments.

Minerals: common subangular to subrounded quartz grains, common subangular calcite, few feldspars.

Inorganic residues of biological origin: dominant faecal spherulites, very frequent phytoliths (frequent articulated), common bone fragments (including burnt bone), few shell fragments.

Anthropogenic elements: very few pottery fragments, common charcoal fragments, common fine micritic aggregates (ash).

Organic: frequent amorphous organic matter.

Micromass: yellowish dusty clay with calcitic crystallitic b-fabric or undifferentiated b-fabric.

Pedofeatures: common Fe hypocoatings and quasicoatings, common weakly impregnated orthic Fe nodules and aggregates, few clay papules, few anorthic Fe nodules (few concentric).

ZEM 57/114

Microstructure and porosity: massive microstructure with planes, vesicles and chambers.

Groundmass: c/f-related distribution pattern is single spaced to close porphyric.

Coarse material:

Rock fragments: common angular to subrounded flint fragments few subangular limestone fragments.

Minerals: common angular calcite, very few pyroxenes, few rounded quartz aggregates, common subangular quartz grains, few subangular feldspars, few muscovite flakes.

Inorganic residues of biological origin: dominant faecal spherulites, very frequent phytoliths, very few bone fragments, very few shell fragments.

Anthropogenic elements: frequent charcoal fragments, common fine micritic aggregates (ash).

Organic: frequent amorphous organic matter, punctuations.

Micromass: yellowish dusty clay with calcitic crystallitic b-fabric.

Pedofeatures: common weakly impregnated orthic Fe nodules and aggregates, few clay papules, few anorthic Fe nodules.

ZEM 58/45

Microstructure and porosity: weakly to highly separated angular to subangular blocky microstructure.

Groundmass: c/f-related distribution pattern is single spaced to close porphyric.

Coarse material:

Rock fragments: common subangular to subrounded flint fragments, few subangular limestone fragments.

Minerals: common subangular to subrounded quartz grains, common muscovite flakes, few angular calcite, few angular feldspars, few pyroxenes.

Inorganic residues of biological origin: very frequent phytoliths, dominant faecal spherulites, common bone fragments (including few burnt bone fragments).

Anthropogenic elements: frequent micritic aggregates (ash), common charcoal fragments, very few pottery fragments.

Organic: common amorphous organic matter.

Micromass: yellowish dusty clay with calcitic crystallitic b-fabric.

Pedofeatures: common clay papules, common orthic Fe/Mn nodules.

ZEM 59/43-45

The thin section ZEM 59 comprises the brownish SU 43 which has at the bottom a thin discontinuous yellowish lense, and SU 45. SU 45 is described in sample ZEM 58/45.

Microstructure and porosity: weakly developed subangular blocky microstructure with vesicles; granular at the bottom of SU 43.

Groundmass: c/f-related distribution pattern is double spaced porphyric; double spaced fine enaulic at the bottom of SU 43.

Coarse material:

Rock fragments: few subrounded limestone fragments, very few subangular to rounded flint fragments.

Minerals: common subangular to subrounded quartz fragments; common subangular feldspars; common angular calcite fragments; few muscovite flakes; few pyroxenes.

Inorganic residues of biological origin: very frequent phytoliths, dominant faecal spherulites.

Anthropogenic elements: common micritic aggregates (ash), common charcoal fragments.

Organic: common tissue and amorphous organic matter.

Pedorelict: few reddish-brown pedorelicts.

Micromass: grayish brown micromass with calcitic crystallitic b-fabric; strial and granostriated b-fabric at the bottom of SU 43.

Pedofeatures: common clay papules, very few clay concentric nodules.

Trench 2:

ZEM 12/100/12 (SU 146)

Microstructure and porosity: massive to channel microstructure.

Groundmass: c/f-related distribution pattern is single spaced to open porphyric

Coarse material:

Rock fragments: common angular to subangular limestone fragments, common subangular to rounded flint fragments.

Minerals: common angular sparitic calcite, frequent angular to subrounded quartz grains, common pyroxenes, frequent muscovite flakes, common phosphates.

Inorganic residues of biological origin: frequent bone fragments

Anthropogenic elements:

Organic:

Pedorelicts: aggregates of pure red clay.

Micromass: dusty clay with granostriated b-fabric.

Pedofeatures: clay papules, Fe /Mn nodules

ZEM 12/101/11 (SU 136)

Microstructure and porosity: lenticular, subangular blocky and granular microstructure with vesicles, channels and chambers.

Groundmass: c/f-related distribution pattern is open porphyric.

Coarse material:

Rock fragments: few very altered (phosphatized) limestone fragments, few rounded flint fragments.

Minerals: very frequent quartz grains, very frequent muscovite flakes, few spatic calcite, few pyroxenes.

Inorganic residues of biological origin: few bone fragments

Anthropogenic elements: few charcoal fragments.

Organic:

Micromass: dusty clay with granostriated and porostriated b-fabric.

Pedofeatures: ice lenses, clay papules, Fe /Mn nodules, clay coatings.

ZEM 12/102/11-10 (SU 130 and SU 138)

SU 130

Microstructure and porosity: subangular blocky to granular microstructure with channels

Groundmass: c/f-related distribution pattern is single spaced to open porphyric.

Coarse material:

Rock fragments: common subangular to rounded limestone fragments (few altered-phosphatized), common angular to rounded flint fragments.

Minerals: common sparitic calcite, frequent quartz grains, frequent muscovite flakes

Inorganic residues of biological origin: frequent bone fragments (including burnt bone).

Anthropogenic elements: very frequent charcoal fragments.

Organic: frequent tissue and amorphous organic matter.

Pedorelicts: red clay aggregates with quartz skeleton, aggregates of yellowish clay with heterogeneous skeleton.

Micromass: dusty clay with granostriated b-fabric.

Pedofeatures: clay papules, fragment of clay coatings, clay infillins.

SU 138

Microstructure and porosity: moderately to weakly developed granular microstructure.

Groundmass: c/f-related distribution pattern is open porphyric.

Coarse material:

Rock fragments: common subangular limestone fragments, common subangular to subrounded flint fragments.

Minerals: frequent quartz grains, few pyroxenes.

Inorganic residues of biological origin: frequent bone fragments.

Anthropogenic elements: frequent charcoal fragments.

Organic: frequent tissue and amorphous organic matter.

Micromass: grano and porostriated b-fabric

Pedofeatures: clay coatings, Fe /Mn nodules, clay papules.

ZEM 12/103/9 (SU 122)

Microstructure and porosity: angular to subangular blocky with channels and chambers.

Groundmass: c/f-related distribution pattern is open porphyric.

Coarse material:

Rock fragments: few rounded flints.

Minerals: frequent angular to rounded quartz grains,

Inorganic residues of biological origin: few spherulites aggregates (fragments of sheep/goat dung).

Anthropogenic elements: very frequent charcoal fragments.

Organic: tissue and amorphous organic matter.

Pedorelicts: reddish pedorelicts with quartz skeleton.

Micromass: dusty clay with granostriated b-fabric.

Pedofeatures: few infillings of spherulites, rolling pedofeatures, clay papules

ZEM 12/104/8 (SU 113 and 118)

Su 118 is composed of mainly organic matter (mostly amorphous and tissue) with few quartz grains and muscovite.

SU 113

Microstructure and porosity: subangular blocky to angular.

Groundmass: c/f-related distribution pattern is open porphyric.

Coarse material:

Rock fragments: few subangular limestone fragments, few angular flint fragments.

Minerals: common angular to subrounded quartz grains, few pyroxenes, common muscovite flakes, phosphates.

Inorganic residues of biological origin: very frequent shell fragments, few spherulites

Anthropogenic elements: frequent charcoal fragments, micritic aggregates (ash).

Organic: amorphous organic matter.

Pedorelicts: red and reddish brown clay aggregates with quartz skeleton, yellowish dusty clay aggregates.

Micromass: dusty clay with calcitic crystallithic and granostriated b-fabric.

Pedofeatures: rolling pedofeatures, clay papules, clay coatings, Fe/Mn nodules (including concentric nodules).

ZEM 12/105/7

Microstructure and porosity: vugly microstructure.

Groundmass: c/f-related distribution pattern is single spaced to open porphyric.

Coarse material:

Rock fragments: few angular flint fragments, common rounded flint fragments.

Minerals: frequent angular to subrounded quartz fragments, few muscovite flakes, micritic aggregates, few angular sparite.

Inorganic residues of biological origin: frequent bone fragments.

Anthropogenic elements: very frequent charcoal fragments, pottery fragments.

Organic: common tissue, frequent amorphous organic matter.

Pedorelicts: red and reddish brown dusty clay aggregates with quartz and muscovite skeleton.

Micromass: dusty clay with undifferentiated b-fabric.

Pedofeatures: rolling pedofeatures, calcite coatings and infillings, clay papules, Fe/Mn nodules

ZEM 12/106/7

Microstructure and porosity: (sub)angular blocky to massive microstructure with vughs.

Groundmass: c/f-related distribution pattern is close porphyric.

Coarse material:

Rock fragments: common subrounded flint fragments, few quartz aggregates, few angular limestone fragments.

Minerals: frequent subangular quartz, few feldspars, common calcite, few phosphates

Inorganic residues of biological origin: few bone fragments, dominant faecal spherulites and phytoliths, few eggshells.

Anthropogenic elements: charcoal fragments, micritic aggregates (ash), pottery fragments.

Organic: punctuations, amorphous organic matter.

Pedorelicts: red dusty clay aggregates with quartz skeleton.

Micromass: dusty clay with calcitic crystallithic b-fabric.

Pedofeatures: few Fe/Mn nodules and intercalations, few clay papulae.

ZEM 12/107/6-5 (SU 109 and overlying unit)

Microstructure and porosity: angular blocky to massive microstructure with vughs.

Groundmass: c/f-related distribution pattern is close porphyric.

Coarse material:

Rock fragments: common subrounded flint fragments, few quartz aggregates, few limestone fragments, few pedorelicts.

Minerals: frequent subangular quartz, few feldspars, common calcite, few phosphates

Inorganic residues of biological origin: few bone fragments, dominant faecal spherulites and phytoliths.

Anthropogenic elements: charcoal fragments, micritic aggregates (ash).

Organic: punctuations, amorphous organic matter.

Micromass: dusty clay with calcitic crystallithic b-fabric.

Pedofeatures: few Fe/Mn nodules and intercalations, few clay papulae.

6.5. Discussion

The grain-size distribution and micromorphological analyses indicate different processes in the deposition of the fine fraction through time.

Paleolithic layers

In trench 3a, the top surface of the lowest group of reddish units (SU 112) is clearly an erosional feature that dips southwards, putting into contact two different sedimentary environments. This reddish unit is probably the colluvium deriving from strongly developed *terra rossa* soils deposited previously outside the cave. The large limestone blocks most probably derive from ceiling breakdown caused by strong cryoturbation. The erosional processes removed the fine component of the sediment, while the large blocks were left in place, with their bottom still included in the red sediment and the top protruding into the overlying levels. At microscopic scale, ice lensing was observed in these levels, indicating deep seasonal frost. In trench 3, mostly in 3b, the sequence directly overlying the gap is made up of levels that plunge into the erosional shape and tend to fill up its depressions. SU 139 is a brownish silty loam including common charcoal, organic matter and bone; it is a domestic waste deposit. Reddish pedorelicts deriving from the underlying levels indicate some reworking (Fig. 6.10). The yellowish unit 142 resembles very closely a loess at eye- and microscopic scale, and may have been deposited in an aridic phase preceding the Mesolithic (Šošić Klindžić et al., 2015).

Mesolithic layers

In trench 3b there is a sequence of two snail middens (SU 134, 135) including reddish sediments resembling the bottom Pleistocene unit, but with some evidence of fine layering or lamination; within each of the shell accumulation levels, the quantity of reddish sediment, which is dominant at the base of the level, decreases upwards. Aggregates of reddish sediment occur also within the middens, and can be easily identified at microscopic scale as pedorelicts deriving from the dismantling of the lowermost reddish units (Fig. 6.9). Here, depositional and erosional processes were continuously alternating, suggesting a phase of relatively strong runoff connected to increased rainfall. This suggests that the anthropic snail accumulations were also somewhat reworked, probably seasonally, by natural erosional processes (Šošić Klindžić et al., 2015). Other Mesolithic units include common charcoal, ashes and bones and are mostly comprised of domestic waste deposits.

Early Bronze Age to Neolithic layers

Almost all of the post-Mesolithic layers are coprogenic and include herbivore dung (sheep/goat/ possibly cattle). In trench 3a the first indicator of stabling is an *in situ* burnt stable layer (the group of SU 64-82-81); it includes a group of greyish ash accumulations with burnt dropping and phytoliths, overlying a dark brown layer of burnt droppings rich in fine organic matter, and a rubefied layer with frequent articulated phytoliths which indicate the presence of a litter, possibly straw spread as bedding for the animals. Based on the absence of pottery, SU 82 and 81 were ascribed to the Mesolithic by the excavators. Micromorphological analysis demonstrates that they should be included in the Neolithic sequence, as integral part of the group of units 64-82-81. This group of units resembles the Neolithic burnt stable layer 116 in trench 3b. Another possible *fumier* lies between units 114 and 45. The other Neolithic (SU 53, 115B, 114, 45) to Bronze Age (SU 40, 43) layers are brown to grayish brown and homogeneous, with spherulites and phytoliths dispersed in the groundmass. An accumulation of incompletely burnt or unburnt herbivore dung is a possible explanation for the difference between the “classical *fumier*” and these layers. The top of the sequence of trench 3 includes yellowish silty clay; at microscopic scale it is made up of an almost pure sediment rich in white mica, very fine quartz, and articulated phytoliths - an intentional accumulation of selected material, a possible prepared surface/floor (Fig. 6.11).

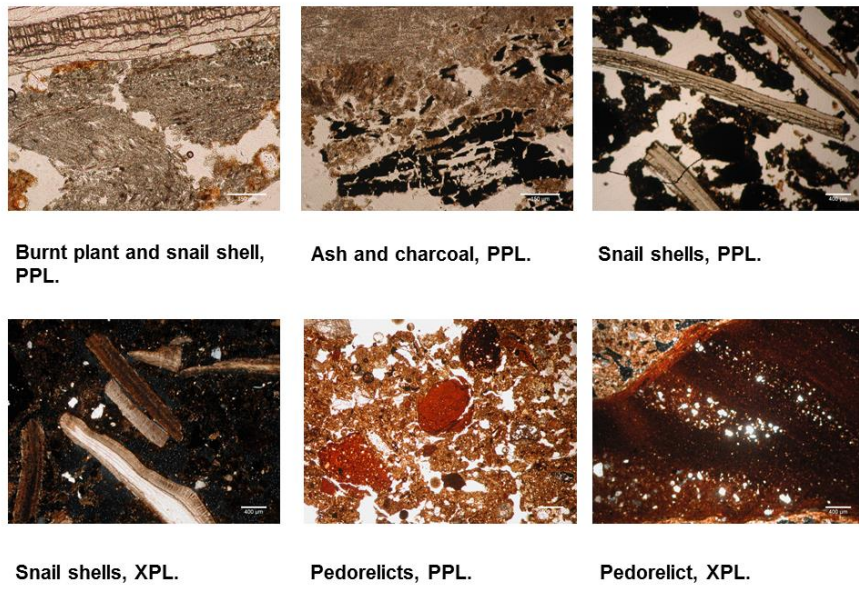


Figure 6.9 SU 134 microphotographs.

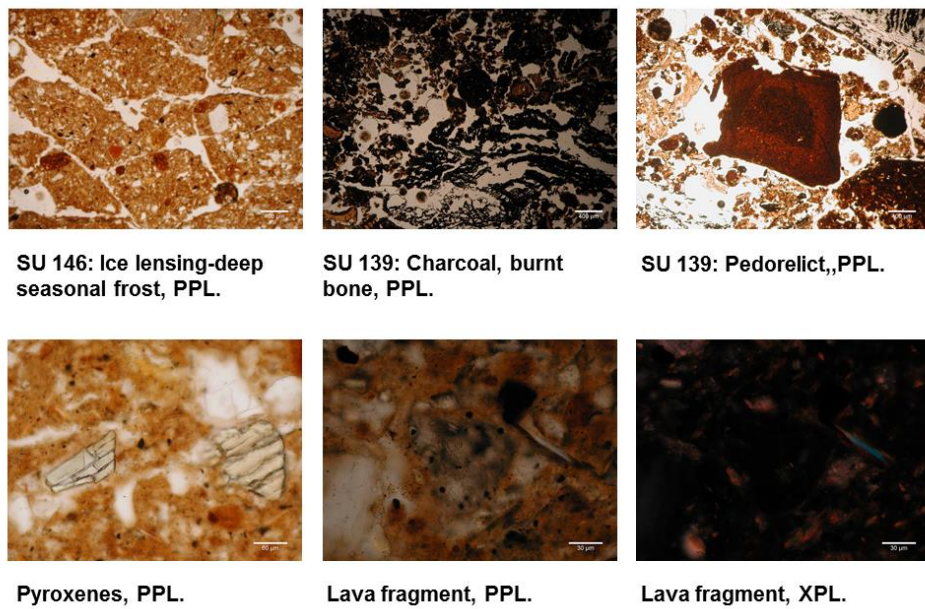


Figure 6.10 Palaeolithic levels microphotographs; possible tephra (bottom row).

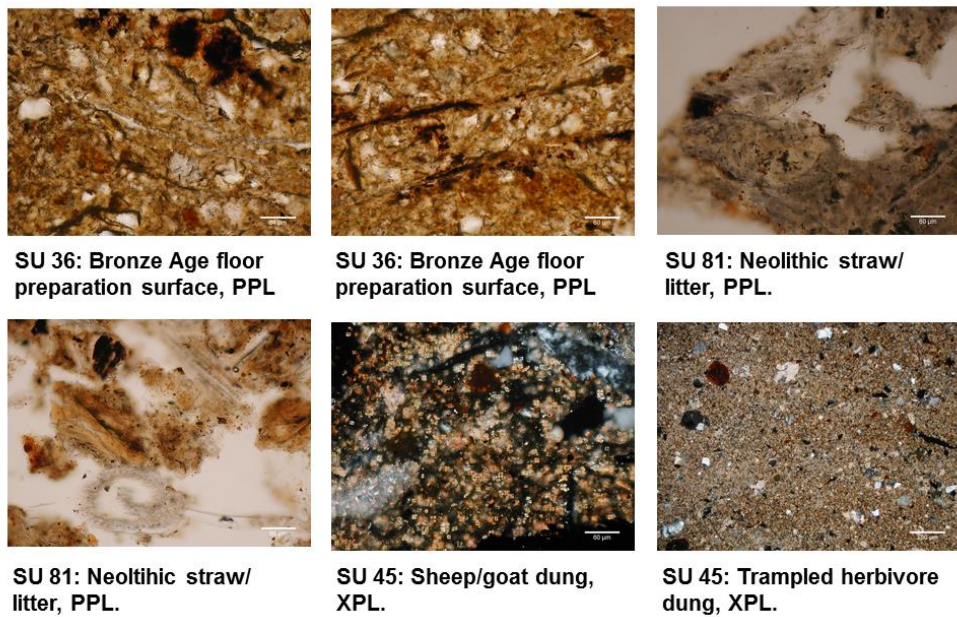


Figure 6.11 Microphotographs of Neolithic and Bronze Age levels.

6.6 Concluding remarks

Geoarchaeological studies indicate strong postdepositional processes, particularly in the lower part of the sequence (Paleolithic-Mesolithic). These processes include reworking and mixing due to erosional processes, cryoturbation, and some hiatuses. Trampling by animals, connected to stabling activities inside the cave, was also observed.

Different use of the cave by humans was confirmed. At Zemunica the Late Upper Palaeolithic levels consist largely of domestic waste residues indicating more intensive frequentation compared to the other studied Paleolithic caves.

The Mesolithic levels mostly comprise domestic waste deposits, including ash, bone fragments and more or less crushed land snails. In the area of Trench 3b, the sequence of thick layers dominated by colluviated land snails and terra rossa pedorelicts probably indicates cyclical reworking of anthropic snail middens by natural erosional processes. The upper part of the Mesolithic sequence may have been affected by Neolithic sheep/goat/cattle trampling.

The Neolithic, Copper, and Bronze Age part of the sequence is characterised by continuous evidence of sheep/goat and probably cattle dung accumulations: *in situ* burnt stable layers – *fumiers* and homogeneous layers – accumulations of incompletely burnt or unburnt herbivore dung. Articulated phytoliths also occur within the cave sediments, indicating the use of straw/litter for these animals.

Micromorphological analyses showed that some of the units labelled as Mesolithic based on the lack of pottery, due to the presence of sheep and possibly goat and cattle dung must be attributed to the Neolithic.

The top of the Bronze Age sequence of trench 3 includes almost pure yellowish sediment with articulated phytoliths - an intentional accumulation of selected material, a possible prepared surface/floor.

7. ROMUALDOVA PEĆINA

7.1 Introduction

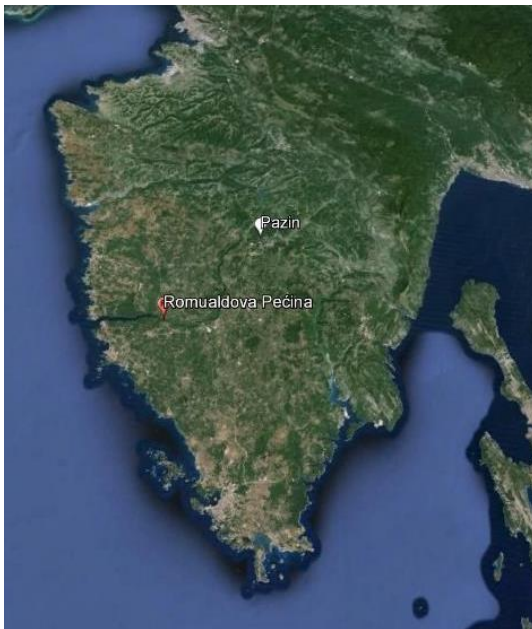


Figure 7.1 Location of Romualdova Pećina (Google Earth).

Romualdova Pećina is situated in Istria (northern Adriatic), on the southern side of the 10 km long Lim Bay (Fig. 7.1).

Although the cave was known since the 16th century, the first investigations conducted by Marchesetti, Gnirs, and Malez date to the late 19th and the 20th centuries (Komšo, 2011). M. Malez excavated the cave systematically in the 1960s and 1970s, when he documented Pleistocene sediments including Upper Paleolithic cultural remains, and Holocene layers with pottery fragments which he ascribed to the Bronze and Iron Age (Malez, 1968; Malez, 1986; Komšo, 2008).

The excavations were resumed in 2006-2008 by D. Komšo (Komšo, 2008; Komšo, 2009), and brought into light a sedimentary sequence including layers containing Middle Paleolithic (Mousterian), Upper Paleolithic, and Bronze Age cultural remains (D. Komšo, 2008; D. Komšo, 2011).²

² In 2014, I. Janković started new investigations in the cave, starting a new trench closer to the cave entrance; these excavations are still in progress and will not be discussed in this thesis.

7.2 Site presentation

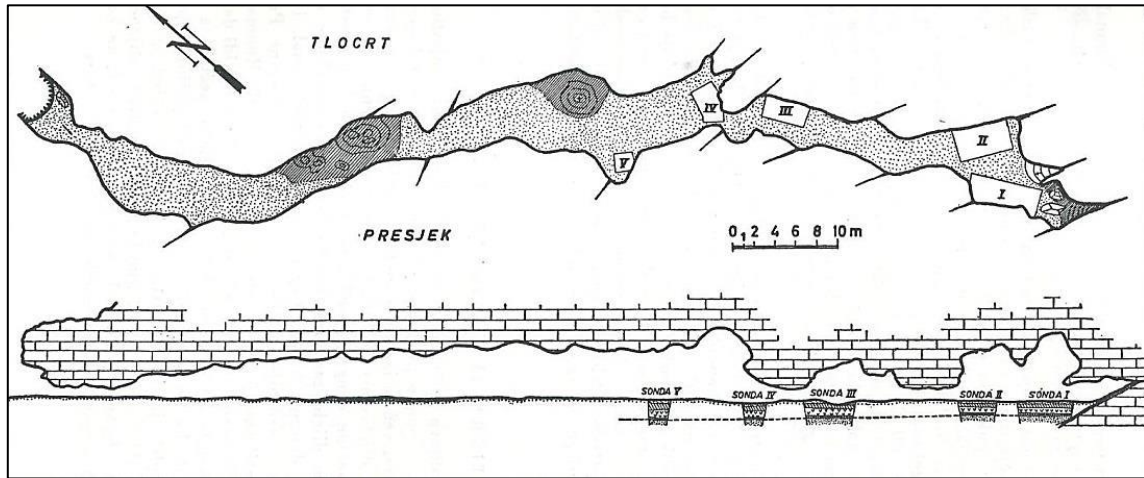


Figure 7.2 Plan and profile of Romualdova Pećina (Malez 1968).

Romualdova Pećina is situated on the southern side of the 10 km long Lim Bay, which is the continuation of the 31 km long Limska Draga karst valley of the river Pazinčica, which springs in a flysch area. The course of the river was stopped in the past by the elevated flysch hills, and directed to the canyon of the present Pazin ponor at the border between flysch and limestone.

Romualdova Pećina is located on the easternmost part of the bay; the entrance to the cave, facing north, is at about 120 m above sea level. The cave is 105 m long; it consists of a corridor which extends in some places into small halls (the widest is cca. 8 m.) (Fig. 7.2). The entrance to the cave is shaped as a rockshelter, with a semi-circular vault, carved in Upper Jurassic thick-bedded limestone. The thickness of the limestone beds varies from 40 cm to over 1 m, and the beds are almost horizontal. The genesis of the cave was controlled by the main direction of the vertical parallel diaclases, which is NW-SE. Speleothems can be seen in some locations of the cave, the most developed ones are located in the largest hall of the cave. A thick flowstone developed along a fissure at the end of the cave (Malez, 1968).

7.3. Archaeological background

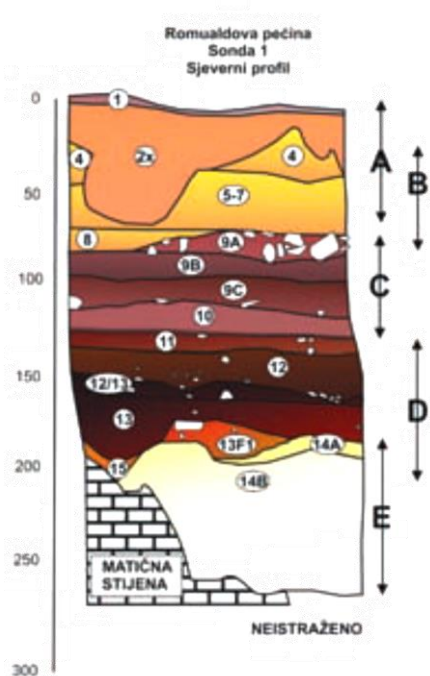


Figure 7.3 Stratigraphic profile of Romualdova Pećina (Komšo, 2008).

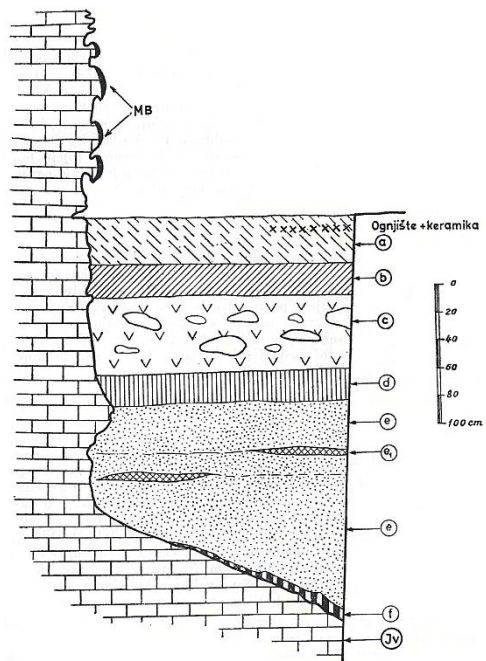


Figure 7.4 Stratigraphic profile of Romualdova Pećina (Malez, 1968).

The sedimentary sequence (Fig. 7.3, Fig. 7.4) of Romualdova Pećina includes Middle Paleolithic, Upper Paleolithic, Bronze and Iron Age cultural remains (Malez, 1968; Komšo, 2011). Unfortunately, absolute dates have not been published yet, and the archaeological materials from the 2007 – 2008 excavations are still under study. A total of 15 layers and some evident disturbances were excavated in Trench 1/2007-8 (sampled for geoarchaeological analysis), which is located in the entrance room of the cave. These layers were grouped into five horizons A – E upon their lithologic characteristics and cultural remain content; the grouping generally resembles the division done by Malez during his excavations in the 1960s and 1970s, however it differs somewhat from it because horizon D includes Middle Palaeolithic remains that had not been previously found (Komšo, 2011). Malez excavated all his trenches only down to the bottom of horizon C, reaching the bedrock only in one trench in the bottom area of the cave (Trench 1/1960s), and did not record any Middle Paleolithic finds. M. Malez marked layer 10 as a separate horizon D, while Komšo included it in his horizon C and ascribed it to the Upper Paleolithic (Komšo, 2008; Komšo, 2011).

Horizon E overlying the limestone bedrock and it includes layers 15, 14A and 14B. A few flint artefacts were collected at the contact with horizon D, from which they probably

migrated due to postdepositional disturbance processes. This horizon corresponds exactly to Malez horizons E and F, and must be contemporary with or predate the Middle Paleolithic (Komšo, 2008; Komšo, 2011).

Horizon D, consists of layers 11, 12 and 13, and was ascribed to the Middle Paleolithic by D. Komšo. In Trench 1/2007-8, numerous Pleistocene fauna, 32 flint artefacts (mostly tools) and a pebble used as hammer for flint knapping were recorded in horizon D. The same horizon in Trench 2/2008 (located opposit to trench 1/2007-8) yielded 36 flint artefacts, but only few of them were tools; a small fireplace was also recorded (Komšo, 2008; Komšo, 2011).

Horizon C comprises layers 9A, 9B, 9C and 10. Relatively numerous remains of Pleistocene fauna and only three flint artefacts ascribed to the Upper Paleolithic were collected in Trench 1/2007-8 (Komšo, 2008).

Horizon B includes layers 4, 5, 6, 7 and 8. Only two flint artefacts, few pottery fragments and very few animal bones were collected here. The layers 4 to 8 can be only dated upon their stratigraphic position between the Bronze Age layers and the Pleistocene horizon C, and can only tentatively be ascribed to the beginning of the Holocene or to the end of the Late Pleistocene. This horizon is generally sterile, the rare finds can be explained by postdepositional processes (Komšo, 2008).

Horizon A comprises layers 1, 2 and 3; it includes Bronze Age and/or recent remains (Komšo, 2008). This horizon is evidently very reworked and it was not sampled for geoarchaeological studies.

The faunal assemblage from the 1960s-70s excavations includes remains from 41 taxa, more than 95% of the remains being *Ursus spelaeus*, indicating that Romualdova Pećina was a cave bear den during the Upper Pleistocene. According to Malez (1968), numerous animal bones were fragmented and gnawed, in a way that is characteristic of hyenas, which means that also cave hyenas must have used the cave periodically as a den (Malez, 1968).

7.4 Results

Samples were taken from one profile of the archaeological Trench 1 (D. Komšo excavations, 2007-08) in the entrance room of the cave. The study of the sequence and the sampling of the lithologic units were carried out after the end of the excavation. A total of 11 samples were collected for grain size analyses and 13 samples for micromorphological analysis. Since the upper part of the sequence, containing Bronze Age cultural remains, showed clear disturbances and reworking already at eye scale observations, no samples were collected for analysis from these levels.

7.4.1 Field observations

The following descriptions are based on the northern profile of Trench 1 (Fig. 7.3, Fig. 7.5). The sequences are described from the bottom upwards.

15 – limestone bedrock.

14 – this unit represents the first clastic sediment overlying the bedrock; silty sand with alternating thin fine grained lenses and coarse layers. Cross-bedding can be observed in some areas at the top of the level. Archaeologically sterile.

14B – laminated at the bottom (dark yellowish brown clayey stratification; level 14B.2. in Figure 7.7.) embedded in coarser whitish sandy sediment with cross-bedding (SU 14B.1). At the top of SU 14B.1 the sediment is a more homogeneous light gray silty sand.

14A – thin yellowish silt loam layer overlaying 14B (probably a remain left in place under the erosion surface filled up by 13F).

13 – reddish brown silty loam with few 1-10 cm subangular altered limestone clasts. The boundary is subhorizontal and clear. Middle Paleolithic cultural remains.

13F – infilling of a depression (probably a channel, as suggested by some crude lamination mostly situated at the bottom of the unit); brown silt loam with very few altered limestone clasts.

12 – yellowish brown silty clay loam with frequent angular to subangular limestone clasts, often parallel to the surface. The boundary is abrupt, subhorizontal. Middle Paleolithic cultural remains.

11 – reddish brown clayey silt with common angular to subangular limestone clasts (about 2-6 cm wide); the boundary is clear and subhorizontal. Middle Paleolithic cultural remains.

10 – homogeneous dark reddish brown silty loam with few angular to subangular limestone clasts (mostly > 3 cm); at the bottom there is a very dark brown silty loam horizon with moderately developed lamellar aggregation; abrupt subhorizontal boundary. Upper Paleolithic cultural remains.

9 – group of superimposed silt loam horizons characterised by different amounts of angular to subangular limestone clasts, with the larger ones concentrated in the top horizons. Upper Paleolithic cultural remains.

9C – frequent medium to fine limestone clasts (frequent 1-3 cm, rare 10 cm) in grayish brown matrix; granular aggregation.

9B – discontinuous layer with few small angular to subangular limestone clasts in brown matrix.

9A – frequent coarse, subangular skeleton (up to about 20 cm, some verticalized) in dark brown matrix; granular aggregation.

5-7 – yellowish brown massive, homogeneous silt loam layer laminated in the middle; very few limestone clasts; the boundary is abrupt. Archaeologically sterile.

4 – yellowish brown loose silt loam with well developed granular aggregation.

2x – reworked loose sediment with subrounded limestone; infilling of a

1 – reworked Bronze Age to recent surface layer

7.4.2 Architecture of the layers and sediment texture

The main stratigraphic units of the Romualdova Pećina infill are shaped as almost continuous approximately horizontal layers. The lowermost group of excavated layers is a grayish to yellowish quartz sand to silty sand, laminated at the bottom (layers 14A, 14B, 14.1) with evident cross-bedding overlying the laminations and a more homogeneous sediment at the top. This group of layers is much thicker on the eastern part of the profile due to the topography of the bedrock. The top of this group of layers is marked by an erosional feature - the sediment of the feature 13F1 fills up a possible channel which eroded partially the underlying layers 13, 14A and 14B. Cryogenic deformation features are visible at the top of layer 14 in the eastern profile of Trench 1/2007-8.

The coarse component of the sediments is calcareous. Grain size analysis (Fig. 7.5 and 7.6) were carried out on the fine grained fraction (<2 mm) of the sediments. The sediments are always poorly sorted. The sand fraction is more abundant (>28%) in the samples from the lowermost layers 14A and 14B.1, where it is always more than 50%. The most common fine

fraction of the overlying layers is always silt, ranging between 36.42% (layer 13) and 71.84% (layer 4) in the undecalcified samples, and between 65.26% (layer 9C) and 85.97% (layer 10) in the decalcified ones. The clay fraction is always less than 22% in decalcified samples, while in undecalcified ones it goes up to 51.29%. Clay is always more abundant in undecalcified samples compared to the decalcified ones. One of the reasons could be the great amount of fine clay-sized Fe oxides which couldn't be disintegrated by the H₂O₂ only, but could be destroyed when attacked by HCl during decalcification. The fine fraction -from sand downwards in the grain-size scale- is dominated by silicate minerals, mostly quartz, feldspars and abundant mica.

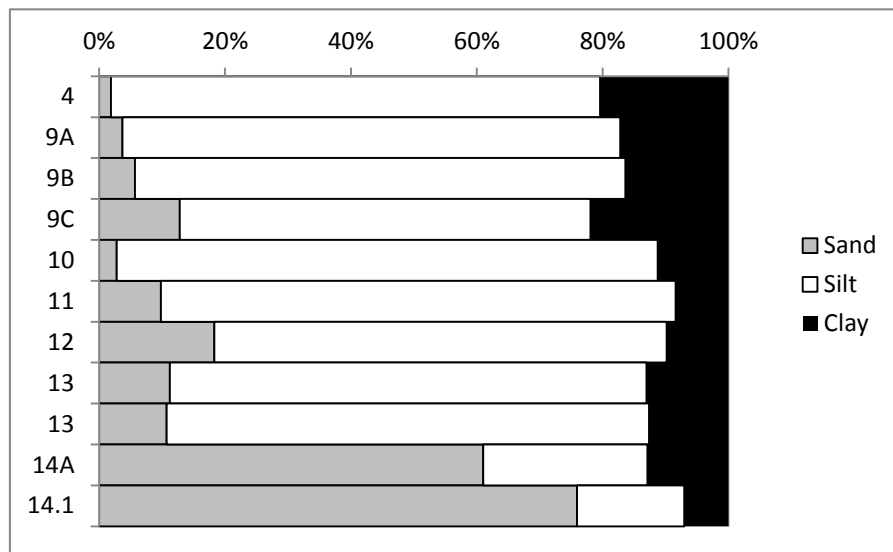


Figure 7.5 Grain-size (Wentworth, 1922) of the <2 mm fraction of decalcified samples.

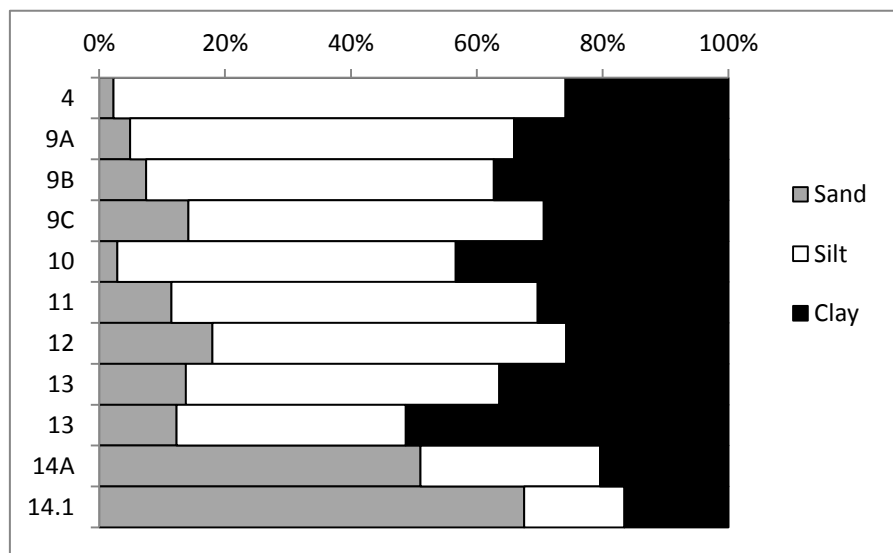


Figure 7.6 Grain-size (Wentworth, 1922) of the <2 mm fraction of undecalcified samples.

4.4.3 Micromorphology



**Figure 7.7 Stratigraphic sequence with the position of the samples
(Trench 1/2008-7, northern profile).**

Micromorphological analyses were carried out on 13 thin sections, approximately one per stratigraphic unit collected from the northern profile of Trench 1/2007-8; in some cases, the samples were collected at the boundary between units. The main micromorphological characteristics of the sediments are summarised in this chapter. The location of the samples collected from the profile is given in Figure 7.7.

ROM 1/14.2

Microstructure and porosity: banded microstructure with channels and vesicles.

Groundmass: c/f-related distribution pattern is single spaced to open porphyric.

Coarse material:

Rock fragments: frequent quartzite, frequent subangular to rounded chert.

Minerals: dominant angular to subrounded quartz grains, few angular to subangular feldspars, frequent muscovite flakes, few rounded glauconite, few rutile, few zircon, few opaques.

Inorganic residues of biological origin: none.

Anthropogenic elements: none.

Organic: none.

Micromass: few dusty clay.

Pedofeatures: clay coatings.

ROM 2/14.1

Microstructure and porosity: banded and lenticular microstructure.

Groundmass: c/f-related distribution pattern is

Coarse material:

Rock fragments: frequent subangular chert

Minerals: dominant angular to subrounded quartz grains, very few zircon, common muscovite flakes, few angular to subangular feldspars.

Inorganic residues of biological origin: none.

Anthropogenic elements: none.

Organic: none.

Micromass: dusty clay.

Pedofeatures: clay coatings, Fe/Mn coating and hypocoatings, ice lenses.

ROM 3/14A

Microstructure and porosity:

Groundmass: c/f-related distribution pattern is

Coarse material:

Rock fragments: common rounded to subrounded chert fragments

Minerals: dominant angular to subrounded quartz grains, few subangular feldspars, common muscovite flakes, few subrounded phosphates.

Inorganic residues of biological origin: none.

Anthropogenic elements: none.

Organic: none.

Micromass: dusty clay, granostriated and porostriated b-fabric.

Pedofeatures: clay coatings, ice lensing, Fe/Mn coatings and hypocoatings.

ROM 4/13

Microstructure and porosity: granular and lenticular microstructure.

Groundmass: c/f-related distribution pattern is double spaced to open porphyric.

Coarse material:

Rock fragments: few quartz aggregates, common rounded chert.

Minerals: common angular to subrounded quartz grains, common rounded to subrounded phosphates, common muscovite flakes, few angular to subangular calcite, very few elongated calcite crystals forming aggregates (recrystallized ash?).

Inorganic residues of biological origin: few bone fragments.

Anthropogenic elements: none.

Organic: few organic matter.

Micromass: dusty clay with stipple speckled and granostriated b-fabric.

Pedofeatures: ice lenses, Fe/Mn hypocoatings, Fe/Mn aggregate nodules.

ROM 5/13

Microstructure and porosity: subangular bocky to granular microstructure.

Groundmass: c/f-related distribution pattern is double spaced to open porphyric.

Coarse material:

Rock fragments: few quartz aggregates, common rounded chert.

Minerals: common angular to subrounded quartz grains, common rounded to subrounded phosphates, common muscovite flakes, few angular to subangular calcite, very few elongated calcite crystals forming aggregates (recrystallized ash?).

Inorganic residues of biological origin: few bone fragments.

Anthropogenic elements: none.

Organic: few organic matter.

Micromass: dusty clay with stipple speckled and granostriated b-fabric.

Pedofeatures: few ice lenses, Fe/Mn hypocoatings, Fe/Mn aggregate nodules, common reddish rounded pedorelicts, few loess like pedorelicts.

ROM 6/12-11

This thin section comprises layers 12 and 11.

Layer 11:

Microstructure and porosity: lenticular microstructure.

Groundmass: c/f-related distribution pattern is open porphyric.

Coarse material:

Rock fragments: common subangular to rounded micritic limestone fragments, few quartz aggregates (sandstone?), common angular to subangular chert fragments.

Minerals: frequent angular to subrounded quartz grains, common subrounded to rounded phosphates (carnivore coprolites), common muscovite flakes, few calcite, few angular feldspars.

Inorganic residues of biological origin: few bone fragments (including digested bone).

Anthropogenic elements: few bone fragments (some digested).

Organic: very few tissue, few amorphous organic matter.

Pedorelicts: very few reddish with quartz skeleton and vesicles (possibly coprolite?)

Micromass: clay with stipple speckled and granostriated b-fabric.

Pedofeatures: ice lenses, common Fe/Mn aggregate nodules, very few nucleic Fe nodules, few clay coatings.

Layer 12:

Microstructure and porosity: granular microstructure.

Groundmass: c/f-related distribution pattern is open porphyric.

Coarse material:

Rock fragments: common subangular to rounded micritic limestone fragments, few quartz aggregates (sandstone?), common angular to subangular chert fragments.

Minerals: frequent angular to subrounded quartz grains, common subrounded to rounded phosphates (carnivore coprolites), common muscovite flakes, few calcite, few angular feldspars (very few microcline).

Inorganic residues of biological origin: few bone fragments.

Anthropogenic elements:

Organic: very few tissue, few amorphous organic matter.

Micromass: clay with stipple speckled and granostriated b-fabric.

Pedofeatures: ice lenses, common Fe/Mn aggregate nodules, very few nucleic Fe nodules, few clay coatings.

ROM 7/10-11

This thin section comprises layers 10 and 11. For layer 11 see thin section ROM 6/12-11.

Microstructure and porosity: subangular blocky to granular microstructure with vesicles and channels, lenticular at the bottom.

Groundmass: c/f-related distribution pattern is double spaced to open porphyric.

Coarse material:

Rock fragments: very few subrounded flint fragments.

Minerals: very frequent angular to subangular quartz grains, very frequent muscovite flakes, few subangular feldspars, few pyroxenes.

Inorganic residues of biological origin: none.

Anthropogenic elements: none.

Organic: frequent tissue (very frequent at the bottom of SU 10), very frequent amorphous organic matter.

Micromass: dusty clay with parallel striated and porostriated b-fabric.

Pedofeatures: few clay coatings, ice lenses.

ROM 8/9C

Microstructure and porosity: granular and in smaller amount lenticular microstructure

Groundmass: c/f-related distribution pattern is double spaced to open porphyric.

Coarse material:

Rock fragments: common subangular to rounded foraminiferal and micritic limestone fragments.

Minerals: frequent subangular to rounded quartz grains, common subrounded to rounded phosphates (carnivore coprolites), few angular to subangular feldspars, very few zircons few pyroxenes).

Inorganic residues of biological origin: common bone fragments (also digested), few microsparite and sparite calcite, common muscovite flakes.

Anthropogenic elements: none.

Organic:

Pedorelicts: few reddish rounded aggregates with quartz skeleton.

Micromass: dusty clay with granostriated b-fabric.

Pedofeatures: common aggregate Fe/Mn nodules, Fe staining few clay papules.

ROM 9/9B

Microstructure and porosity: lenticular and in smaller amount granular microstructure with vesicles.

Groundmass: c/f-related distribution pattern is double spaced to open porphyric.

Coarse material:

Rock fragments: few rounded chert fragments, very few angular flint fragments.

Minerals: very frequent angular to subrounded quartz grains, frequent phosphates (carnivore coprolites), very frequent muscovite flakes, few angular to subangular feldspars, few sparitic calcite.

Inorganic residues of biological origin: few bone fragments.

Anthropogenic elements: very few charcoal fragments.

Organic: few tissue.

Micromass: dusty clay with granostriated, porostriated and monostriated b-fabric.

Pedofeatures: Fe/Mn nodules, Fe concentric nodules, Fe aggregate nodules, few clay papules.

ROM 10/9A

Microstructure and porosity: granular and crumb microstructure with channels and vesicles and chambers. Banded fabric in the upper part of the thin section can be observed.

Groundmass: c/f-related distribution pattern is double spaced to open porphyric.

Coarse material:

Rock fragments: none.

Minerals: frequent angular to subrounded quartz grains, frequent muscovite flakes, few feldspars (very few microclines), very few pyroxenes.

Inorganic residues of biological origin: few bone fragments.

Anthropogenic elements: few charcoal fragments.

Organic: common tissue and amorphous organic matter.

Micromass: dusty clay with granostriated and porostriated b-fabric.

Pedofeatures: few clay coatings, very few ice lenses, common Fe/Mn nodules and impregnations, clay hypocoatings and quasicoatings.

ROM 11/5-7a

Microstructure and porosity: massive microstructure with vesicles, chambers and channels.

Groundmass: c/f-related distribution pattern is single spaced to open porphyric.

Coarse material:

Rock fragments: none.

Minerals: few pyroxenes, frequent angular to subangular quartz grains, very frequent muscovite flakes, common biotite, few feldspars.

Inorganic residues of biological origin: none.

Anthropogenic elements: very few charcoal fragments.

Organic: few tissue and amorphous organic matter .

Micromass: clay with stipple-speckled and strial b-fabric; banded fabric.

Pedofeatures: clay papules, Fe hypocoatings and quasicoatings, Fe/Mn nodules.

ROM 11/5-7b

Microstructure and porosity: massive, and weakly to moderately developed granular microstructure (at the bottom) with vesicles, chambers and channels.

Groundmass: c/f-related distribution pattern is single spaced to open porphyric.

Coarse material:

Rock fragments: none.

Minerals: few pyroxenes, frequent angular to subangular quartz grains, very frequent muscovite flakes, common biotite, few feldspars.

Inorganic residues of biological origin: none.

Anthropogenic elements: very few charcoal fragments.

Organic: few tissue and amorphous organic matter .

Pedorelicts: dark brown rounded aggregates with quartz skeleton (at the bottom of the thin section).

Micromass: clay with stipple-speckled and porostriated b-fabric; banded fabric.

Pedofeatures: clay papules, Fe hypocoatings and quasicoatings, Fe/Mn nodules, and few clay coatings at the bottom of the thin section.

ROM 12/4

Microstructure and porosity: highly developed granular microstructure.

Groundmass: c/f-related distribution pattern is single spaced to open porphyric.

Coarse material: none.

Rock fragments: very few angular flint fragments.

Minerals: common pyroxenes, frequent angular to subangular quartz grains, very frequent muscovite flakes, few biotite, few feldspars, very few rounded phosphates.

Inorganic residues of biological origin: very few bones.

Anthropogenic elements: very few charcoal fragments.

Organic: common tissue and amorphous organic matter.

Micromass: dusty clay with stipple-speckled b-fabric; fan-like fabric.

Pedofeatures: Fe/Mn intercalations, “rolling” pedofeatures, Fe/Mn nodules.

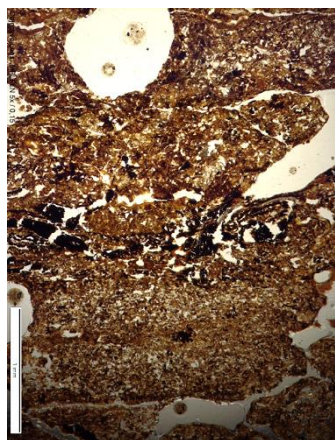


Figure 7.8 Microphotograph of the organic layer between unit 10 and 11 (leaves, twigs etc.).

7.5 Discussion

The main characteristic of Romualdova Pećina sediments is that the sediments were mostly formed by natural processes, as suggested by the scanty cultural remains that were found in all levels, and also by the micromorphological analyses, which did not put into evidence clear traces of human activity. The coarse calcareous skeleton, mainly composed of subangular limestone fragments of climatic origin (frost shattering of the cave walls and ceiling) is often altered by surface dissolution, probably because of the low pH of the sediment, which is rich in clay. The most evident microscopic features of the freezing and thawing cycles are lenticular microstructures (layers 14A, 11, bottom of 10, 9B) and ice lensing pedofeatures.

Another characteristic of some of the layers are phosphate aggregates which could be interpreted as animal coprolites, at least some of them being most probably hyena coprolites.

Clay coatings, especially in the lower part of the stratigraphic sequence, indicate some clay illuviation processes, which testify to some phase of strong water input into the cave, as dripwater or possibly also in-wash. Moderate- or low-energy water flow, also possibly due to in-wash, is indicated by laminated levels within units 5-7.

The texture and cross-stratification of the lowermost layer 14B indicates relatively high-energy sediment transport. The mineralogy of these sediments (quartz is dominant, but quartzite, chert, feldspars, mica, glauconite, rutile, and zircon also occur) indicates a possible fluvial(?) transport of dismantled flysch deposits observable in the Pazin basin (Toševski, Grgec and Padovan, 2012).³ However, the sedimentary structures observed within this level do not give hints about the direction of flow; consequently, it cannot be determined whether these sands originated from the flow of an underground vadose karstic system, or if they were washed into the cave by a former river flowing in the Limski Kanal.

The grain-size of all the studied layers overlying the quartz sands of the horizon E (layers 14) lies within the limits of the primary loess field. The texture fits both the palaeosols (the grain-size distribution of palaeosols of Susak is similar to that of loess) and loess in the Susak Island loess sequences (Cremaschi, 1990b; Mikulčić Pavlaković et al., 2011; Wacha et al., 2011; Wacha, 2011).

³ “Quartz diagenetic sediments” (known also as “quartz sands” or “quartz sandstones”) occur within limestones in three separate layers (0.5 - 6 m thick) trending in two directions: NE-SW (Tinjan-Pula region) and NW-SE (Savudrija-Buje-Optalj region). These sediments are composed mostly of idiomorphic authigenic quartz crystals, microcrystalline quartz aggregates and cryptocrystalline to microcrystalline chert-like clusters (Durn et al. 2003).

Sediments belonging to horizon D are associated with the Middle Paleolithic Mousterian industry. Different microstructures (subangular blocky to granular in layer 13, granular in layer 12 and lenticular in layer 11) testify to variable climatic conditions; the lenticular microstructure of layer 11 is characteristic of deep-seasonal frost processes (freezing-thawing of impregnating water on sediments).

A few cm thick dark brown stratum at the bottom of layer 10 divides horizon D (Middle Paleolithic) from horizon C (Upper Paleolithic). Micromorphological analyses showed that it consists of organic matter of vegetal origin (leaves, twigs, etc.) (Fig. 7.8) embedded in silty matrix, settled parallel or subparallel to the surface of the layers. It is archaeologically sterile and it probably represents a hiatus in the occupation of the cave. It was probably accumulated inside the cave by low-energy surface flow due to intense precipitations, which transported into the cave vegetal debris accumulated in woody areas.

In layer 10, the limestone rubble is almost absent, whereas a moderate increase in the amount and size of the limestone rubble is observable in layer 9C; the rubble is again rare in layer 9B, and it increases considerably in size and quantity in layer 9A. These sediments belonging to horizon C, ascribed to the Upper Paleolithic, indicate cyclical dismantling of the cave ceiling and/or walls caused by cryoclastic processes (frost shattering) and may reflect cyclically alternating cool-wet and cool-dry climatic conditions. In fact, further evidence of different intensity of freeze-thaw effects between those layers were observed at micromorphological scale, ash alternating lenticular (bottom of layer 10 and layer 9B) and granular microstructures with some minor ice lensing pedofeatures (top of layer 10, and layers 9C and 9A). According to Van Vliet-Lanoë (2010) lenticular microstructure is typical of frost-affected soils with low content of coarse material, while granular microstructure occurs in the upper part of frost-affected soils. The micromass shows often a granostriated or porostriated b-fabric, corresponding to stress features formed by alignment of clay particles at the surface of the aggregates under the pressure of the growth of ice crystals (Van Vliet-Lanoë, 2010).

Layers 5-7 of the B horizon include graded layering resulting from rapid decrease in flow velocity that caused progressively finer suspended sediment particles to settle on the bottom of the cave. Micromorphological analyses confirmed that layer 4 of the same horizon B in fact shows the same graded stratification, but it was reworked *ab antiquo* and is no longer visible at eye scale.

Phosphate aggregates that can be identified at microscopic level as fragments of carnivore coprolites in almost all of the layers from horizons C and D; they probably belong

to hyenas (Kolska Horwitz and Goldberg, 1979; Goldberg, 1980) and possibly other cave animals (cave bear?).

7.6 Concluding remarks

Sedimentological and micromorphological analyses showed that the fine component of the sediments overlying horizon E is mainly made up of poorly altered loess. This may represent cold and arid climatic conditions alternating with somewhat wetter conditions, as indicated by limestone rubble deriving from roof spall.

The thin dark brown stratum dividing horizon D (Middle Paleolithic) from horizon C (Upper Paleolithic) consists of organic matter of vegetal origin (leaves, twigs, etc.). The vegetal remains were probably transported into the cave by low-energy surface flow due to intense precipitations.

It is noteworthy that deep seasonal freeze pedofeatures (ice lensing) are common in the Romualdova Pećina sediments, which is in contrast with what was observed for the sediments of the caves of the Trieste Karst during the Pleistocene, where no deep seasonal freeze pedofeatures were present (Boschian and De Santis, 2011). The alternations of layers with frequent and rare limestone rubble as well as the alternation of granular and lenticular microstructure indicate climate variability during the whole Late Pleistocene. Unfortunately, no geochromometric data are available at present for Romualdova Pećina, making it impossible to correlate the local climate during MIS 3 and MIS 2 with the global climatic conditions.

The anthropogenic input in the sediments of the cave is rather scanty. In contrast, paleontological (Malez, 1968) and micromorphological analyses (coprolites) showed that the cave was used frequently as cave bear and hyena den.

8. VELIKA PEĆINA – KLIČEVICA

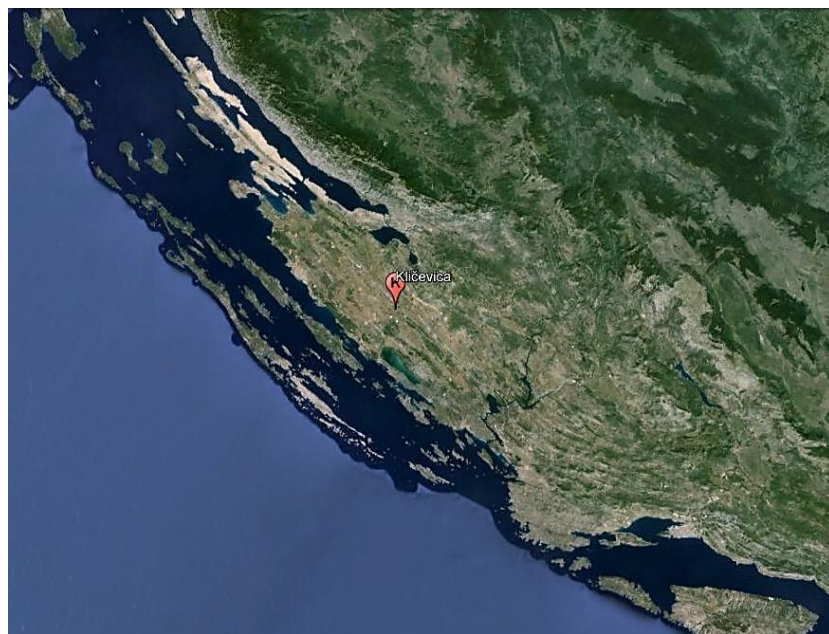


Figure 8.1 Location of Velika Pećina-Kličevica (Google Earth).

8.1 Introduction

Velika pećina is located in the area of Ravní Kotari near the town of Benkovac in Northern Dalmatia (Fig. 8.1). M. Savić reported already in 1984 some stone finds now kept in the Benkovac Local History Museum (Karavanić et al., 2014.). Several artefacts from the cave are stored at the Institute of Palaeontology and Geology of the Quaternary of the Croatian Academy of Sciences and Arts, probably collected by M. Malez (Karavanić et al., 2014). During the 2006 excavation several depressions of the cave surface were observed, pointing to the possibility of prior sondage excavations at the site (Karavanić and Čondić, 2006), which was later confirmed during the 2012-13 excavations of the Trench D-E/15-16. During a trial excavation in 2006, directed by I. Karavanić, a small sondage measuring 2x1 m was excavated in the main tunnel of the cave down to a depth of about 1.5 m. All of the layers excavated so far except the topsoil (mixed Holocene and Pleistocene finds) and two sterile layers directly overlying the bedrock, yielded Middle Paleolithic Mousterian culture remains (Karavanić, Čondić and Vukosavljević, 2007; Karavanić et al., 2014).

8.2 Site presentation

Velika pećina is situated in the canyon of the stream Kličevica. The stream is 14.5 km long; it springs at the foot of Biljanski vrh and flows into Nadinsko blato; one part of its course runs through the canyon on whose northern side are located two caves, Velika and Mala Pećina (Velika and Mala Kličevica), distant about thirty meters from each other (Karavanić and Čondić, 2006). The area of Ravni Kotari is a karstic area characterized by fertile flysch valleys.

The present-day entrance to the cave faces south-east, and is located at about 125 m a.s.l. (Karavanić et al., 2014). The first plan and cross-section of the cave were published by S. Božičević (1987). The cave includes 92 m of tunnels (Fig. 8.2); the main one veers left after about 30 m from the entrance and forks off after another ten metres (Božičević, 1987; Janković, Mihelić and Karavanić, 2011).

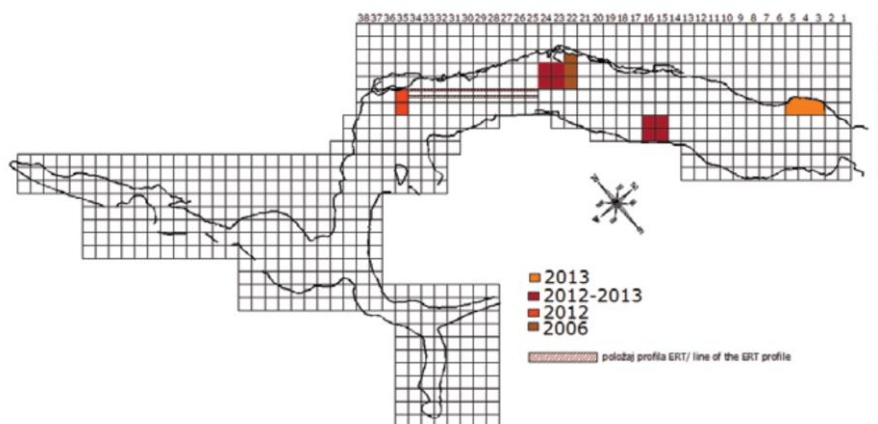


Figure 8.2 Velika Pećina cave map with the location of the trenches (Karavanić et al., 2014).

8.3 Archaeological background

Velika Pećina in Kličevica near Benkovac is the first Palaeolithic cave site in northern Dalmatia with the established stratigraphy (Karavanić and Čondić, 2006). Since the excavations are still ongoing, only very preliminary conclusions are available about the lithic finds. The lithic assemblage, belonging to the late Mousterian, in addition to tools on flakes, contains various débitage artefacts. The discovered tools are small (the so-called micro-Mousterian) and made on local cherts (Karavanić et al., 2014).

Six layers were excavated in Trench H-J/22-24. Except from the surface layers (A and B), all the others (C, D, E, and F) yielded only Mousterian artefacts together with some animal remains. The overall stratigraphy is relatively short; in the deepest part of the trench, the limestone bedrock was reached after 1.5 meters (Karavanić et al., 2014). The excavators documented a dark brown surface organic layer (A) overlaying a clayey brownish sediment with coarse sand (layer B). Below, there was a reddish sediment C which was divided in two parts (upper C1 and lower C2) by a flowstone. In most of the trench, layer D – a reddish brown clayey sediment – overlies the bedrock, but in a small southern part of the trench two more layers were identified between D and the bedrock – a darker clay loam layer E and a somewhat lighter layer F (Karavanić and Čondić, 2006; Karavanić, Čondić and Vukosavljević, 2007). There were numerous badger tunnels cutting through most of the layers. As a result, large part of the infill was intensively reworked.

A part of what was probably an old sondage became evident during the excavations of Trench D-E/15-16. Much of the sediments were disturbed and reworked also by animal activity (badger tunnels). A block of reddish sediment (layer C) with coarse limestone skeleton is probably the only *in situ* remnant of what was once the upper part of the sequence. Four more layers were identified in the lower part of the sequence; layers G and H which included flint artefacts, and layers I and J which were archaeologically sterile (Karavanić et al., 2014).

Adjacent to the entrance of the cave, along the north-eastern cave wall, a new trench was opened in 2013, in squares G-H/3-5. The entire area near the entrance to the cave was covered by medium to large stones and blocks. Immediately below the stones some recent human remains were found; medieval pottery was also collected in the uppermost sediments. Excavations of this trench are still in progress and it will not be the subject of this study.

A fragment of a long bone of an ungulate from layer D was dated to $39,240 \pm 740$ uncal BP (Beta-228733) by the radiocarbon method (AMS) (Karavanić, Čondić and Vukosavljević, 2007). Another animal bone from layer D was sent for an AMS radiocarbon dating. One sample of a half of this bone was prepared for the AMS in the standard way and yielded the result of $35,110 \pm 310$ uncal BP (Beta-372935), while the other sample was prepared by ultrafiltration and gave a date of $32,520 \pm 240$ uncal BP (Beta-372934) (Karavanić et al., 2014)⁴.

⁴ What might have caused different dates derived from the same bone is still unclear, the problem is addressed in Karavanić et al., 2014.

8.4 Results

Samples were collected from two trenches inside the cave (Trench H-J/22-24 and Trench D-E/15-16) (Fig. 8.2); sample X is from a sediment remain attached to the cave wall, opposite Trench D-E/15-16 (Fig. 8.3). A total of seven samples for grain-size analysis and 17 samples for micromorphology were studied.

8.4.1 Field observations

Evident traces of at least two levels of pre-existing sediments, one dark brown and the other reddish, can be observed on the walls of the cave (Fig. 8.3; Fig. 8.4.). These layers were from few decimetres up to more than a metre thick, respectively in the entrance hall and in the back of the cave.



Figure 8.3 North eastern cave wall opposite Trench D-E/15-16 with remains of reddish sediment (with bones inside).



Figure 8.4 Interior of the cave with remains of dark brown and reddish sediment on the walls.

The following descriptions are based on the north western profile of Trench H-J/22 excavated in 2006 (Fig. 8.5) and the south eastern profile of Trench D-E/15-16 (Fig. 8.6) excavated in 2012 – 2013.

Profile H-I/21-22

The sequence is described from the bottom upwards. The bedrock was covered in part by a flowstone.

D.3 –few cm thick wavy lens situated in a limited area in the southern part of the trench, following the topography of the bedrock under layer D.

D – dark brown stoneless silty loam with fine granular aggregation; the sediment is partly reworked and loose. This layer is discontinuous subhorizontal, slightly dipping towards southeast, and following the flowstone that covers the bedrock. It is disturbed by a badger tunnel in several places. The boundary is clear.

C2 – reddish silt loam, compact. The, boundary is abrupt or unclear. The unit is partly cut and reworked by a badger tunnel. A 10-20 cm thick discontinuous flowstone overlies this layer.

C1 – reddish silt loam with very few limestone clasts, more compact than C2. This unit lies upon the flowstone covering C2.; Sharp boundary, the top of this layer is clearly eroded.

B –Dark brown silt loam with subrounded and altered gravel and pebble-size (about 3-15 cm) skeleton; skeleton supported structure, fine granular aggregation. Abrupt boundary.

A – fresh bat guano accumulation.

In the southern part of the trench two more layers (visible in the southeastern profile) were excavated:

E – reddish brown silt loam, representing the top of layer F. Reworked by bager tunnels.

F – the lowermost clastic unit is a red silt loam with fine granular aggregation, with few limestone gravel to pebble-size (7-15 cm) clasts, mostly arranged vertically; on the southern part of the profile the boundary is clear, on the northern part it is diffuse. It is a funnelshaped infill inbetween the flowstone and a large limestone block.. Thickness about 50 cm; reworked.

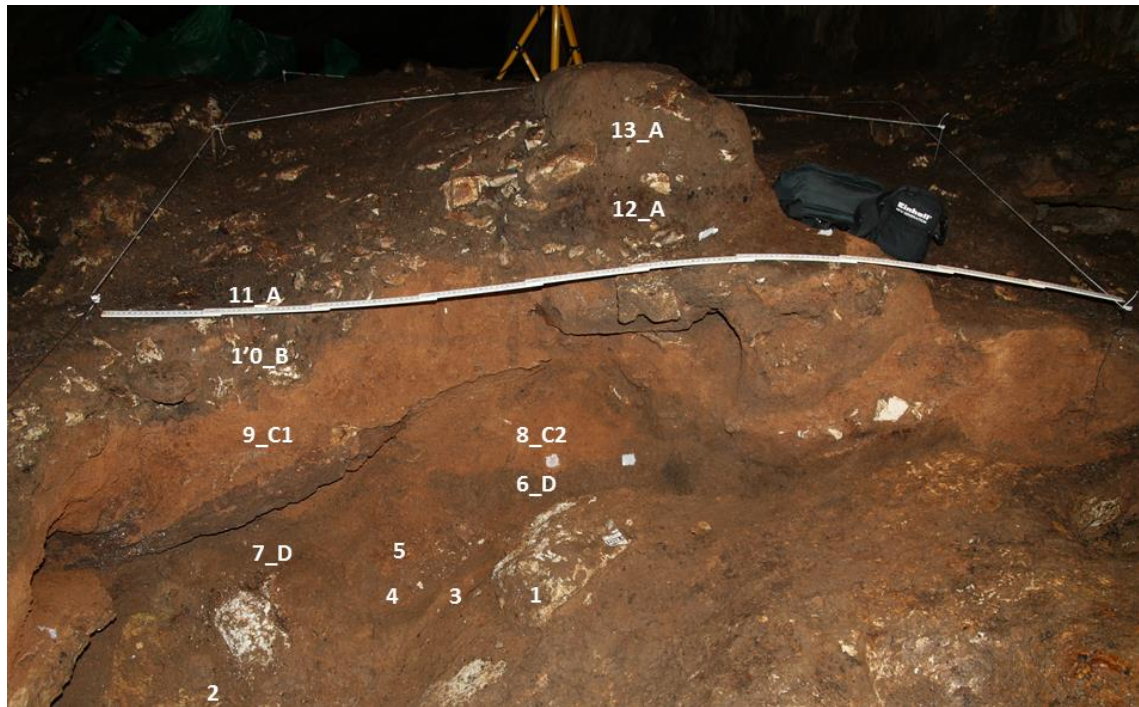


Figure 8.5 North western profile of Trench H-I/22.

Profile D-E/15-16

The infilling of this trench is mostly reworked and cut by several animal dens (Fig. 8.6).

The lowermost clastic sediment (J) is a yellowish brown sandy silt loam, few cm thick with an abrupt boundary. Above this layer there is a grayish-white silt loam lens (layer H) few cm thick and with abrupt boundary.

In the upper part of the sequence there is a block of reddish sediment which seems moderately *in situ*. This sediment can be divided in two parts: the upper one is a light red silt loam with few surrounded altered (decalcified and covered by manganese) limestone clasts. At the top there are two levels of stones gently sloping towards the south east; the lower part is a somewhat darker reddish brown silt loam with iso-oriented limestone skeleton made up of medium gravel (the size of the stones is few cm).

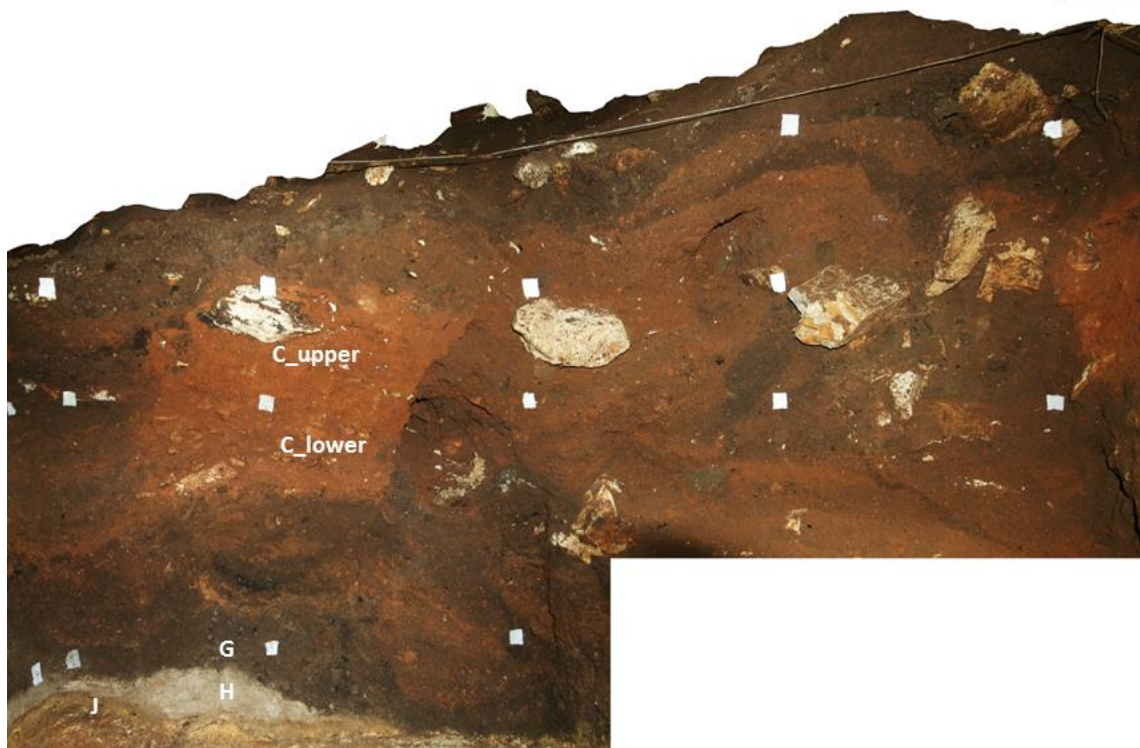


Figure 8.6 South eastern profile of Trench D-E/14-15.

8.4.2 Sediment texture

The coarse component of the sediments is usually calcareous. Grain size analyses (Fig. 8.7; Fig. 8.8) have been carried out on the fine grained fraction (<2 mm) of the sediments. Since most of the layers are strongly reworked, the granulometric analyses were conducted only on the sediments that looked in situ in the field. These include layer D, layer C1, C2, and layer G. A sample X was collected from the remains of the reddish sediment attached to the cave wall opposite Trench D-E/15-16. The sediments are always very poorly sorted and coarse skewed.

The sand fraction is always less than 30% (from 20.74% to 29.34% in undecalcified samples and from 13.7% to 21.93% in decalcified samples). The most common fine fraction of the layers in undecalcified samples is always clay, ranging between 36.67% (sample X) and 52.01% (layer G). In decalcified samples, the most common fraction is silt, always about 50%. In decalcified samples, the clay fraction is always less than 34%. As it was observed in Romualdova Pećina, clay is always more abundant in undecalcified samples compared to the decalcified ones also in sediments of Velika Pećina-Kličevica. One of the reasons could be the great amount of fine Fe oxides which couldn't be disintegrated by the H₂O₂ only, but could be destroyed when attacked by HCl.

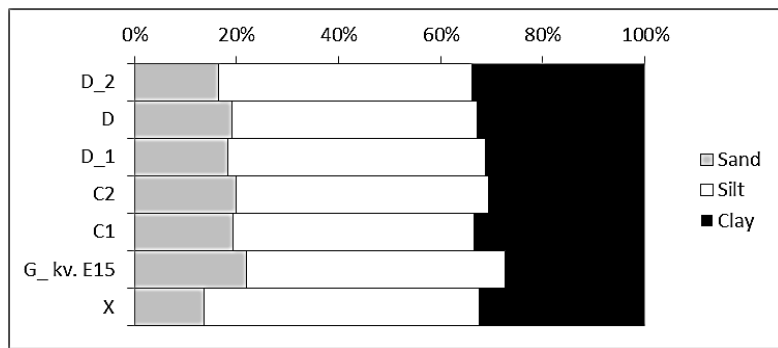


Figure 8.7 Grain-size (Wentworth, 1922) of the <2 mm fraction of decalcified samples.

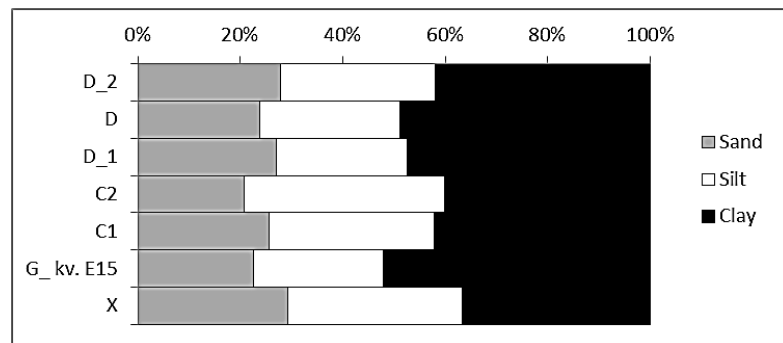


Figure 8.8 Grain-size (Wentworth, 1922) of the <2 mm fraction of undecalcified samples.

8.4.3 Micromorphology

Micromorphological analyses were carried out on 17 thin sections, approximately one per layer; in some cases, the samples were collected at the boundary between units. The main micromorphological characteristics of the sediments are summarised in this chapter.

VPK 12/H 22_23/12-13 (layer A)

Microstructure and porosity: angular and subangular blocky to granular microstructure with channels and chambers.

Groundmass: c/f-related distribution pattern is open porphyric.

Coarse material:

Rock fragments: common quartzitic fragments.

Minerals: frequent angular to subrounded quartz grains, common subangular to rounded phosphates, common muscovite flakes, few pyroxenes, few feldspars.

Inorganic residues of biological origin:

Anthropogenic elements: frequent charcoal fragments.

Organic: common organic matter.

Pedorelicts:

Micromass: dusty clay with some granostriated b-fabric.

Pedofeatures: fragments of clay coatings, clay infillings, Fe/Mn nodules.

VPK 12/H 22_23/10 (layer B)

Microstructure and porosity: angular and subangular blocky to granular microstructure with channels and chambers.

Groundmass: c/f-related distribution pattern is open porphyric.

Coarse material:

Rock fragments: phosphatic speleothems, few subangular to subrounded micritic limestone fragments.

Minerals: few rounded hematite, frequent angular to subrounded quartz grains, common subangular to rounded phosphates, common muscovite flakes, few pyroxenes, few feldspars.

Inorganic residues of biological origin: few bone fragments.

Anthropogenic elements: frequent charcoal fragments.

Organic: amorphous organic matter.

Pedorelicts: aggregates of yellowish dusty clay with few quartz skeleton.

Micromass: dusty clay.

Pedofeatures: red limpid clay infillings, fragments of clay coatings, clay infillings, Fe/Mn nodules.

VPK 12/H22_23/9 (layer C1)

Microstructure and porosity: subangular blocky to granular microstructure

Groundmass: c/f-related distribution pattern is open porphyric.

Coarse material:

Rock fragments: few speleothem fragments, few subangular micritic limestone fragments, very few rounded flint fragments, few quartzite fragments.

Minerals: few sparitic calcite, very frequent angular to subrounded quartz grains, very frequent subangular to subrounded phosphates (carnivore coprolites are the most frequent, but other phosphates-possibly altered bone fragments-are common too), few angular feldspars.

Inorganic residues of biological origin: few bone fragments

Anthropogenic elements:

Organic:

Pedorelicts: few reddish silty clay pedorelict with very few quartz skeleton, rounded calcitic aggregates.

Micromass: dusty clay with granostriated b-fabric or calcitic crystallithic b-fabric.

Pedofeatures: Fe/Mn nodules, infillings, coatings, hypocoatings and quasicoatings, rolling pedofeatures, calcite coatings and hypocoatings on channels, few ice lenses.

VPK 12/H22_23/8 (layer C2)

This thin section is the same as VPK 12/H22_23/9 (layer C1) except from 3 cm in the middle of the thin section (a thin lens in the field) which will be described here.

Microstructure and porosity: pellicular grain microstructure.

Groundmass: c/f-related distribution pattern is chitonic and close to single spaced porphyric.

Coarse material:

Rock fragments: common rounded quartzite fragments.

Minerals: dominant angular to subrounded quartz grains, few muscovite flakes, few feldspars, few opaques.

Inorganic residues of biological origin: none.

Anthropogenic elements: none.

Organic: none.

Pedorelicts: aggregates of reddish silty clay sediment (they are the same as the sediment in the upper and lower part of the thin section, same as VPK 12/H22_23/9).

Micromass: dusty clay with undifferentiated or granostriated b-fabric.

Pedofeatures: Fe/Mn nodules and infillings.

VPK 12/H22_23/6 (layer D)

The upper part of the thin section is the same as VPK 12/H22_21/D. The lower part of the thin section is described here.

Microstructure and porosity: angular blocky microstructure (often banded fabric), becoming gradually granular in the lower part of the thin section; vesicles and chambers.

Groundmass: c/f-related distribution pattern is single spaced to open porphyric.

Coarse material:

Rock fragments: few quartz aggregates.

Minerals: very frequent angular to subrounded quartz grains, very few phosphates (carnivore coprolites), common phosphates (probably altered bone fragments, and other phosphates), few pyroxenes.

Inorganic residues of biological origin: common bone fragments (often altered).

Anthropogenic elements: few microcharcoal.

Organic: common amorphous organic matter.

Micromass: dusty clay with granostriated and porostriated b-fabric.

Pedofeatures: ice lenses, layered fragments of clay coatings, Fe/Mn nodules, impregnations, hypocoatings and punctuations.

VPK 12/H 22_23/5 (lens below layer D)

Microstructure and porosity: angular to subangular blocky with chambers and channels, at the bottom of the thin section it is platy.

Groundmass: c/f-related distribution pattern is open porphyric.

Coarse material:

Rock fragments: few speleothem fragments, few subangular micritic limestone fragments, very few rounded flint fragments, few quartzite fragments.

Minerals: few hematite, very frequent angular to subrounded quartz grains, very frequent subangular to subrounded phosphates, few angular feldspars.

Inorganic residues of biological origin: few bone fragments

Anthropogenic elements:

Organic:

Pedorelicts: rounded calcitic aggregates.

Micromass: dusty clay with granostriated b-fabric or calcitic crystallitic b-fabric.

Pedofeatures: Fe/Mn nodules, infillings, coatings, hypocoatings and quasicoatings, rolling pedofeatures, calcite coatings and hypocoatings on channels.

VPK 12/H 22_23/4-3 (lenses overlying the bedrock)

Microstructure and porosity: granular microstructure with channels and chambers.

Groundmass: c/f-related distribution pattern is open porphyric.

Coarse material:

Rock fragments: few quartzite fragments, very few flint fragments.

Minerals: very frequent angular to subrounded quartz grains, very frequent subangular to subrounded phosphates, few angular feldspars

Inorganic residues of biological origin: few bone fragments.

Anthropogenic elements:

Organic:

Pedorelicts: common reddish clay aggregates with quartz skeleton.

Micromass: dusty clay with granostriated b-fabric.

Pedofeatures: Fe/Mn nodules, infillings, coatings, hypocoatings and quasicoatings,

VPK 12/H23/C1

Microstructure and porosity: angular to subangular blocky with chambers and channels, at the bottom of the thin section it is platy.

Groundmass: c/f-related distribution pattern is open porphyric.

Coarse material:

Rock fragments: few speleothem fragments, few subangular micritic limestone fragments, very few rounded flint fragments, few quartzite fragments.

Minerals: very frequent angular to subrounded quartz grains, very frequent subangular to subrounded phosphates (carnivore coprolites are the most frequent, but other phosphates-possibly altered bone fragments-are common too), few angular feldspars.

Inorganic residues of biological origin: few bone fragments

Anthropogenic elements:

Organic:

Pedorelicts: rounded calcitic aggregates.

Micromass: dusty clay with granostriated b-fabric or calcitic crystallitic b-fabric.

Pedofeatures: Fe/Mn nodules, infillings, coatings, hypocoatings and quasicoatings, rolling pedofeatures, calcite coatings and hypocoatings on channels.

VPK 12/H22_21/D

Microstructure and porosity: granular microstructure with vesicles.

Groundmass: c/f-related distribution pattern is single spaced to open porphyric.

Coarse material:

Rock fragments: few flowstone fragments, few subangular limestone fragments, common quartz aggregates.

Minerals: very frequent angular to subrounded quartz grains, frequent phosphates (including carnivore coprolites, probably alter bone fragments, and other phosphates), few pyroxenes.

Inorganic residues of biological origin: common bone fragments (often altered).

Anthropogenic elements: few microcharcoal.

Organic: common amorphous organic matter.

Pedorelicts: common silty clay pedorelicts with few quartz skeleton.

Micromass: dusty clay with granostriated and porostriated b-fabric.

Pedofeatures: layered fragments of clay coatings, Fe/Mn nodules, impregnations, hypocoatings and punctuations.

VPK 12/H22_21/F

Microstructure and porosity: granular microstructure (some granules have banded fabric composed of clay, silty clay, and sandy clay loam, often are in inclined position); channels.

Groundmass: c/f-related distribution pattern is open porphyric.

Coarse material:

Rock fragments: none.

Minerals: frequent angular to subangular quartz grains, few biotite, common white mica, few hematite, few phosphates (frequent at the bottom of the thin section, probably altered bone fragments).

Inorganic residues of biological origin: few bone fragments (altered, phosphatized).

Anthropogenic elements: none.

Organic: none.

Pedorelicts: common silty clay pedorelicts with few quartz skeleton.

Micromass: dusty clay with granostriated, cross striated, circular striated and striae b-fabric

Pedofeatures: fragments of layered clay coatings, clay coatings, Fe/Mn nodules, Fe impregnations and coatings

VPK 13/H24/D (lens inside layer D)

Microstructure and porosity: intergrain microaggregate microstructure.

Groundmass: c/f-related distribution pattern is close to single spaced enaulic.

Coarse material:

Rock fragments: none.

Minerals: dominant angular to subrounded phosphates, common angular to subrounded quartz grains.

Inorganic residues of biological origin:

Anthropogenic elements: none.

Organic: none.

Micromass: dusty clay with granostriated b-fabric.

Pedofeatures: clay infillings, clay papules and clay coatings.

VPK 13/E16/C_upper

Microstructure and porosity: angular to subangular blocky with vesicles, chambers and channels.

Groundmass: c/f-related distribution pattern is open porphyric.

Coarse material:

Rock fragments: very few subrounded micritic limestone fragments.

Minerals: very frequent angular to subangular quartz fragments, dominant subangular to rounded phosphates (carnivore coprolites) at the bottom of the thin section and common through the thin section, common muscovite flakes, few feldspars.

Inorganic residues of biological origin: few bone fragments.

Anthropogenic elements: very few charcoal fragments.

Organic: few organic matter.

Pedorelicts:

Micromass: dusty clay with granostriated b-fabric.

Pedofeatures: clay papules, phosphatic and iron staining coating and hypocoatings on limestone fragments, Fe nodules, Mn hypo, rolling pedofeatures, .

VPK 13/E16/C_lower

Microstructure and porosity: angular to subangular blocky and granular microstructures with vesicles and chambers and channels.

Groundmass: c/f-related distribution pattern is single spaced to open porphyric

Coarse material:

Rock fragments: very frequent phosphatic crusts (often verticalized), subrounded few quartzite.

Minerals: very frequent subangular to rounded phosphates (carnivore coprolites), very frequent angular to subrounded quartz grains, few angular feldspars.

Inorganic residues of biological origin: few bone fragments.

Anthropogenic elements: few charcoal fragments.

Organic: none.

Micromass: granostriated b-fabric

Pedofeatures: Fe staining coatings and hypocoatings, limpid clay papules, Fe/Mn nodules, few ice lenses.

VPK 13/E16/G-H

This thin section consist of two layers, G and H, for the description of layer H see VPK 13/E16/H.

Microstructure and porosity: granular and angular blocky microstructure with vesicles and channels.

Groundmass: c/f-related distribution pattern is open porphyric.

Coarse material:

Rock fragments: common subangular to sub rounded quartzite fragments.

Minerals: very frequent angular to subrounded quartz grains, common muscovite flakes, very few pyroxene, very few zircon?

Inorganic residues of biological origin: none.

Anthropogenic elements: very frequent charcoal fragments.

Organic: frequent tissue and amorphous organic matter.

Pedorelicts: dusty clay aggregates.

Micromass: dusty clay with undifferentiated or porostriated b-fabric.

Pedofeatures: calcite coatings and hypocoatings on channels, clay papules.

VPK 13/E16/H

Microstructure and porosity: massive or angular to subangular blocky microstructure with vesicles and channels.

Groundmass: c/f-related distribution pattern is single spaced to open porphyric.

Coarse material:

Rock fragments: few angular to rounded flint fragments, very few sandstone, few quartz aggregates.

Minerals: frequent angular to subangular quartz grains, common muscovite flakes, common angular to subangular phosphates (altered bone fragments?), few feldspars very few zircon?

Inorganic residues of biological origin: none.

Anthropogenic elements: frequent charcoal fragments.

Organic: none

Micromass: dusty clay with cross striated, granostriated porostriated b-fabric

Pedofeatures: clay coatings and infillings, depletions, calcite coatings on channels, Mn impregnations, Fe punctuations.

VPK 13/E16/J

Microstructure and porosity: subangular blocky and granular microstructures with frequent channels and vesicles; undulated fabric.

Groundmass: c/f-related distribution pattern is open porphyric.

Coarse material:

Rock fragments: none.

Minerals: common subangular to subrounded quartz grains, very few muscovite flakes, frequent phosphates (phosphatic crusts).

Inorganic residues of biological origin: none.

Anthropogenic elements: none.

Organic: none.

Micromass: dusty clay with granostriated, porostriated, parallel striated and striae b-fabric.

Pedofeatures: clay coatings and hypocoatings, calcite coatings and infillings, Fe/Mn impregnations.

VPK 12/X

The thin section was prepared from the sample of the reddish sediment attached to the north eastern cave wall opposite Trench D-E/15-16 (Figure 8.3.).

Microstructure and porosity: complex microstructure (subangular blocky, platy, granular) with very frequent channels.

Groundmass: c/f-related distribution pattern is open porphytic.

Coarse material:

Rock fragments: fragments of speleothems, few quartz aggregates (quartzite?).

Minerals: frequent subangular to subrounded phosphates (carnivore coprolites and other phosphates), frequent angular to subrounded quartz grains, common muscovite flakes, few feldspars.

Inorganic residues of biological origin: few bone fragments.

Anthropogenic elements: none.

Organic: none.

Micromass: dusty clay with calcitic crystallitic b-fabric.

Pedofeatures: calcite coatings and hypocoatings on channels, Fe/Mn coatings and impregnations, calcite infillings, Fe/Mn nodules, excrement infillings

8.5 Discussion

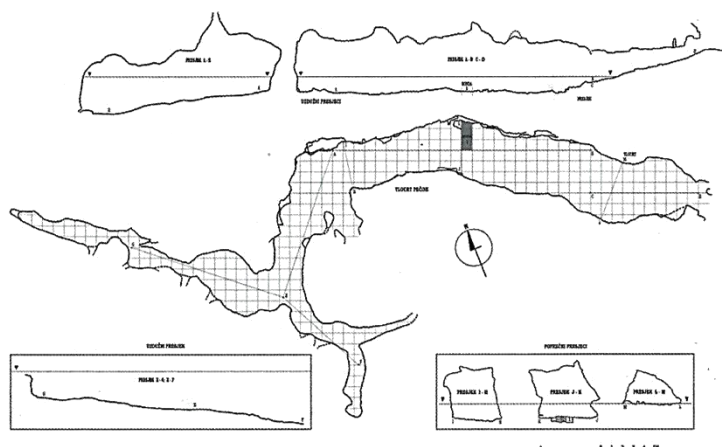


Figure 8.9 Cave plan and sections (Karavanić and Čondić, 2006).

The traces of sediments on the wall of the cave indicate that sediment was removed from this cave, probably for fertilising fields, as reported by local people. Pleistocene cave sediments are enriched in phosphates resulting from the alteration in acidic environment of the bones of megafauna which used the caves (Hubbard, 2012). Accumulations of bat guano are another source of phosphates and are also often used as fertilizer for gardens and fields.

In contrast to the other two studied caves with Middle Paleolithic cultural remains (Mujina Pećina and Romualdova Pećina), not one of the sediments from Velika Pećina-Kličevica lies within the limits of the primary loess field, although a relatively high percent of silt in decalcified samples (around 50% in all of the analysed layers) may indicate the input of reworked loess which was deposited outside the cave, altered by soil-forming processes, and then colluviated inside .

As it is the case with Mujina Pećina and Romualdova Pećina, phosphate aggregates that can be identified at microscopic level as fragments of carnivore coprolites, possibly hyenas (Miller, Macphail, pers. comm.; Kolska Horwitz and Goldberg, 1979; Goldberg,

1980) are a relevant component of the sediments of almost all layers, except from the lowermost layers I and J which are sterile and were probably derived from the alteration of the flowstones and/or bedrock, and the surface bat guano layer.

Even though most of sediments from this cave were strongly reworked and disturbed, in some of the layers (most evidently in some parts of layer C1) ice lensing testifying deep seasonal frost has been preserved. In layer D, banded fabric characterized by sorted coarse grain sands and lenticular aggregates may have the same meaning (Van Vliet-Lanoë, 2010). Another indication of cryogenic processes may be recognized in some verticalized elements (few clasts at macroscopic and microscopic level). One of the most evident postdepositional processes is clay illuviation; layered clay coatings testify to different phases of these processes.

8.6 Concluding remarks

A large amount of the sediment was removed from the cave and probably used as fertilizer for agricultural activities, thus some archaeological layers may have been destroyed in the process. Most of the sediments were disturbed by recent faunal activity (badger channels); some of them were eroded and reworked *ab antiquo* (layer C1).

Very frequent carnivore (and possibly other) coprolites indicate that the cave was often used as a den during the Pleistocene.

It is noteworthy that large part of the bone has been very strongly altered by dephosphatization; this may possibly be one of the causes for “bad” dates, because of the complex geochemical behaviour of percolating phosphates with the organic matter and iron included in the sediment.

9. CONCLUSIONS

Sedimentological and micromorphological analysis of stratigraphic sequences of five caves – Mujina Pećina, Zala, Zemunica, Romualdova Pećina and Velika Pećina-Kličevica – contributed to the understanding of site formation process (including postdepositional processes) of archaeological cave sites and the extent and type of human activities in the caves of the eastern Adriatic coast and its hinterland. By the identification of these processes, some conclusions can be drawn about the environmental and climatic conditions during the late Pleistocene and Holocene in the studied area. The analyses confirmed the hypothesis of different cave use by Middle Paleolithic, Upper Paleolithic, Mesolithic, Neolithic and Bronze Age humans.

The identified site formation processes are polygenetic in origin and can generally be divided in geogenic, non-human biogenic processes and processes derived by anthropic activities (Bar-Yosef, 1993; Farrand, 2000; Goldberg and Macphail, 2006).

As it is usually the case with caves, geological deposits include both sediments from inside (autochthonous/endogenous) and outside (allochthones/exogenous) the cave (Goldberg and Macphail, 2006).

Autochthonous deposits include coarse calcareous skeleton mainly composed of limestone fragments derived from the breakdown of the walls and ceiling of the cave bedrock. In Europe, the main process of detachment of large blocks and smaller sized rock debris is of cryogenic origin; it is caused by freezing and thawing of water that has percolated into cracks and fissures in the bedrock (Barton and Clark, 1993; Goldberg and Macphail, 2006). These processes usually indicate colder climatic conditions at the time of deposition. Cryoclastic deposition of large amount of clastic accumulation in caves cannot always be explained by freeze-thaw effects, as proposed by Farrand for Franchthi Cave in Greece (see also Barton and Clark, 1993). In our case, the cryogenic origin of this processes was corroborated by micromorphology; lenticular microstructures (ice lensing), silt cappings, verticalized and/or frost shattered coarse fragments and banded fabric – which are all clear indicators of frost affected sediments – were observed at microscopic scale. Cryoturbations have been recognized in Pleistocene sediments (both with Middle and Upper Paleolithic remains) from all of the studied caves. One peculiarity has been observed in Zala Cave, where also Holocene Mesolithic and at least some of the Bronze Age sediments have similar microscopic characteristic. It may be argued that deep seasonal frost may not fit the age and supposed

warm climate corresponding to the deposition of the upper part of the sequence in Zala, which took place during the Medium-Late Holocene (Bronze Age remains). Nonetheless, it can be observed that the depression where Zala is situated is a peculiar ecotope, where the characteristics of the present-day floral biocenosis indicate average temperatures lower than in the surroundings. Such peculiarity may have also enhanced the effects of low temperatures during the Late Glacial and the Early Holocene, causing strong cryoturbation in the cave sediments. In Zala, cryoturbations such as convolutions, injection features and ice wedges most certainly moved the Paleolithic, and Mesolithic finds vertically and horizontally through the sequence during the Late Pleistocene and Early Holocene.

In general, it can be observed that presently the inner temperature of the caves corresponds roughly to the yearly average of the exterior. Even if changes in the entrance breadth -mostly a generalised reduction due to accumulation processes- may have influenced the inside temperature régime through time, it is noteworthy that frost inside caves must have resulted from very severe outside temperatures. These climatic conditions also caused a generalised in-depth decrease of the rock mass, fostering ice formation within the underground systems. However, the traces of deep *seasonal* frost also suggest that temperatures varied dramatically through the year, indicating strong seasonal contrast.

Running water from the cave interior transported fluvial sediments into the entrance (habitation) hall of Zala Cave. The underground river flow must have been much stronger than the present-day one during the late Late Pleistocene-Early Holocene, as demonstrated by the coarser grain-size of the sediments and by the well-developed lateral accretion deposits. This peculiarity may be in agreement with information from Pupićina Peć and Vešanska Peć (Miracle, 2007) in north-eastern Istria: those data show that Vela Draga gorge (flowing down from Učka) was periodically subject to strong water discharge, probably flash-floods triggered by strong rainfall in the nearby area. The small size of the Vela Draga imbriferous basin, and the proximity of a high mountain like Učka (1'234 m), may have enhanced the effects of rainstorms or snow melting in some cases, but all these data point to some evidence of periodical strong rainfall in the area (Boschian and Fusco, 2007; Boschian and Gerometta, 2015). The texture and cross-stratification of the lowermost layer 14B in Romualdova Pećina indicates relatively high-energy sediment transport. The mineralogy of these sediments indicates a possible fluvial transport of dismantled flysch deposits. However, the sedimentary structures observed within this level do not give enough information about the direction of flow; consequently, it cannot be determined whether these sands were transported into the

entrance hall by running water from the cave system, or if they were washed into the cave from the outside.

Allotogenous materials, coming from more or less distant areas, were introduced into the caves by movements of slope debris outside the caves. Evidence of slope processes and colluvium of soils developed outside the cave are also confirmed by soil micromorphology: the pedorelicts and/or papules indicate inputs of sediment or soil, previously deposited outside the cave and transported into it by in-wash. Grain-size and micromorphological analyses demonstrate that at least some of the sediments are made up of poorly to moderately altered loess (Mujina Pećina, Romualdova Pećina) and transported into caves by similar processes.

It may be concluded that the cave sediments demonstrate climate variability during the whole Upper Pleistocene (Middle and Upper Paleolithic); cold and arid climatic conditions were alternating with somewhat wetter conditions.

Non-human biogenic input in sediments is visible from the remains of denning activities by carnivores and omnivores (Goldberg and Macphail, 2006). These have been recognized at microscopic scale as hyena and possibly bear coprolites and digested bones in Pleistocene sediments (Velika Pećina-Kličevica, Mujina Pećina, Romualdova Pećina). Bat guano was observed on the cave's surface in Romualdova Pećina, and Velika Pećina-Kličevica where it was most probably removed by recent human activities together with large quantities of older reddish sediment (traces are still visible on the cave walls).

In some of the caves part of the bone has been very strongly altered by dephosphatization; this may possibly be one of the causes for "bad" dates, because of the complex geochemical behaviour of percolating phosphates with the organic matter and iron included in the sediment.

Anthropogenic activities are also responsible for bringing sedimentary components into the studied caves.

The main characteristic of sediments containing Middle Paleolithic cultural remains is that the sediments were mostly formed by natural processes, as suggested by sedimentological and micromorphological analyses, which did not demonstrate many traces of human activity. Boschian (2003) argues that the small groups of Neandertals used the caves only occasionally for temporary shelters and campsites. This behaviour was discussed for the Trieste Karst, Friuli and northern Slovenia, but may also be true for the wider area of the eastern Adriatic coast. The environmental data from the sediments do not show particular connection between climate and human presence in Romualdova and Velika Pećina-Kličevica (Boschian, 2003). The data from Mujina Pećina differ in some extent. The human presence in the cave was more

frequent during the earlier warmer phases and the rather arid event corresponding to loess deposition. The phase of more intense and continuous use of the cave by humans was during the deposition of unit E3C.

Scanty traces of human activities in caves during the Upper Paleolithic are also observed in Romualdova Pećina and Zala. At Zemunica the Late Upper Palaeolithic levels consist largely of domestic waste residues.

The Mesolithic levels mostly comprise domestic waste deposits, including ash, bone fragments and more or less crushed land snails in Zemunica. In Zala the Mesolithic levels are characterized by ash accumulations and abundant fish bone, and can also be interpreted as domestic use of space.

Soil micromorphology provided valuable information also about the infilling processes and on-site Neolithic to Bronze Age human activities. In Zemunica, this part of the sequence is characterised by continuous evidence of sheep/goat and probably cattle dung accumulations. One indicator of stabling are *in situ* burnt stable layers – *fumiers*. More homogeneous layers with spherulites and phytoliths dispersed in the groundmass can be interpreted as accumulations of incompletely burnt or unburnt herbivore dung. Phytoliths also occur within the cave sediments, indicating the use of straw litter for these animals. The top of the Bronze Age sequence of trench 3 includes almost pure yellowish sediment with articulated phytoliths - an intentional accumulation of selected material, a possible prepared surface/floor. In Zala Cave during the Bronze Age, the cave was first used for short-term domestic activities, with a shift to seasonal pastoral activities in later stages of the Bronze Age. The interpretation of these sediments relies mostly on micromorphological and microstratigraphic observations, as well as on geo-ethnoarchaeological considerations (Brochier, J. E., Villa, P. and Giacomarra, M., 1992). The archaeological importance of animal droppings is much more diagnostic than that of the zooarchaeological data because animals may not have been butchered on-site. Therefore, “Dung is sounder evidence of the presence of flocks than sheep bones are” (Boschian and Montagnari-Kokelj, 2000, 347). Caves and rock-shelters are typical spots of the landscape where flocks can be stabled and find shelter from rain and predators. They were used for stabling animals from the Neolithic onwards throughout Mediterranean Europe (Boschian and Montagnari Kokelj, 2000; Angelucci et al., 2009).

Bibliography

- Angelucci. 2009. Appunti di Geoarcheologia I (Corso di Metodologie della Ricerca Archeologica I per il Corso di Laurea Magistrale in Conservazione e Gestione dei Beni Culturali). Università degli Studi di Trento, Dipartimento di Lettere e Filosofia.
- Angelucci, D. E., Boschian G., Fontanals M., Pedrotti A. and Vergès J.M. Shepherds and karst: the use of caves and rock-shelters in the Mediterranean region during the Neolithic. *World Archaeology* 44 (2009): 191-204.
- Angelucci, Diego. 2010. Appunti di Geoarcheologia II (Corso di Metodologie della Ricerca Archeologica I per il Corso di Laurea Magistrale in Conservazione e Gestione dei Beni Culturali). Università degli Studi di Trento, Dipartimento di Lettere e Filosofia.
- Bahun, S. «Geološka osnova krške zavale Ogulin – Plaški.» *Krš Jugoslavije* 7.1 (1970): 1-20.
- Barton, M. C. and Clark, G. A. “Cultural and Natural Formation Processes in Late Quaternary Cave and Rockshelter Sites of Western Europe and Near East.” Goldberg, P., Nash, D. T. and Petraglia, M. D. *Formation Processes in Archaeological Context*. Vol. Monographs in World Archaeology 17. Madison, Wisconsin: Prehistory Press, 1993. 33-52.
- Bar-Yosef, O. “Site Formation Processes from Levantine Viewpoint.” Goldberg, P., Nash, D. T. and Petraglia, M. D. (eds.). *Formation Processes in Archaeological Context*. Vol. Monographs in World Archaeology 17. Madison, Wisconsin: Prehistory Press, 1993. 13-32.
- Bognar, A. “Geomorfološka regionalizacija Hrvatske.” *Acta Geographica Croatica* 34 (1994) (2001): 7-29.
- Bognar, A., Faivre, S., Buzjak, N., Pahtnik, M and Bočić, N. “Recent Landform Evolution in the Dinaric and Pannonian Regions of Croatia.” Lóczy, D., Stankoviansky, M. and Kotarba, A. (eds.). *Recent Landform Evolution*. Heidelberg, London, New York: Springer, 2012. 313-344.
- Boschian, G. and Montagnari-Kokelj, E. Prehistoric Shepherds and Caves in the Trieste Karst (Northeastern Italy). *Geoarchaeology: An International Journal* 15(4) (2000): 31-371.
- Boschian, G. and De Santis, A. “Bears and sediments at Caverna degli Orsi/Medvedja jama (Trieste, Italy).” *Fragments of Ice Age environments. Proceedings in Honour of Ivan Turk's Jubilee*. Ed. B. Toškan. Ljubljana: ZRC SAZU, 2011. 181-201.
- Boschian, G., Gerometta, K., Elwood, B. B. and Karavanić, I. “Late Neandertals in Dalmatia: climate change, human activity and site formation processes at Mujina Pećina, Croatia.” (in prep.).

- Boschian, G. "Geoarchaeology of Pupićina Cave / Geoarheologija Pupićine peći." Miracle, P. T., Forenbaher, S. (eds.). *Prehistoric herders of northern Istria. The archaeology of Pupićina Cave. / Pretpovijesni stočari sjeverne Istre. Arheologija Pupićine peći.* Monografije i katalozi 14. Vol. 1. Pula: Arheološki muzej Istre, 2006. 123-162.
- Božičević, S. "Speleološke pojave benkovačkog kraja i njihovo značenje." *Benkovački kraj kroz vjekove.* Vol. Zbornik 1. Benkovac, 1987. 29-35.
- Božičević, Hidrogeologija. Bertoša, S., Matijašić, R. (eds.). *Istarska enciklopedija.* Leksikografski zavod Miroslav Krleža, 2008, <http://istra.lzmk.hr/clanak.aspx?id=1113>.
- Brewer, R. *Fabric and mineral analysis of soils.* New York: John Wiley & Sons, 1964.
- Brochier, J. E., Villa, P. and Giacomarra, M. "Sheperds and Sediments: Geoethnoarchaeology of Pastoral Sites." *Journal of Anthropological Archaeology* 11 (1992): 47-102.
- Bullock, P., Fedoroff, N., Jungerius, A., Stoops, G., Tursina T. and Babel U. *Handbook for Soil Thin Section Description.* Wolverhampton: Waine Research Publications, 1985.
- Butzer, K. W. *Archaeology as Human Ecology.* Cambridge: Cambridge University Press, 1982.
- Butzer, K. W. *Environment and Archaeology: An Ecological Approach to Prehistory.* Chicago: Aldine Publishing Company, 1964.
- Canti, M. "The Production and Preservation of Faecal Spherulites: Animals, Environment and Taphonomy." *Journal of Archaeological Science* 26 (1999): 251-258.
- Catt, J. A. (ed.). "Paleopedology Manual." *Quaternary International* 6 (1991): 1-95.
- Chapman, J., Shields, R. and Batović, Š. *The changing face of Dalmatia: archaeological and ecological studies in a Mediterranean landscape.* Leicester: Leicester University Press, 1996.
- Cornwall, I. W. *Soils for the Archaeologist.* New York: Macmillan Company, 1958.
- Cottignoli, A., Boschian, G., Di Maggio, C., Masini, F. and Petruso, D. "Pedostratigraphic notes on the middle-late Pleistocene of Capo San Vito Peninsula (NW Sicily)." *Il Quaternario* 15.1 (2002): 89-96.
- Coutard, J. and Mücher, H. J. "Deformation of laminated silt loam due to repeated freezing and thawing cycles." *Earth Surface Processes and Landforms* 10 (1985) (1983): 309-319.
- Cremašchi, M. "Depositional and Post-depositional Processes in Rock Shelters of Northern Italy during the Late Pleistocene: their Paleoclimatic and Paleoenvironmental Significance." *Quaternaire* 1 (1990b): 51-64.

- Cremaschi, M. *Manuale di Geoarcheologia*. Bari: Manuali Laterza, 2000.
- Cremaschi, M. "Stratigraphy and palaeoenvironmental significance of the loess deposits on Susak Island (Dalmatian archipelago)." *Quaternary International* 5 (1990b): 97-106.
- Cremaschi, M. "The Loess in Northern and Central Italy: a Loess Basin Between the Alps and the Mediterranean Sea." Cremaschi, M. (ed.). *The Loess in Northern and Central Italy: a Loess Basin Between the Alps and the Mediterranean Sea*. Milano: C.N.R., Centro di Studio per la Stratigrafia e Petrografia delle Alpi Centrale, 1990a. 15-19.
- Di Maggio, C., Incandela, A., Masini, F., Petruso, D., Renda, P., Simonelli, C. and Boschian, G. "Oscillazioni eustatiche, biocronologia e depositi continentali quaternari e neotettonica nella Sicilia nord-occidentale (Penisola di S. Vito lo Capo – Trapani)." *Il Quaternario* 12.1 (1999): 25-49.
- Durn, G., Ottner F. and Slovenec, D. "Mineralogical and geochemical indicators of the polygenetic nature of terra rossa in Istria, Croatia." *Geoderma* 91 (1999): 125-150.
- Durn, G. "Terra Rossa in the Mediterranean Region: parent materials, composition and origin." *Geologia Croatica* 56.1 (2003): 83-100.
- Durn, G., Ottner, F., Tišljar, J., Mindszenty, A. and Barudžija, U. *Regional Subaerial Unconformities in Shallow-Marine Carbonate*. Ed. I. and Tišljar, J. Vlahović. Opatija: 22nd IAS Meeting of Sedimentology, 2003.
- Farrand, W. R. *Depositional History of Franchthi Cave. Sediments, Stratigraphy, and Chronology*. Vols. Excavations at Franchthi Cave, Greece. Fascicle 12. Bloomington, Indianapolis: Indiana University Press, 2000.
- Friganović, M. «Regionalni pregled.» Crkvenčić, I., Derado, K., Friganović, M., Kalodera, A., Mirković,
D., Radica, T., Riđanović, J., Rogić, V., Roglić, J., Stražičić, N., and Šegota, T. *Geografija SR Hrvatske. Južno Hrvatsko primorje*. A. Cvitanović (ed.). Vol. 6. Zagreb: Školska knjiga, 1974. 94-218.
- Goldberg, P. "Micromorphology in Archaeology and Prehistory." *Paleorient* 6 (1980): 159-164.
- Goldberg, P. and Macphail, R. I. *Practical and Theoretical Geoarchaeology*. Oxford: Blackwell Publishing, 2006.
- Gutiérrez-Castorena, M. C. and Effland, W. R. "Pedogenetic and Biogenic Siliceous Features." Stoops, G., Marcelino, V. and Mees, F. (eds.). *Interpretation of Micromorphological Features of Soils and Regoliths*. Amsterdam, Oxford: Elsevier, 2010. 471-496.
- Hubbard Jr., D. A. "Saltpetre Mining." *Encyclopedia of Caves*. Ed. W. B. and Culver, D. C. White. Second Edition. Oxford: Elsevier, 2012. 676-679.

Jalžić, B. and Božičević, S. "Pećina Zala u kanjonu Bistraca." *Speleolog* XVIII-XIX (1970-71): 3-5.

Janković, I., Mihelić S. and Karavanić, I. *Put neandertalca / The Neandertal trail*. Zagreb: Arheološki muzej u Zagrebu, 2011.

Karavanić, I. and Bilich-Kamenjarin, I. "Musterijensko nalazište Mujina Pećina kod Trogira, rezultati trogodišnjih iskopavanja." *Opuscula archaeologica* 21 (1997): 195-204.

Karavanić, I., Ahern, J., Šošić, R. and Vukosavljević, N. "Pećina Zala." *Hrvatski arheološki godišnjak* 3/2006 (2007): 213-217.

Karavanić, I., Čondić, N. and Vukosavljević, N. "Velika pećina u Kličevici." *Hrvatski arheološki godišnjak* (2007): 345-347.

Karavanić, I., Čondić, N. and Vukosavljević, N. "Velika pećina u Kličevici." *Hrvatski arheološki godišnjak* 3 (2006) (2007): 347.

Karavanić, I., Čondić, N. "Probno sondiranje Velike pećine u Kličevici." *Obavijesti Hrvatskog arheološkog društva* XXXVIII.2 (2006): 45-50.

Karavanić, I., Golubić, V., Kurtanjek, D., Šošić, R and Zupanić, J. "Litička analiza materijala iz Mujine pećine / Lithic analysis of materials from Mujina Pećina." *Vjesnik za arheologiju i povijest Dalmatinsku* (2008): 29-58.

Karavanić, I., Miracle, P. T., Culiberg, M., Kurtanjek, D., Zupanić, J., Golubić, V., Paunović, M., Mauch Lenardić, J., Malez, V., Šošić, R., Janković, I. and Smith, F. H. "The Middle Paleolithic from Mujina Pećina, Dalmatia, Croatia." *Journal of Field Archaeology* 33.3 (2008): 259-277.

Karavanić, I., Šošić R., Ahern, J. and Vukosavljević, N. "Špilja Zala." *Hrvatski arheološki godišnjak* 4/2007 (2008a): 238-239.

Karavanić, I., Šošić, R., Vukosavljević, N., Ahern, J. "Sustavna arheološka istraživanja špilje Zale kod Tounja." *Modruški zbornik* 2 (2008b): 31-35.

Karavanić, I., Vukosavljević, N., Šošić Klindžić, R., Ahern, J. C. M., Čondić, N., Becker, R., Zubčić, K., Šuta, I., Gerometta, K. and Boschian, G. "Projekt "Kasni musterijen na istočnom Jadranu – temelj za razumijevanje identiteta kasnih neandertalaca i njihovog nestanka": sažetak 1. godine istraživanja / The Late Mousterian in the eastern Adriatic – towards understanding of late Neanderthals' identi." *Prilozi Instituta za arheologiju u Zagrebu* 31 (2014): 139-157.

Karkanas, P. "Cave Sediment Studies in Greece: A Contextual Approach to the Archaeological Record." Mavridis, F. and Jensen, J. T. *Stable Places and Changing Perceptions: Cave Archaeology in Greece*. Vol. S2558. BAR International Series, 2013. 73-82.

- Kolska Horwitz, L. and Goldberg, P. "A study of Pleistocene and Holocene hyaena coprolites." *Journal of Archaeological Science* 16 (1989): 71-94.
- Komšo, D. and Vukosavljević, N. "Connecting coast and inland: Perforated marine and freshwater snail shells in the Croatian Mesolithic." *Quaternary International* 244.1 (211): 117-125.
- Komšo, D. "Limski kanal." *Hrvatski arheološki godišnjak* 4 (2007) (2008): 264-268.
- Komšo, D. "Srednji paleolitik u Istri. Romualdova pećina i Campanož / Middle Palaeolithic in Istria. Romualdova pećina and Campanož." Janković, I., Mihelić, S. and Karavanić, I. *Put Neandertalca / The Neandertal Trail*. Zagreb: Arheološki muzej u Zagrebu, 2011. 193-205.
- Kubiëna, W. L. *Micropedology*. Ames, Ia.: Collegiate press, 1938.
- Malez, M. and Rukavina, D. "Krioturbacijske pojave u gornjopleistocenskim naslagama pećine Vindije u sjeverozapadnoj Hrvatskoj." *Rad Jugoslavenske akademije znanosti i umjetnosti* 371.17 (1975): 245–265.
- Malez, M. "Pregled paleolitičkih i mezolitičkih kultura na području Istre." *Arheološka istraživanja u Istri i Hrvatskom primorju. Izdanja Hrvatskog arheološkog društva*. Vol. 11. Zagreb: Hrvatsko arheološko društvo, 1987. 1 (1986) vols. 3-47.
- Malez, M. *Tragovi paleolita u Romualdovoj pećini kod Rovinja u Istri*. Vols. Poseban otisak iz knjige "Arheološki radovi i rasprave" - knjiga šesta. Zagreb: Jugoslavenska akademija znanosti i umjetnosti, 1968.
- Malez, M., Šimunić An. and Šimunić, Al. "Geološki, sedimentološki i paleoklimatski odnosi špilje Vindije i bliže okolice." *Rad Jugoslavenske akademije znanosti i umjetnosti* 411 (1984): 231-264.
- Marinčić, S., Magaš, N. and Borović, I. "Osnovna geološka karta SFR 1:100000, list Split." Beograd: Institut za geološka istraživanja Zagreb, 1971.
- Mihevc, A., Prelovšek, M. "Geographical Position and General Overview." Mihevc, A., Prelovšek, M. and Zupan Hajna, N. (eds.). *Introduction to the Dinaric Karst*. Postojna: Karst Research Institute at ZRC SAZU, 2010. 6-8.
- Mikulčić Pavlaković, S., Crnjaković, M., Tibljaš, D., Šoufek, M., Wacha, L., Frechen, M. and Lacković, D. "Mineralogical and geochemical characteristics of Quaternary sediments from the Island of Susak (Northern Adriatic, Croatia)." *Quaternary International* 234 (2011): 32-49.
- Miller Rosen, Arlene. *Cities of Clay: The Geoarchaeology of Tells*. Chicago: University of Chicago Press, Prehistoric Archeology and Ecology Series, 1986.

Miracle, P. "Late Mousterian subsistence and cave use in Dalmatia: the zooarchaeology of Mujina Pećina, Croatia." *International Journal of Osteoarchaeology* 15 (2005): 84-105.

Nizek, R. and Karavanić, I. "Prostorna analiza nalaza musterijenskih razina D2, E1, E2 i E3 Mujine pećine / The spatial analysis of finds from Mousterian levels D2, E1, E2 and E3 at Mujina pećina." *Prilozi Instituta za arheologiju u Zagrebu* 29 (2012): 25-56.

Olujić, B. and Perković, I. "Analiza i obrada keramičkog materijala iz istraživanja lokaliteta Zala." Vukosavljević, N. and Karavanić, I. *Arheologija špilje Zale. Od paleolitičkih lovaca skupljača do rimske osvajača.* Vol. Modruški zbornik. Posebna izdanja. Knjiga 2. Modruš: Katedra Čakavskog sabora Modruše, 2015. 175-208.

Pavić, R. «Gorski kotar i ogulinsko-plaščanska udolina.» Bognar, A., Pavić, R., Riđanović, J., Rogić, V.

and Šegota, T. *Geografija SR Hrvatske. Gorska Hrvatska.* A. Cvitanović (ed.). Vol. 4. Zagreb: Školska knjiga, 1975. 61-96.

Riđanović, J. «Istra.» Riđanović, J., Rogić, V., Roglić, J. and Šegota, T. *Geografija SR Hrvatske. Sjeverno Hrvatsko primorje.* A. Cvitanović (ed.). Vol. 5. Zagreb: Školska knjiga, 1975. 170-205.

Rink, W. J., Karavanić, Ivor, Pettitt, P. B., van der Plicht, J., Smith, F. H. and Bartoll, J. "ESR and AMS-based 14C dating of Mousterian levels at Mujina Pećina, Dalmatia, Croatia." *Journal of Archaeological Science* 29 (2002): 943-952.

Roglić, V. «Prirodna osnova.» Riđanović, J., Rogić, V., Roglić, J. and Šegota, T. *Geografija SR Hrvatske. Sjeverno Hrvatsko primorje.* A. Cvitanović (ed.). Vol.5. Zagreb: Školska knjiga, 1975. 5-28.

Schiffer, M. B. "Toward the Identification of Formation Processes." *American Antiquity* 48.4 (1983): 675-706. <<http://www.jstor.org/stable/279771>>.

Seierstad, I.K, Abbott, P.M., Bigler, M., Blunier, T., Bourne, A.J., Brook, E., Buchardt, S.L., Buizert, C., Clausen, H.B., Cook, E., Dahl-Jensen, D., Davies, S.M., Guillevic, M., Johnsen, S.J., Pedersen, D.S., Popp, T.J., Rasmussen, S.O., Severinghaus, J. "Consistently dated records from the Greenland GRIP, GISP2 and NGRIP ice cores for the past 104 ka reveal regional millennial-scale $\delta^{18}\text{O}$ gradients with possible Heinrich event imprint." *Quaternary Science Reviews* 106 (2014): 29-46.

Stoops, G. *Guidelines for Analysis and Description of Soil and Regolith Thin Section.* Madison, Wisconsin: Soil Science Society of America, Inc., 2003.

Stoops, G., Marcelino, V. and Mees, F. (eds.). *Interpretation of Micromorphological Features of Soils and Regoliths.* Amsterdam, Oxford: Elsevier, 2010.

Šošić Klindžić, R., Karavanić, I., Vukosavljević, N. and Ahern, J. C. M. "Smještaj, stratigrafija, kronologija i tijek iskopavanja špilje Zale." *Arheologija špilje Zale. Od*

paleolitičkih lovaca skupljača do rimskih osvajača. Vol. Modruški zbornik. Posebna izdanja. Knjiga 2. Modruš: Katedra Čakavski sabora Modruše, 2015. 15-48.

Šošić Klindžić, R., Radović, S., Težak-Gregl, T., Šlaus, M., Perhoč, Z., Altherr, R., Hulina, M., Gerometta, K., Boschian, G., Vukosavljević, N., Ahern, J. C. M., Janković, I., Richards, M. and Karavanić, I. "Late Upper Paleolithic, Early Mesolithic and Early Neolithic from the cave site Zemunica near Bisko (Dalmatia, Croatia)." *Eurasian Prehistory* (2015): 3-46.

Šošić, R. and Karavanić, I. "Pećina Zemunica." *Hrvatski arheološki godišnjak* 2 (2006): 376-378.

Van Vliet-Lanoë, B. "Dynamique periglaciaire actuelle et passée. Apport de l'étude micromorphologique et de l'expérimentation." *Bulletin de l'Association française pour l'étude du Quaternaire* 3 (1987): 113-132.

Van Vliet-Lanoë, B. "Frost Action." Stoops, G., Marcelino, V. and Mees, F. (eds.). *Interpretation of Micromorphological Features of Soils and Regoliths*. Amsterdam, Oxford: Elsevier, 2010. 81-108.

Van Vliet-Lanoë, B. "Frost Effects in Soils." Boardman, J. (ed.). *Soils and Quaternary Landscape Evolution*. London: Wiley, 1985. 117-158.

Van Vliet-Lanoë, B. "Traces de ségrégation de glace en lentilles associées aux sols et phénomènes periglaciaires." *Biuletyn Peyglacjalny* 26 (1976): 41-54.

Vlahović, I., Tišljar, J. and Velić, I. Geologija. Bertoša, S., Matijašić, R. (eds.). *Istarska enciklopedija*. Leksikografski zavod Miroslav Krleža, 2008, <http://istra.lzmk.hr/clanak.aspx?id=956>.

Vrsaljko, D., Bošnjak, M. and Japundžić, D. "Geomorfologija Ogulinsko-plaščanske udoline." Vukosavljević, N. and Karavanić, I. (eds.). *Arheologija špilje Zale. Od paleolitičkih lovaca skupljača do rimskih osvajača*. Vol. Modruški zbornik. Posebna izdanja. Knjiga 2. Modruš: Katedra Čakavskog sabora Modruše, 2015. 9-14.

Wacha, L., Mikulčić Pavlaković, S., Frechen, M. and Crnjaković, M. "The Loess Chronology of the Island of Susak, Croatia." *Quaternary Science Journal* 60.1 (2011): 153-169.

Weiner, S. *Microarchaeology: beyond the visible archaeological record*. New York: Cambridge University Press, 2010.

Zupan Hajna, N. "Geology." Mihevc, A., M. Prelovšek and N. Zupan Hajna (eds.). *Introduction to the Dinaric Karst*. Postojna: Karst Research Institute at ZRC SAZU, 2010. 14-19.

List of Figures

| | |
|--|----|
| Figure 2.1 Study area: 1. Romualdova Pećina, 2. Pećina Zala, 3. Velika Pećina-Kličevica, 4. Mujina Pećina, 5. Pećina Zemunica..... | 5 |
| Figure 2.2 Hydrogeological map of Croatia (Bognar et al., 2012)..... | 5 |
| Figure 2.3 Underground hydrography of Istria (http://www.pazinska-jama.com/index_en.php?link=postanak), 9 November 2015..... | 7 |
| Figure 2.4 Figure 2.4. Geology of Istria (Tišljar et al., 2008)..... | 7 |
| Figure 2.5 Hydrogeology of Istria (Božičević, 2008)..... | 7 |
| Figure 2.6 Underground hydrography of the Ogulin area (Pavić, 1975)..... | 9 |
| Figure 2.7 Geology of the Ogulin-Plaški Valley. 1. Paleozoic and Triassic clastics, 2. Dogger and Malm and Lower Cretaceous dolomites, 3. Triassic, Liassic and partly Malm dolomites, 4. Malm dolomites and limestones, 5. Cretaceous limestones, 6. permanent spring, 7. periodical spring, 8. ponor, 9. permanent surface water stream, 10. periodical surface water stream (Pavić, 1975)..... | 9 |
| Figure 2.8 Ravn Kotari and Bukovica (Chapman, J., Shields, R. and Batović, 1996)..... | 9 |
| Figure 2.9 Geology of Ravn Kotari and Bukovica (Chapman, J., Shields, R. and Batović, 1996)..... | 10 |
| Figure 2.10 Geological sketch of Dalmatia: 1. sands and lacustrine deposits (Late Neogene), 2. recent alluvial sediments, 3. recent gravel and sandy debris, 4. alluvium and terra rossa (Quaternary), 5. lacustrine clay and marl deposits (Late Neogene), 6. limestone conglomerates (Paleogene) intercalated with sandstones and marl, 7. platy and stratified/layered flysch (Paleogene), 8. marls and conglomerates (Paleogene), 9. flysch-like deposits (Mesozoic), 10. limestone breccia (mostly Upper and Lower Cretaceous), 11. stratified and banked karstified limestone (Mesozoic), 12. limestones and dolomites (mostly Mesozoic), 13. dolomites (mostly Mesozoic) (Roglić, 1975) | 11 |
| Figure 4.1 Location map of Mujina Pećina (Boschian et al., in prep.)..... | 20 |
| Figure 4.2 Plan of Mujina Pećina. Stars mark the main sampling locations for sedimentology and soil micromorphology..... | 21 |
| Figure 4.3 View of the SW side of the karstic gorge crossing Labinštica hills. The cave is situated at the foot of a limestone cliff, close to the toe of a small scree. Continuous line: fault line (Boschian et al., in prep)..... | 21 |

| | |
|--|----|
| Figure 4.4 Reference stratigraphic sequence along the longitudinal profile, in excavation square D6 (Boschian et al., in prep.)..... | 27 |
| Figure 4.5 Stratigraphic Profile A from Mujina Pećina (Karavanić and Bilich-Kamenjarin, 1997)..... | 28 |
| Figure 4.6 Grain-size (Wentworth, 1922) of the <2 mm fraction of decalcified samples..... | 30 |
| Figure 4.7 Grain-size (Wentworth, 1922) of the <2 mm fraction of undecalcified samples..... | 31 |
| Figure 4.8 Microphotographs of sediment thin sections from Mujina Pećina. a: silt cappings on limestone fragments, PPL. b: as in a, XPL. c: chert, PPL. d: as in c, XPL. e: pedorelic with quartz skeleton, PPL. f: as in e, XPL..... | 37 |
| Figure 4.9 Microphotographs of sediment thin sections from Mujina Pećina. a: phosphate-probable carnivore coprolite and a bone fragment, PPL. b: as in a, XPL. c: as in a, infrared FLUO. d: as in a, blue FLUO. e: silt capping on limestone fragment with red clay pedorelic and muscovite flake inside, PPL. f: as in e, XPL..... | 38 |
| Figure 4.10 Microphotographs of sediment thin sections from Mujina Pećina. a: burnt bone, “bone sand”, amorphous organic matter, nodules, granostriated b-fabric, PPL. b: as in a, XPL. c: as in a, infrared fluorescence. d: “rolling” pedofeature, XPL..... | 38 |
| Figure 5.1 Location map of Zala Cave..... | 42 |
| Figure 5.2 Lacation of Zala Cave..... | 42 |
| Figure 5.3 Cave system Đula - Medvedica with surface and underground hydrology. (http://161.53.55.11/speleo/DjulaMedvedica/images/SOVelebitHidroloska%20karta.JPG).... | 43 |
| Figure 5.4 Cave plan, modified and redrawn from Jalžić & Božičević (1966)..... | 44 |
| Figure 5.5 Plan and profiles of the entrance chamber. 1: old excavation area; 2: present-day excavation area; 3: main profile view. Modified and redrawn after Šošić Klindžić..... | 44 |
| Figure 5.6 Main transversal profile across the entrance hall with the location of samples. In black – granulometry; in red – micromorphology. The details for the yellow square are given in Figure 5.9..... | 46 |

| | |
|---|----|
| Figure 5.7 Strongly convoluted and disrupted laminae and possible ice wedge..... | 47 |
| Figure 5.8 Stratigraphic unit SJ85, sand grains from the grain-size class 100-710 µm..... | 47 |
| Figure 5.9 Bronze Age anthropogenic and geogenic units; detail of Figure 9 with the locations of the samples..... | 49 |
| Figure 5.10 Granulometric analyses of Zala Cave sediments. 1. decalcified, 2. undecalcified..... | 50 |
| Figure 5.11 Harris matrix (Šošoć Klindžić et al., 2015)..... | 51 |
| Figure 5.12 Photomicrographs: a) SU 100, lenticular microstructure, PPL; b) SU 100, lenticular microstructure, XPL; c) SU 90, banded fabric and silt cappings, PPL; d) SU 90, banded fabric and silt cappings, XPL; e) SU 100, stratified silt capping on limestone fragment; f) SU 90, lenticular microstructure, PPL..... | 60 |
| Figure 5.13 Photomicrographs, SU 65: a) spherulites, phytoliths and ash in PPL; b) spherulites, phytoliths and ash in XPL; c) same as a, detail; d) same as b, detail; e) recrystallized ashes, spherulites, phytoliths, PPL; f) recrystallized ashes, spherulites, phytoliths, XPL..... | 61 |
| Figure 5.14 Photomicrographs, SU 49, phosphatic dropping..... | 61 |
| Figure 6.1 Location map of Zemunica (Šošić Klindžić et al. , 2015)..... | 67 |
| Figure 6.2 Cave plan (Šošić Klindžić et al., 2015)..... | 68 |
| Figure 6.3 Profile V 17-18-19, trench 3a..... | 69 |
| Figure 6.4 Profile S 19-20, trench 3b..... | 70 |
| Figure 6.5 Profile G 18-19, trench 2..... | 70 |
| Figure 6.6 Grain-size (Wentworth, 1922) of the <2 mm fraction of decalcified samples..... | 78 |
| Figure 6.7 Grain-size (Wentworth, 1922) of the <2 mm fraction of undecalcified samples..... | 79 |
| Figure 6.8 Location of the samples for micromorphological analyses: a) SU 106, b) SU 139 lower, c) SU 139 upper, d) SU 135 (134 middle), e) SU 134 (134 upper), f) SU 115 lower, g) | |

| | |
|--|-----|
| SU 115 upper, h) SU 114, i) SU 45, j) SU 43-45, k) SU 116lower-115 upper, l) SU116 upper..... | 80 |
| Figure 6.9 SU 134 microphotographs..... | 100 |
| Figure 6.10 Palaeolithic levels microphotographs; possible tephra (bottom row)..... | 101 |
| Figure 6.11 Microphotographs of Neolithic and Bronze Age levels..... | 101 |
| Figure 7.1 Location of Romualdova Pećina (Google Earth)..... | 103 |
| Figure 7.2 Plan and profile of Romualdova Pećina (Malez 1968)..... | 104 |
| Figure 7.3 Stratigraphic profile of Romualdova pećina (Komšo, 2008)..... | 105 |
| Figure 7.4 Stratigraphic profile of Romualdova pećina (Malez, 1968)..... | 105 |
| Figure 7.5 Grain-size (Wentworth, 1922) of the <2 mm fraction of decalcified samples..... | 109 |
| Figure 7.6 Grain-size (Wentworth, 1922) of the <2 mm fraction of undecalcified samples..... | 109 |
| Figure 7.7 Straigraphic sequence with the position of the samples (Trench 1/2008-7, northern profile)..... | 110 |
| Figure 7.8 Microphotograph of the organic layer between unit 10 and 11 (leaves, twigs etc.)..... | 118 |
| Figure 8.1 Location of Velika Pećina-Kličevica (Google Earth)..... | 122 |
| Figure 8.2 Velika Pećina cave map with the location of the trenches (Karavanić et al., 2014)..... | 123 |
| Figure 8.3 North eastern cave wall opposite Trench D-E/15-16 with remains of reddish sediment (with bones inside)..... | 125 |
| Figure 8.4 Interior of the cave with remains of dark brown and reddish sediment on the walls..... | 125 |
| Figure 8.5 North western profile of Trench H-I/22..... | 127 |
| Figure 8.6 South eastern profile of Trench D-E/14-15..... | 128 |

| | |
|---|-----|
| Figure 8.7 Grain-size (Wentworth, 1922) of the <2 mm fraction of decalcified samples..... | 129 |
| Figure 8.8 Grain-size (Wentworth, 1922) of the <2 mm fraction of undecalcified samples..... | 129 |
| Figure 8.9 Cave plan and sections (Karavanić and Čondić, 2006)..... | 140 |

List of Tables

| | |
|---|----|
| Table 5.1 Grouping and colour of the analysed lithologic units..... | 50 |
| Table 6.1 Sediment colour under wet and dry conditions..... | 75 |

Biography

Katarina Gerometta was born in Pula (1982), has achieved three M. A.'s: History of Art and Italian Language and Literature, and Archaeology (2009) from the University of Zagreb, and is now a PhD candidate in Archaeology at the same University. She has been employed by the Juraj Dobrila University of Pula as Research Assistant since 2010 (courses taught: *Prehistory of Croatia, History of Civilizations, and History of Mesopotamia*). She attended soil micromorphology training courses and workshops in Pisa, London, Tübingen, and Cambridge. Her research interests are in Geoarchaeology, Archaeological Soil Micromorphology, Prehistory, Landscape Archaeology, and Stratigraphy. Since 2004 she participated in archaeological excavations on more than 30 sites in Croatia, Italy, France, Greece, Serbia, Bosnia and Herzegovina, Montenegro and conducted geoarchaeological sampling and research in several caves, rock shelters, and open-air sites in Croatia and abroad. She currently participates in two projects: "ARCHAEOOLIM: Archaeological investigations into the Late Pleistocene and Early Holocene of the Lim Channel, Istria" (P. I. Ivor Janković, PhD; Institute for Anthropological Research, Zagreb), Roman Age Transformation and Reuse of Prehistoric Hillforts in Istria – analysis and case study" (P. I. Prof. Klara Buršić-Matijašić, PhD., Juraj Dobrila University of Pula).

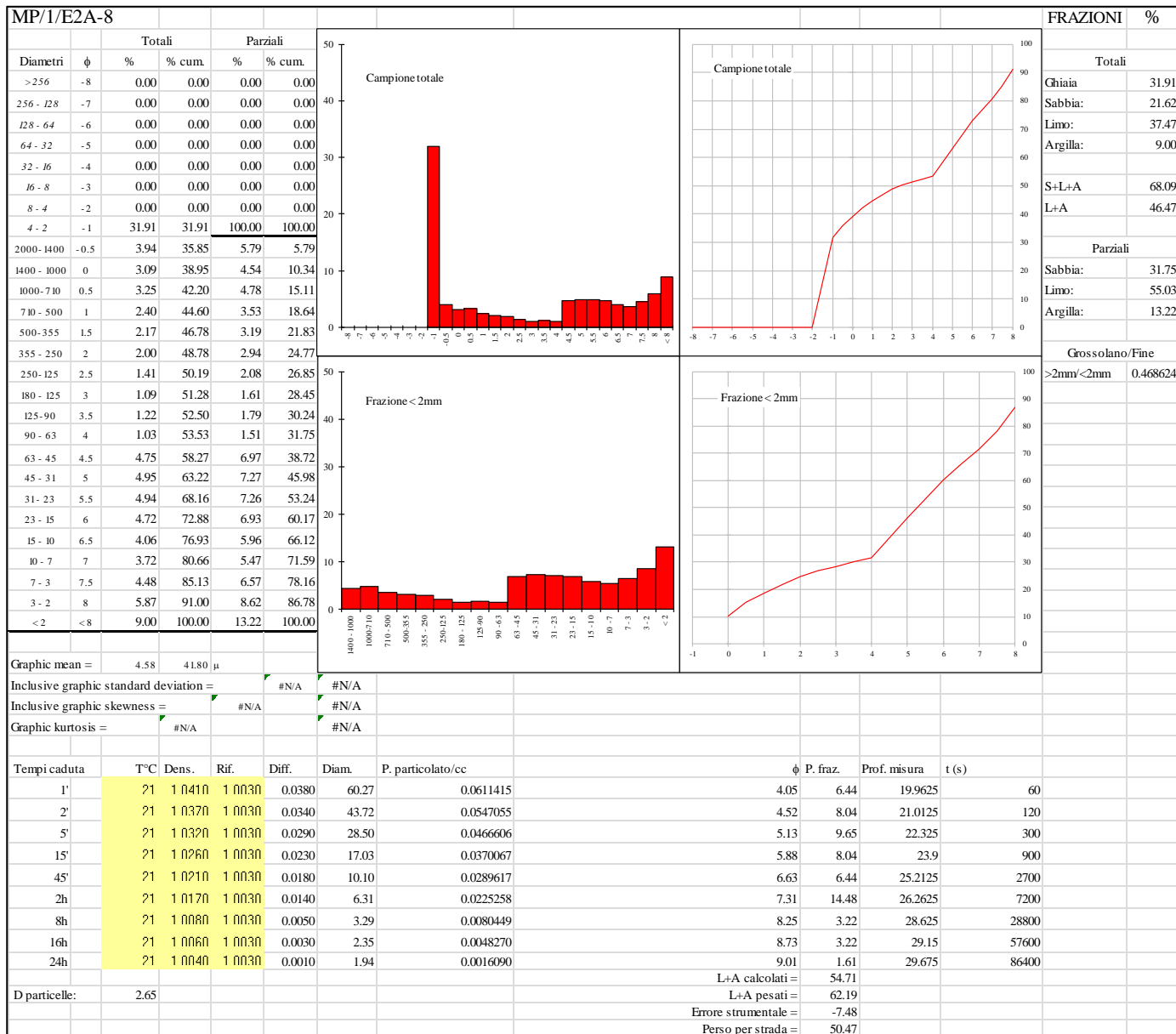
Bibliography: bib.irb.hr, unipu.academia.edu, scholar.google.hr

Životopis

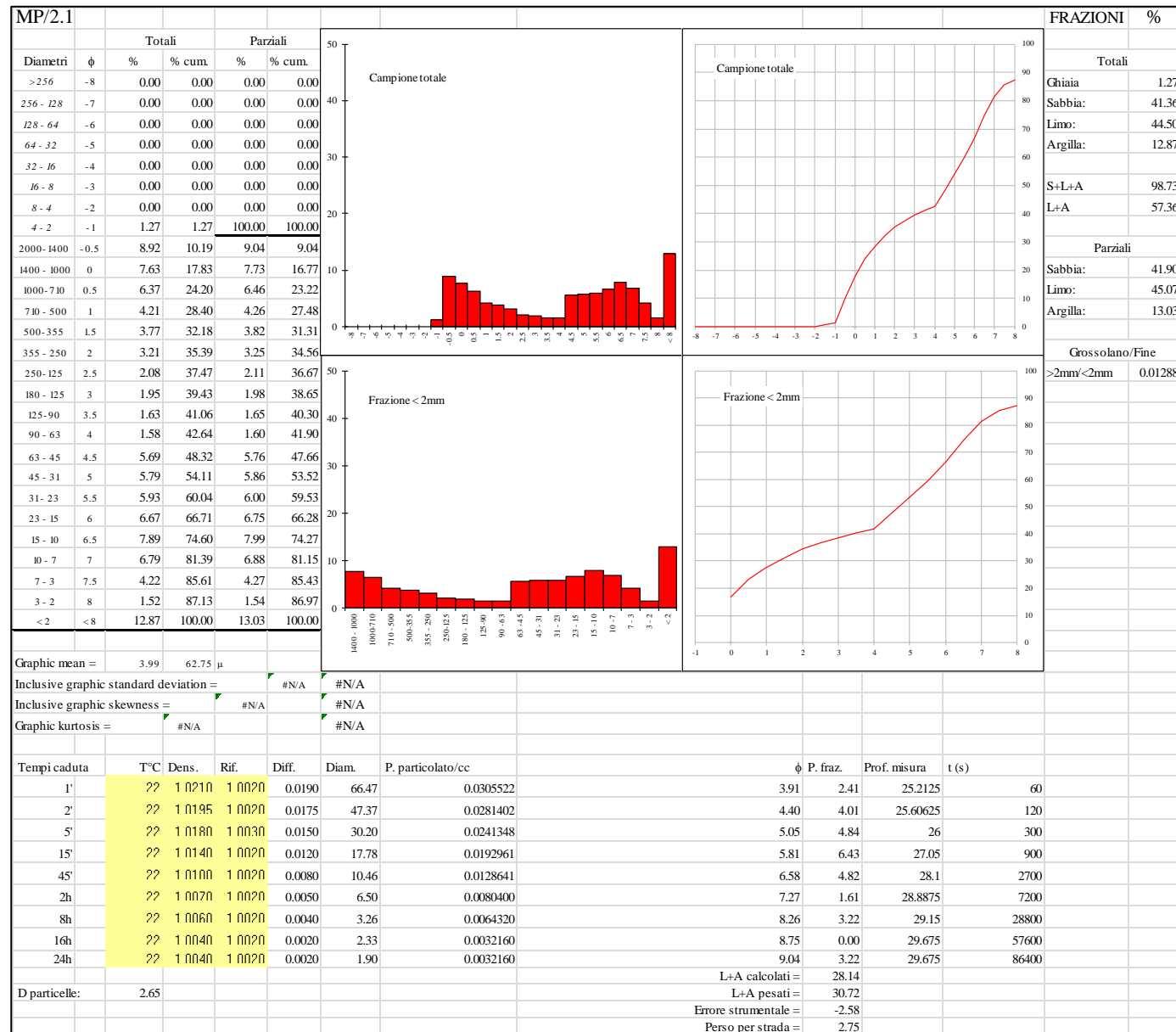
Katarina Gerometta rođena je u Puli (1982.), diplomirala je arheologiju, povijest umjetnosti i talijanistiku na Filozofskome fakultetu Sveučilišta u Zagrebu. Godine 2009. na istom je sveučilištu upisala Poslijediplomski doktorski studij arheologije. Znanstvena je novakinja na Odsjeku za povijest Filozofskoga fakulteta Sveučilišta Jurja Dobrile u Puli, gdje je zaposlena od prosinca 2010. g. (predaje predmete: Prapovijest hrvatskih zemalja, Povijest civilizacija, Povijest Mezopotamije). Stručno se usavršavala iz mikromorfologije tla na sveučilištima u Pisi, Londonu, Tübingenu i Cambridgeu. Sudjelovala je u brojnim arheološkim istraživanjima u Hrvatskoj, Italiji, Grčkoj, BiH, Srbiji, Francuskoj i Crnoj Gori. Područja istraživanja: geoarheologija, mikromorfologija, stratigrafija, interakcija čovjeka i okoliša u prošlosti. Suradnica je na projektima *Arheološka istraživanja kasnog pleistocena i ranog holocena u Limskom kanalu, Istra* (voditelj doc. dr. sc. I. Janković) i *Rimskodobne preobrazbe prapovijesnih gradina u Istri* (voditeljica prof. dr. sc. K. Buršić-Matijašić).

Bibliografija: bib.irb.hr, unipu.academia.edu, scholar.google.hr

**Appendix 1.1. Grain-size
(Wentworth, 1922) of the <2 mm
fraction of undecalcified samples
from Mujina Pećina, SU E2A.**

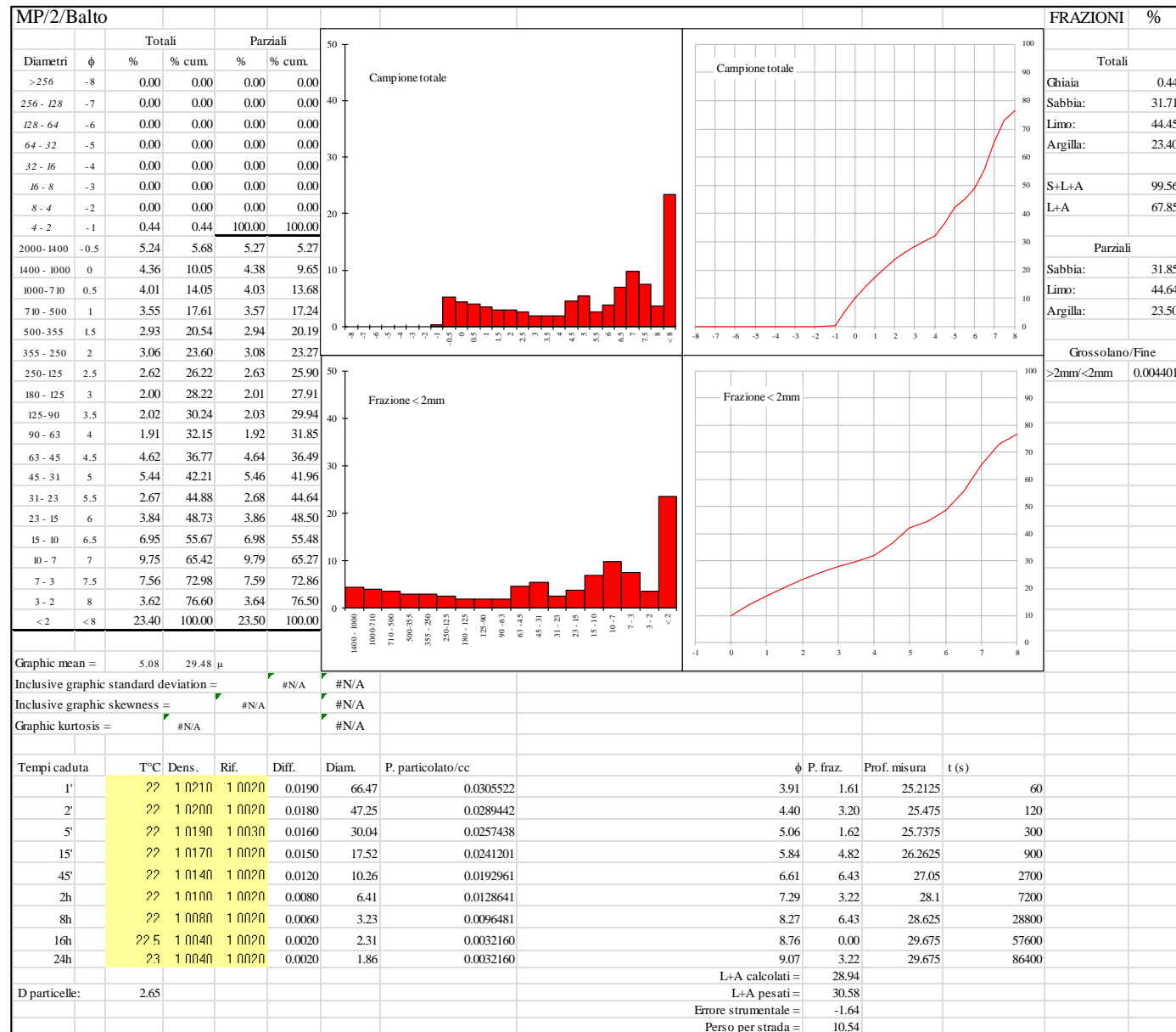


**Appendix 1.2. Grain-size
(Wentworth, 1922) of the <2 mm
fraction of undecalcified samples
from Mujina Pećina, SU B.**

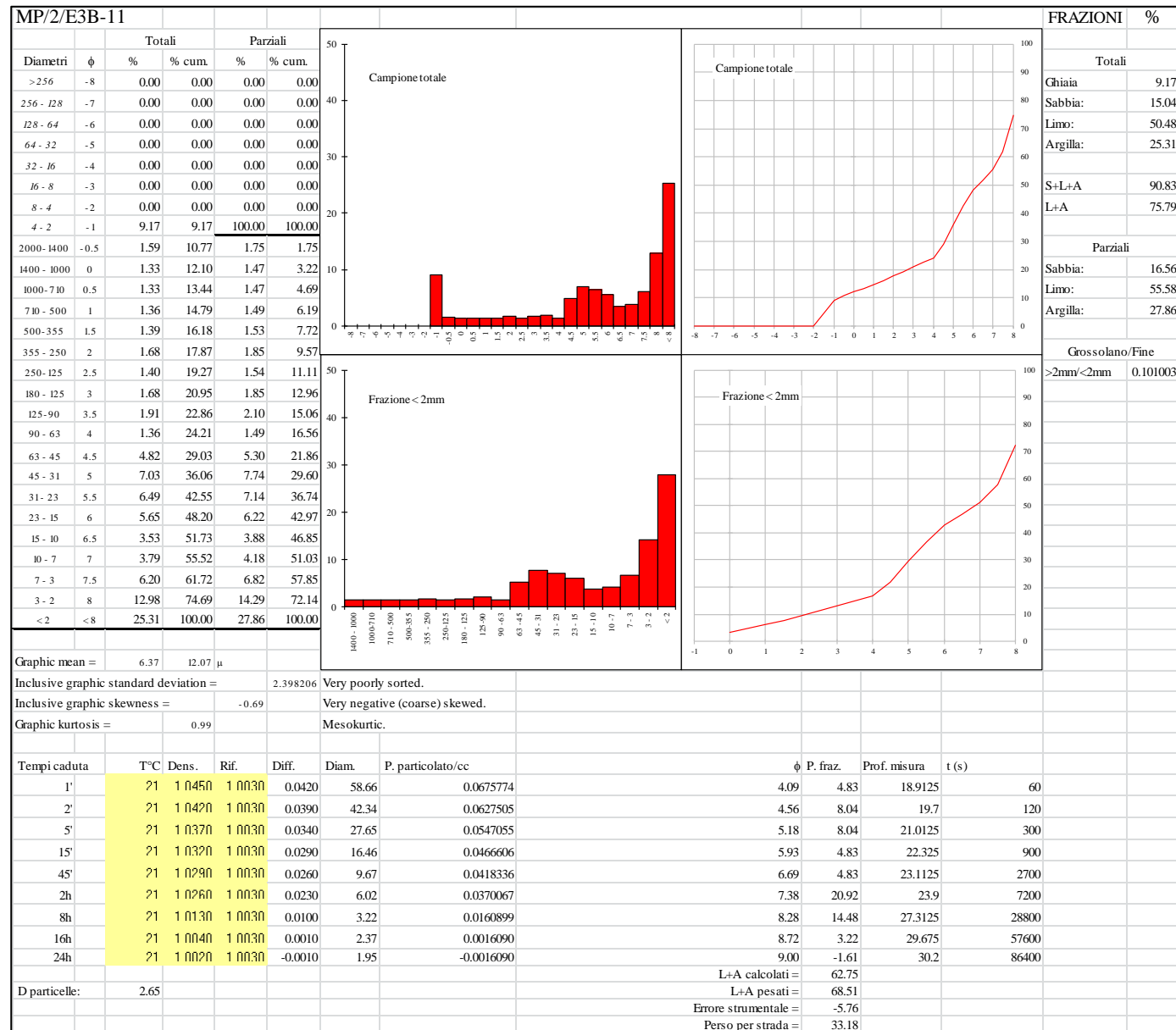


**Appendix 1.3. Grain-size
(Wentworth, 1922) of the <2 mm
fraction of undecalcified samples
from Mujina Pećina, SU B.**

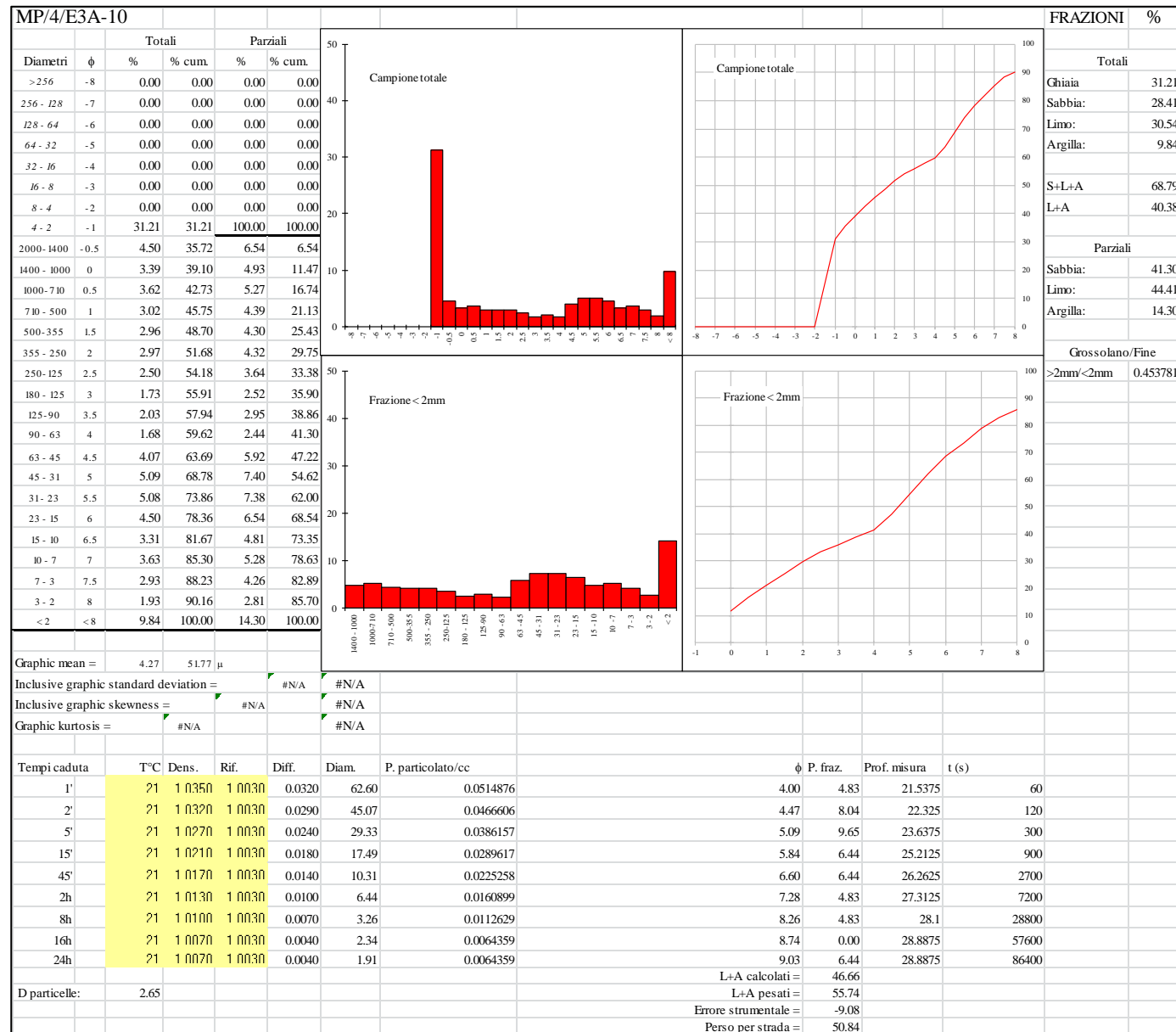
•



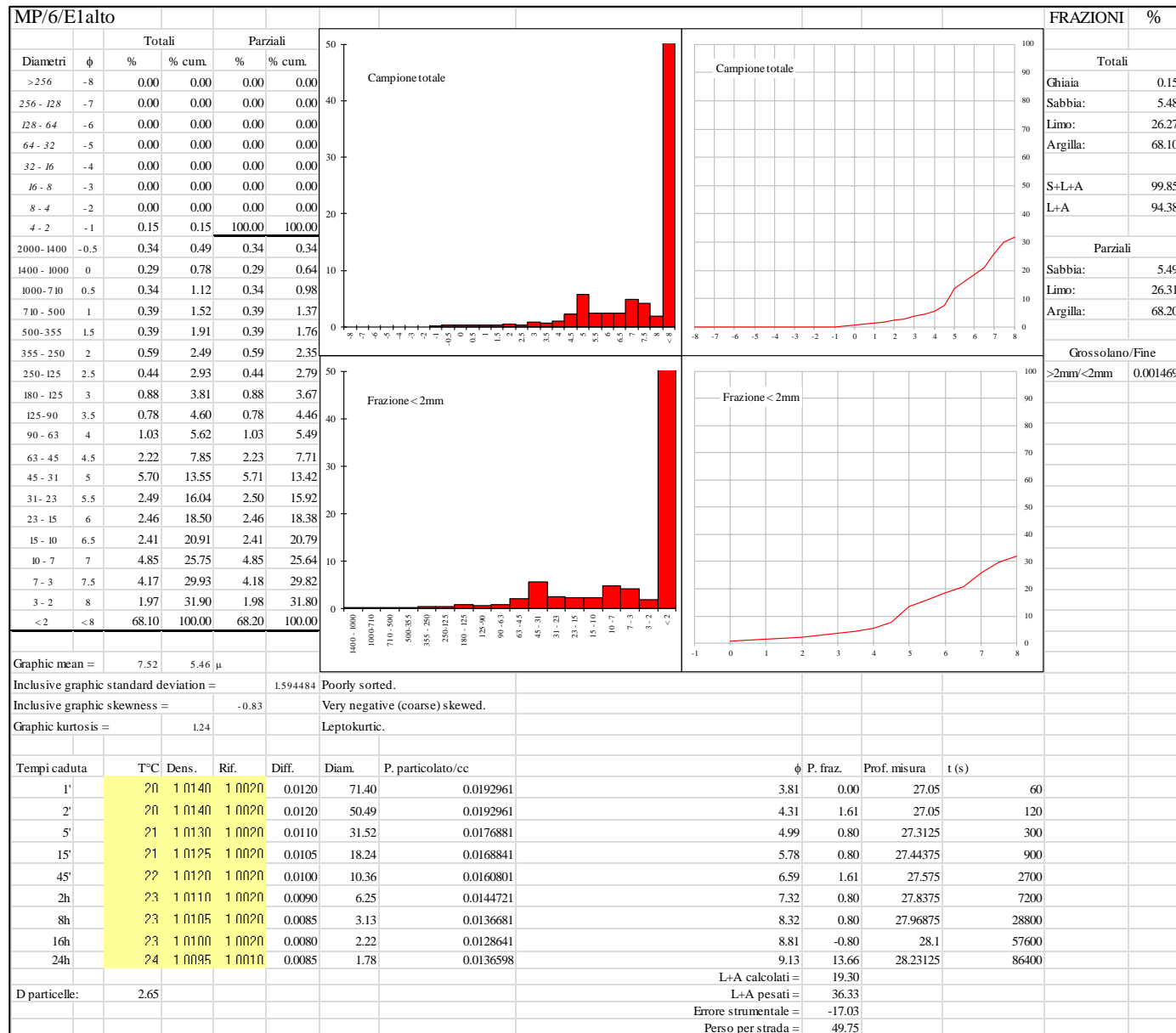
**Appendix 1.4. Grain-size
(Wentworth, 1922) of the <2 mm
fraction of undecalcified samples
from Mujina Pećina, SU E3B.**



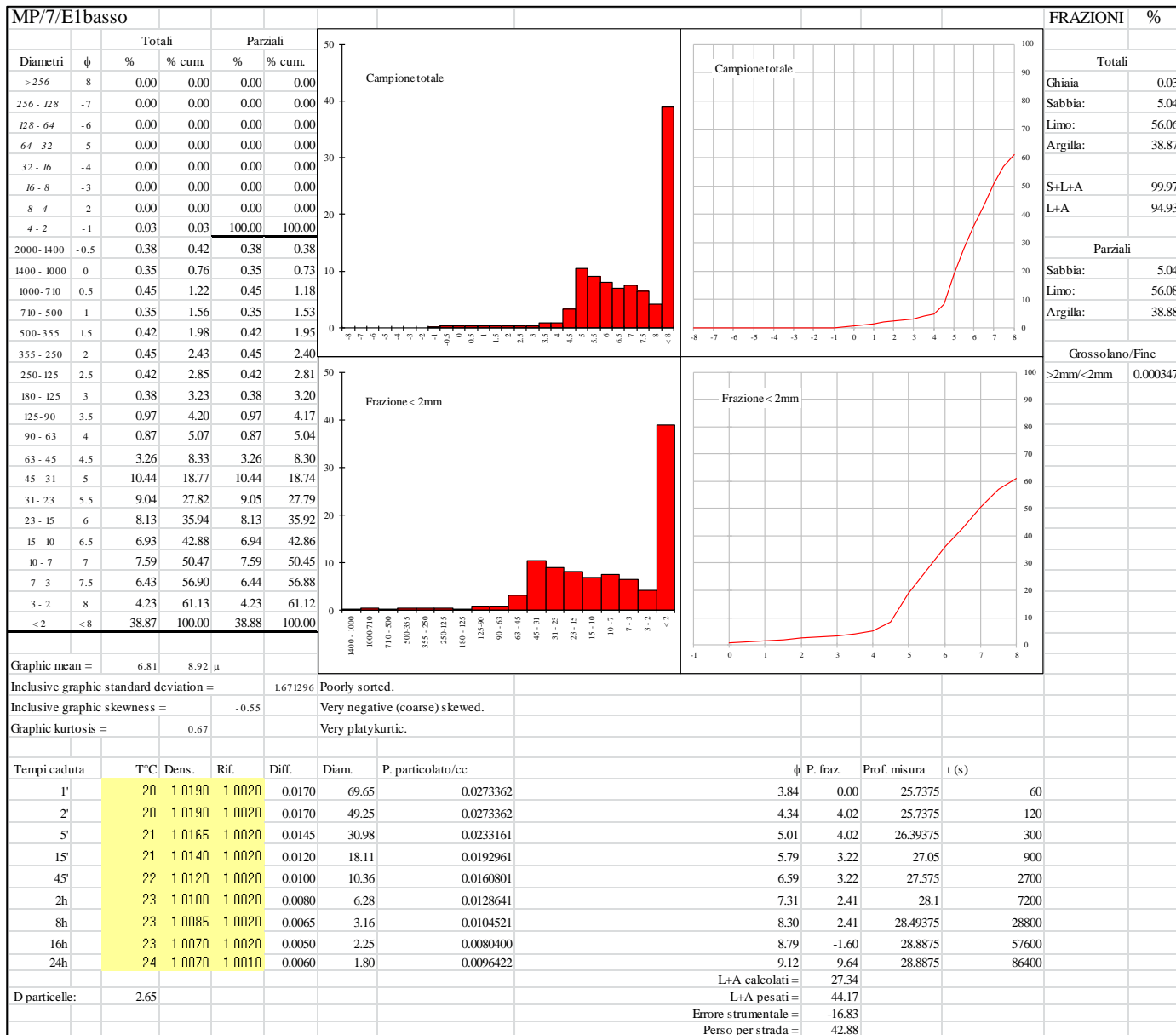
**Appendix 1.5. Grain-size
(Wentworth, 1922) of the <2 mm
fraction of undecalcified samples
from Mujina Pećina, SU E3A.**



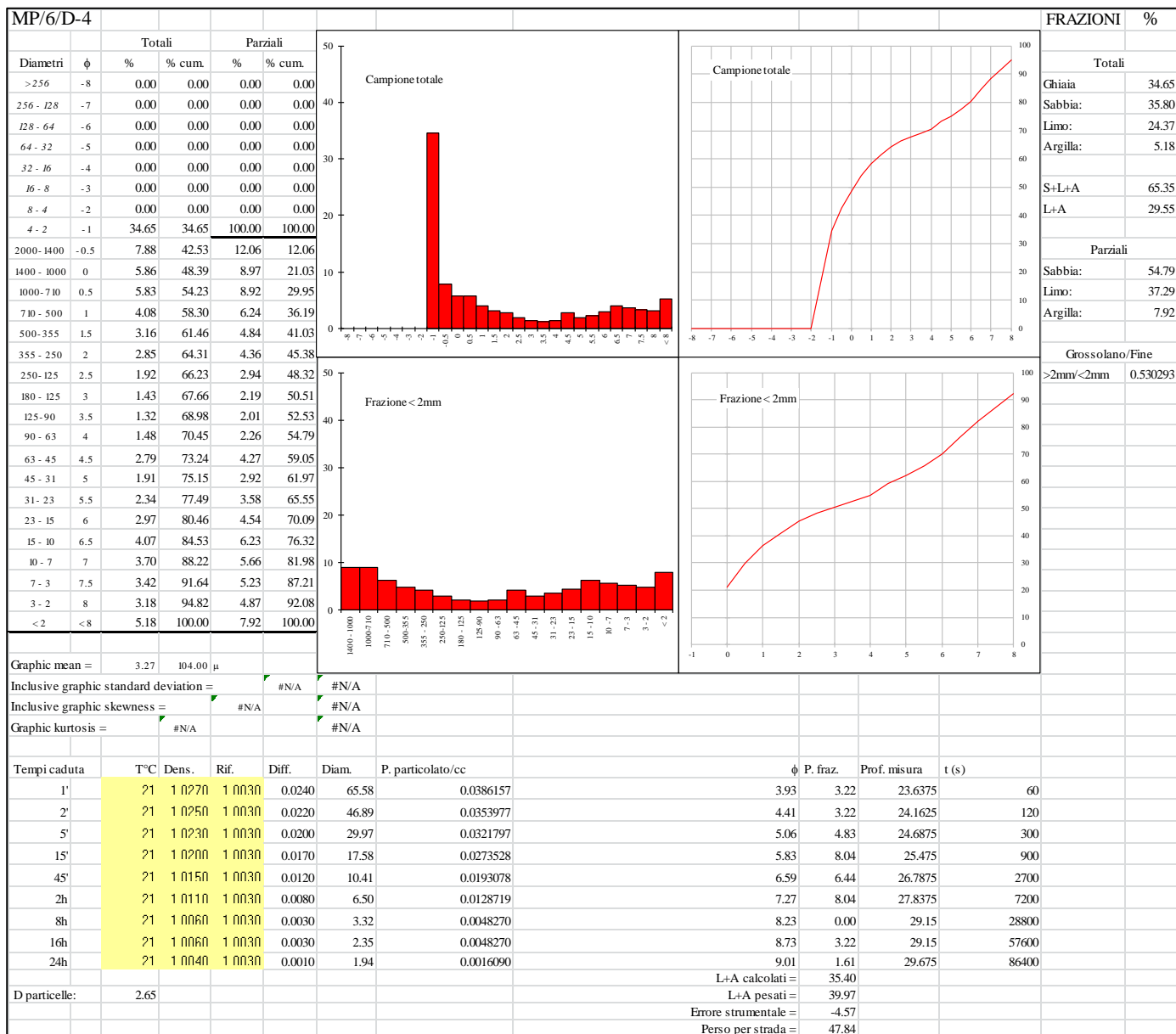
**Appendix 1.6. Grain-size
(Wentworth, 1922) of the <2 mm
fraction of undecalcified samples
from Mujina Pećina, SU E1.**



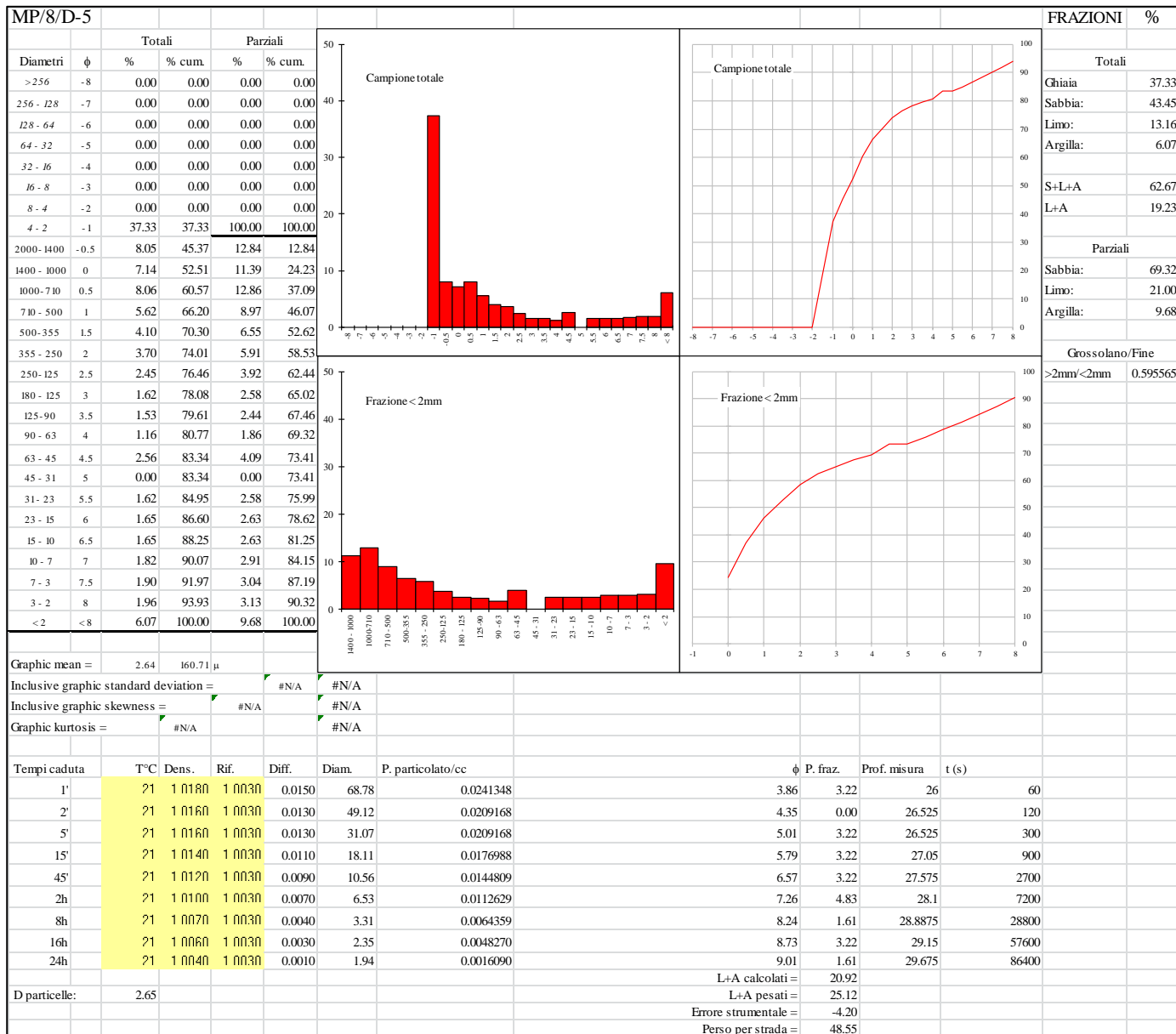
**Appendix 1.7. Grain-size
(Wentworth, 1922) of the <2 mm
fraction of undecalcified samples
from Mujina Pećina, SU E1.**



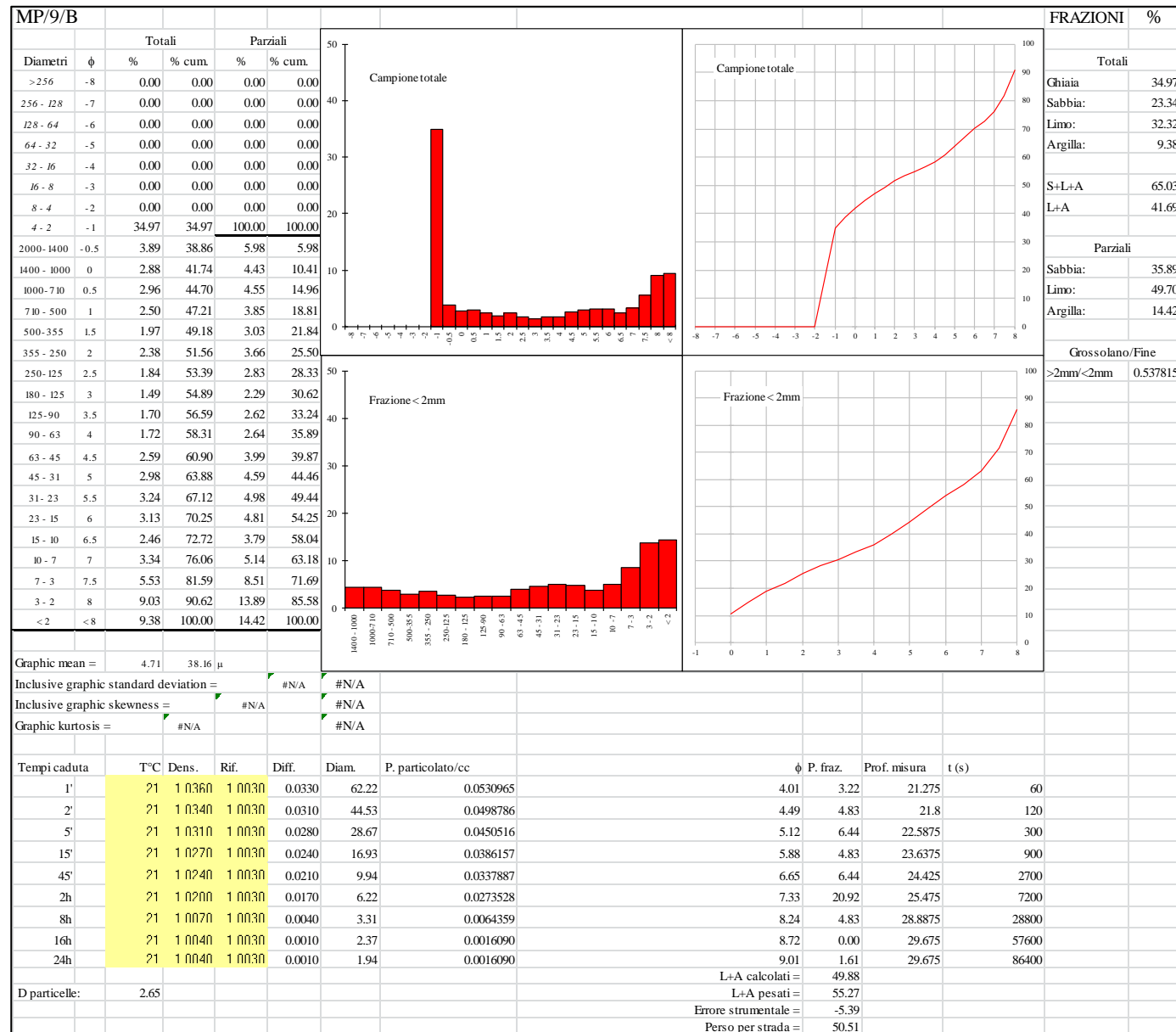
**Appendix 1.8. Grain-size
(Wentworth, 1922) of the <2 mm
fraction of undecalcified samples
from Mujina Pećina, SU D.4.**



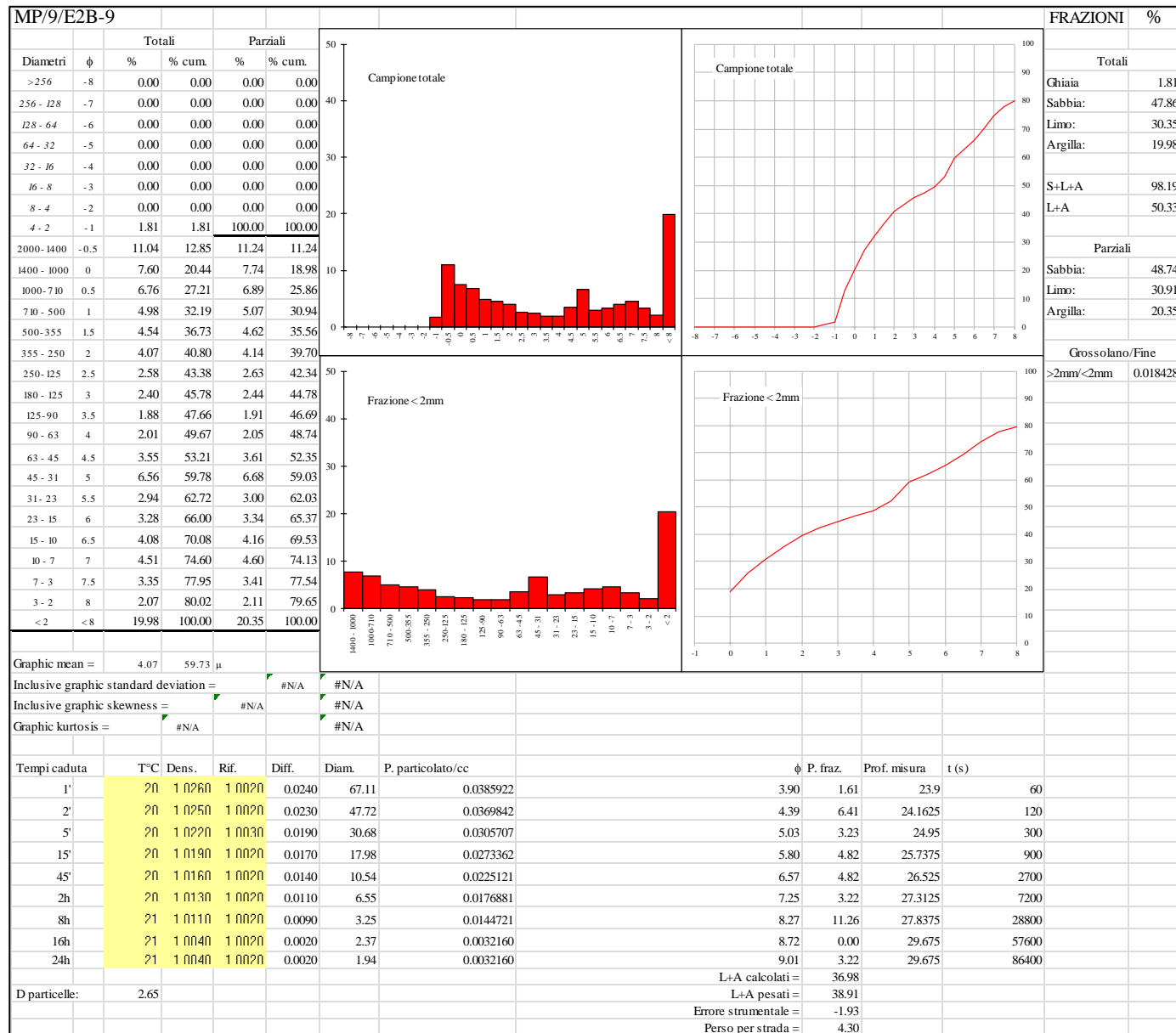
**Appendix 1.9. Grain-size
(Wentworth, 1922) of the <2 mm
fraction of undecalcified samples
from Mujina Pećina, SU D.5.**



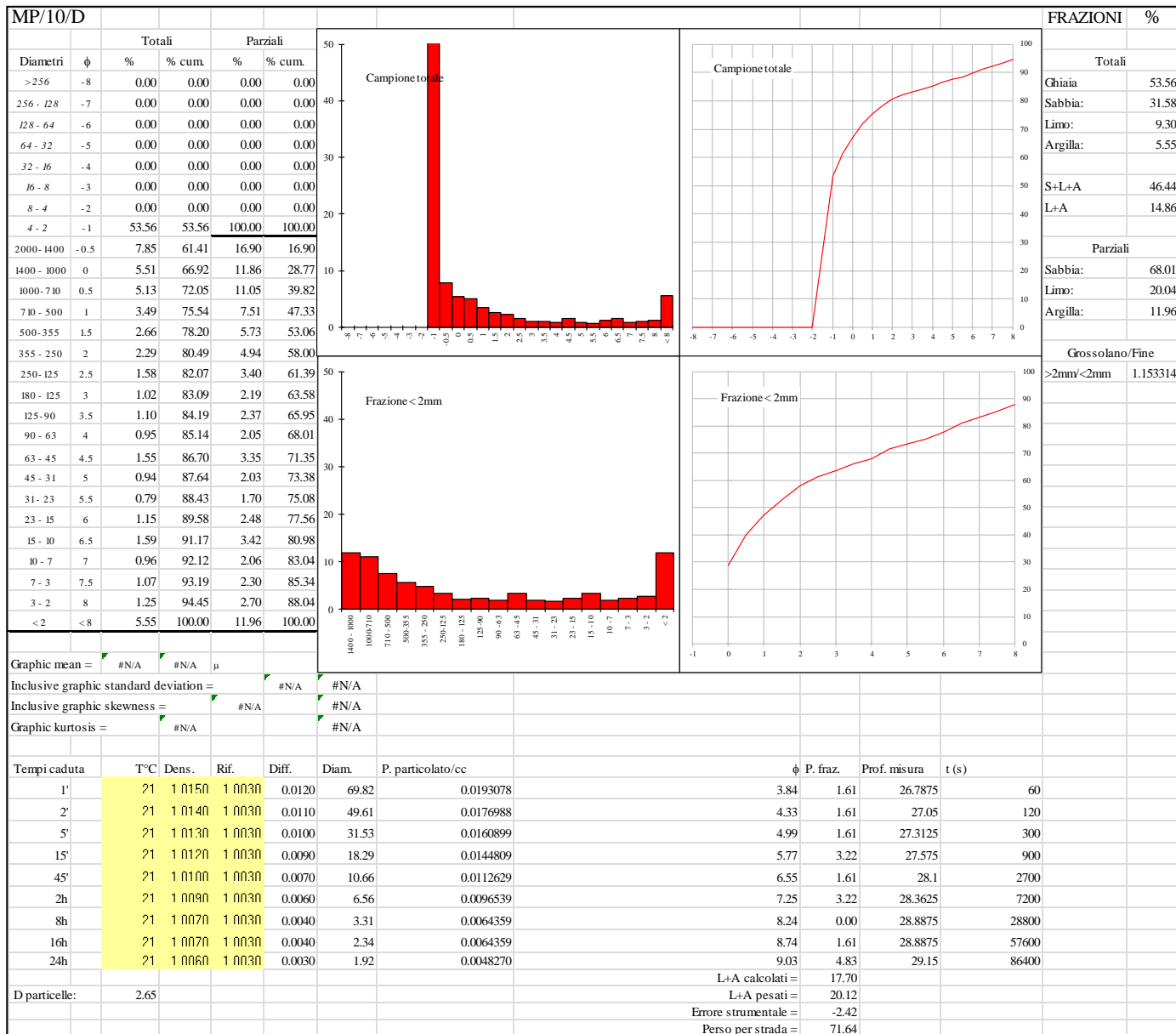
**Appendix 1.10. Grain-size
(Wentworth, 1922) of the <2 mm
fraction of undecalcified samples
from Mujina Pećina, SU B.**



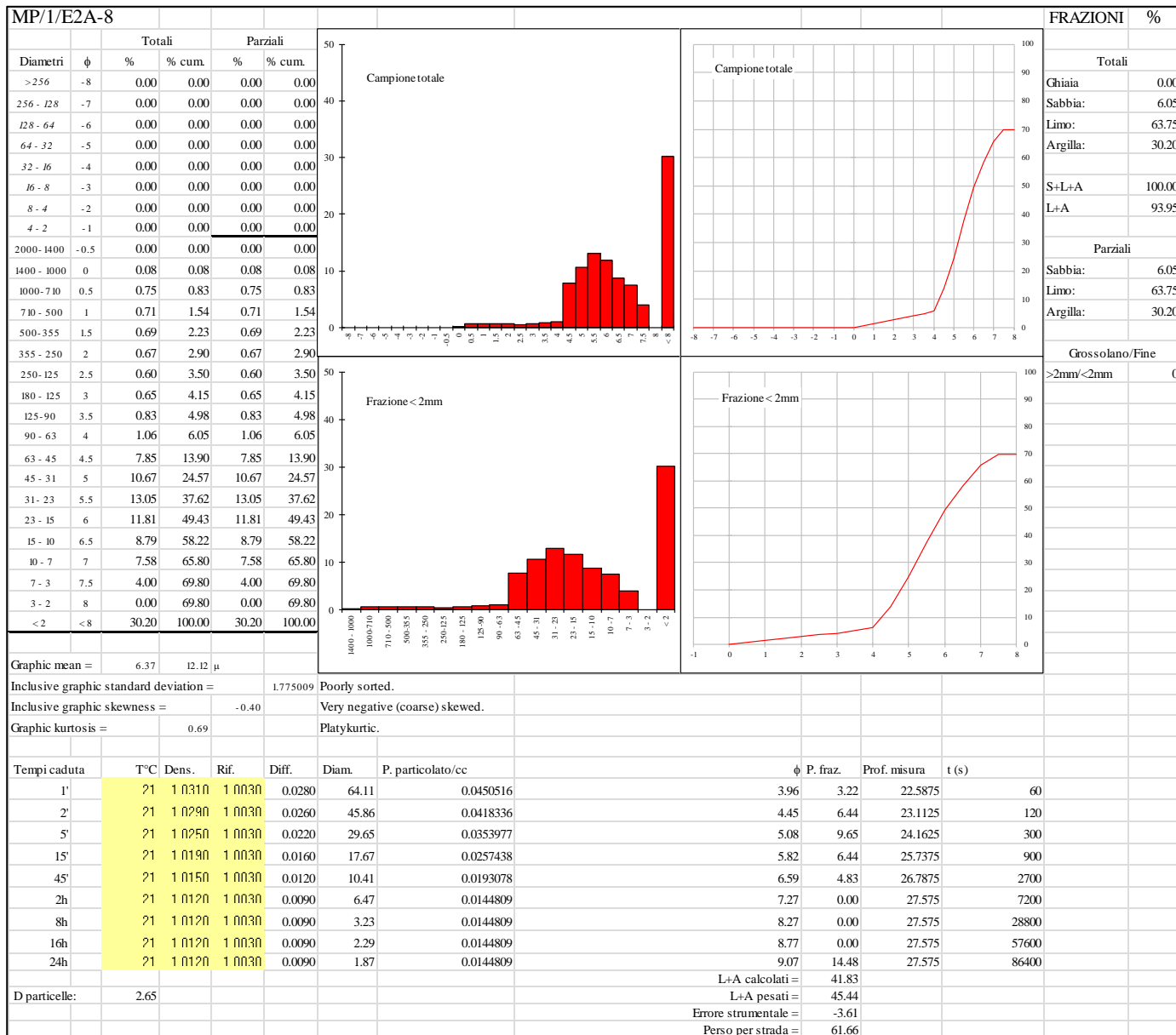
**Appendix 1.11. Grain-size
(Wentworth, 1922) of the <2 mm
fraction of undecalcified samples
from Mujina Pećina, SU E2B.**



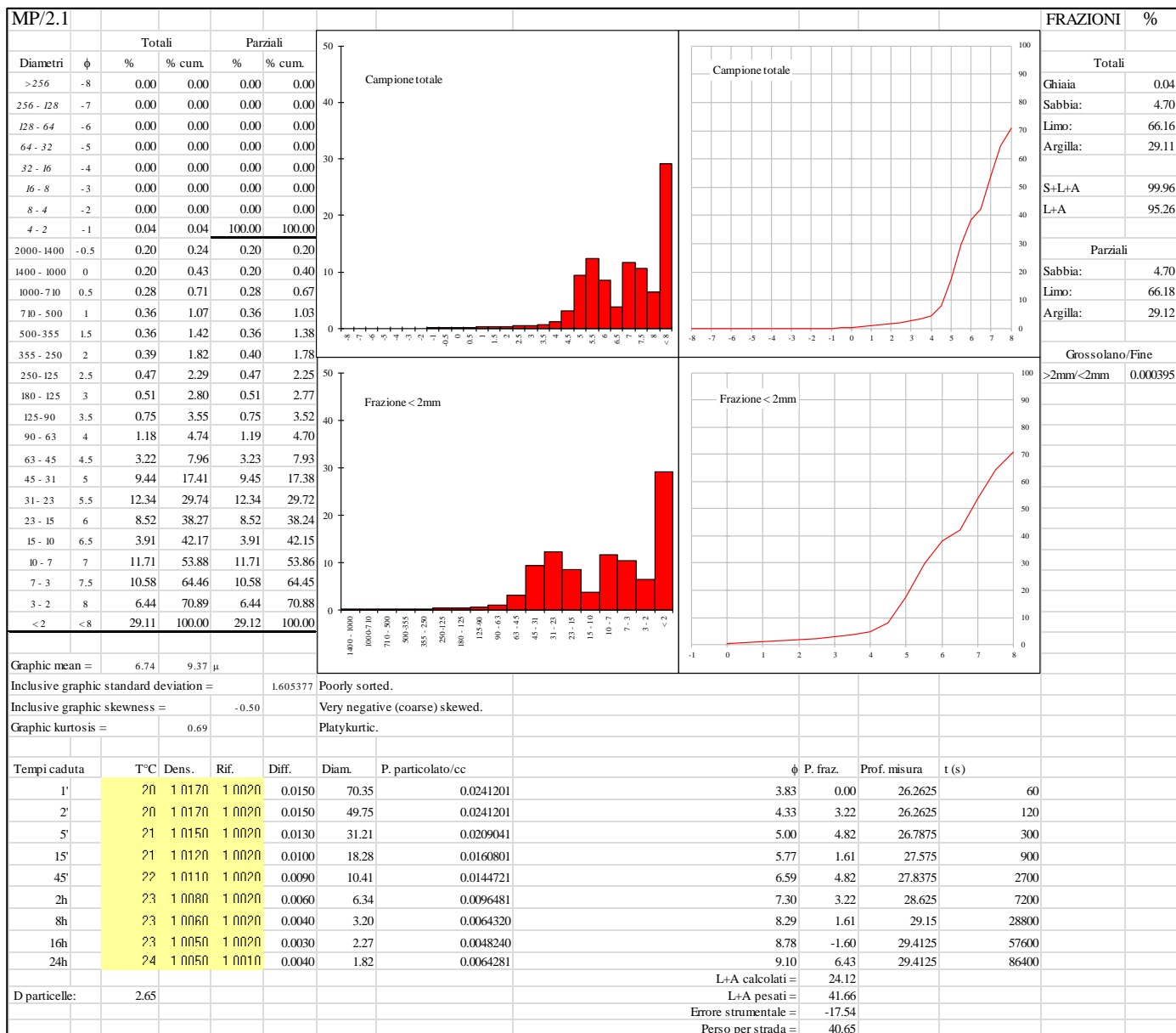
**Appendix 1.12. Grain-size
(Wentworth, 1922) of the <2 mm
fraction of undecalcified samples
from Mujina Pećina, SU D.**



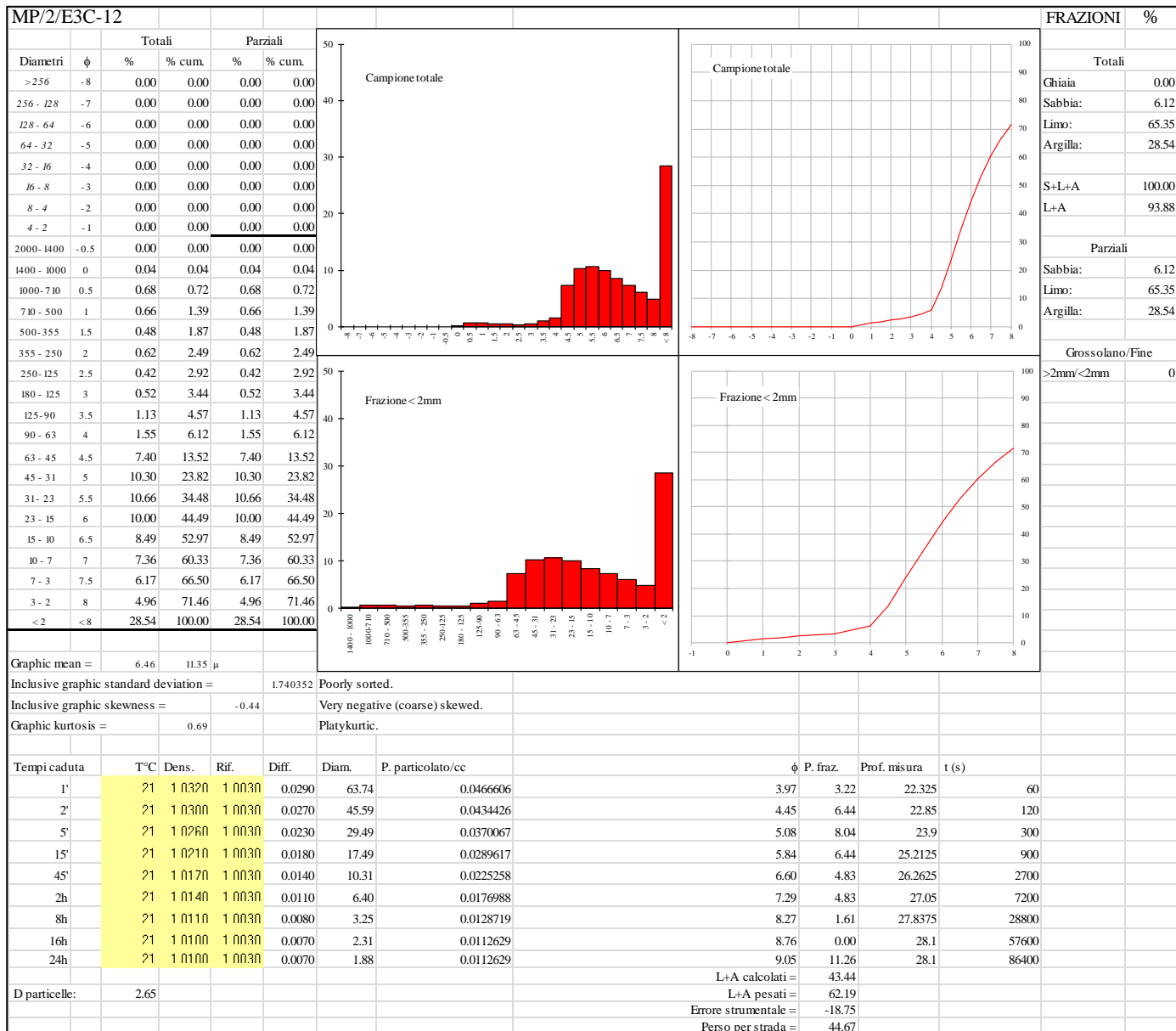
**Appendix 2.1. Grain-size
(Wentworth, 1922) of the <2 mm
fraction of decalcified samples
from Mujina Pećina, SU E2A.**



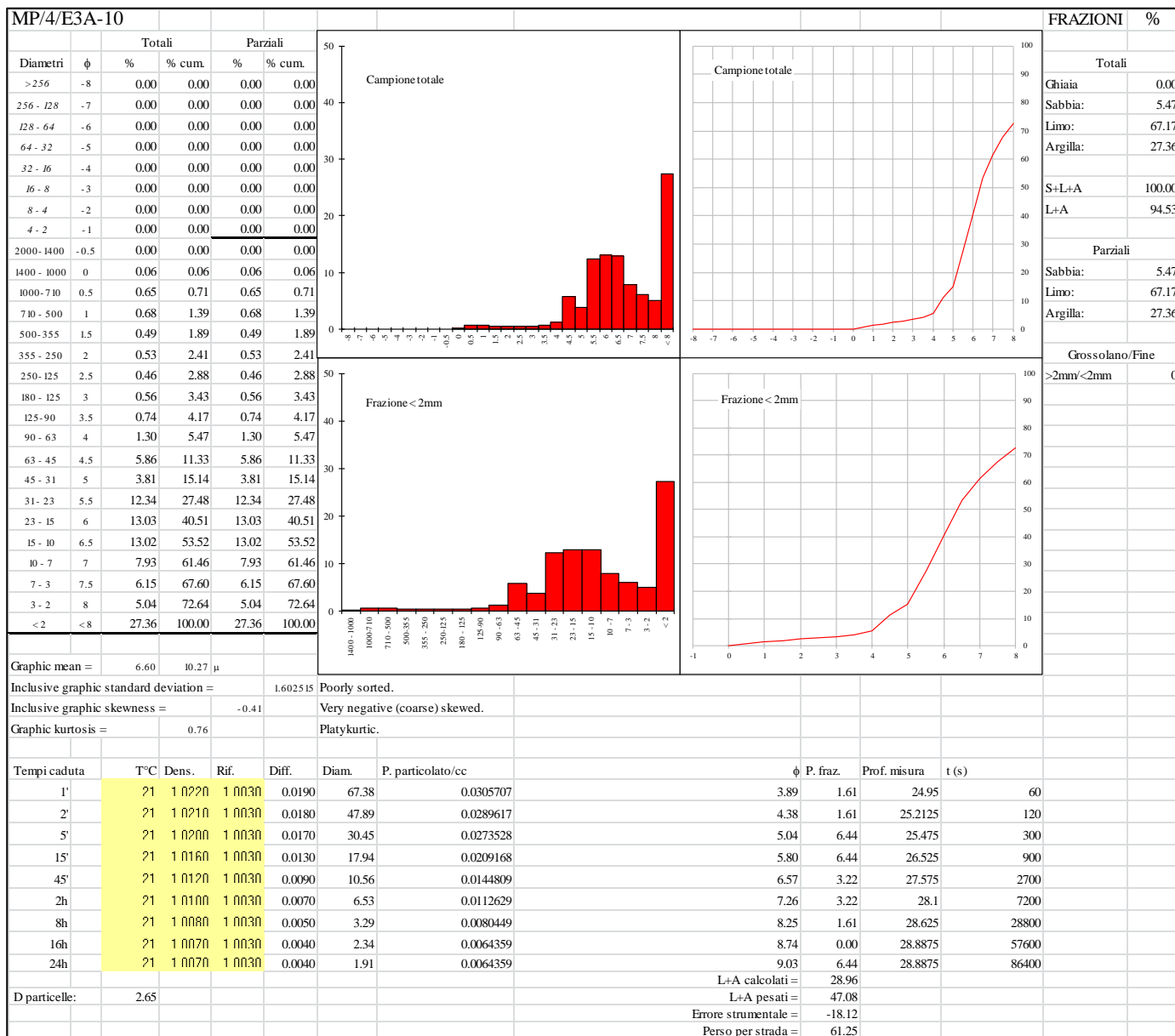
**Appendix 2.2. Grain-size
(Wentworth, 1922) of the <2 mm
fraction of decalcified samples
from Mujina Pećina, SU B.**



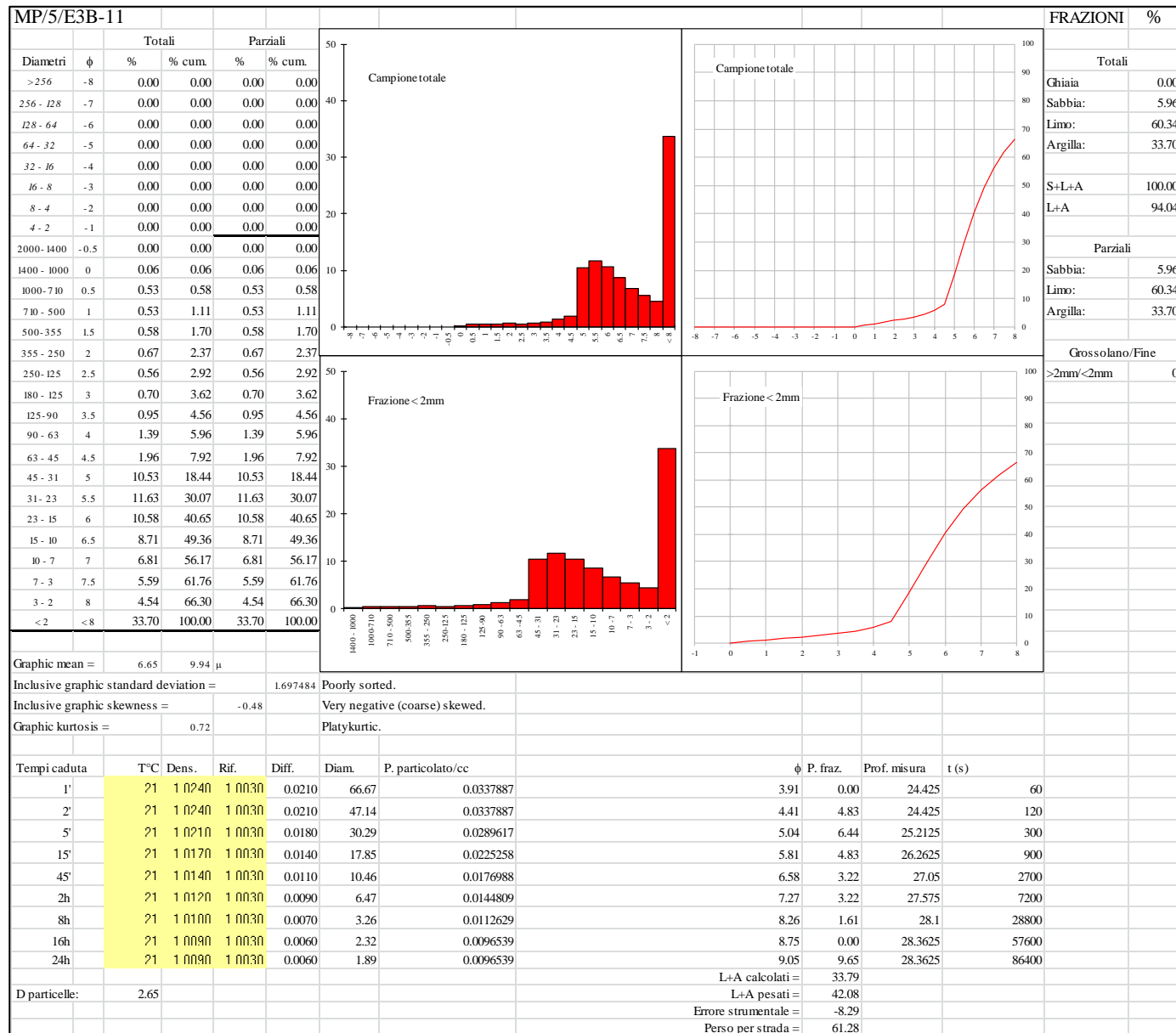
**Appendix 2.3. Grain-size
(Wentworth, 1922) of the <2 mm
fraction of decalcified samples
from Mujina Pećina, SU E3C**



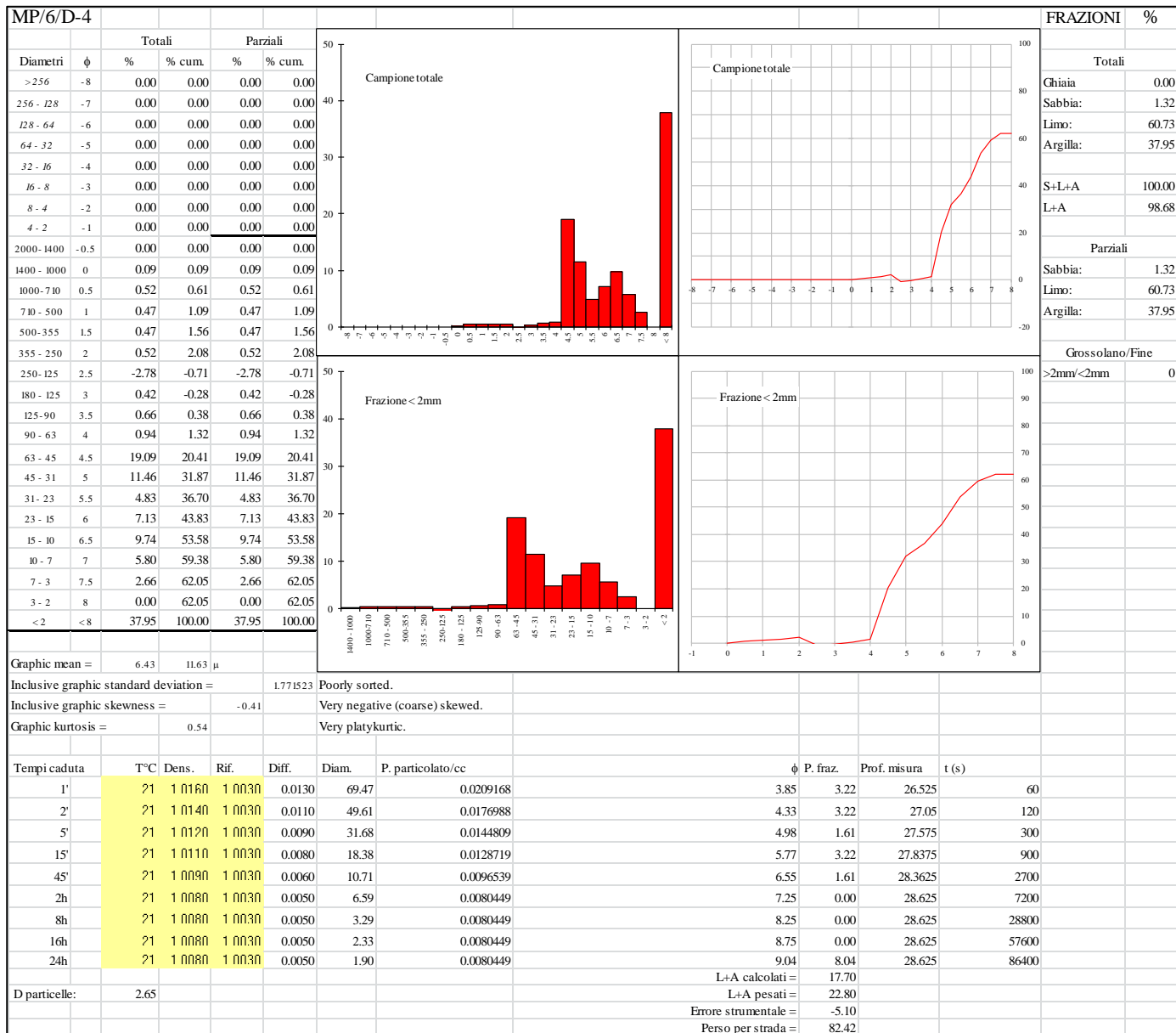
**Appendix 2.4. Grain-size
(Wentworth, 1922) of the <2 mm
fraction of decalcified samples
from Mujina Pećina, SU E3A.**



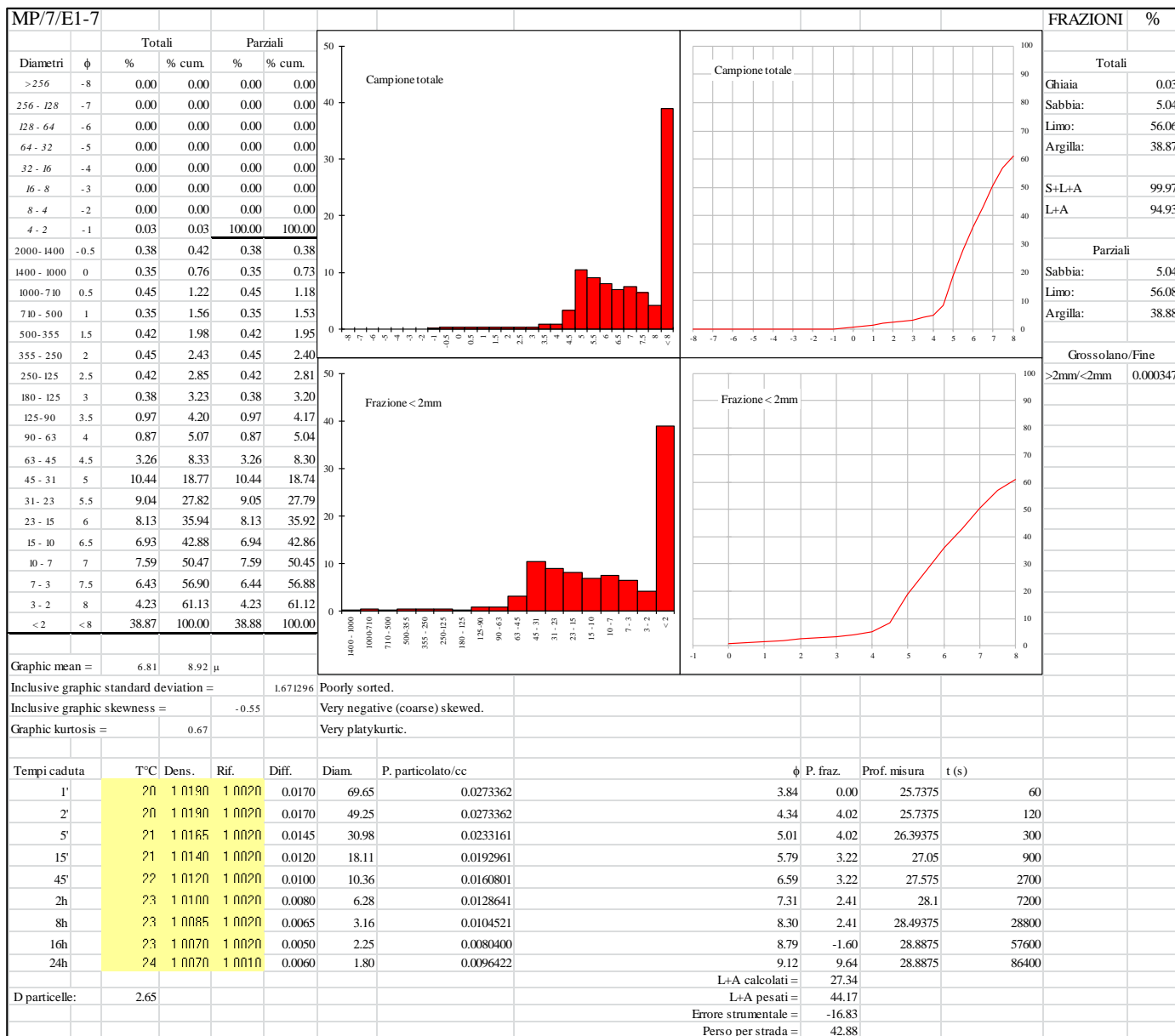
**Appendix 2.5. Grain-size
(Wentworth, 1922) of the <2 mm
fraction of decalcified samples
from Mujina Pećina, SU E3B.**



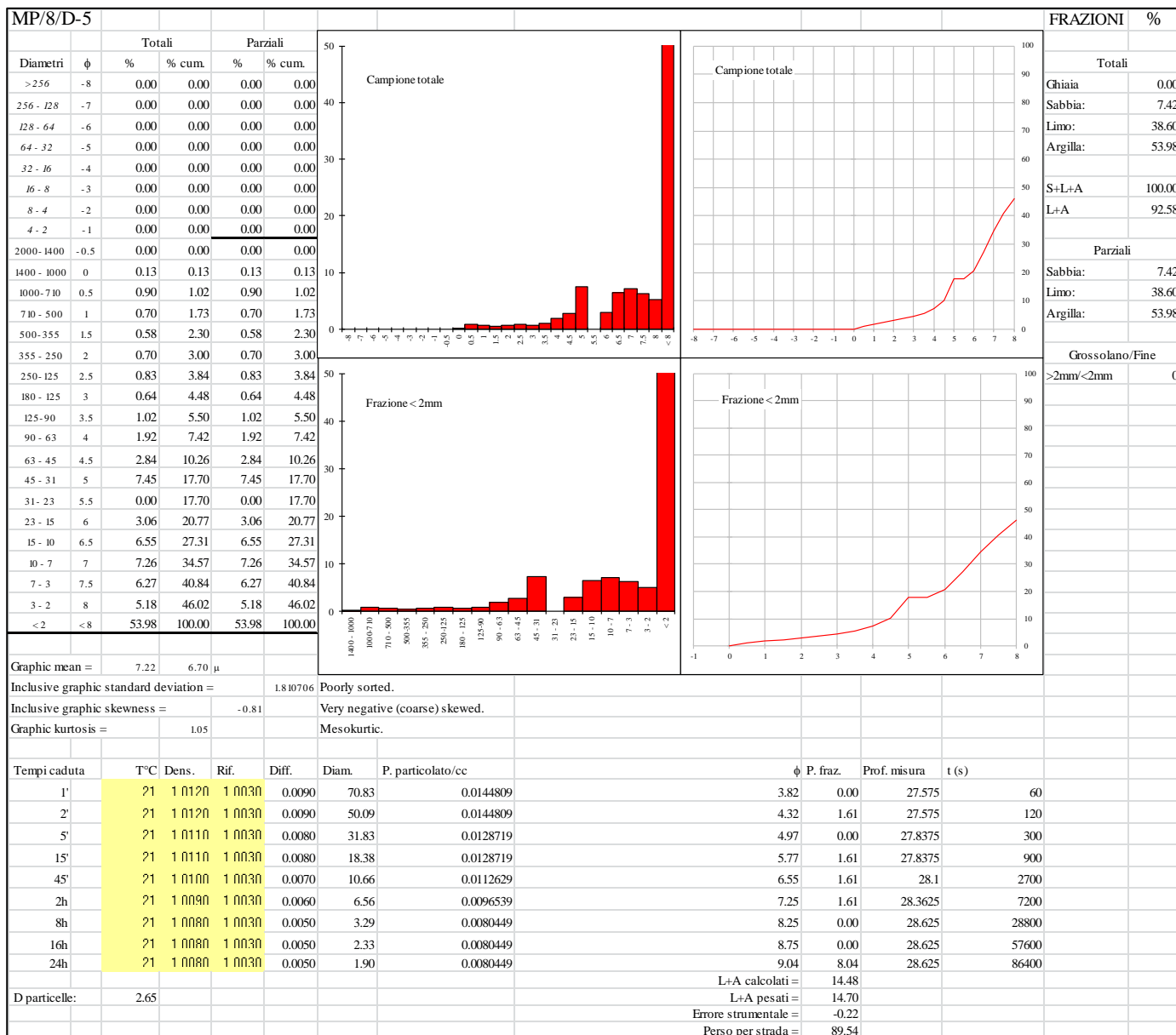
**Appendix 2.6. Grain-size
(Wentworth, 1922) of the <2 mm
fraction of decalcified samples
from Mujina Pećina, SU D.4.**



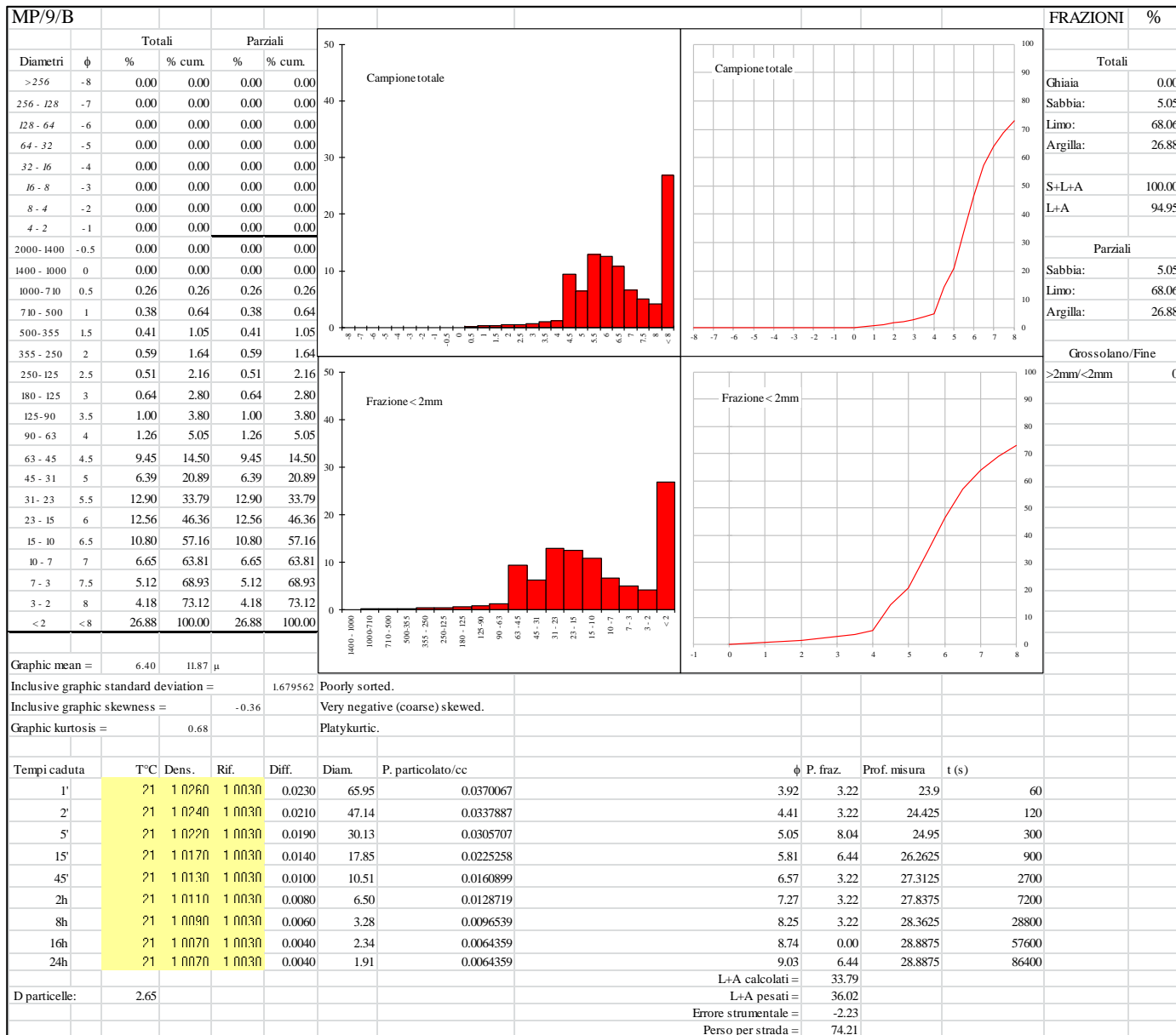
**Appendix 2.7. Grain-size
(Wentworth, 1922) of the <2 mm
fraction of decalcified samples
from Mujina Pećina, SU E1.**



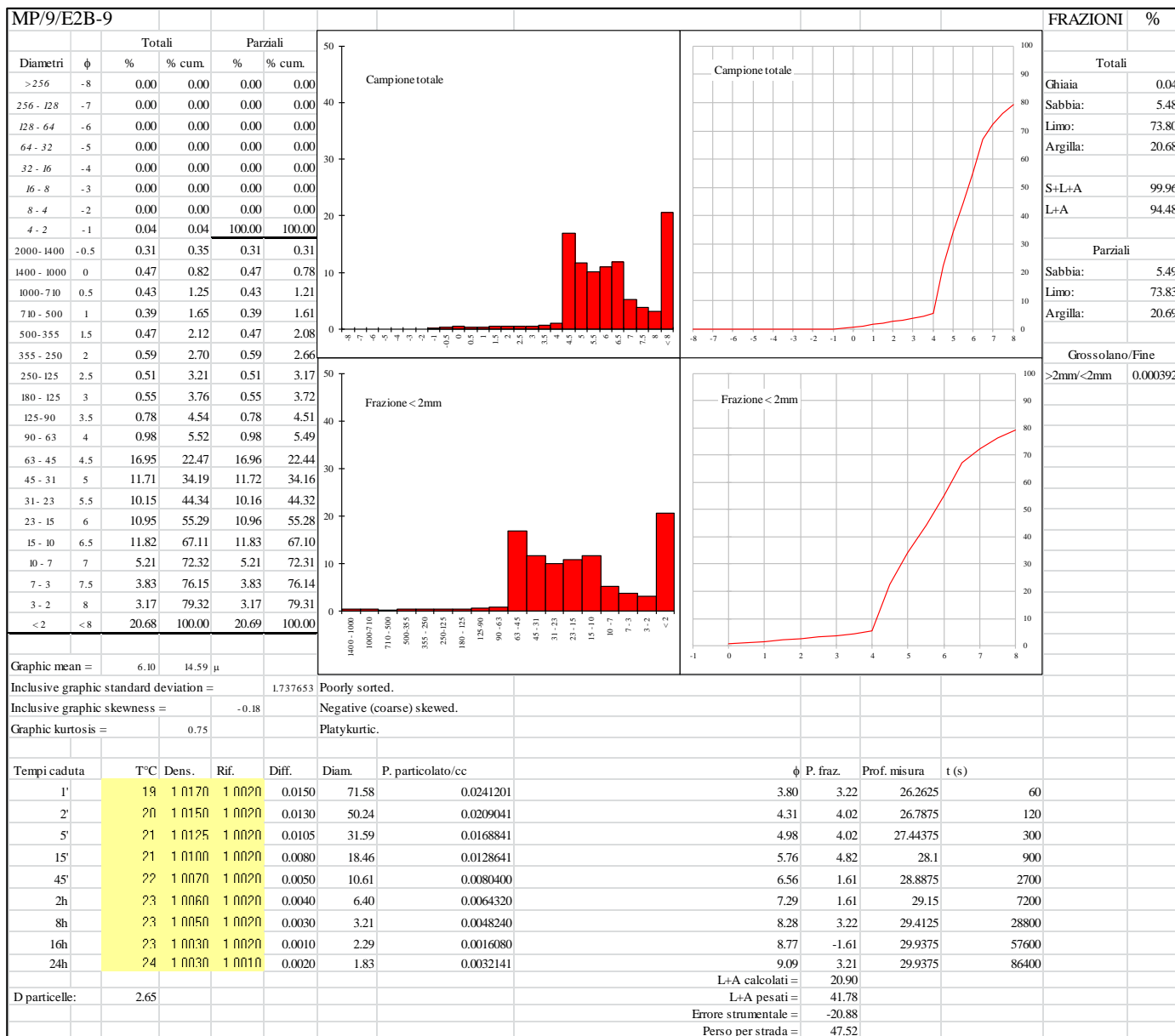
**Appendix 2.8. Grain-size
(Wentworth, 1922) of the <2 mm
fraction of decalcified samples
from Mujina Pećina, SU D.5.**



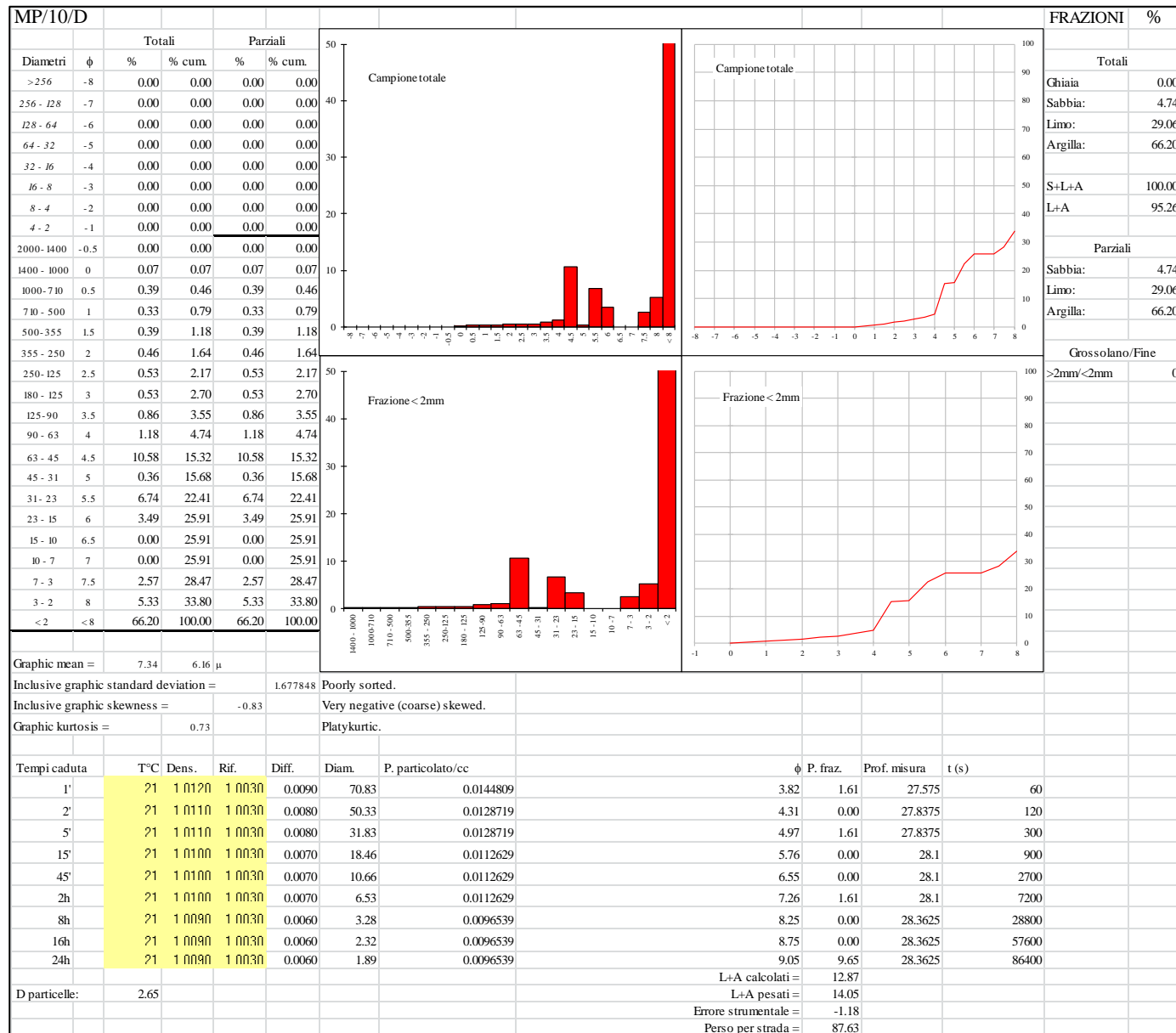
**Appendix 2.9. Grain-size
(Wentworth, 1922) of the <2 mm
fraction of decalcified samples
from Mujina Pećina, SU B.**



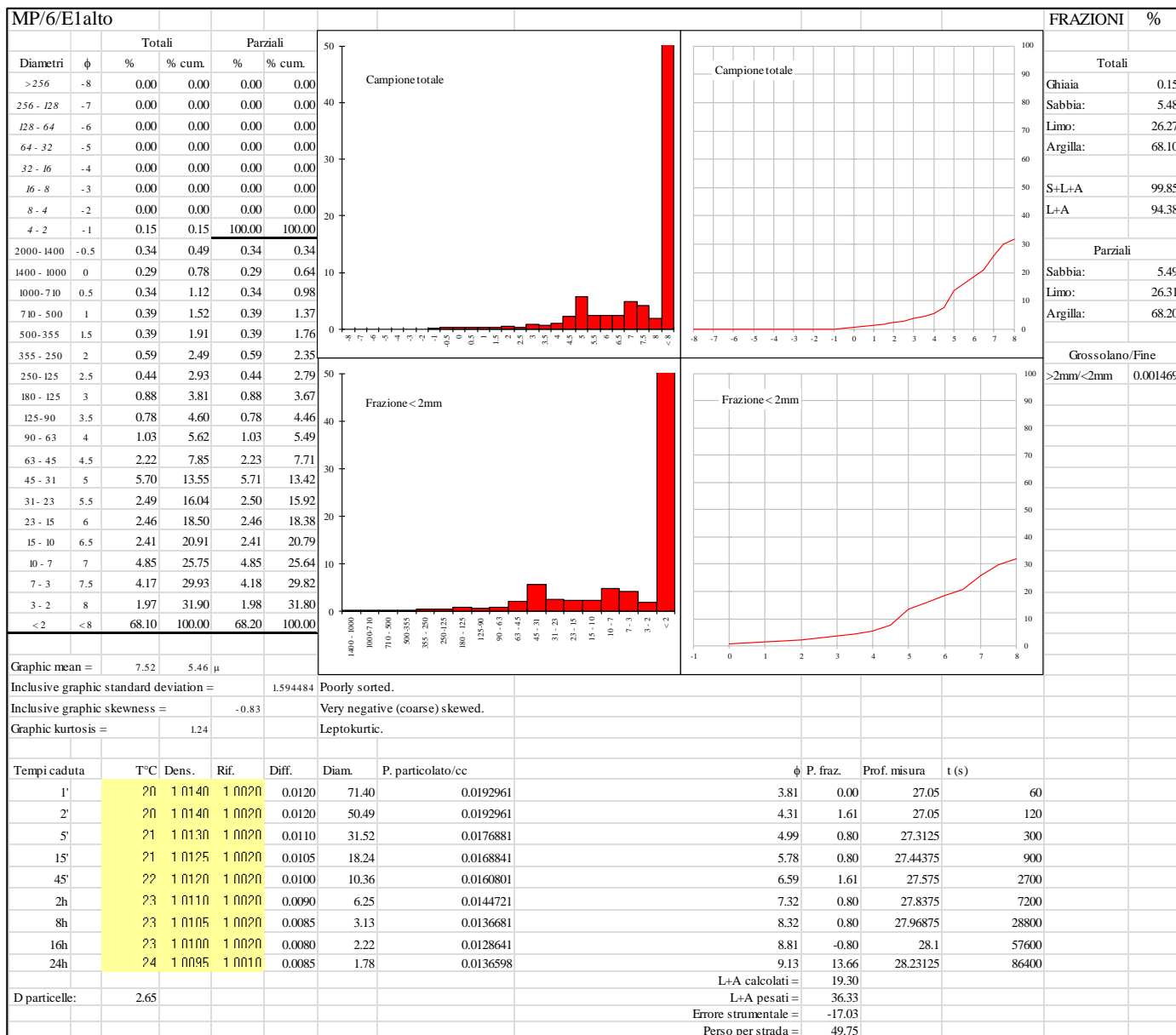
**Appendix 2.10. Grain-size
(Wentworth, 1922) of the <2 mm
fraction of decalcified samples
from Mujina Pećina, SU E2B.**



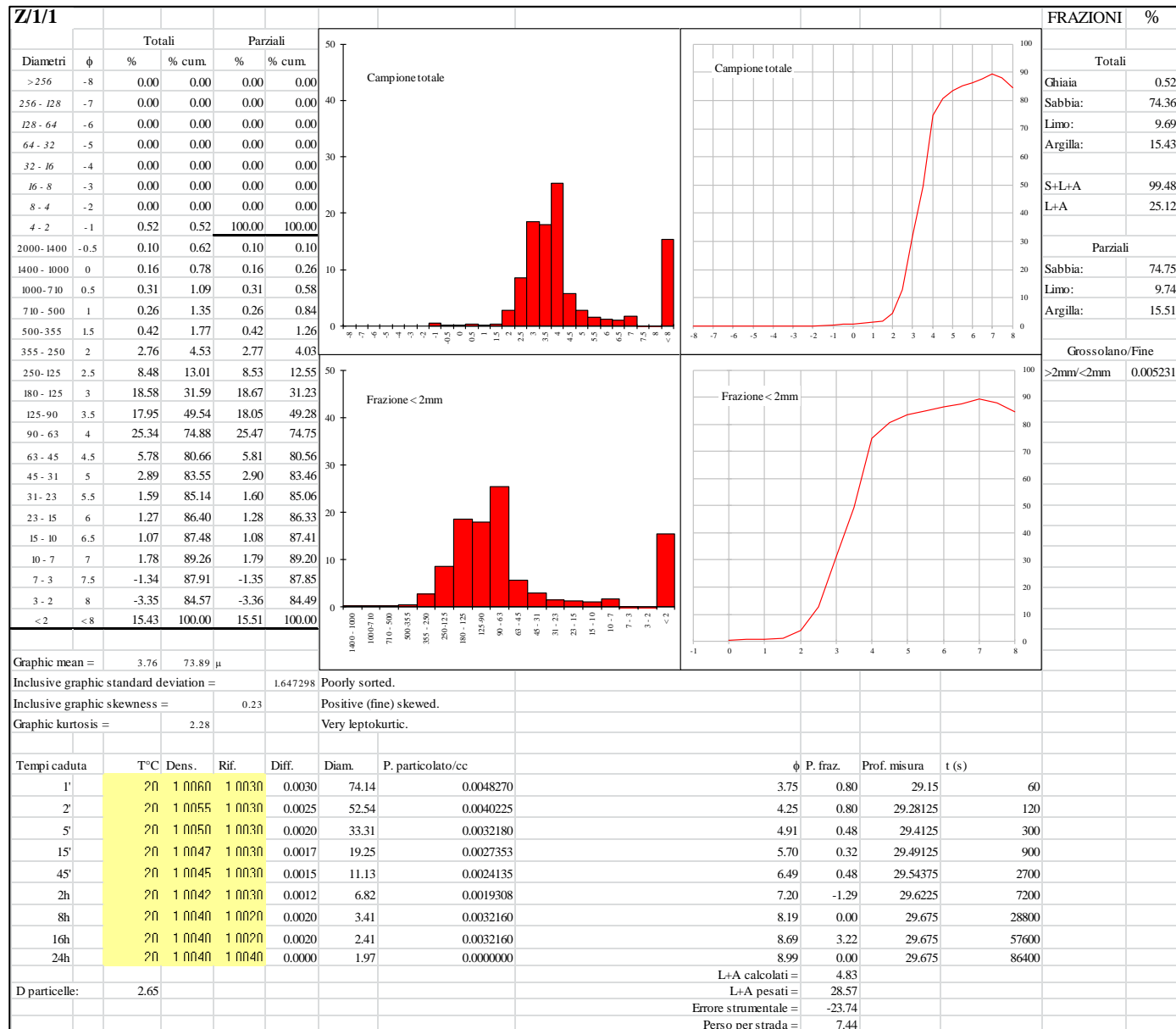
**Appendix 2.11. Grain-size
(Wentworth, 1922) of the <2 mm
fraction of decalcified samples
from Mujina Pećina, SU D.**



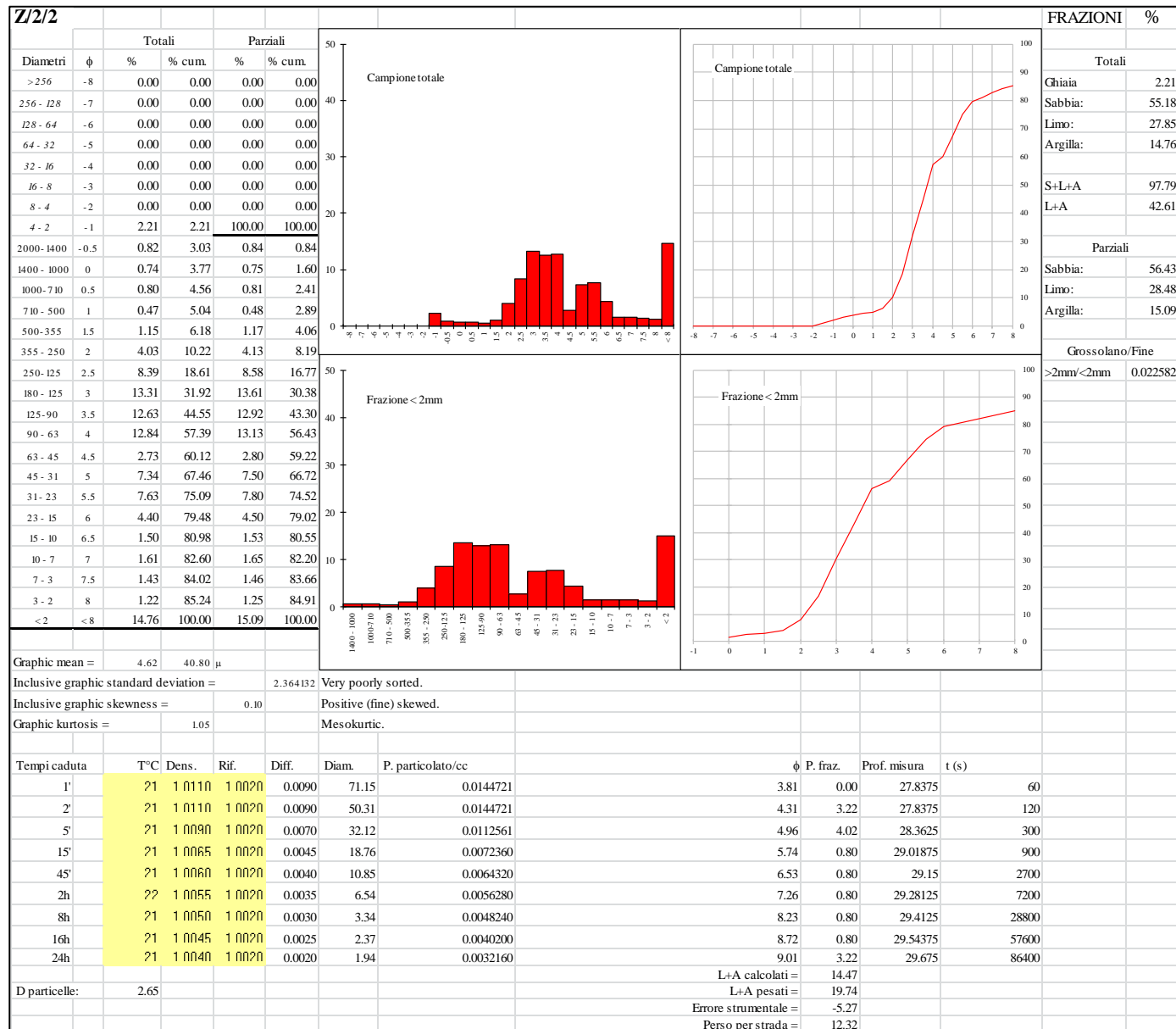
**Appendix 2.12. Grain-size
(Wentworth, 1922) of the <2 mm
fraction of decalcified samples
from Mujina Pećina, SU E1.**



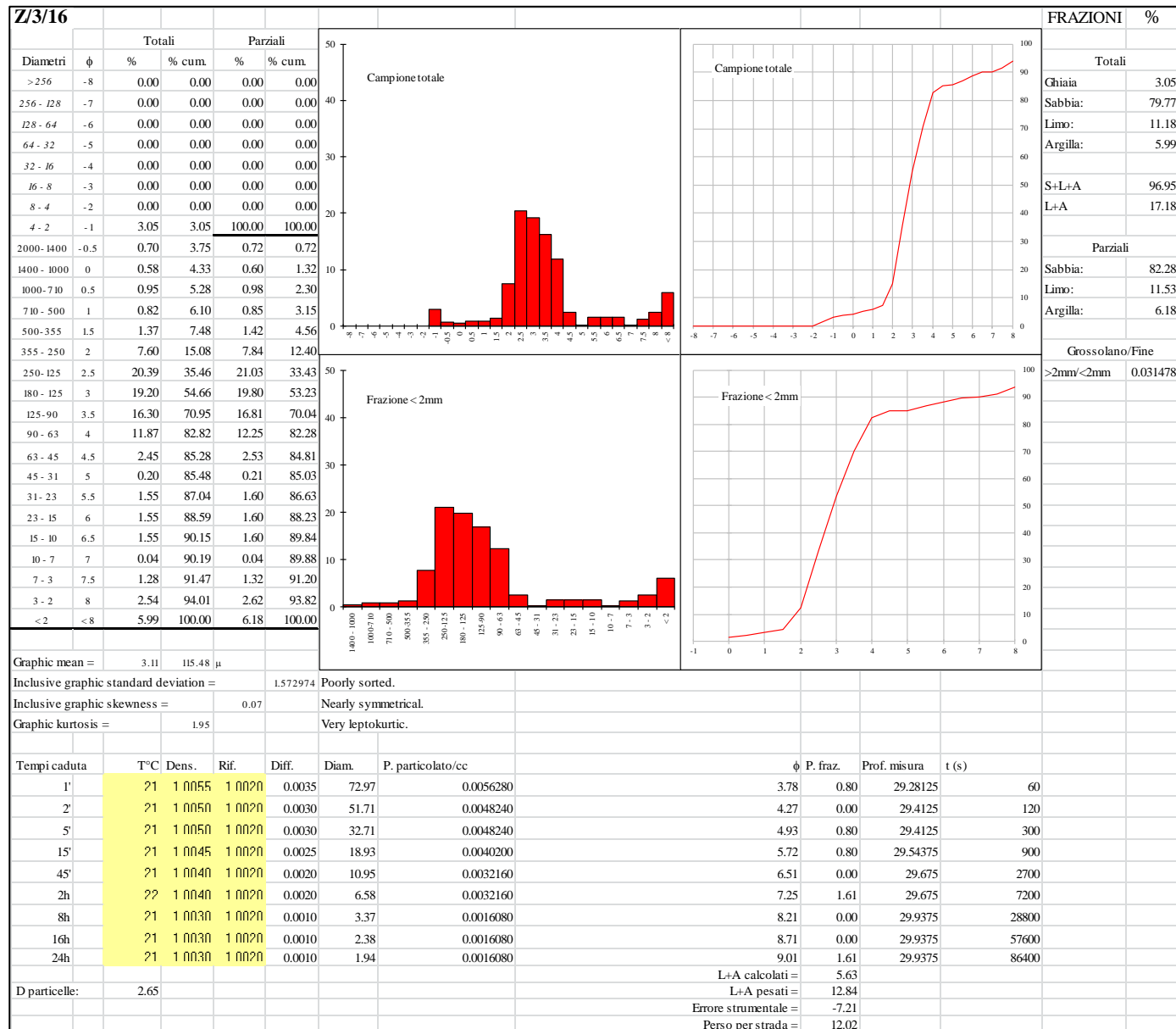
**Appendix 3.1. Grain-size
(Wentworth, 1922) of the <2 mm
fraction of undecalcified samples
from Zala Cave, SU 1.**



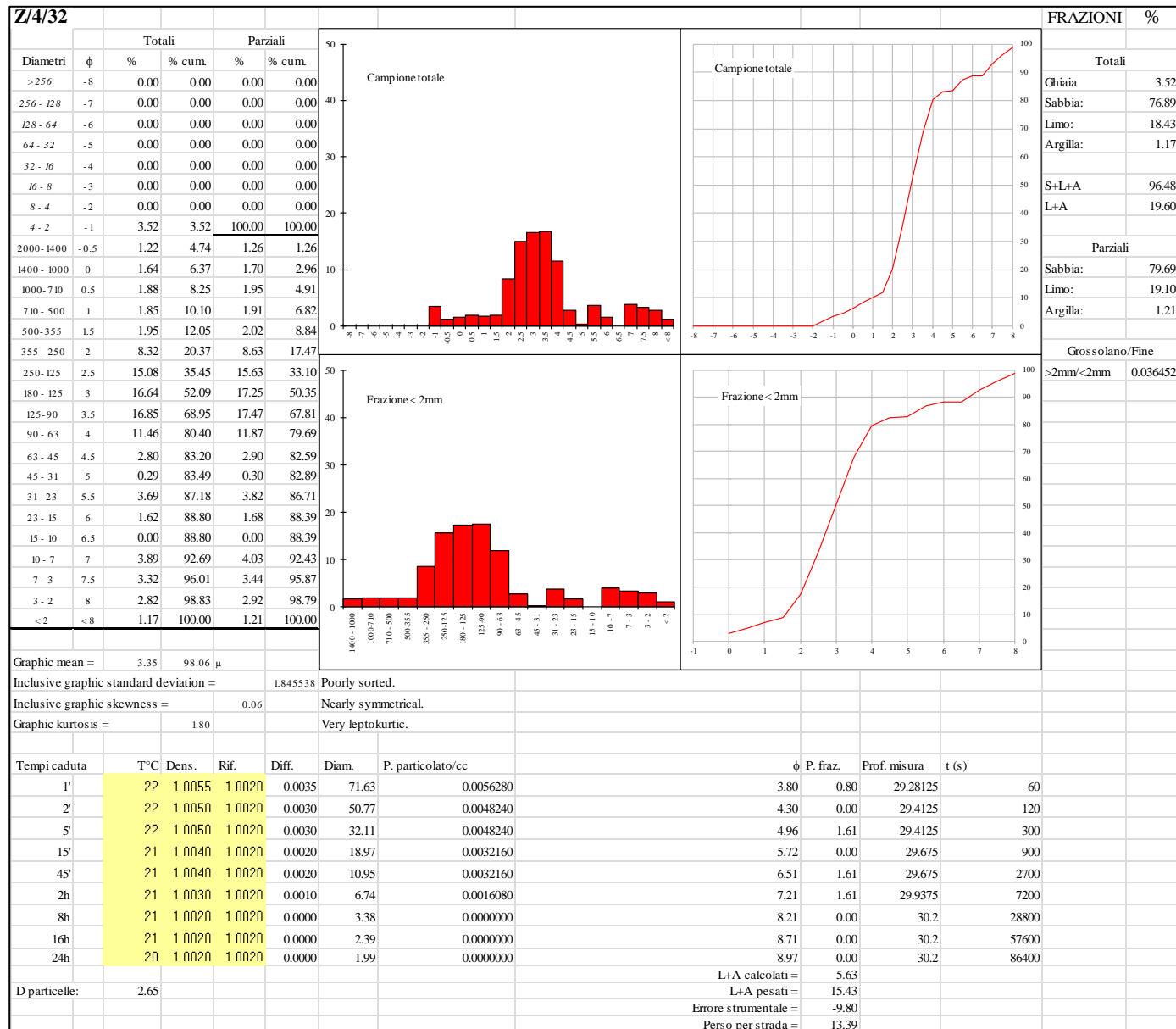
**Appendix 3.2. Grain-size
(Wentworth, 1922) of the <2 mm
fraction of undecalcified samples
from Zala Cave, SU 2.**



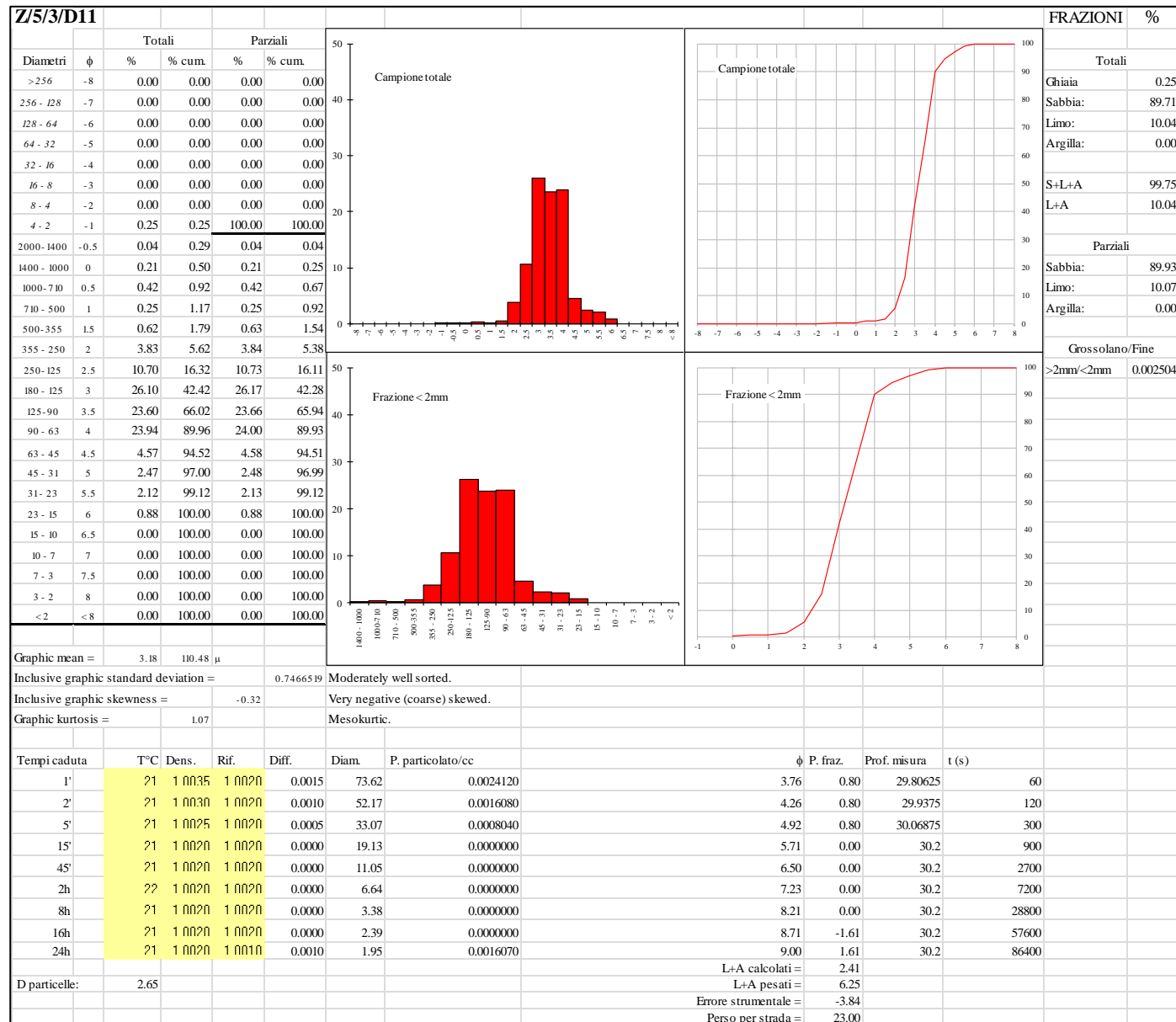
**Appendix 3.3. Grain-size
(Wentworth, 1922) of the <2 mm
fraction of undecalcified samples
from Zala Cave, SU 16.**



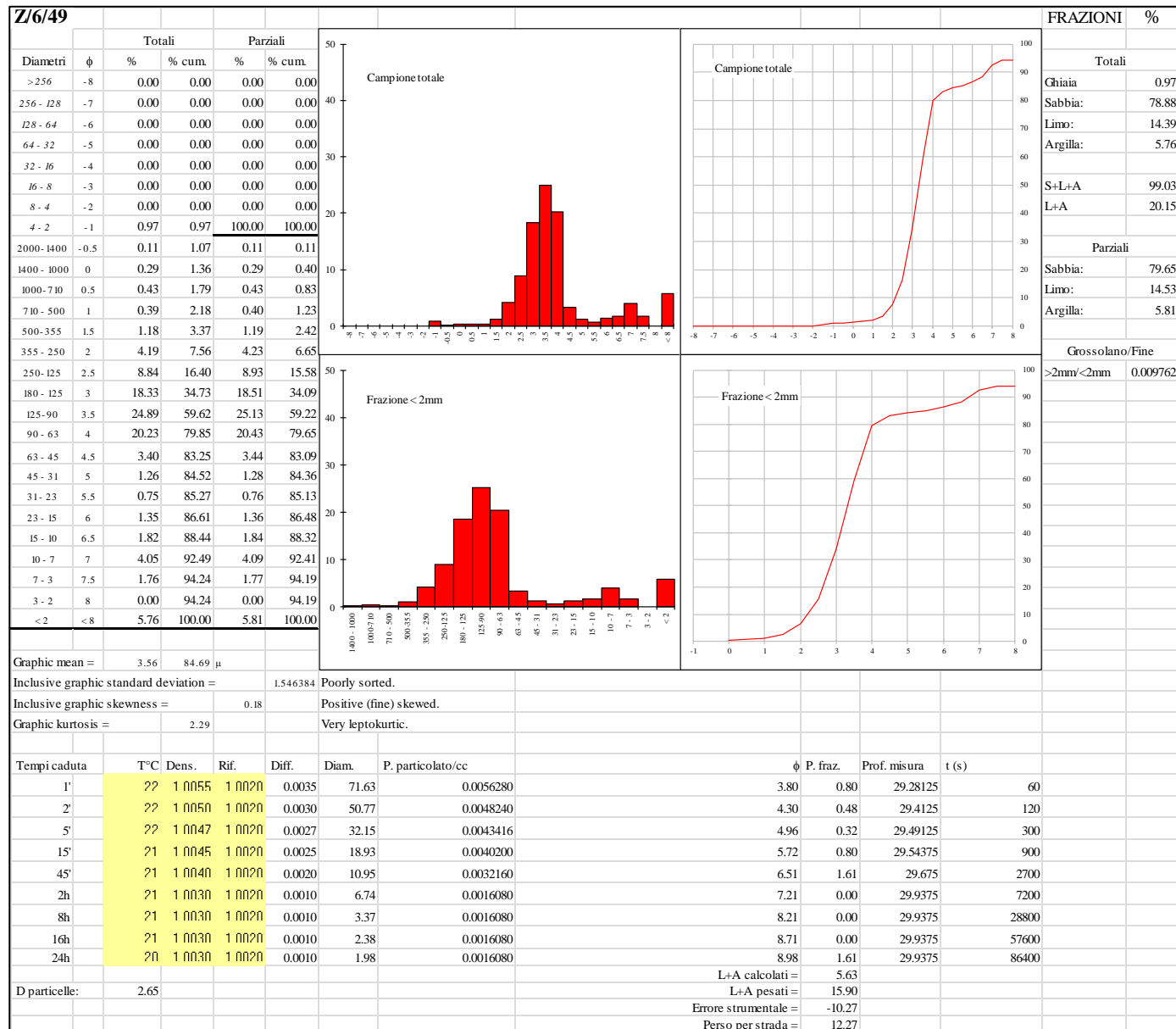
**Appendix 3.4. Grain-size
(Wentworth, 1922) of the <2 mm
fraction of undecalcified samples
from Zala Cave, SU 32.**



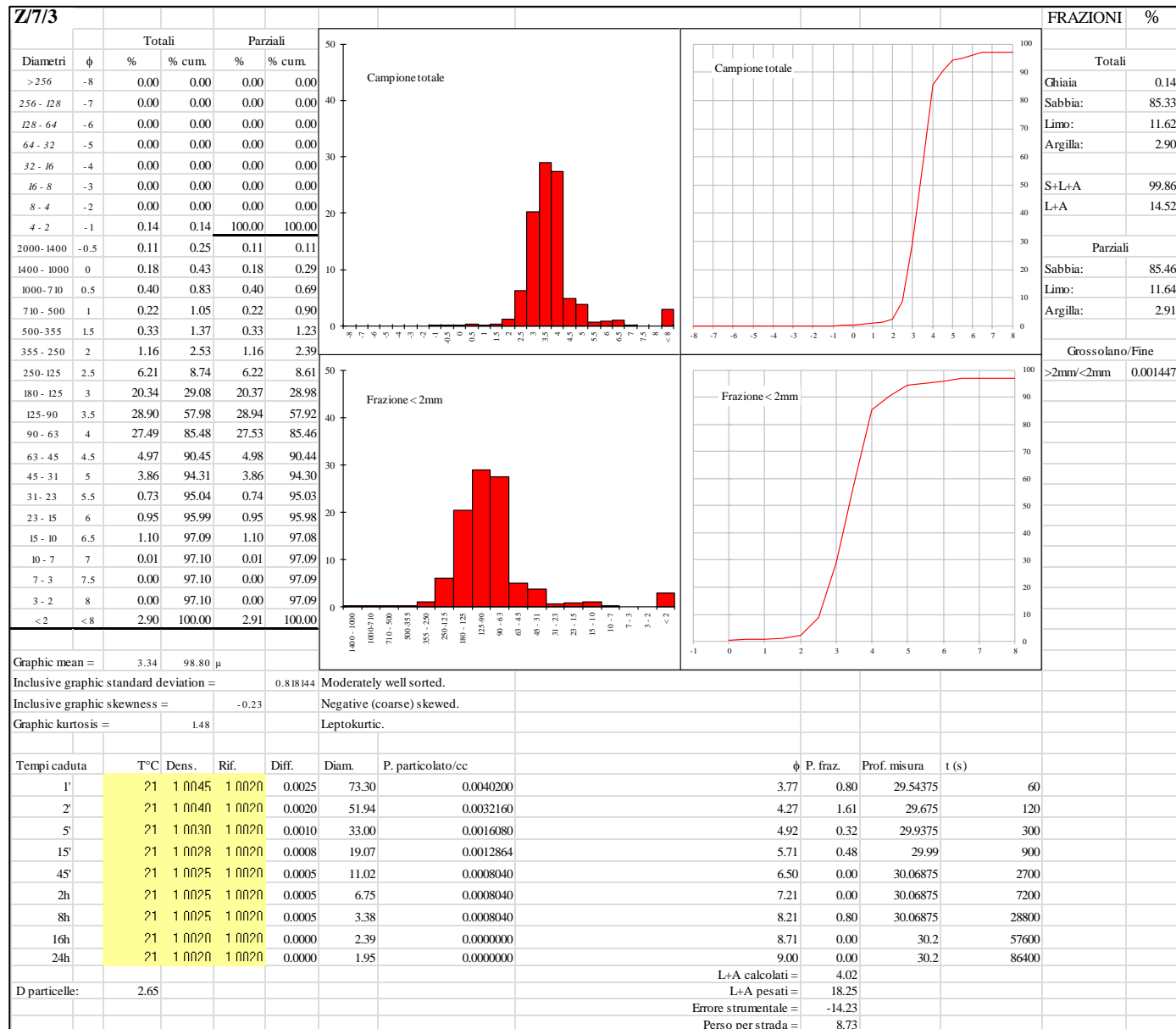
**Appendix 3.5. Grain-size
(Wentworth, 1922) of the <2 mm
fraction of undecalcified
samples from Zala Cave, SU 3.**



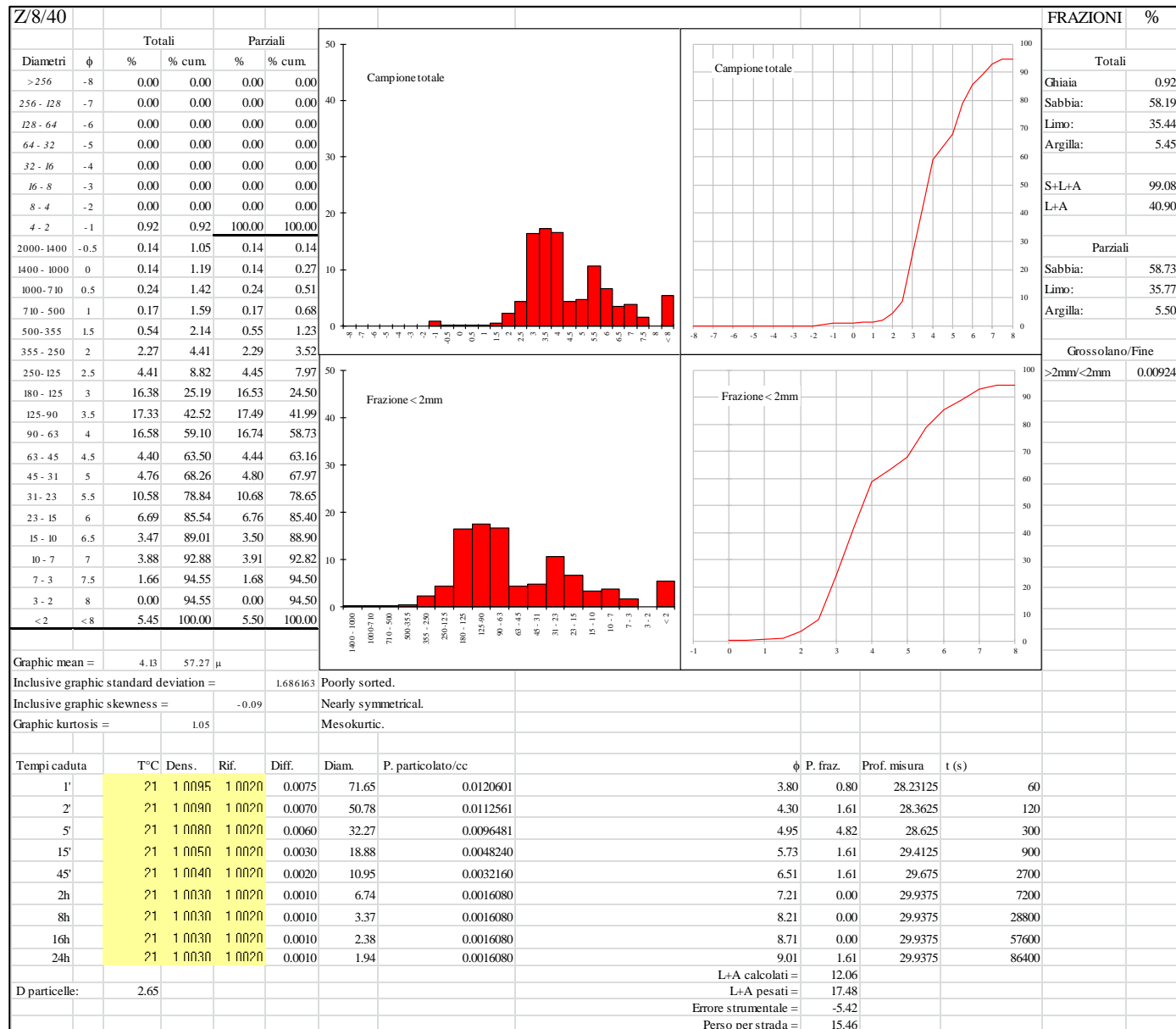
**Appendix 3.6. Grain-size
(Wentworth, 1922) of the <2 mm
fraction of undecalcified samples
from Zala Cave, SU 49_D11.**



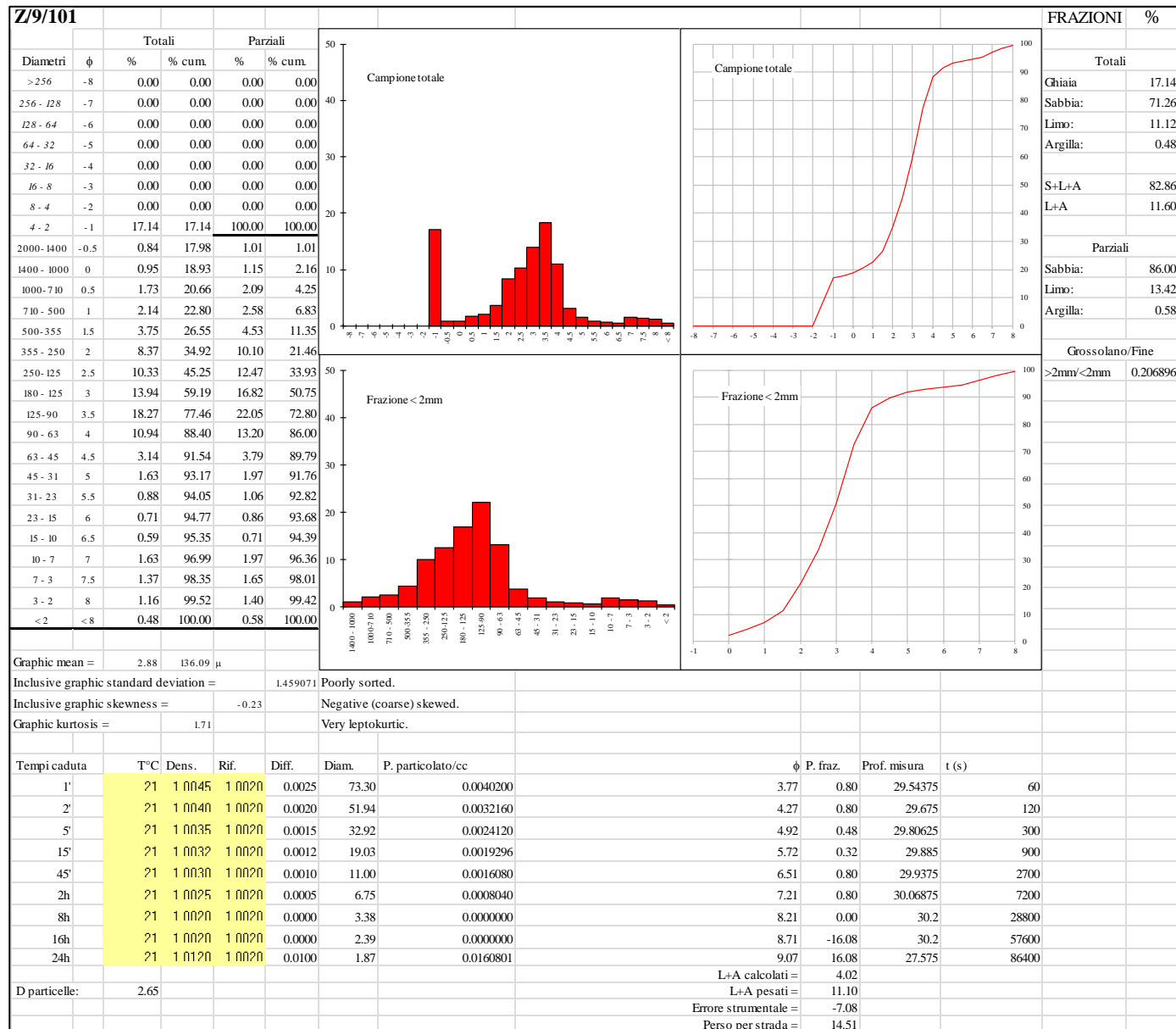
**Appendix 3.7. Grain-size
(Wentworth, 1922) of the <2 mm
fraction of undecalcified samples
from Zala Cave, SU 3b.**



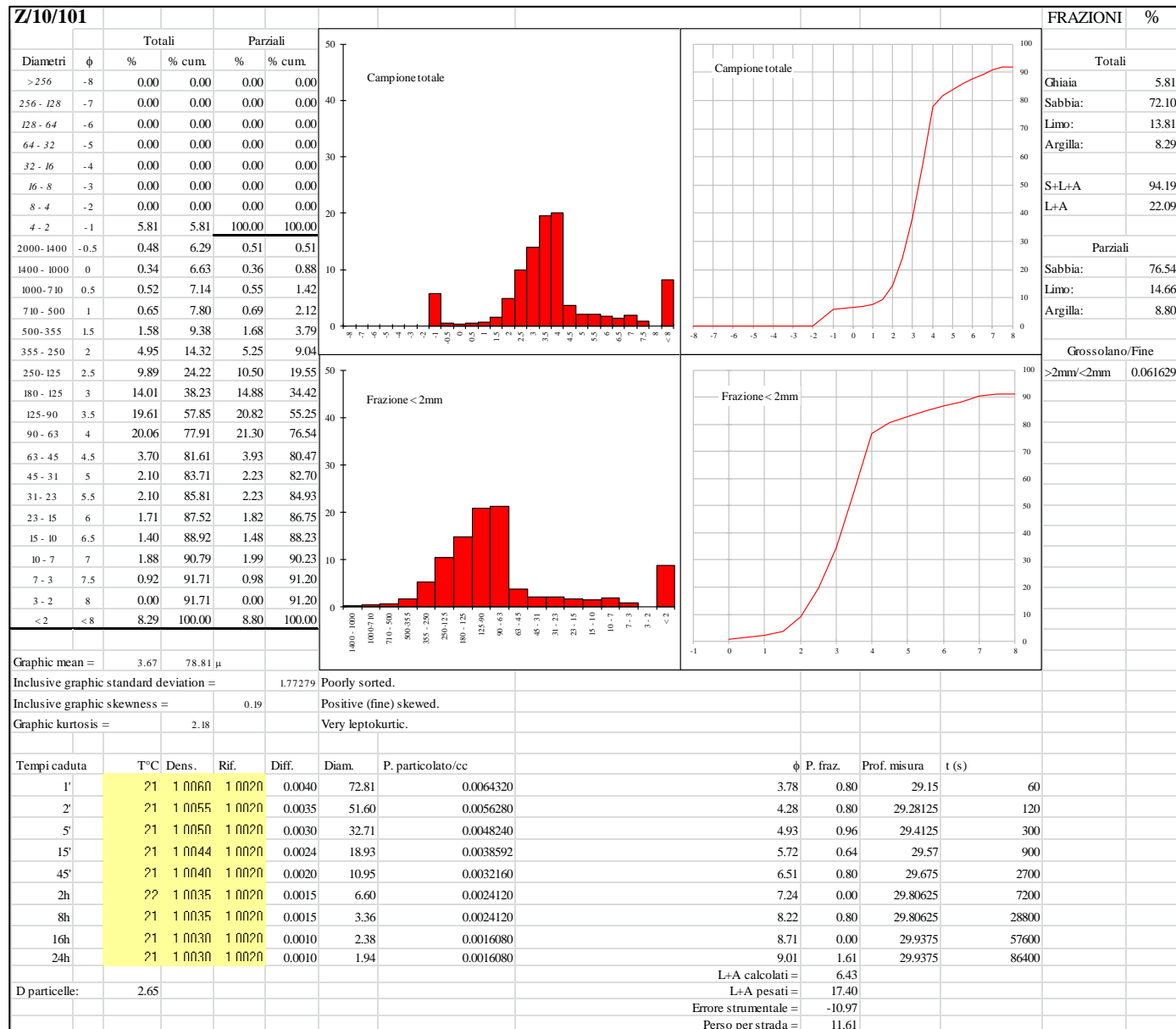
**Appendix 3.8. Grain-size
(Wentworth, 1922) of the <2 mm
fraction of undecalcified samples
from Zala Cave, SU 40.**



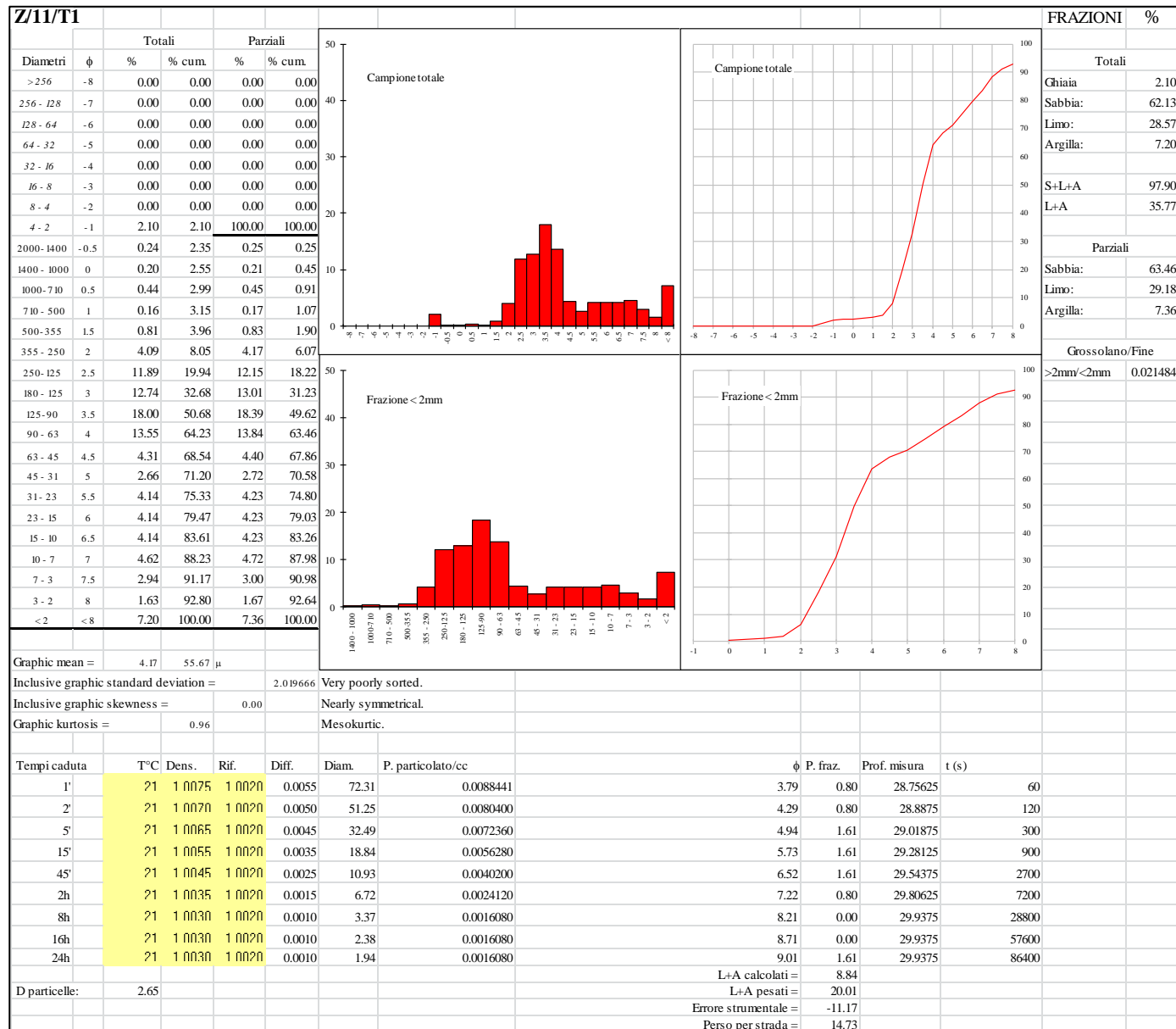
**Appendix 3.9. Grain-size
(Wentworth, 1922) of the <2 mm
fraction of undecalcified samples
from Zala Cave, SU 101.**



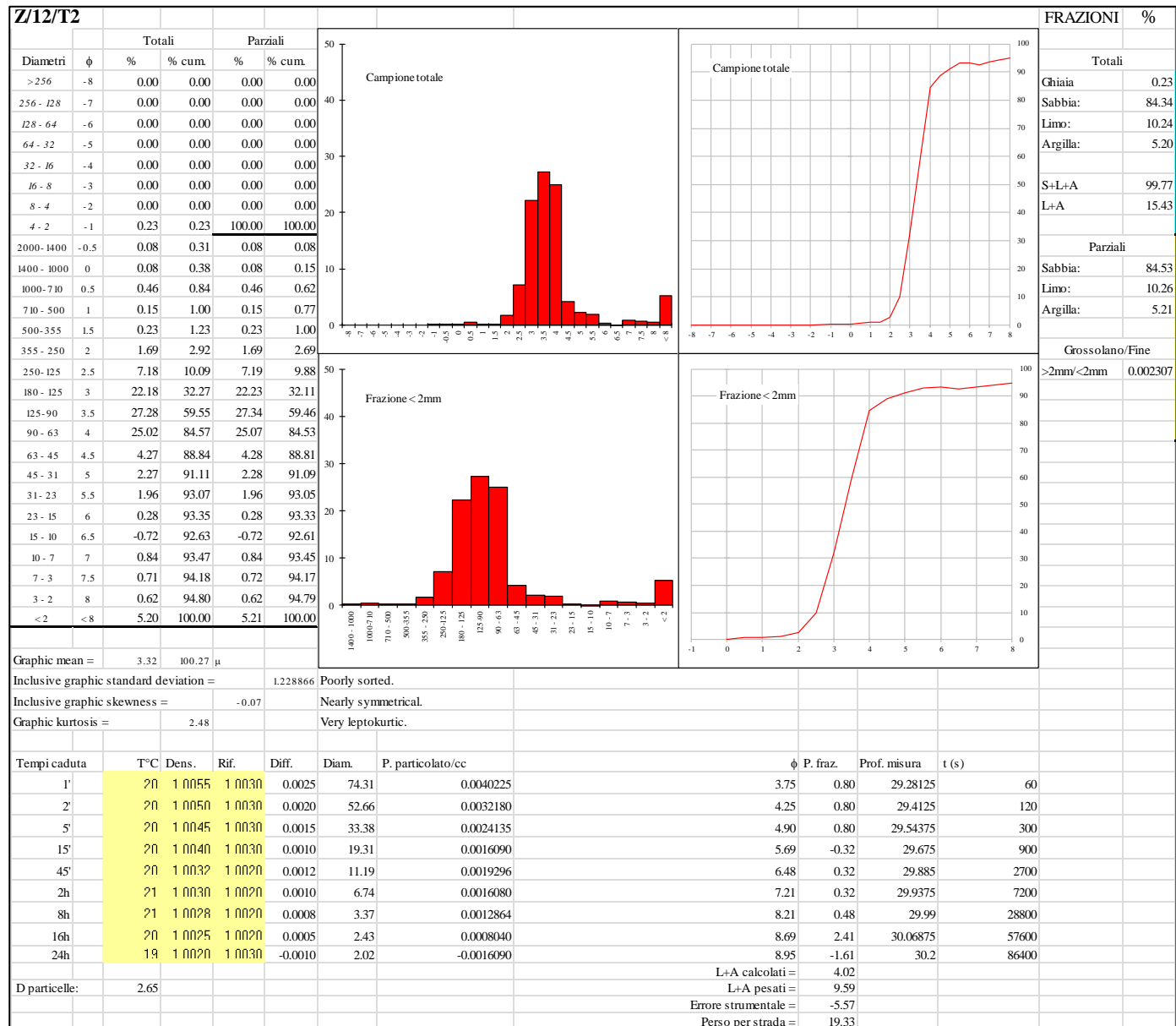
**Appendix 3.10. Grain-size
(Wentworth, 1922) of the <2 mm
fraction of undecalcified samples
from Zala Cave, SU 101.**



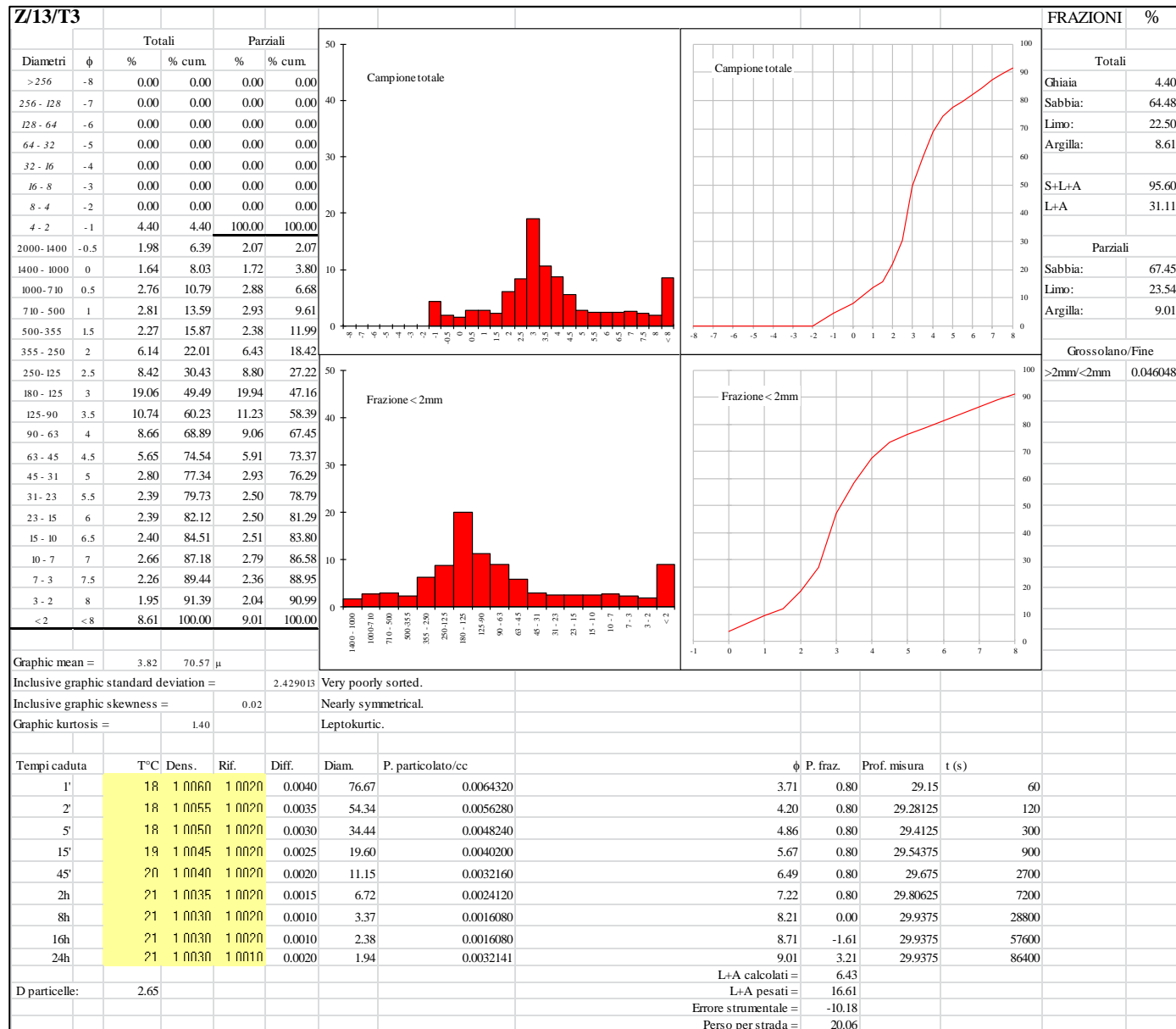
**Appendix 3.11. Grain-size
(Wentworth, 1922) of the <2 mm
fraction of undecalcified samples
from Zala Cave, SU 49.**



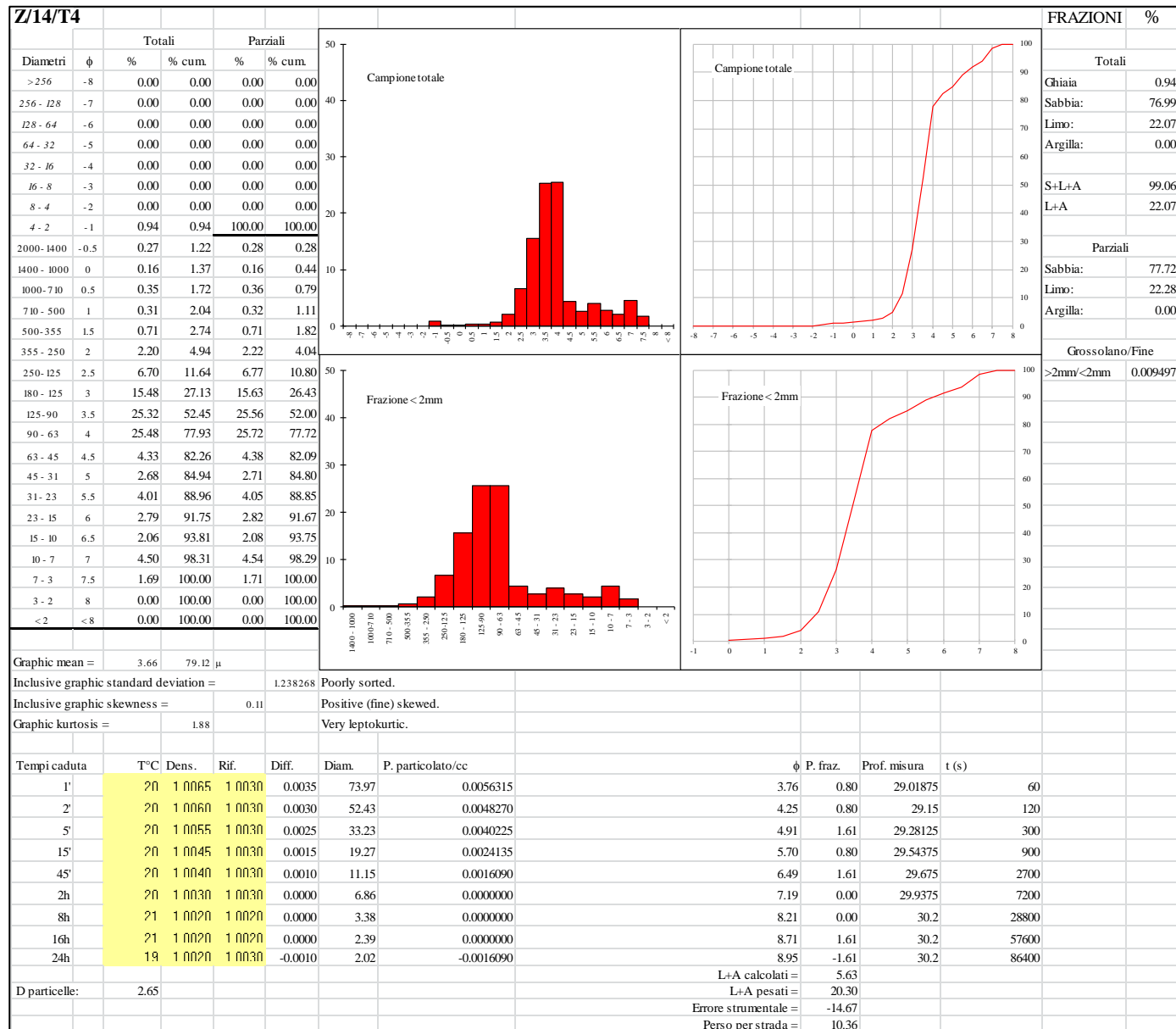
**Appendix 3.12. Grain-size
(Wentworth, 1922) of the <2 mm
fraction of undecalcified samples
from Zala Cave, SU 3c.**



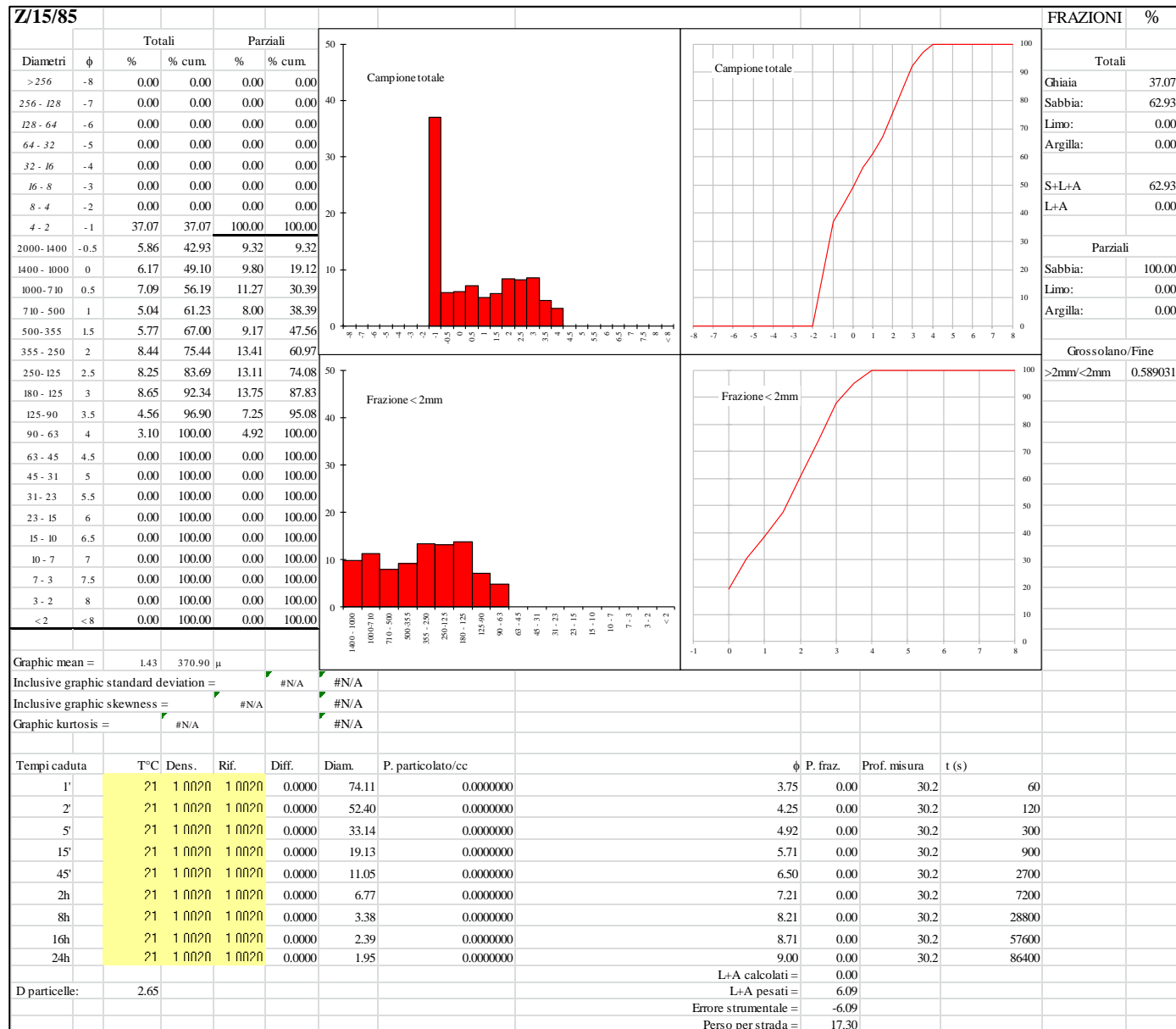
**Appendix 3.13. Grain-size
(Wentworth, 1922) of the <2 mm
fraction of undecalcified samples
from Zala Cave, SU 65.**



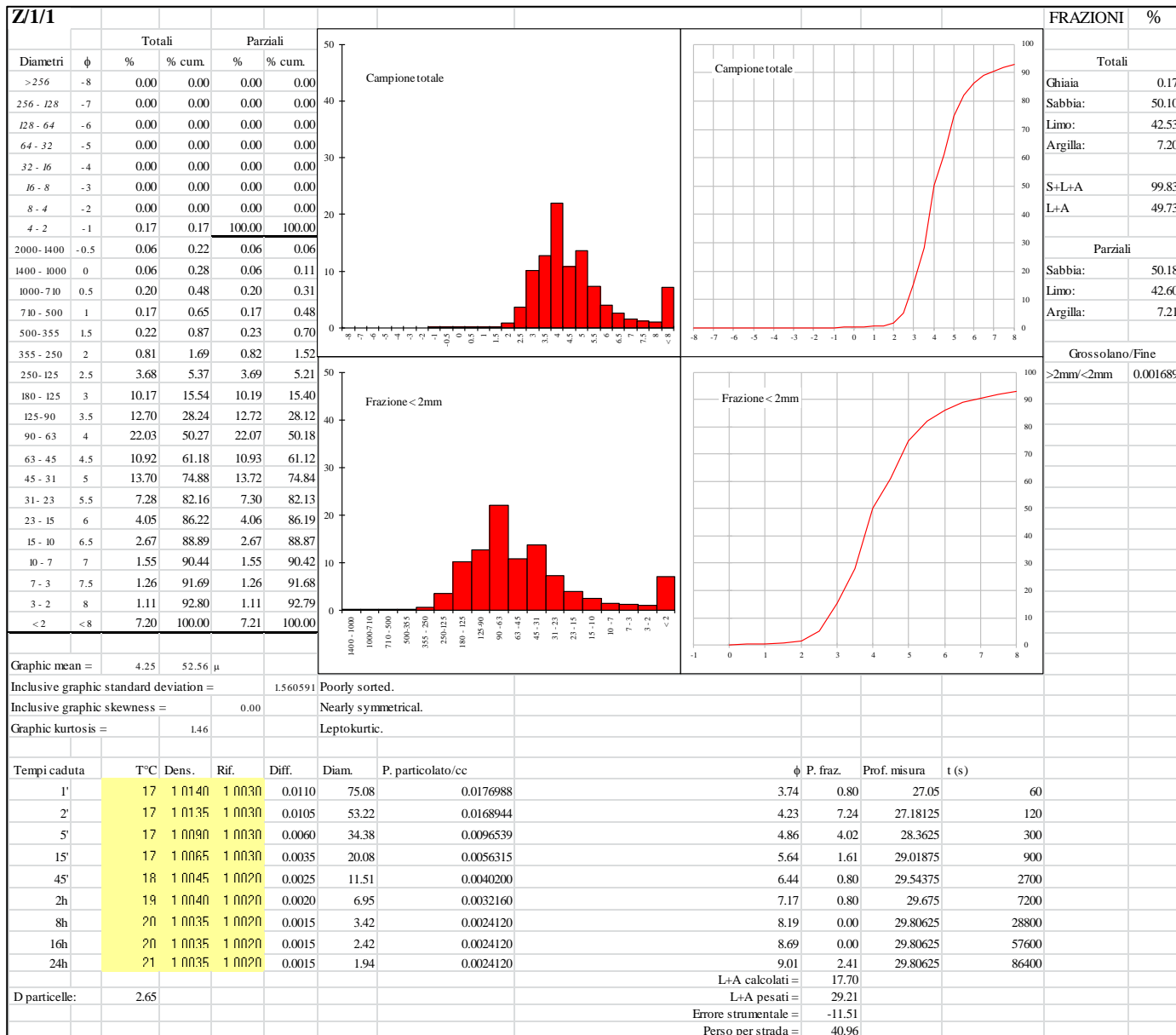
**Appendix 3.14. Grain-size
(Wentworth, 1922) of the <2 mm
fraction of undecalcified samples
from Zala Cave, SU 71.**



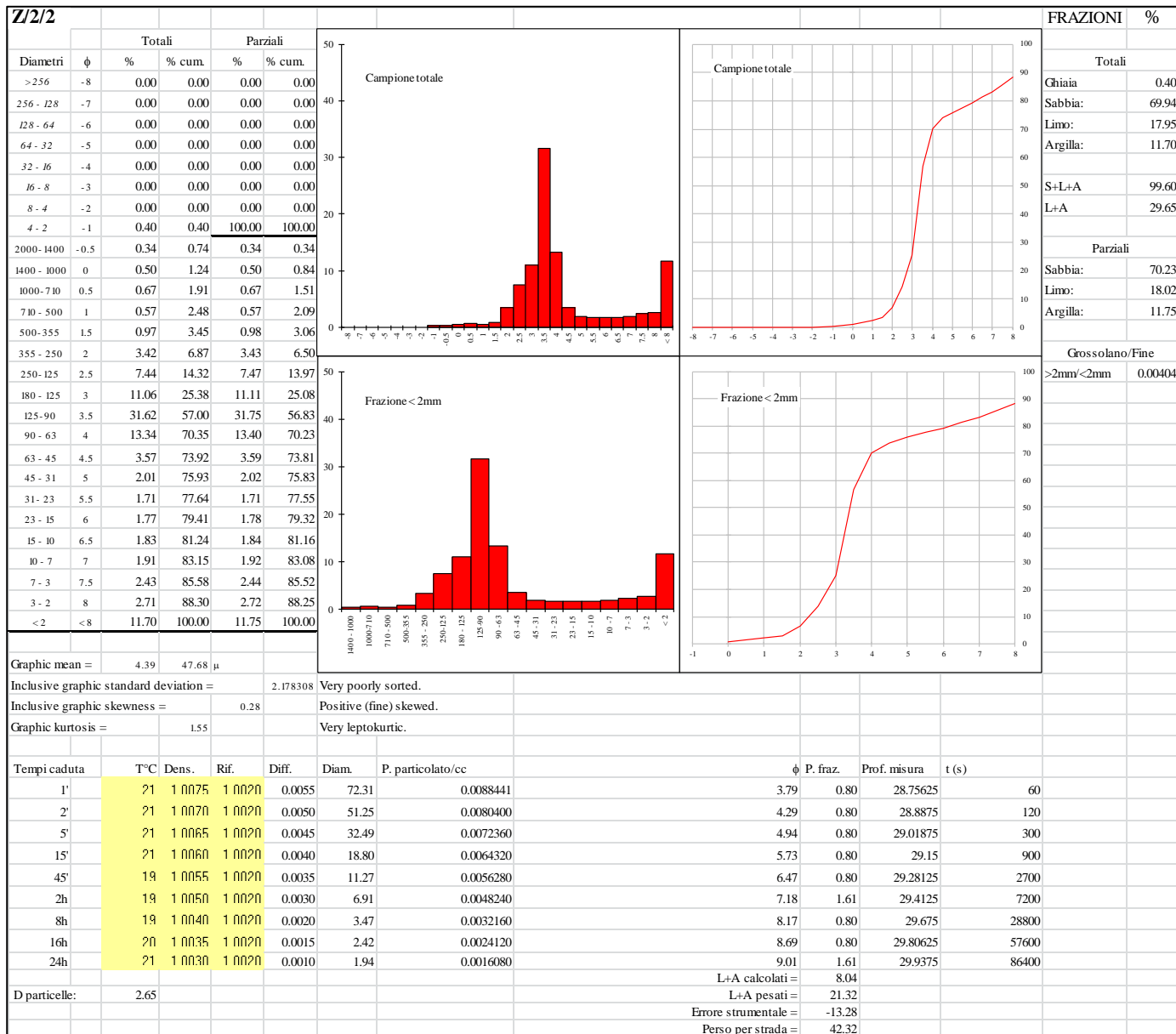
**Appendix 3.15. Grain-size
(Wentworth, 1922) of the <2 mm
fraction of undecalcified samples
from Zala Cave, SU 85.**



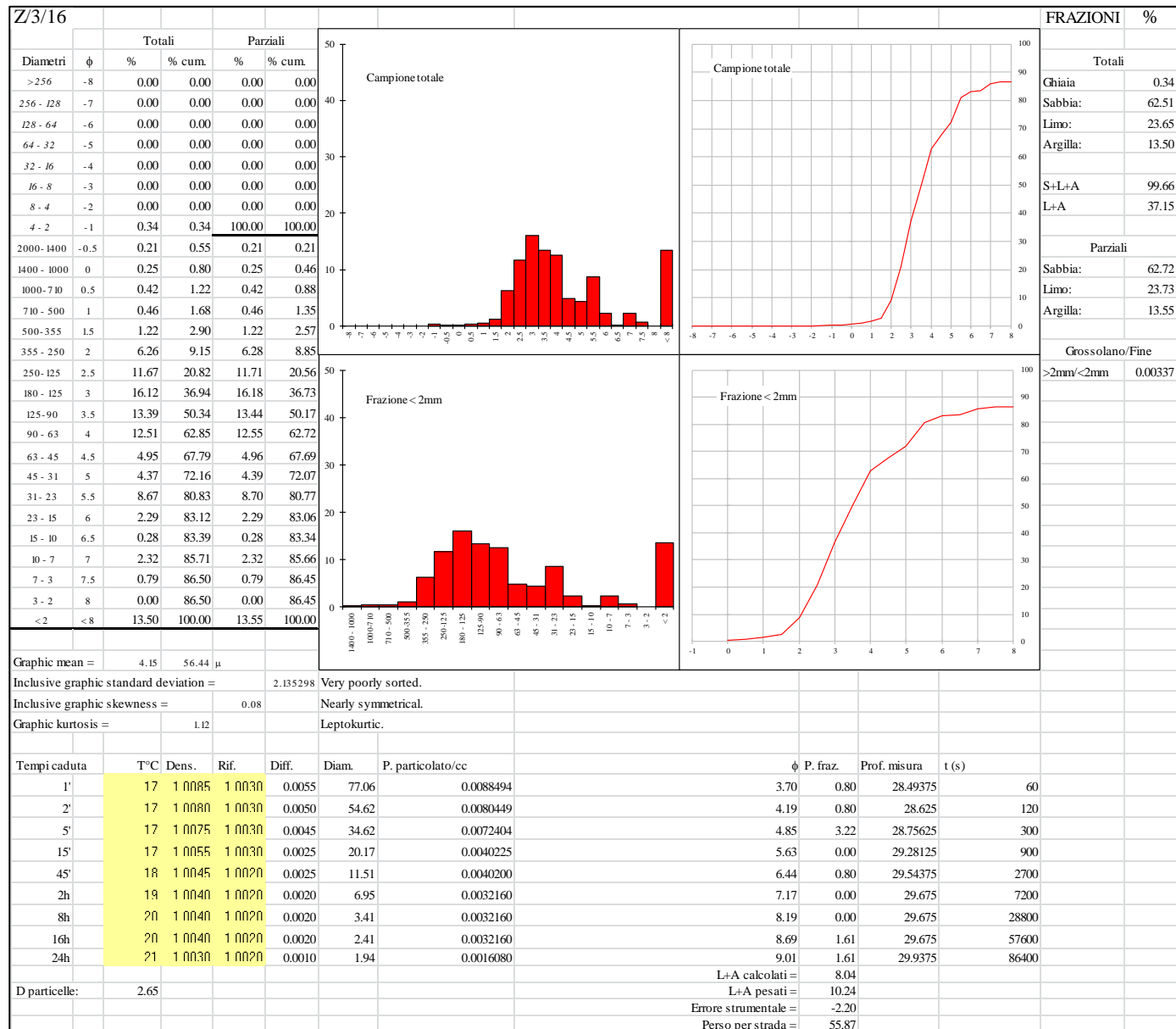
**Appendix 4.1. Grain-size
(Wentworth, 1922) of the <2 mm
fraction of decalcified samples
from Zala Cave, SU**



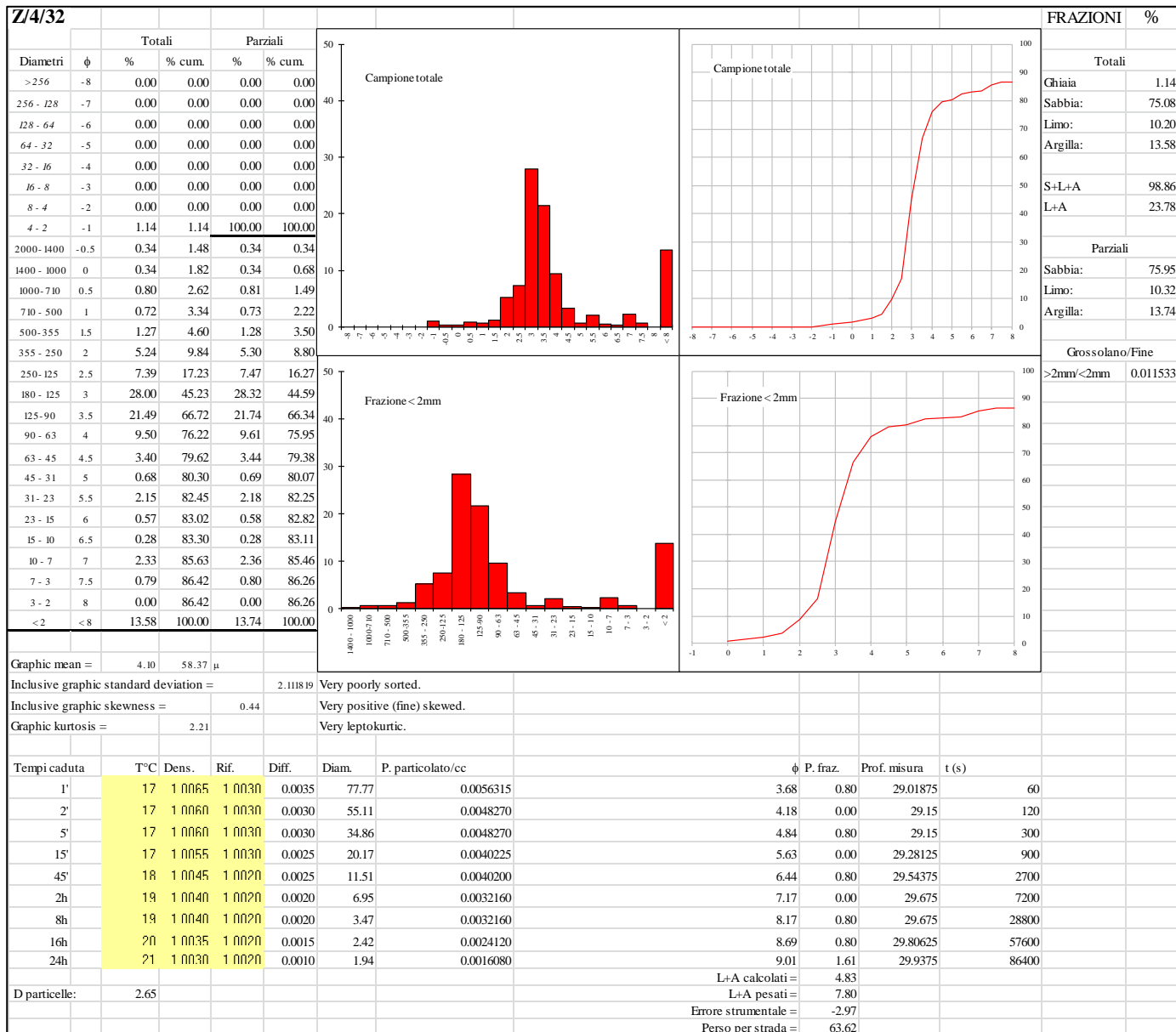
**Appendix 4.2. Grain-size
(Wentworth, 1922) of the <2 mm
fraction of decalcified samples
from Zala Cave, SU 2.**



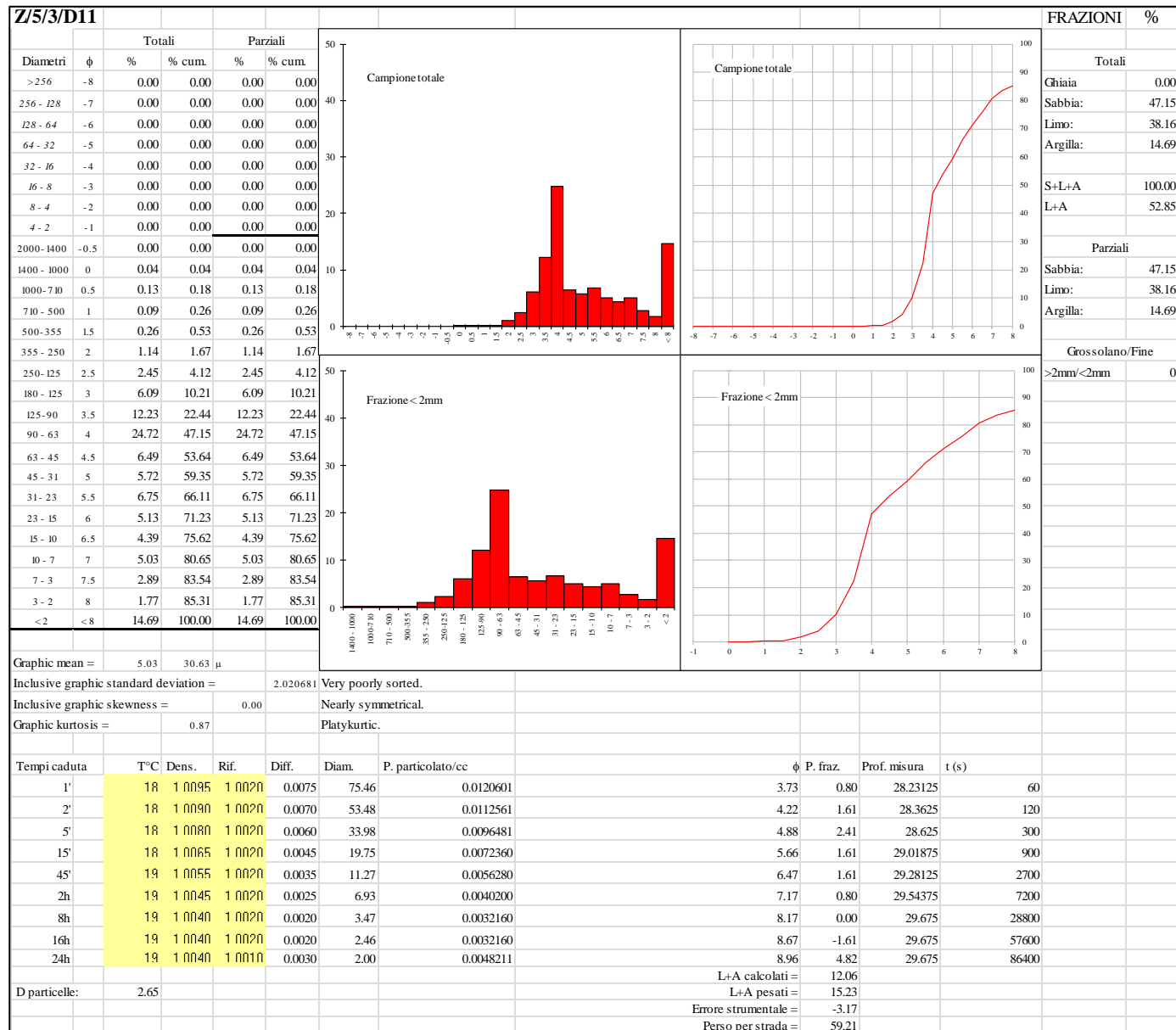
**Appendix 4.3. Grain-size
(Wentworth, 1922) of the <2 mm
fraction of decalcified samples
from Zala Cave, SU 16.**



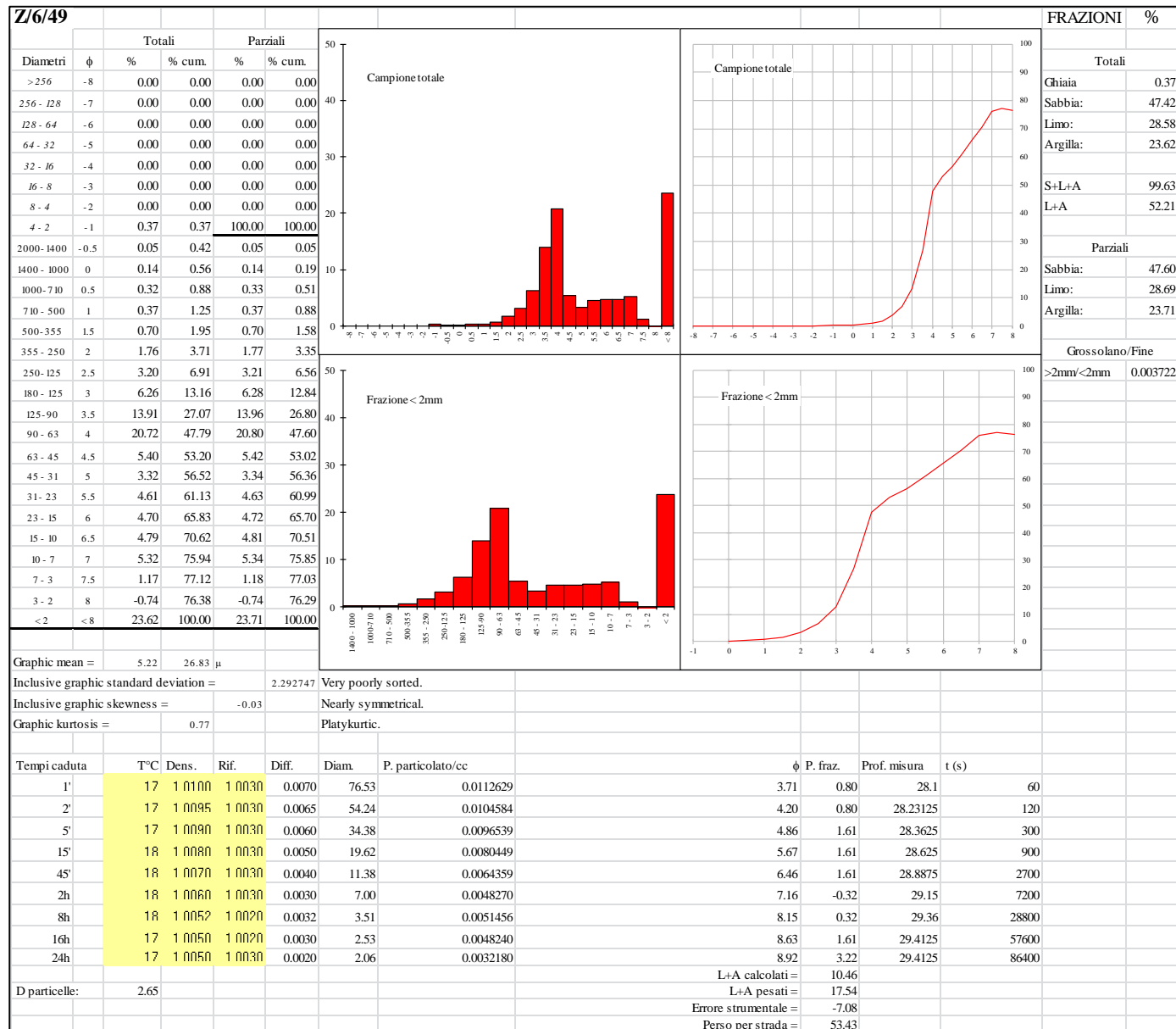
**Appendix 4.4. Grain-size
(Wentworth, 1922) of the <2 mm
fraction of decalcified samples
from Zala Cave, SU 32.**



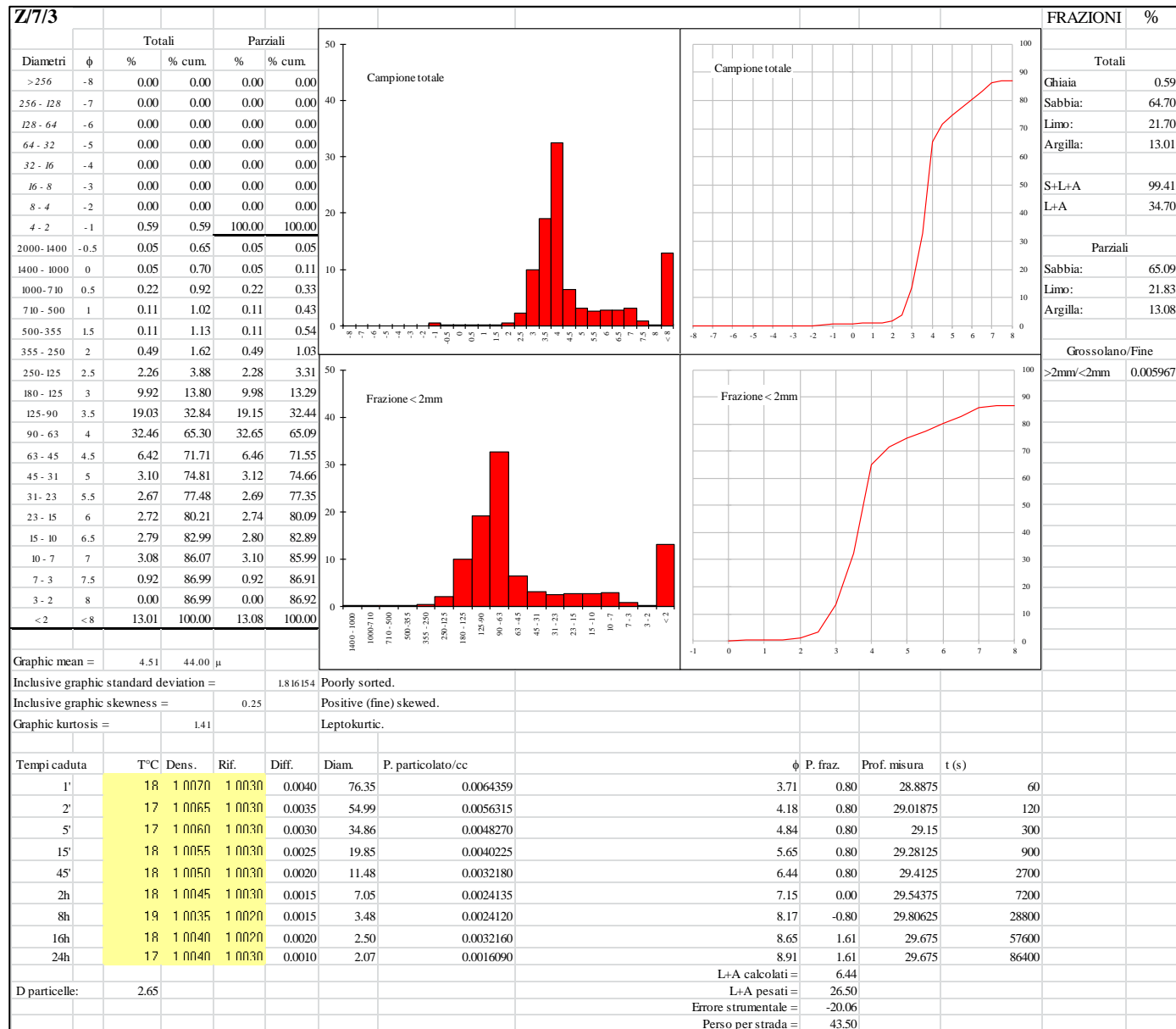
**Appendix 4.5. Grain-size
(Wentworth, 1922) of the <2 mm
fraction of decalcified samples
from Zala Cave, SU 3.**



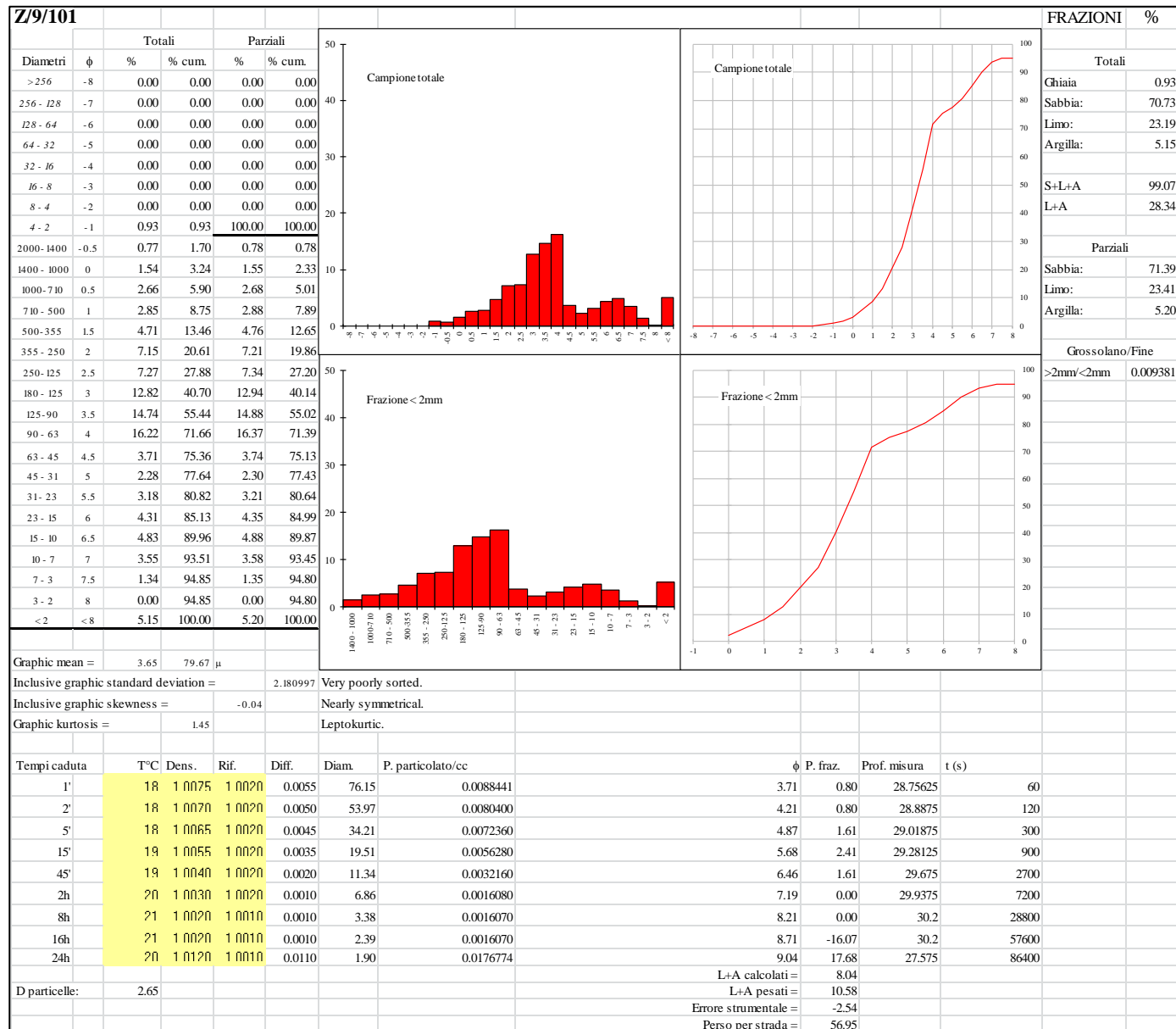
**Appendix 4.6. Grain-size
(Wentworth, 1922) of the <2 mm
fraction of decalcified samples
from Zala Cave, SU 49_D11..**



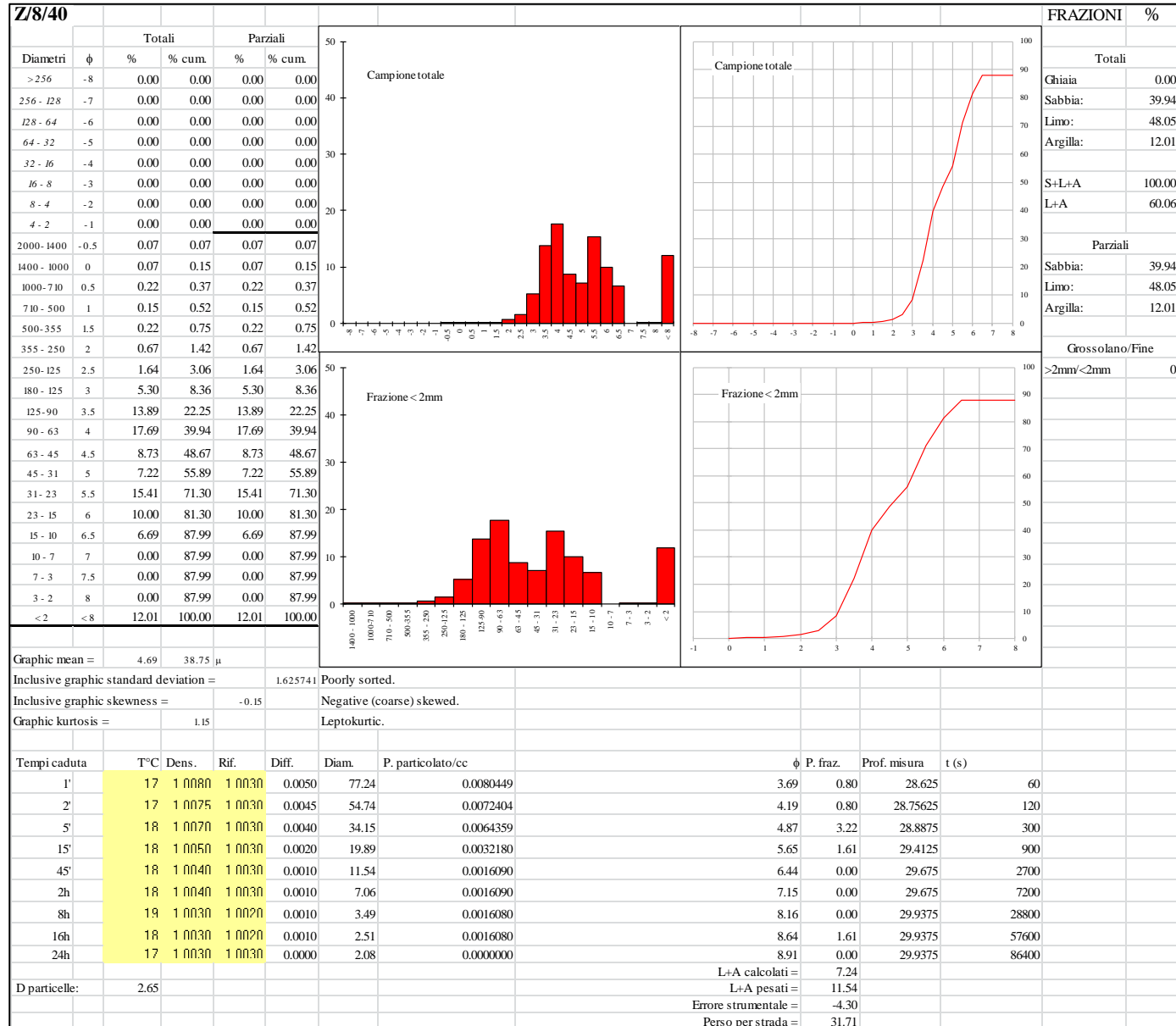
**Appendix 4.7. Grain-size
(Wentworth, 1922) of the <2 mm
fraction of decalcified samples
from Zala Cave, SU 3b.**



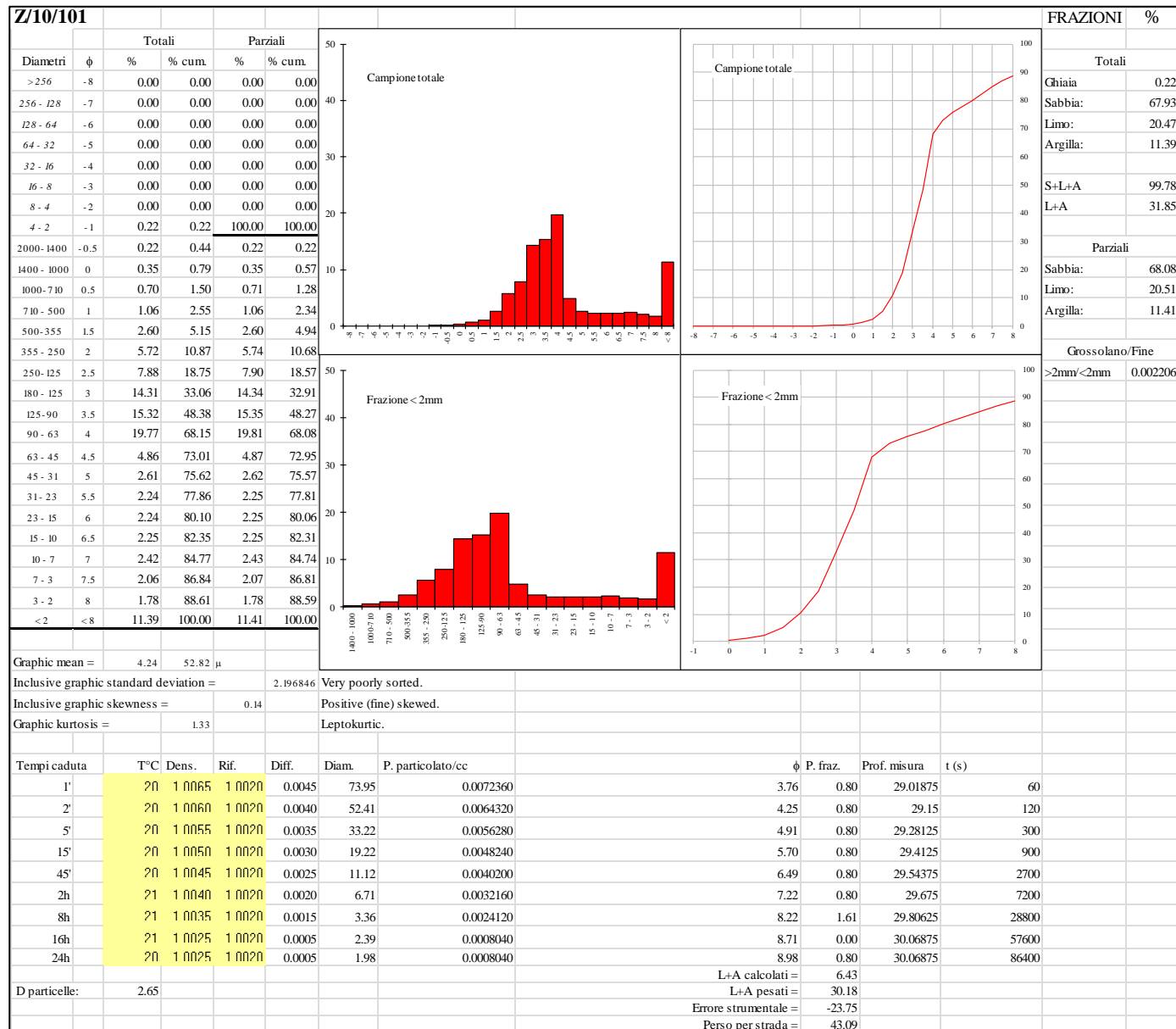
**Appendix 4.8. Grain-size
(Wentworth, 1922) of the <2 mm
fraction of decalcified samples
from Zala Cave, SU 101.**



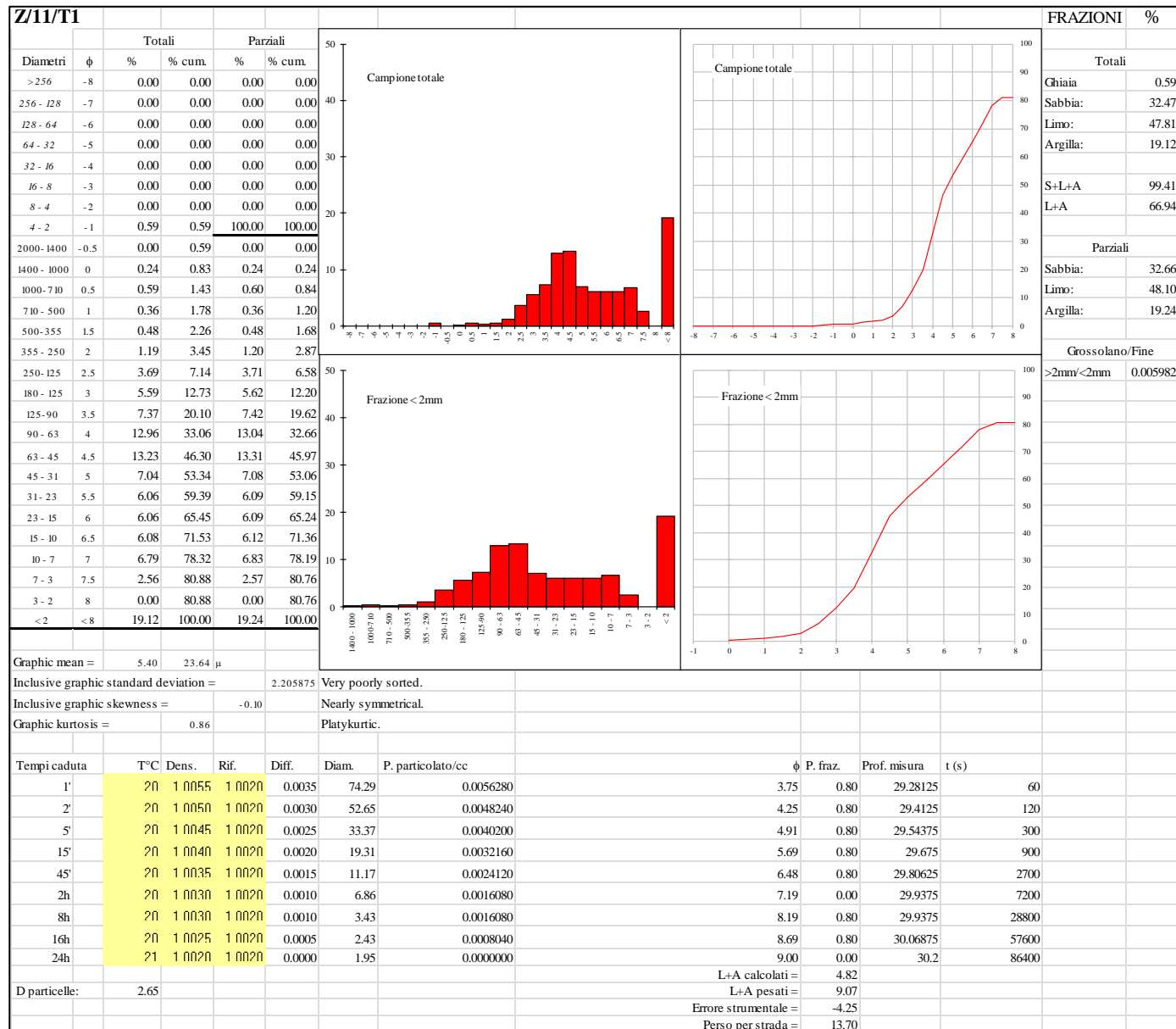
Appendix 4.9. Grain-size (Wentworth, 1922) of the <2 mm fraction of decalcified samples from Zala Cave, SU 40.



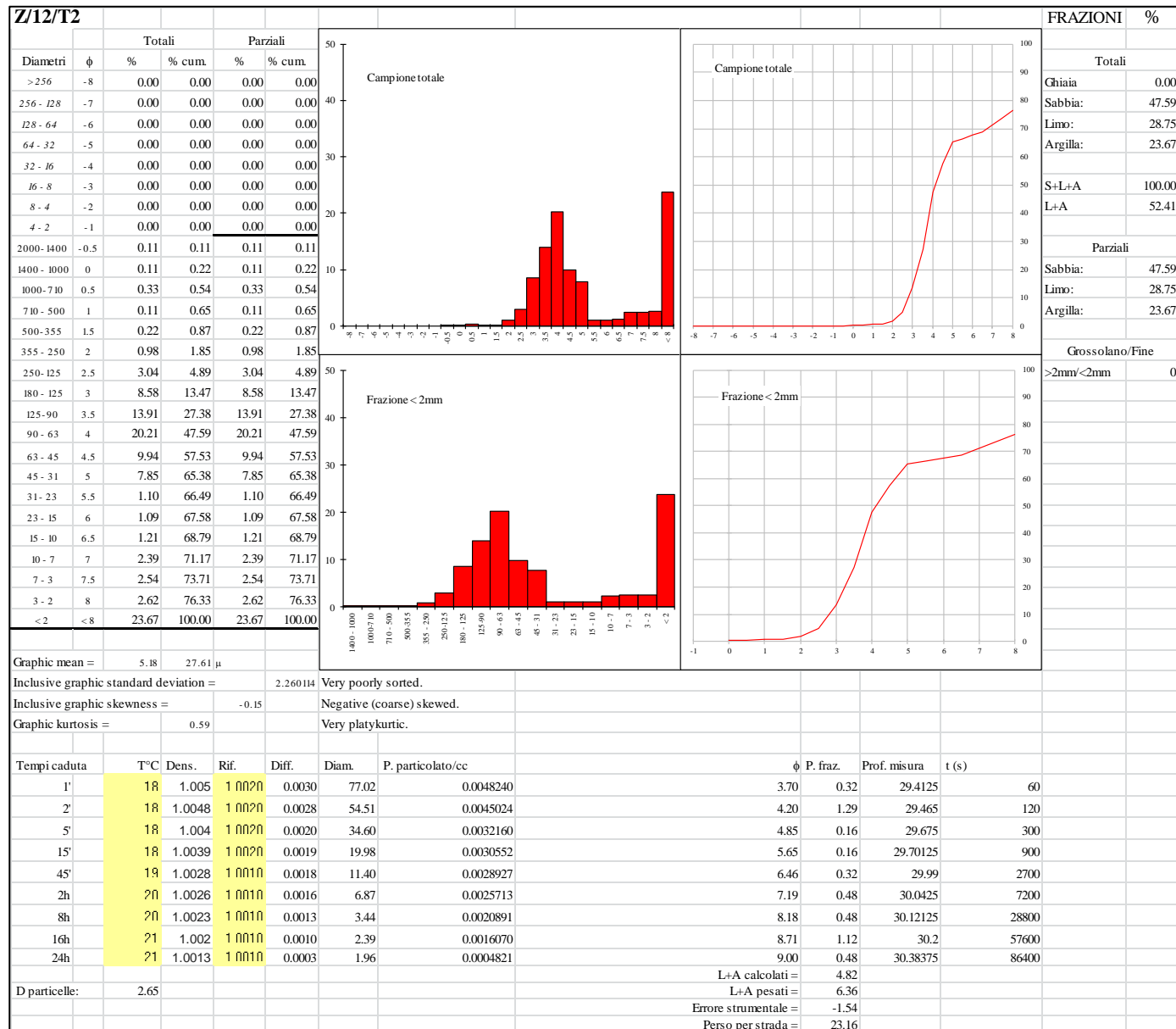
**Appendix 4.10. Grain-size
(Wentworth, 1922) of the <2 mm
fraction of decalcified samples
from Zala Cave, SU 101.**



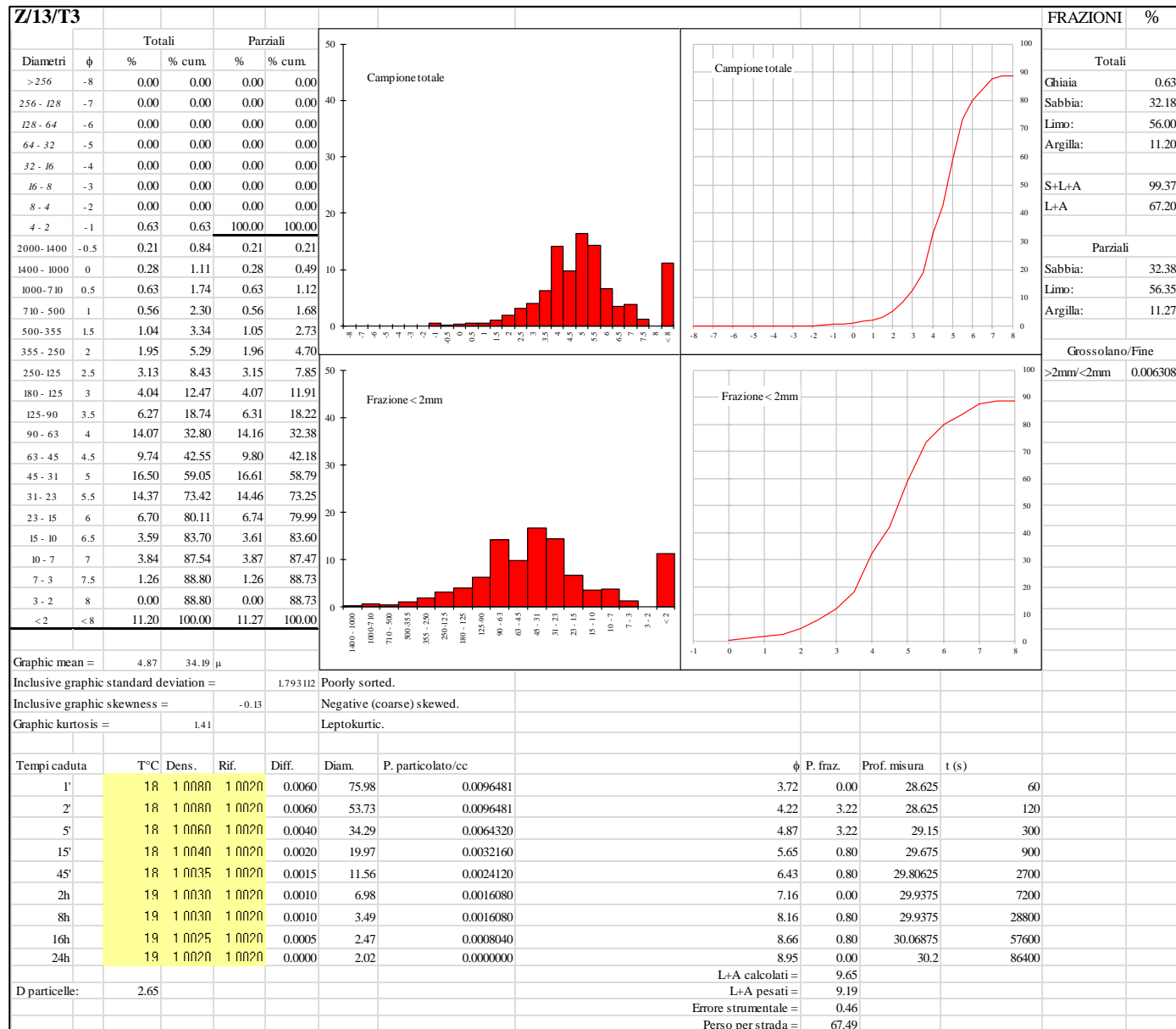
**Appendix 4.11. Grain-size
(Wentworth, 1922) of the <2 mm
fraction of decalcified samples
from Zala Cave, SU 49.**



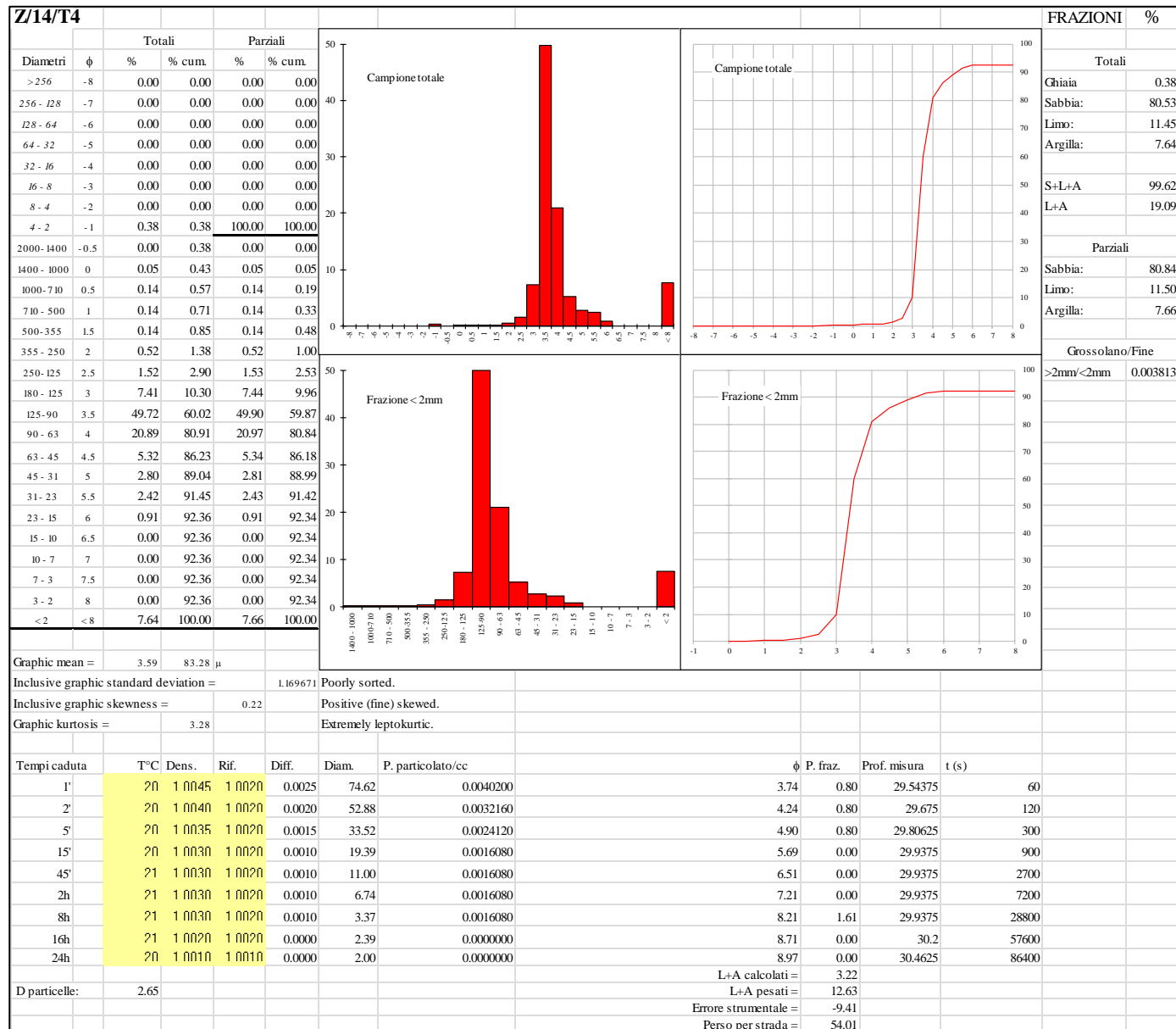
**Appendix 4.12. Grain-size
(Wentworth, 1922) of the <2 mm
fraction of decalcified samples
from Zala Cave, SU 3c.**



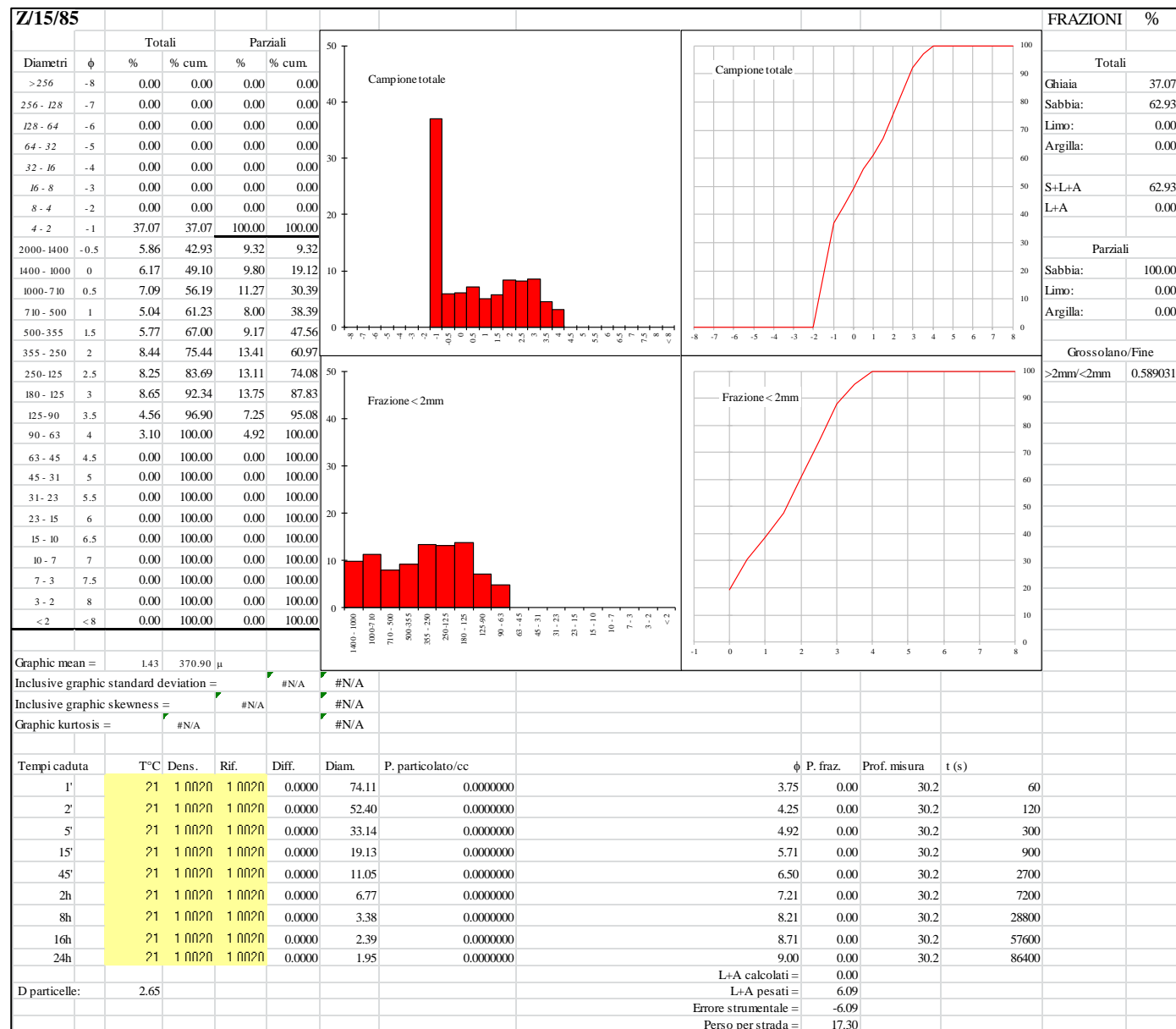
**Appendix 4.13. Grain-size
(Wentworth, 1922) of the <2 mm
fraction of decalcified samples
from Zala Cave, SU 65.**



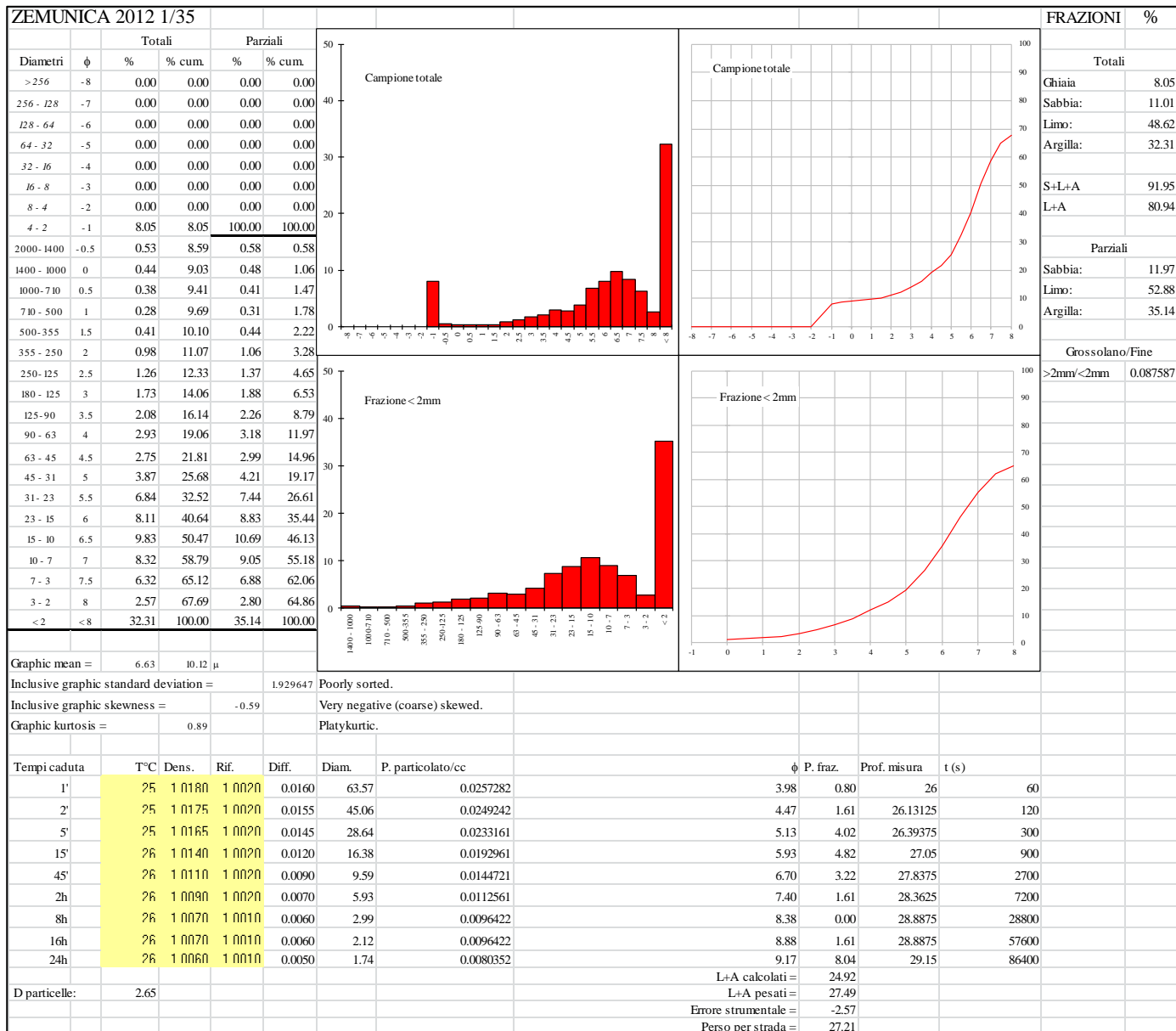
**Appendix 4.14. Grain-size
(Wentworth, 1922) of the <2 mm
fraction of decalcified samples
from Zala Cave, SU 71.**



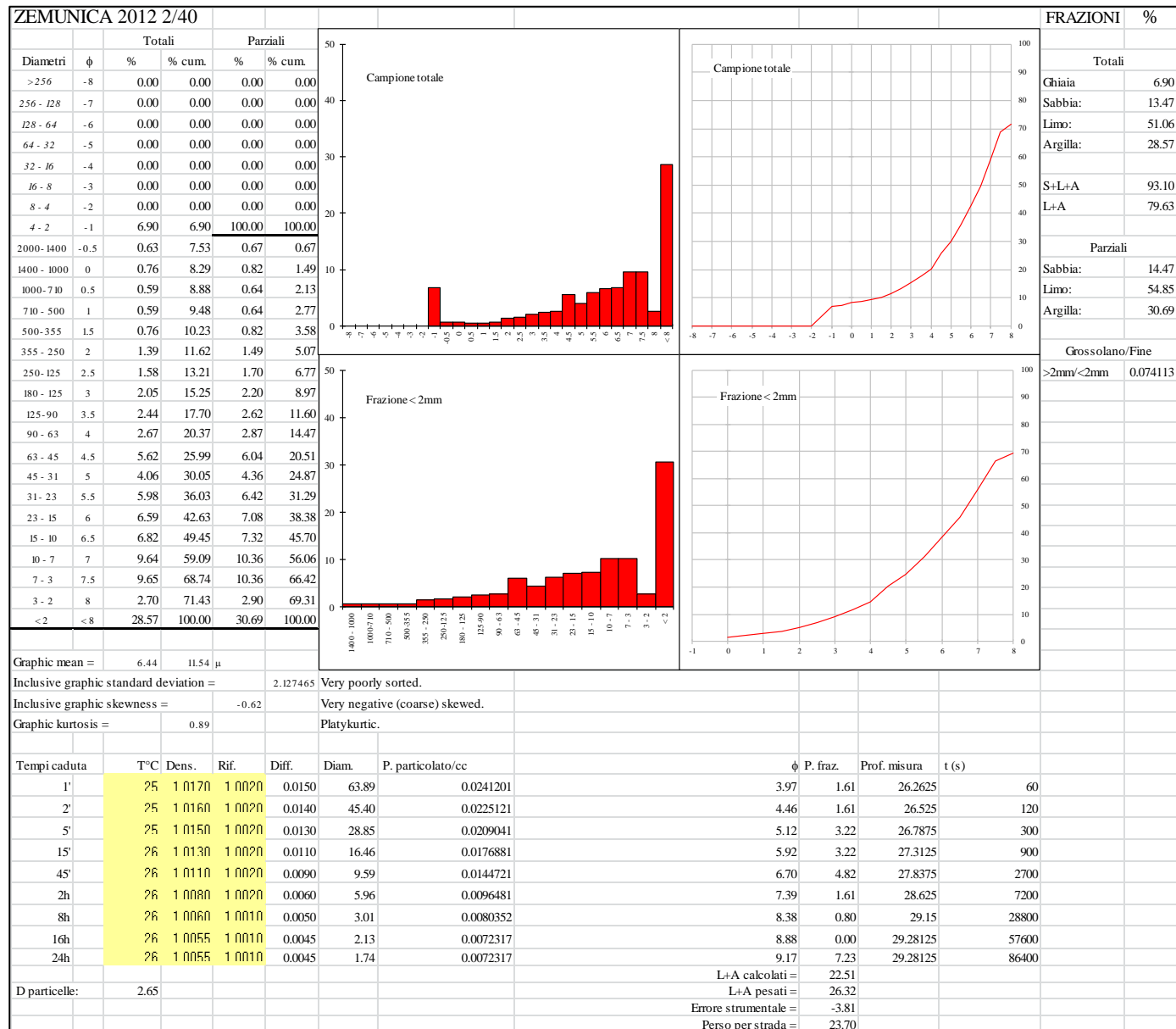
**Appendix 4.15. Grain-size
(Wentworth, 1922) of the <2 mm
fraction of decalcified samples
from Zala Cave, SU 85.**



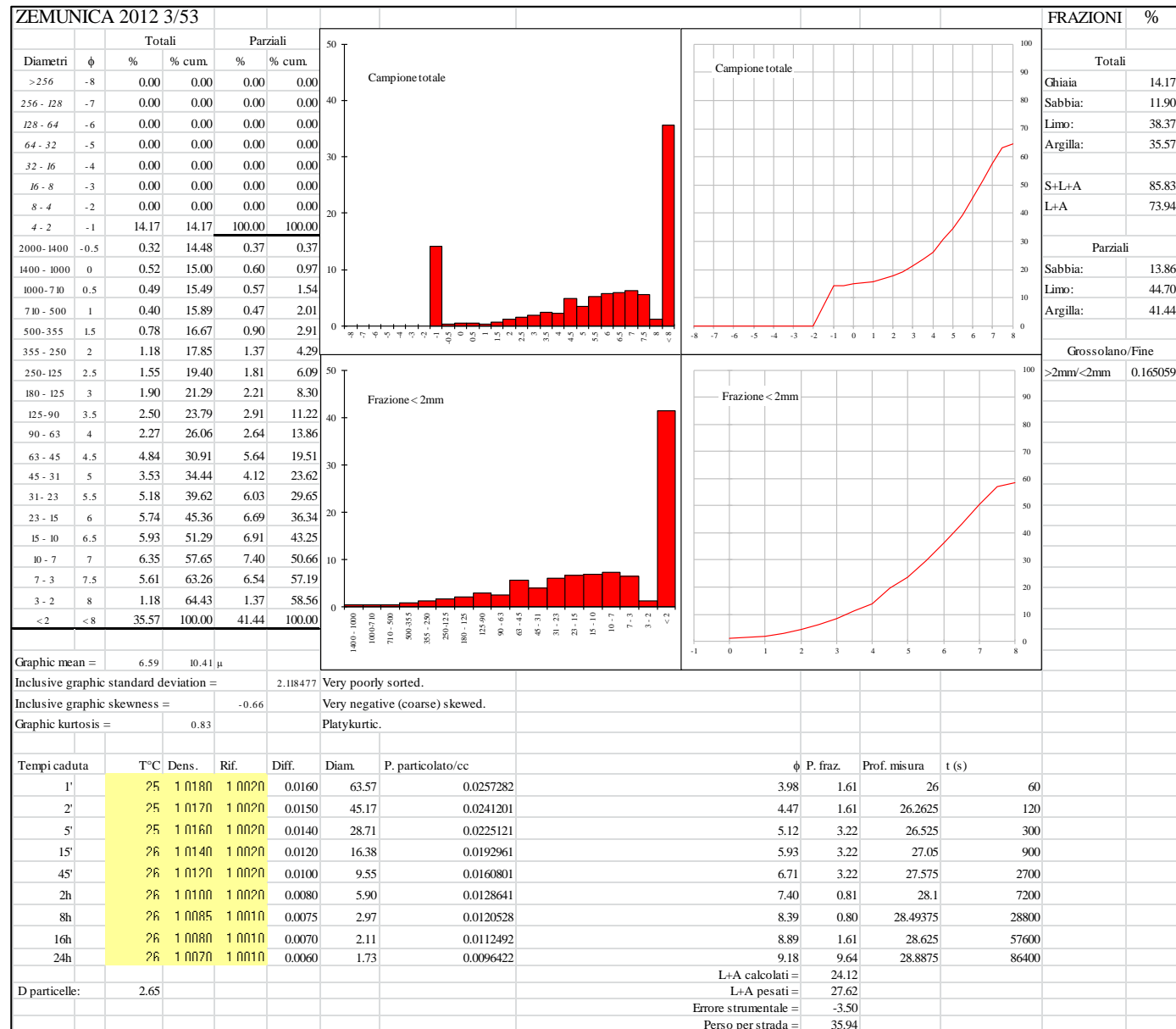
**Appendix 5.1. Grain-size
(Wentworth, 1922) of the <2 mm
fraction of undecalcified samples
from Zemunica, SU 35 (Trench
3a).**



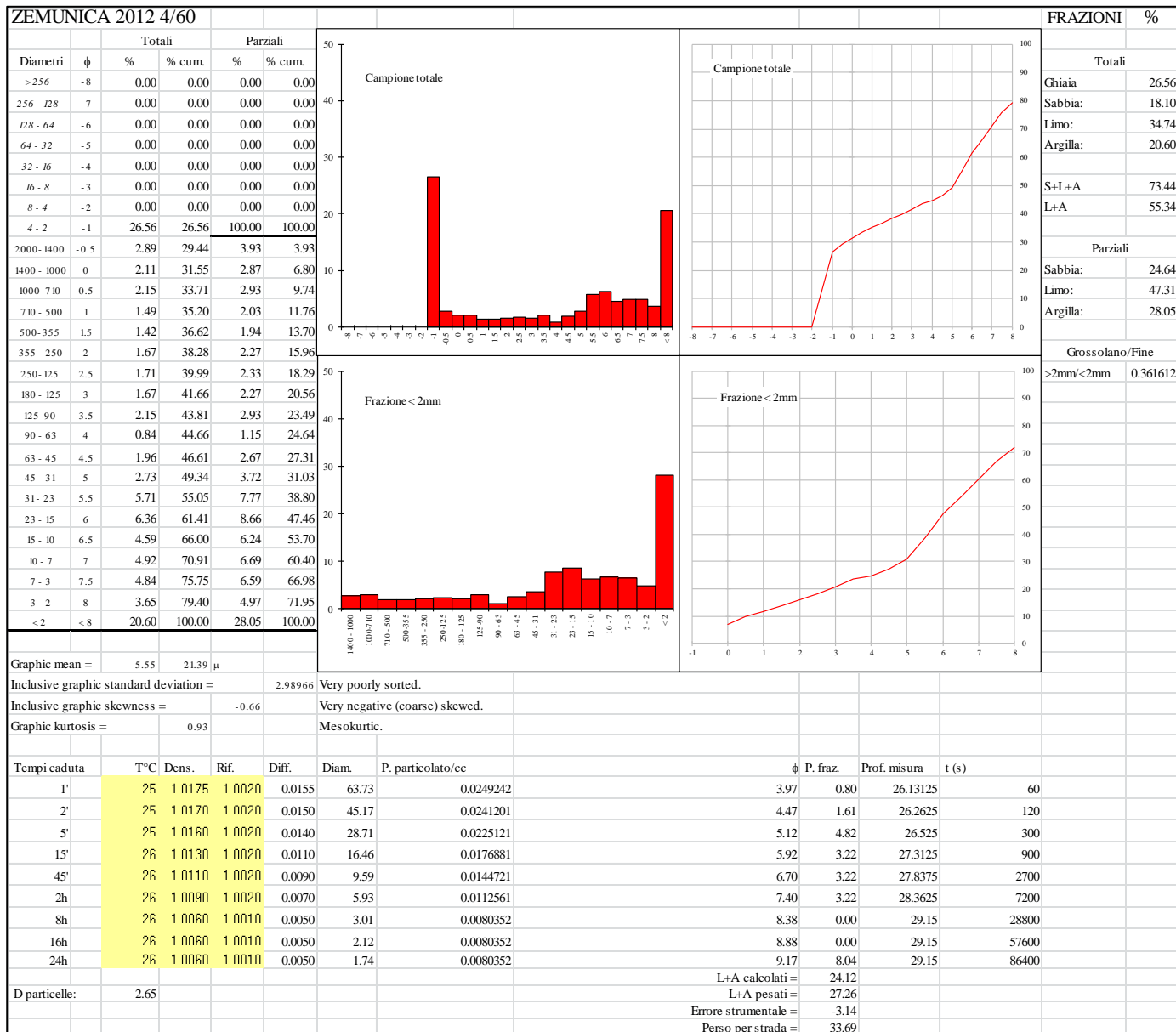
**Appendix 5.2. Grain-size
(Wentworth, 1922) of the <2 mm
fraction of undecalcified samples
from Zemunica, SU 40 (Trench
3a).**



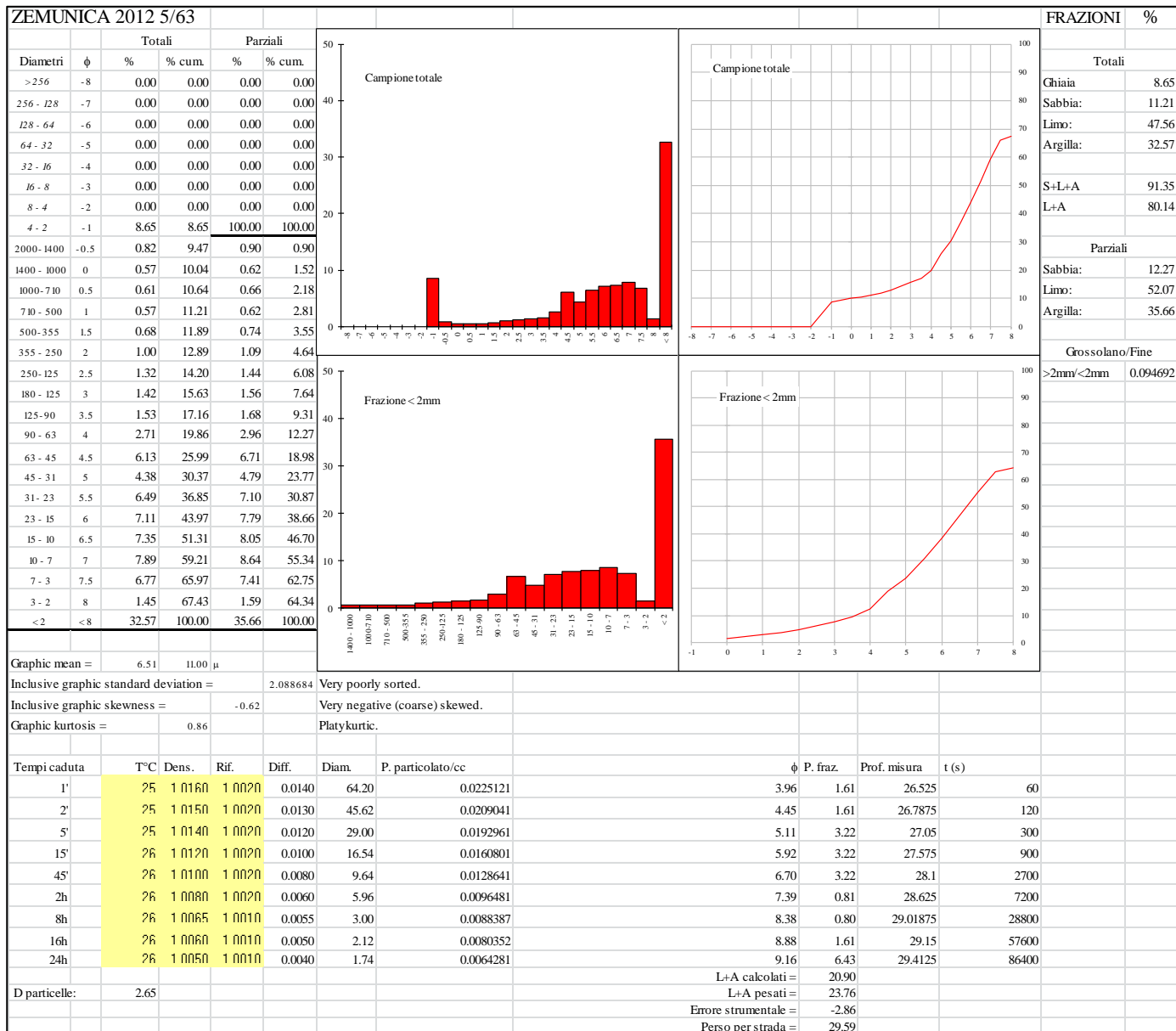
Appendix 5.3. Grain-size (Wentworth, 1922) of the <2 mm fraction of undecalcified samples from Zemunica, SU 53 (Trench 3a).



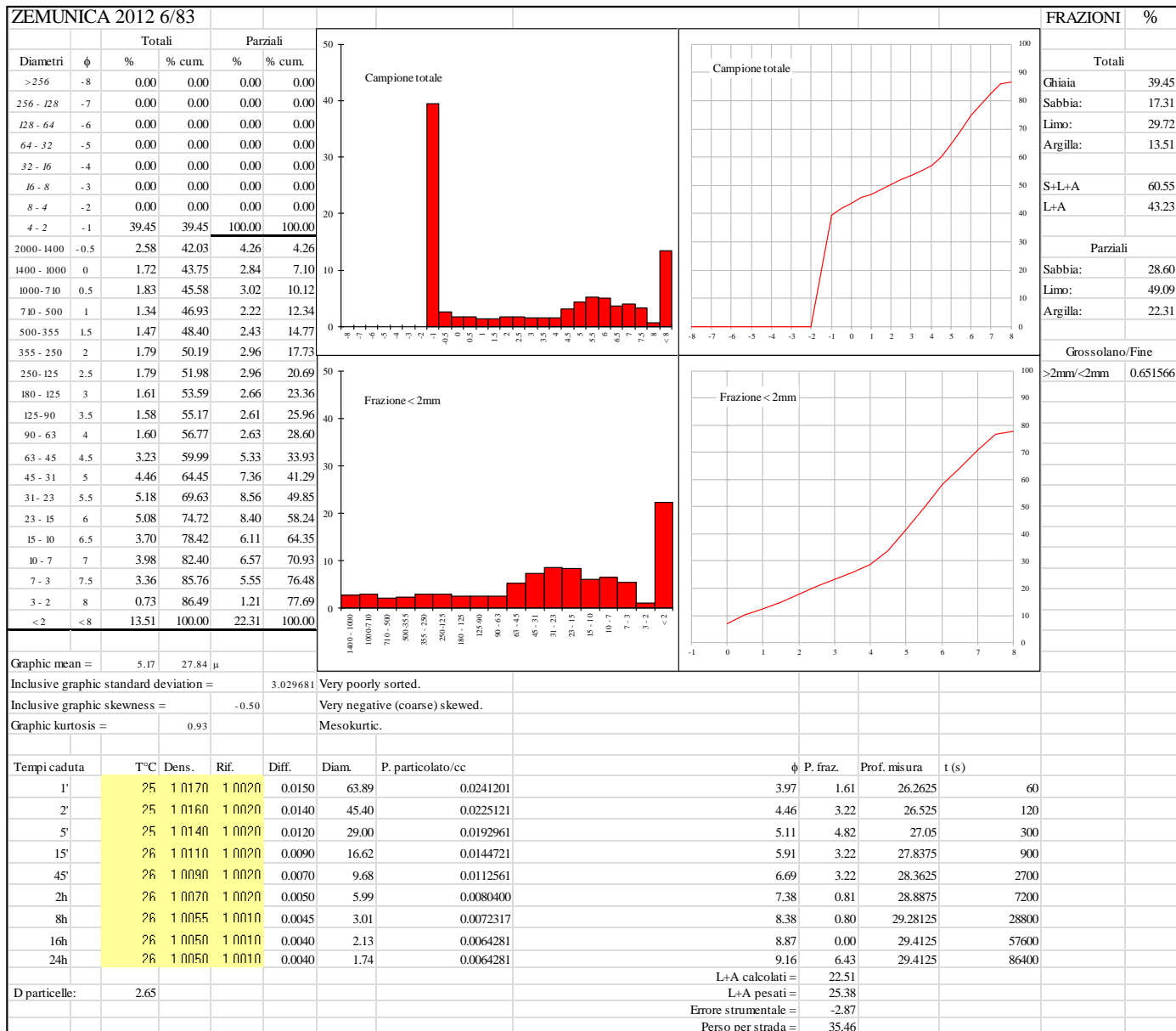
**Appendix 5.4. Grain-size
(Wentworth, 1922) of the <2 mm
fraction of undecalcified samples
from Zemunica, SU 60 (Trench
3a).**



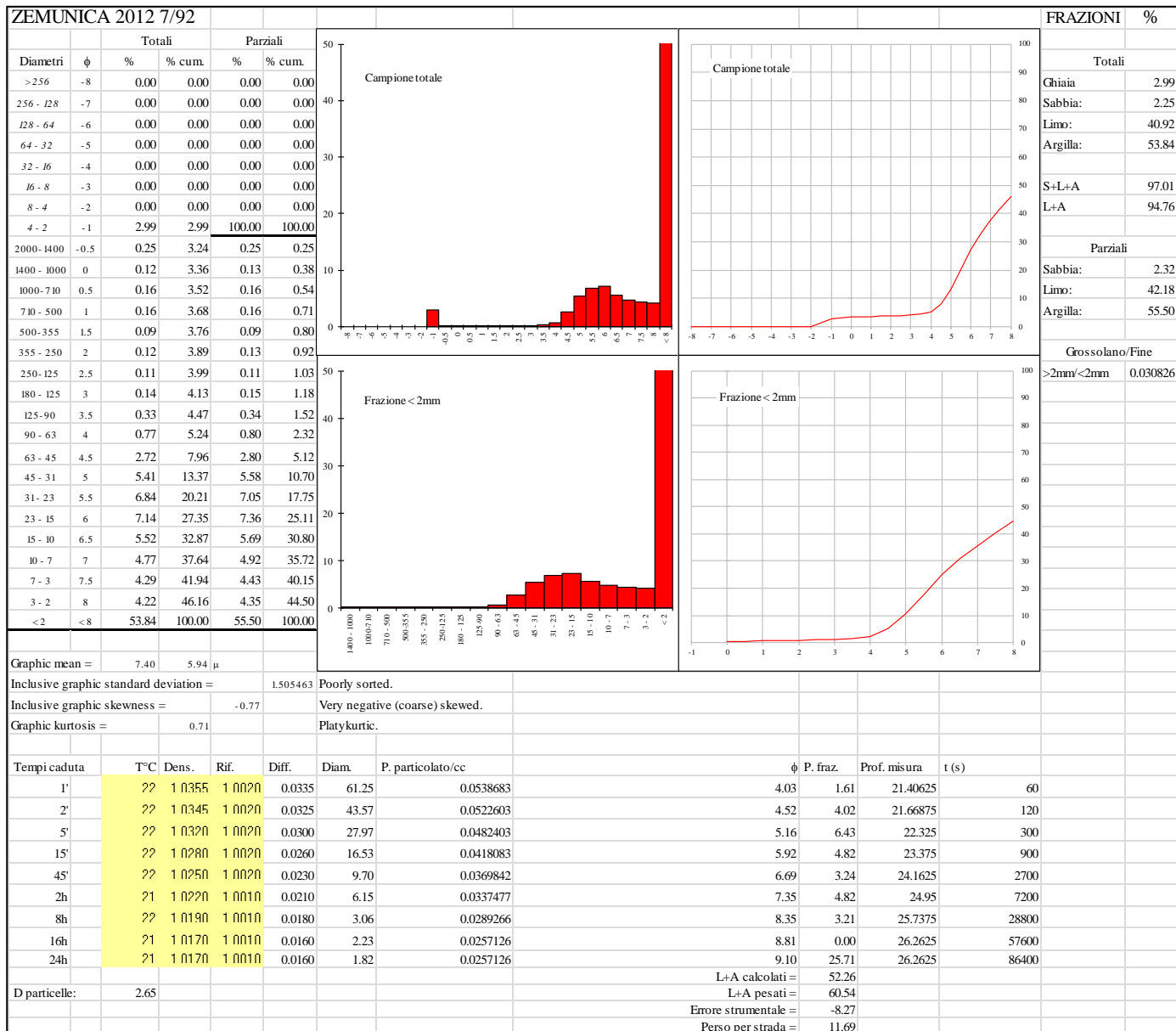
**Appendix 5.5. Grain-size
(Wentworth, 1922) of the <2 mm
fraction of undecalcified samples
from Zemunica, SU 63 (Trench
3a).**



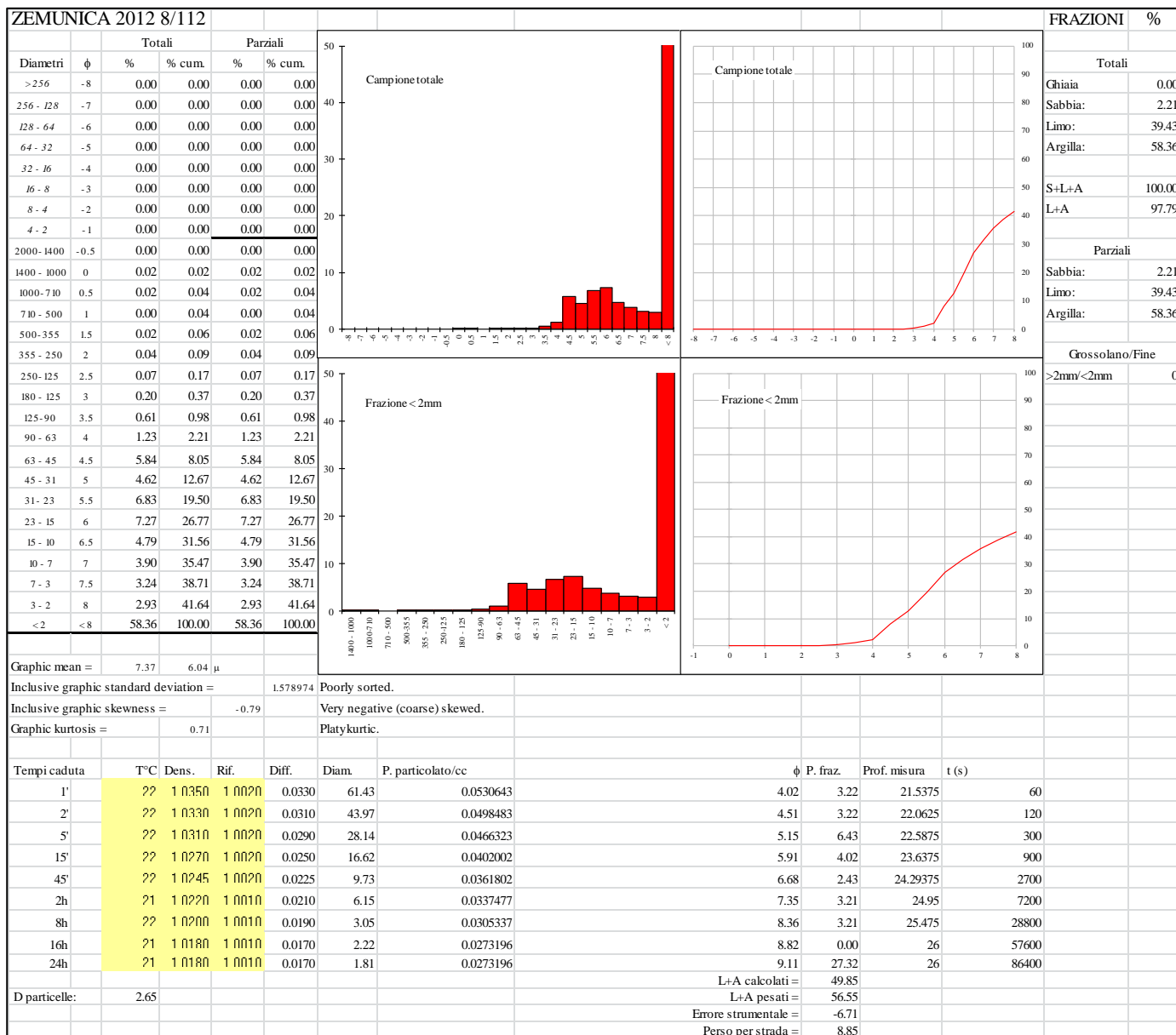
**Appendix 5.6. Grain-size
(Wentworth, 1922) of the <2 mm
fraction of undecalcified samples
from Zemunica, SU 83 (Trench
3a).**



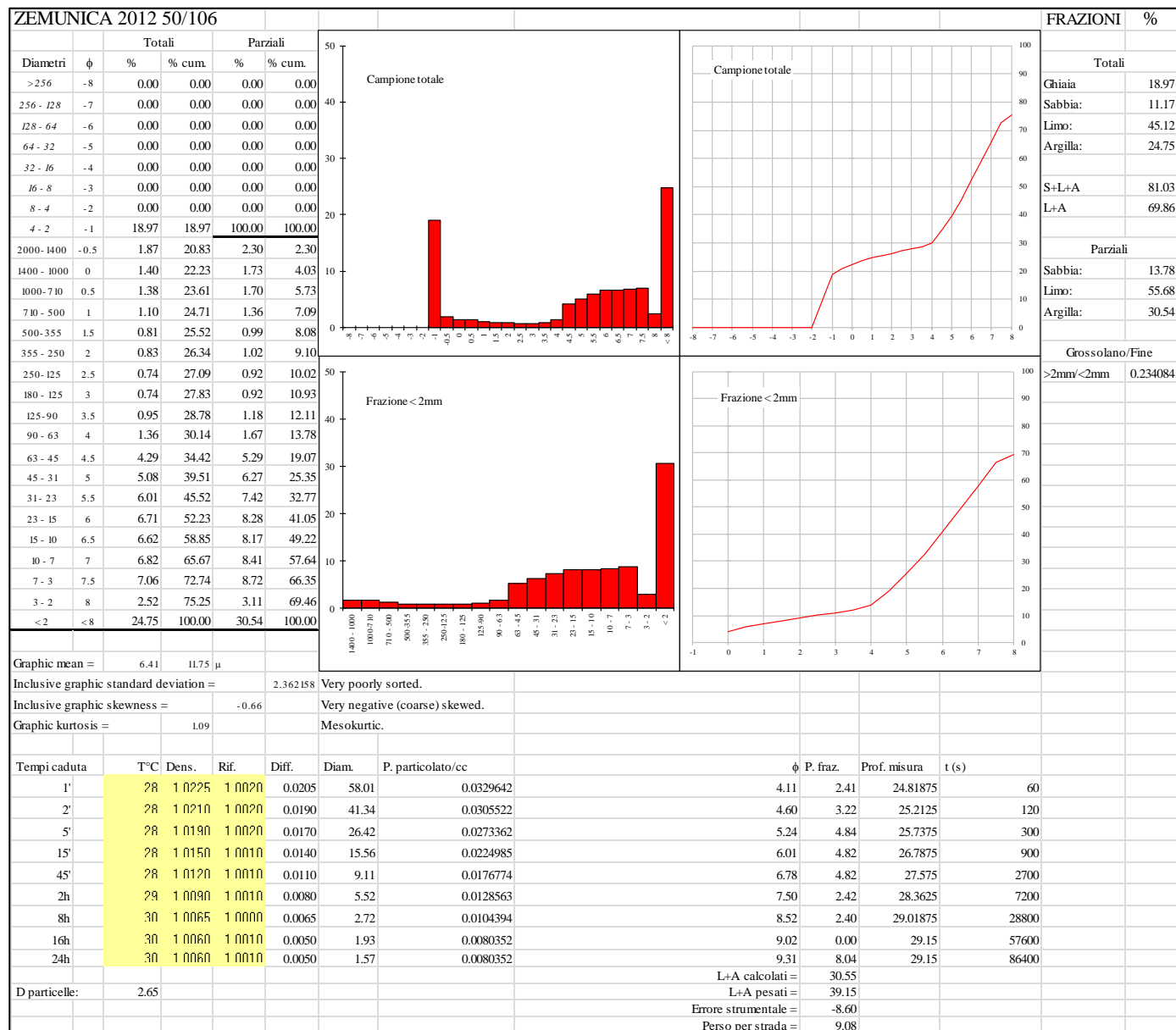
**Appendix 5.7. Grain-size
(Wentworth, 1922) of the <2 mm
fraction of undecalcified samples
from Zemunica, SU 92 (Trench
3a).**



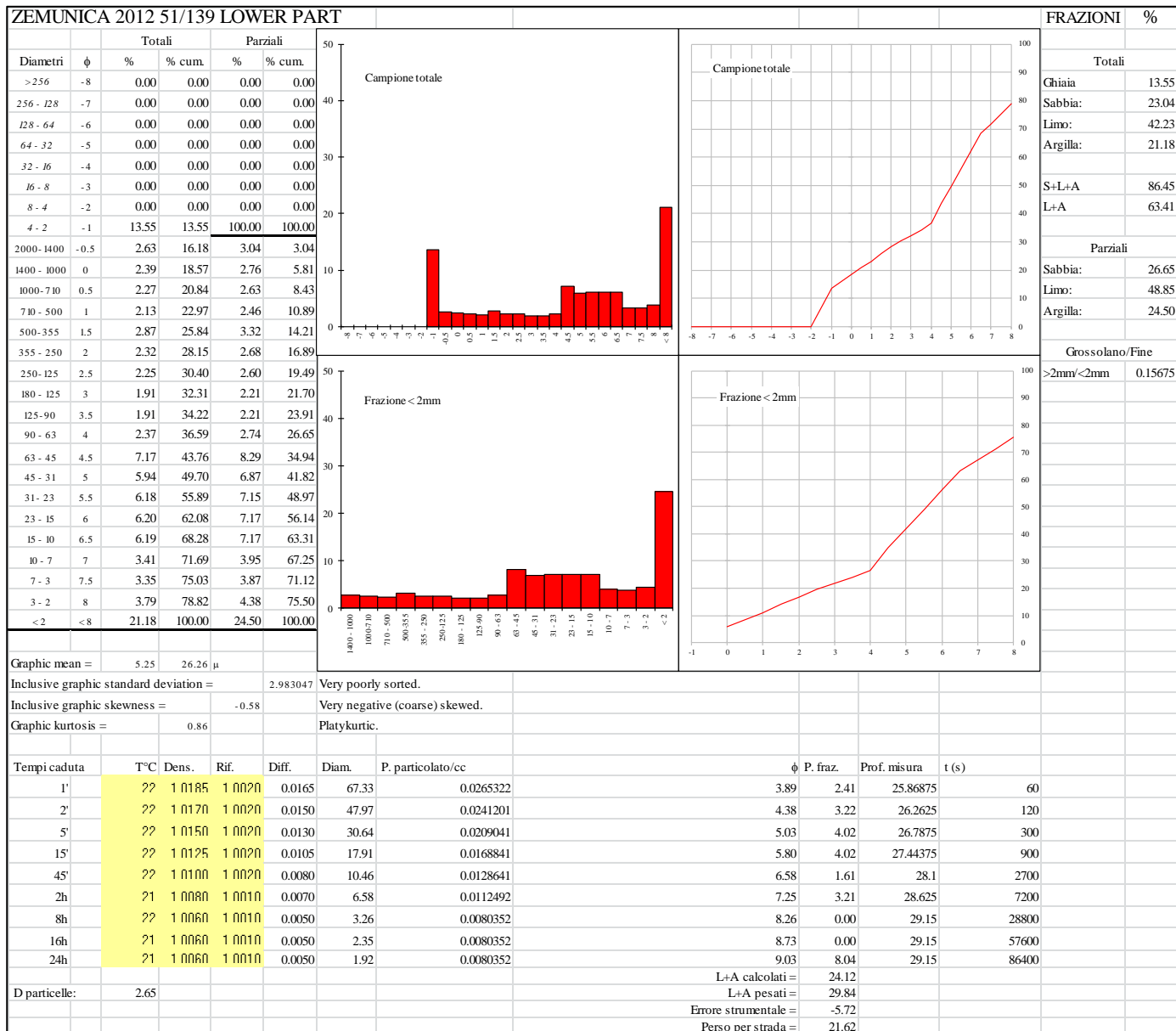
**Appendix 5.8. Grain-size
(Wentworth, 1922) of the <2 mm
fraction of undecalcified samples
from Zemunica, SU 106 lower
part, between large stones SU
112 (Trench 3a).**



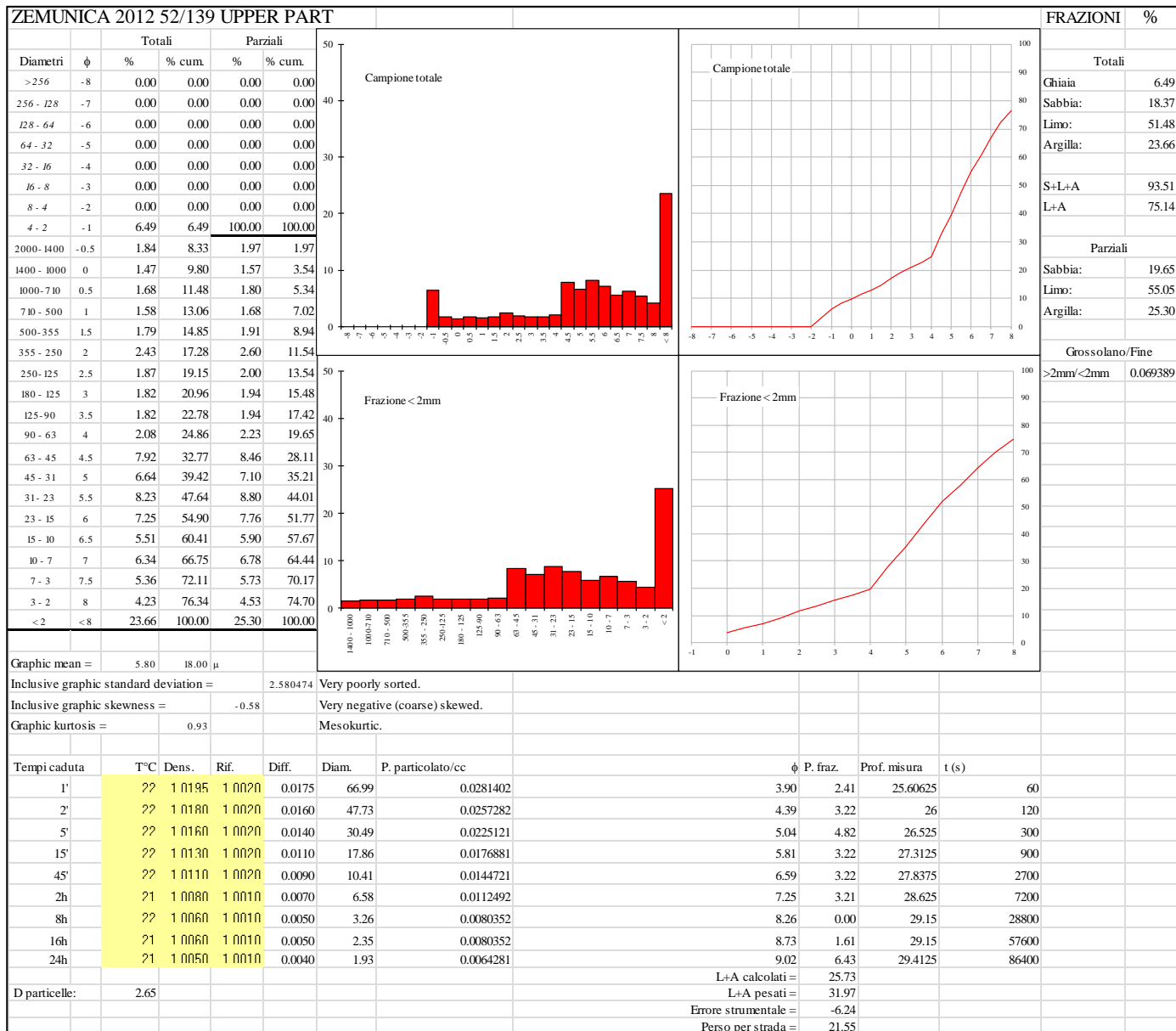
**Appendix 5.9. Grain-size
(Wentworth, 1922) of the <2 mm
fraction of undecalcified samples
from Zemunica, SU 106 (Trench
3b).**



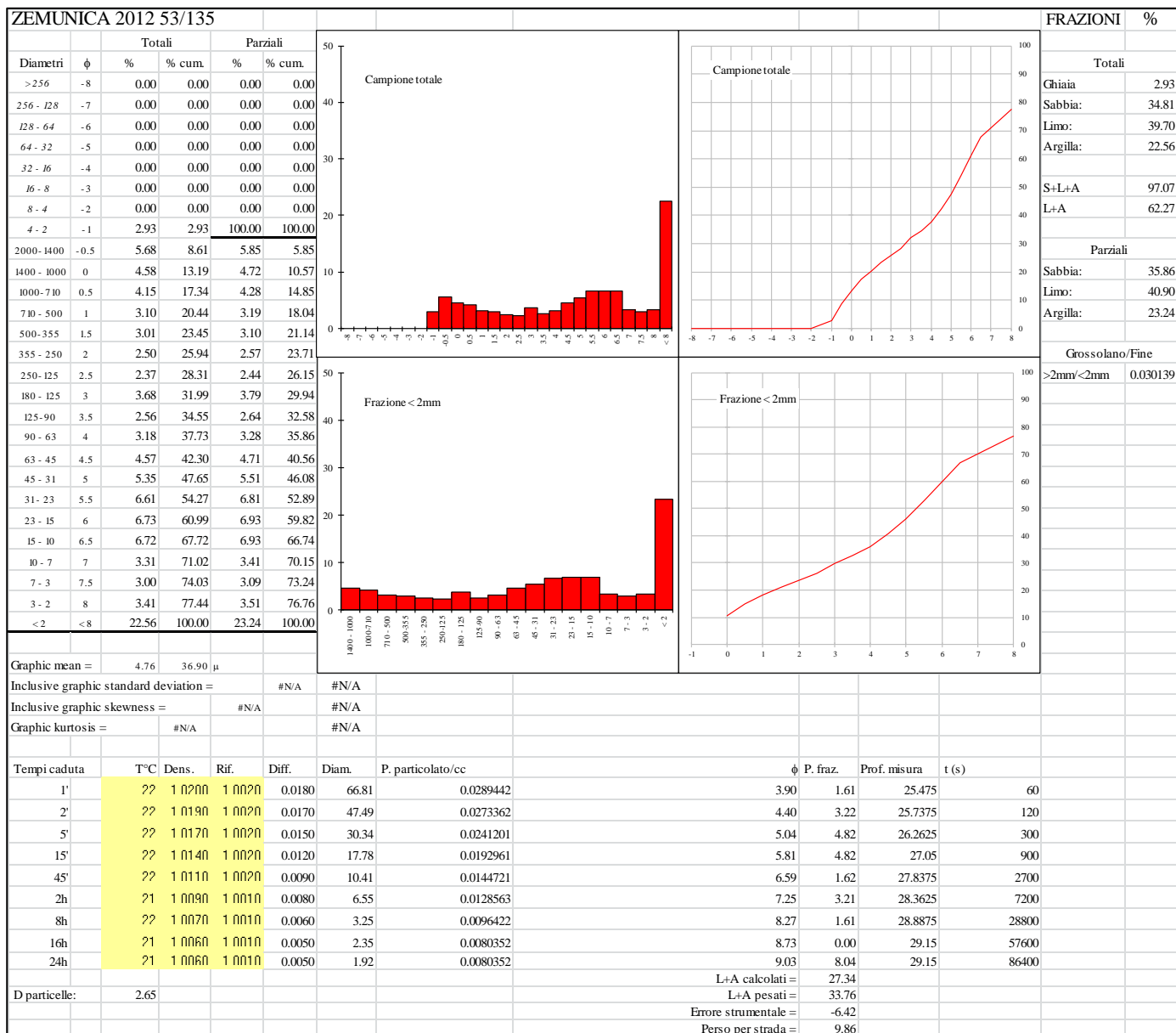
**Appendix 5.10. Grain-size
(Wentworth, 1922) of the <2 mm
fraction of undecalcified samples
from Zemunica, SU 139_lower
part (Trench 3b).**



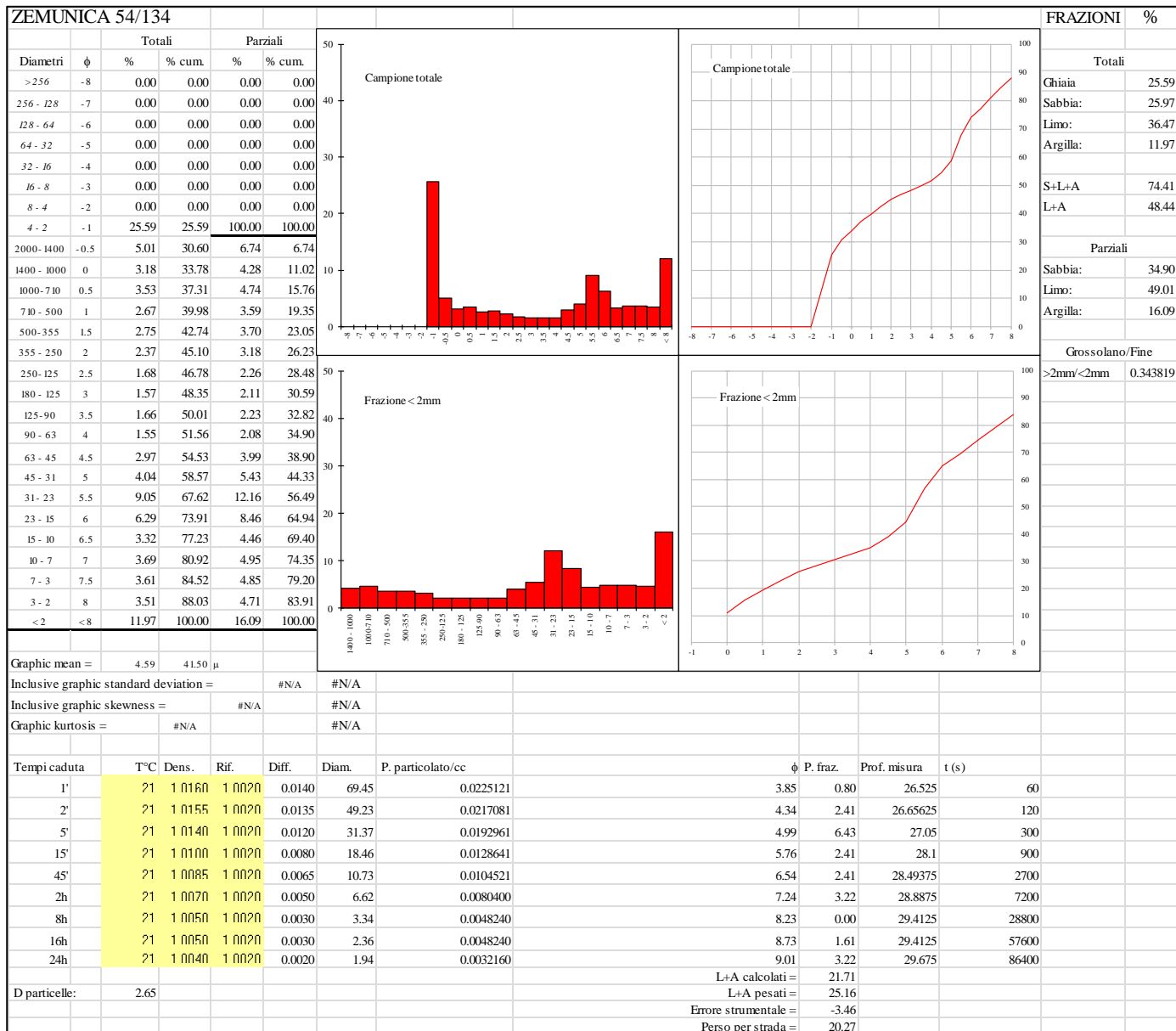
**Appendix 5.11. Grain-size
(Wentworth, 1922) of the <2 mm
fraction of undecalcified samples
from Zemunica, SU 139_upper
part (Trench 3b).**



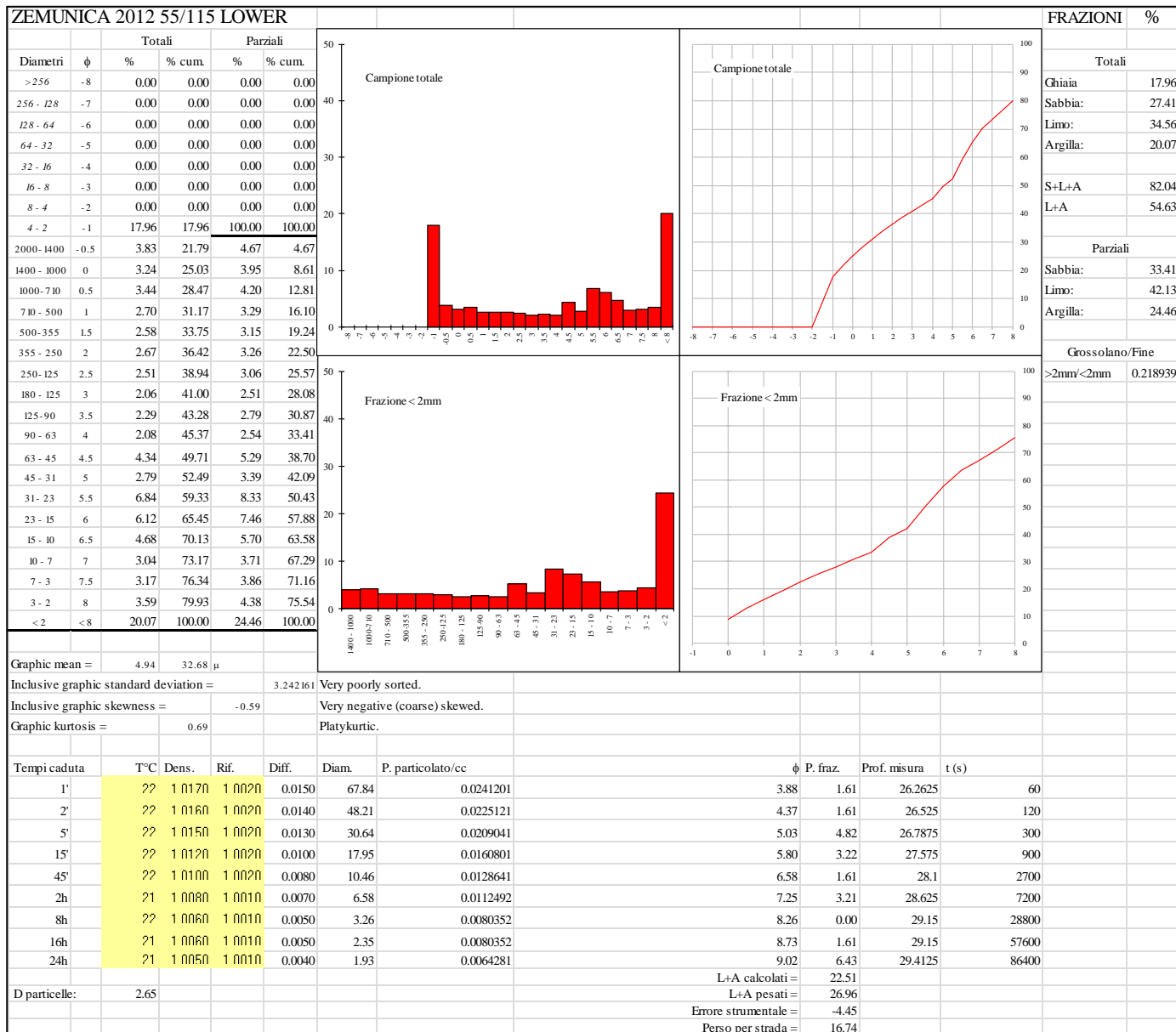
**Appendix 5.12. Grain-size
(Wentworth, 1922) of the <2 mm
fraction of undecalcified samples
from Zemunica, SU 135 (Trench
3b).**



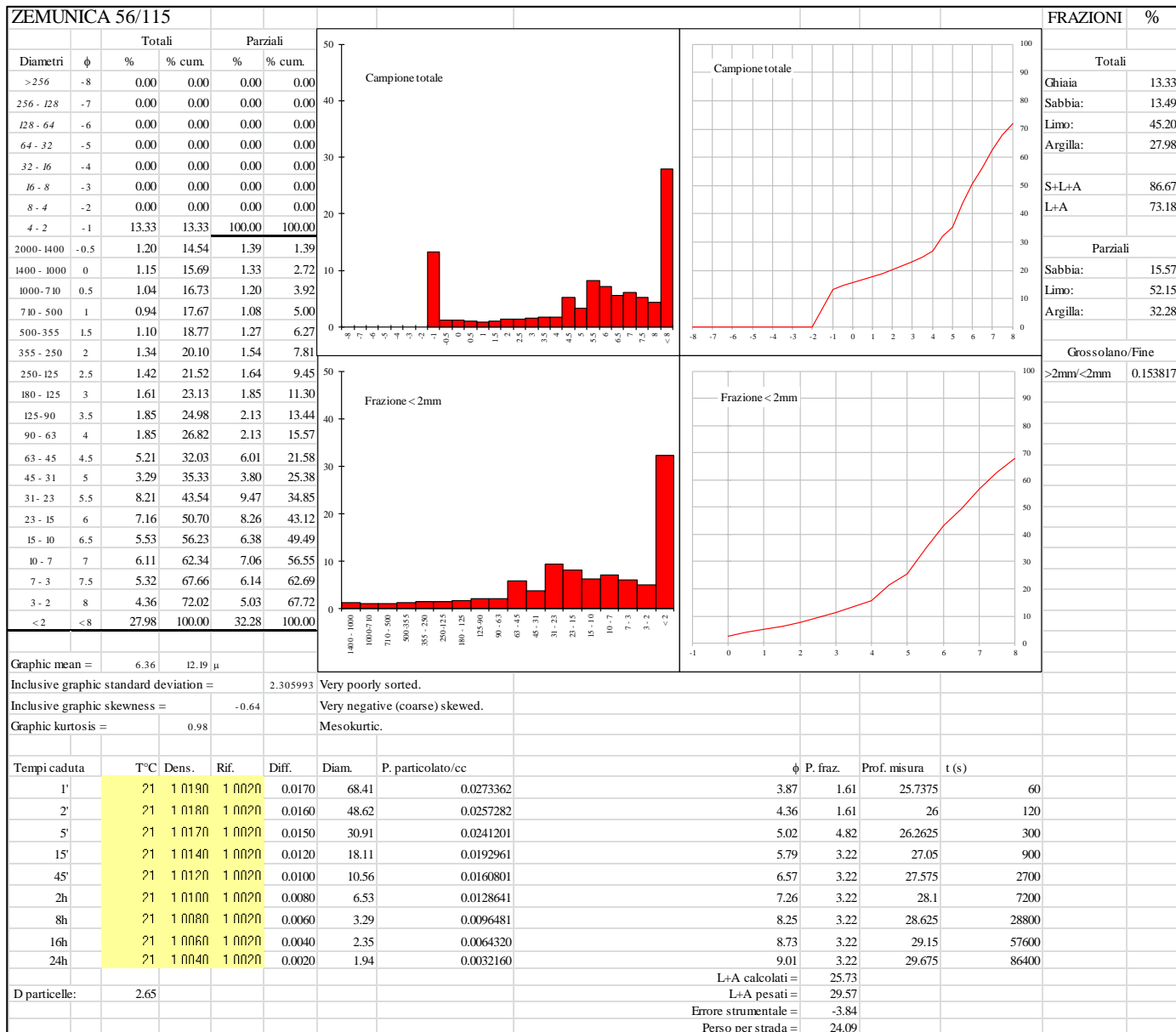
**Appendix 5.13. Grain-size
(Wentworth, 1922) of the <2 mm
fraction of undecalcified samples
from Zemunica, SU 134 (Trench
3b).**



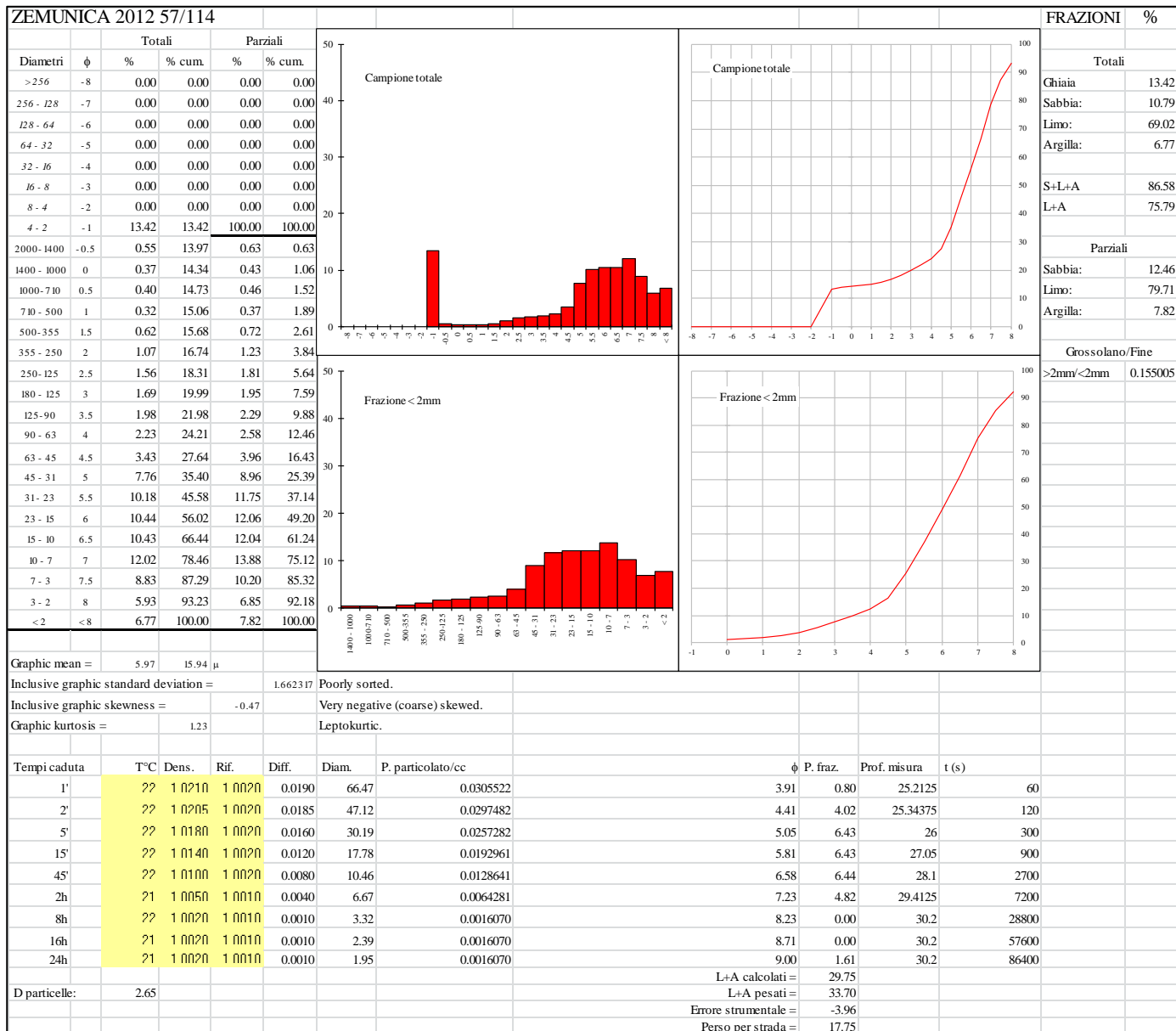
**Appendix 5.14. Grain-size
(Wentworth, 1922) of the <2 mm
fraction of undecalcified samples
from Zemunica, SU 115_lower
part (Trench 3b).**



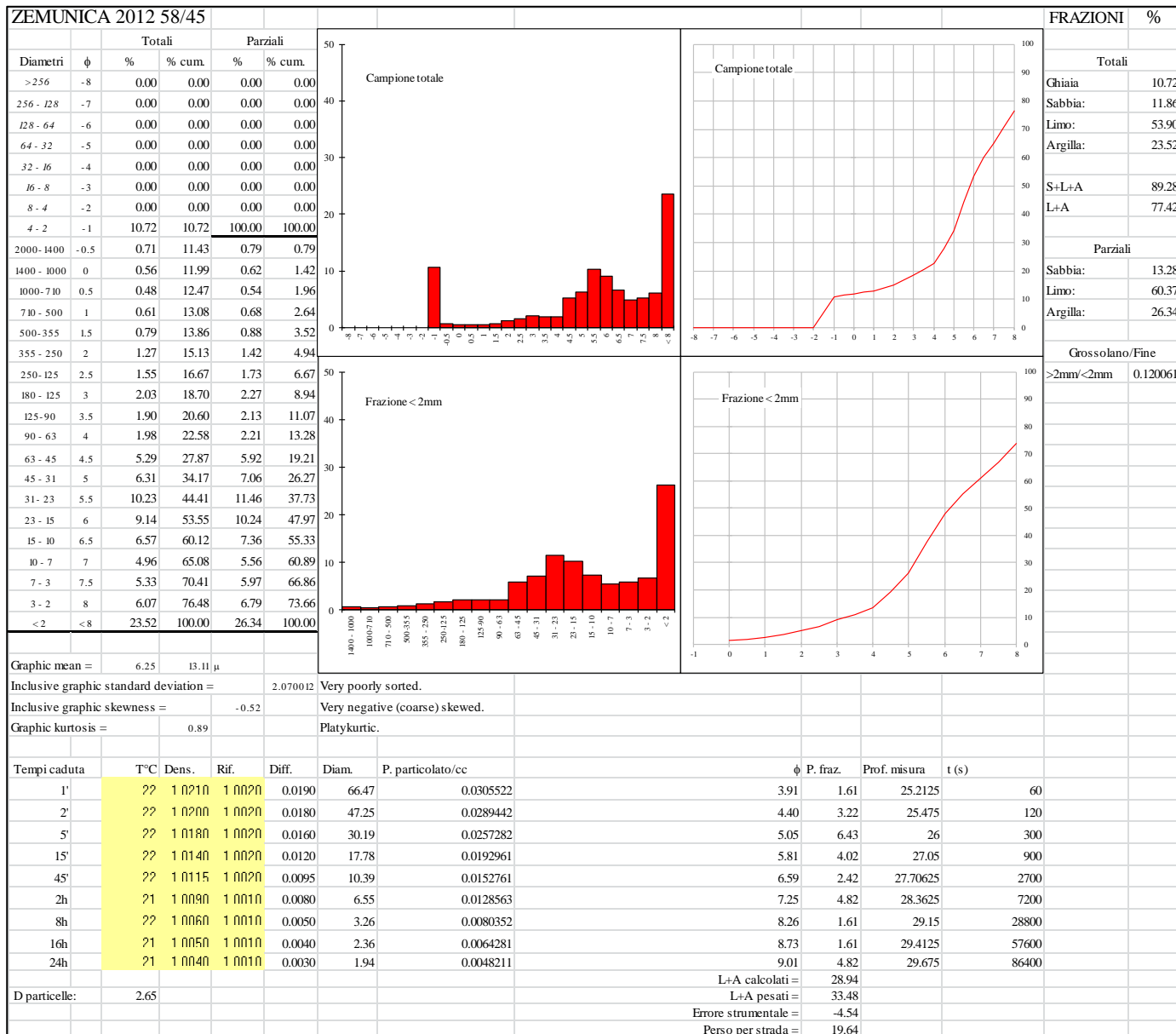
**Appendix 5.15. Grain-size
(Wentworth, 1922) of the <2 mm
fraction of undecalcified samples
from Zemunica, SU 115_upper
part (Trench 3b).**



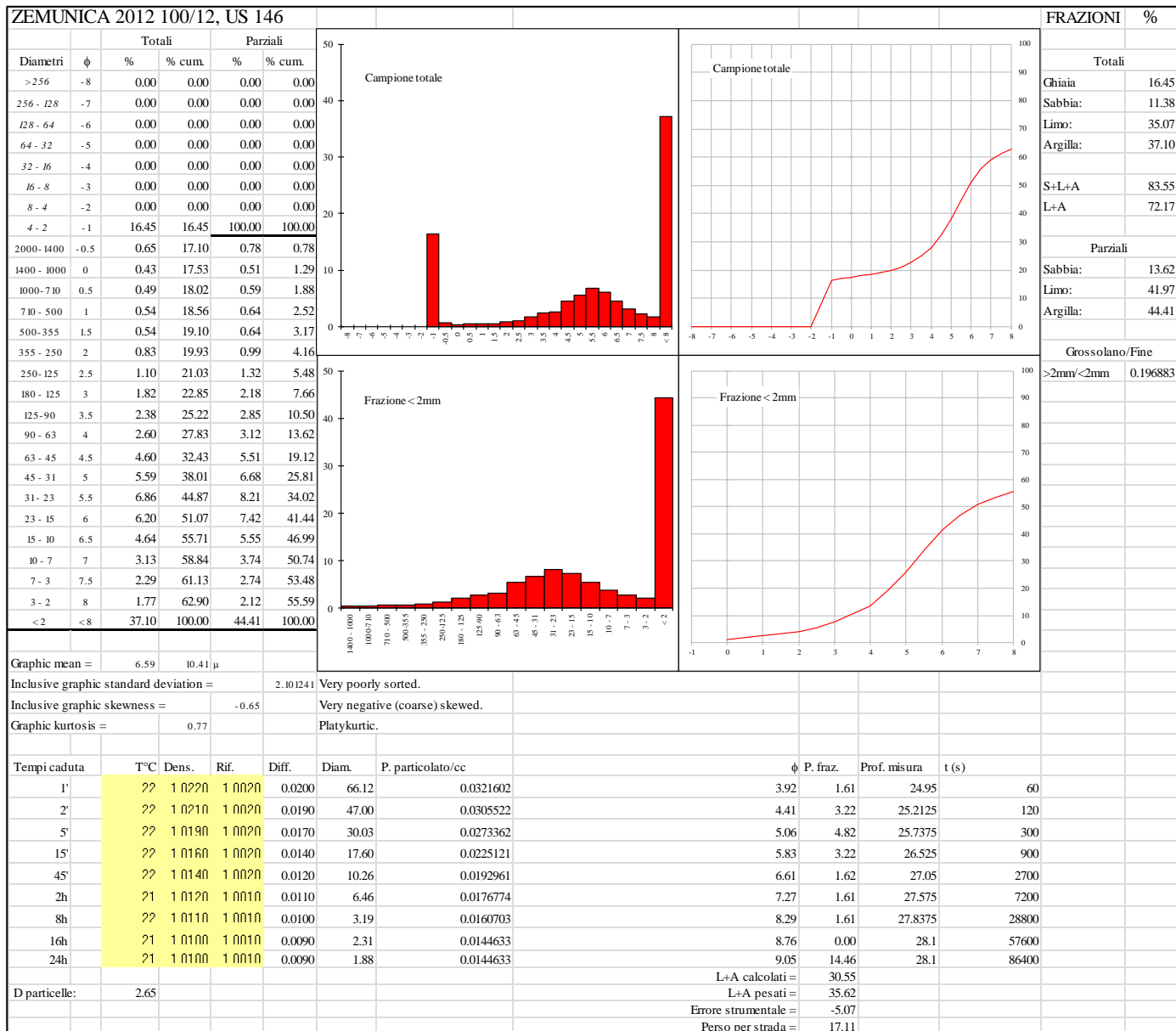
**Appendix 5.16. Grain-size
(Wentworth, 1922) of the <2 mm
fraction of undecalcified samples
from Zemunica, SU 114 (Trench
3b).**



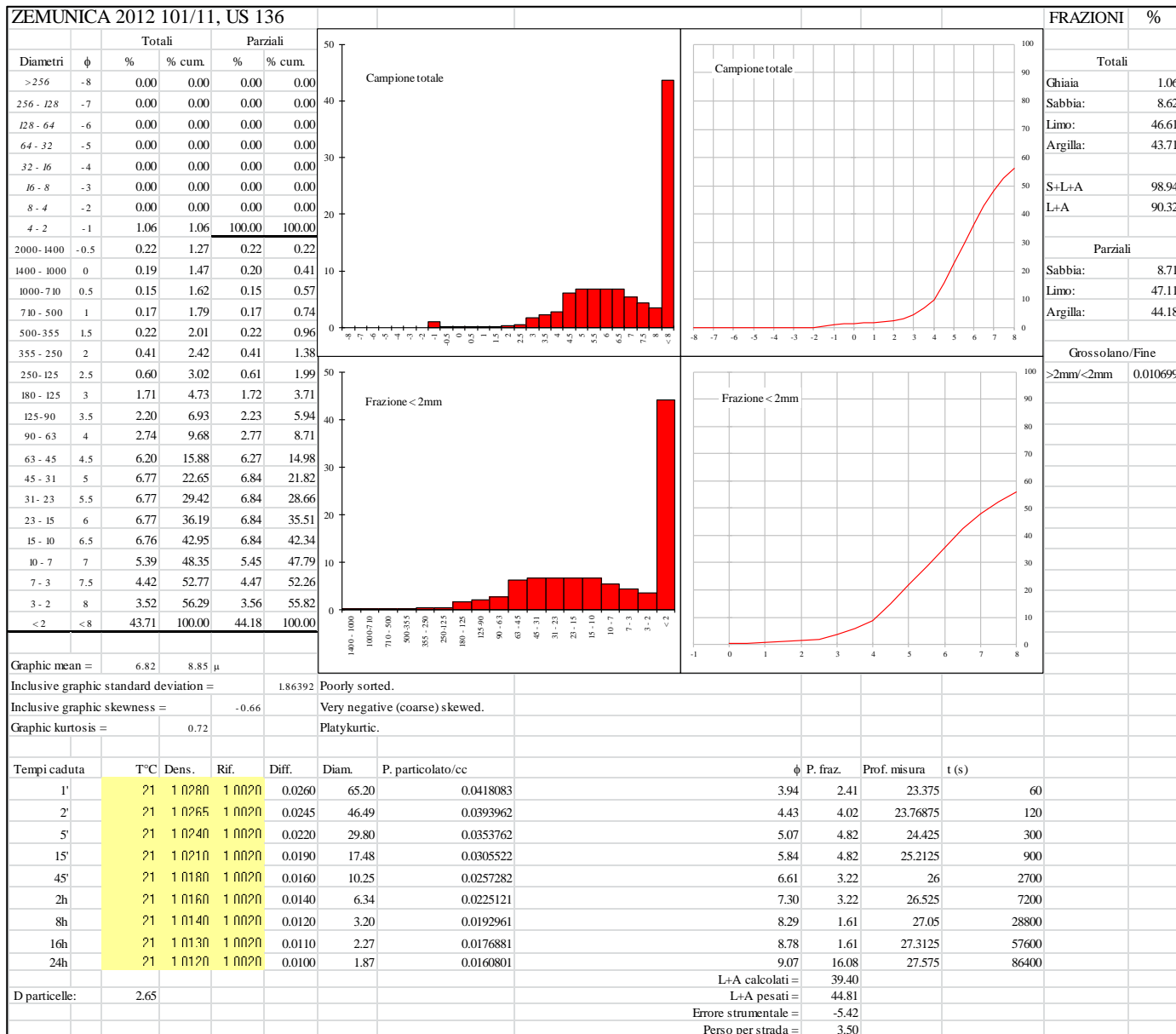
**Appendix 5.17. Grain-size
(Wentworth, 1922) of the <2 mm
fraction of undecalcified samples
from Zemunica, SU 45 (Trench
3b).**



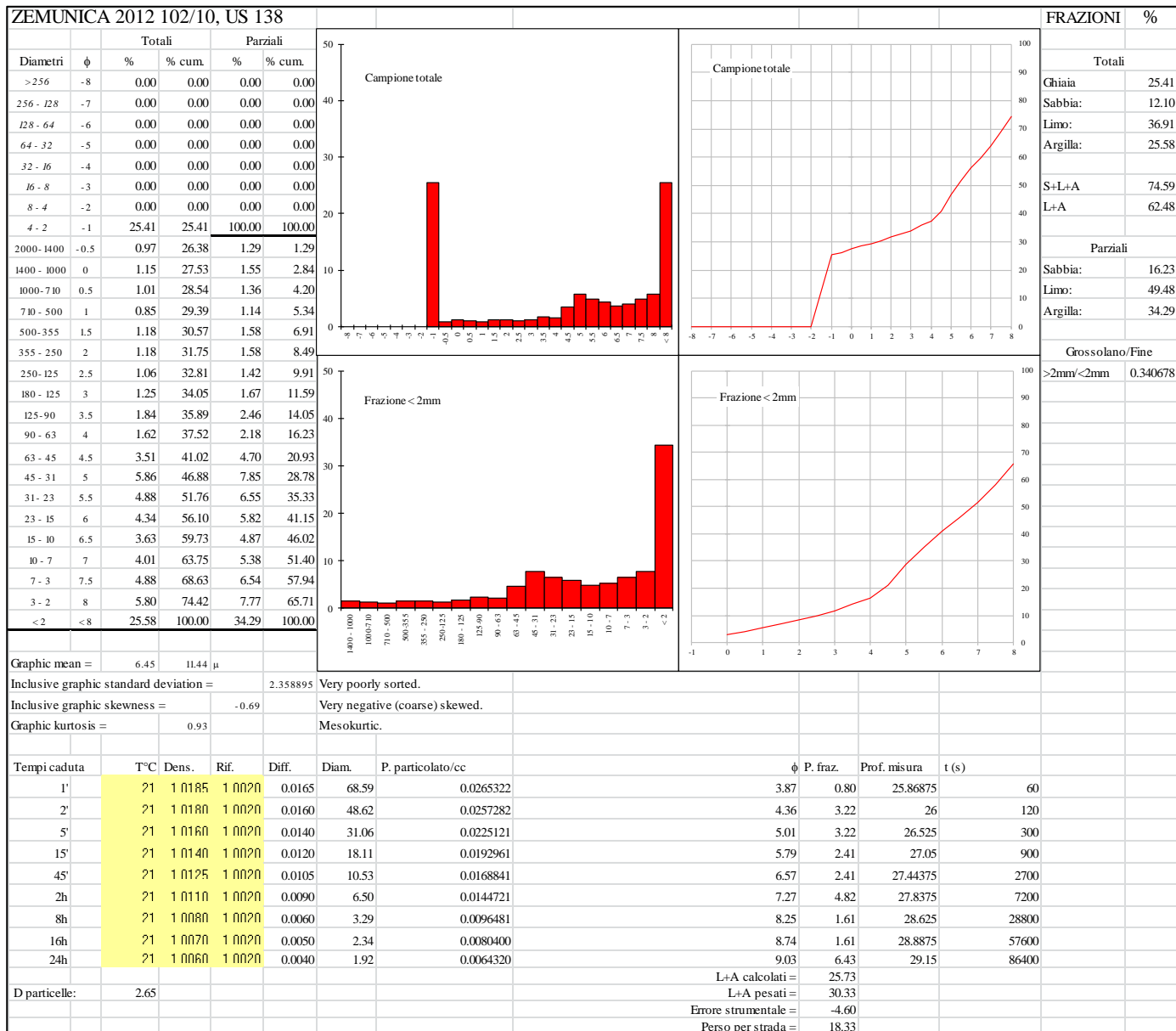
**Appendix 5.18. Grain-size
(Wentworth, 1922) of the <2 mm
fraction of undecalcified samples
from Zemunica, SU 146 (Trench
2).**



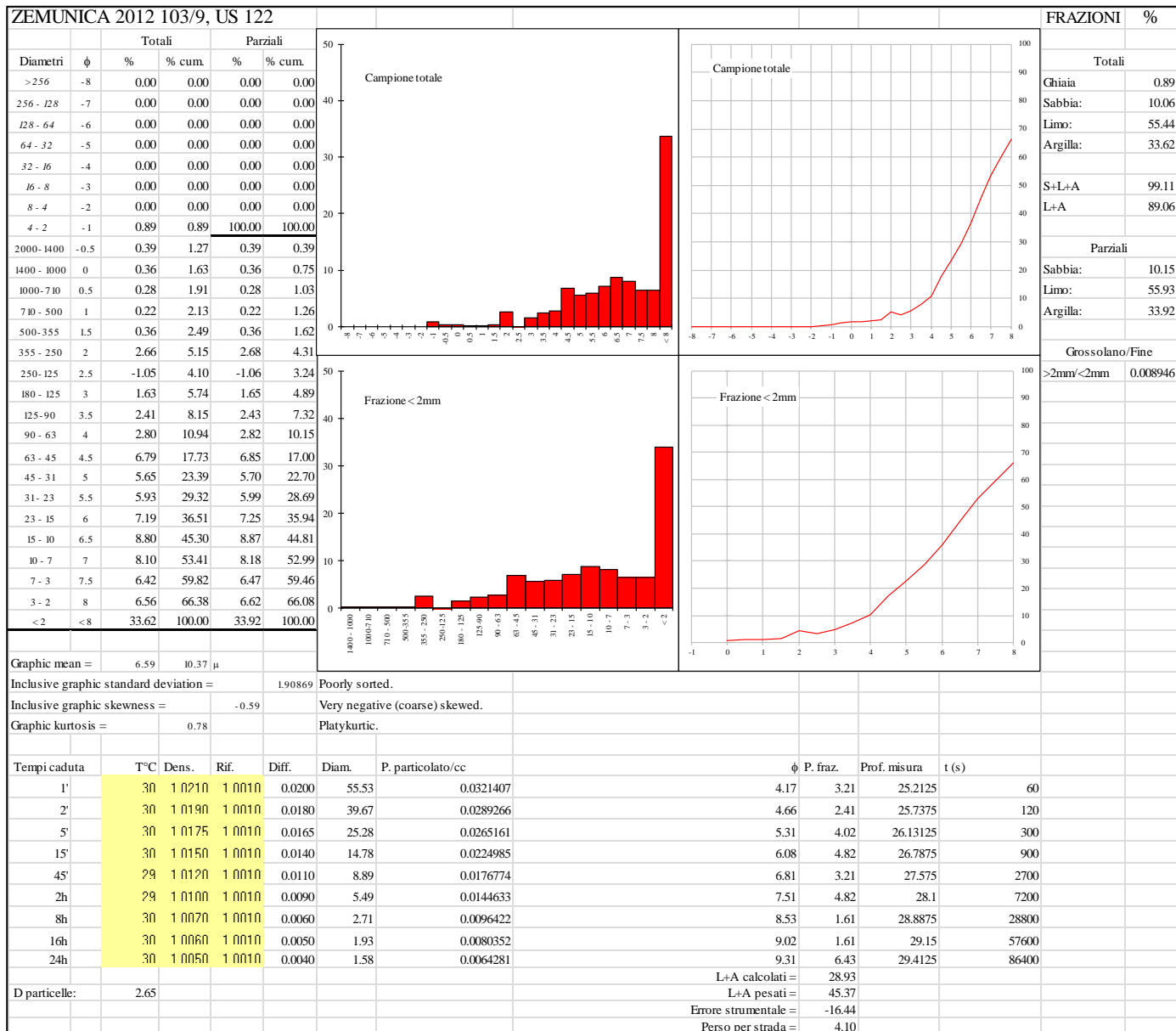
**Appendix 5.19. Grain-size
(Wentworth, 1922) of the <2 mm
fraction of undecalcified samples
from Zemunica, SU 136 (Trench
2).**



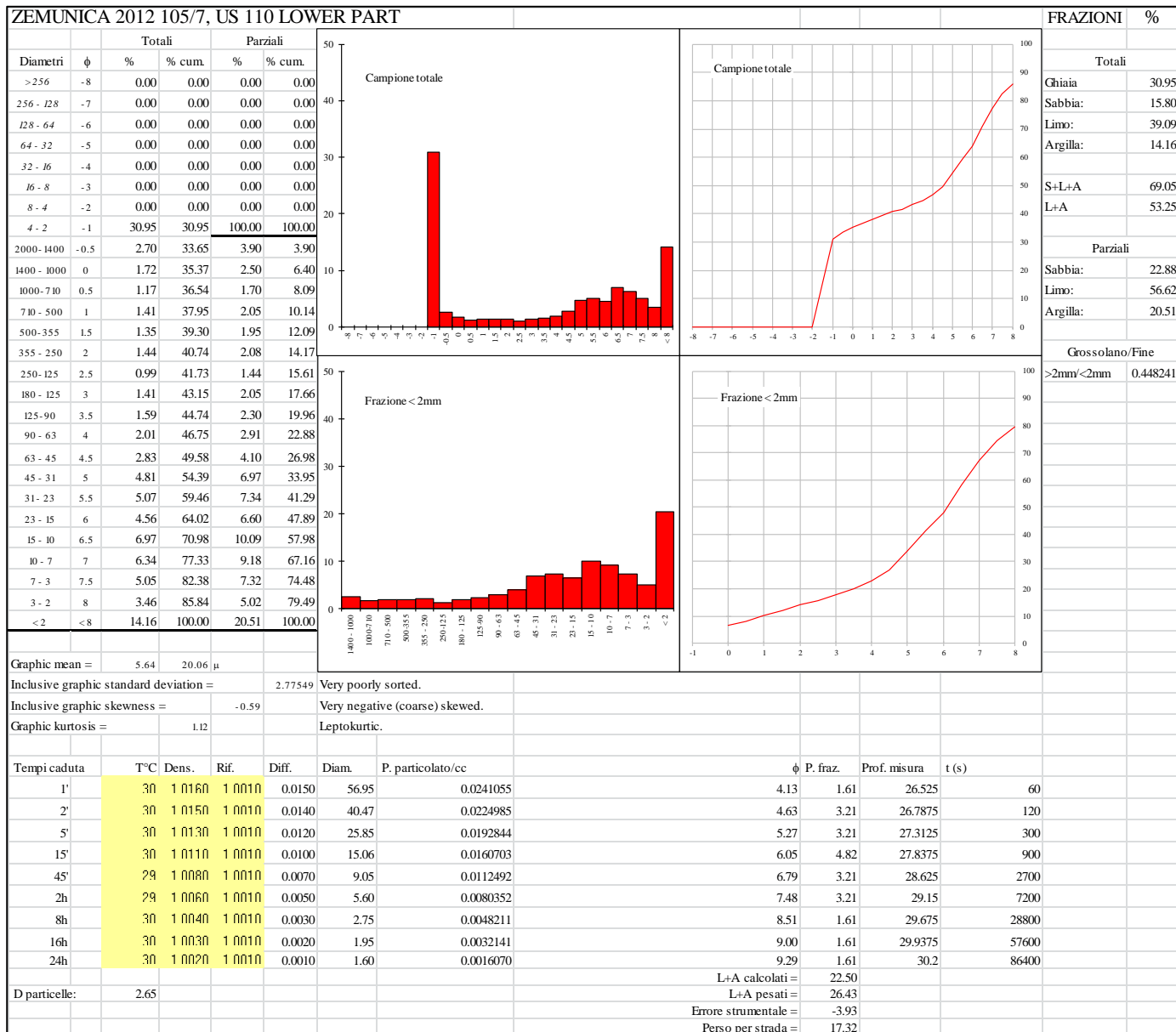
**Appendix 5.20. Grain-size
(Wentworth, 1922) of the <2 mm
fraction of undecalcified samples
from Zemunica, SU 138 (Trench
2).**



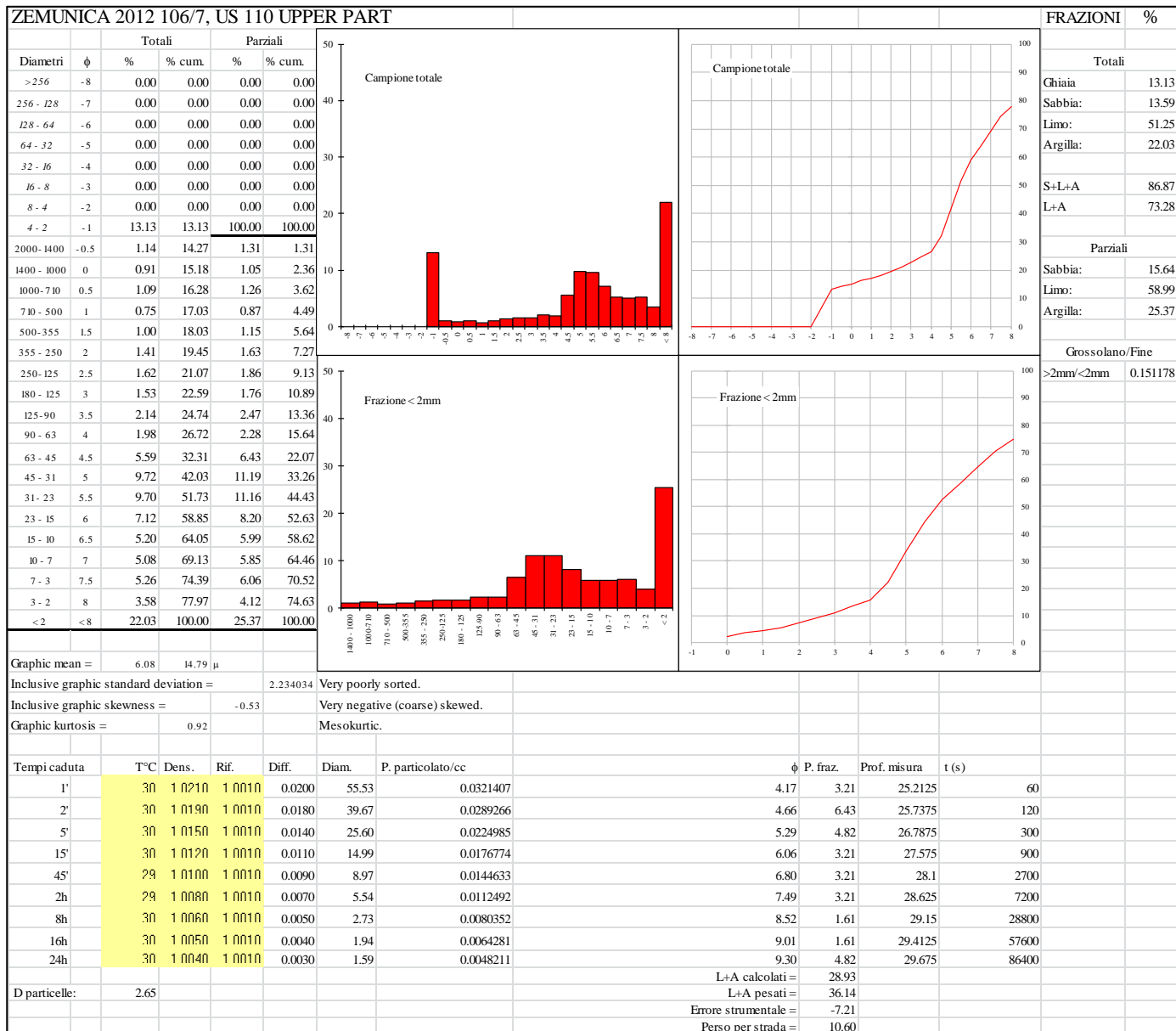
**Appendix 5.21. Grain-size
(Wentworth, 1922) of the <2 mm
fraction of undecalcified samples
from Zemunica, SU 122 (Trench
2).**



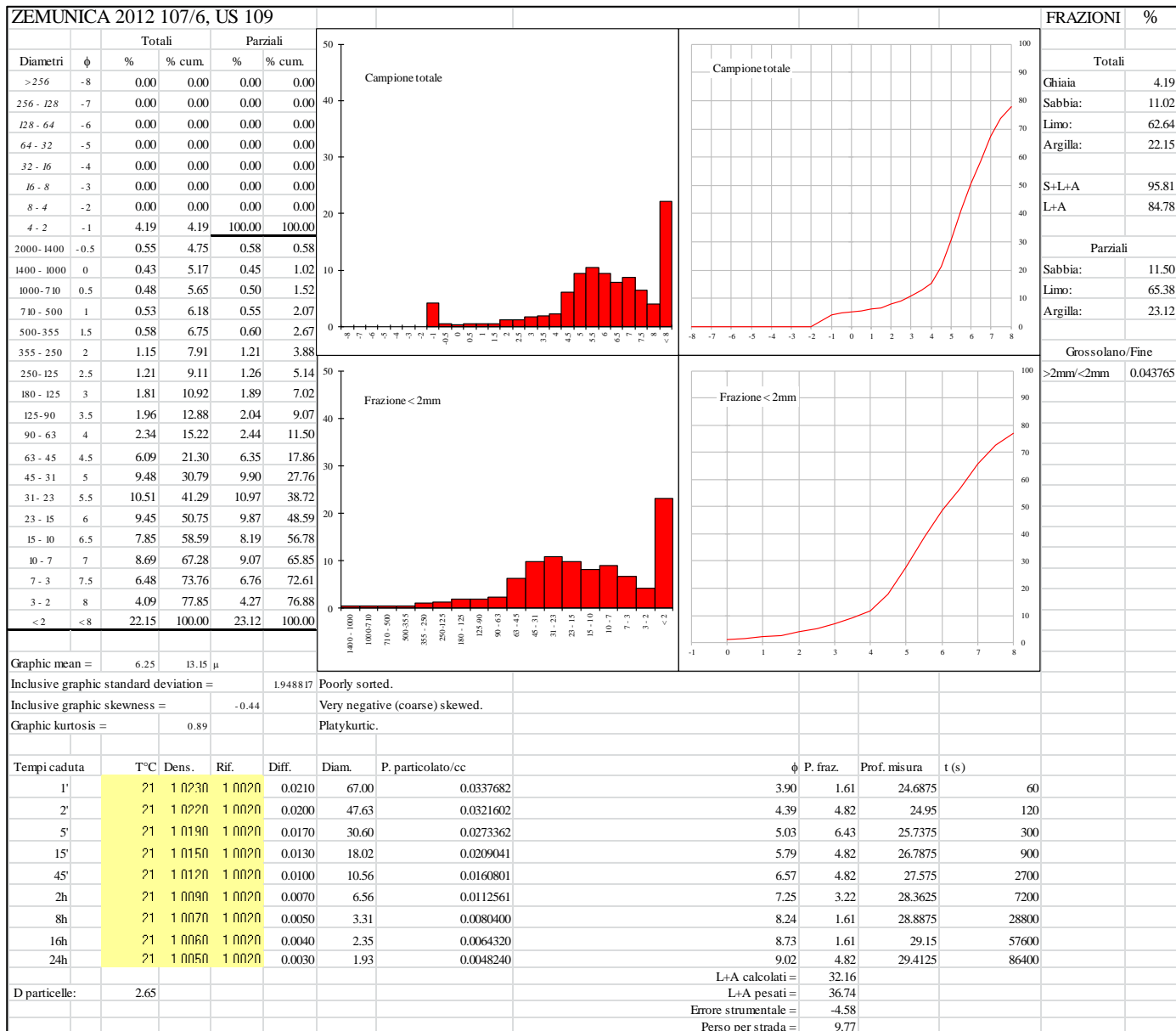
**Appendix 5.22. Grain-size
(Wentworth, 1922) of the <2 mm
fraction of undecalcified samples
from Zemunica, SU 110_lower
part (Trench 2).**



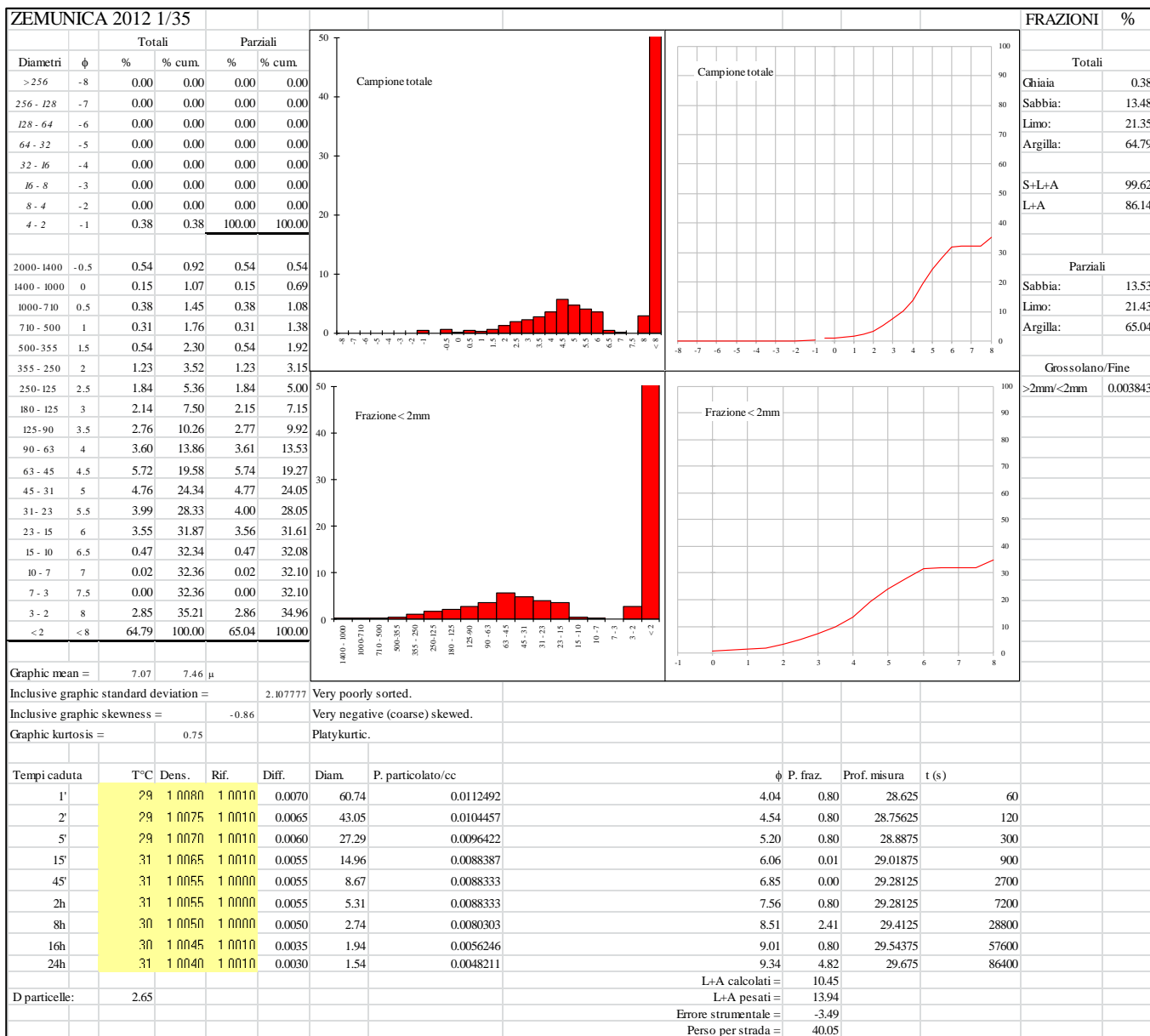
**Appendix 5.23. Grain-size
(Wentworth, 1922) of the <2 mm
fraction of undecalcified samples
from Zemunica, SU 110_upper
part (Trench 2).**



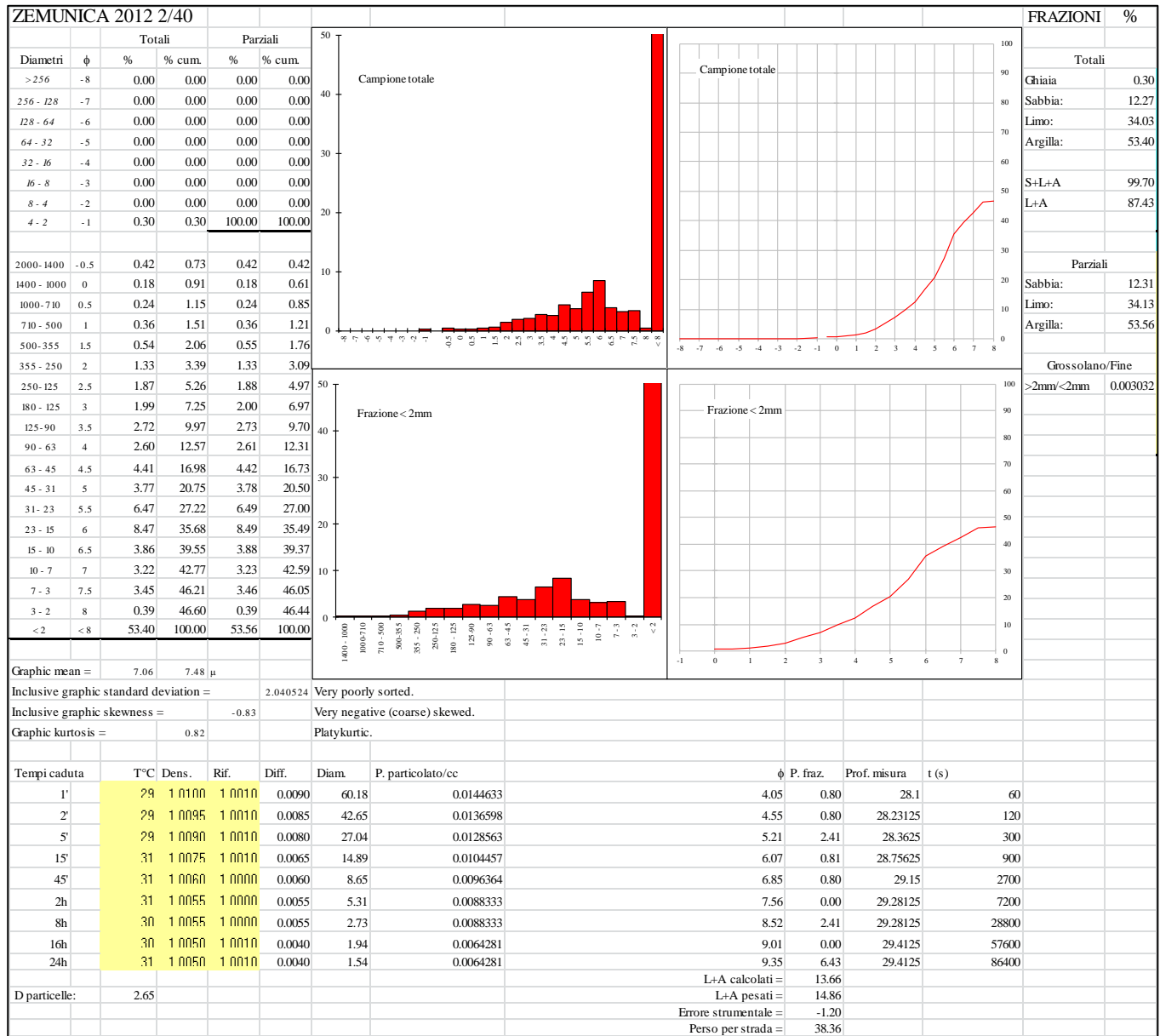
**Appendix 5.24. Grain-size
(Wentworth, 1922) of the <2 mm
fraction of undecalcified samples
from Zemunica, SU 109 (Trench
2).**



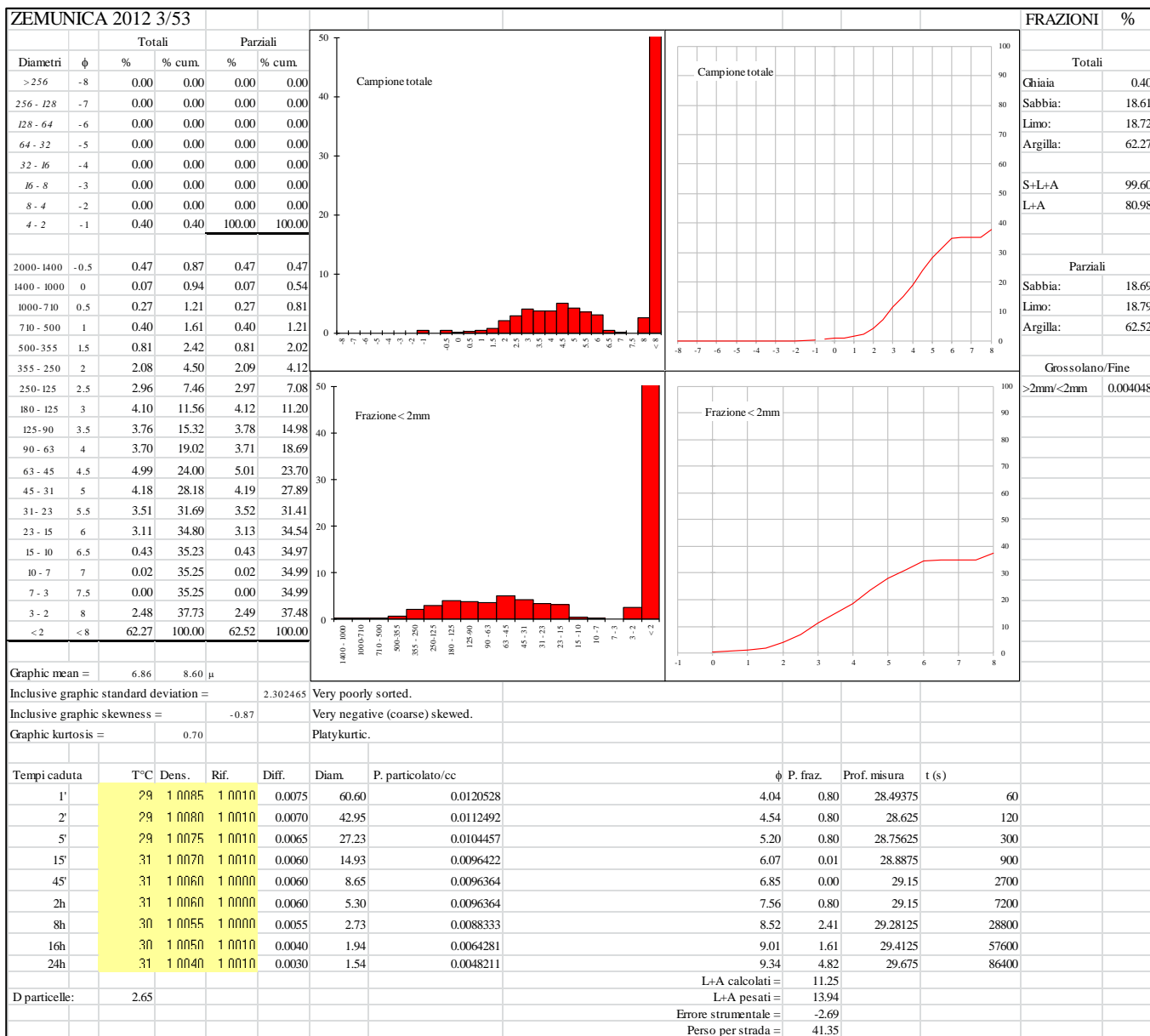
**Appendix 6.1. Grain-size
(Wentworth, 1922) of the <2 mm
fraction of decalcified samples
from Zemunica, SU 35 (Trench 3a).**



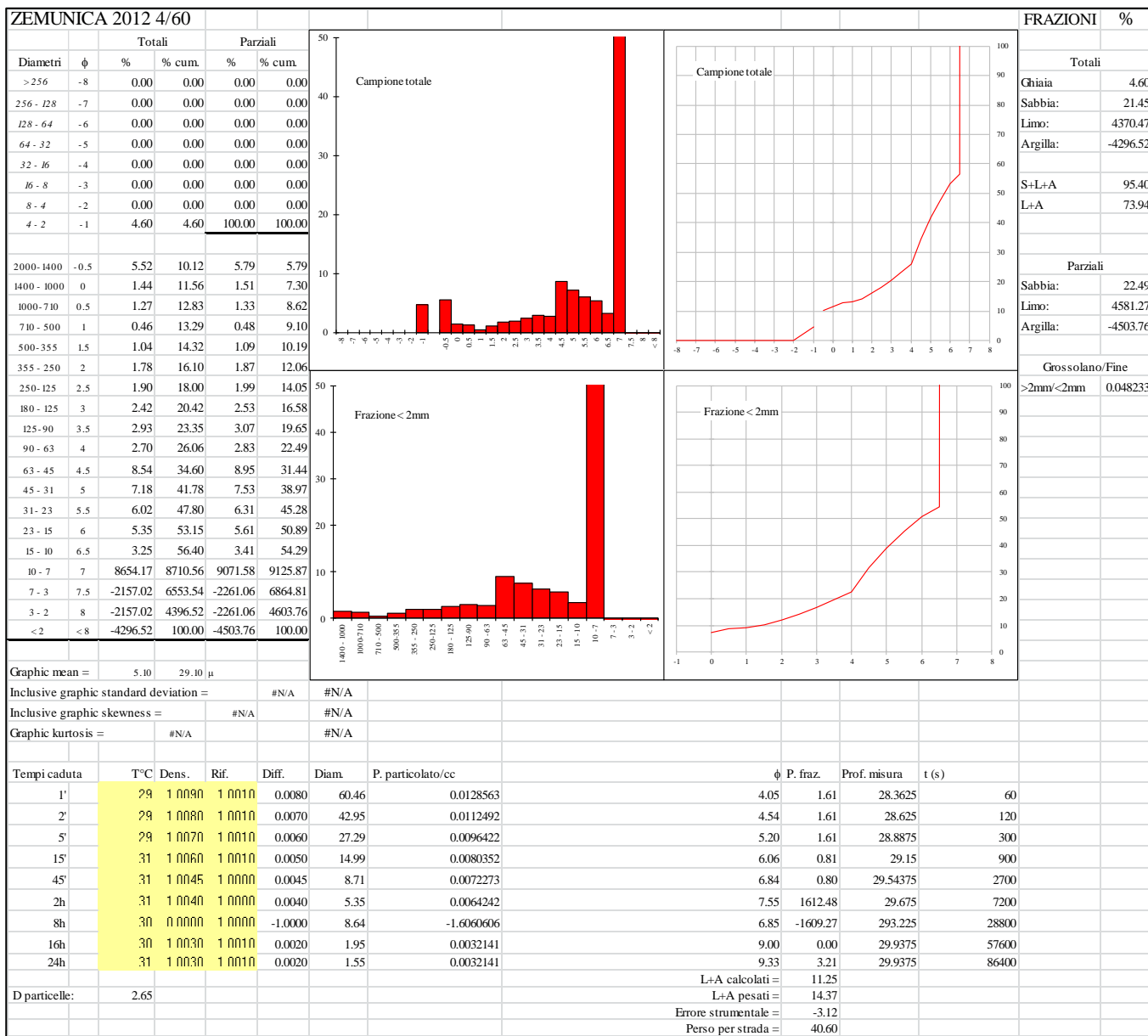
Appendix 6.2. Grain-size (Wentworth, 1922) of the <2 mm fraction of decalcified samples from Zemunica, SU 40 (Trench 3a).



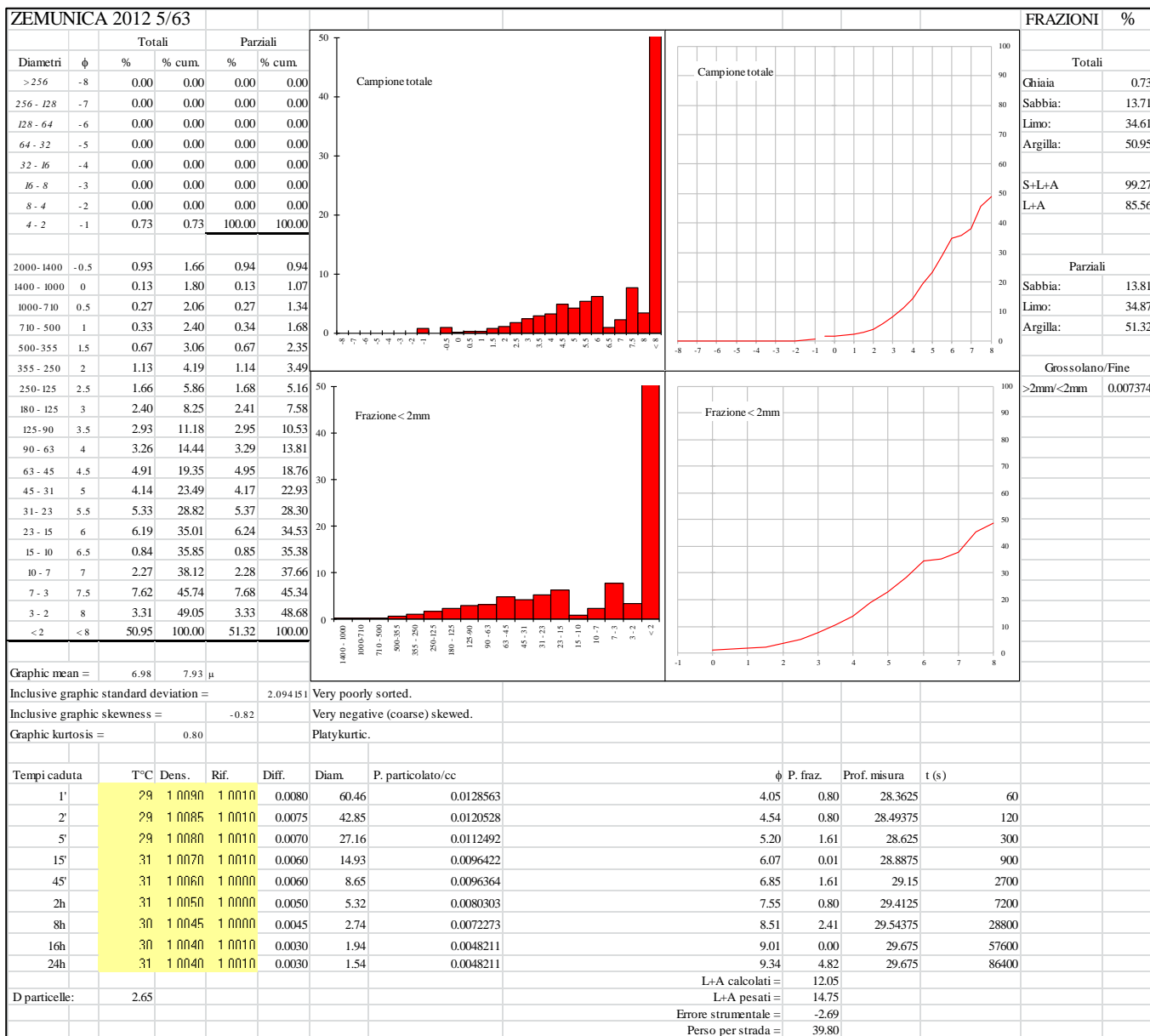
**Appendix 6.3. Grain-size
(Wentworth, 1922) of the <2 mm
fraction of decalcified samples
from Zemunica, SU 53 (Trench 3a).**



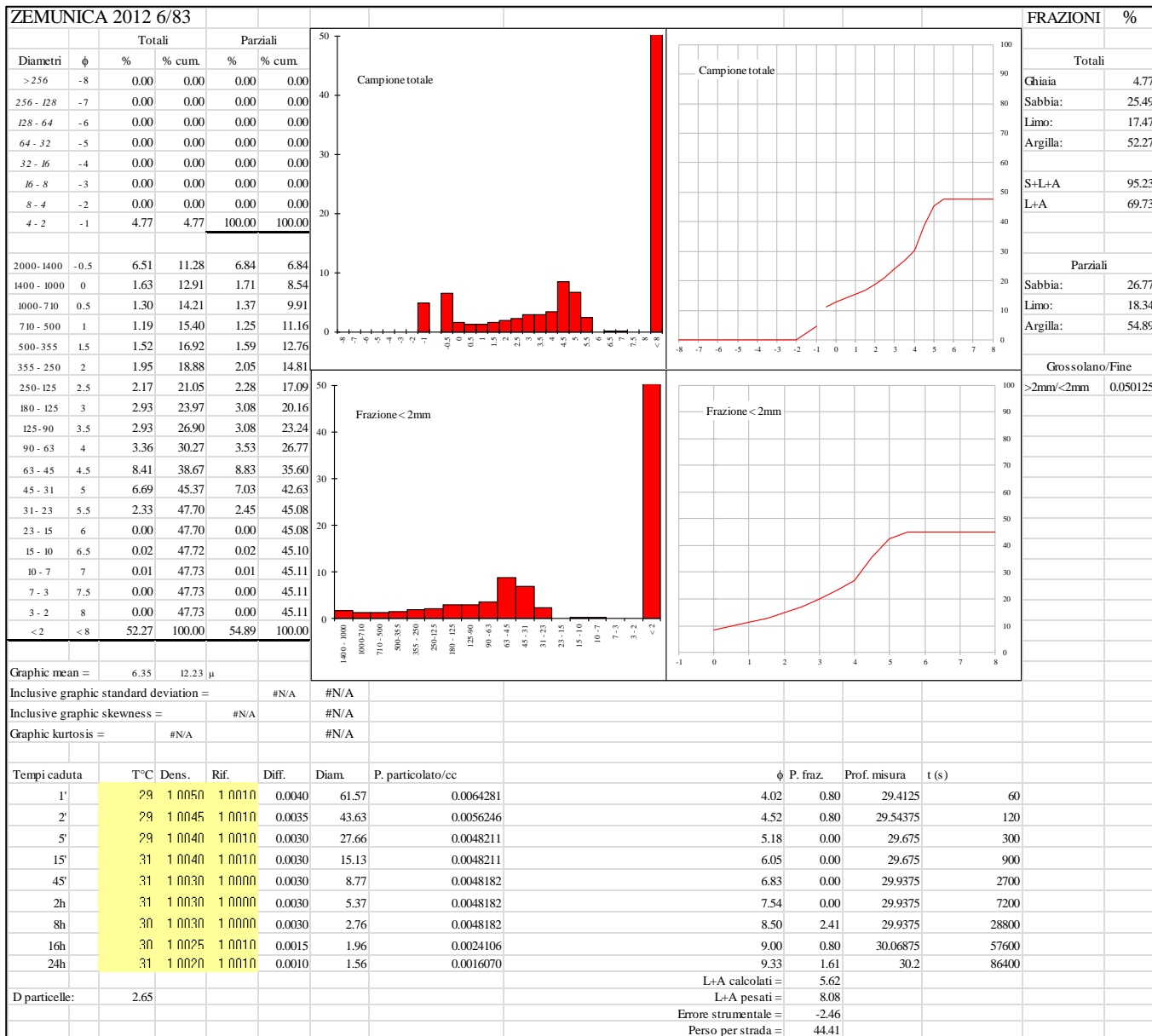
**Appendix 6.4. Grain-size
(Wentworth, 1922) of the <2 mm
fraction of decalcified samples
from Zemunica, SU 60 (Trench 3a).**



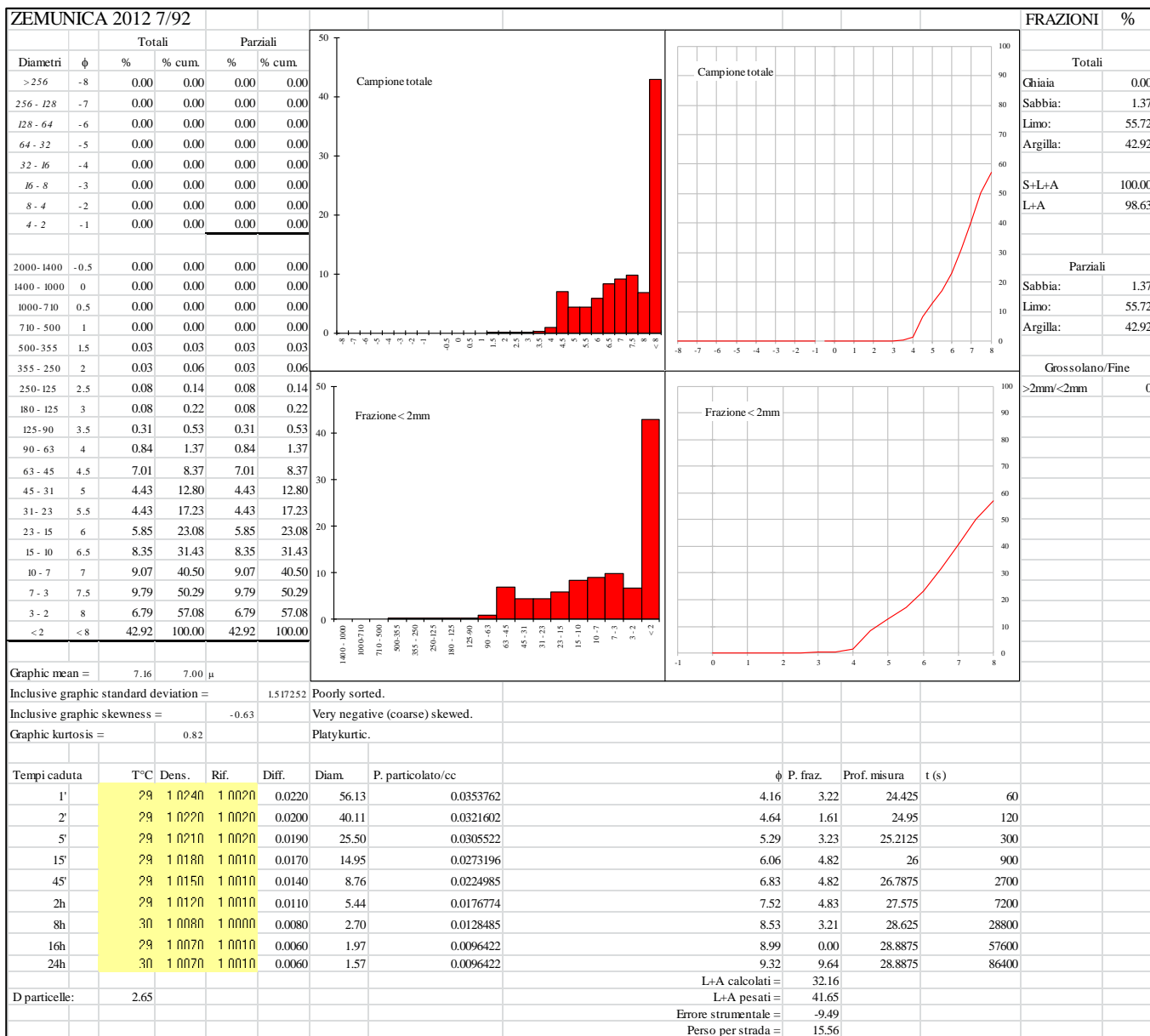
**Appendix 6.5. Grain-size
(Wentworth, 1922) of the <2 mm
fraction of decalcified samples
from Zemunica, SU 63 (Trench 3a).**



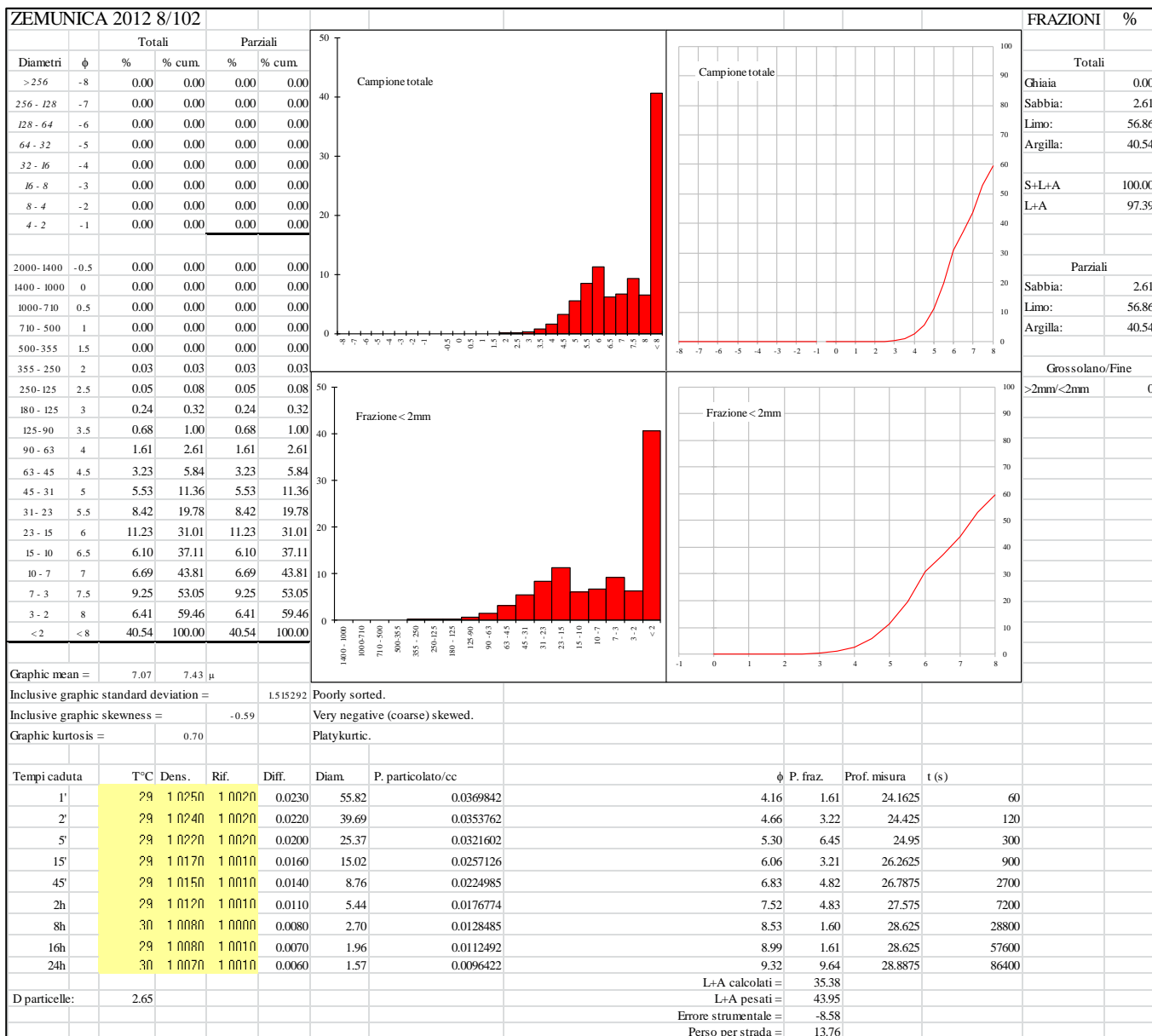
**Appendix 6.6. Grain-size
(Wentworth, 1922) of the <2 mm
fraction of decalcified samples
from Zemunica, SU 683 (Trench
3a).**



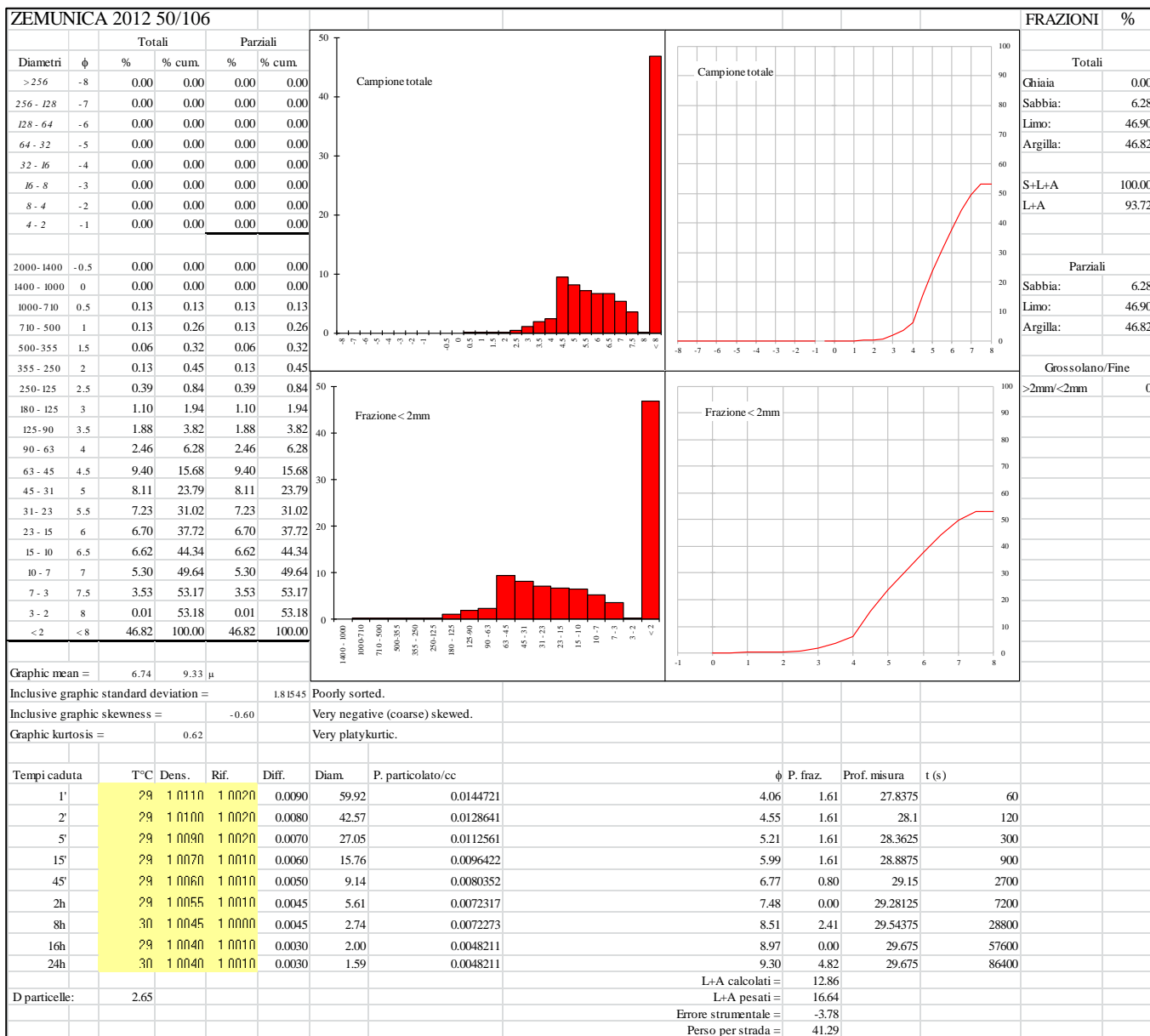
**Appendix 6.8. Grain-size
(Wentworth, 1922) of the <2 mm
fraction of decalcified samples
from Zemunica, SU 92 (Trench 3a).**



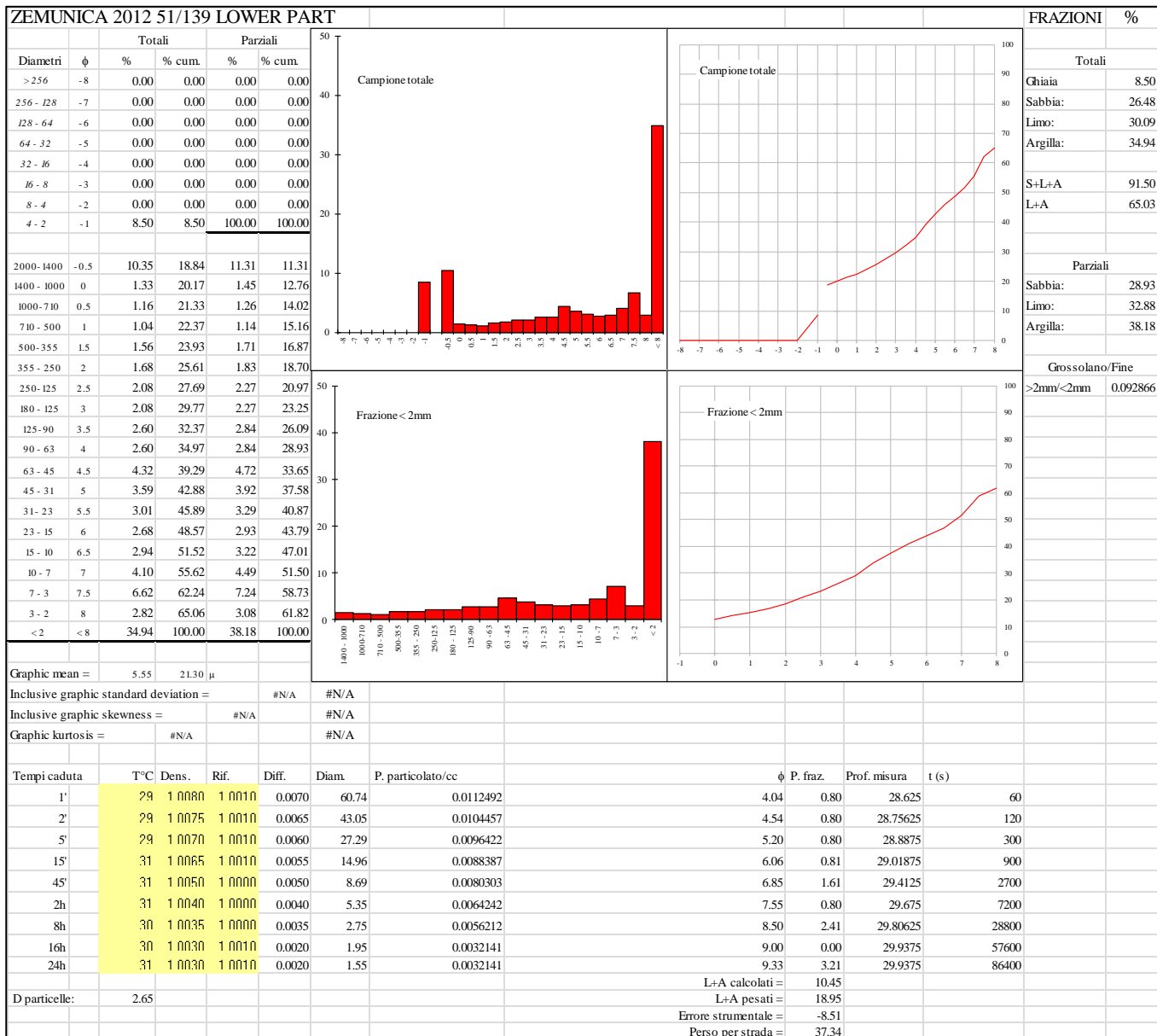
**Appendix 6.9. Grain-size
(Wentworth, 1922) of the <2 mm
fraction of decalcified samples
from Zemunica, SU 106 lower part,
between large stones SU 112
(Trench 3a).**



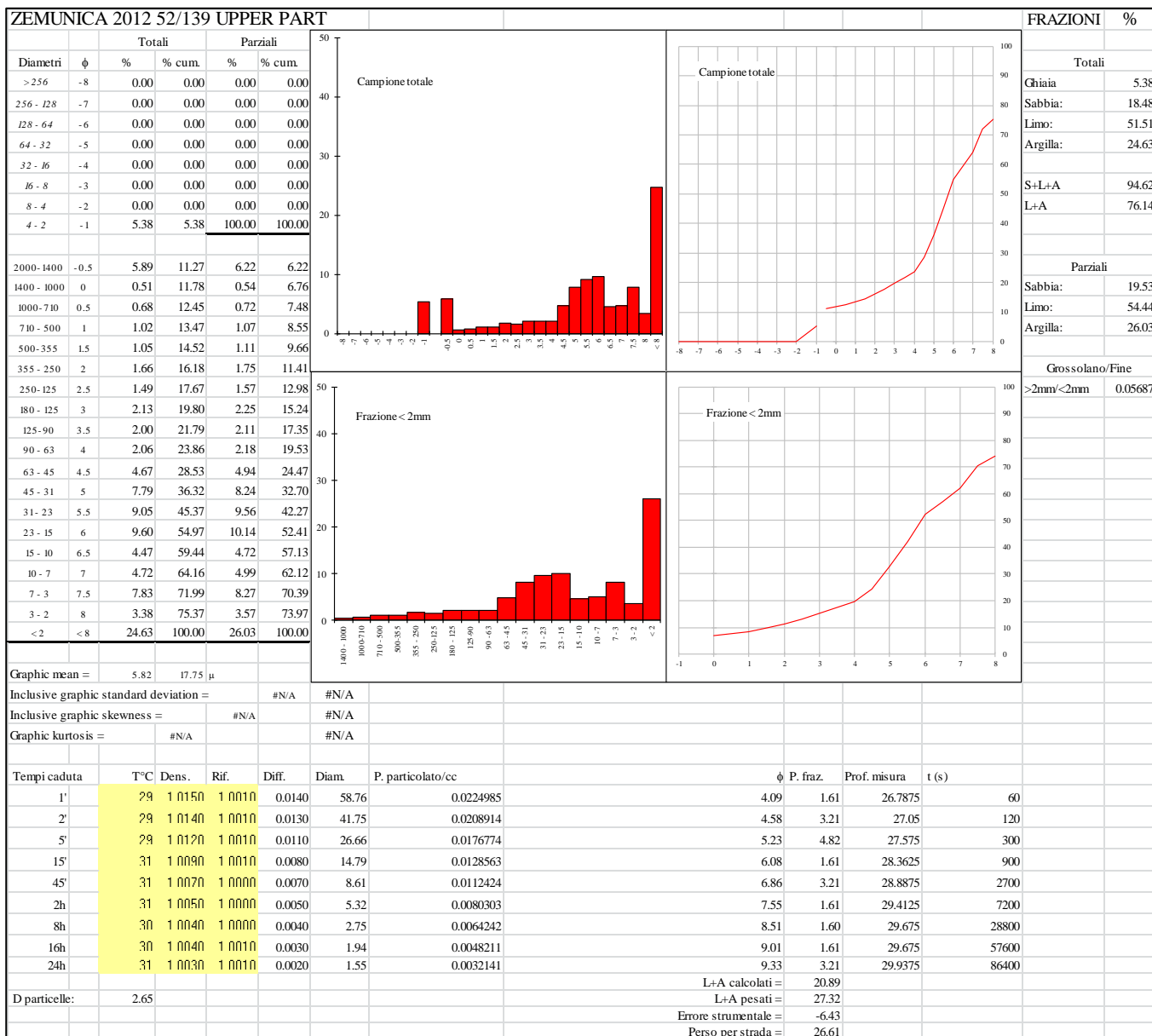
**Appendix 6.10. Grain-size
(Wentworth, 1922) of the <2 mm
fraction of decalcified samples
from Zemunica, SU 106 (Trench
3b).**



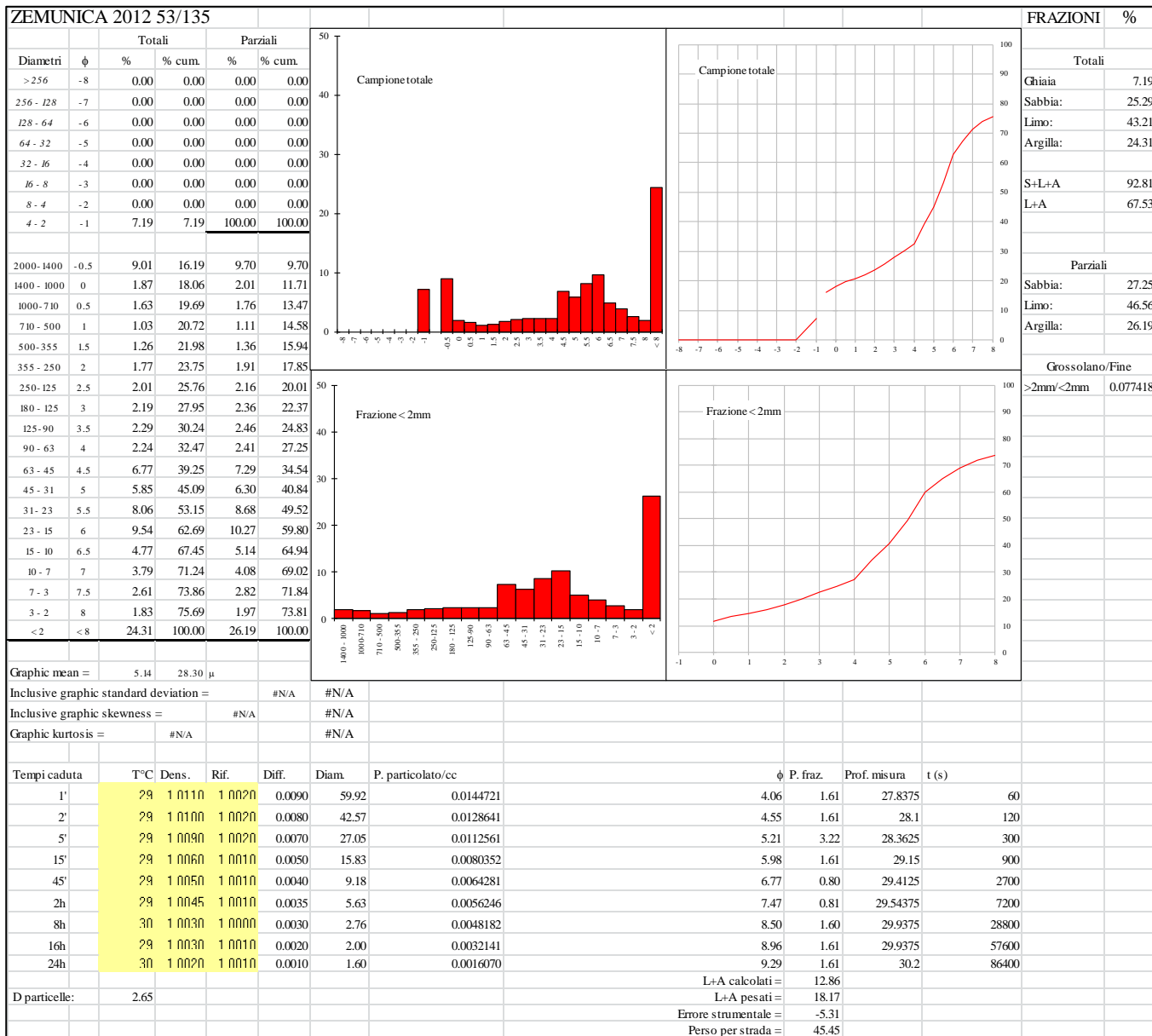
**Appendix 6.11. Grain-size
(Wentworth, 1922) of the <2 mm
fraction of decalcified samples
from Zemunica, SU 139_lower part
(Trench 3b).**



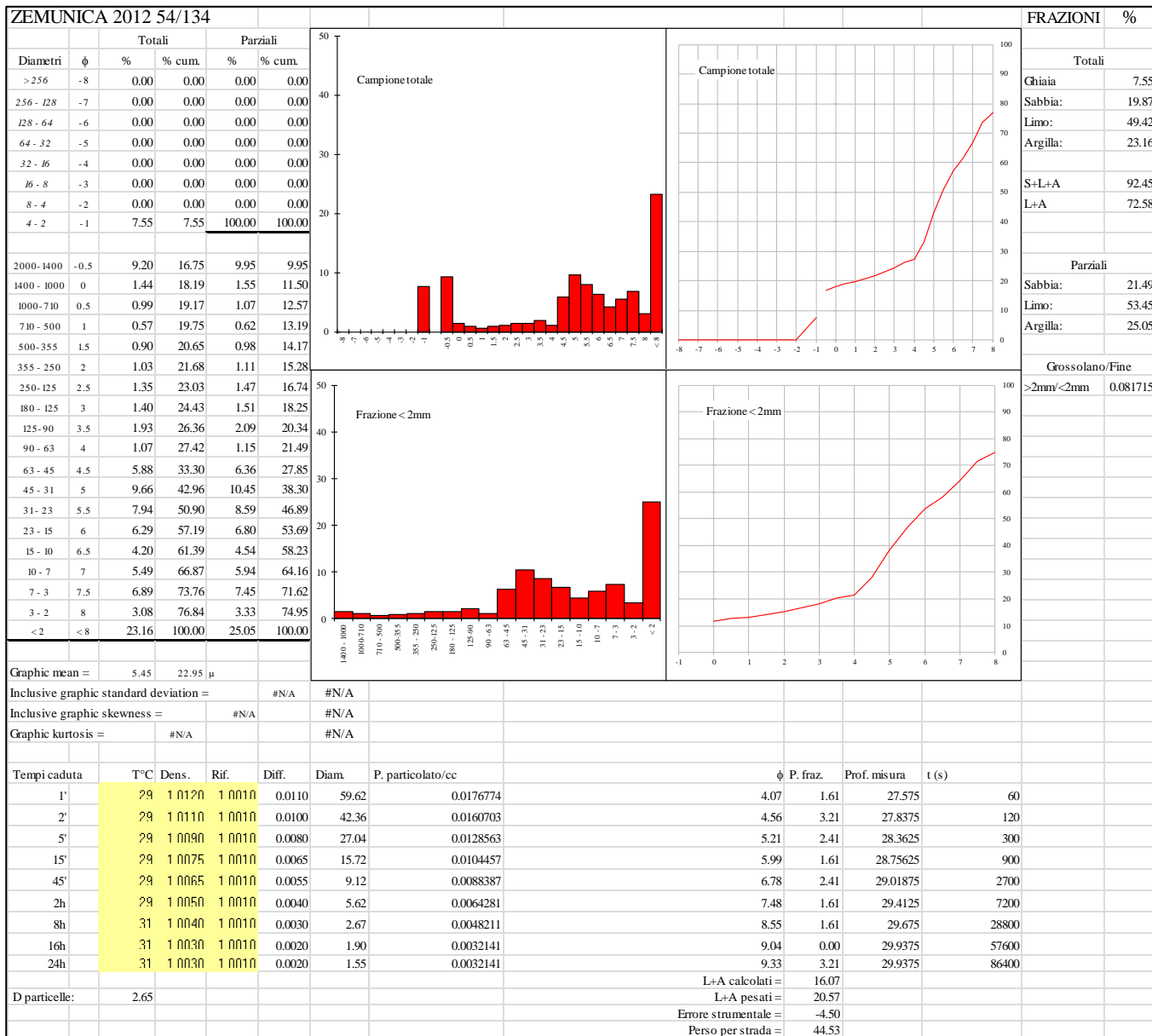
**Appendix 6.12. Grain-size
(Wentworth, 1922) of the <2 mm
fraction of decalcified samples
from Zemunica, SU 139_upper
part (Trench 3b).**



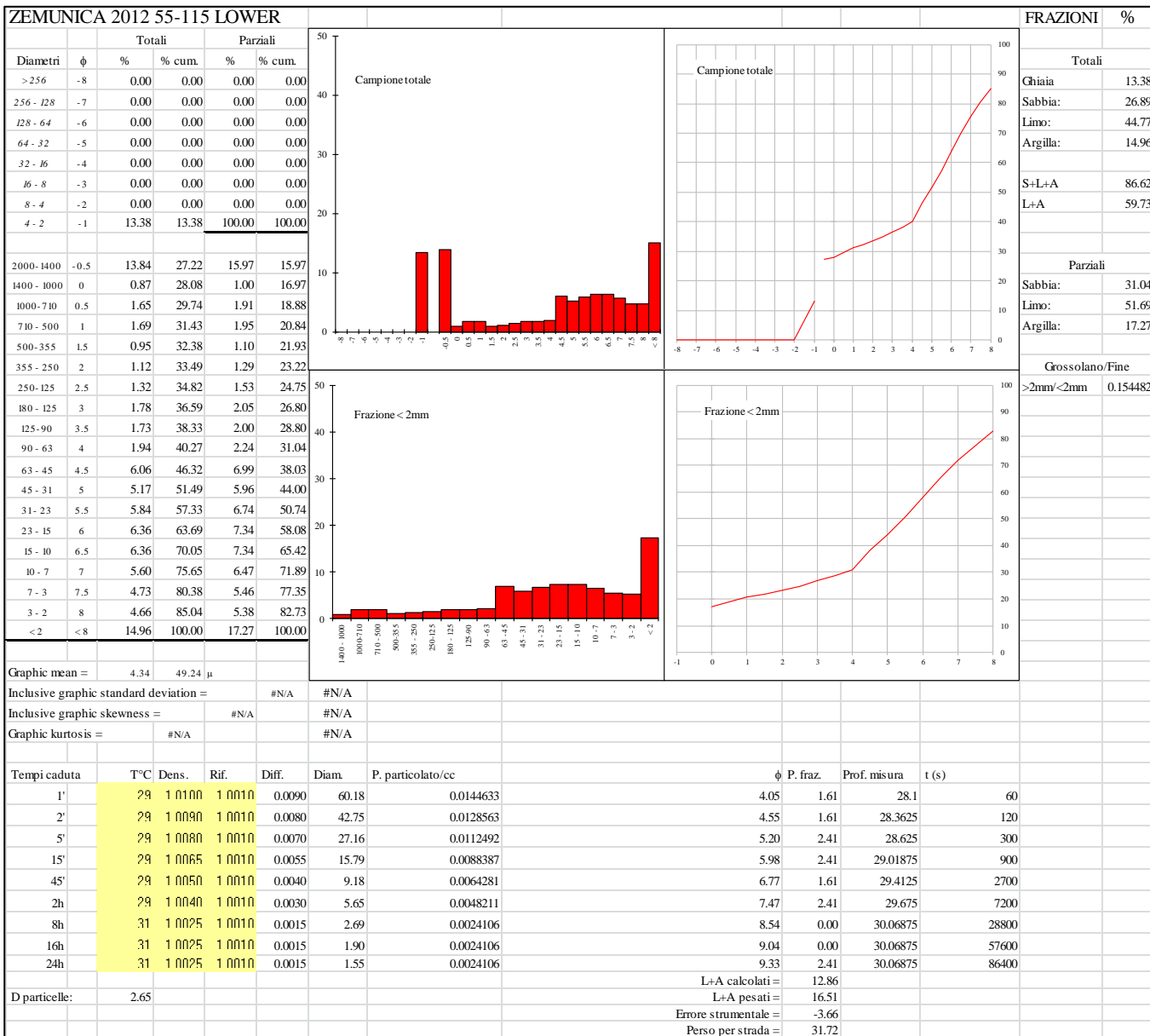
Appendix 6.13. Grain-size (Wentworth, 1922) of the <2 mm fraction of decalcified samples from Zemunica, SU 135 (Trench 3b).



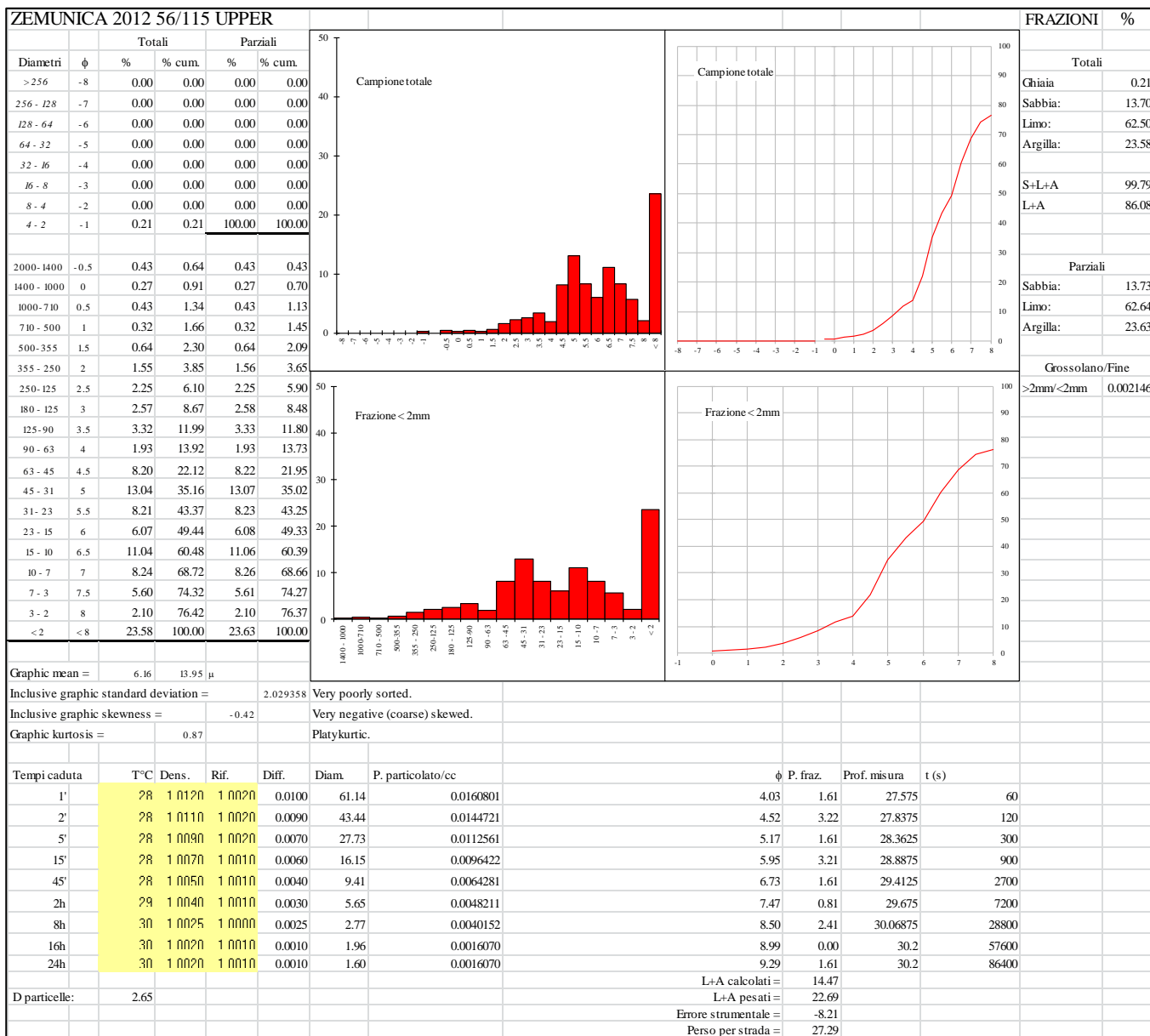
Appendix 6.14. Grain-size (Wentworth, 1922) of the <2 mm fraction of decalcified samples from Zemunica, SU 134 (Trench 3b).



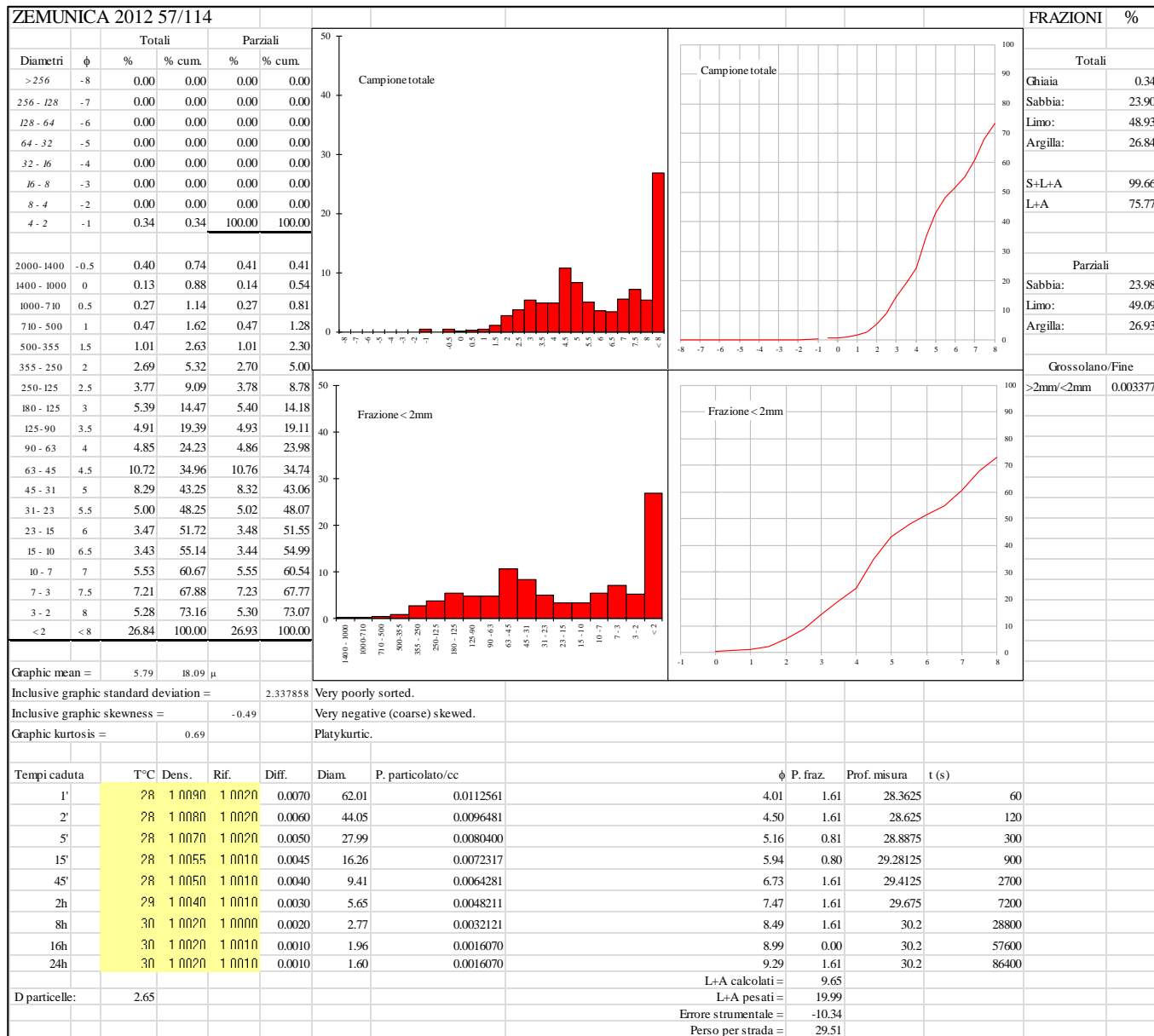
**Appendix 6.15. Grain-size
(Wentworth, 1922) of the <2 mm
fraction of decalcified samples
from Zemunica, SU 115_lower part
(Trench 3b).**



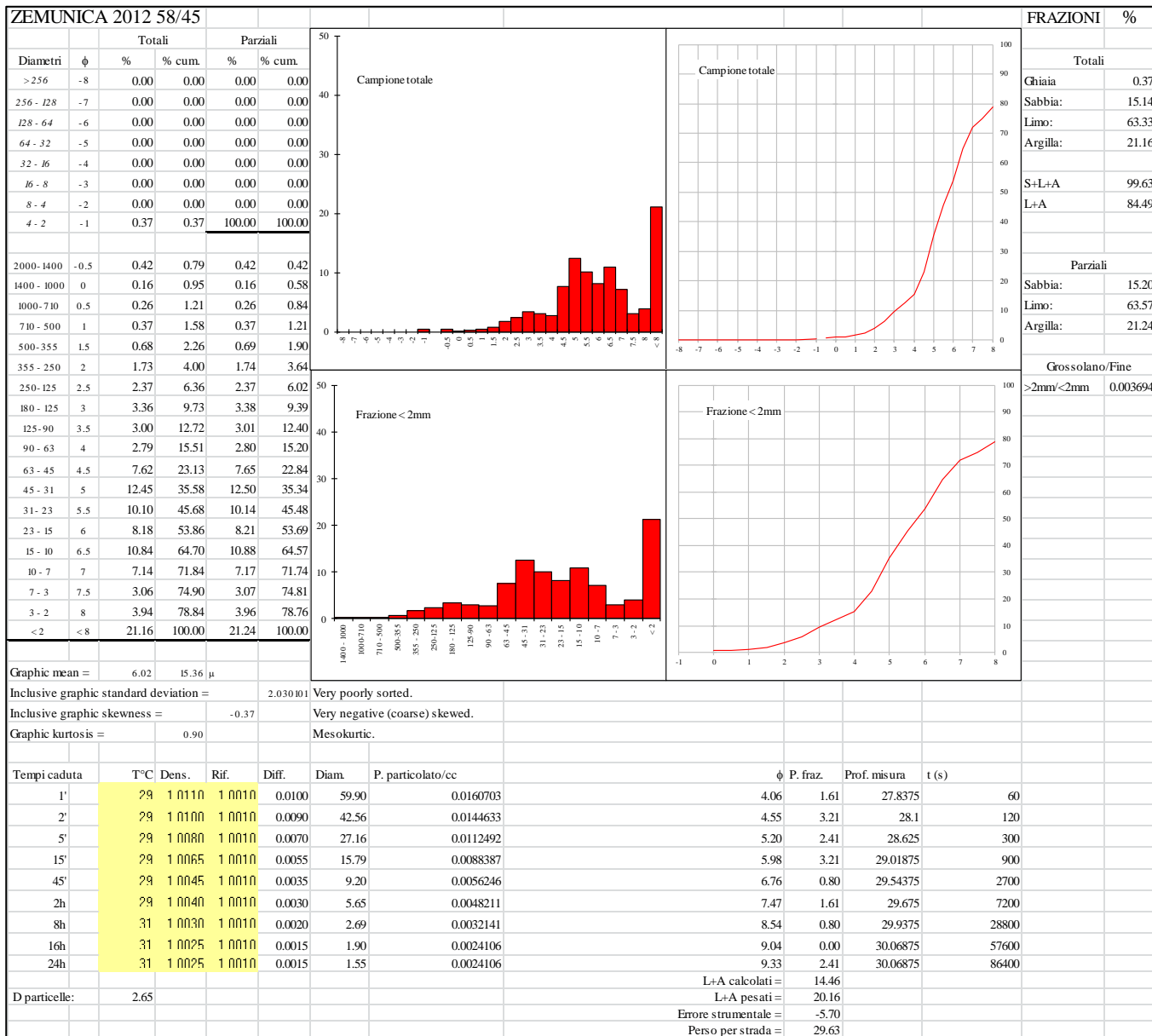
Appendix 6.16. Grain-size (Wentworth, 1922) of the <2 mm fraction of decalcified samples from Zemunica, SU 115_upper part (Trench 3b).



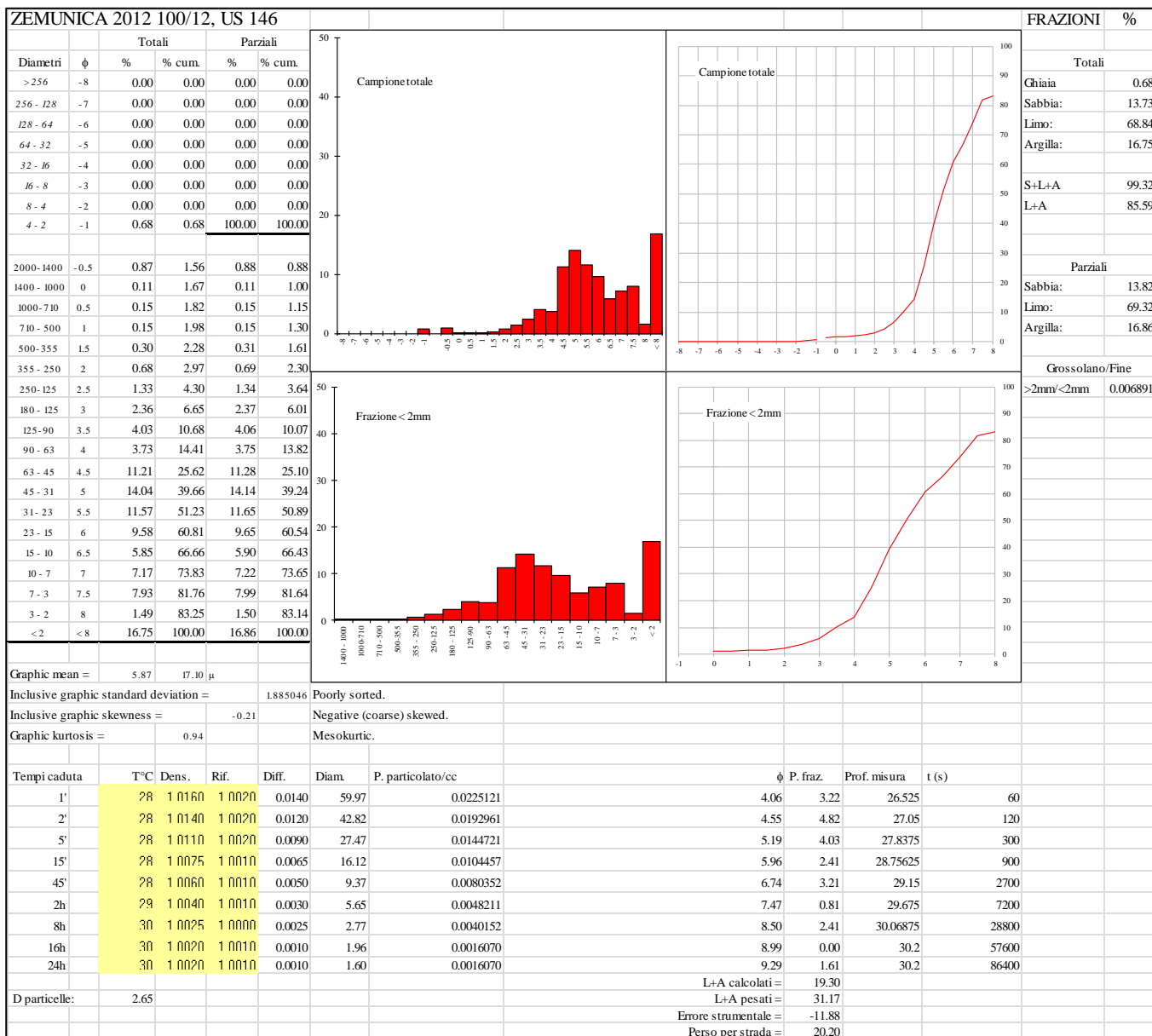
Appendix 6.17. Grain-size (Wentworth, 1922) of the <2 mm fraction of decalcified samples from Zemunica, SU 114 (Trench 3b).



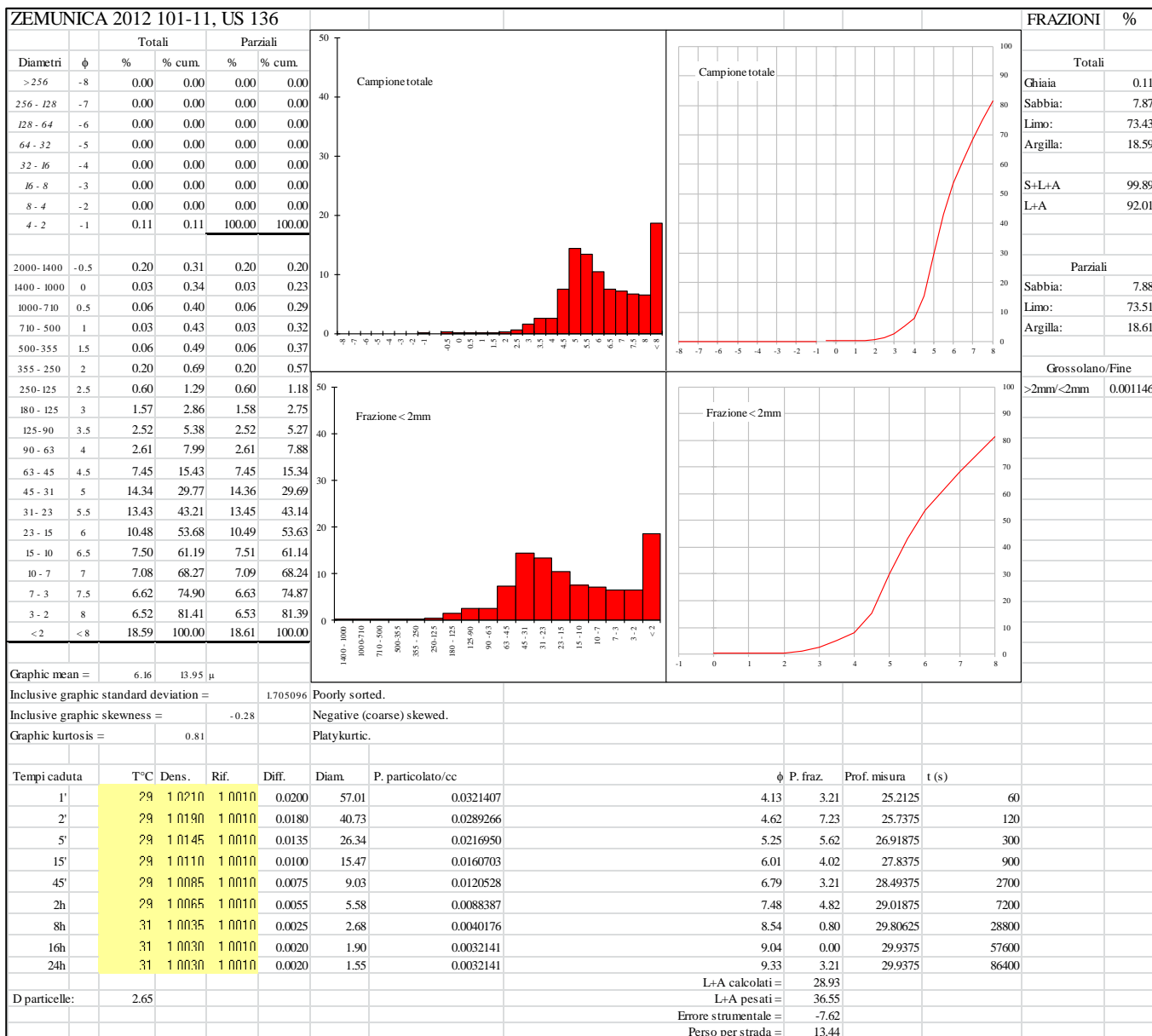
**Appendix 6.18. Grain-size
(Wentworth, 1922) of the <2 mm
fraction of decalcified samples
from Zemunica, SU 45 (Trench
3b).**



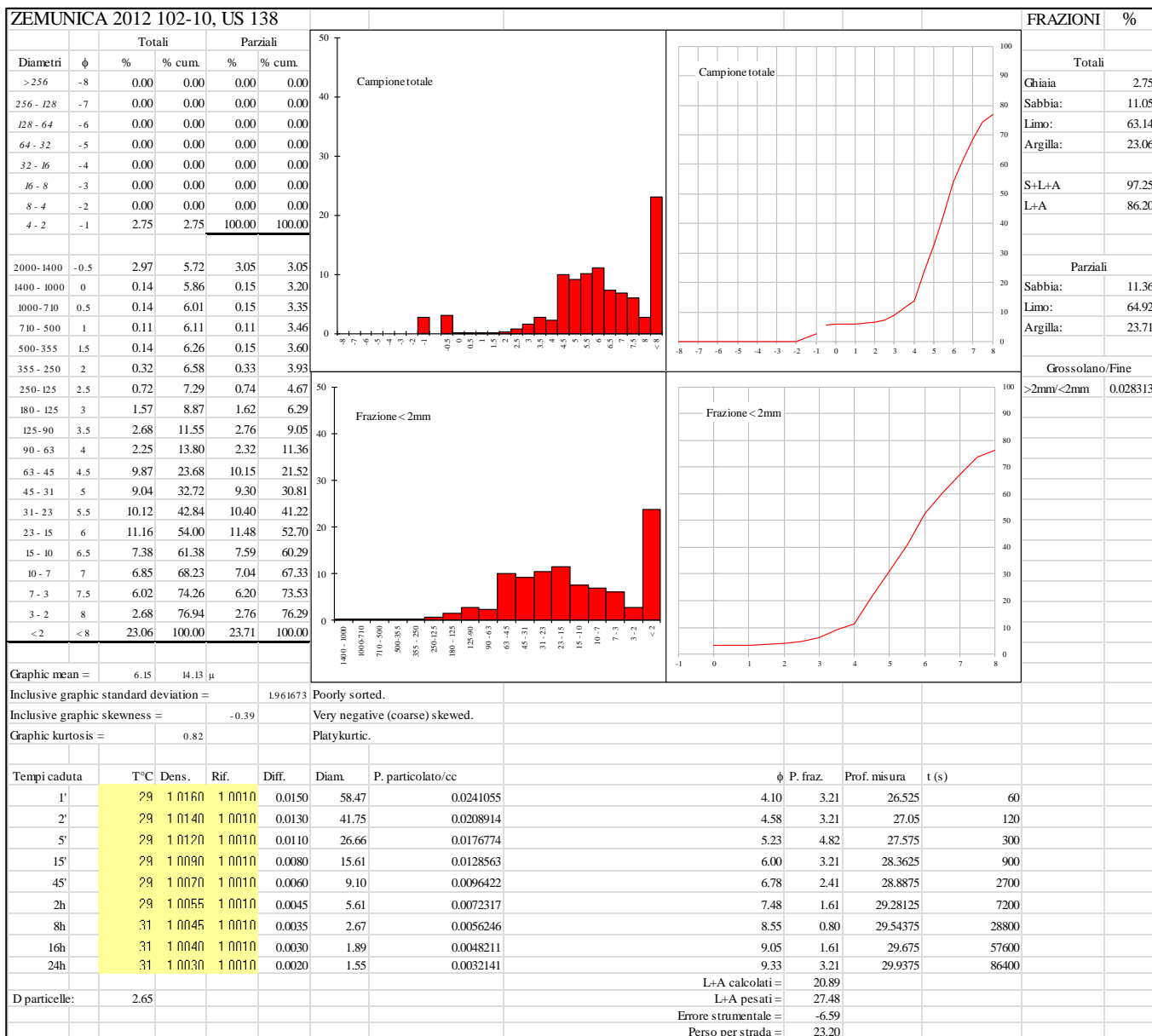
**Appendix 6.19. Grain-size
(Wentworth, 1922) of the <2 mm
fraction of decalcified samples
from Zemunica, SU 146 (Trench 2).**



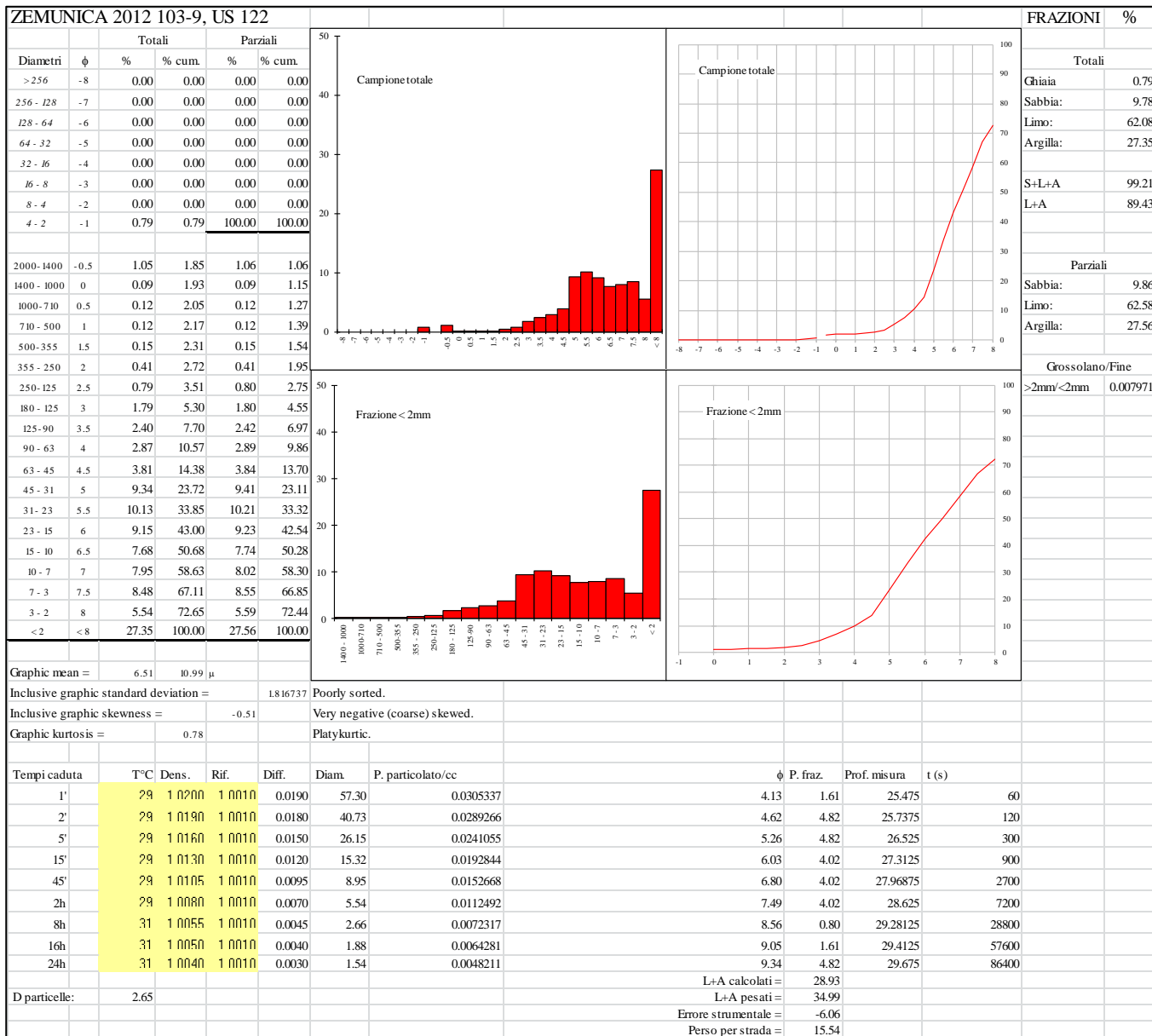
**Appendix 6.20. Grain-size
(Wentworth, 1922) of the <2 mm
fraction of decalcified samples
from Zemunica, SU 136 (Trench 2).**



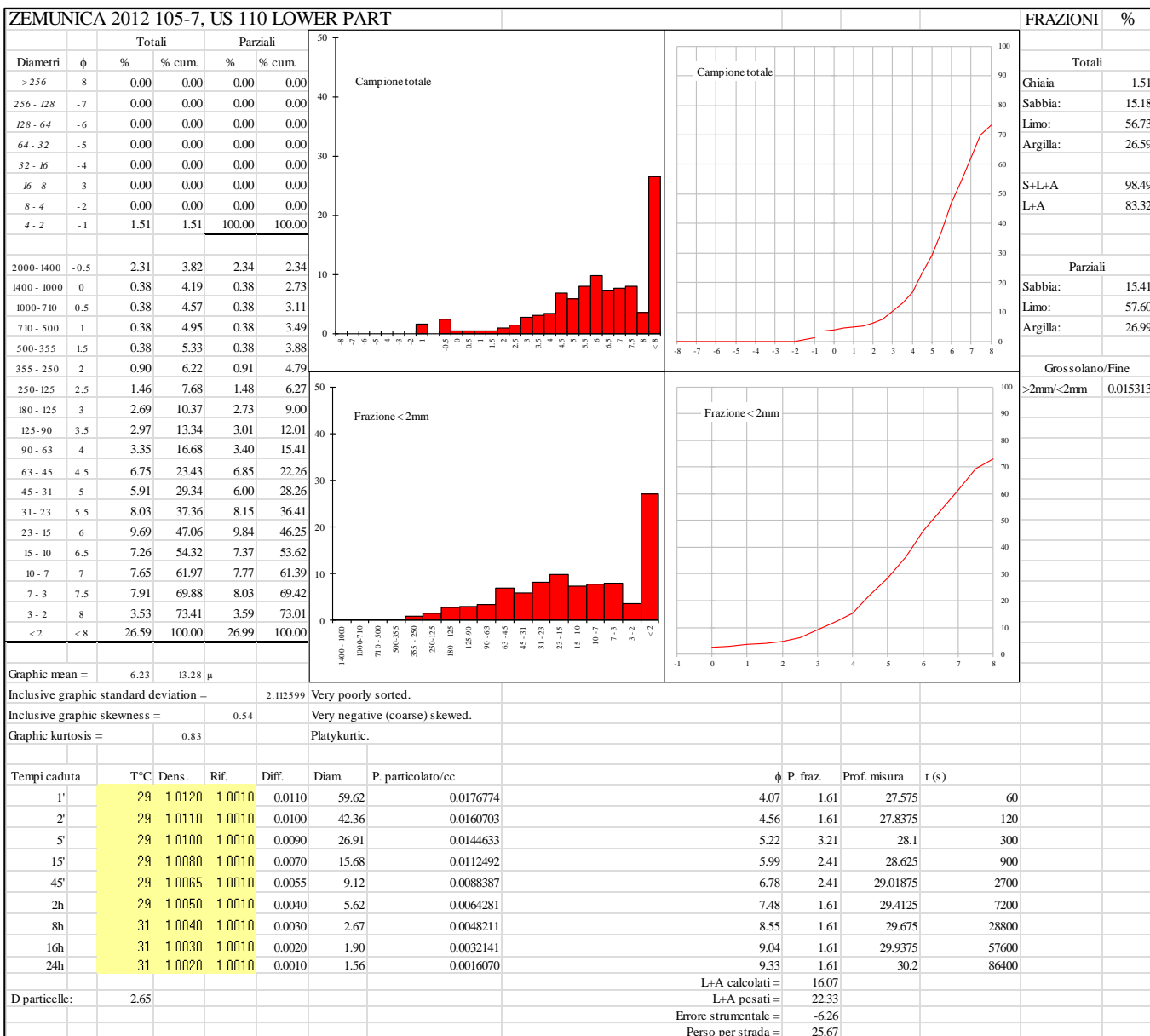
**Appendix 6.21. Grain-size
(Wentworth, 1922) of the <2 mm
fraction of decalcified samples
from Zemunica, SU 138 (Trench 2).**



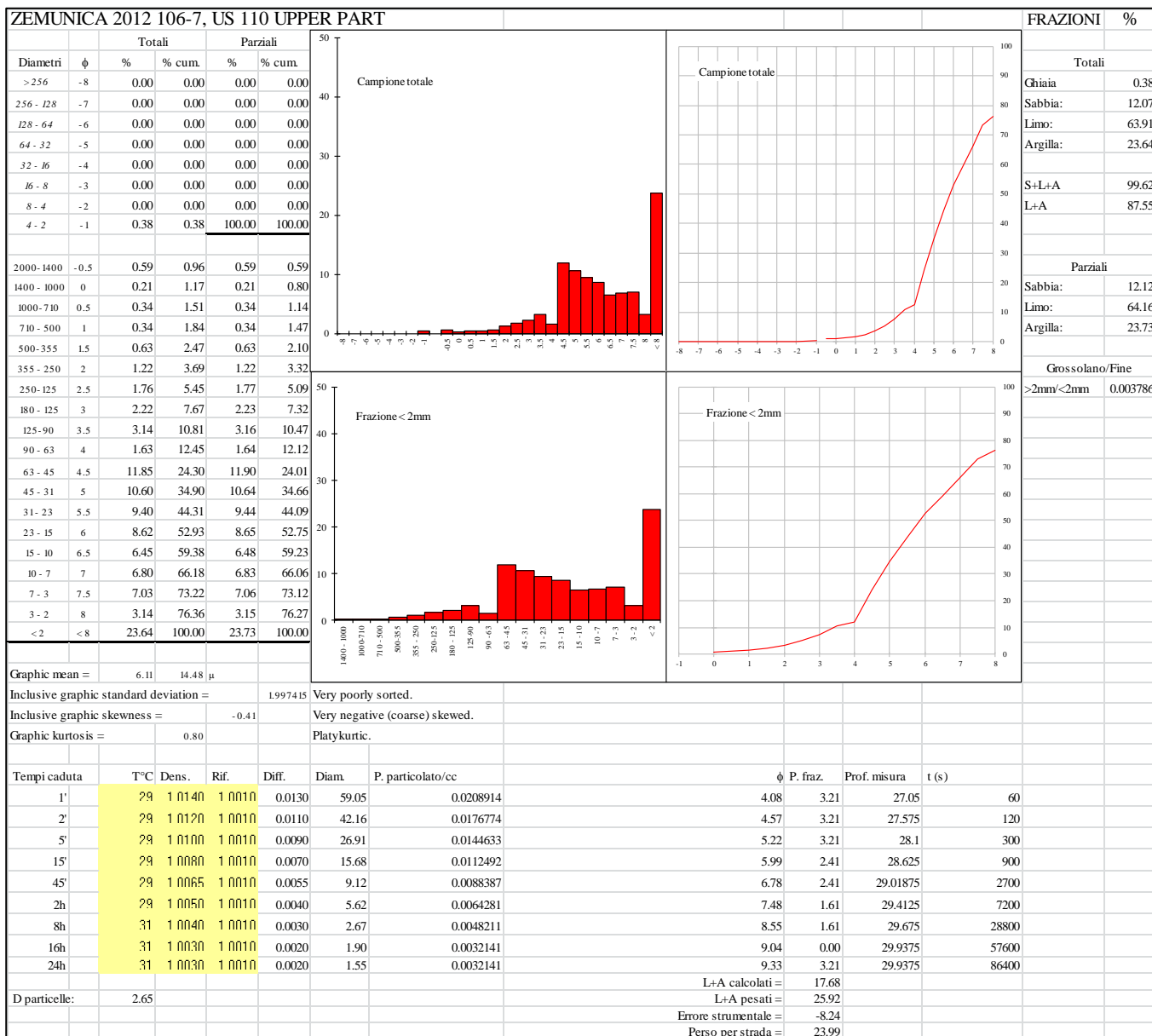
**Appendix 6.22. Grain-size
(Wentworth, 1922) of the <2 mm
fraction of decalcified samples
from Zemunica, SU 122 (Trench 2).**



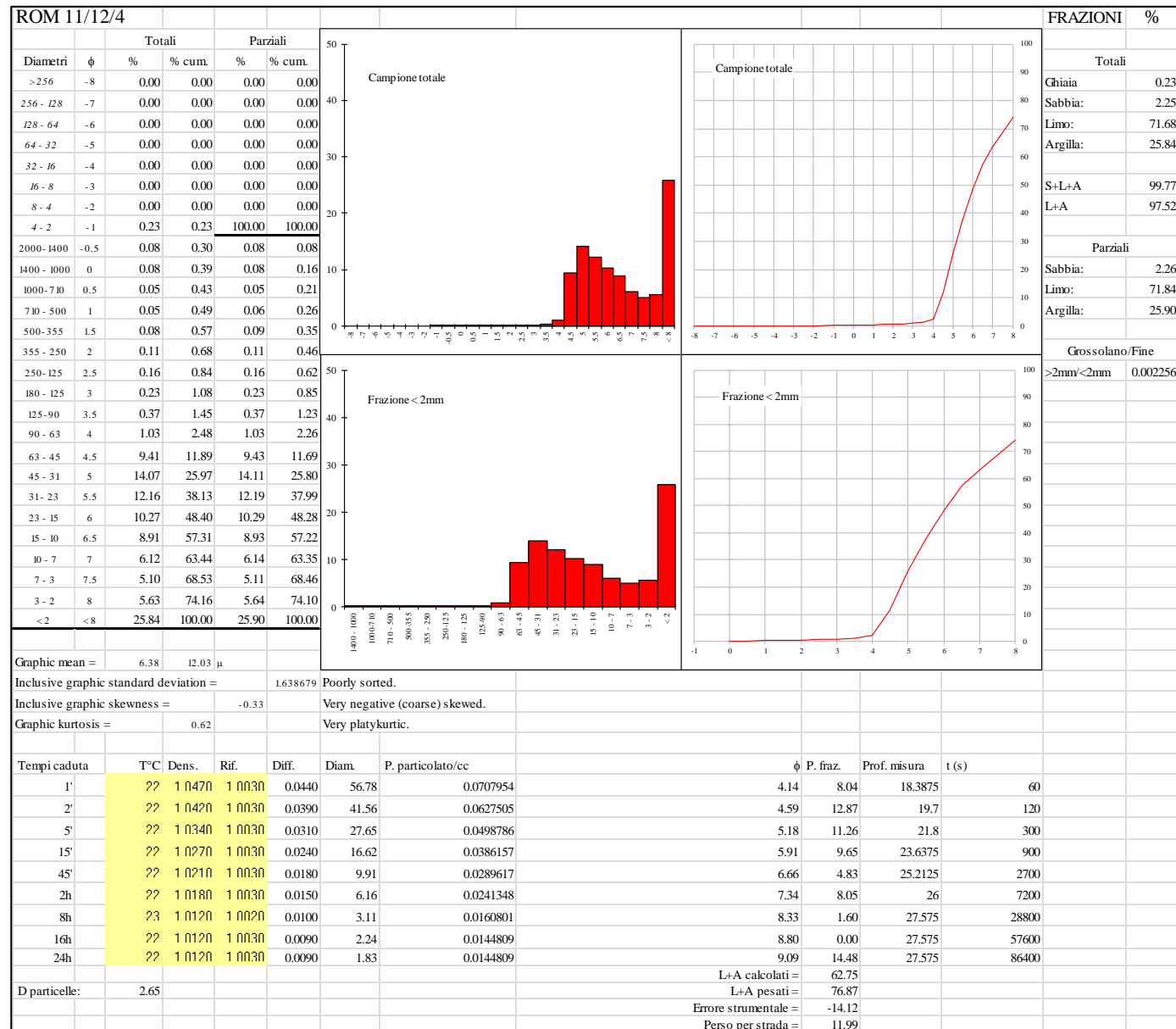
**Appendix 6.23. Grain-size
(Wentworth, 1922) of the <2 mm
fraction of decalcified samples
from Zemunica, SU 110_lower part
(Trench 2).**



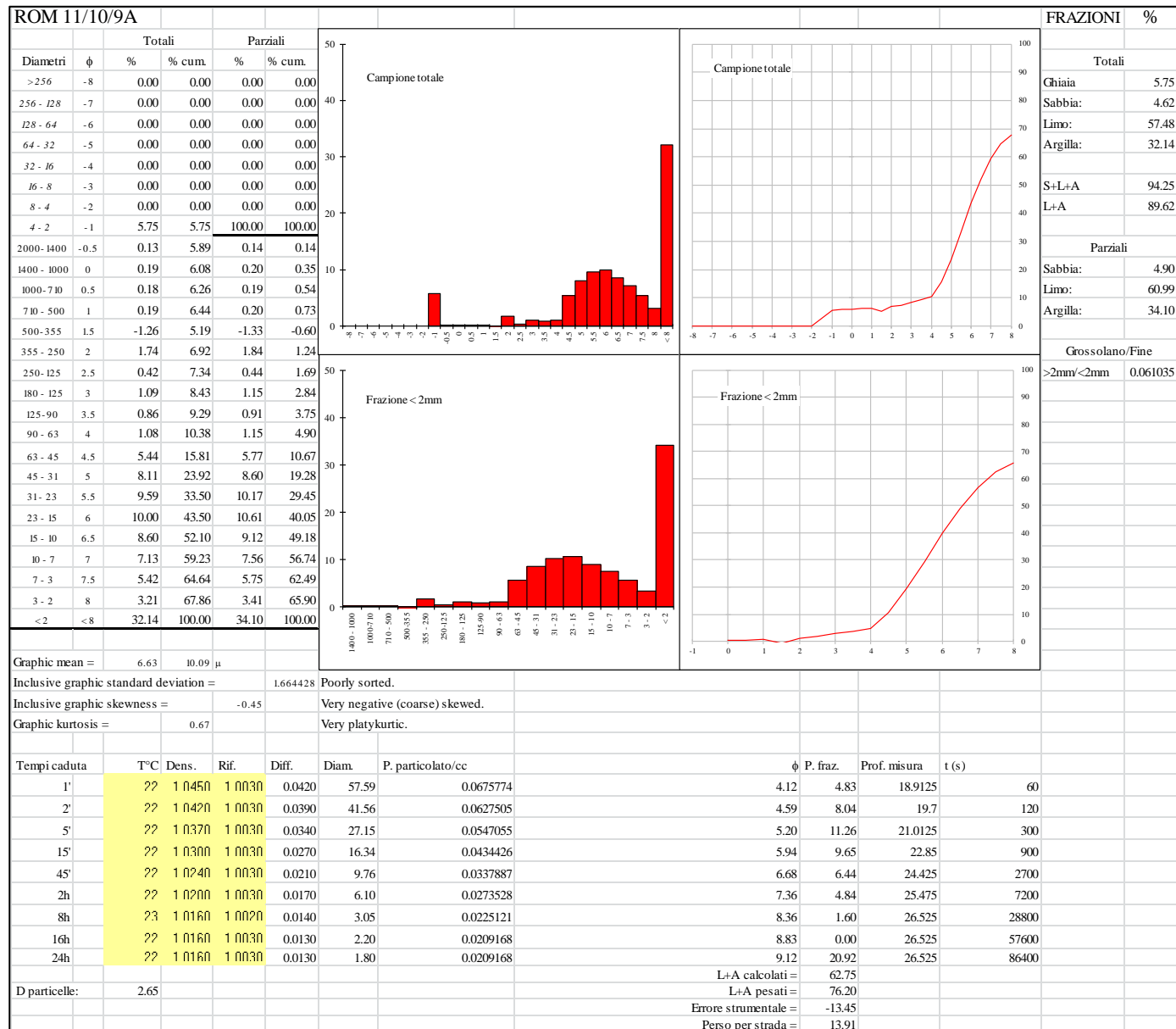
**Appendix 6.24. Grain-size
(Wentworth, 1922) of the <2 mm
fraction of decalcified samples
from Zemunica, SU 110_upper
part (Trench 2).**



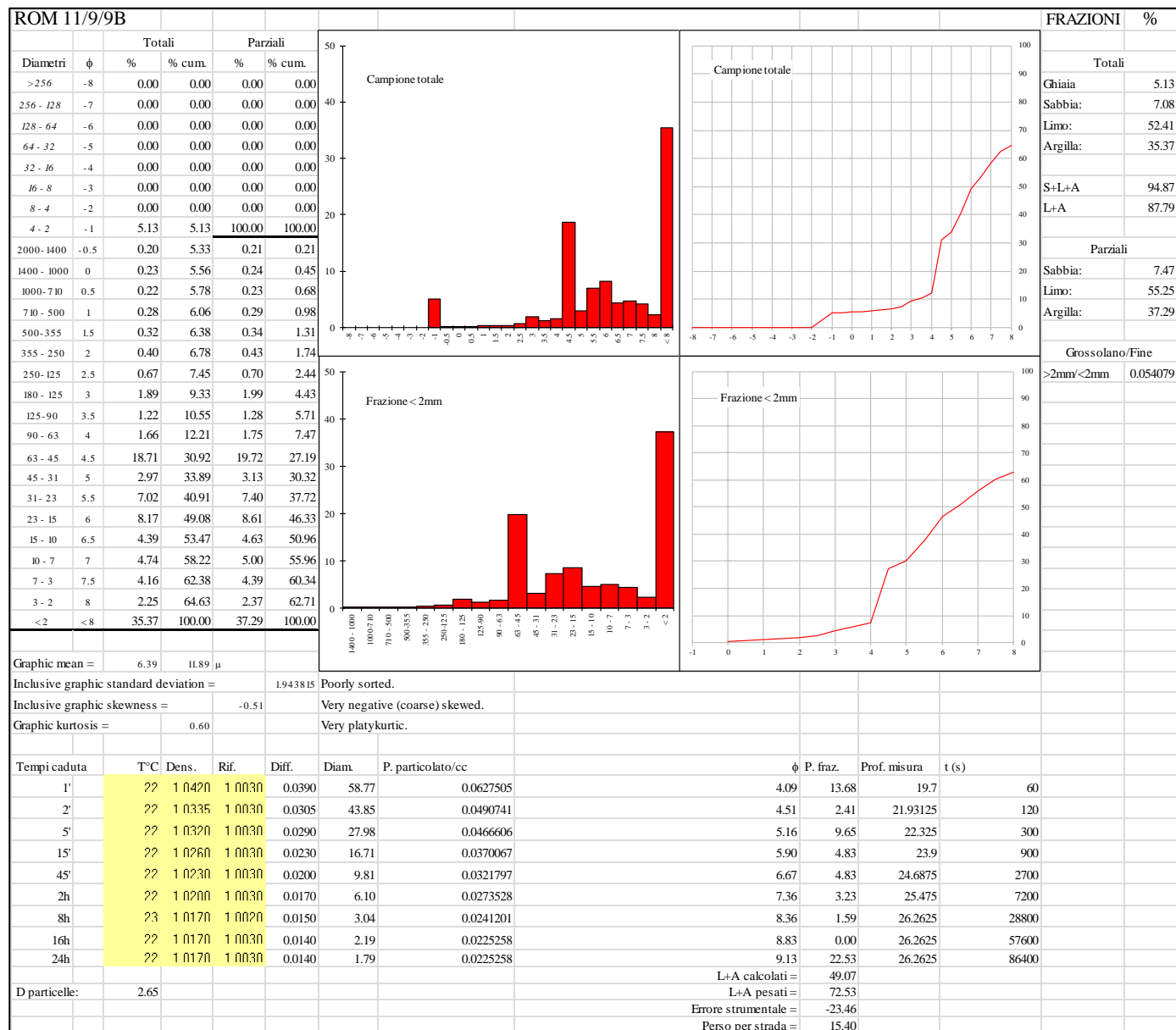
**Appendix 7.1. Grain-size
(Wentworth, 1922) of the <2 mm
fraction of undecalcified samples
from Romualdova Pećina, SU 4.**



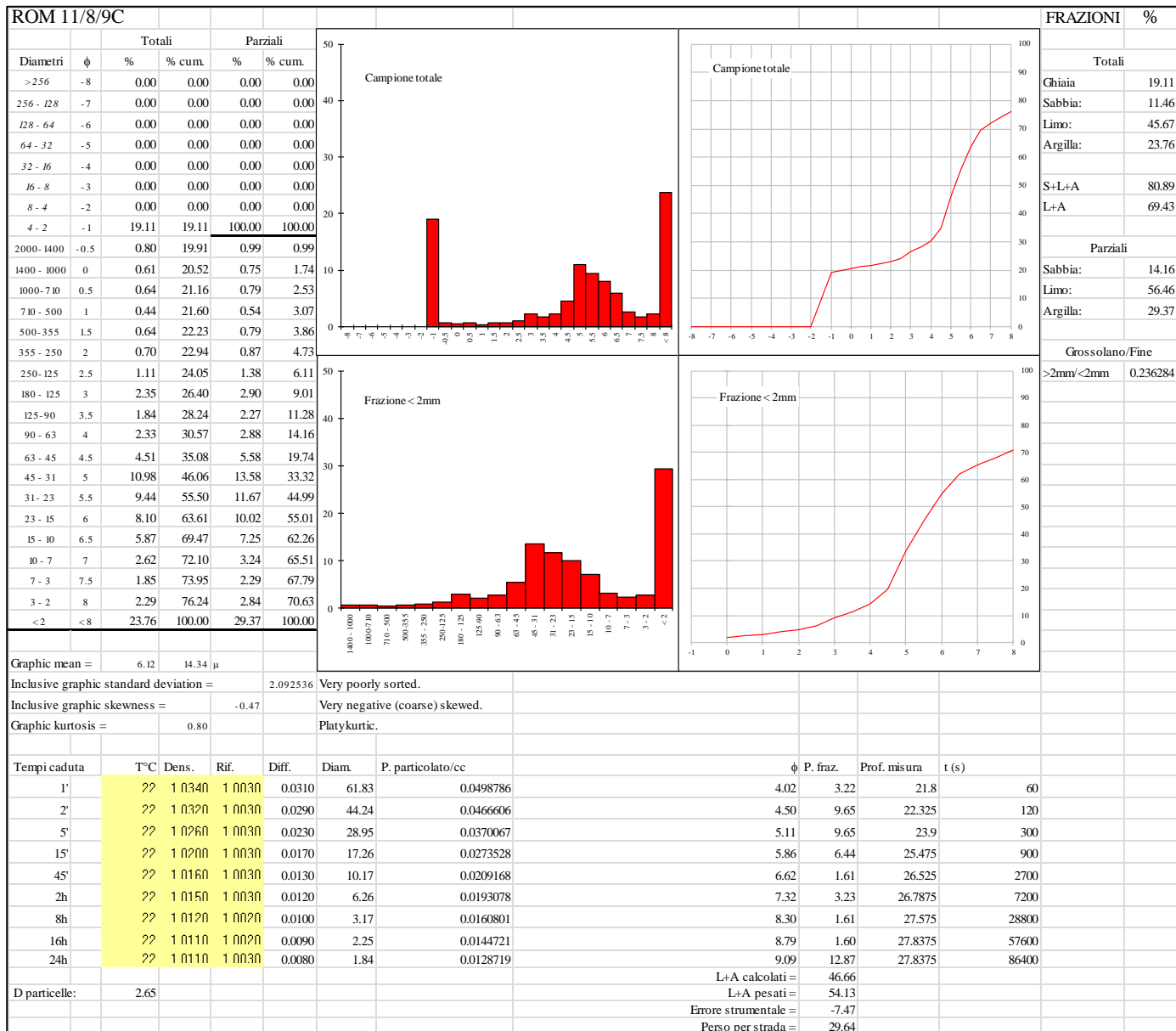
**Appendix 7.2. Grain-size
(Wentworth, 1922) of the <2 mm
fraction of undecalcified samples
from Romualdova Pećina, SU
9A.**



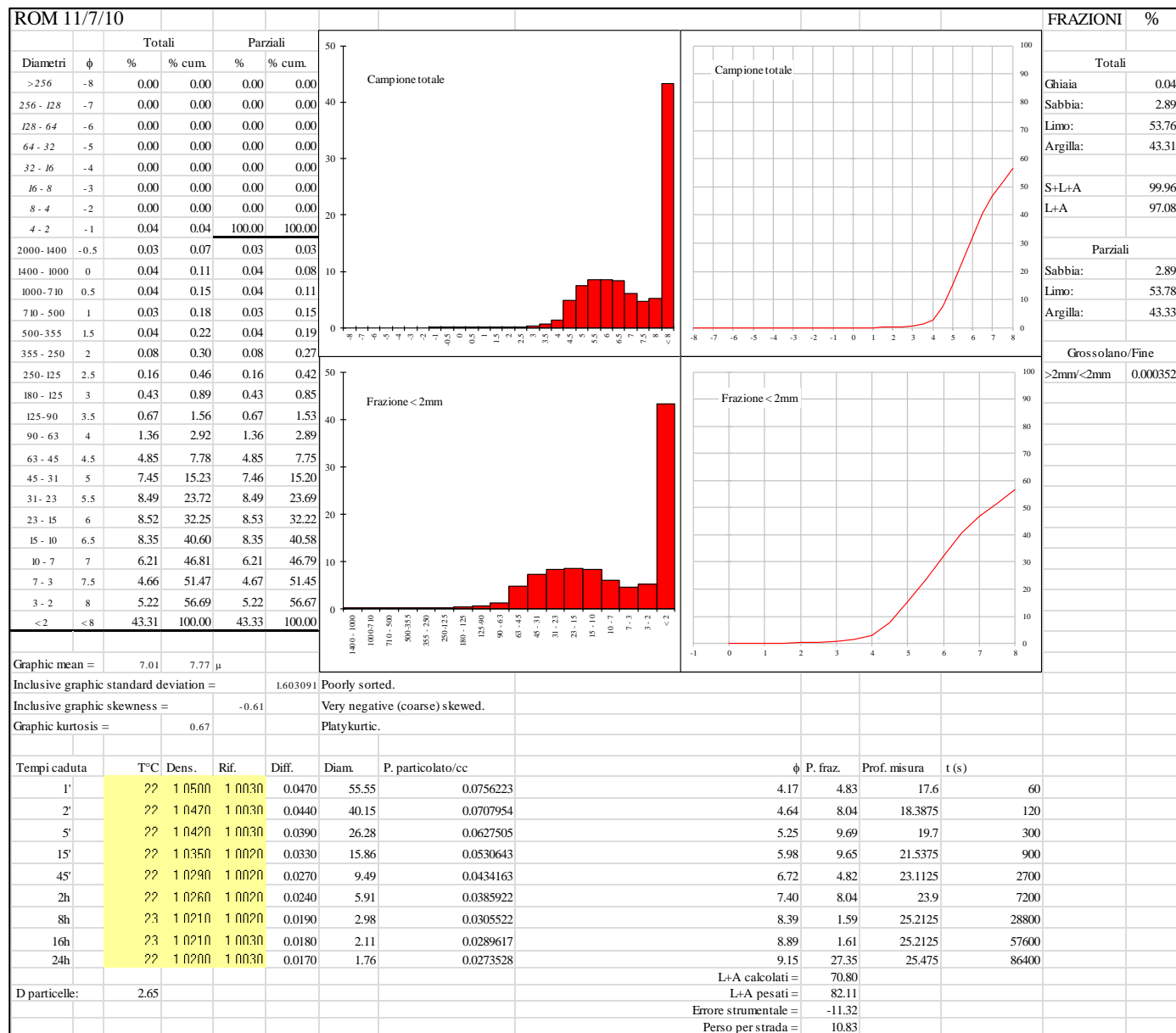
**Appendix 7.3. Grain-size
(Wentworth, 1922) of the <2 mm
fraction of undecalcified samples
from Romualdova Pećina, SU 9B.**



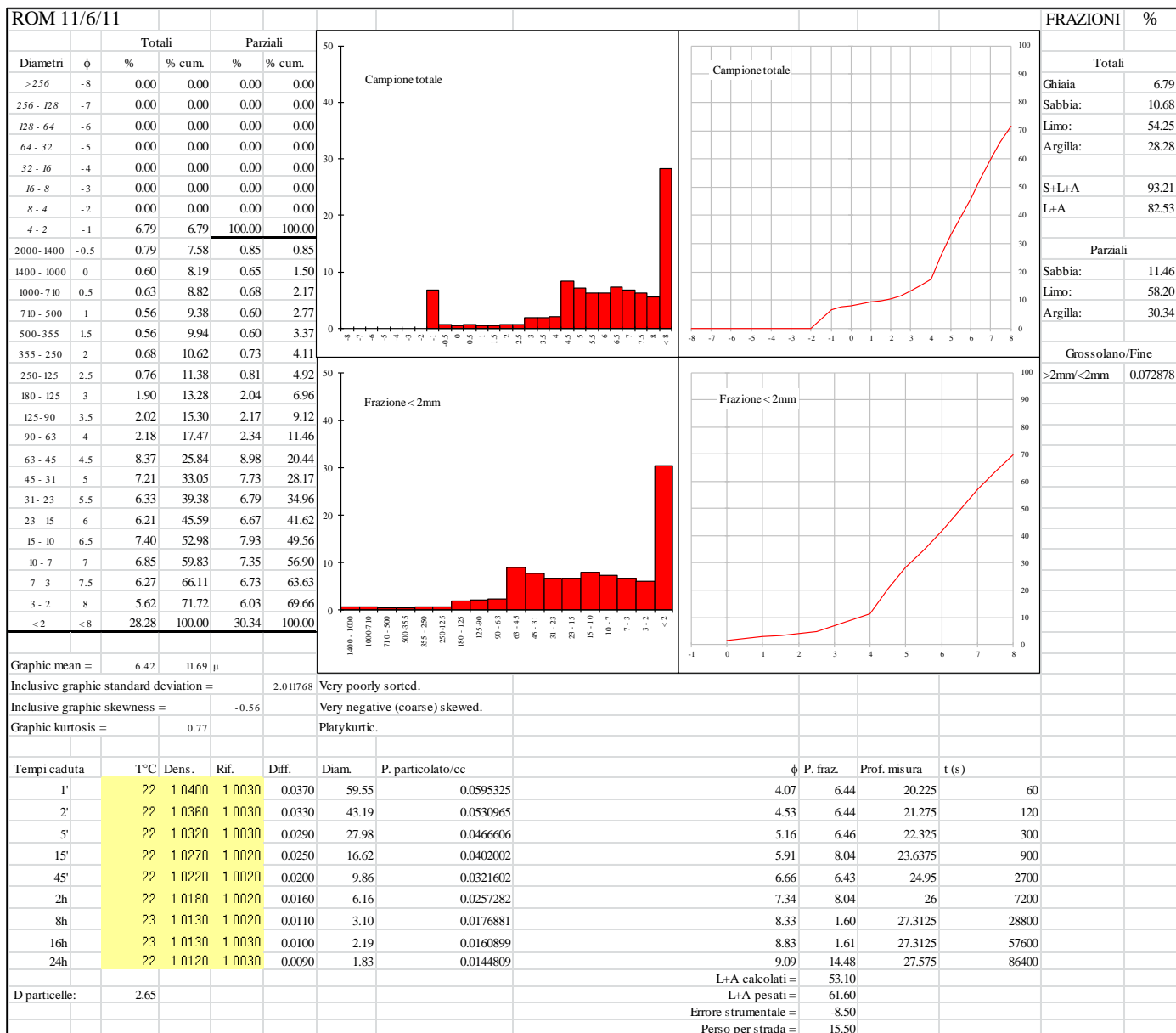
**Appendix 7.4. Grain-size
(Wentworth, 1922) of the <2 mm
fraction of undecalcified samples
from Romualdova Pećina, SU
9C.**



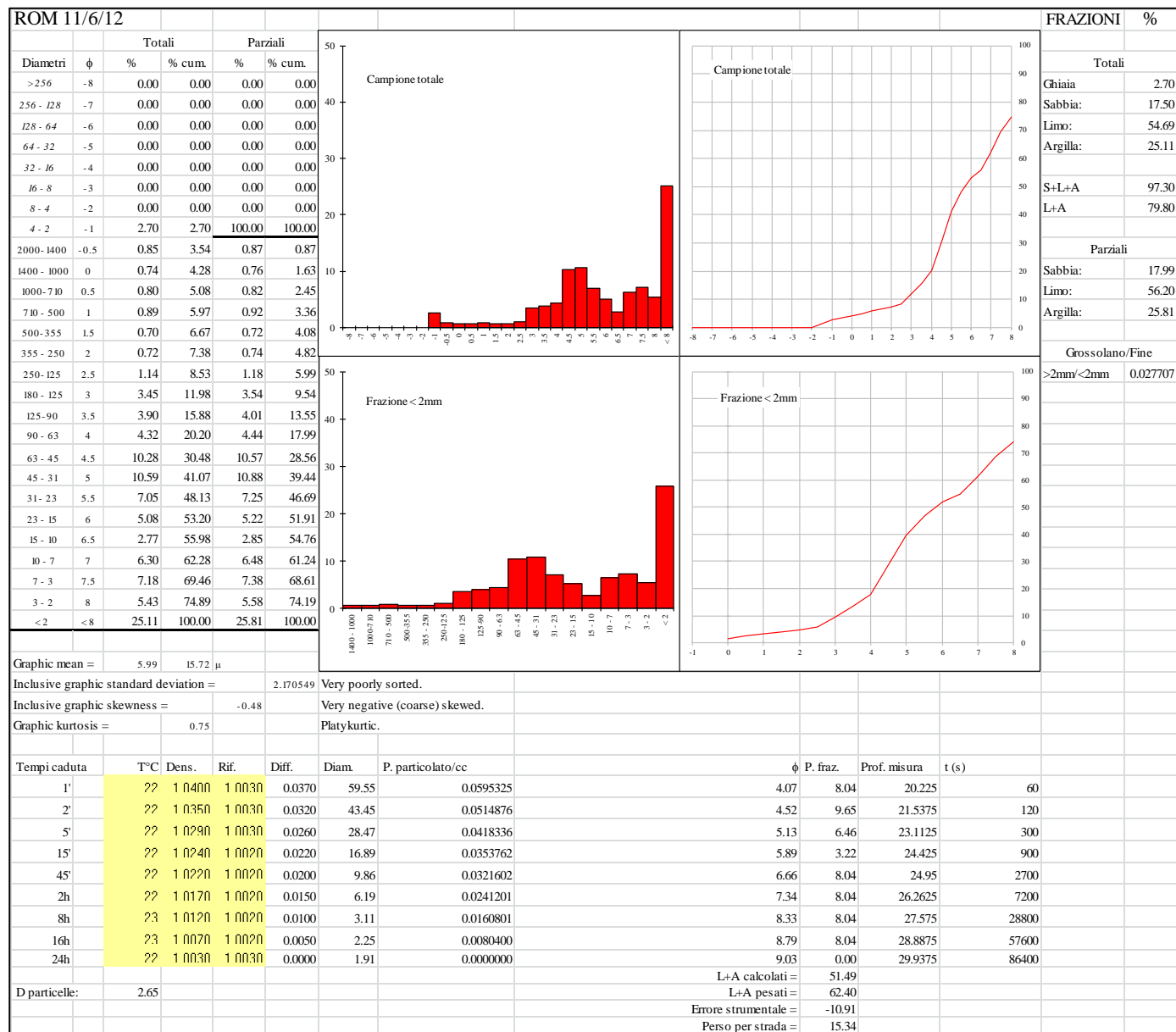
**Appendix 7.5. Grain-size
(Wentworth, 1922) of the <2 mm
fraction of undecalcified samples
from Romualdova Pećina, SU 10.**



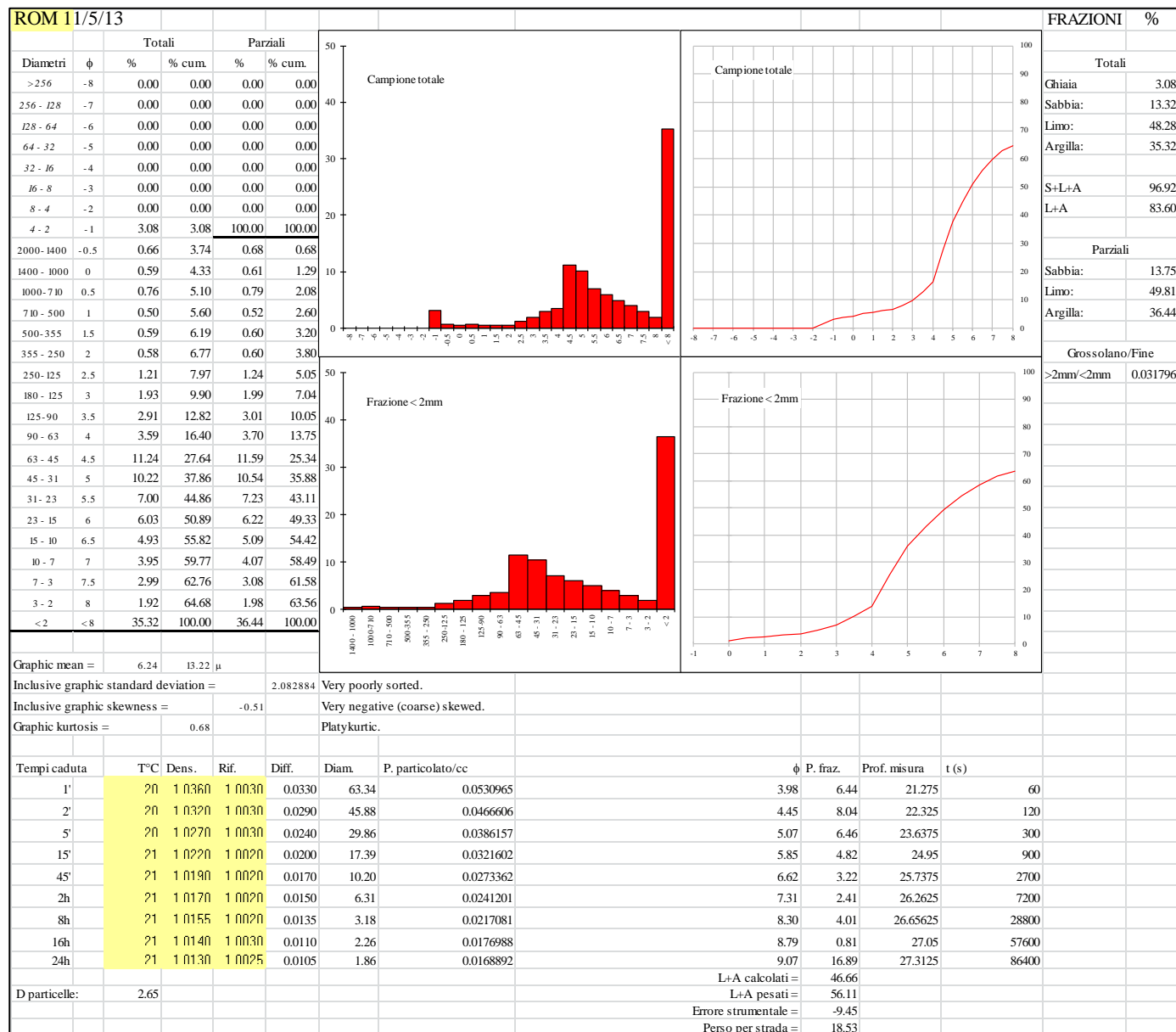
**Appendix 7.6. Grain-size
(Wentworth, 1922) of the <2 mm
fraction of undecalcified samples
from Romualdova Pećina, SU 11.**



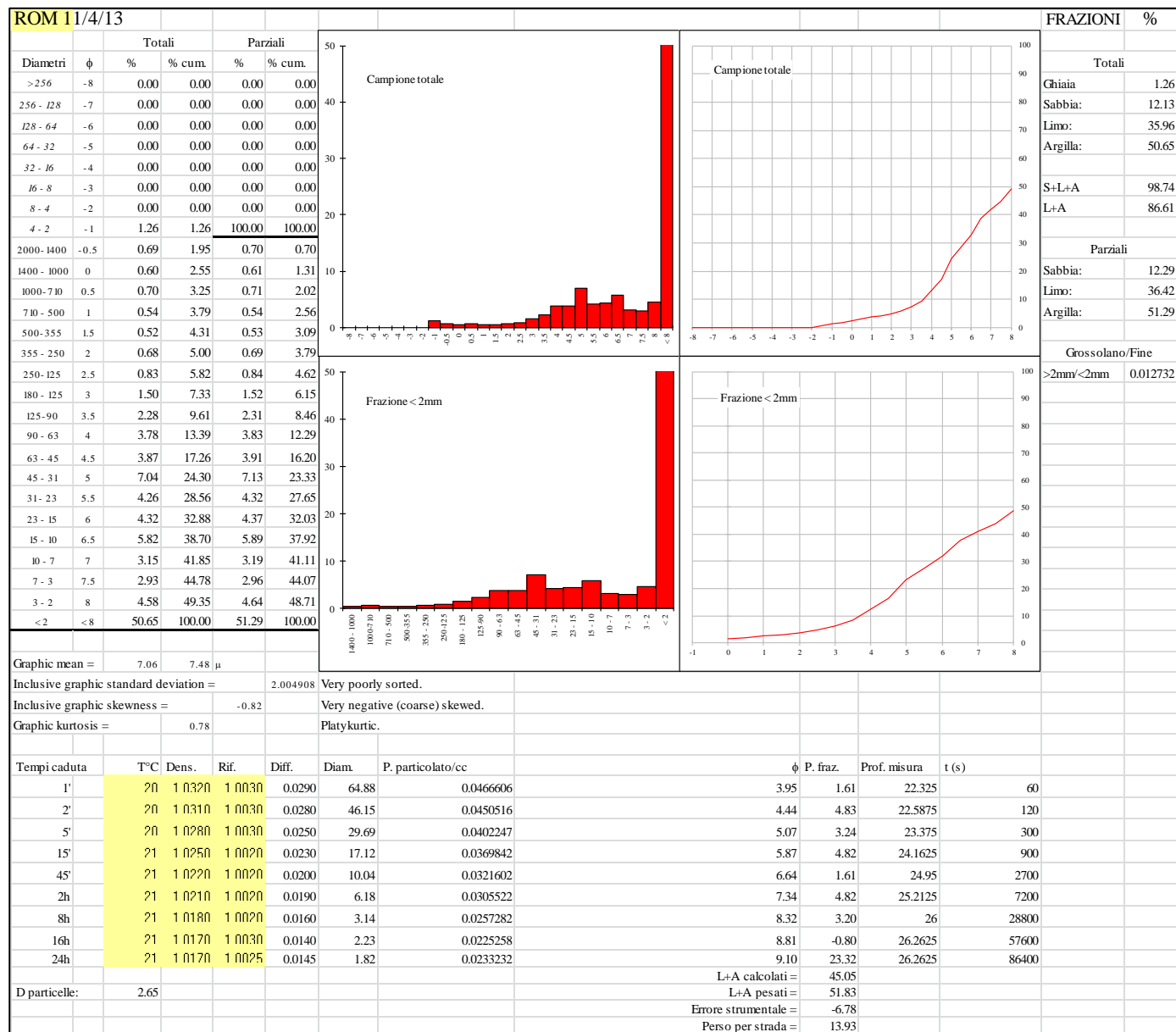
**Appendix 7.7. Grain-size
(Wentworth, 1922) of the <2 mm
fraction of undecalcified samples
from Romualdova Pećina, SU 12.**



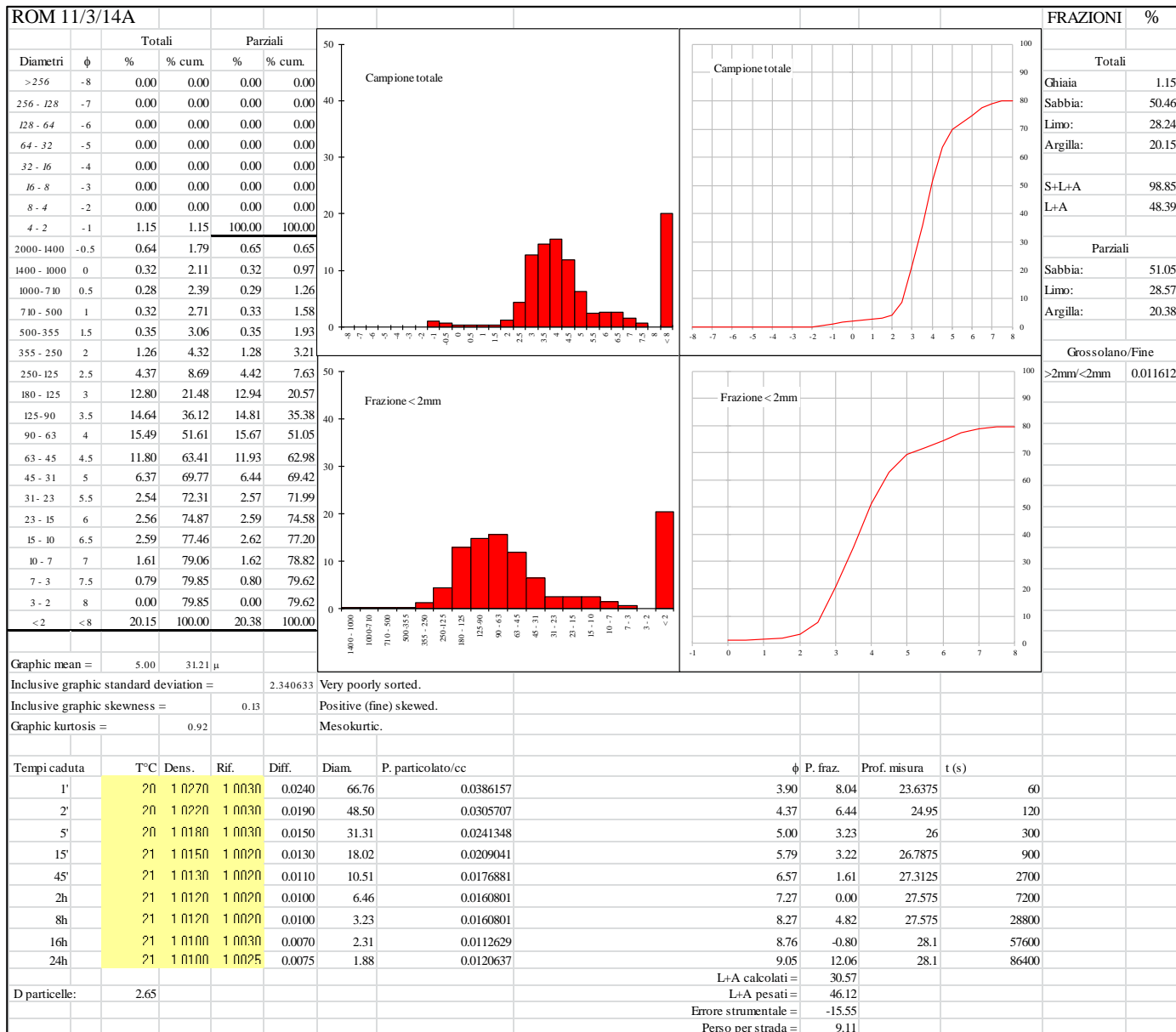
**Appendix 7.8. Grain-size
(Wentworth, 1922) of the <2 mm
fraction of undecalcified samples
from Romualdova Pećina, SU 13.**



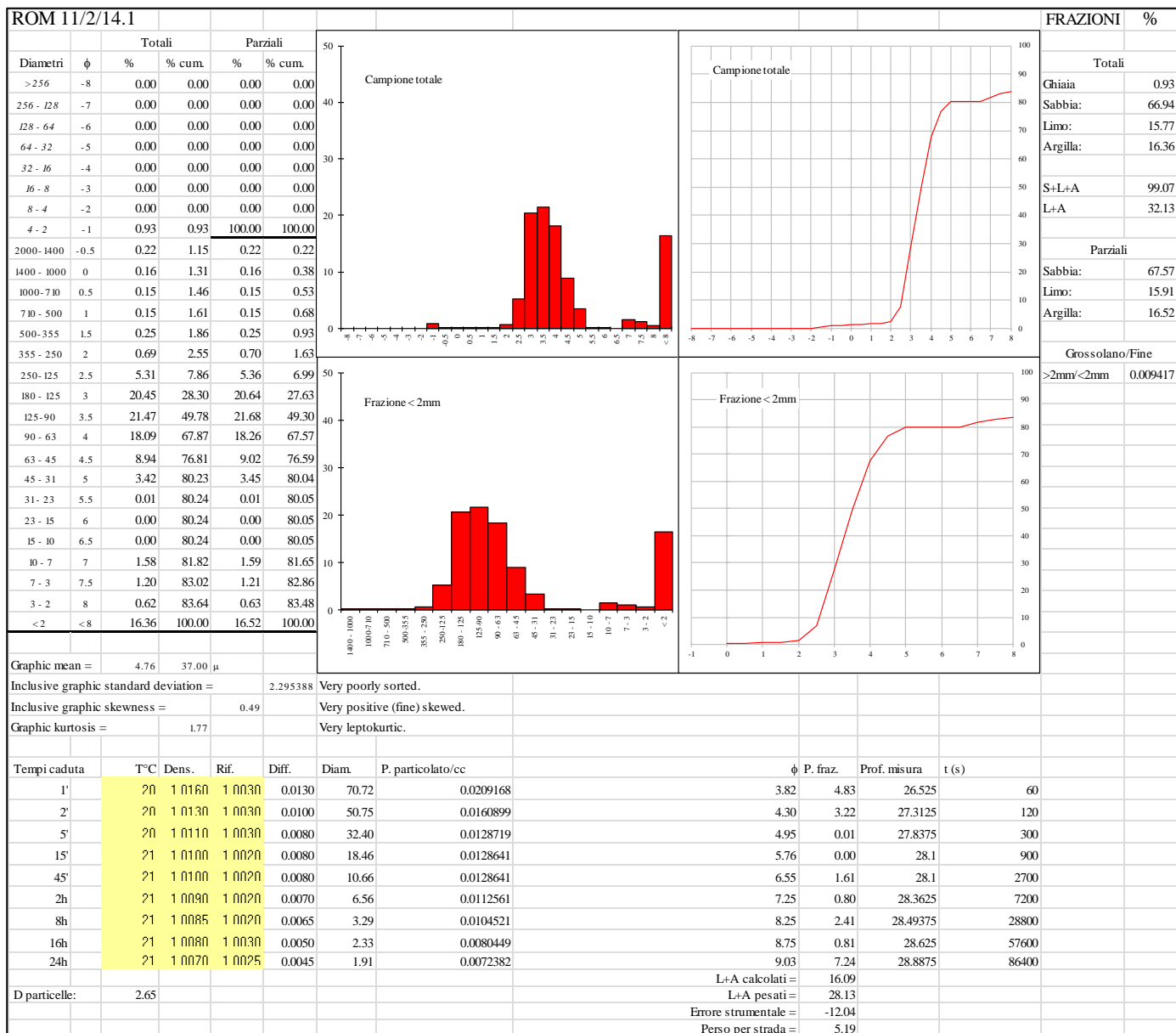
**Appendix 7.9. Grain-size
(Wentworth, 1922) of the <2 mm
fraction of undecalcified samples
from Romualdova Pećina, SU 13.**



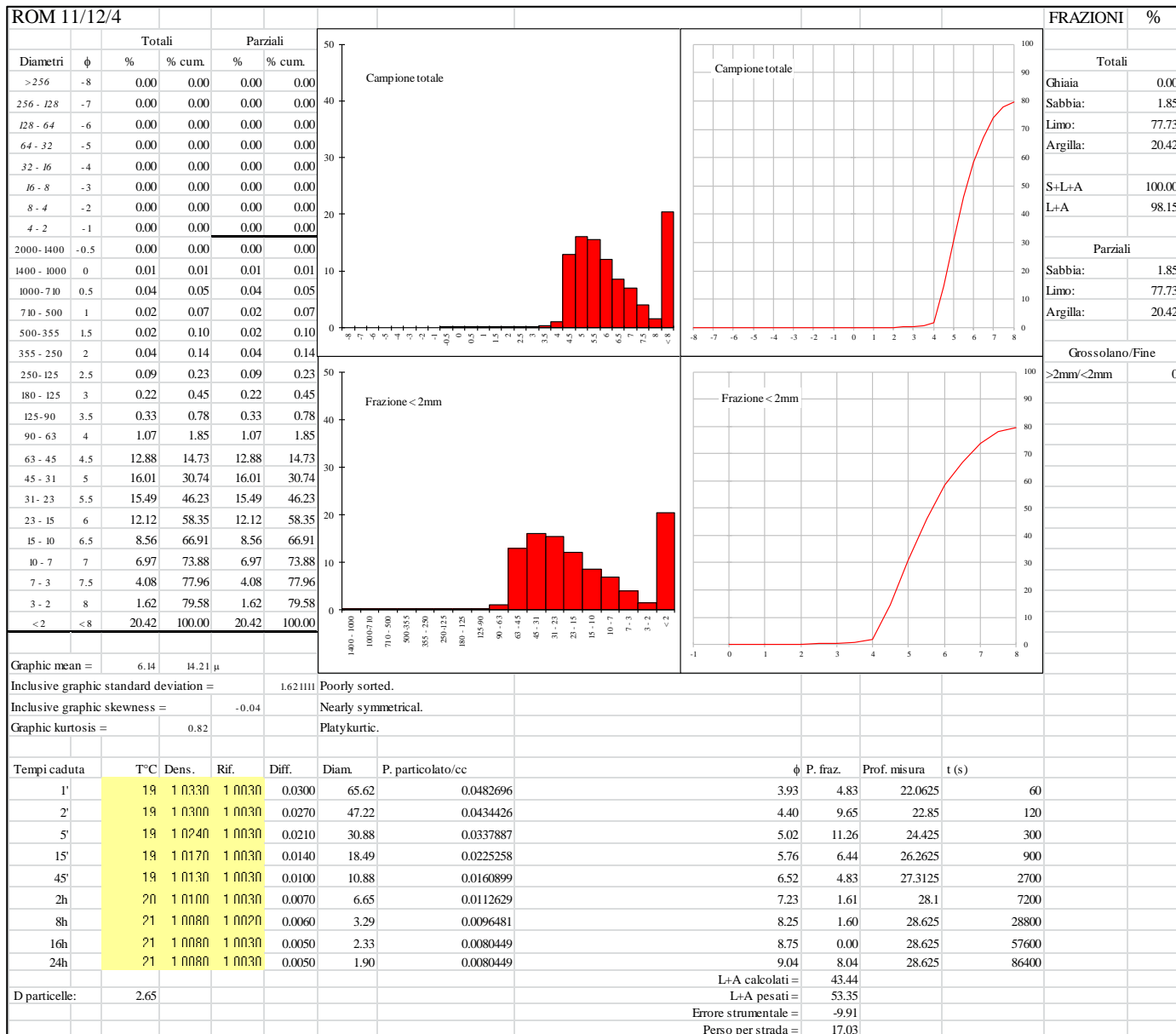
**Appendix 7.10. Grain-size
(Wentworth, 1922) of the <2 mm
fraction of undecalcified samples
from Romualdova Pećina, SU
14A.**



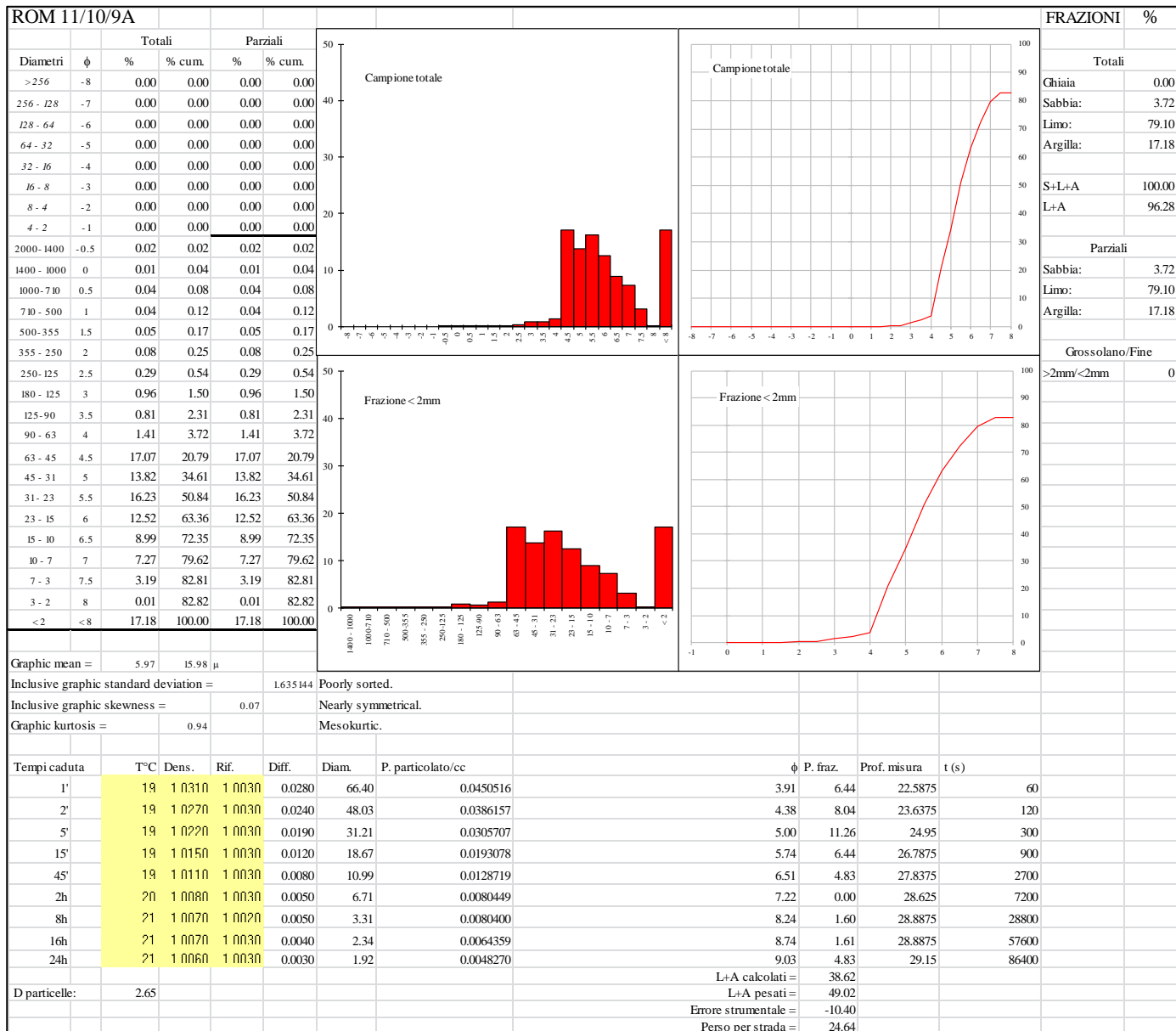
**Appendix 7.11. Grain-size
(Wentworth, 1922) of the <2 mm
fraction of undecalcified samples
from Romualdova Pećina, SU
14B.**



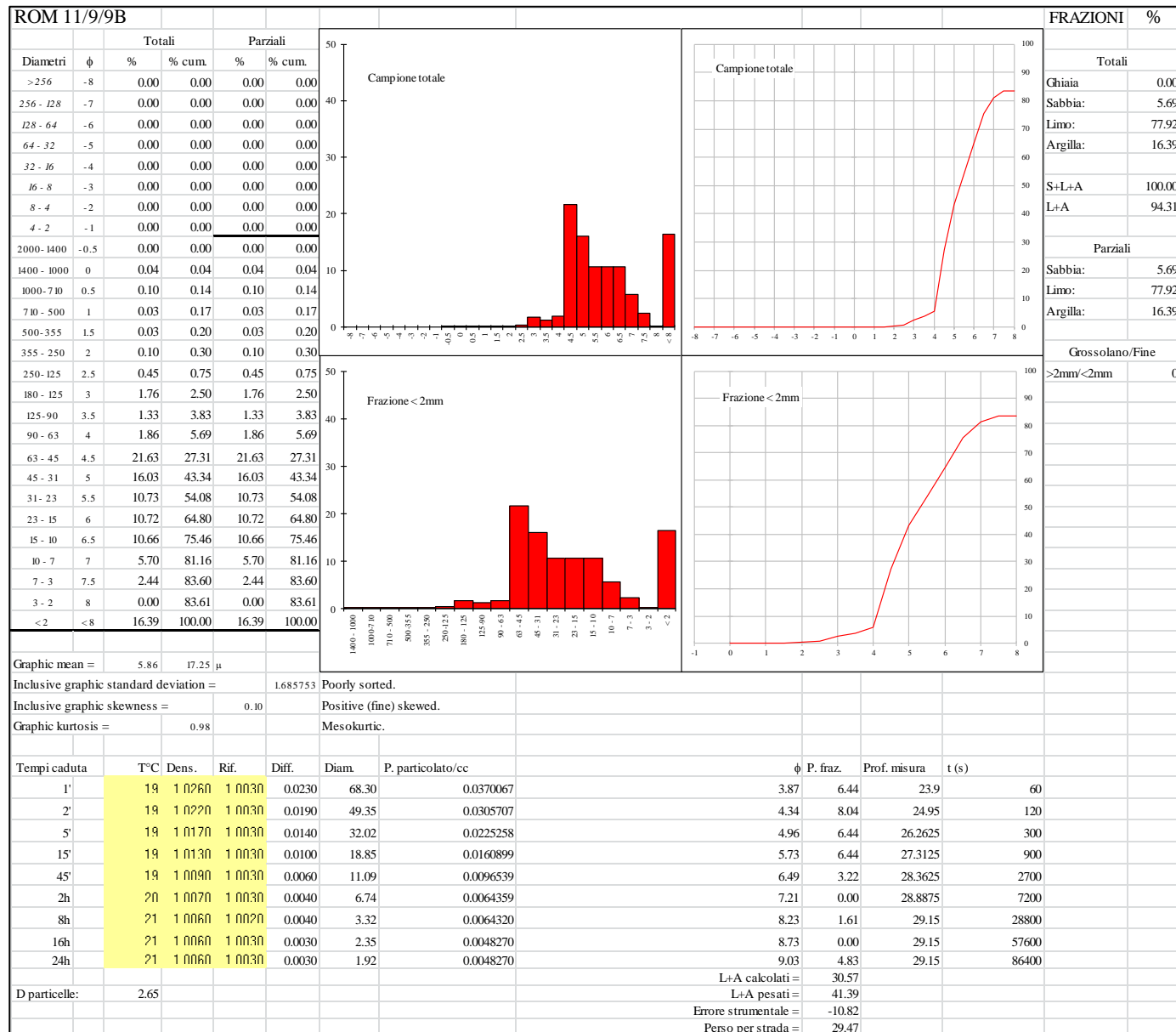
**Appendix 8.1. Grain-size
(Wentworth, 1922) of the <2 mm
fraction of decalcified samples
from Romualdova Pećina, SU 4.**



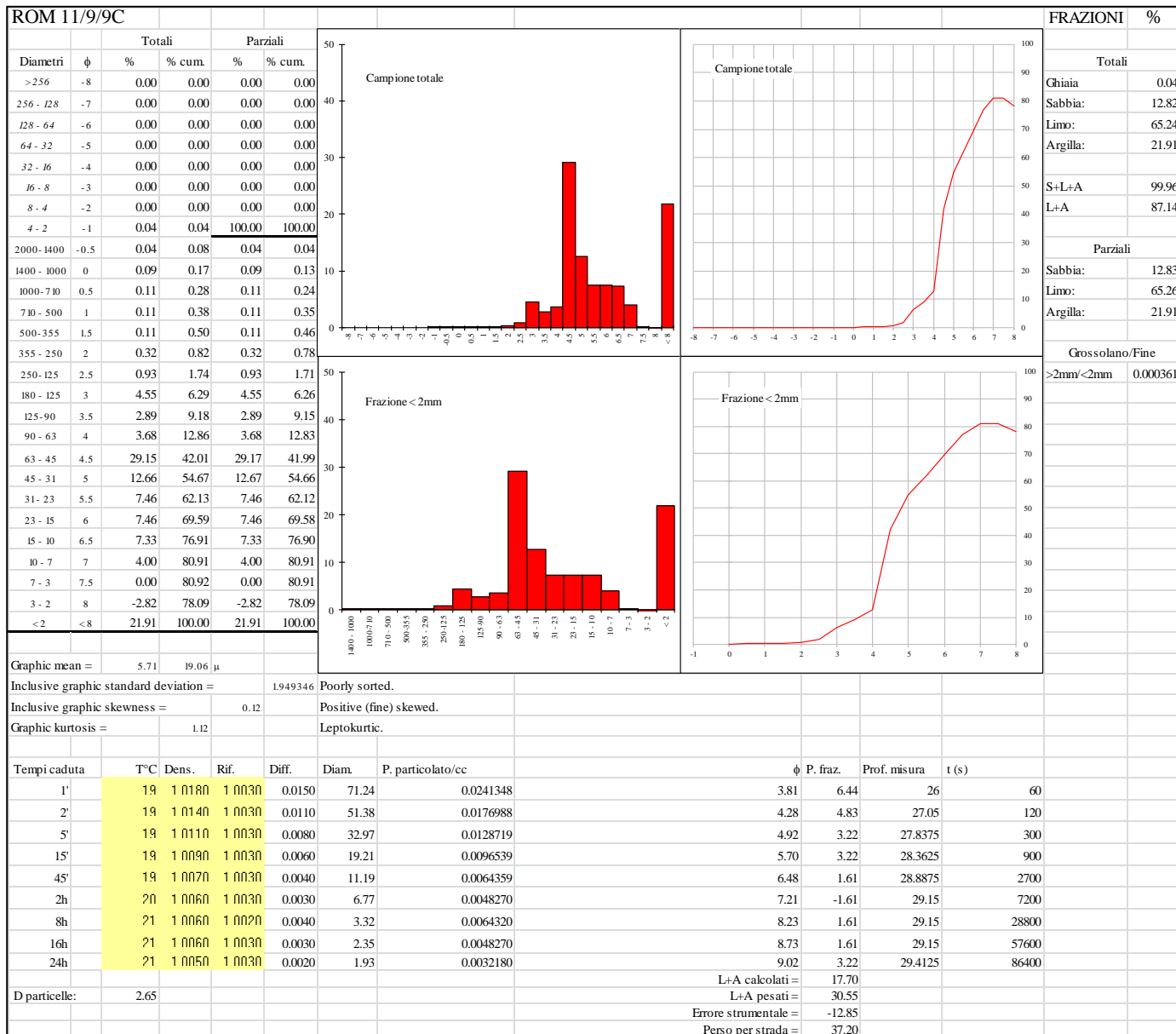
**Appendix 8.2. Grain-size
(Wentworth, 1922) of the <2 mm
fraction of decalcified samples
from Romualdova Pećina, SU
9A.**



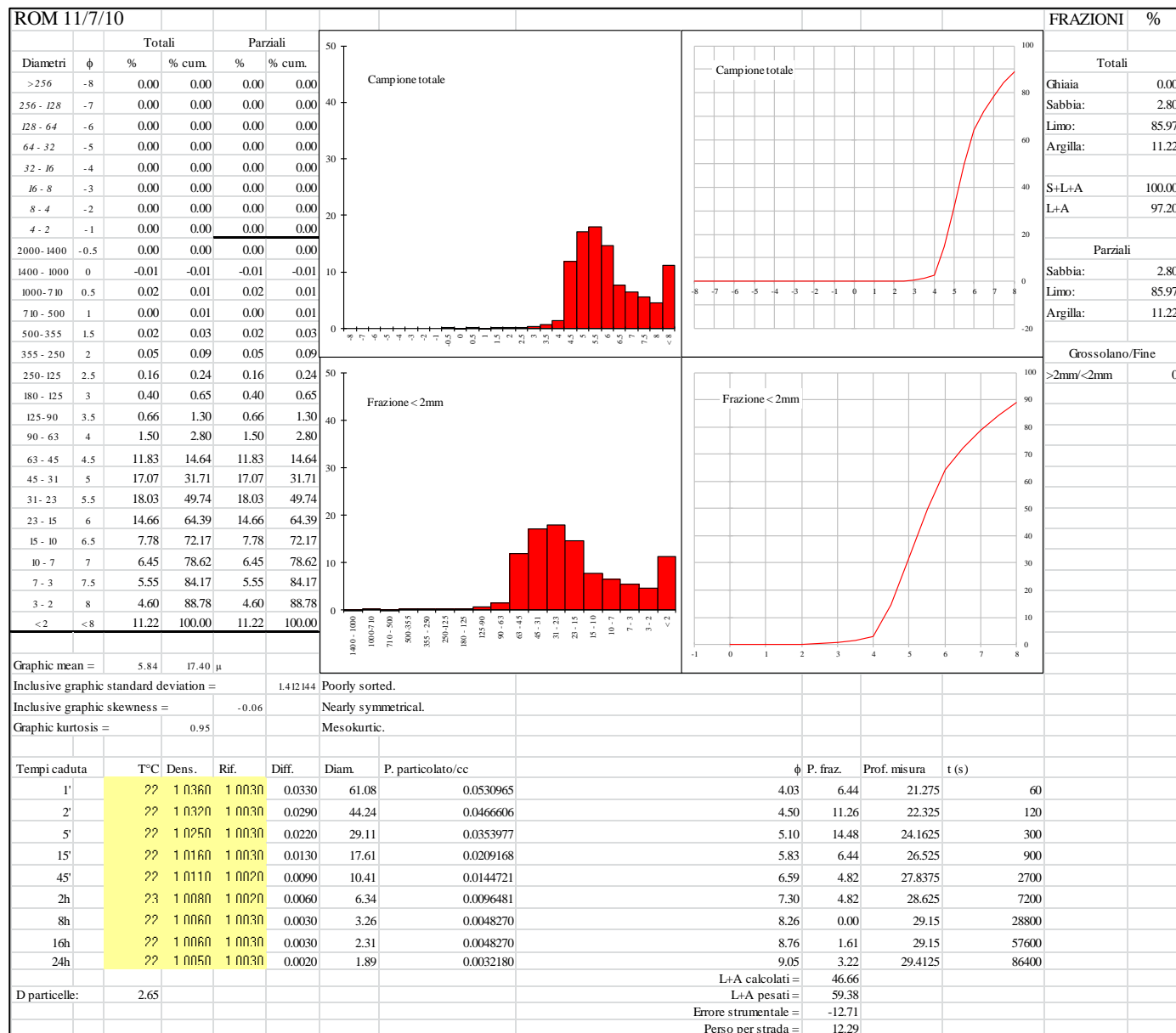
**Appendix 8.3. Grain-size
(Wentworth, 1922) of the <2 mm
fraction of decalcified samples
from Romualdova Pećina, SU 9B.**



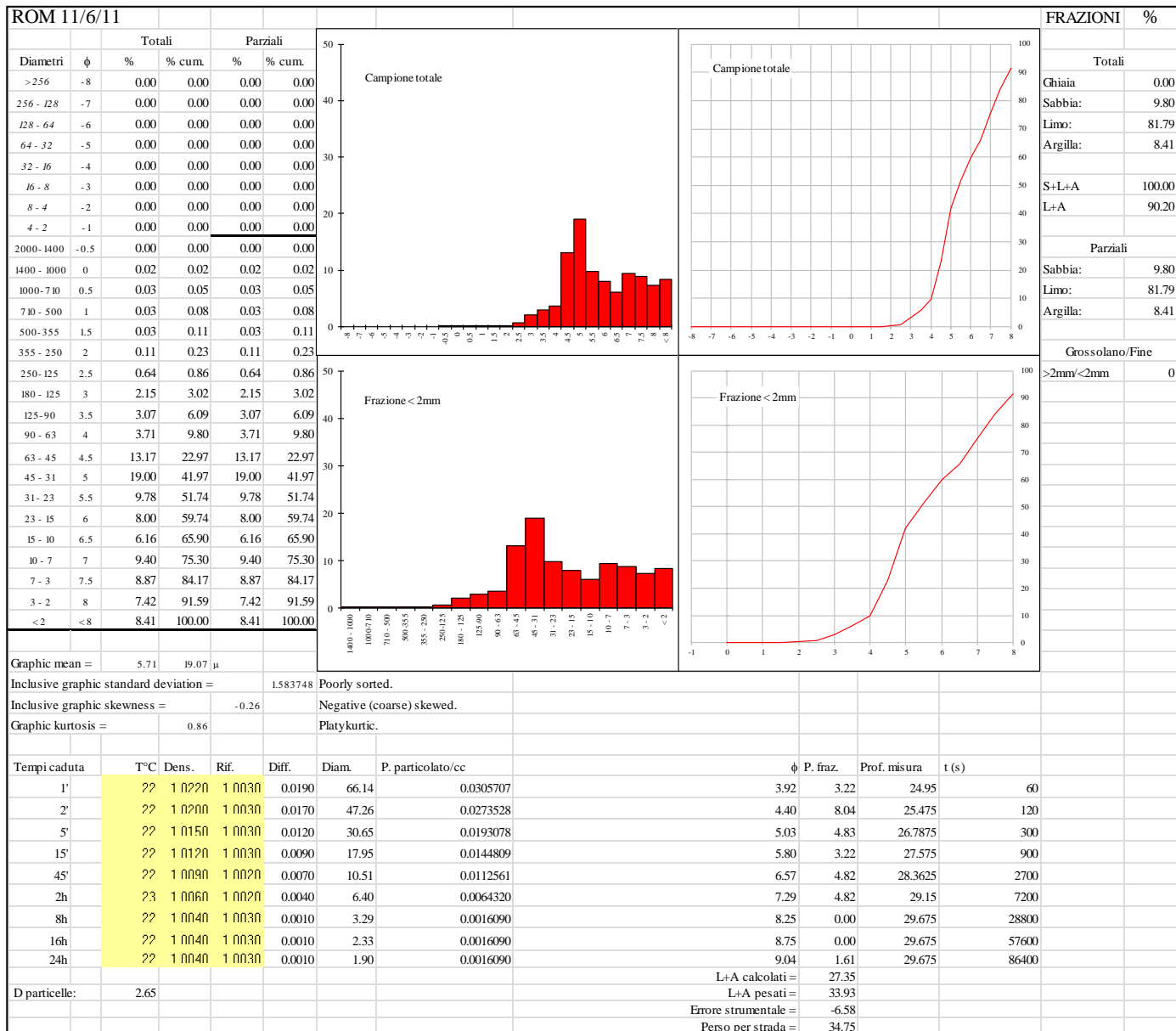
**Appendix 8.4. Grain-size
(Wentworth, 1922) of the <2 mm
fraction of decalcified samples
from Romualdova Pećina, SU
9C.**



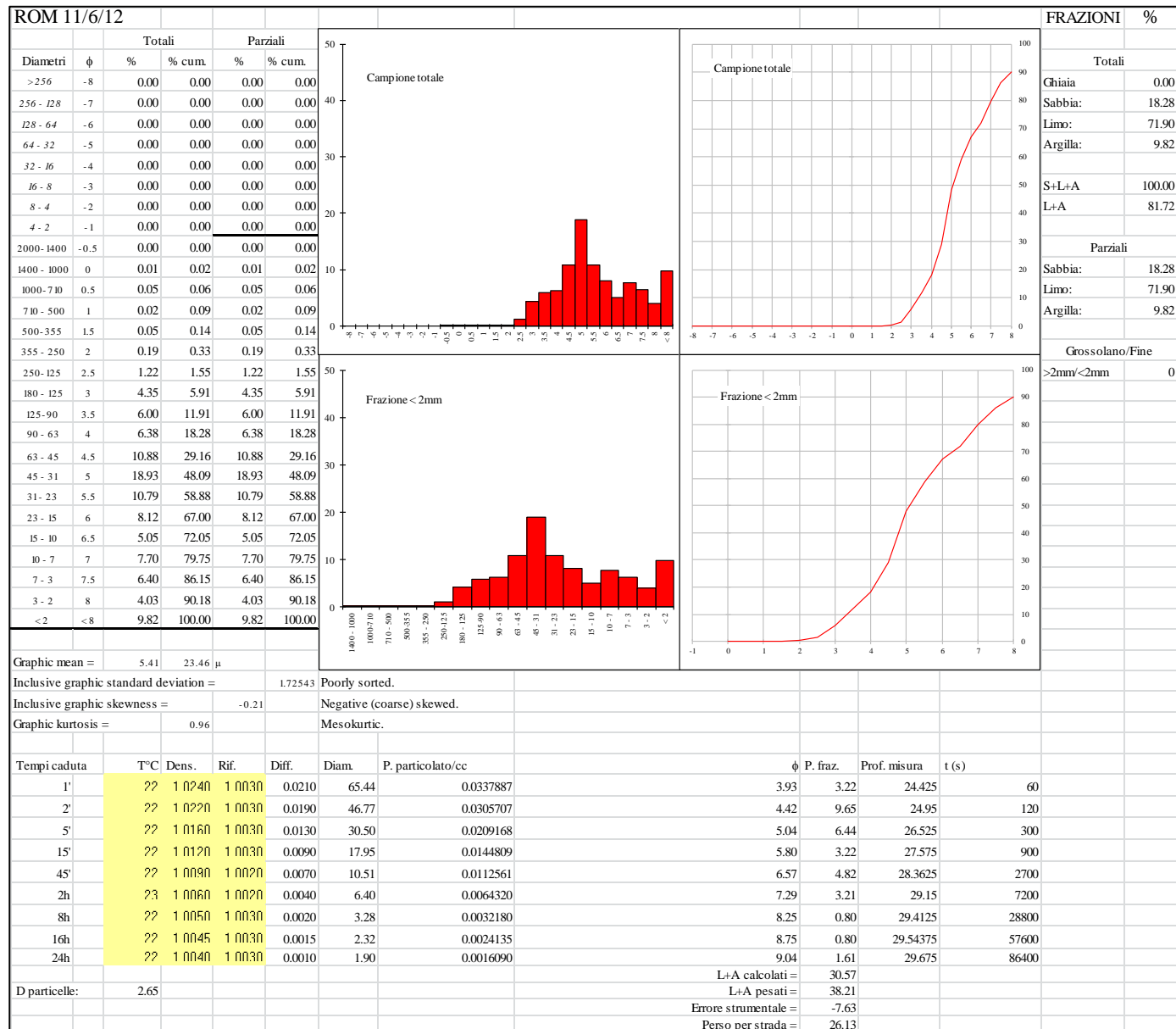
**Appendix 8.5. Grain-size
(Wentworth, 1922) of the <2 mm
fraction of decalcified samples
from Romualdova Pećina, SU 10.**



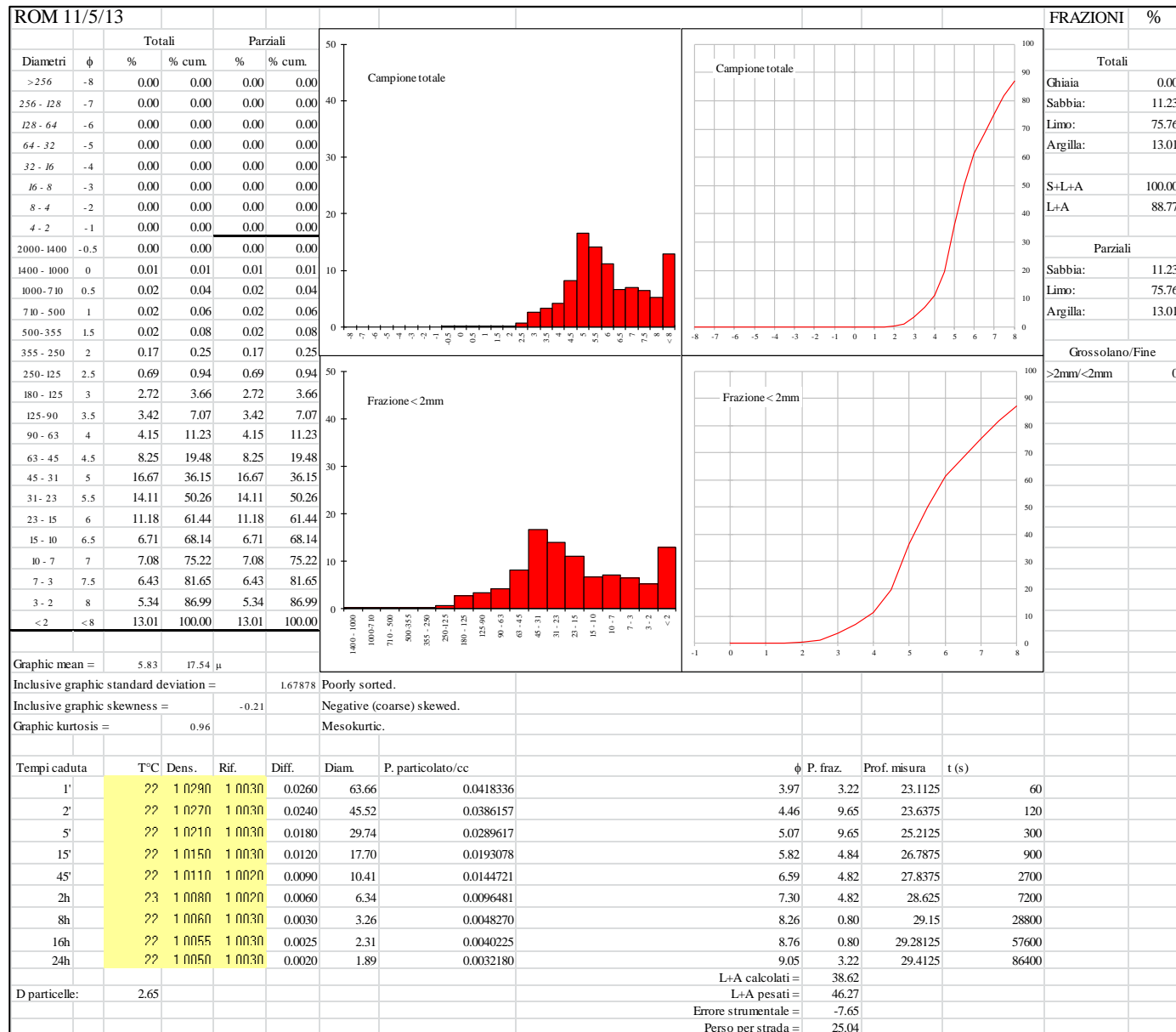
**Appendix 8.6. Grain-size
(Wentworth, 1922) of the <2 mm
fraction of decalcified samples
from Romualdova Pećina, SU 11.**



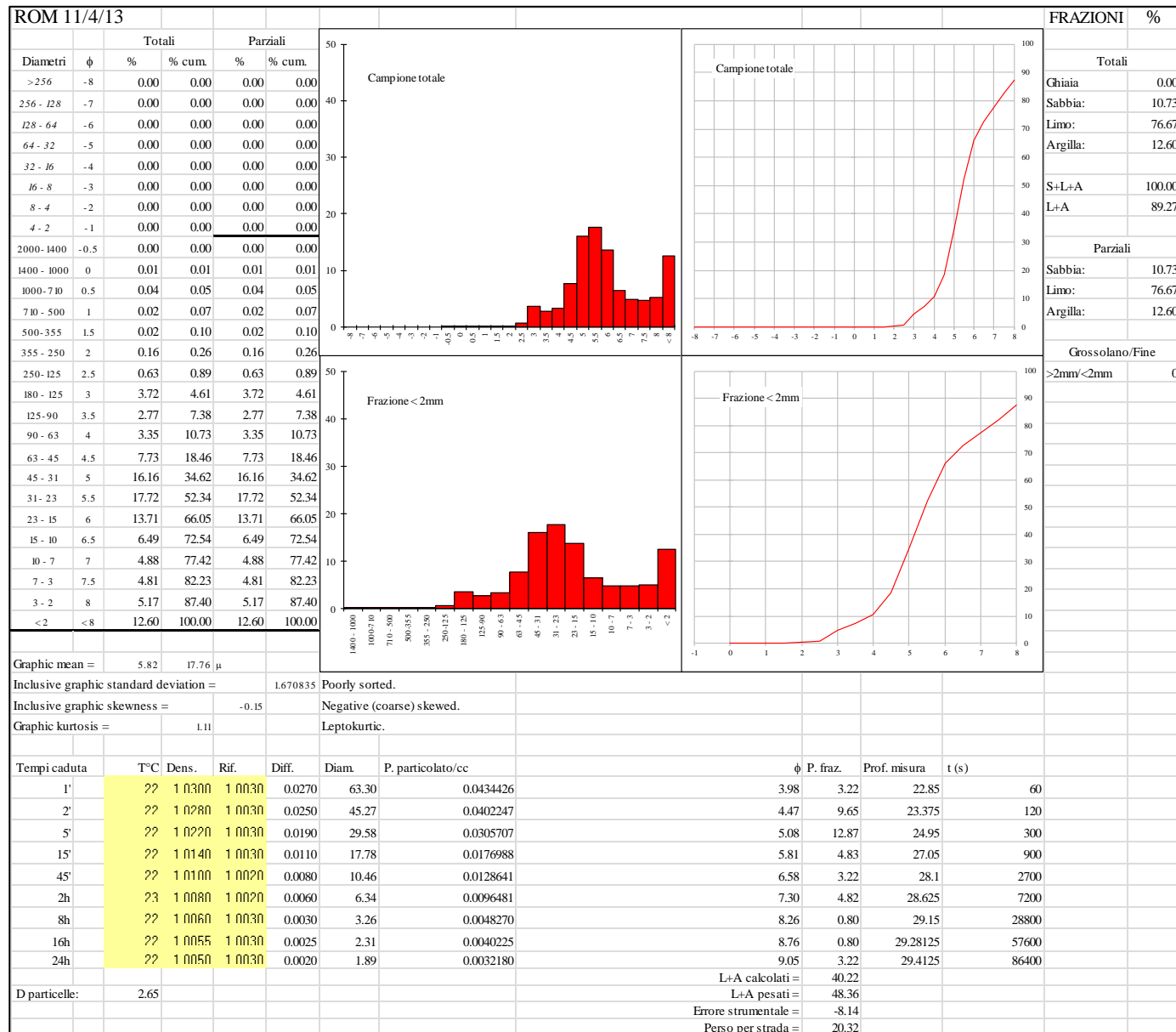
**Appendix 8.7. Grain-size
(Wentworth, 1922) of the <2 mm
fraction of decalcified samples
from Romualdova Pećina, SU 12.**



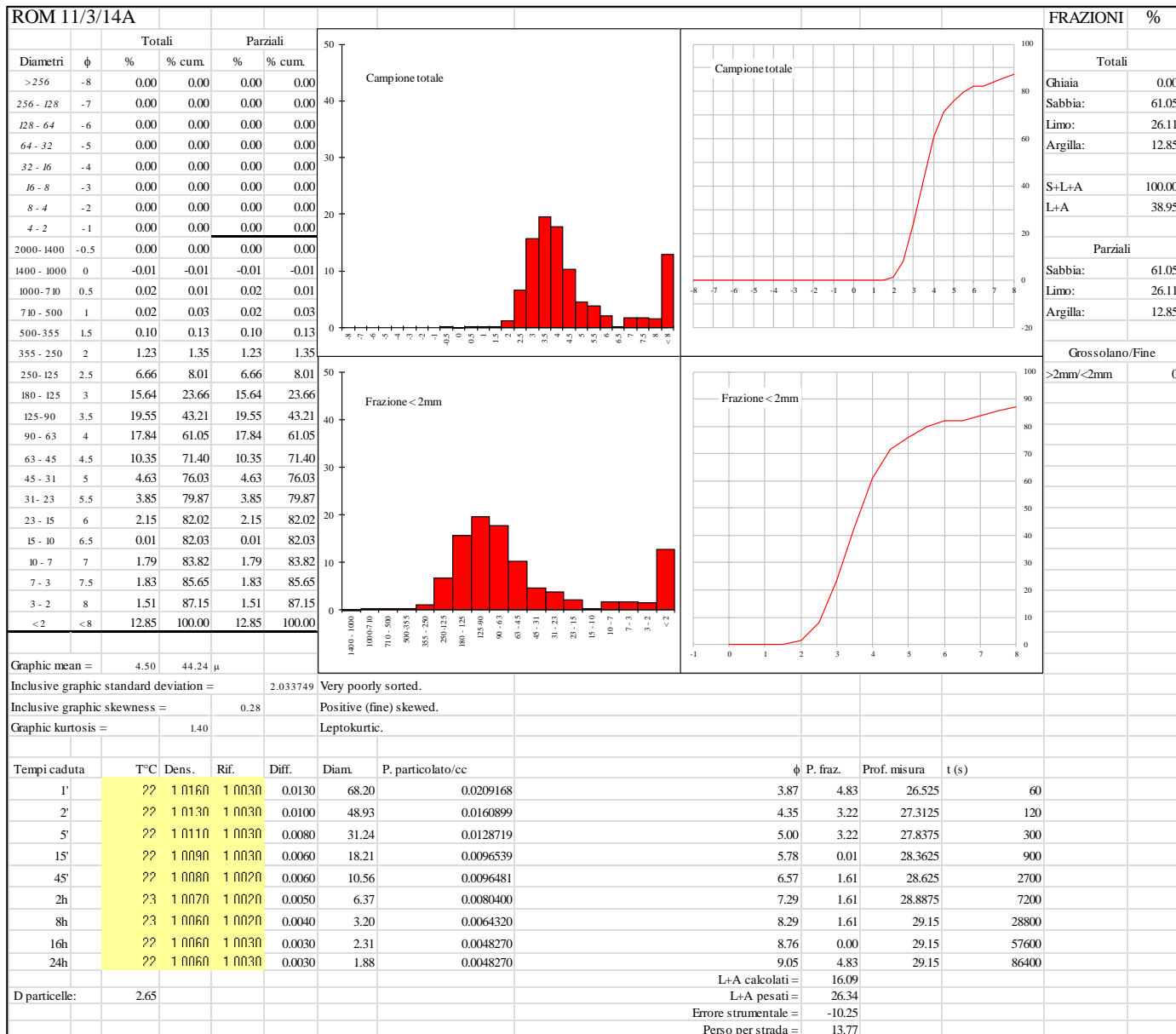
**Appendix 8.8. Grain-size
(Wentworth, 1922) of the <2 mm
fraction of decalcified samples
from Romualdova Pećina, SU 13.**



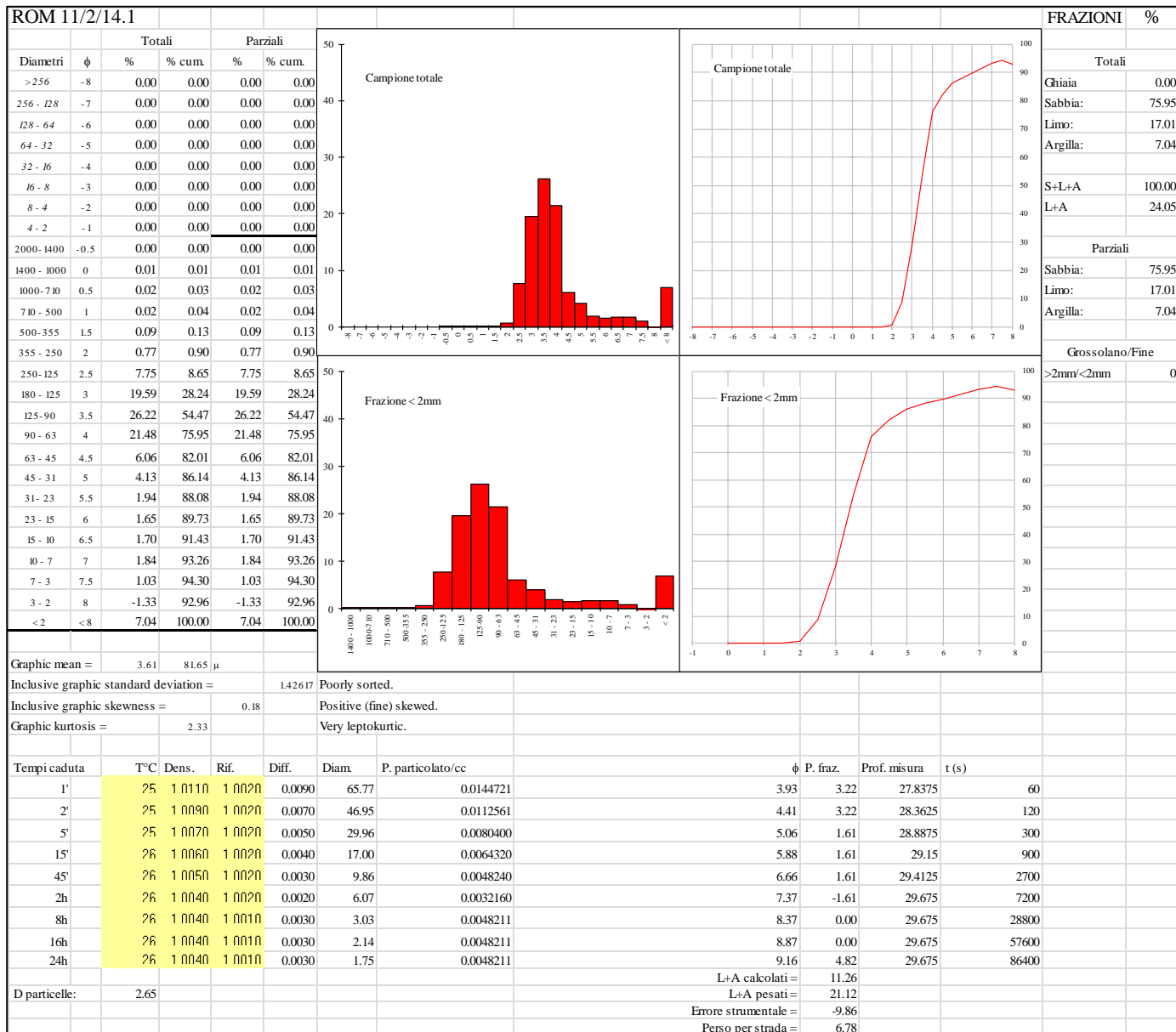
**Appendix 8.9. Grain-size
(Wentworth, 1922) of the <2 mm
fraction of decalcified samples
from Romualdova Pećina, SU 13.**



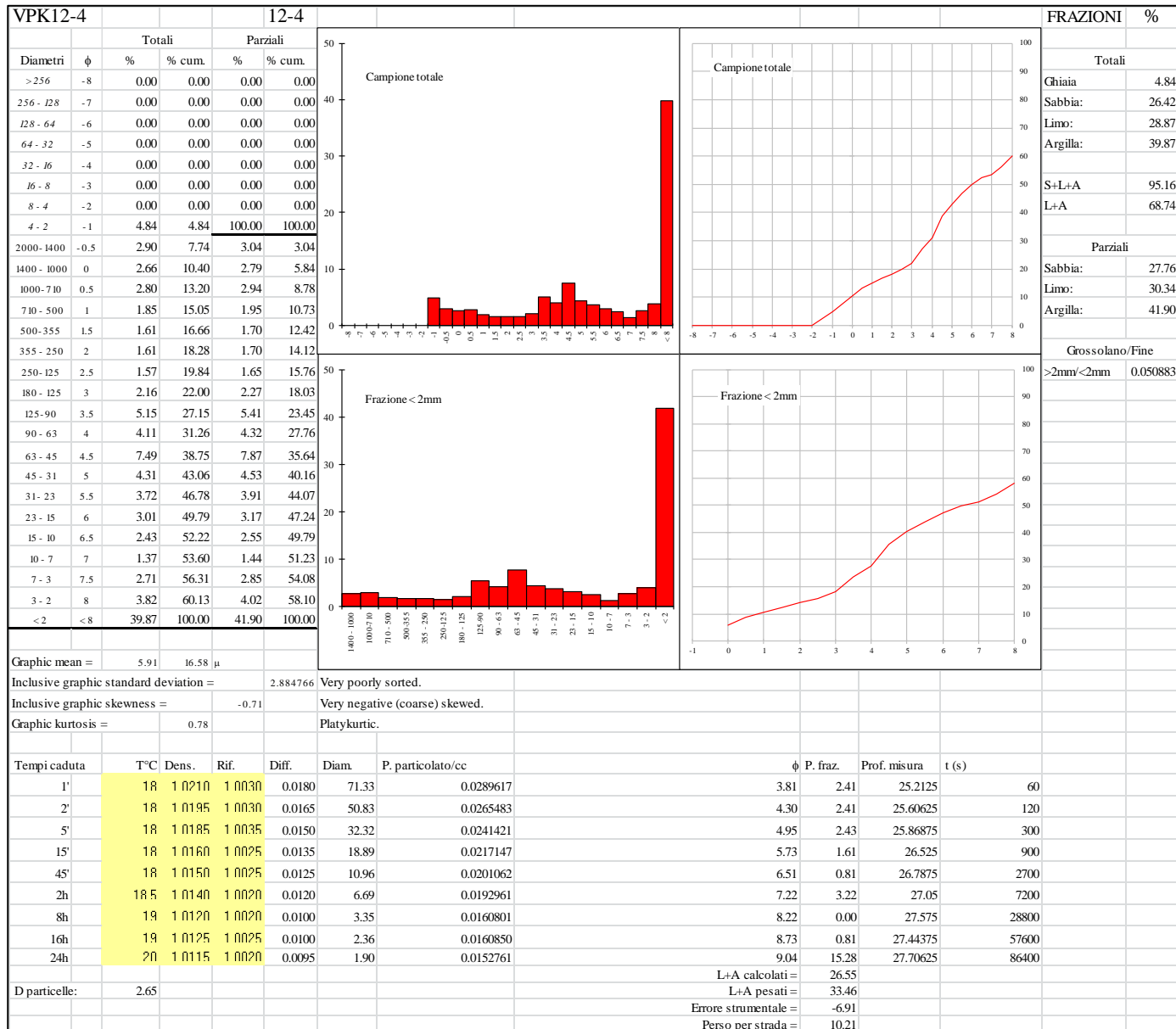
**Appendix 8.10. Grain-size
(Wentworth, 1922) of the <2 mm
fraction of decalcified samples
from Romualdova Pećina, SU
14A.**



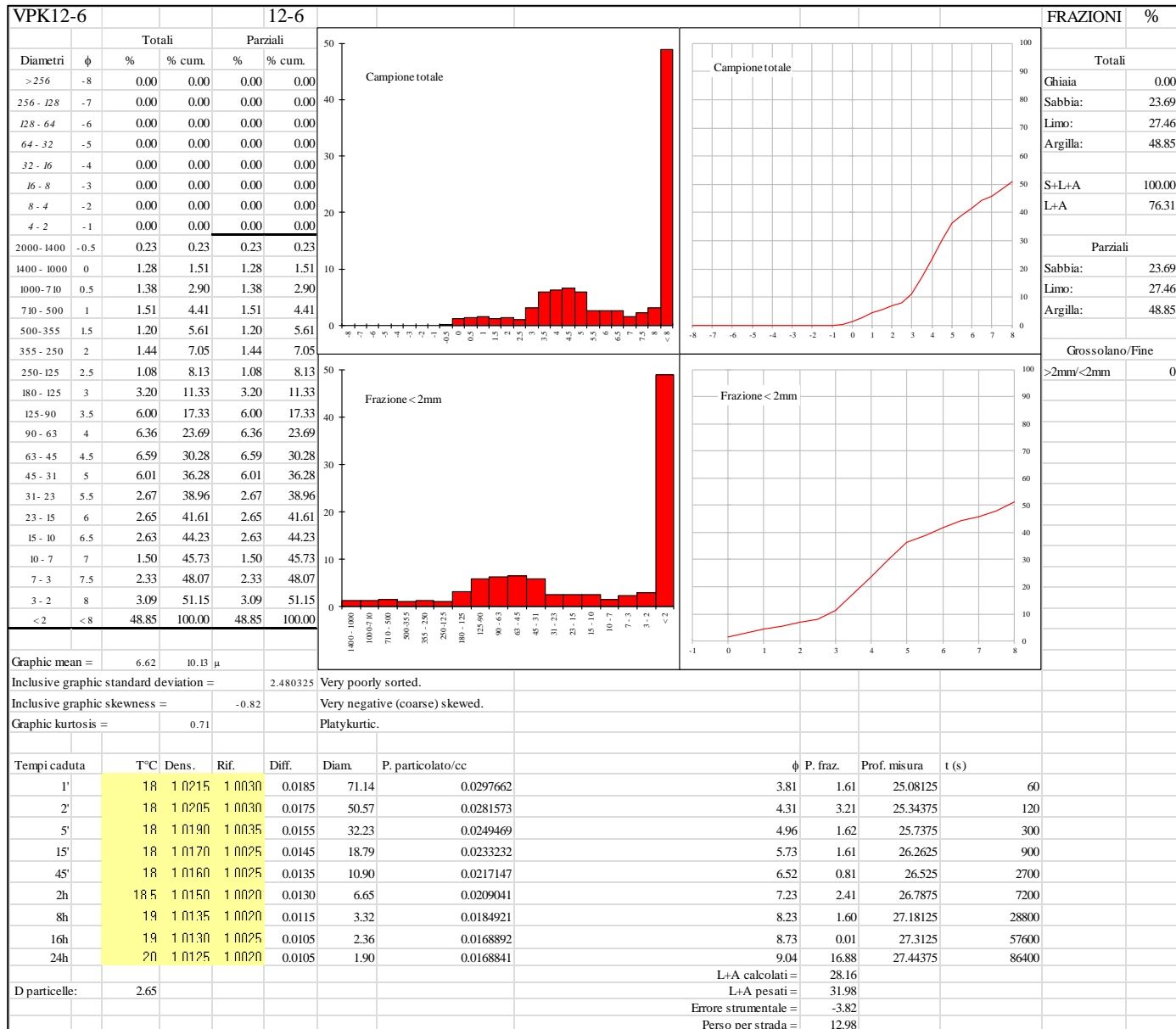
**Appendix 8.11. Grain-size
(Wentworth, 1922) of the <2 mm
fraction of decalcified samples
from Romualdova Pećina, SU
14B.**



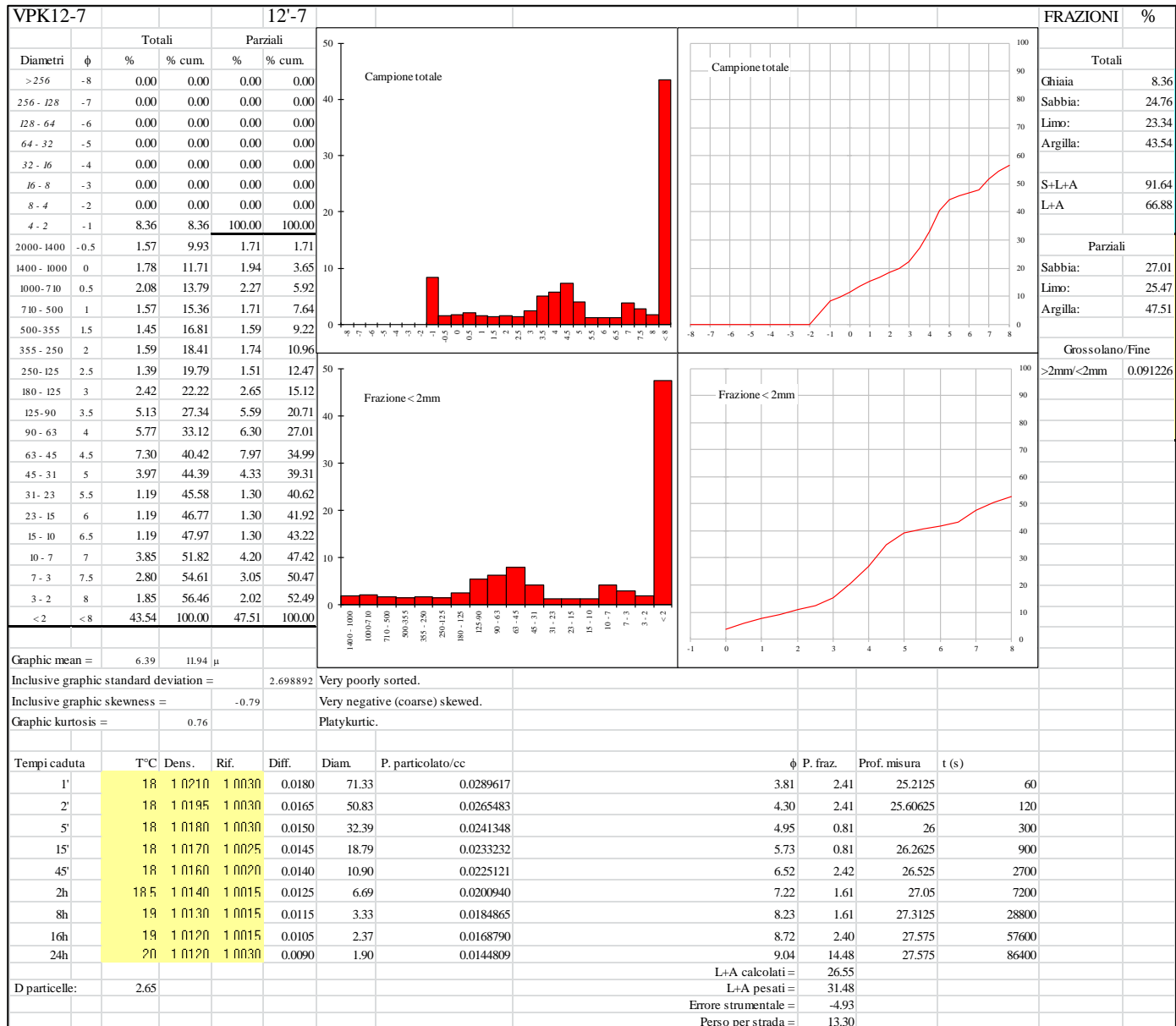
Appendix 9.1. Grain-size (Wentworth, 1922) of the <2 mm fraction of undecalcified samples from Velika Pećina - Kličevica, SU D_2.



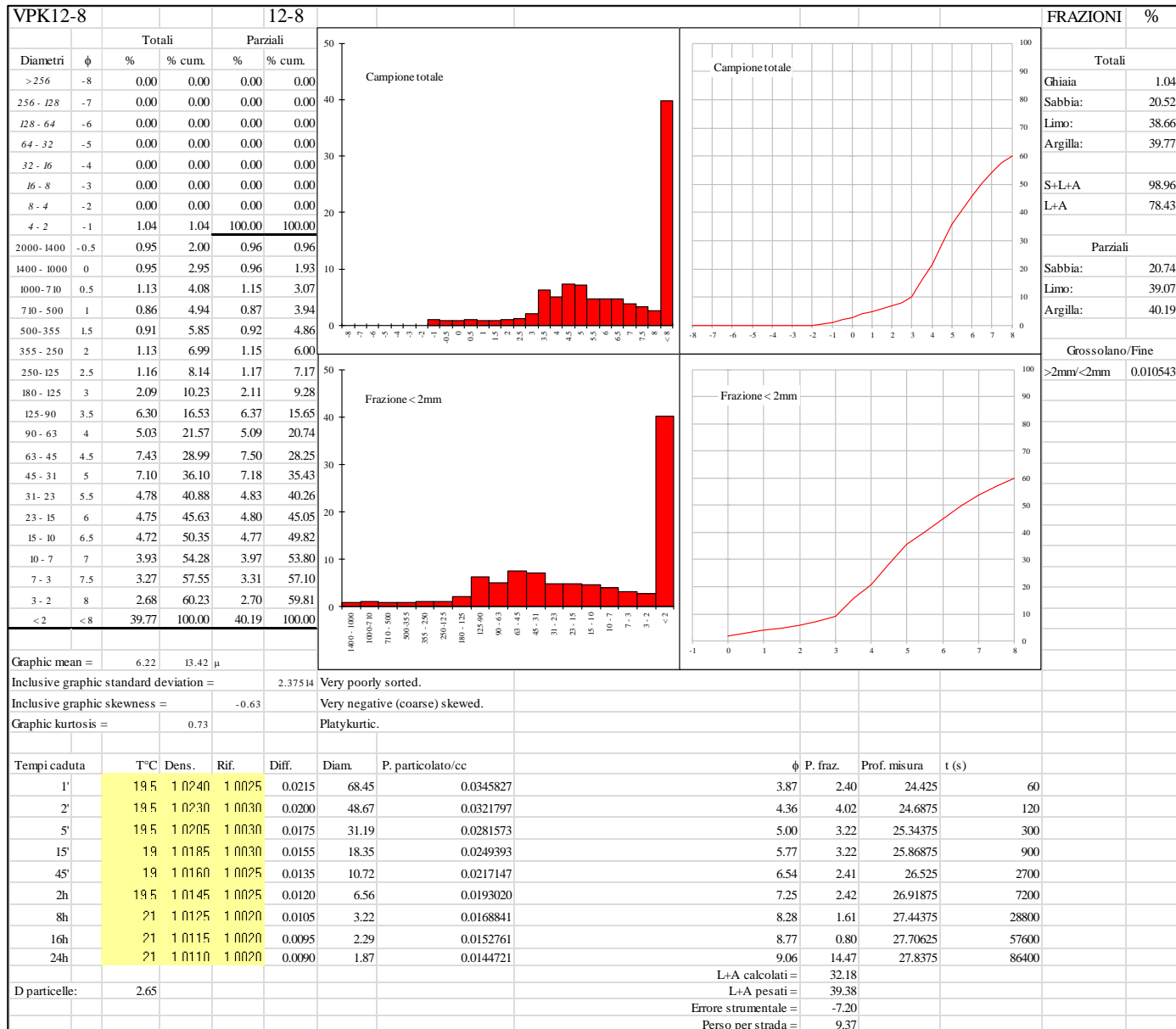
Appendix 9.2. Grain-size (Wentworth, 1922) of the <2 mm fraction of undecalcified samples from Velika Pećina - Kličevica, SU D.



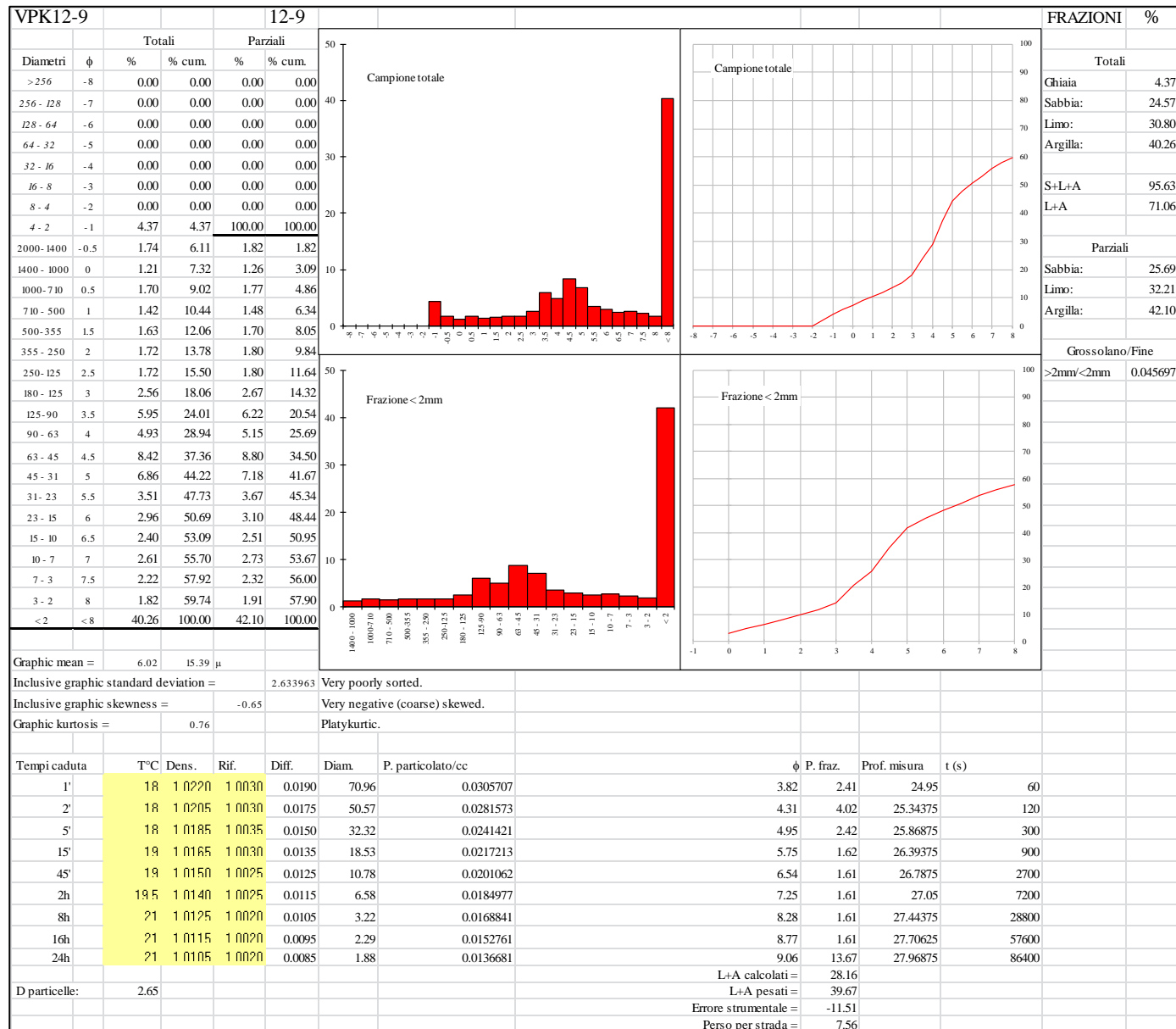
Appendix 9.3. Grain-size (Wentworth, 1922) of the <2 mm fraction of undecalcified samples from Velika Pećina - Kličevica, SU D_1.



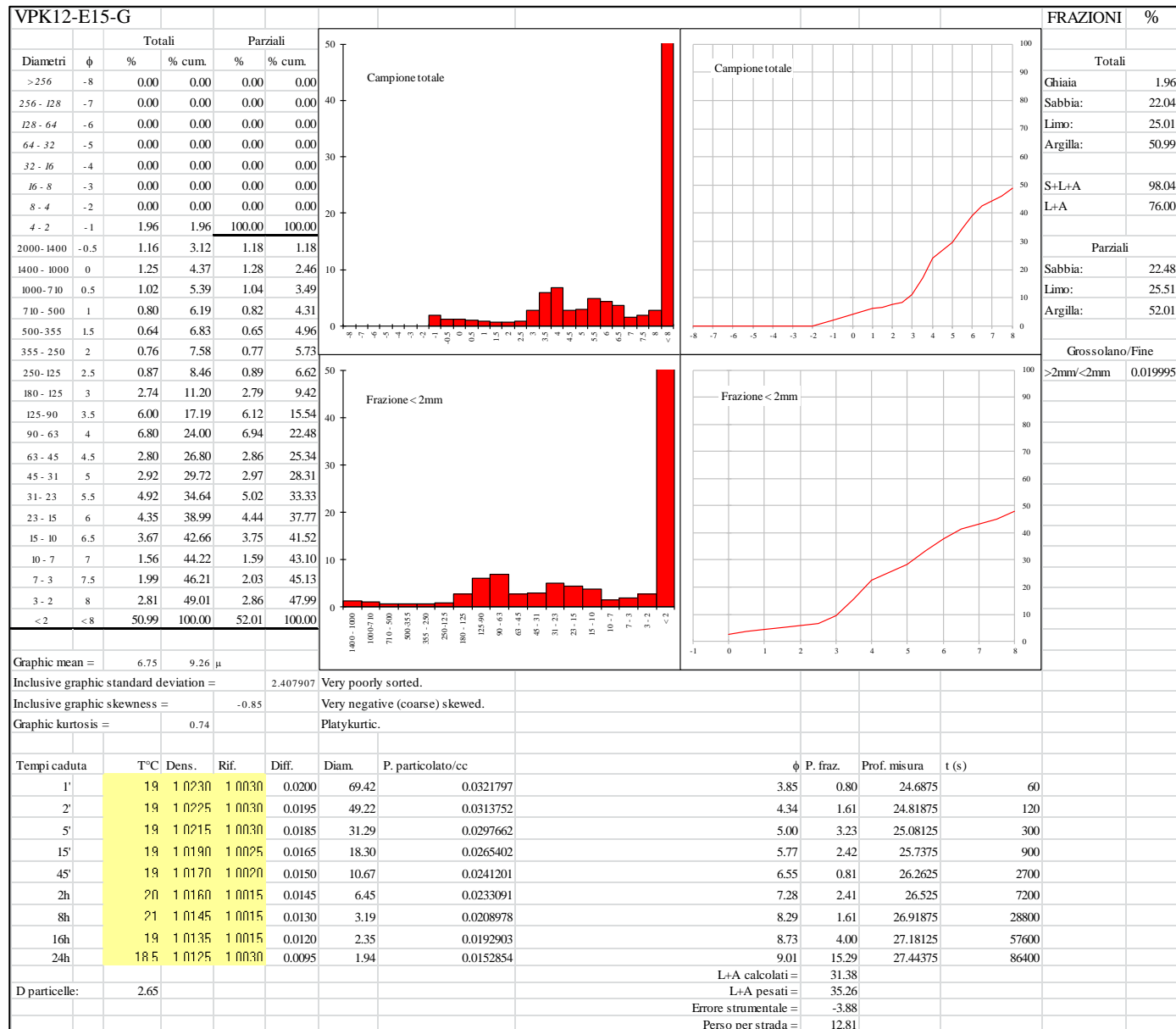
Appendix 9.4. Grain-size (Wentworth, 1922) of the <2 mm fraction of undecalcified samples from Velika Pećina - Kličevica, SU C2.



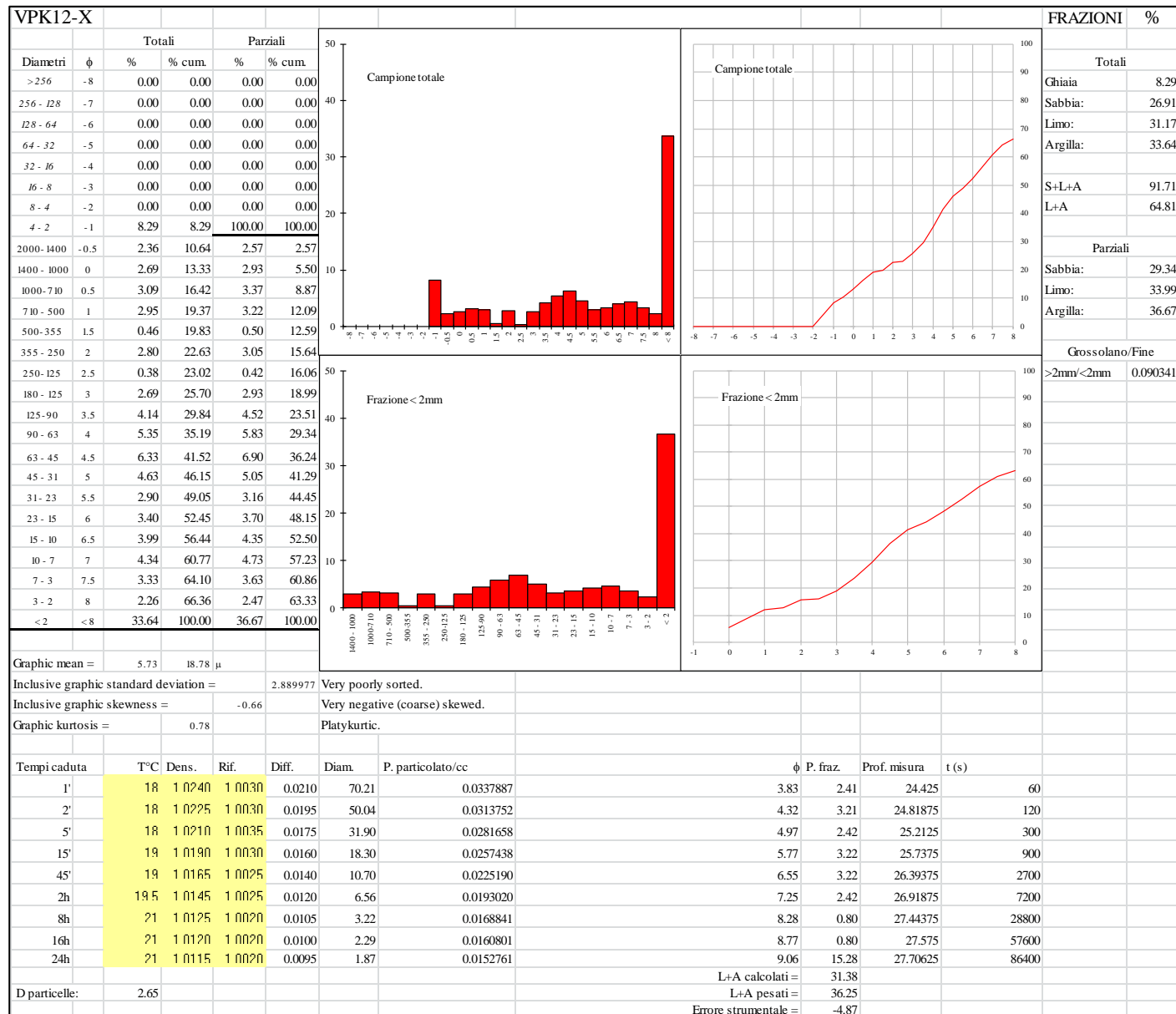
**Appendix 9.5. Grain-size
(Wentworth, 1922) of the <2 mm
fraction of undecalcified samples
from Velika Pećina - Kličevica,
SU C1.**



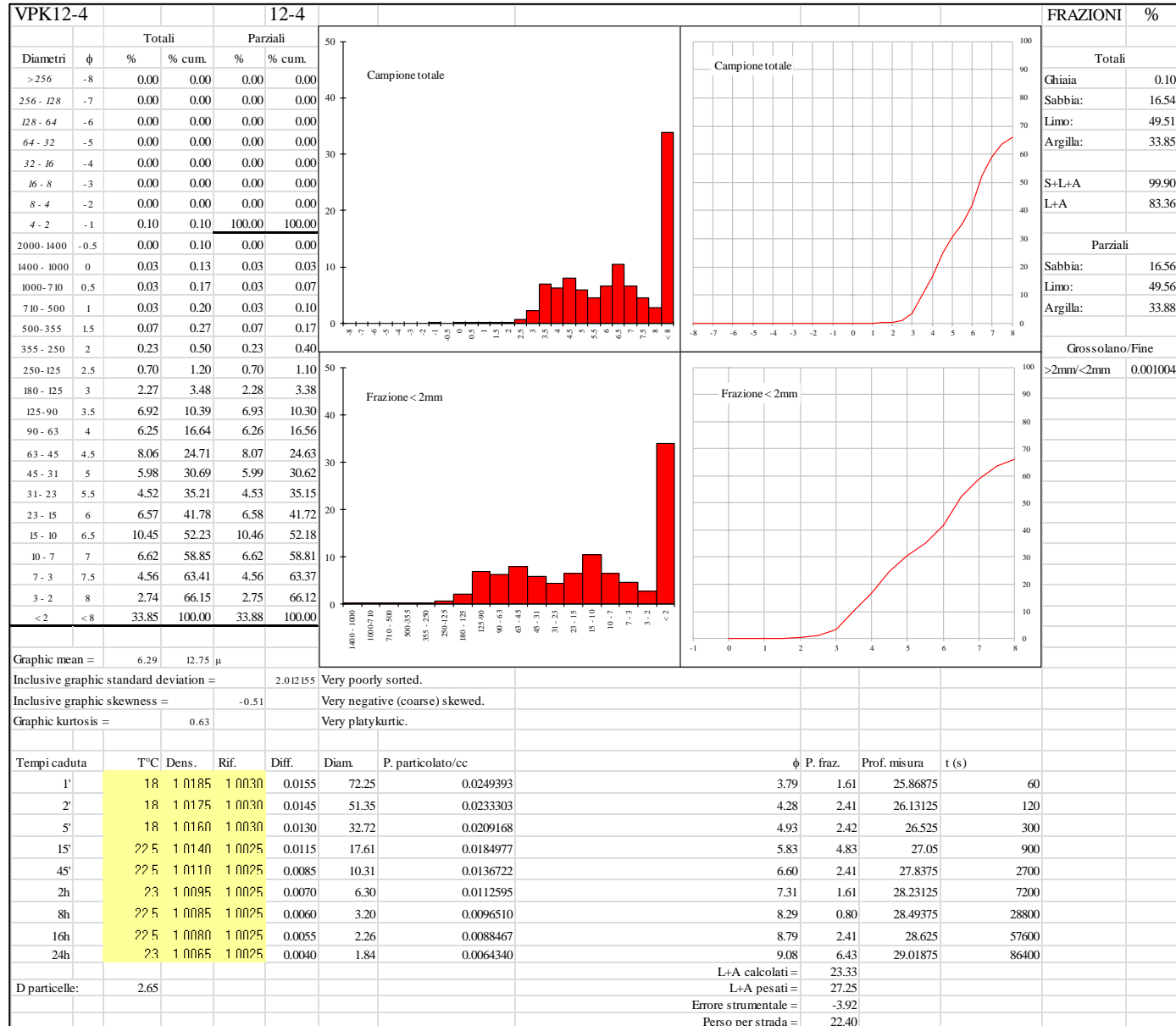
**Appendix 9.6. Grain-size
(Wentworth, 1922) of the <2 mm
fraction of undecalcified samples
from Velika Pećina - Kličevica,
SU G.**



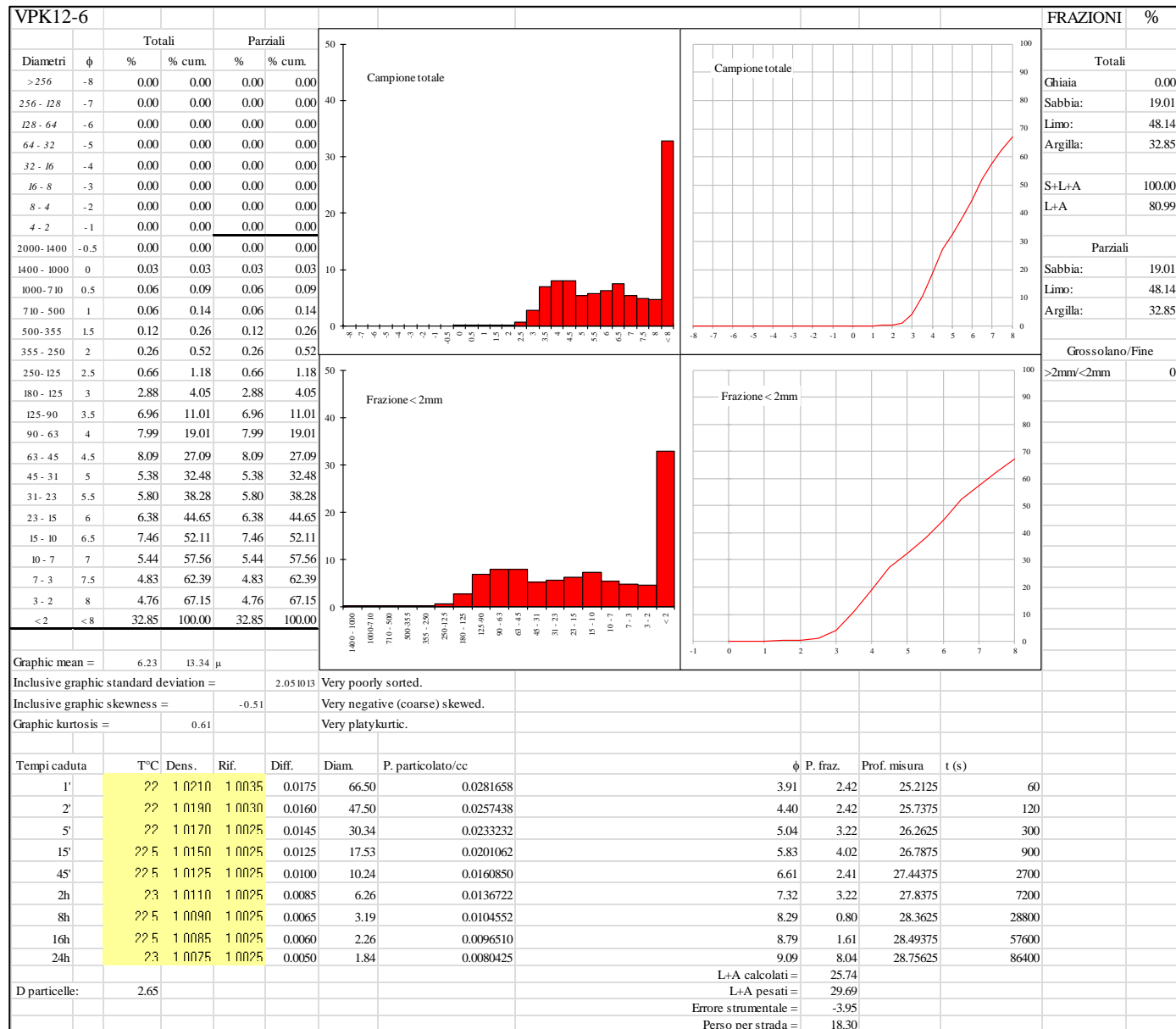
**Appendix 9.7. Grain-size
(Wentworth, 1922) of the <2
mm fraction of undecalcified
samples from Velika Pećina -
Kličevica, SU X.**



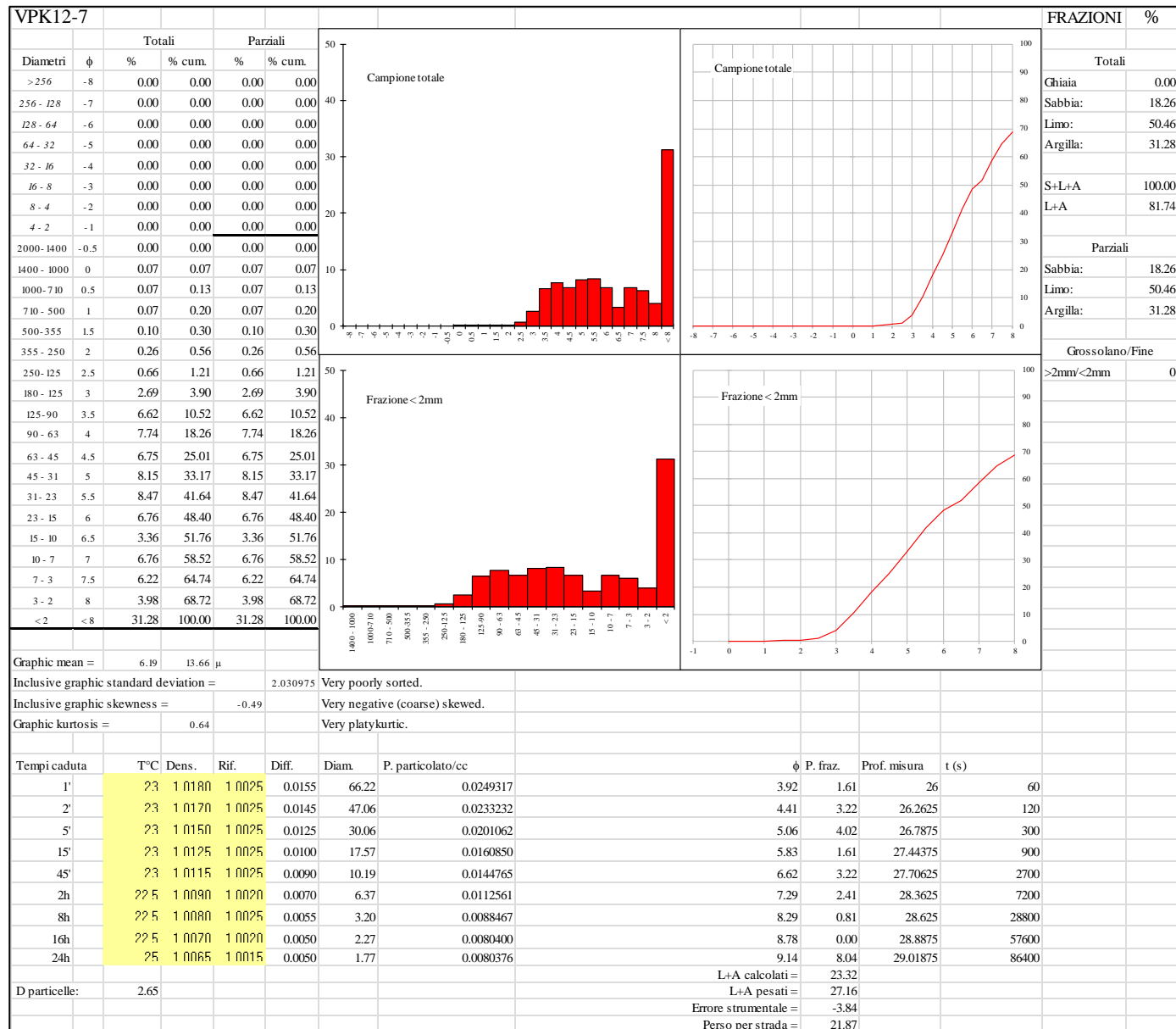
Appendix 10.1. Grain-size (Wentworth, 1922) of the <2 mm fraction of decalcified samples from Velika Pećina - Kličevica, SU D_2.



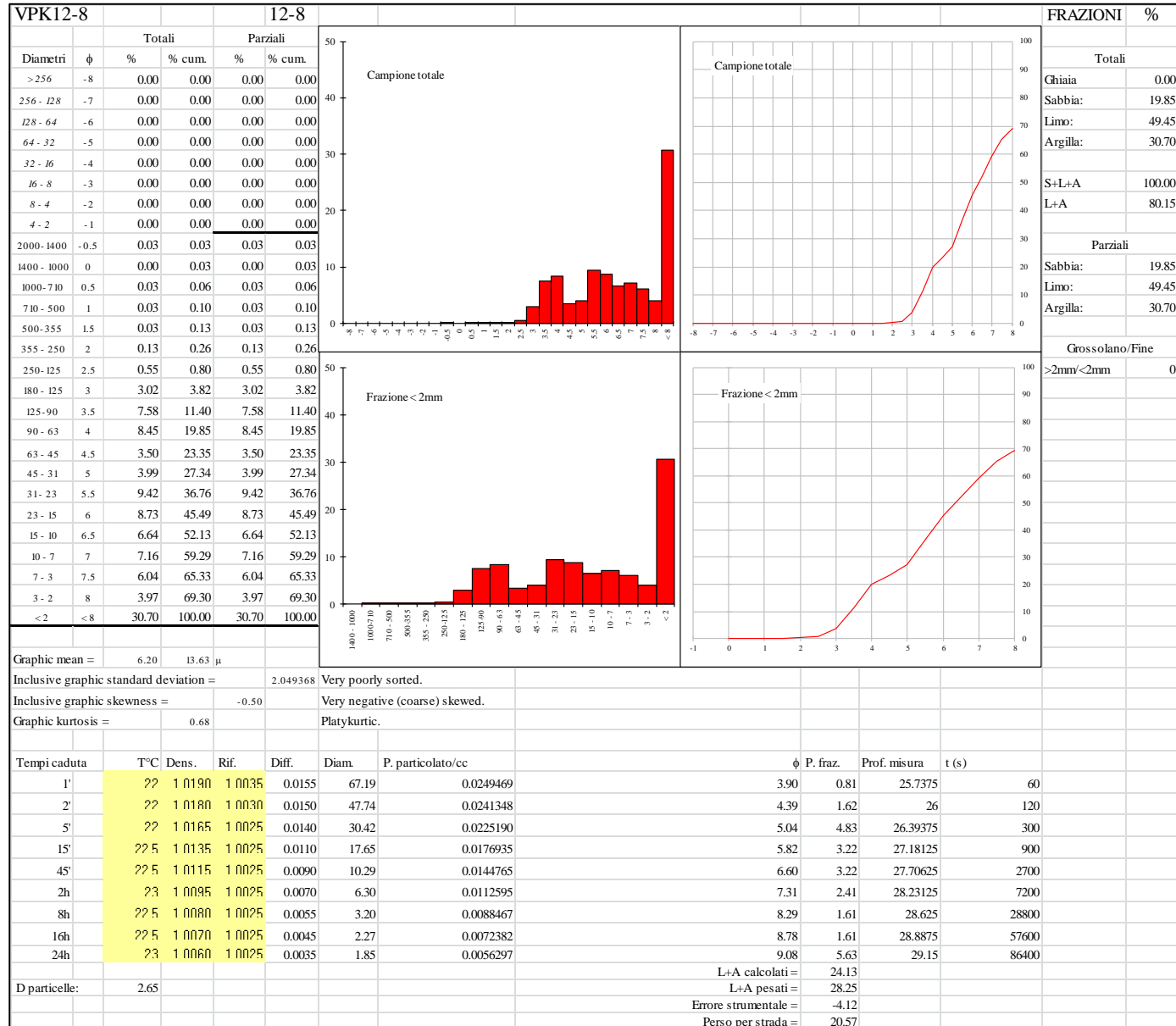
**Appendix 10.2. Grain-size
(Wentworth, 1922) of the <2 mm
fraction of decalcified samples
from Velika Pećina - Kličevica,
SU D.**



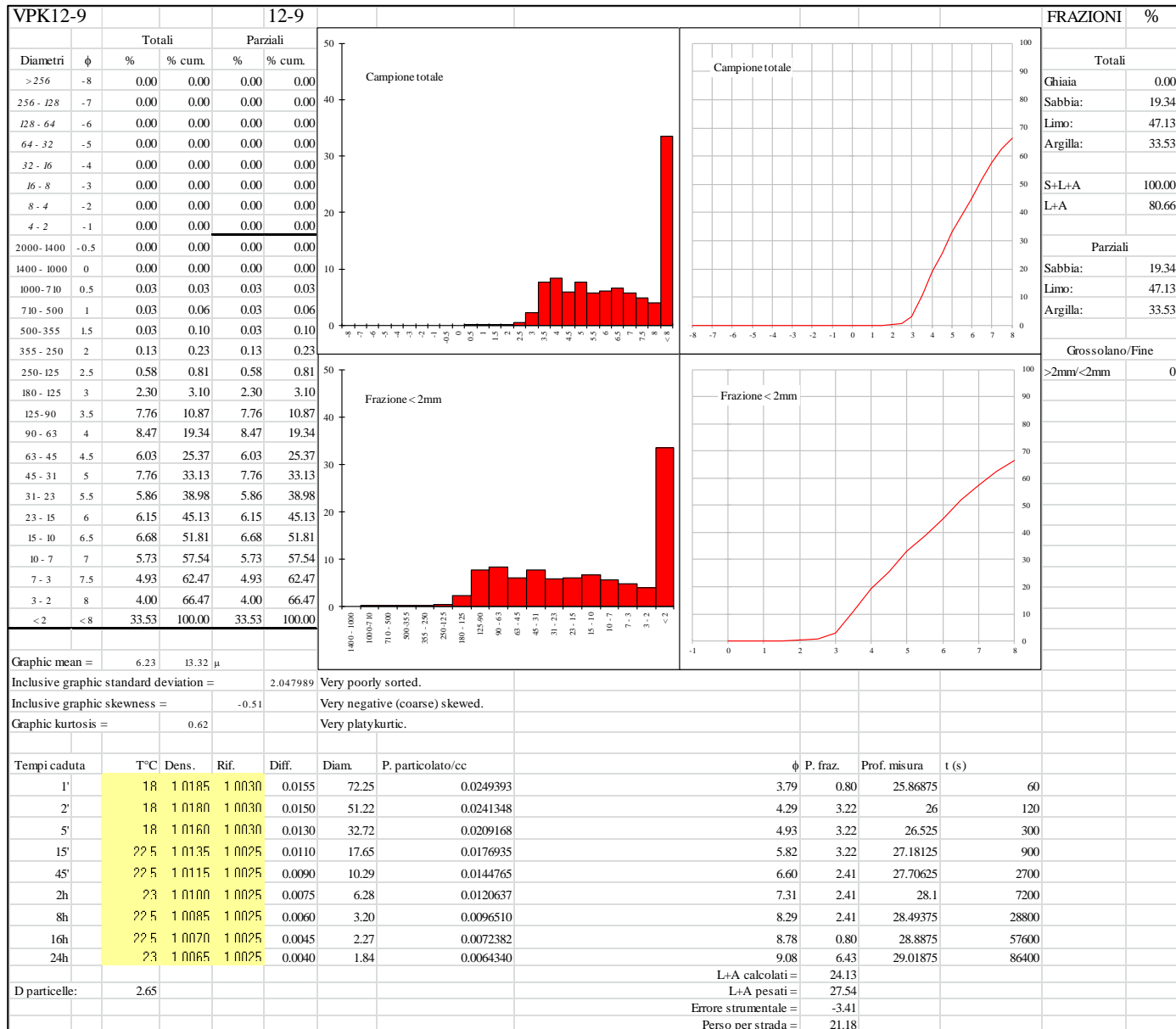
**Appendix 10.3. Grain-size
(Wentworth, 1922) of the <2 mm
fraction of decalcified samples
from Velika Pećina - Kličevica,
SU D_1.**



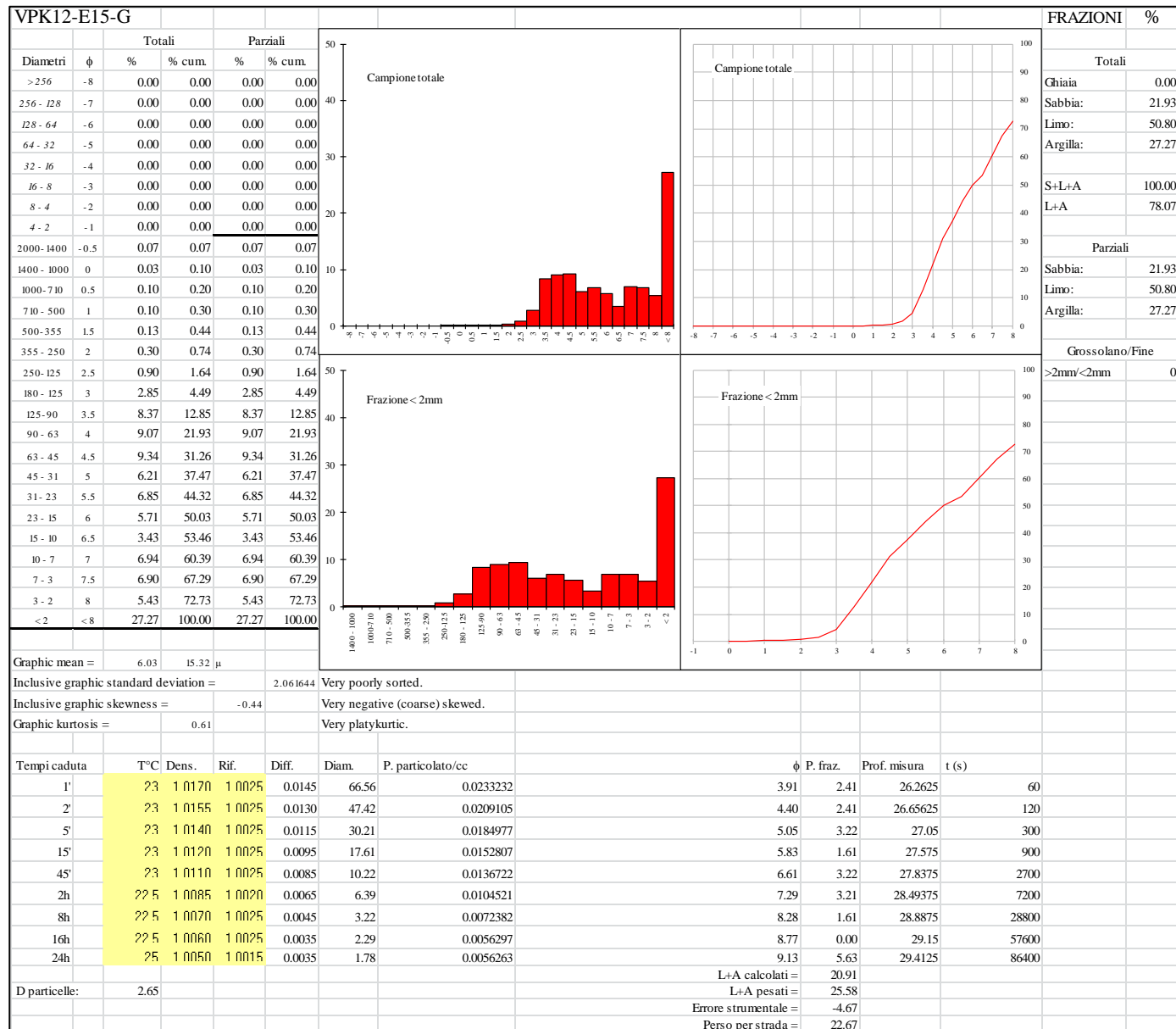
Appendix 10.4. Grain-size (Wentworth, 1922) of the <2 mm fraction of decalcified samples from Velika Pećina - Kličevica, SU C2.



Appendix 10.5. Grain-size (Wentworth, 1922) of the <2 mm fraction of decalcified samples from Velika Pećina - Kličevica, SU C1.



**Appendix 10.6. Grain-size
(Wentworth, 1922) of the <2 mm
fraction of decalcified samples
from Velika Pećina - Kličevica,
SU G.**



Appendix 10.7. Grain-size (Wentworth, 1922) of the <2 mm fraction of decalcified samples from Velika Pećina - Kličevica, SU X.

